THE UNIVERSITY
of EDINBURGH

Development and application of low-cost monitoring approaches for atmospheric ammonia, acid gases and ammonium aerosols

THE UNIVERSITY
of EDINBURGH

Yuk Sim Tang

A thesis submitted in fulfilment of the requirements
for the degree of Doctor of Philosophy

The University of Edinburgh

2020

Declaration

Parts of this work have been published in and/or submitted to:

Tang, Y. S., Braban, C. F., Dragosits, U., Dore, A.J., Simmons, I., van Dijk, N., Poskitt, J., Dos Santos Pereira, G., Keenan, P. O., Conolly, C., Vincent, K., Smith, R. I., Heal, M. R., and Sutton, M. A.: Drivers for spatial, temporal and long-term trends in atmospheric ammonia and ammonium in the UK, Atmos. Chem. Phys., 18(2), 705–733, https://doi.org/10.5194/acp-18-705-2018, 2018.

Tang, Y. S., Braban, C. F., Dragosits, U., Simmons, I., Leaver, D., van Dijk, N., Poskitt, J., Thacker, S., Patel, M., Carter, H., Pereira, M. G., Keenan, P. O., Lawlor, A., Conolly, C., Vincent, K., Heal, M. R., and Sutton, M. A.: Acid gases and aerosol measurements in the UK (1999–2015): regional distributions and trends, Atmos. Chem. Phys., 18(22), 16293–16324, https://doi.org/10.5194/acp-18-16293-2018, 2018.

Tang, Y. S., Flechard, C. R., Dämmgen, U., Vidic, S., Djuricic, V., Mitosinkova, M., Uggerud, H. T., Sanz, M. J., Simmons, I., Dragosits, U., Nemitz, E., Twigg, M., van Dijk, N., Fauvel, Y., Sanz, F., Ferm, M., Perrino, C., Catrambone, M., Braban, C. F., Leaver, D., Cape, J. N., Heal, M. R., and Sutton, M. A.: Pan-European rural atmospheric monitoring network shows dominance of NH_3 gas and NH_4NO_3 aerosol in inorganic pollution load, Atmos. Chem. Phys. Discuss., https://doi.org/10.5194/acp-2020-275, in review, 2020.

Some subjects of this thesis are also related to other publications I have contributed to:

Martin, N. A., Ferracci, V., Cassidy, N., Hook, J., Battersby, R. M., di Meane, E. A., Tang, Y. S., Stephens, A. C. M., Leeson, S. R., Jones, M. R., Braban, C. F., Gates, L., Hangartner, M., Stoll, J - M., Sacco, P., Pagani, D., Hoffnagle, J. A., and Seitler, E.: Validation of ammonia diffusive and pumped samplers in a controlled atmosphere test facility using traceable Primary Standard Gas Mixtures, Atmos. Environ., 199, 453–462, https://doi.org/10.1016/ j.atmosenv. 2018.11. 038, 2019.

Twigg, M. M., Llyinskaya, E., Beccaceci, S., Green, D. C., Jones, M. R., Langford, B., Leeson, S. R., Lingard, J. J. N., Pereira, G. M., Carter, H., Poskitt, J., Richter, A., Ritchie, S., Simmons, I., Smith, R. I., Tang, Y.S., van Dijk, N., Vincent, K., Nemitz, E., Vieno, M., and Braban, C. F.: Impacts of the 2014–2015 Holuhraun eruption on the UK atmosphere, Atmos. Chem. Phys., 16 (17), 11415-11431. https://doi.org/10.5194/acp-16-11415-2016, 2016.

Vieno, M., Heal, M. R., Hallsworth, S., Famulari, D., Doherty, R. M., Dore, A. J., Tang, Y. S., Braban, C. F., Leaver, D., Sutton, M. A., and Reis, S.: The role of long-range transport and domestic emissions in determining atmospheric secondary inorganic particle concentrations across the UK, Atmos. Chem. Phys., 14(16), 8435–8447, https://doi.org/10.5194/acp-14-8435-2014, 2014.

Yuk Sim Tang

July 2020

Abstract

Ammonia (NH_3) is the major alkaline gas in the atmosphere, with around 90 % of the total anthropogenic emissions in Europe coming from agriculture-related sources. Following emission to the atmosphere, the neutralisation reaction between NH_3 and the acid gases sulfur dioxide (SO_2), nitric acid (HNO_3) and hydrochloric acid (HCl) produces secondary inorganic aerosols (ammonium nitrate (NH_4NO_3), ammonium sulfate ($(NH_4)_2SO_4$) and ammonium chloride (NH_4Cl)). With longer atmospheric lifetimes than the gases, the aerosols also contribute to transboundary pollution problems. The gases and aerosols are removed from the atmosphere by wet (in precipitation) or dry (direct uptake by vegetation and surfaces) deposition processes. Together, they can negatively impact the natural environment through the input of excess acidity and nutrient nitrogen and harm human health through the formation of aerosols that contributes to fine-mode particulate matter ($PM_{2.5}$). They can also potentially influence climate change from the radiative forcing properties of the aerosols and the inputs of nitrogen that can alter the carbon cycle.

Monitoring data are necessary for assessing the spatial and temporal extent of pollution and as evidence to detect changes in pollutant concentrations in response to current and future policies to mitigate emissions of NO_x, SO_2 and NH_3. Combined with models, the concentration data are also used to estimate the different fractions of the total sulfur or nitrogen input and different chemical forms of the pollutants. Since the spatial and temporal patterns and atmospheric behaviours of gases and aerosols differ, measurements therefore need to distinguish between the phases.

The development of simple, low-cost, time-integrated air sampling methods and their application in cost-efficient monitoring strategies to assess temporal, spatial and trends in the gas and aerosol pollutants in the UK and across Europe is described. An active diffusion denuder method (DELTA®) and a passive sampler (ALPHA®) are implemented at a large number of sites (> 70) in the UK National Ammonia Monitoring Network (NAMN, established 1996) to measure NH_3 with a monthly frequency. An extension of the DELTA® method

provided additional, monthly measurements of particulate NH_4^+ (for the NAMN) and of the acid gases (SO_2, HNO_3, HCl) and aerosol species (NO_3^-, SO_4^{2-}, Cl^-, Na^+, Ca^{2+}, Mg^{2+}) for the UK Acid Gas and Aerosol network (AGANet, established 1999) at a subset of NAMN sites. The close integration of the two networks demonstrated the cost-effectiveness of the DELTA® approach, which provided quality assured, concurrent speciated measurement data on multiple pollutants at multiple sites, and also simplicity of operation by a large network of site operators, some of whom have no technical or scientific background. The DELTA® approach and quality protocol developed in the UK networks was further applied to a pan-European NitroEurope (NEU) DELTA® network (20 countries: 2006 – 2010), with knowledge sharing and collaboration between multiple laboratories and research organisations.

Important features in the spatial variability and seasonality in the gas and aerosol components were captured in the UK and European networks. The gases, with shorter lifetimes in the atmosphere were found to be spatially more heterogeneous, with a wider range of concentrations than their aerosol counterparts. Variations on a spatial scale were correlated with distributions and magnitude of emission sources, e.g. NH_3 and NH_4^+ concentrations were highest in intensively farmed areas (e.g. East Anglia in eastern England, NAMN) and countries (e.g. the Netherlands, NEU DELTA®). In the UK, evidence is also presented of the contribution by long-range transboundary sources to enhancement of concentrations of NH_4NO_3 and $(NH_4)_2SO_4$.

Distinct and contrasting seasonal cycles in the gas and aerosol phase components were established, important for identifying periods of pollution and for targeting abatement measures. The observed variations were attributed to seasonal changes in emission sources, atmospheric interactions and the influence of climate on partitioning between the gases and aerosols. For NH_3, peaks in concentrations occur from increased volatilisation promoted by warm, dry conditions (summer) and also from agriculture-related emissions, with a main peak in spring and a smaller peak in autumn. Concentrations of SO_2 were higher in winter (increased combustion), except in Southern Europe where the

peak period was in summer. HNO_3 concentrations were more complex, with small peaks in the seasonal cycle related to traffic and industrial emissions, photochemistry, meteorology and the influence of climate on HNO_3:NH_4NO_3 equilibrium. In comparison, the springtime peak in NH_4NO_3 was attributed to the reaction of a surplus of NH_3 with HNO_3 to form NH_4NO_3 in the aerosol phase under cooler, wetter conditions. A summertime peak in particulate SO_4^{2-} was observed in Southern Europe, coinciding also with peaks in SO_2, NH_3 and HNO_3 concentrations. While the high HNO_3 concentrations suggests increased oxidative capacity for formation of H_2SO_4 (from SO_2) and reaction with NH_3 to form $(NH_4)_2SO_4$, the absence of an NH_4^+ peak illustrates the larger influence of the more abundant NH_4NO_3 in controlling the seasonality of particulate NH_4^+.

Important changes in the atmospheric concentrations and partitioning between the different gas and aerosol components were captured. The measurement data highlighted the dominance of NH_3 and NH_4NO_3 in rural air, as the emissions of SO_2 and NO_x continues to fall, against a backdrop of increasing NH_3 emissions in the UK and across Europe since 2013. The observed shift in the form of NH_4^+ aerosol from the stable $(NH_4)_2SO_4$ to the semi-volatile NH_4NO_3 is expected to maintain a larger fraction of the NH_3 and HNO_3 in the gas phase. NH_4NO_3 can act as a reservoir and release the gases in warm weather, which may partly explain the observed non-linearity between emissions and measured concentrations of NH_3 in the UK data. The current and projected trends in the emissions of the gases SO_2, NO_x and NH_3 suggest that NH_3 and NH_4NO_3 can be expected to continue to dominate the inorganic pollution load over the next decades.

Lay Summary

Sulfur dioxide (SO_2), nitrogen oxides (NO_x), hydrogen chloride (HCl) and ammonia (NH_3) are short-lived airborne pollutant gases that are released to the atmosphere from both natural and man-made sources. Sulfuric acid (H_2SO_4) and nitric acid (HNO_3) are produced from SO_2 and NO_x, respectively. As a major alkaline gas in the atmosphere, NH_3 combines with these acids and also HCl to produce longer-lived ammonium-containing particles. The gases and particles are removed from the atmosphere either by wet deposition ("acid rain"), or dry deposition (direct uptake by vegetation and surfaces) processes. Unlike the gases which deposit locally close to sources, the particles can be transported longer distances and contribute to pollution in places far from sources, including across national boundaries. Together, these air pollutants have wide-ranging environmental effects, from damaging sensitive natural habitats (e.g. decline in species and biodiversity), to harming human health and influencing climate change.

Monitoring programmes provide the necessary data in support of evidence-based policies to improve air quality and assess environmental impacts. The different pollutants are unevenly dispersed in the atmosphere and require monitoring at a large number of sites to assess the geographic variations. Measurements must also be able to accurately measure the different forms of the pollutants at the same time and provide long-term, continuous data.

Simple air monitoring methods with low unit costs, suitable for implementation in high-density networks, have been developed to measure the concentrations of the different air pollutants. The main method (DELTA®) uses a small air pump to collect air and trap the gases and particles on a sample train consisting of chemically coated glass tubes and filters over a period of a month. The DELTA® method is deployed at a large number of sites in two UK air quality monitoring networks (established in the 1990s) and was also used in a pan-European network over a 4 year period (2006 – 2010). A second method is the passive air sampler (ALPHA®). These are little plastic air samplers (3 cm x 2.5 cm) that do not require power. The ALPHA® samplers are used to

measure NH_3 at remote sites and increased the UK network density. The UK and European networks relied on a network of local site contacts who swapped the air samples every month and posted exposed samples back to a chemical laboratory for analysis.

Information on the concentrations and distribution of the different gases and particles in the UK and across Europe highlighted where the "hotspots" are and months that they occur and where effects are likely to occur. The gases, in particular were spatially variable in the landscape because of their short lifetimes and uneven distribution of emission sources. Particles varied less in concentrations than the gases as they have longer lifetimes and have more time to mix and dilute in the atmosphere.

The smallest concentrations of air pollutants were measured in Northern Europe (Scandinavia), with the lowest emissions of the pollutant gases. Sulfur dioxide concentrations were highest in Central and Eastern Europe with larger SO_2 emissions. Around 90% of NH_3 in the UK and across Europe comes from agriculture. This is reflected in the data where NH_3 concentrations were highest in intensively farmed areas, e.g. in East Anglia (pig & poultry farming) in the UK, and in countries with larger NH_3 emission densities (e.g. the Netherlands and Italy). Peak periods for NH_3 emissions and concentrations in agricultural areas are spring and autumn when manure spreading usually takes place. In summer, warmer, drier conditions also enhances release of NH_3 from the ground (manure, fertiliser etc.) and this gives rise to a summer peak in concentrations. The main sources of SO_2 are from fossil fuel combustion, and elevated concentrations were seen in winter (increased energy demand for heating), except in Southern Europe where the peak period was in summer. The highest concentrations of particles were generally where concentrations of the gases were largest, peaking in spring when there was a surplus of NH_3 to react with acid gases.

Concentrations of the acid gases are shown to have fallen to low levels, in line with reported trends in emissions of the gases, in particular in SO_2. There were however little change in NH_3 concentrations, which continued to exceed safe

levels for sensitive habitats at large numbers of sites across the UK and Europe. Ammonia pollution is also implicated in causing premature deaths through the formation of fine particles. Emissions of NH_3, in particular from the agricultural sector, have also instead been increasing in the UK and across Europe since 2013. The current and projected trends in the emissions of the different gases suggests that NH_3 pollution will remain a problem over the next decades. Mitigating NH_3, in particular from the agricultural sector is likely to deliver the largest improvement in air quality and reduce impacts on the environment and human health. The monitoring programmes described delivered cost-effective measurements of the different gases and particles. Continuation and wider adoption of the monitoring programmes will inform policy decisions.

Acknowledgements

The work presented in this thesis was made possible by the large numbers of dedicated local site operators (LSO) in the UK and European networks, and site owners / host organisations, to whom I would like to express my gratitude for their contributions and continuing support. Colleagues also provided invaluable assistance and support and I would like to thank the following:

- Antje Branding, Ben Miners: my predecessors, for laying the groundwork to the UK NAMN.
- Celia Milford, Mhairi Coyle: training, advice and friendship when I started. Carrying a heavy duty post-driver 2 miles up Allt á Mharcaidh and back with Celia on my first field trip was memorable.
- Robert Storeton-West, Ian Leith, Ivan Simmons and field team: setting up sites, maintaining equipment / field sites and LSO duties.
- Eiko Nemitz, Neil Cape, David Fowler, Ron Smith: science advice.
- Ulli Dragosits: network/Glenshee measurements in the beginning, science advice, GIS guru, support / encouragement and a good friend.
- Gordon Elphinstone, Dave McEwan: building DELTA/misc. equipment, making the first prototype ALPHA samplers and tackling the various engineering/workshop requests I threw at them, with good humour.
- Chris Bennett, George Rutherford, Albert Johnston: building wind-solar systems and workshop/engineering support.
- Alan Warwick, Cyril Barrett, Phil Farrand: building new DELTA II systems, site upgrades/servicing, workshop/engineering support.
- Kate Crowe, Gary Fitchie, admin/facilities staff for their kind assistance.

I am very privileged to have Mark Sutton, Mat Heal and Christine Braban as my PhD supervisors and I would like to thank them for their encouragement, patience and guidance in my scientific endeavours.

To friends, family and in particular to my partner Alan Mitchell, I reserve special thanks for their support and being there for me.

The PhD was funded by UKCEH.

Contents

List of Figures

List of Tables

Chapter 1 Introduction

1.1 Ammonia, acid gases and aerosols

Atmospheric pollutants that form the focus of this thesis are ammonia (NH_3), nitric acid (HNO_3), sulfur dioxide (SO_2), hydrochloric acid (HCl) and the secondary inorganic aerosols (SIAs) ammonium sulfate ($(NH_4)_2SO_4$), ammonium nitrate (NH_4NO_3) and ammonium chloride (NH_4Cl). The aerosols are reaction products from the neutralisation reaction between the alkaline NH_3 gas with HCl and the atmospheric acid gases formed through the oxidation of nitric oxides, NO_x (HNO_3) and SO_2 (H_2SO_4) (Fig. 1.1) (Huntzicker et al., 1980; AQEG, 2012).

As a chemically reactive and water-soluble alkaline gas, NH_3 has a relatively short atmospheric lifetime (a few hours to ~ 5 days) in the atmosphere (Fig. 1.1, Table 1.1). By comparison, NH_4^+ aerosols have longer atmospheric residence time of 3 - 25 days and may be transferred much longer distances (100 to >1000 km) and contribute to pollution in places far from sources (Fig. 1.1, Table 1.1).

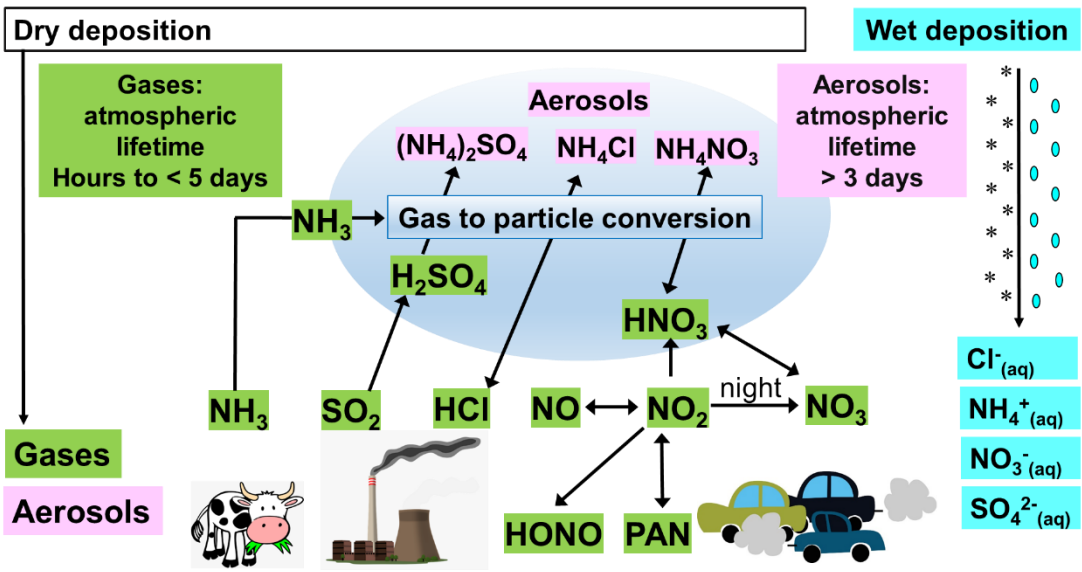

Figure 1.1: Reaction scheme showing the emissions, atmospheric chemistry and fate of NH_3, acid gases and NH_4^+ aerosols. PAN = peroxyacetyl nitrate, HONO = nitrous acid.

The atmospheric lifetimes of NH_3 and NH_4^+ aerosols are influenced by the following processes: i) short range dispersion and deposition of NH_3 gas, ii) chemical reaction and formation of longer-lived NH_4^+ aerosols, and the long-range transport and deposition of the NH_4^+ aerosols, and iii) changing ratio of NH_3 and acid gases (ROTAP, 2012). The actual transport distance also depends on wind, climate and meteorological conditions (Fowler et al., 2015), as well as emission height. When pollutants are emitted at higher levels, e.g. from tall stacks, the atmospheric residence time and transport distance increases (ROTAP, 2012).

Removal of the pollutants from the atmosphere occur either by dry deposition (direct uptake by vegetation and surfaces), wet deposition (in rain/snow) or by occult deposition in fog and cloud (ROTAP, 2012). The dry deposition velocity of NH_3 is typically at least an order of magnitude higher than for the NH_4^+ aerosols (Table 1.1). Loss of NH_3 from the atmosphere through dry deposition is therefore more rapid than for NH_4^+ aerosols, and a significant fraction of the emitted NH_3 is dry deposited within 2 - 5 km of its source (e.g. Fowler et al., 1998; ROTAP, 2012). By contrast, NH_4^+ aerosols are mainly removed by wet deposition (ROTAP, 2012).

Loss of NH_3 through chemical reaction with atmospheric acids is estimated to further deplete NH_3 by approximately 5% per hour (van Jaarsveld and Bleeker, 2004) to 30 % per hour (Asman et al, 1998; Asman, 2001). Since the reaction between NH_3 and acidic species is very fast, the time it takes for converting gaseous NH_3 to NH_4^+ aerosols depends on the availability and formation rates of H_2SO_4 and HNO_3 (Fowler et al., 2015). For example, when the concentrations of SO_2 are in large molar excess over NH_3, McKay (1971) showed that 50 % of available NH_3 was converted into $(NH_4)_2SO_4$ in about 35 minutes. Any significant reduction in NH_3 through chemical reaction therefore occurs at distances of several tens of kilometres from a source, with dry deposition processes contributing to removal of a larger fraction of emitted NH_3 close to sources.

Table 1.1: Comparison of atmospheric lifetimes, dry deposition velocities (V_d) and transport distances of NH_3 and NH_4^+ aerosols in Europe.

	Ammonia gas	Ammonium aerosols
Atmospheric lifetime	0.8 days (Moller and Schieferdecker, 1985) 1 – 5 days (Warneck, 1988) 1 day (Seinfeld and Pandis, 1998) 3.5 hrs (dry deposition) (Flechard and Fowler, 1998) 1 day (Wichink Kruit et al., 2012) A few hours (Fowler et al., 2015) Several hours (Hendriks et al., 2016) Atmospheric half-life: 1.93 hrs (day) - 3.85 hrs (night) (Erisman et al., 1988)	7-10 days (Seinfeld and Pandis, 1998) 1 – 15 days (Perrino et al., 2002) 4 -15 days (ROTAP, 2012) 3 – 25 days (Długosz-Lisiecka and Henryk, 2012) A few days to a week (Fowler et al., 2015)
Transport distance	< 1 km to 100 km (Asman et al., 1998) 14 km (night) - 35 km (day) (Erisman et al., 1988) 50 km (Moorland) (Flechard and Fowler, 1998) 50km (Ferm, 1998) 20 – 100km (RoTAP, 2012)	up to 1500 km (Asman et al., 1998) > 1000 km (ROTAP, 2012)
Deposition velocity, V_d (mm s^{-1})	Coniferous forest: median = 21 (5 – 33) Mixed forest: median = 12 (4 – 30) Deciduous forest: median = 9 (3 – 18) Semi-natural: median = 7 (1 – 18) Urban: median = 8 (1 – 11) Water: median = 6 (5 – 9) Agricultural: median = 4 (2 – 71) (Schrader et al., 2014)	Coniferous forest: 0.7 (Hicks et al., 1982) Deciduous forest: 0.6 (Hicks et al., 1989) Moorland: 1.9 (Sutton, 1992) Heathland: 1.8 (Duyzer, 1994) Forest: 11.5 (Ruijgrok et al., 1997) Land: 1 (Ferm, 1998) Low vegetation: 1.4 (Asman, 2001) Coniferous forests: 8.4 ± 2.5 (Horvath, 2003)

Together, these gases and aerosols are linked to negative impacts on ecosystem and human health at local to transboundary scales, as well as playing an important role in climate forcing (ROTAP, 2012; EMEP, 2019). They are major contributors to input of acidity (acidification) and nutrient nitrogen (N) (eutrophication) to terrestrial and freshwater ecosystems (ROTAP, 2012; EMEP, 2019). The accumulation of acidity and/or N in soil, vegetation and water bodies affects the competitive balance of plant species by shifting the pH and chemical balance of nutrients. This can lead to a reduction in both soil and water quality, decline in sensitive species and biodiversity and ecosystem change (e.g. Bobbink et al., 2010; Sheppard et al., 2011). Exposure of vegetation to the pollutant gases above ecosystem thresholds can also cause damage directly (Harmens et al., 2012).

The aerosols formed are mainly in the 'fine' mode. They make up a significant fraction of fine particulate matter (PM) with diameters less than 2.5 µm ($PM_{2.5}$) (AQEG, 2015; Vieno et al., 2014), known to be harmful to human health (e.g. Kim et al., 2015; Brunekreef et al., 2015). The input of airborne N to the biosphere also influences climate through the closely coupled N and carbon (C) cycle (Reis et al., 2012; Sutton et al., 2013; Zaehle and Dalmonech, 2011). The radiative scattering properties of the aerosols in the stratosphere can exert climate-cooling effects *via* aerosol-radiation and aerosol-cloud interactions that reflect solar radiation back into space (Hayward, 2016).

1.2 Air quality policies

A number of EU policies and international agreements specifically target reducing the environmental impacts of SO_2, NO_x and NH_3 (and also PM). These include:

UNECE Convention on Long-Range Transboundary Air Pollution (CLRTAP) 1999 Gothenburg Protocol (amended 2012) to abate acidification, eutrophication and ground-level ozone (UNECE, 2012). This sets maximum permitted level of emissions of SO_2, NO_x and NH_3, relative to the emissions in

2005, for the years 2020 to 2029, with greater reduction commitments from 2030.

EU National Emissions Ceilings Directive (NECD, 2016/2284/EU) sets binding emission reduction commitments equal to those required by the Gothenburg protocol (EU, 2016). Emissions of $PM_{2.5}$ are also included for the first time.

2008/50/EC Ambient Air Quality Directive, with target ambient concentration values in relation to SO_2, NO_2 and PM (EC, 2008).

2010/75/EU Industrial Emissions Directive (IED) on industrial emissions (under the pollution prevention and control (PPC) regulations) to prevent and control emissions from industrial activities into air, water or soil, in relation to polluting substances, including N (EC, 2010). In 2017, more stringent targets were set for emissions of NO_x, SO_2 and PM concentrations from large combustion plants, including many large coal-fired power stations, giving the operators four years to meet the standards, as detailed in the Decision (EU) 2017/1442 under Directive 2010/75/EU (EC, 2017).

A host of Directives that limit emissions of these gases from specific sources, including legislation for road transport exhausts (Euro 5 and 6 Regulation (EC) No 715/2007) (EC, 2007), non-road mobile machinery (EU Regulation (2016/1628) (EC, 2016), shipping (sea and inland waterways; MARPOL 73/78) (IMO, 1978), and ammonia pollution of the aquatic environment (76/464) (EC, 1976).

Emissions of SO_2 and NO_x have been decreasing across Europe over the past 20 years and are projected to decrease further under the revised Gothenburg Protocol and NECD. Substantial reductions in SO_2 have been achieved in the UK (−96 %; 173 kt in 2017) (NAEI, 2020) and across Europe (−83 %; 4700 kt in 2016) (EEA, 2020) since 1990. The decrease in NO_x has been smaller, decreasing by 72 % in the UK (873 kt in 2017) and by 54 % across Europe (8586 kt in 2016). By contrast, the commitments to reduce NH_3 emissions have been more modest and decreased more slowly than either SO_2 or NO_2 in the UK (−13 %; 283 kt in 2017) (NAEI, 2020) and Europe (−18 %; 4717 kt in 2016)

(EEA, 2020) since 1990. Since 2013, the decreasing trend in NH_3 was reversed, with an increase of around 4 % since 2014 in the UK and across Europe. As a result, the importance of N pollution, and in particular NH_3, is expected to continue to increase over the next decades relative to the other nitrogen and sulfur (S) pollutants, playing a significant role in contributing to ecosystem effects through acid and N deposition and to the formation of fine PM.

1.3 The role of air monitoring

The environmental impacts of air pollutants described in Sect. 1.1 occur as result of both the direct effects of concentrations above ecosystem/human exposure thresholds and the deposition/input of acidity (acidification) and nutrient N (eutrophication) to sensitive habitats. In Europe, ecosystem effects assessments apply the “critical levels” and “critical loads” approach (CLRTAP, 2014). By comparing critical levels with measured air pollutant concentrations, and critical loads with total reactive N and S deposition, the complementary approaches provide an estimate of exceedance of ecosystem thresholds at designated sites (e.g. Natura 2000 sites) (Hallsworth et al., 2010; Rowe et al., 2017). The risk of change to ecosystems resulting from exposure to air pollutants can also be assessed in this way.

Measurement data are necessary to provide information on the atmospheric composition, spatial, temporal and long-term trends, and to assess atmospheric transport and chemistry models (e.g. Simpson et al., 2006; Vieno et al., 2016). Air concentrations may be measured, but depositions are more usually estimated using atmospheric models (e.g. Dore et al., 2015; Flechard et al., 2011). This requires the availability of measurement data at sufficient resolution and spatial coverage to run the model and to map atmospheric deposition inputs at an appropriate scale for assessing effects (e.g. EMEP, 2019; ROTAP, 2012). Estimating N dry deposition is particularly challenging due to the different forms and routes of N input. Consequently, it remains a

key source of uncertainty in quantifying net N inputs to terrestrial ecosystems for effects assessment (e.g. Flechard et al., 2011; Fowler et al., 2007; Sutton et al., 2007).

Under the 2012 UNECE Gothenburg protocol and EU NECD, member states must jointly cut their emissions of NH_3, SO_2 and NO_x (precursor to HNO_3) between 2005 and 2020, with further NECD targets set for 2030. As a precursor to PM, controlling NH_3 will also reduce the contribution of NH_3 to $PM_{2.5}$ and PM_{10}. In the light of policies to reduce atmospheric emissions, it is important to be able to measure ambient concentrations of these pollutants on a continuous, long-term basis to detect changes in pollutant concentrations. This provides the evidence to assess the effectiveness of current and future abatement policies and inform policy decisions. The measurement data are also key for assessing changes and potential recovery in ecosystem responses to emissions reductions of air pollutants under Article 9 of the NECD (EC, 2012) and reporting under the Habitats Directive (EC, 1992).

An integrated approach to the monitoring of these air pollutants provides a better understanding of the atmospheric composition. The measurement of the different gases and aerosols at the same time and on a sufficient scale and duration allows interactions between them to be investigated in a changing chemical climate.

In designing a network, both spatial and temporal sampling considerations should reflect the variability and gradients in the air pollutant concentrations. Owing to their atmospheric reactivity, high deposition velocities and heterogeneous sources, the acid gases, and NH_3 in particular, have higher spatial variability than the NH_4^+ aerosols. Consequently, a larger number of sites will be needed to get a representative concentration field (e.g. country-scale) for the reactive gases than for the aerosols. Areas with low concentrations may have fewer sites, while focussing more monitoring in areas with larger and more variable concentrations. The choice of possible monitoring methods and the number of sites are then based on meeting

measurement objectives (single *vs* multi-pollutant), the ability of the network to identify pollution episodes, or describe seasonal and/or annual average values of air pollution, while minimising the cost of the network (see e.g. Trujillo-Ventura and Ellis, 1991).

1.4 Measurement approaches for reactive gases and aerosols

A review of the range of available methods for measuring reactive gases (NH_3, HNO_3, SO_2, HCl) and aerosols (NH_4^+, NO_3^-, SO_4^{2-}, Cl^-) in ambient air is presented. The key focus is on simple, low-cost time-integrated methods that can distinguish between the gas and aerosol phase and that are suitable for implementation at multi-sites in long-term monitoring networks. Automatic methods, including the latest state-of-the-art instrumentation are also described, but these are more suited to measurements at a few key sites, or for campaign measurements of short duration.

1.4.1 Integrative atmospheric sampling methods

Integrative atmospheric sampling methods provide atmospheric concentrations averaged over a prescribed sampling period. These include passive and active air samplers. Passive samplers rely on the passive diffusion of gases to a collection surface (Sect. 1.4.1.1). Active air samplers require the active pumping of air and include impingers/bubblers (Sect. 1.4.1.2), filter packs (Sect. 1.4.1.3) and diffusion denuder methods (Sect. 1.4.1.4).

1.4.1.1 Passive diffusion samplers

Passive diffusion samplers are widely used in monitoring NO_2 and NH_3 (e.g. Krupa et al. 2000; Martin et al., 2019; Tang et al. 2001). Since they are simple, low-cost and do not need power, large numbers may be deployed easily and cheaply to provide detailed spatial and temporal surveys. They are very useful for site representativeness studies (e.g. Lolkema et al., 2015), studies in source areas (e.g. Vogt et al., 2013) and in complementing other air quality measurements in national networks (e.g. Butler et al., 2016; Lolkema et al.,

2015). Passive samplers for monitoring SO_2 (e.g. Ayers et al., 1998; Plaisance et al., 2002; Hien et al., 2014) and HNO_3 (e.g. Bytnerowitz et al., 2005; Ferm et al., 2005; Place et al., 2018) have also been reported, but are not routinely used. In the case of HNO_3, adsorption losses of HNO_3 gas to the PTFE membrane at the inlet can lead to under-estimation of HNO_3 concentration (Place et al., 2018).

There are three main types of passive samplers: tube, badge and radial types (Fig. 1.2). The sampling rates and therefore sensitivity of the different designs are determined by their geometry (Tang et al., 2001). Sampler types should therefore be matched to measurement requirements.

Tube-type samplers are typically of low sensitivity because of the large length to area ratio (Fig. 1.2). Examples include the original design of the open Palmes tube (7.1 cm long; Palmes, 1976; Thijsse et al., 1996) and shorter Gradko diffusion tubes with a membrane air inlet (3.5 cm long; Thijsse et al., 1996, Sutton et al., 2001a; Tang et al., 2001; Martin et al., 2019).

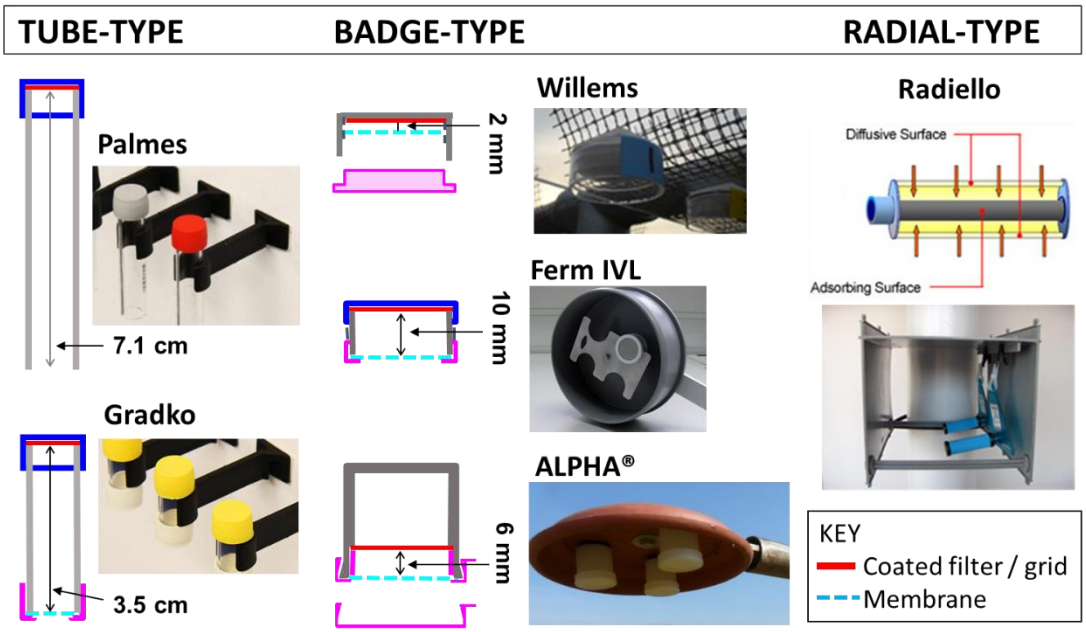

Figure 1.2: Types of passive diffusion samplers.

The sensitivity of diffusion tubes are sufficient for monitoring NO_2 concentrations that are generally > 10 ppb and for monitoring NH_3 close to sources, with concentrations > 5 ppb (Loubet et al., 2009). They are however unsuitable for monitoring ambient concentrations of NH_3, where concentrations at background sites can be < 1 ppb (Sutton et al., 2001a). Palmes-type diffusion tubes are used to measure nitrogen dioxide (NO_2) in a UK diffusion tube network (NO_2-net) (Conolly et al., 2016). Established in 1990, the network provides a rural background for the UK modelling of NO_2 for annual compliance mapping against Air Quality Objectives. The rural measurements supplements continuous NO_x measurements made with automatic methods (Sect. 1.4.2.3) in the UK Automatic Urban and Rural Network (https://uk-air.defra.gov.uk/networks/ network-info?view=aurn).

Badge-type samplers (Fig. 1.2) are more sensitive and can be used to monitor low concentrations of NO_2 and NH_3 in background areas, but may not be suitable for monitoring in source regions or for long-term exposures (1 month or more) due to potential saturation problems (Tang et al., 2001). For example, the Willems badge sampler (Willems, 1993) was used to map NH_3 concentration across the Republic of Ireland in 1990 (de Kluizenaar and Farrell, 2000), repeated in 2013 (Doyle and Cummins, 2014). In order to avoid saturation, weekly (in 1990) and 2-weekly (in 2013) exposure periods were used to derive annual mean concentrations, which demanded greater effort and resources.

With a sampling rate that is intermediate between the Willems sampler and diffusion tubes, the IVL Ferm sampler is suitable for ambient air monitoring with longer (monthly) exposure period, (Ferm, 1991; Ferm and Svanberg, 1998). However, the use of the IVL sampler is restricted as the company does not sell the components and offers a measurement service only. In the absence of a suitable passive sampler on the market, the CEH ALPHA® sampler (Tang et al., 2001) was developed specifically to permit accurate and sensitive monitoring of ambient NH_3 concentrations on a monthly timescale. This replaced the Gradko membrane diffusion tubes that were used at the

beginning in the UK National Ammonia Monitoring Network (Sutton et al., 2001a) (see Chapter 2).

The Radiello™ sampler is a high sensitivity radial-type diffusive sampler (Fig. 1.2), used widely in the US (Butler et al., 2016; Puchalski et al., 2011). Its cylindrical outer surface acts as the diffusive membrane, with gases moving axially parallel towards an adsorbent bed which is also cylindrical and coaxial to the diffusive surface. Owing to the design, the samplers need to be exposed inside specially designed shelters to protect them from rain.

While the passive samplers are simple to use, well-defined quality protocol and validation against a reference active sampling method is essential, to assess the performance of the samplers and to calibrate the uptake rate of the samplers. In a recent assessment, the ALPHA® outperformed all other passive samplers tested in an inter-comparison exercise across a range of ambient NH_3 concentrations (Martin et al., 2019). Key elements to the success of the ALPHA® samplers are the implementation of quality protocol developed and described in this thesis (Chapter 2) that were applied to the NH_3 measurements.

1.4.1.2 Impingers/Bubblers

In this classical method, reactive gases such as SO_2 and NH_3 are collected in an absorbing solution in a bubbler or on an impinger (Fig. 1.3) (Egner and Eriksson, 1955; Hayman et al., 2004), with offline analysis of the chemical species in the aqueous sample. Since there is potential interference from collection of aerosol NH_4^+, the method is unsuited to the measurement of atmospheric NH_3, but it was widely used in the 1980s to measure SO_2 (NEGTAP, 2001; ROTAP, 2012). In the UK, a hydrogen peroxide bubbler instrument was implemented in the former rural SO_2 network (1991 – 2000) with 31 sites at which concentrations of SO_2 were measured on a daily to weekly basis (Hayman et al., 2004). The sensitivity of the method is however limited by the large volume of the absorption/extraction solution and it was replaced by a filter-pack method (see Sect. 1.4.1.3) in 2001, when SO_2

concentrations in the UK declined to levels that were at or below the limit of detection of the bubblers (Hayman et al., 2004).

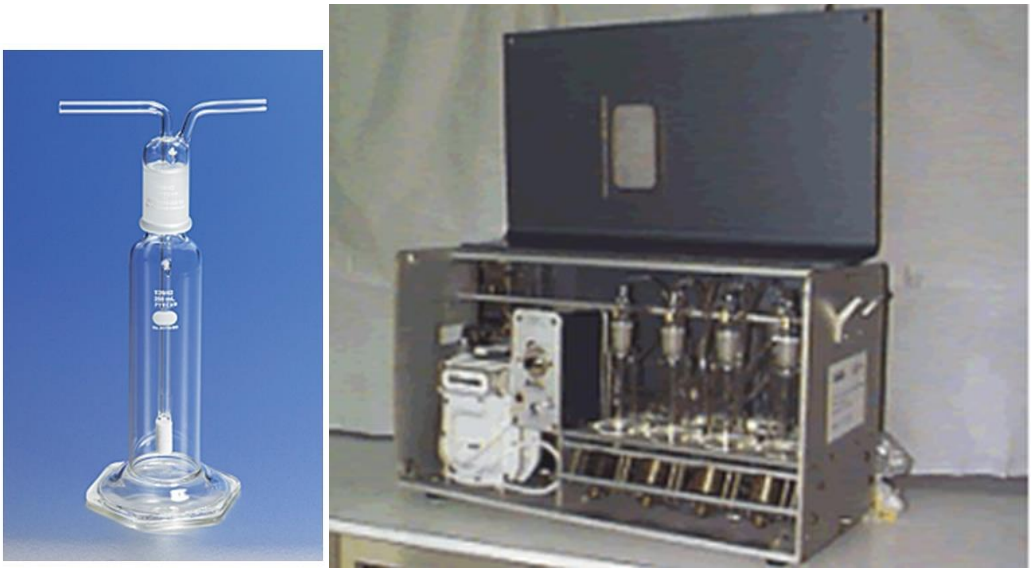

Figure 1.3: (LEFT) Picture of a typical glass bubbler, consisting of a cylindrical glass bottle which is filled with an absorption solution and an impinger tube and frit to "bubble" gas into the absorbing solution. (RIGHT) Bubbler sampler instrument in which a known volume of air is pumped through a chemical solution in each of the glass bubbler for a prescribed period of time.

1.4.1.3 Filter Packs

The filter-pack method is one of the early methods developed to separately measure gas and particulate phase inorganic pollutants (e.g. EMEP, 2014; Kitto and Colbeck, 2017; Sickles et al., 1999). This consists of a pre-filter to capture particulate phase, usually made of Teflon, followed by one or more filters to collect gases (Fig. 1.4). The filters are housed within an airtight holder, and air is actively pumped through the holder, using an air pump, with air flow monitored with a gas meter. The method was used for determination of SO_2 and particulate SO_4^{2-} in the UK rural SO_2 network from 2001 to 2005 with a fortnightly and later, monthly frequency (Hayman et al., 2004), which replaced the bubbler method described in Sect. 1.4.1.2).

Figure 1.4: An example 2-stage open-face filter pack sampler.

Although the method is considered to be robust for sampling SO_2 concentrations, there are potential artefacts in sampling HNO_3 and HCl, due to interactions with NH_3 and the volatility of NH_4NO_3 and NH_4Cl aerosol (EMEP, 2014; Kitto and Colbeck, 2017; Sickles et al., 1990). Disturbance of atmospheric gas-particle equilibrium during sampling (temperature, relative humidity or acidity change in the filter and pressure drop across the filter) may cause volatilisation of NH_4NO_3 and NH_4Cl from the filter, with the release of HNO_3, NH_3 and HCl in the gas phase (Kitto and Colbeck, 2017; Sickles et al., 1999). Evolved gases will be collected on downstream filters intended for gases, resulting in a positive bias in gaseous components and a negative bias on particulates. Ammonia can also be retained on the front filter of a filter pack, either by adsorption or reaction with the collected particulate matter, to give a positive bias in particulate NH_4^+ (Kitto and Colbeck, 2017).

The filter-pack method continues to be used in the European Monitoring and Evaluation Program (EMEP) network on a daily timescale (Torseth et al., 2012). EMEP is a Europe-scale monitoring program developed and implemented by the cooperative programme for monitoring and evaluation of the long-range transmission of air pollutants in Europe, linked to the Convention on Long-range Transboundary Air Pollution (CLRTAP) (EMEP, 2019). Due to uncertainty in the partitioning between the gas and aerosol

phase nitrogen concentrations just described, the results are typically reported as the sum of Total Inorganic Nitrogen (TIN: HNO_3 + NO_3^-) and sum of Total Inorganic Ammonium (TIA: NH_3 + NH_4^+) (Torseth et al., 2012).

1.4.1.4 Diffusion Denuder

The diffusion denuder is a technique that selectively removes reactive gases on chemically coated denuders, followed by collection of particulates on aerosol filters placed downstream, if required (e.g. Ferm, 1979; Perrino et al., 1990; 2001; Sutton et al., 2001b). In this approach, potential artefacts caused by phase interactions that may be associated with bubblers (Sect. 1.4.1.2) and filter packs (Sect. 1.4.1.3) are avoided. When a laminar air stream passes through a tube coated on the inside with, for example, an acid, NH_3 is captured by the acid walls, whereas NH_4^+ aerosol pass through unaffected and may be collected on a post-denuder aerosol filter. Conversely, the use of a base coating will collect acid gases such as HNO_3, SO_2 and HCl. The separation of particles from gaseous species is achieved due to the much more rapid diffusion of gaseous species to the tube wall compared with that of particles (Ferm, 1979). In this case, partition equilibrium is undisturbed, since the residence time in the denuder is of the order of tenths of seconds.

Ferm denuders

In the most basic form, a simple glass tube may be used as a diffusion denuder. The simplest is the original design of Ferm (1979), although this is intended for short-term sampling (1 - 24 hrs). The Ferm denuders are 0.5 m long to achieve > 95 % collection efficiencies at a high flow rate of 4 L min^{-1}, with associated issues of practicality in terms of handling and sending the long, denuders in the post.

DELTA® system

The DEnuder for Long Term Atmospheric sampling (DELTA®) system (Fig. 1.5) (Sutton et al., 2001b; Tang et al., 2009, 2018a, 2018b) samples air more slowly (0.2 – 0.4 L min^{-1}) and uses shorter, robust glass tubes (10 – 15 cm long x 1 cm external diameter) that can be put in the post. It was developed

specifically to provide monthly measurements of NH_3 and later also particulate NH_4^+ for the UK NAMN (Fig. 1.6) (Chapter 2). An extension of the denuder-filter sample train in the method was used to additionally measure acid gases (HNO_3, SO_2, HCl) and aerosols (NO_3^-, SO_2, SO_4^{2-}, HCl, Cl^- and base cations) (Fig. 1.7) in the UK Acid Gas and Aerosol Network (AGANet, Chapter 3) and a pan-European network (Chapter 4). The DELTA® method is therefore economical, since it makes concurrent speciated measurement of the gases and aerosols. It also has the required sensitivity to measure down to the low concentrations encountered in the UK and Europe. Simplicity of the method makes it easy to set up in the field and requires little training for field operators to carry out the required monthly exchange of samples.

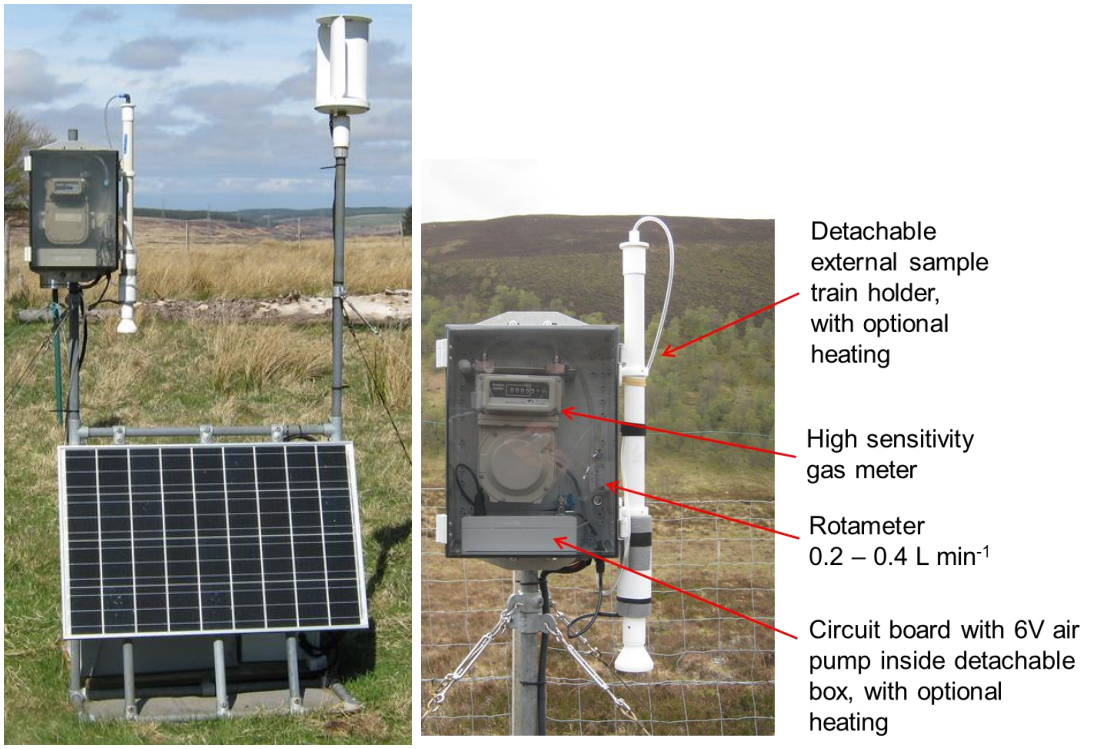

Figure 1.5: (LEFT) Wind-solar powered DELTA® system. (RIGHT) Low voltage DELTA® system (new design since 2016). DELTA® denuder-filter pack sample trains are housed within the detachable external holder.

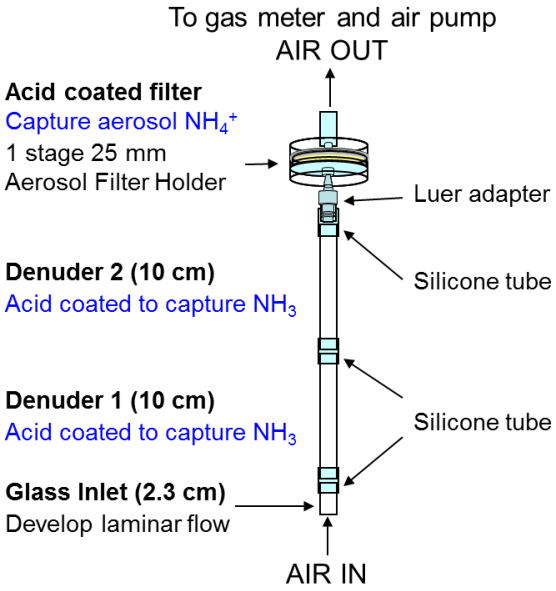

Figure 1.6: DELTA® denuder-filter sample train for speciated collection of NH_3 gas and particulate NH_4^+.

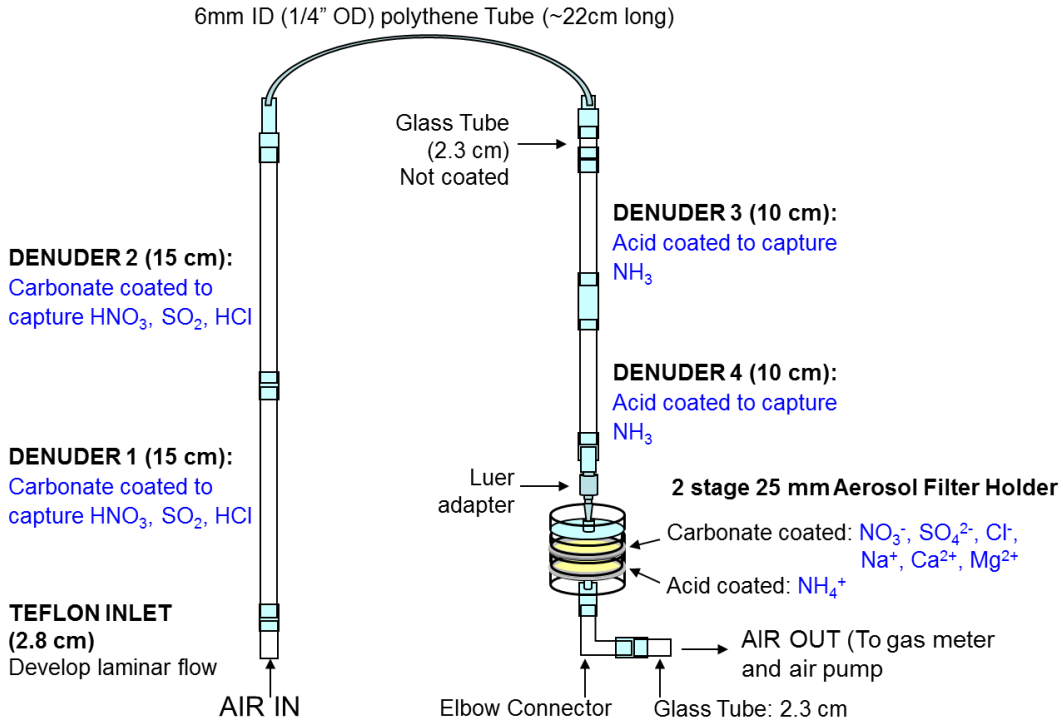

Figure 1.7: DELTA® extended denuder-filter pack sample train for speciated collection of NH_3, acid gases and aerosols, deployed between 1999 to 2015. This was replaced by a sample train with a linear configuration in 2016 (Tang et al. 2015).

Annular and honeycomb denuder systems

More complex denuders include annular and honeycomb denuders (Fig. 1.8) that are designed for short-term sampling of between 1-24 hours and operate at much higher flow rate of 10 - 15 L min^{-1} (e.g. Possanzini et al., 1999; Koutrakis et al., 1993). The design of annular denuders consists of coaxial tubes, forcing the sample stream to flow through the annular space between the outer and inner tubes (Fig. 1.8). The configuration increases the surface area for retaining reactive gases, thereby allowing higher operative flow rate and a shorter length of collection tube. A honeycomb denuder, as the name implies, is made up of hexagonal flow channels (Fig. 1.8), with one such system consisting of 212 channels of 2 mm diameter (Koutrakis et al., 1993). This results in a more compact design. The high costs of the equipment and running these types of measurements necessarily limits operations to a few sites or to campaign measurements.

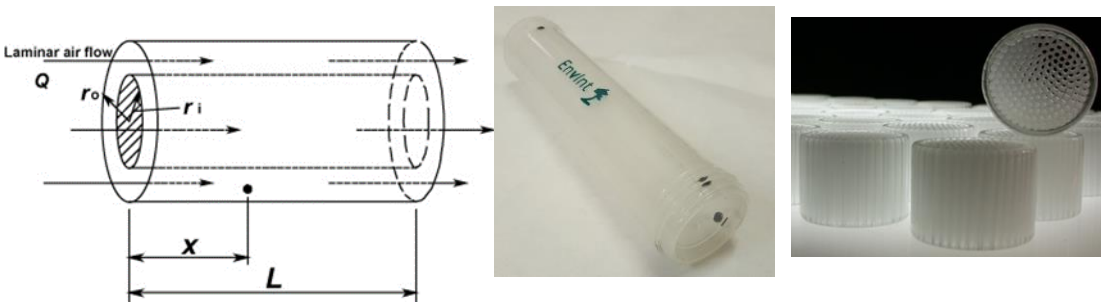

Figure 1.8: (LEFT) Annular denuders. (RIGHT) Honeycomb denuders**.**

Although annular denuder systems (ADS) are recommended by the US EPA (USEPA, 1997) and also by EMEP (EMEP, 2014), daily monitoring using the ADS is hard work, requiring repeated manual extraction and recoating of the denuders. The large numbers of samples for chemical analysis also incur high laboratory costs. Commercially available annular denuders are also both expensive and fragile. The ADS is therefore labour-intensive and prohibitively expensive for long-term measurement at multiple sites. It is estimated to be about 30-50 times more costly than DELTA® monthly monitoring, based on

experience of operating the 2 methods in parallel over a one-year period in the UK AGANet (Chapter 3; Tang et al., 2018b). In the EMEP network, an ADS is used at a small number of sites to provide speciated data, in support of TIN/TIA measurements made at filter pack sites (Sect. 1.4.1.3) for modelling purpose (EMEP, 2016).

1.4.2 Continuous air measurement methods

Continuous air monitoring methods include wet denuders and diffusion scrubbers with on-line chemical analysis (1.4.2.1), as well as various spectroscopic methods (Sect. 1.4.2.3; see also review by Lööv et al., 2014 and Blohm et al., 2020). Their main benefit is to provide high time-resolution data, and so identify peaks in concentration, duration of 'acute' exposures, and to associate such episodes with particular weather conditions. However, because of their cost, requirement for electrical power and skilled personnel, they are not well suited to monitoring the spatial extent of gases such as NH_3 that has high spatial variability.

1.4.2.1 Continuous wet denuders

Continuous wet annular denuder methods with on-line analysis for atmospheric monitoring of NH_3 include AMOR (Fig. 1.9) (Ammonia MOnitoR, Berkhout et al., 2017) and AMANDA (Ammonia Measurement by ANnular Denuder sampling with online Analysis (Wyers et al., 1993; Moring et al., 2017). The AMOR system operates with an hourly time resolution and was used in the Netherlands to provide the concentration field for atmospheric NH_3 at 8 stations in the Dutch NH_3 monitoring network (Buijsman 1998; Van Pul et al., 2004; van Zanten et al., 2017). A disadvantage of the method is the use of reagents which have to be frequently refilled, disposal of waste solutions, and the need for frequent calibration. This led to the replacement of the AMOR by a mini-DOAS method (see Sect. 1.4.2.3) across the Dutch network in 2016 (Berkhout et al; 2017; van Zanten et al., 2017). The AMANDA gradient system is similar to the AMOR, but operates with a higher time resolution, applied in a

large number of studies measuring NH_3 fluxes (Erisman et al., 2001, Sutton et al., 2009; Moring et al., 2017).

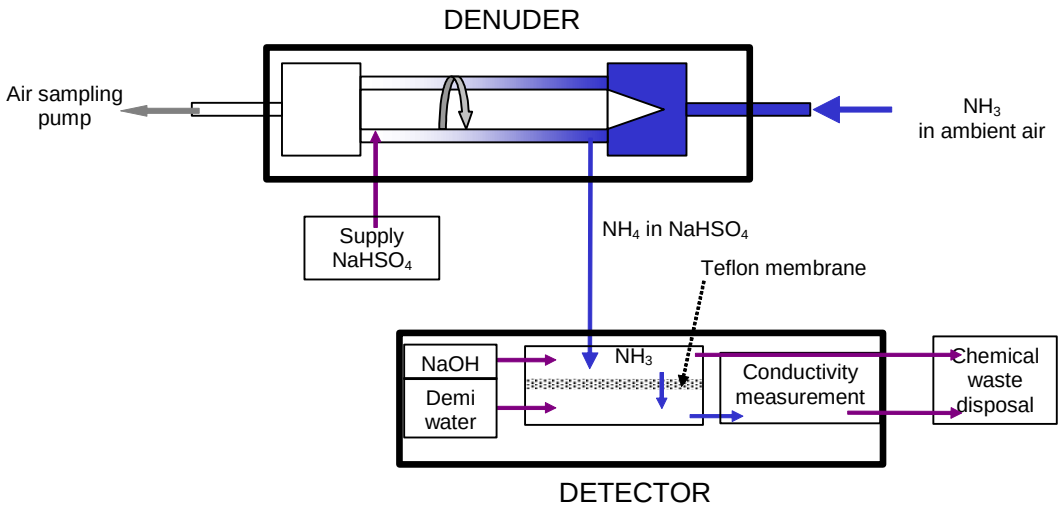

Figure 1.9: Schematic representation of the measurement principle of AMOR.

The GRAEGOR (Gradient of Aerosols and Gases Online Registrator) is a further development and extension of the AMANDA system (Genfa et al. 2003; Jonegejan et al. 1997; Ramsey et al., 2018; ten Brink et al. 2007; Thomas et al., 2009). It has a wet rotating annular denuder (WRD) to collect water-soluble reactive trace gases (NH_3, HNO_3, HONO, HCl, and SO_2) and a steam-jet aerosol collector (SJAC) to collect aerosol species (NH_4^+, NO_3^-, NO_2^-, Cl^-, SO_4^{2-}), with online analysis of inorganic ions by ion chromatography.

The MARGA (Monitor for AeRosols and Gases, Applikon Analytical BV) is a commercial system, based on the AMANDA and GRAEGOR instruments (Fig. 1.10) (Twigg et al., 2016). This can provide unattended continuous, simultaneous measurements of the water-soluble reactive gases and aerosol components for up to 2 weeks (Rumsey and Walker, 2016; Stieger et al., 2018; Thomas et al., 2009; Twigg et al., 2016). In addition, the use of size-selective inlets further provide speciated PM measurements in the different size ranges (e.g. $PM_{1.0}$, $PM_{2.5}$ or PM_{10}). The high cost and large size of the equipment, coupled to the requirement for calibration/operation by skilled personnel

necessarily restrict it to a small number of sites. The MARGA is currently operated on a continuous basis at two EMEP supersites in the UK (Twigg et al., 2016), and as part of the US Environmental Protection Agency's Clean Air Status and Trends Network (CASTNet) (Rumsey et al., 2014).

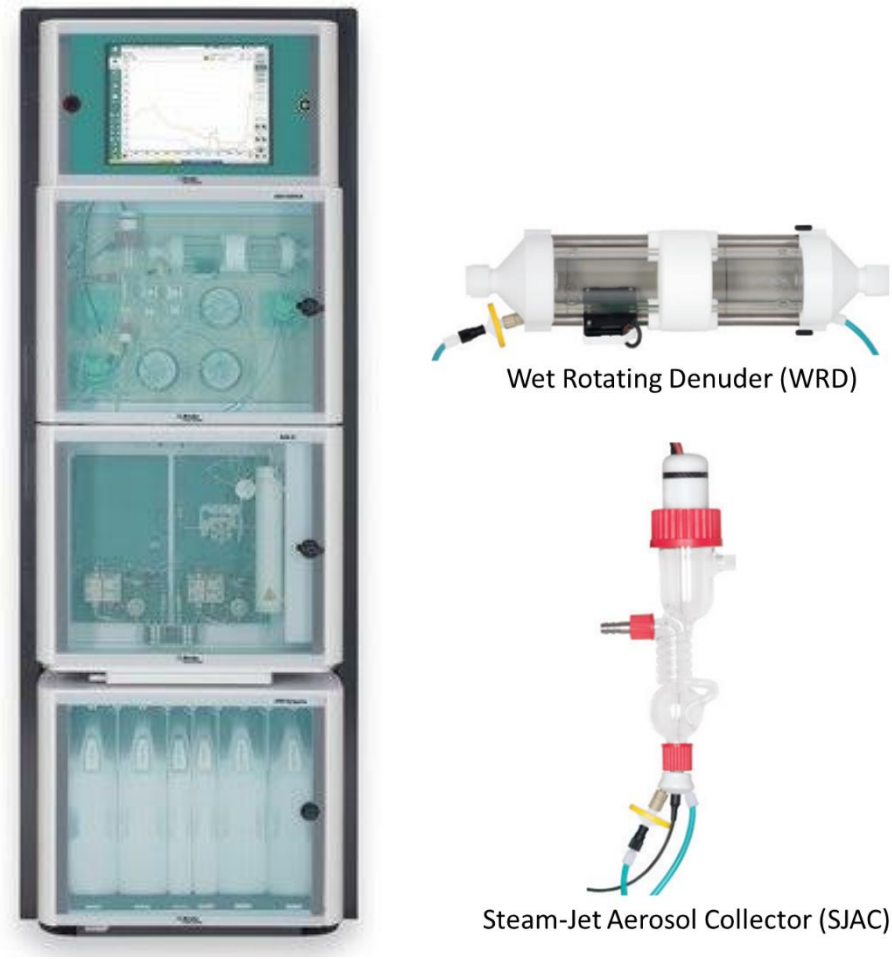

Figure 1.10: (LEFT) The Monitor for AeRosols and Gases in Ambient air (MARGA) for continuous monitoring of water-solube gases and aerosols. (RIGHT) Wet rotating denuder for collection of water-soluble reactive gases and stean-jet aerosol collector for collection of water-soluble aerosols (https://www.metrohm.com/).

1.4.2.2 Continuous Diffusion scrubbers

Diffusion scrubbers are membrane-based, in which the sample air flows on one side of the membrane and a suitable scrubber liquid flows on the other side (Dasgupta, 1984; Neftel et al., 1998, Sorenson et al., 1994). Such systems typically collect 10-30% of the NH_3 passing through, and are calibrated according to their collection efficiency. An example commercial system is the AiRRmonia Automated Ammonia Analyzer (Fig. 1.11) (RR Mechatronics, Netherlands). This contains a membrane stripping system for quantitative sampling of gas-phase NH_3 (Fig. 1.11). After diffusion through the membrane, NH_3 is absorbed in a sampling solution, while NH_4^+-containing aerosols pass through the sampler. The sample solution is then pumped continuously through the detector for conductivity measurement (Fig. 1.11). This method is used in high-resolution measurements to estimate emissions and fluxes (e.g. Riddick et al., 2016; Spirig et al., 2010; von Bobrutski et al., 2010).

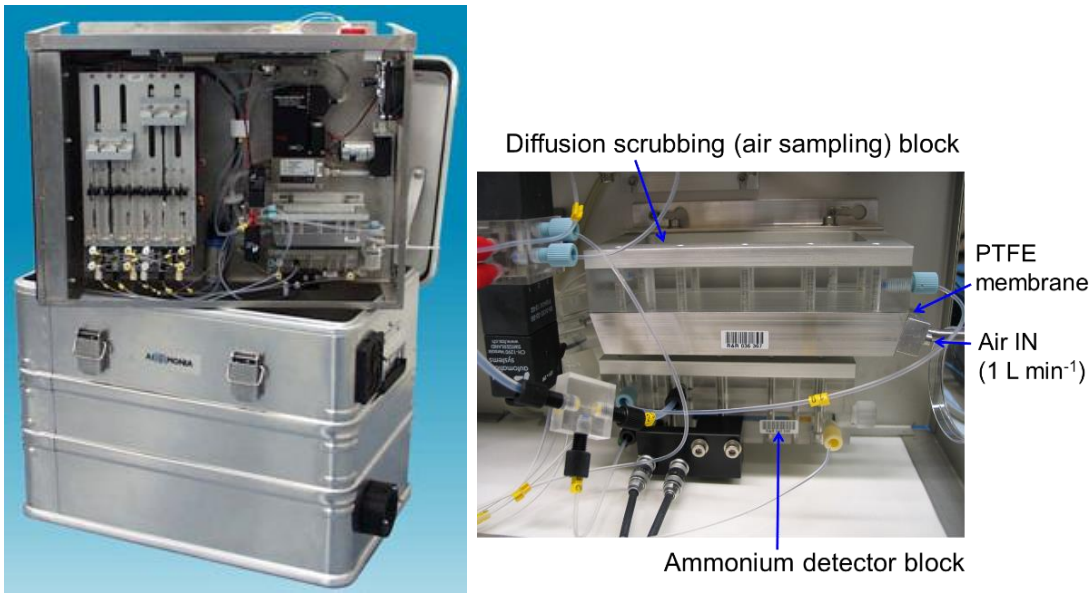

Figure 1.11: (LEFT) AiRRmonia Automated Ammonia Analyzer (RR Mechatronics, Netherlands). (RIGHT) Diffusion scrubber ontop of and ammonium detector.

1.4.2.3 Optical spectroscopic methods

Automatic, optical spectroscopic methods are routinely used in compliance monitoring against air quality objectives across Europe. These include reference methods recommended by the EU for the measurement of SO_2 (UV fluorescence; EC, 2005) and NO_x (chemiluminescence; EC, 2012).

UV fluorescence

SO_2: The measurement of SO_2 is based on fluorescence spectroscopy principles. SO_2 exhibits a strong ultraviolet absorption spectrum between 200 and 240 nm. When SO_2 absorbs UV from this, emissions of photons occur (300–400 nm). The amount of fluorescence emitted is directly proportional to the SO_2 concentration.

Chemiluminescence

NO_x**:** Instruments measure NO by chemiluminescence that is emitted from the NO_2 produced from the reaction of NO with ozone. Excess ozone is produced *in situ* in the instrument from oxygen in the inlet air. The instruments measure NO_x (i.e. the sum of NO and NO_2) when the air passes through a heated Mo-converter (converting NO_2 to NO), while only NO is measured when the Mo-converter is bypassed. Other oxidized N compounds, in particular PAN and HNO_3, are also (at least partially) converted to NO by the Mo-converter and can interfere with the measurement of NO_x. NO_2 concentrations are calculated within the reference method by subtracting the concentration of NO from the concentration of NO_x.

NH_3: One of the earliest continuous monitors for NH_3 was based on a chemiluminescence detector for NO_x, where the sampled air stream is passed through a catalytic converter to convert NH_3 quantitatively to NO (Demmers et al. 1999; Riddick et al., 2016; von Bobrutski et al., 2010). This technique has a relatively high detection limit, especially where background NO_x levels are high, because the NH_3 signal is derived as (usually) a small difference between two large numbers. Any inefficiencies in converting different forms of oxidised

and reduced N compounds to NO lead to large bias in the result. Particulate NH_4^+ can also cause an interference in the NH_3 detection.

Other state-of-the-art methods

A range of state-of-the-art instrumentation has been developed for high resolution, precise and selective continuous monitoring of air pollutants. These include advanced optical methods (see review by Blohm et al., 2020), e.g. Tunable Diode Laser Absorption Spectroscopy (TDLAS) (Clemitshaw, 2004), LOng Path liquid Absorption Photometer (LOPAP) (Clemitshaw, 2004; Kleffmann et al., 2007, 2008; Villena et al., 2011) and Differential Optical Absorption Spectroscopy (DOAS) methods for NO_2, SO_2 (Avino and Manigrasso, 2008), and also for NH_3 (Berkhout et al., 2017). The technique makes use of the characteristic absorption features of gas molecules along a path of known length in the open atmosphere. A miniaturised mini-DOAS system was developed to provide high-resolution continuous NH_3 measurements in the Dutch NH_3 network from 2016 (Berkhout et al., 2017).

Instruments are developing continuously, and photo-acoustic spectroscopy is now used in commercially available NH_3 monitors. Recent developments include cavity ring-down instruments (Fig. 1.12) (CRDS; Bobrutzki et al., 2010) and quantum cascade laser-based ammonia sensor (QCL: Miller et al., 2014; Martin et al., 2016, 2019; Zöll et al., 2016), with detection down to parts-per-billion (ppb).

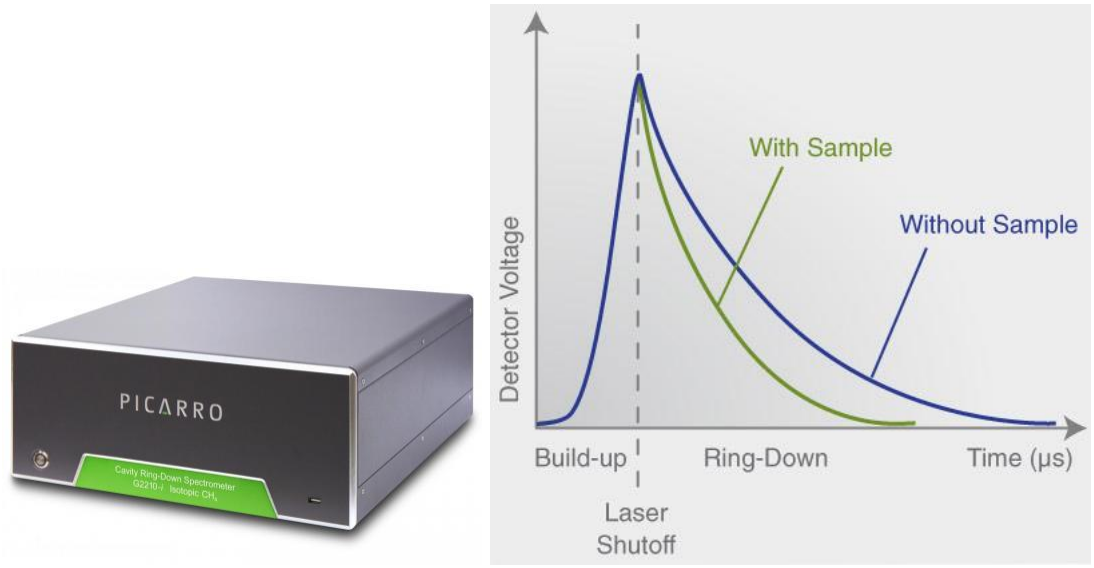

Figure 1.12: (LEFT) An example Cavity Ring-Down Spectroscopy (CRDS) instrument by Picarro (https://www.picarro.com/). (RIGHT) Measurement principle of CRDS, which compares light intensity as a function of time with and without a sample having resonant absorbance. Optical loss (due to absorption by sample, e,g. NH_3 gas) is converted to real time concentration measurement

1.5 Multi-pollutant air monitoring strategies

In devising a multi-pollutant monitoring strategy, the level of ambition has to be balanced against the most cost-effective way of delivering those objectives with available resources. In the EMEP '3 level' approach (EMEP 2014; Sutton et al., 2004; Torseth 2003), measurement requirements at each level are matched to specific measurement objectives, such as temporal and spatial changes in air concentrations and deposition, development and validation of models and source-receptor relationships (Fig. 1.13). Measurement methods suitable for monitoring at the different levels are summarised in Table 1.2.

By using low temporal resolution measurements in high density networks for the assessment of spatial patterns and trends (Sect. 1.5.1), and focusing process measurements at a few key sites (Sect. 1.5.2), overall science delivery of the combined levels strategy is maximised, based on the resources available. The selection of appropriate methods to meet measurement requirements needs to consider the following:

- Single or multi-pollutant.
- Measurement resolution: weekly / monthly time-integrated average, or time resolved continuous data.
- Required limit of detection limit.
- Degree of automation.
- Available resources (capital and personnel).

The determination of NH_3 and HNO_3 in air can also be complicated by interference from particle-borne NH_4^+ and NO_3^- ions. Measurement techniques must therefore be able to accurately determine the gas and particulate phase concentrations without disturbing the partition existing in the atmosphere at the time of sampling.

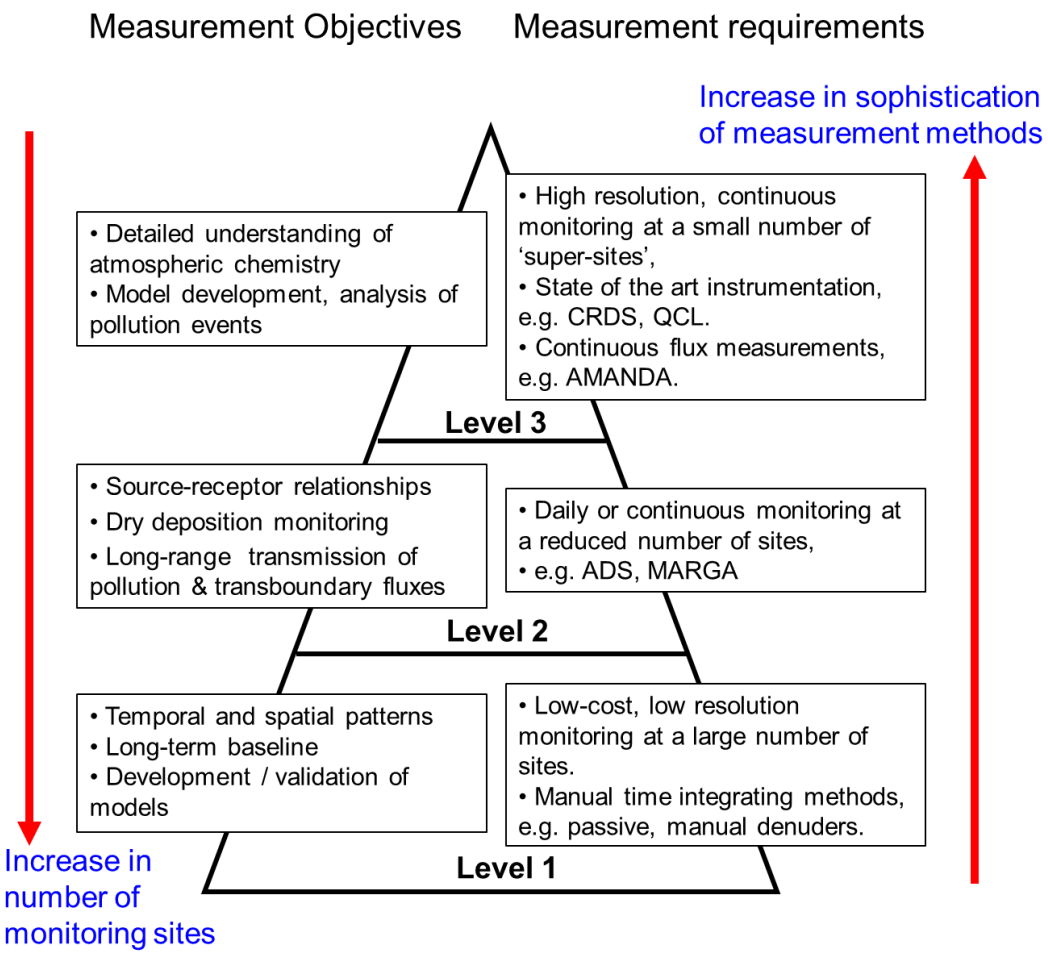

Figure 1.13. EMEP 3-Level monitoring strategy. Adapted from Sutton et al. (2004).

Table 1.2. Matching monitoring methods to measurement objectives for NH_3, acid gases (HNO_3, NO_x, SO_2, HCl) and NH_4^+ aerosols, including base cations**.**

Methods	Measurement Ambition			Species measured	Comments
	Level 1	Level 2	Level 3		
INTEGRATIVE					
Passive samplers	✓			NH_3, HNO_3, SO_2, NO_x	Gases only. Single gas per sampler.
Bubblers	✓	✓		SO_2, SO_4^{2-}	Method not reliable for NH_3 - interference from NH_4^+
Filter packs	✓	✓		SO_2, SO_4^{2-} Sum (HNO_3, NO_3^-) Sum (NH_3, NH_4^+)	Phase uncertainty Reported as: TIN (HNO_3 + NO_3^-) TIA (NH_3 + NH_4^+)
Simple denuders (Ferm)	✓	✓		Gases: NH_3, HNO_3, HONO, SO_2, HCl Particles: NH_4^+, NO_3^-, SO_4^{2-}, Cl^-, Na^+, Ca^{2+}, Mg^{2+} Collected at same time	High sampling rate (4 L min^{-1}): hourly to daily monitoring
Simple denuders (DELTA®)	✓				Low sampling rate (0.2 – 0.4 L min^{-1}): weekly to monthly monitoring
Annular (ADS) + honeycomb denuders		✓	✓		High sampling rate (10 - 15 L min^{-1}): hourly to daily monitoring
CONTINUOUS					
Wet denuders: AMOR		✓		NH_3	Hourly resolution. Used in Dutch NH_3 network (1995 – 2016)
Wet denuders: AMANDA			✓	NH_3	High resolution flux measurements
Wet denuders with steam jet aerosol collector: MARGA, GRAEGOR			✓	Same as for denuders	Hourly resolution. Used at two UK EMEP supersites
Spectroscopic: UV fluorescence			✓	SO_2	EU Reference method for SO_2
Spectroscopic: DOAS			✓	NH_3	Mini-DOAS in Dutch NH_3 network (from 2016)
Spectroscopic: Chemiluminescence			✓	NO_x NH_3	EU Ref. method for NO_x Method not reliable for NH_3 - interference from NO_x
Spectroscopic: TDLAS			✓	NH_3 HNO_3	High resolution.
Spectroscopic: QCL, CRDS			✓	NH_3	High resolution, new emerging technologies

1.5.1 Level 1: seasonal, spatial patterns and trends

To assess spatial patterns and temporal trends, level 1 monitoring can be achieved cost-effectively by the implementation of low-cost methods at many sites in a network with a low temporal frequency (Table 1.2). Key requirements of monitoring methods include:

(a) *Adequate spatial coverage:* Air pollutants are often unevenly dispersed in the environment. For mapping concentration fields, data are required at resolutions which match the spatial variability of any given pollutant and which reflects the resolution of the atmospheric models being applied. For more spatially variable species such as NH_3 (Dragosits et al., 2002), there is a need for denser monitoring. For example, NH_3 is monitored at > 70 sites in the UK NAMN (Chapter 2). With respect to secondary pollutants, with low spatial variability and low formation rates, fewer sites are required. For example, ammonium aerosols are measured at only 30 sites in the UK AGANet (Chapter 3). Measurements to assess spatial variability requires the deployment of many samplers simultaneously. Consequently, unit costs must be kept low.

(b) *Sufficient temporal resolution:* Information on seasonal variations will allow investigation of atmospheric processes and model improvements, as well as analysis of individual pollution events, important for assessing human health and ecosystem impacts. Monthly is considered optimal and provides the most effective resolution to derive annual mean concentrations and to examine seasonality in the data.

(c) *Long-term monitoring*: This is important for establishing baselines to allow detection of trends.

(d) *Co-located and concurrent monitoring* of all relevant components to allow an assessment of their interactions.

(e) *Standardised methods and quality protocols* with adequate quality control and quality assurance procedures to provide accurate and reproducible measurement data with a consistent methodology over time.

Passive samplers are the lowest cost option (Sect. 1.4.1.1). These alone will provide a good measure of the spatial extent of NH_3 concentrations, but will not measure NH_4^+ aerosols. Alternatively, a simple diffusion denuder (DELTA®) method (Sect. 1.4.1.4) could provide simultaneous measurements of reactive gases and aerosols. The DELTA® is used in the UK to monitor both NH_3 and NH_4^+ in the UK NAMN (see Chapter 2) and which also provides measurement of acid gases and aerosols (HNO_3, SO_2, HCl, Na^+, Ca^{2+}, Mg^{2+}) in the UK AGANet (see Chapter 3) on a monthly timescale. The ALPHA®samplers are also deployed in the UK NAMN. While the DELTA® method provides the main regional patterns in NH_3 and also NH_4^+, the ALPHA® method permits measurements at remote sites with no access to power. The lower unit costs of the ALPHA® also makes it possible to increase network density in source areas to explore source-receptor relationships and for model validation. Compared with expensive high frequency sampling (Sect. 1.4.2; a level 2 approach) (Table 1.2), the low-cost DELTA® approach, complemented by passive ALPHA® NH_3 monitoring represents a very effective use of resources.

1.5.2 Levels 2/3: Intensive measurements

Intensive daily manual sampling methods (e.g. filter packs, Sect 1.4.1.3; annular denuders, Sect. 1.4.1.4) and new high-resolution technologies (e.g. CRDS, Sect. 1.4.2) are for investigating process interactions (Table 1.2). These may be classed as Level 2 and 3 activities. For intensive measurements, daily (or even hourly) monitoring of aerosol and gases are useful at a few selected locations for detailed analysis and model testing. However, given the costs, it is clear that daily manual sampling is not advisable for assessing long-term trends or spatial patterns. Expensive high frequency measurement is better suited to validation of high-resolution atmospheric chemistry/transport models, source-receptor relationships and rapid temporal changes. State-of-the-art measurements also require support of research groups, further increasing the costs and resource requirements.

1.6 Reactive gas and aerosol monitoring in Europe

In the 1980s, wet deposition measurements were coordinated across Europe under the EMEP pan-European programme, to understand the contributions and effects of SO_2 emissions to acid rain (e.g. EMEP, 2019; ROTAP, 2012). Atmospheric measurements were later added to provide a more detailed understanding of atmospheric composition, provide information on the concentrations and deposition of air pollutants, as well as the quantity and significance of the long-range transport of air pollutants and their fluxes across boundaries (UNECE, 2004; Torseth et al., 2012).

The EMEP observations include measurements of the S and N pollutants that are linked to acidification and eutrophication effects, addressed by the UNECE Gothenburg protocol. Atmospheric measurements of sulfur (SO_2, SO_4^{2-}) and N (NH_3, HNO_3, NH_4^+, NO_3^-) are made by a daily filter pack method (Sect.1.4.1.3) across the EMEP networks since 1985 that provide data for evaluating wet and dry deposition models (EMEP 2016; Torseth et al., 2012). As discussed in Sect. 1.4.1.3, the method does not distinguish between the gas and aerosol phase N species. Speciated measurements by an expensive and labour-intensive daily annular denuder method (Sect. 1.4.1.4) are also made (Torseth et al., 2012), but are necessarily restricted to a small number of sites, due to high costs associated with this type of measurement.

There are also networks with specific focus on particular S or N components, for example, air quality compliance monitoring across Europe in the case of SO_2 and NO_x and the national NH_3 monitoring networks in the Netherlands (van Zanten et al., 2017) and in the US (Puchalski et al., 2015). In the UK, monitoring of atmospheric pollutants initially focused on SO_2 to assess effects of acid rain (ROTAP, 2012). Other networks include the NO_2 diffusion tube network (NO_2-net) at rural locations established in the 1980s to map rural concentrations in the UK (Conolly et al., 2016).

A need exists for speciated and concurrent measurement data for the respective gas and aerosol phase at sufficient spatial scales. Such data would help to, 1) improve estimates of N deposition, 2) contribute to development and validation of long-range transport models, e.g. EMEP (Simpson et al, 2006) and EMEP4UK (Vieno et al. 2014, 2016), 3) interpret interactions between the gas and aerosol phases, and 4) interpret other ecological responses to N (e.g. ecosystem biodiversity or net carbon exchange).

The spatial variability of NH_3 and SO_2 and potentially even HNO_3 near ground level (1-2 m) is actually very large. Therefore, monitoring would be required to provide data at a resolution matching the expected spatial variability. Secondary pollutants, with low spatial variability and low formation rates require fewer sites. Although there is a very wide range of possible measurement methods, only a limited number satisfy the criteria of being simple, robust, low-cost, with the required sensitivity and which can distingush between the gas and aerosol phase components (Table 1.2). These include passive samplers (Sect. 1.4.1.1) which can be used to monitor gases (NH_3), and simple diffusion denuder methods (Sect. 1.4.1.4) that fulfil all the requirements.

1.7 Objectives of the thesis

The thesis is organised into the following sections and objectives:

Chapter 2 describes the development and application of two low-cost, simple, robust measurement approaches (ALPHA® passive NH_3 sampler and DELTA® diffusion denuder system) to measure ambient atmospheric NH_3 and particulate NH_4^+ concentrations in the UK National Ammonia Monitoring network (NAMN). The extensive dataset (1998 – 2014) was analysed to provide an understanding on key drivers influencing seasonal, temporal and long-term trends in variations of NH_3 and NH_4^+.

Chapter 3 describes further development and extension of the DELTA® method to provide additional, simultaneous measurements of atmospheric acid gases (HNO_3, SO_2, HCl) and aerosol (NO_3^-, SO_4^{2-}, Cl^-, Na^+, Ca^{2+}, Mg^{2+}) concentrations in the UK Acid Gas and Aerosol Network (AGANet). This provided an extensive dataset that was analysed to assess interactions between the pollutants on changes in atmospheric composition, long-term trends and in partitioning between the gas and aerosol phase components.

Chapter 4 presents the application of the UK DELTA® monitoring approach on a pan-European network. The implementation of a harmonised DELTA® method by multiple laboratories, coupled to quality protocols involving regular laboratory inter-comparisons provided an extensive quality-assured dataset on the acid gases and aerosols at the same time. The data were analysed to highlight differences in spatial and seasonal patterns in the components and also changes in the chemical climate across Europe.

Chapter 5 presents a summary of the findings from the UK and Europe-scale monitoring and their implication in air quality polices and effects assessment. The chapter concludes with recommendations for future research to address issues and questions identified by the work carried out in the thesis.

References

AQEG, Fine Particulate Matter ($PM_{2.5}$) in the United Kingdom, AIR QUALITY EXPERT GROUP report prepared for: Department for Environment, Food and Rural Affairs; Scottish Executive; Welsh Government; and Department of the Environment in Northern Ireland, http://uk-air.defra.gov.uk, 2012.

AQEG, Mitigation of United Kingdom $PM_{2.5}$ Concentrations, AIR QUALITY EXPERT GROUP report prepared for: Department for Environment, Food and Rural Affairs; Scottish Executive; Welsh Government; and Department of the Environment in Northern Ireland, http://uk-air.defra.gov.uk, 2015.

Asman W. A. H.: Modelling the atmospheric transport and deposition of ammonia and ammonium: an overview with special reference to Denmark, Atmos. Environ., 35(11), 1969-1983, doi:10.1016/S1352-2310(00)00548-3, 2001.

Asman, W. A. H., Sutton M. A., and Schjorring, J. K.: Ammonia: Emission, atmospheric transport and deposition, New Phytologist, 139(1), 27-48, doi:10.1046/j.1469-8137.1998.00180.x, 1998.

Avino, P. and Manigrasso, M.: Ten-year measurements of gaseous pollutants in urban air by an open-path analyzer, Atmos. Environ., 42(18), 4138-4148, doi:10.1016/j.atmosenv.2008.01.024, 2008.

Ayers, G. P., Keywood, M. D., Gillett, R., Manins, P. C., Malfroy, H., and Bardsley, T.: Validation of passive diffusion samplers for SO_2 and NO_2, Atmos. Environ., 32(20), 3587–3592, doi:10.1016/S1352-2310(98)00079-X, 1998.

Balzani Lööv, J. M., Alfoldy, B., Gast, L. F. L., Hjorth, J., Lagler, F., Mellqvist, J., Beecken, J., Berg, N., Duyzer, J., Westrate, H., Swart, D. P. J., Berkhout, A. J. C., Jalkanen, J.-P., Prata, A. J., van der Hoff, G. R., and Borowiak, A.: Field test of available methods to measure remotely SO_x and NO_x emissions from ships, Atmos. Meas. Tech., 7(8), 2597–2613, doi:10.5194/amt-7-2597-2014, 2014.

Berkhout, A. J. C., Swart, D. P. J., Volten, H., Gast, L .F .L., Haaima, M., Verboom, H., Stefess, G., Hafkenscheid, T., and Hoogerbrugge, R.: Replacing the AMOR with the miniDOAS in the ammonia monitoring network in the Netherlands, Atmos. Meas. Tech., 10, 4099–4120, doi:10.5194/amt-10-4099-2017, 2017.

Blohm, A., Sieburg, A., Popp, J., and Frosch, T.: 6 - Detection of gas molecules by means of spectrometric and spectroscopic methods, Editor(s): Lucian, B., Zsolt, P., Klara, H., and Monica, B.: In Micro and Nano Technologies, Advanced Nanostructures for Environmental Health, Elsevier, 251-294, doi:10.1016/B978-0-12-815882-1.00006-9, 2020.

Bobbink, R., Hicks, K., Galloway, J., Spranger, T., Alkemade, R., Ashmore, M., Bustamante, M., Cinderby, S., Davidson, E., Dentener, F., Emmett, B., Erisman, J., Fenn, M., Gilliam, F., Nordin, A., Pardo, L., and De Vries, W.: Global assessment of nitrogen deposition effects on terrestrial plant diversity: a synthesis, Ecol. App., 20: 30-59. doi:10.1890/08-1140.1, 2010.

Brunekreef, B., Harrison, R. M., Künzli, N., Querol, X., Sutton, M. A., Heederik, D. J. J., and Sigsgaard, T.: Reducing the health effect of particles from agriculture, The Lancet Respiratory Medicine, 3(11), 831–832, doi:10.1016/S22132600(15) 00413-0, 2015.

Buijsman, E., Aben, J. M. M., Van Elzakker, B. G., and Mennen, M. G.: An automatic atmospheric ammonia network in the Netherlands set-up and results, Atmos. Environ., 32(3), 17-324, doi:10.1016/S1352-2310(97)00233-1, 1998

Butler, T., Vermeylen, F., Lehmann, C. M., Likens, G. E., and Puchalski, M.: Increasing ammonia concentration trends in large regions of the USA derived from the NADP/AMoN network, Atmos. Environ., 146, 132-140, doi:10.1016/j.atmosenv .2016.06.033, 2016.

Bytnerowicz, A., Sanz, M. J., Arbaugh, M. J., Padgett, P. E., Jones, D. P., and Davila, A.: Passive sampler for monitoring ambient nitric acid (HNO_3) and nitrous acid (HNO_2) concentrations, Atmos. Environ., 39 (14), 2655-2660, doi:10.1016/ j.atmosenv.2005.01.018, 2005.

CLRTAP: Manual on Methodologies and Criteria for Modelling and Mapping Critical Loads and Levels and Air Pollution Effects, Risks and Trends. Umwelbundesamt, Berlin, 2004.

Clemitshaw, K.C.: A review of instrumentation and measurement techniques for ground-based and airborne field studies of gas-phase tropospheric chemistry, Crit. Rev. Env. Sci. Technol., 34 (1), 1-108, doi:10.1080/10643380490265117, 2004.

Conolly, C., Davies, M., Knight, D., Vincent, K., Sanocka, A., Lingard, J., Richie, S., Donovan, B., Collings, A., Braban, C., Tang, Y. S., Stephens, A., Twigg, M., Jones, M., Simmons, I., Coyle, C., Kentisbeer, J., Leeson, S., van Dijk, N., Nemitz, E., Langford, B., Bealey, W., Leaver, D., Poskitt, J., Carter, H., Thacker, S., Patel, M., Keenan, P., Pereira, G., Lawlor, A., Warwick, A., Farrand, P. and Sutton, M. A.: UK Eutrophying and Acidifying Atmospheric Pollutants (UKEAP) Annual Report 2015, 2016.

Dasgupta, P. K.: A diffusion scrubber for the collection of atmospheric gases, Atmos. Environ. (1967), 18(8), 1593-1599, doi:10.1016/0004-6981(84)90381-0, 1984.

Demmers T, G, M., Burgess L, R., Short J, L., Philips V, R., Clark J, A., and Wathes C,M.: Ammonia emissions from two mechanically ventilated UK livestock buildings, Atmos. Environ., 33 (2): 217-227, doi:10.1016/S1352-2310(98)00150-2, 1999.

Dore, A. J., Carslaw, D. C., Braban, C., Cain, M., Chemel, C., Conolly, C., Derwent, R. G., Griffiths, S. J., Hall, J., Hayman, G., Lawrence, S., Metcalfe, S. E., Redington, A., Simpson, D., Sutton, M. A., Sutton, P., Tang, Y. S., Vieno, M., Werner, M., and Whyatt, J. D.: Evaluation of the performance of different atmospheric chemical transport models and inter-comparison of nitrogen and sulphur deposition estimates for the UK, Atmos. Environ., 119, 131-143, doi:10.1016/j.atmosenv2015.08.008, 2015.

De Kluizenaar, Y. and Farrell, E. P.: Ammonia Monitoring in Ireland - Final Report. R & D Report Series No. 8. Environmental Protection Agency, Ireland, 2000.

Długosz-Lisiecka, M. and Henryk B.: Determination of the mean aerosol residence times in the atmosphere and additional ^{210}Po input on the base of simultaneous determination of ^{7}Be, ^{22}Na, ^{210}Pb, ^{210}Bi and ^{210}Po in urban air, Journal of radioanalytical and nuclear chemistry, 293 (1), 135-140, doi:10.1007/s10967-012-1690-5, 2012.

Doyle, B. C. and Cummins, T.: The spatial distribution of ambient atmospheric ammonia concentrations in Ireland. Agricultural Research Forum. 10th & 11th March 2014. Tullamore, Co Offaly. ISBN: 978-1-84170-605-4, 2014.

Dragosits, U., Theobald, M. R., Place, C. J., Lord, E., Webb, J., Hill, J., ApSimon, H. M., and Sutton, M. A.: Ammonia emission, deposition and impact assessment at the field scale: a case study of sub-grid spatial variability, Environ. Poll., 117, 147-158, doi:10.1016/s0269-7491(01)00147-6, 2002.

Duyzer, J.: Dry deposition of ammonia and ammonium aerosols over heathland. J. geophys. res., 99, 18757 – 18763, doi:10.1029/94JD01210, 1994.

EC: Council Directive 76/464/EEC of 4 May 1976 on pollution caused by certain dangerous substances discharged into the aquatic environment of the Community, Official Journal L 129, 18/05/1976 P. 0023 – 0029, 1976.

EC: Directive (EU) 2008/50/EC of the European Parliament and of the Council of 21 May 2008 on ambient air quality and cleaner air for Europe, 2008.

EC: Decision (EU) 2017/1442 Commission Implementing Decision (EU) 2017/1442 of 31 July 2017 establishing best available techniques (BAT) conclusions, under Directive 2010/75/EU of the European Parliament and of the Council, for large combustion plants (notified under document C(2017) 5225), 2017.

EC: Habitats Directive (EU) Council Directive 92/43/EEC of 21 May 1992 on the conservation of natural habitats and of wild fauna and flora, 1992.

EC: EU reference method: BS EN14212: 2005 (SO_2). Ambient air quality Standard method for the measurement of the concentration of sulphur dioxide by ultraviolet fluorescence, published March 2005.

EC: EU reference method: BS EN14211: 2005 (NO_x). Ambient air. quality Standard method for the measurement of the concentration of nitrogen dioxide and nitrogen monoxide by chemiluminescence, published 30 September 2012.

EC: Regulation (EC) No 715/2007 of the European Parliament and of the Council of 20 June 2007 on type approval of motor vehicles with respect to emissions from light passenger and commercial vehicles (Euro 5 and Euro 6) and on access to vehicle repair and maintenance, 2007.

EC: Regulation (EU) 2016/1628 of the European Parliament and of the Council of 14 September 2016 on requirements relating to gaseous and particulate pollutant emission limits and type-approval for internal combustion engines for non-road mobile machinery, amending Regulations (EU) No 1024/2012 and (EU) No 167/2013, and amending and repealing Directive 97/68/EC, 2016.

EEA: Datasource: https://www.eea.europa.eu/data-and-maps/dashboards/ air-pollutant-emissions-data-viewer-2, accessed 15 January 2020.

Egnér H. and Eriksson E.: Current data on the chemical composition of air and precipitation, Tellus 7, 134-137, doi:10.3402/tellusa.v7i1.8763, 1955.

EMEP: EMEP Manual for Sampling and Analysis. Revised February 2014, www.nilu.no/projects/ccc/manual/, 2014.

EMEP: Transboundary particulate matter, photooxidants, acidifying and eutrophying components, EMEP Status Report 1/2019, http://www.diva-portal.org/smash/record.jsf?pid=diva2%3A1371039&dswid=-7800, 2019.

EMEP: Air pollution trends in the EMEP region between 1990 and 2012, CCC-Report 1/2016, http://www.ivl.se/download/18.7e136029152c7d48c202d81/1466685735821/C206.pdf), 2016.

Erisman, J. W., Vermetten, A. W. M., Asman, W. A. H., Waijers-Ijpelaan, A., and Slanina, J.: Vertical distribution of gases and aerosols: The behaviour of ammonia and related components in the lower atmosphere, Atmos. Environ., (1967), 22(6), 1153-1160, doi:10.1016/0004-6981(88)90345-9, 1988.

Erisman, J. W., Hensen, A., Fowler, D., Flechard, C. R., Grüner, A., Spindler, G., Duyzer, J. H., Weststrate, H., Römer, F., Vonk, A. W., and Jaarsveld, H. V.: Dry Deposition Monitoring in Europe, WASP: Focus 1,17–27, doi:10.1023/A:1013 105727252, 2001.

Erisman, J. W., Otjes, R., Hensen, A., Jongejan, P., van den Bulk, P., Khlystov, A., Mols, H., and Slanina S.: Instrument development and application in studies and monitoring of ambient ammonia. Atmos. Environ. 35 (11): 1913-1922, doi:10.1016/S1352-2310(00)00544-6, 2001.

EU: Directive (EU) 2016/2284 of the European Parliament and of the Council of 14 December 2016 on the reduction of national emissions of certain atmospheric pollutants, amending Directive 2003/35/EC and repealing Directive 2001/81/EC, 2016.

Ferm, M.: Method for determination of atmospheric ammonia, Atmos. Environ., 13, 1385-1393, doi:10.1016/0004-6981(79)90107-0, 1979.

Ferm, M.: A sensitive diffusional sampler, IVL Report L91-172, Swedish Environmental Research Institute, Göteborg, Sweden, 1991.

Ferm, M.: Atmospheric ammonia and ammonium transport in Europe and critical loads: a review, Nutr. Cyc. Agroecosys., 51, 5–17, doi:10.1023/A:1009780030477, 1998.

Ferm, M. and Svanberg, P-A.: Cost-efficient techniques for urban- and background measurements of SO_2 and NO_2, Atmos. Environ., 32, 1377-1381, doi:10.1016/S1352-2310(97)00170-2, 1999.

Ferm, M., De Santis, F., and Varotsos, C.: Nitric acid measurements in connection with corrosion studies, Atmos. Environ., 39 (35), 6664-6672, 2005, doi:10.1016/j.atmosenv.2005.07.044, 2005.

Flechard, C. R. and Fowler, D.: Atmopheric ammonia at a Moorland site: I: The meteorological control of ambient ammonia concenttrations and the influence of local sources. Q.J.R. Meterol. Soc., 124, 733-757, doi:10.1002/qj.49712454705, 1998.

Flechard, C. R., Nemitz, E., Smith, R. I., Fowler, D., Vermeulen, A. T., Bleeker, A., Erisman, J. W., Simpson, D., Zhang, L., Tang, Y. S., and Sutton, M. A.: Dry deposition of reactive nitrogen to European ecosystems: a comparison of inferential models across the NitroEurope network, Atmos. Chem. Phys., 11, 2703-2728, doi:10.5194/acp-11-2703-2011, 2011.

Fowler, D. and Reis, S.: Challenges in quantifying biosphere-atmosphere exchange of nitrogen species, Environ. Poll., 150, 125-139, doi:10.1016/j.envpol. 2007.04.014, 2007.

Fowler, D., Steadman, C. E., Stevenson, D., Coyle, M., Rees, R. M., Skiba,U. M., Sutton, M. A., Cape, J. N., Dore, A. J., Vieno, M., Simpson, D., Zaehle, S., Stocker, B. D., Rinaldi, M., Facchini, M. C., Flechard, C. R., Nemitz, E.,Twigg, M., Erisman, J. W., Butterbach-Bahl, K., and Galloway, J. N.: Effects of global change during the 21st century on the nitrogen cycle. [In special issue: Atmospheric composition

change: science for policy] Atmos. Chem. Phys., 15 (24). 13849-13893. doi:10.5194/acp-15-13849-2015, 2015.

Genfa, Z., Slanina, S., Boring, C. B., Jongejan, P. A. C., and Dasgupta, P. K.: Continuous wet denuder measurements of atmospheric nitric and nitrous acids during the 1999 Atlanta Supersite, Atmos. Environ., 37, 1351-1364, doi:10.1016/S1352-2310(02)01011-7, 2003.

Haywood, J. Chapter 27 - Atmospheric Aerosols and Their Role in Climate Change, Editor(s): Trevor M. Letcher, Climate Change (Second Edition), Elsevier, 449-463, doi:10.1016/B978-0-444-63524-2.00027-0, 2016.

Hendriks, C., Kranenburg, R., Kuenen, J. J. P., Van den Bril, B., Verguts, V., and Schaap, M.: Ammonia emission time profiles based on manure transport data improve ammonia modelling across north western Europe, Atmos. Environ., 131, 83-96, doi:10.1016/j.atmosenv.2016.01.043, 2016.

Hicks, B. B., Wesely, M. L., Durham, J. L., and Brown, M.: A. Some direct measurements of atmospheric sulfur fluxes over a pine plantation, Atmos. Env., (1967), 16(12), 2899-2903, doi:10.1016/0004-6981(82)90040-3, 1982.

Hicks, B. B., Matt, D. R., and McMillen, R. T.: A micrometeorological investigation of surface exchange of O3, SO2 and NO: A case study. Boundary-Layer Meteo., 47(1-4), 321-336. doi:10.1007/BF00122337, 1989.

Hien, P. D., Hangartner, M., Fabian, S., and Tan, P. M.: Concentrations of NO_2, SO_2, and benzene across Hanoi measured by passive diffusion samplers, Atmos. Env., 88, 66-73, doi:10.1016/j.atmosenv.2014.01.036, 2014.

Horvath L.: Dry deposition velocity of $PM_{2.5}$ ammonium sulfate particles to a Norway spruce forest on the basis of S- and N-balance estimations, Atmospheric Environment, 37(31), 4419-4424, doi:10.1016/S1352-2310(03)00584-3, 2003.

Huntzicker, J. J., Robert A. Cary, R. A., and Ling, C-S.: Neutralization of sulfuric acid aerosol by ammonia, Environ. Sci. Technol., 14 (7), 819-824, doi:10.1021/es60167a009, 1980.

IMO: MARPOL 73/78: International Convention for the Prevention of Pollution from Ships, 1973 as modified by the Protocol of 1978, http://www.imo.org/en/About/conventions/listofconventions/pages/international-convention-for-the-prevention-of-pollution-from-ships-(marpol).aspx, 1978.

Jongejan, P. A. C., Bai, Y., Veltkamp, A. C., Wyers, G. P., and Slanina, J.: An automated field instrument for the determination of acidic gases in air, Intern. J. Environ. Anal. Chem., 66, 241-251, doi:10.1080/03067319708028367, 1997.

Kim, K-H., Kabir, E., and Kabir, S.: A review on the human health impact of airborne particulate matter, Env. Int., 74, 136-143, doi:10.1016/j.envint.2014.10.005, 2015.

Kitto, A. and Colbeck, I.: Chapter 4: Filtration and denuder sampling techinques, In: Analytical Chemistry of Aerosols: Science and Technology, Editor Kvetoslav R. Spurny Publisher Routledge, ISBN1351466577, 2017.

Kleffmann, J., Gavriloaiei, T., Elshorbany, Y., Ródenas, M., and Wiesen, P.: Detection of nitric acid (HNO_3) in the atmosphere using the LOPAP technique, J. Atmos. Chem., 58. 131-149, doi:10.1007/s10874-007-9083-9, 2007.

Kleffmann, J. and Wiesen, P.: Technical Note: Quantification of interferences of wet chemical HONO LOPAP measurements under simulated polar conditions, Atmos. Chem. Phys., 8, 6813–6822, doi:10.5194/acp-8-6813-2008, 2008.

Koutrakis, P., Ferguson, S. T., Wolfso, J. M., Mulik, J. D., and Burton, R. M.: Development and evaluation of a glass honeycomb denuder/filter pack system to collect atmospheric gases and particle, Environ. Sci. Technol., 27(12), 2497-2501, doi:10.1021/es00048a029,1993.

Krupa, S. V. and Legge, A. H.: Passive sampling of ambient, gaseous air pollutants: an assessment from an ecological perspective, Environ. Poll., 107, 31-45, doi:10.1016/S0269-7491(99)00154-2, 2000.

Lolkema, D. E., Noordijk, H., Stolk, A. P., Hoogerbrugge, R., van Zanten, M. C., and van Pul, W. A. J.: The Measuring Ammonia in Nature (MAN) network in the Netherlands, Biogeosciences, 12, 5133–5142, doi:10.5194/bg-12-5133-2015, 2015.

Loubet B., Asman, W. A. H., Theobald, M. R., Hertel, O., Tang, Y. S., Robin, P., Hassouna, M., Dämmgen, U., Genermont, S., Cellier, P., and Sutton, M. A.: Ammonia Deposition Near Hot Spots: Processes, Models and Monitoring Methods. In: Sutton M.A., Reis S., Baker S.M. (eds) Atmospheric Ammonia. Springer, Dordrecht, doi:10.1007/978-1-4020-9121-6_15, 2009.

Martin, N. A., Ferracci, V., Cassidy, N., Hook, J., Battersby, R. M., di Meane, E. A., Tang, Y. S., Stephens, A. C. M., Leeson, S. R., Jones, M. R., Braban, C. F., Gates, L., Hangartner, M., Stoll, J-M., Sacco, P., Pagani, D., Hoffnagle, J. A., and Seitler, E.: Validation of ammonia diffusive and pumped samplers in a controlled atmosphere test facility using traceable Primary Standard Gas Mixtures, Atmos. Environ., 199. 453-462, doi:10.1016/ j.atmosenv.2018.11.038, 2019

McKay, H. A. C.: The atmospheric oxidation of sulphur dioxide in water droplets in presence of ammonia, Atmos. Environ (1967), 5(1), 7-14, doi:10.1016/0004-6981(71)90039-4, 1971.

Milford, C., Theobald, M. R., Nemitz, E., Hargreaves, K. J., Horvath, L., Raso, J., Dämmgen, U., Neftel, A., Jones, S. K., Hensen, A., Loubet, B., Cellier, P., and Sutton, M. A.: Ammonia fluxes in relation to cutting and fertilization of an intensively managed grassland derived from an inter-comparison of gradient measurements, Biogeosciences, 6, 819–834, doi:10.5194/bg-6-819-2009, 2009.

Miller, D. J., Sun, K., Tao, L., Khan, M. A., and Zondlo, M. A.: Open-path, quantum cascade-laser-based sensor for high-resolution atmospheric ammonia measurements, Atmos. Meas. Tech., 7, 81–93, doi:10.5194/amt-7-81-2014, 2014.

Móring, A., Vieno, M., Doherty, R. M., Milford, C., Nemitz, E., Twigg, M. M., Horváth, L., and Sutton, M. A.: Process-based modelling of NH_3 exchange with grazed grasslands, Biogeosciences, 14, 4161–4193, doi:10.5194/bg-14-4161-2017, 2017.

Moller D. and Schiferdecker H.: A relationship between agricultural NH_3 emissions and the atmospheric SO_2 content over industrial areas. Atmospheric Environment, 19, 695-700, doi:10.1016/0004-6981(85)90056-3, 1985.

NAEI, http://naei.beis.gov.uk/data/, accessed: 19 December 2019.

NEGTAP: Transboundary Air Pollution: Acidification, Eutrophication and Ground Level ozone in the UK. Report of the National Expert Group on Transboundary Air Pollution, DEFRA, London, 2001.

Neftel A., Blatter A., Gut A., Hoegger D., Meixner F. X, Ammann C., and Nathaus F. J.: NH_3 soil and soil surface gas measurements in a triticale wheat field. Atmos. Environ., (Ammonia Special Issue), 32 (3), 499-506, doi:10.1016/S1352-2310(97)00162-3,1, 1998.

Perrino, C., De Santis, F., and Febo, A.: Criteria for the choice of a denuder sampling technique devoted to the measurement of atmospheric nitrous and nitric acids, Atmos. Environ., Part A. General Topics, 24, 617-626, doi:10.1016/0960-1686(90)90017-H, 1990.

Perrino, C., Ramirez, D., and Allegrini, I.: Monitoring acidic air pollutants near Rome by means of diffusion lines: development of a specific quality control procedure, Atmos. Environ., 35(2), 331-341, doi:10.1016/ S1352-2310(00)00144-8, 2001.

Perrino, C., Catrambone, M., Di Menno Di Bucchianico, A., and Allegrini, I.: Gaseous ammonia in the urban area of Rome, Italy and its relationship with traffic emissions, Atmos. Environ., 36(34), 5385-5394, doi:10.1016/S1352-2310(02)00469-7, 2002.

Philips, D. A. and Dasgupta, P.K.: A Diffusion Scrubber for the Collection of Gaseous Nitric Acid, Separation Sci. Technol., 22:4, 1255-1267, doi:10.1080/ 01496398708057178, 1987.

Place, B. K., Young, C. J., Ziegler, S. E., Edwards, K. A., Salehpoor, L., and VandenBoer, T. C.: Passive sampling capabilities for ultra-trace quantitation of atmospheric nitric acid (HNO_3) in remote environments, Atmos. Environ., 191, 360-369, doi:10.1016/j.atmosenv.2018.08.030, 2018.

Plaisance, H., Sagnier, I., Saison, J. Y., Galloo, J. C., and Guillermo, C.: Performances and Application of a Passive Sampling Method for the Simultaneous Determination of Nitrogen Dioxide and Sulfur Dioxide in Ambient Air, Environ Monit Assess., 79, 301–315, doi:10.1023/A:1020205230396, 2002.

Possanzini M., De Santis F., and Di Palo V.: Measurements of nitric acid and ammonium salts in lower Bavaria, Atmos. Environ., 33 (22): 3597-3602, doi:10.1016/S1352-2310(99)00096-5, 1999

Puchalski, M. A., Rogers, C. M., Baumgardner, R., Mishoe, K. P., Price, G., Smith, M. J., Watkins, N., and Lehmann, C. M.: A statistical comparison of active and passive ammonia measurements collected at Clean Air Status and Trends Network (CASTNET) sites, Environ. Sci.-Proc. Imp., 17, 358–369, doi:10.1039/ c4em00531g, 2015.

Ramsay, R., Di Marco, C. F., Heal, M. R., Twigg, M. M., Cowan, N., Jones, M. R., Leeson, S. R., Bloss, W. J., Kramer, L. J., Crilley, L., Sörgel, M., Andreae, M., and Nemitz, E.: Surface–atmosphere exchange of inorganic water-soluble gases and associated ions in bulk aerosol above agricultural grassland pre- and postfertilisation, Atmos. Chem. Phys., 18, 16953–16978, doi:10.5194/acp-18-16953-2018, 2018.

Reis, S., Grennfelt, P., Klimont, Z., Amann, M., ApSimon, H., Hettelingh, J.-P., Holland, M., LeGall, A.-C., Maas, R., Posch, M., Spranger, T., Sutton, M. A., and Williams, M.: From acid rain to climate change, Science 338, 1153–1154, doi:10.1126/science.1226514, 2012.

Riddick, S. N., Blackall, T. D., Dragosits, U., Daunt, F., Newell, M., Braban, C. F., Tang, Y. S., Schmale, J., Hill, P. W., Wanless, S., Trathan, P., and Sutton, M. A.:

Measurement of ammonia emissions from temperate and sub-polar seabird colonies, Atmos. Environ., 134, 40-50, doi:10.1016/j.atmosenv.2016.03.016, 2016.

ROTAP: Review of Transboundary Air Pollution: Acidification, Eutrophication, Ground Level Ozone and Heavy Metals in the UK. Contract Report to the Department for Environment, Food and Rural Affairs. Centre for Ecology & Hydrology, http://www.rotap.ceh.ac.uk/, 2012.

Rowe, E. C., Jones, L., Dise, N. B., Evans, C. D., Mills, G., Hall, J., Stevens, C. J., Mitchell, R. J., Field, C., Caporn, S. J. M., Helliwell, R. C., Britton, A. J., Sutton, M. A., Payne, R. J., Vieno, M., Dore, A. J., and Emmett, B. A.: Metrics for evaluating the ecological benefits of decreased nitrogen deposition, Biol. Cons., 212(B), 454-463, doi:10.1016/j.biocon.2016.11.022, 2017.

Ruijgrok, W., Tieben H., and Eisinga, P.: The dry deposition of particles to a forest canopy: A comparison of model and experimental results, Atmos. Environ., 31(3), 399-415, doi:10.1016/S1352-2310(96)00089-1, 1997.

Rumsey, I. C., Cowen, K. A., Walker, J. T., Kelly, T. J., Hanft, E. A., Mishoe, K., Rogers, C., Proost, R., Beachley, G. M., Lear, G., Frelink, T., and Otjes, R. P.: An assessment of the performance of the Monitor for AeRosols and GAses in ambient air (MARGA): a semi-continuous method for soluble compounds, Atmos. Chem. Phys., 14, 5639–5658, doi:10.5194/acp-14-5639-2014, 2014.

Rumsey, I. C. and Walker, J. T.: Application of an online ion-chromatography-based instrument for gradient flux measurements of speciated nitrogen and sulfur, Atmos. Meas. Tech., 9, 2581–2592, doi:10.5194/amt-9-2581-2016, 2016.

Schaap, M., Otjes, R. P., and Weijers, E. P.: Illustrating the benefit of using hourly monitoring data on secondary inorganic aerosol and its precursors for model evaluation, Atmos. Chem. Phys., 11, 11041–11053, doi:10.5194/acp-11-11041-2011, 2011.

Schrader, F. and Brummer, C.: Land use specific ammonia deposition velocities: a review of recent studies (2004 – 2013), WASP, 225, 2114 – 2125, doi:10.1007/s11270-014-2114-7, 2014.

Seinfeld J. H. and Pandis S. N.: Atmospheric Chemistry and physics. From Air Pollution to climate change. Wiley. New York, 1998.

Sheppard, L. J., Leith, I. D., Mizunuma, T., Cape, J. N, Crossley, A., Leeson, S., Sutton, M. A., van, Dijk, N., and Fowler, D.: Dry deposition of ammonia gas drives species change faster than wet deposition of ammonium ions: evidence from a long-term field manipulation, Global Change Biol., 17, 3589-3607, doi:10.1111/j.1365-2486.2011.02478.x, 2011.

Sickles, I. J. E., Hodson, L. L., and Vorburger, L. M.: Evaluation of the filter pack for long-duration sampling of ambient air, Atmos. Environ., 33, 2187-2202, doi:10.1016/S1352-2310(98)00425-7, 1999.

Simpson, D., Butterbach-Bahl, K., Fagerli, H., Kesik, M., Skiba, U., and Tang, Y.: Deposition and emissions of reactive nitrogen over European forests: A modelling study, Atmos. Environ., 40. 5712-5726. doi:10.1016/j.atmosenv.2006.04.063, 2006.

Sørensen, L. L., Granby, K., Nielsen, H., and Asman, W. A. H.: Diffusion scrubber technique used for measurements of atmospheric ammonia, Atmos. Environ., 28(22), 3637-3645, doi:10.1016/1352-2310(94)00189-R, 1994.

Spirig, C., Flechard, C. R., Ammann, C., and Neftel, A.: The annual ammonia budget of fertilised cut grassland – Part 1: Micrometeorological flux measurements and emissions after slurry application, Biogeosciences, 7, 521–536, doi:10.5194/bg-7-521-2010, 2010.

Stieger, B., Spindler, G., Fahlbusch, B., Müller, K., Grüner, A., Poulain, L., Thöni, L., Seitler, E., Wallasch, M., and Herrmann, H.: Measurements of PM_{10} ions and trace gases with the online system MARGA at the research station Melpitz in Germany – A five-year study, J. Atmos. Chem., 75, 33–70, doi:10.1007/s10874-017-9361-0, 2018.

Sutton, M. A., Moncrieff, J. B., and Fowler, D.: Deposition of atmospheric ammonia to moorlands, Environ. Poll., 75(1), 15-24, doi:10.1016/0269-7491(92)90051-B, 1992.

Sutton, M. A., Tang, Y. S., Dragosits, U., Fournier, N., Dore, A. J., Smith, R. I., Weston, K. J., and Fowler, D.: A spatial analysis of atmospheric ammonia and ammonium in the UK, Scientific World Journal. Nov 28;1 Suppl 2:275-86, doi:10.1100/tsw.2001.313, 2001a.

Sutton, M. A., Tang, Y. S., Miners, B., and Fowler, D.: A new diffusion denuder system for long-term, regional monitoring of atmospheric ammonia and ammonium, WASP: Focus 1: 145, doi:10.1023/A:1013138601753, 2001b.

Sutton, M. A., Smith, R., Cape, J. N., Nemitz, E., and Fowler, D.: European monitoring of transboundary air pollution – the challenge to expand the EMEP network without unrealistic additional resources, Report to TFMM, CEH Edinburgh, 2004.

Sutton, M. A., Nemitz, E., Erisman, J. W., Beier, C., Bahl, K. B., Cellier, P., de Vries, W., Cotrufo, F., Skiba, U., Di Marco, C., Jones, S., Laville, P., Soussana, J. F., Loubet, B., Twigg, M., Famulari, D., Whitehead, J., Gallagher, M. W., Neftel, A., Flechard, C. R., Herrmann, B., Calanca, P. L., Schjoerring, J. K., Daemmgen, U., Horvath, L., Tang, Y. S., Emmett, B. A., Tietema, A., Penuelas, J., Kesik, M., Brueggemann, N., Pilegaard, K., Vesala, T., Campbell, C. L., Olesen, J. E., Dragosits, U., Theobald, M. R., Levy, P., Mobbs, D. C., Milne, R., Viovy, N., Vuichard, N., Smith, J. U., Smith, P., Bergamaschi, P., Fowler, D., and Reis, S.: Challenges in quantifying biosphere-atmosphere exchange of nitrogen species, Environ. Poll., 150, 125-139, doi:10.1016/j.envpol.2007.04.014, 2007.

Sutton, M. A., Reis, S., Riddick, S. N., Dragosits, U., Nemitz, E., Theobald, M. R., Tang, Y.S., Braban, C.F., Vieno, M., and Dore, A.J.: Towards a Climate-Dependent Paradigm of Ammonia Emission and Deposition, Philos. Trans. R. Soc. B Biol. Sci., 368, 20130166, doi:10.1098/rstb.2013.0166, 2013.

Sutton, M. A., Nemitz, E., Theobald, M. R., Milford, C., Dorsey, J. R., Gallagher, M. W., Hensen, A., Jongejan, P. A. C., Erisman, J. W., Mattsson, M., Schjoerring, J. K., Cellier, P., Loubet, B., Roche, R., Neftel, A., Hermann, B., Jones, S. K., Lehman, B. E., Horvath, L., Weidinger, T., Rajkai, K., Burkhardt, J., Löpmeier, F. J., and Daemmgen, U.: Dynamics of ammonia exchange with cut grassland: strategy and implementation of the GRAMINAE Integrated Experiment, Biogeosciences, 6, 309–331, doi:10.5194/bg-6-309-2009, 2009.

Tang, Y.S., Cape, J.N., and Sutton, M. A.: Development and types of passive samplers for monitoring atmospheric NO_2 and NH_3 concentrations, ScientificWorldJournal, 1, 513-529, doi:10.1100/tsw.2001.82, 2001.

Tang, Y. S., Simmons, I., van Dijk, N., Di Marco, C., Nemitz, E., Dammgen, U., Gilke, K., Djuricic, V., Vidic, S., Gliha, Z., Borovecki, D., Mitosinkova, M., Hanssen, J. E., Uggerud, T. H., Sanz, M. J., Sanz, P., Chorda, J. V., Flechard, C. R., Fauvel, Y., Ferm, M., Perrino, C., and Sutton, M. A.: European scale application of atmospheric reactive nitrogen measurements in a low-cost approach to infer dry deposition fluxes, Agric, Ecosys. Environ., 133, 183-195, doi:10.1016/j.agee. 2009.04.027, 2009.

Tang, Y. S., Cape, J. N., Braban, C. F., Twigg, M. M., Poskitt, J., Jones, M. R., Rowland, P., Bentley, P., Hockenhull, K., Woods, C., Leaver, D., Simmons, I., van Dijk, N., Nemitz, E., and Sutton, M. A.: Development of a new model DELTA sampler and assessment of potential sampling artefacts in the UKEAP AGANet DELTA system: summary and technical report, London, Defra, CEH Project no. C04544, C04845, available at: https://uk-air. defra.gov.uk/library/reports?report_ id=861, 2015.

Tang, Y. S., Braban, C. F., Dragosits, U., Dore, A. J., Simmons, I., van Dijk, N., Poskitt, J., Pereira, M. G., Keenan, P. O., Conolly, C., Vincent, K., Smith, R. I., Heal, M. R., and Sutton, M. A.: Drivers for spatial, temporal and long-term trends in atmospheric ammonia and ammonium in the UK, Atmos. Chem. Phys., 18, 705-733, doi:10.5194/acp-18-705-2018, 2018a.

Tang, Y. S., Braban, C. F., Dragosits, U., Simmons, I., Leaver, D., van Dijk, N., Poskitt, J., Thacker, S., Patel, M., Carter, H., Pereira, M. G., Keenan, P. O., Lawlor, A., Connolly, C., Vincent, K., Heal, M. R., and Sutton, M. A.: Acid gases and aerosol measurements in the UK (1999–2015): regional distributions and trends, Atmos. Chem. Phys., 18, 16293-16324. doi:10.5194/acp-18-16293-2018, 2018b.

ten Brink, H., Otjes, R., Jongejan, P., and Slanina, S.: An instrument for semi-continuous monitoring of the size-distribution of nitrate, ammonium, sulphate and chloride in aerosol, Atmos. Environ., 41, 2768-2779, doi:10.1016/j.atmos env.2006.11.041. 2007.

Thijsse, Th. R., Duyzer, J. H., Verhagen, H. L. M., Wyers, G. P., Wayers, A., and Möls, J. J.: Measurement of ambient ammonia with diffusion tube samplers, Atmos. Environ. (Ammonia Special Issue), 32(3), 333-337, doi:10.1016/S1352-2310(97)00278-1, 1998

Thomas, R. M., Trebs, I., Otjes, R., Jongejan, P. A. C., ten Brink, H., Phillips, G., Kortner, M., Meixner, F. X., and Nemitz, E.: An automated analyzer to measure surface-atmosphere exchange fluxes of water soluble inorganic aerosol compounds and reactive trace gases, Env. Sci. Technol., 43, 1412–1418, doi:10.1021/es8019403, 2009.

Thöni, L., Brang, P., Braun, S., Seitler E., and Rihm, B.: Ammonia Monitoring in Switzerland with Passive Samplers: Patterns, Determinants and Comparison with Modelled Concentrations, Env. Monit. Assess., 98, 93–107, doi:10.1023/B:EMAS. 0000038181.99603.6e, 2004.

Torseth, K. and Hov, O.: (Eds) The EMEP monitoring strategy for 2004-2009. EMEP Report 9/2003, 2003.

Tørseth, K., Aas, W., Breivik, K., Fjæraa, A. M., Fiebig, M., Hjellbrekke, A. G., Lund Myhre, C., Solberg, S., and Yttri, K. E.: Introduction to the European Monitoring and Evaluation Programme (EMEP) and observed atmospheric composition

change during 1972-2009, Atmos. Chem. Phys., 12, 5447-5481, doi:10.5194/acp-12-5447-2012, 2012.

Trujillo-Ventura, A. and Ellis, J.H.: Multiobjective air pollution monitoring network design, Atmospheric Environment. Part A. General Topics, 25(2), 469-479, doi:10.1016/0960-1686(91)90318-2, 1991.

Twigg, M. M., Ilyinskaya, E., Beccaceci, S., Green, D. C., Jones, M. R., Langford, B., Leeson, S. R., Lingard, J. J. N., Pereira, G. M., Carter, H., Poskitt, J., Richter, A., Ritchie, S., Simmons, I., Smith, R. I., Tang, Y. S., Van Dijk, N., Vincent, K., Nemitz, E., Vieno, M., and Braban, C. F.: Impacts of the 2014–2015 Holuhraun eruption on the UK atmosphere, Atmos. Chem. Phys., 16, 11415–11431, doi:10.5194/acp-16-11415-2016, 2016.

UNECE: Protocol to Abate Acidification, Eutrophication and Ground-level Ozone, the 1999 Gothenburg Protocol to Abate Acidification, Eutrophication and Ground-level Ozone, http://www.unece.org/env/lrtap/multi_h1.html, last accessed March 2018.

Harmens, H., Mills, G., Hayes, F., and Norris, D.: Air Pollution and Vegetation, ICP Vegetation1 Annual Report 2011/2012, https://icpvegetation.ceh.ac.uk/sites /default/files/ICPVegetationannualreport2011-12_0.pdf, September 2012.

van Jaarsveld, J.A. and Bleeker, A.: Evaluation of Ammonia Emission Reductions in the Netherlandands using Measurements and the OPS Model. In: Gryning SE., Schiermeier F.A. (eds) Air Pollution Modeling and Its Application XIV. Springer, Boston, MA, doi:10.1007/0-306-47460-3_72004.

Van Pul, A., Van Jaarsveld, H., Van Der Meulen, T., and Velders, G.: Ammonia concentrations in the Netherlands: Spatially detailed measurements and model calculations, Atmos. Environ., 38, 4045-4055, doi:10.1016/j.atmosenv.2004. 03.051, 2004.

van Zanten, M. C., Wichink Kruit, R. J., Hoogerbrugge, R., Van der Swaluw, E., and van Pul, W. A. J.: Trends in ammonia measurements in the Netherlands over the period 1993–2014, Atmos. Environ., 148, 352-360, doi:10.1016/j.atmosenv. 2016.11.007, 2017.

Villena, G., Bejan, I., Kurtenbach, R., Wiesen, P., and Kleffmann, J.: Development of a new Long Path Absorption Photometer (LOPAP) instrument for the sensitive detection of NO_2 in the atmosphere, Atmos. Meas. Tech., 4, 1663–1676, doi:10.5194/amt-4-1663-2011, 2011.

Vogt, E., Braban, C. F.,Dragosits, U.,Theobald, M. R., Billett, M. F., Dore, A. J., Tang, Y. S., van Dijk, N., Rees, R. M., McDonald, C., Murray, S., Skiba, U., and Sutton, M. A.: Estimation of nitrogen budgets for contrasting catchments at the landscape scale, Biogeosciences, 10 (1), 119-133, doi:10.5194/bg-10-119-2013, 2013.

von Bobrutzki, K., Braban, C. F., Famulari, D., Jones, S.K., Blackall, T., Smith, T., Blom, M., Coe, H., Gallagher, M., Ghalaieny, M., McGillen, M. R., Percival, C. J., Whitehead, J. D., Ellis, R., Murphy, J., Mohacsi, A., Pogany, A., Junninen, H., Rantanen, S., Sutton, M. A., and Nemitz, E.: Field inter-comparison of eleven atmospheric ammonia measurement techniques, Atmos. Meas. Tech., 3, 91-112, doi:10.5194/amt-3-91-2010, 2010.

Warneck, P.: Chemistry of the Natural Atmosphere. Academic Press, London, 1988.

Wichink Kruit, R. J., Schaap, M., Sauter, F. J., van Zanten, M. C., and van Pul, W. A. J.: Modeling the distribution of ammonia across Europe including bi-directional

surface–atmosphere exchange, Biogeosciences, 9, 5261–5277, doi:10.5194/bg-9-5261-2012, 2012.

Willems, J. J. H.: Low-cost methods for measuring air pollutants (a training program). Report R-635. Wageningen (Nl) Agricultural University, Department of Air Quality, Wageningen, Netherlands, 1993.

Wyers, G. P, Otjes, R. P., and Slanina, J.: A continuous-flow denuder for the measurement of ambient concentrations and surface-exchange fluxes of ammonia, Atmos. Environ., Part A. General Topics, 27(13), 2085-2090, doi:10.1016/0960-1686(93)90280-C, 1993.

Zaehle, S. and Dalmonech, D.: Carbon–nitrogen interactions on land at global scales: current understanding in modelling climate biosphere feedbacks, Current Opinion in Environmental Sustainability, 3(5), 311-320, doi:10.1016/j.cosust.2011.08.008, 2011.

Zöll, U., Brümmer, C., Schrader, F., Ammann, C., Ibrom, A., Flechard, C. R., Nelson, D. D., Zahniser, M., and Kutsch, W. L.: Surface–atmosphere exchange of ammonia over peatland using QCL-based eddy-covariance measurements and inferential modeling, Atmos. Chem. Phys., 16, 11283–11299, doi:10.5194/acp-16-11283-2016, 2016.

Chapter 2 Drivers for spatial, temporal and long-term trends in atmospheric ammonia and ammonium in the UK

This chapter is based on the research paper published in `*Atmospheric Chemistry and Physics' (Tang Y. S., Braban, C. F., Dragosits, U, Dore, A. J., Simmons, I., van Dijk, N., Poskitt, J., Pereira, M. G., Keenan, P. O., Connolly, C., Vincent, K., Smith, R. I., Heal, M. R., and Sutton, M. A.: Drivers for spatial, temporal and long-term trends in atmospheric ammonia and ammonium in the UK, Atmos. Chem. Phys., 18 (2). 705-733, https://doi.org/10.5194/acp-18-705-2018, 2018).*

Author contributions:

As network manager for the NAMN (1997 – 2016), I coordinated the measurement and collection of data with the support of a large network of local site operators (monthly exchange of air samples), UKCEH Lancaster chemical laboratory (from 2009 for sample preparation and chemical analysis) and UKCEH / Ricardo EE field teams (site / equipment maintenance). I developed and implemented improved protocols in NH_3 measurements with the DELTA® and Gradko membrane diffusion tubes, and made all network measurements up to 2009. Ivan Simmons helped with building DELTA® systems, site establishment and equipment maintenance. Netty van Dijk assisted with measurements. Mark Sutton designed the DELTA® system, and conceived and established the NAMN. Mark Sutton and I designed and developed the ALPHA® NH_3 passive gas sampler and extended the DELTA® method to include particulate NH_4^+ measurements. Tony Dore provided FRAME modelled NH_3 concentrations. Ulli Dragosits assisted with network measurements and logistics (early on), provided modelled data and advice on NH_3 emissions and dominant emission source sectors, and training/advice on GIS. Ron Smith provided advice on statistics. Christine Braban is project coordinator for UKEAP, of which NAMN is a component network. Keith Vincent supported data submission to the Defra UK-AIR website. I performed the data

collection, data analysis (including statistics) and wrote the manuscript, with input from all co-authors. Mark Sutton, Mat Heal, Christine Braban and Ulli Dragosits provided valuable advice on the interpretation of results and feedback on the manuscript.

2.1 Abstract

A unique long-term dataset from the UK National Ammonia Monitoring Network (NAMN) is used here to assess spatial, seasonal and long-term variability in atmospheric ammonia (NH_3: 1998–2014) and particulate ammonium (NH_4^+: 1999–2014) across the UK. Extensive spatial heterogeneity in NH_3 concentrations is observed, with lowest annual mean concentrations at remote sites (< 0.2 µg m^{-3}) and highest in the areas with intensive agriculture (up to 22 µg m^{-3}), while NH_4^+ concentrations show less spatial variability (e.g. range of 0.14 to 1.8 µg m^{-3} annual mean in 2005). Temporally, NH_3 concentrations are influenced by environmental conditions and local emission sources. In particular, peak NH_3 concentrations are observed in summer at background sites (defined by 5 km grid average NH_3 emissions < 1 kg N ha^{-1} yr^{-1}) and in areas dominated by sheep farming, driven by increased volatilization of NH_3 in warmer summer temperatures. In areas where cattle, pig and poultry farming is dominant, the largest NH_3 concentrations are in spring and autumn, matching periods of manure application to fields. By contrast, peak concentrations of NH_4^+ aerosol occur in spring, associated with long-range transboundary sources. An estimated decrease in NH_3 emissions by 16 % between 1998 and 2014 was reported by the UK National Atmospheric Emissions Inventory. Annually averaged NH_3 data from NAMN sites operational over the same period (n = 59) show an indicative downward trend, although the reduction in NH_3 concentrations is smaller and nonsignificant: Mann–Kendall (MK), −6.3 %; linear regression (LR), −3.1 %. In areas dominated by pig and poultry farming, a significant reduction in NH_3 concentrations between 1998 and 2014 (MK: −22 %; LR: −21 %, annually averaged NH_3) is consistent with, but not as large as the decrease in estimated

NH_3 emissions from this sector over the same period (−39 %). By contrast, in cattle-dominated areas there is a slight upward trend (non-significant) in NH_3 concentrations (MK: +12 %; LR: +3.6 %, annually averaged NH_3), despite the estimated decline in NH_3 emissions from this sector since 1998 (−11 %). At background and sheep-dominated sites, NH_3 concentrations increased over the monitoring period. These increases (non-significant) at background (MK: +17 %; LR: +13 %, annually averaged data) and sheep-dominated sites (MK: +15 %; LR: +19 %, annually averaged data) would be consistent with the concomitant reduction in SO_2 emissions over the same period, leading to a longer atmospheric lifetime of NH_3, thereby increasing NH_3 concentrations in remote areas. The observations for NH_3 concentrations not decreasing as fast as estimated emission trends are consistent with a larger downward trend in annual particulate NH_4^+ concentrations (1999–2014: MK: −47 %; LR: −49 %, $p < 0.01$, $n = 23$), associated with a lower formation of particulate NH_4^+ in the atmosphere from gas phase NH_3.

2.2 Introduction

Atmospheric ammonia (NH_3) gas is assuming increasing importance in the global pollution climate, with effects on local to international (transboundary) scales (Fowler et al., 2016). While substantial reductions in SO_2 emissions and limited reductions in NO_x emissions have been achieved in Europe and North America following legislation designed to improve air quality, NH_3 emissions, primarily from the agricultural sectors (94 % of total NH_3 emissions in Europe in 2014) have seen much smaller reductions (EEA, 2016). In the period 2000–2014, NH_3 emissions are estimated to have decreased in the EU-28 (28 member states of the European Union) by only 8 % from 4.3 to 3.9 million tonnes, with the UK contributing 7.2 % in 2014 (EEA, 2016). SO_2 emissions are estimated to have declined by 69 % and NO_x by 39 % across the EU-28 over the same period.

NH_3 is known to contribute significantly to total nitrogen (N) deposition to the environment, and causes harmful effects through eutrophication and

acidification of land and freshwaters. This can lead to a reduction in both soil and water quality, loss of biodiversity and ecosystem change (e.g. Pitcairn et al., 1998; Sheppard et al., 2011). In the atmosphere, NH_3 is the major base for neutralization of atmospheric acid gases, such as SO_2 and NO_x emitted from combustion processes (vehicular and industrial) and from natural sources, to form ammonium-containing particulate matter (PM): primarily ammonium sulfate ($(NH_4)_2SO_4$) and ammonium nitrate (NH_4NO_3). This secondary PM is mainly in the "fine" mode with diameters of less than 2.5 µm (i.e. $PM_{2.5}$ fraction) (Vieno et al., 2014). The effects of PM on atmospheric visibility, radiative scattering, cloud formation (and resultant climate effects) and on human health (bronchitis, asthma, coughing) are well documented (e.g. Kim et al., 2015; Brunekreef et al., 2015). Inputs of NH_3 and NH_4^+ (collectively termed NH_x) are the dominant drivers of ecological effects of deposited N, compared with wet deposited NH_4^+ in rain (UNECE, 2016), and the importance of NH_x can be expected to increase further, relative to oxidized N, as NO_x emissions have been decreasing faster than NH_3 emissions (Reis et al., 2012; EEA, 2016; EU, 2016).

In gaseous form, NH_3 has a short atmospheric lifetime of about 24 h (Wichink Kruit et al., 2012). It is primarily emitted at ground level in the rural environment, and is associated with large dry deposition velocities to vegetation (Sutton and Fowler, 2002). High NH_3 concentrations can lead to acute problems at a local scale, for example, at nature reserves located in intensive agricultural landscapes (Sutton et al., 1998; Cape et al., 2009a; Hallsworth et al., 2010; Vogt et al., 2013). The NH_3 remaining in the atmosphere generally partitions to PM where the NH_4^+ can have a lifetime of several days (Vieno et al., 2014). Although NH_4^+ dry deposits at the surface, the primary removal mechanism for NH_4^+ is thought to be through scavenging of PM by cloud and rain, leading to wet deposition of NH_4^+ (Smith et al., 2000). Characterizing the relationship between NH_3 emissions and the formation of PM is, however, not straightforward; an increase in NH_3 emissions does not automatically translate into a proportionate increase in NH_4^+ (Bleeker et al.,

2009). The relationship depends on climate and meteorology as well as the concentration of other precursors to PM formation such as SO_2 and NO_x (Fowler et al., 2009). Since UK particulate NH_4^+ is generally dominated by NH_4NO_3 and $(NH_4)_2SO_4$ (see e.g. Twigg et al., 2016; Malley et al., 2016) and NH_3 gas is present in excess, then gas-particle transfer of NH_3 to NH_4^+ is the dominant pathway for forming NH_4^+ in PM. While it is clear that reductions in NH_3 emissions will lead to reductions in overall NH_4^+ concentrations (Vieno et al., 2016), the relative changes in gaseous NH_3 and NH_4^+ particles remains poorly quantified.

International targets have been agreed to reduce NH_3 emissions to move towards protection against its harmful effects. These include the UNECE Convention on Long-Range Transboundary Air Pollution (CLRTAP) Gothenburg Protocol and the recently revised EU National Emission Ceilings Directive (NECD 2016/2284) (EU, 2016). The 1999 UNECE Gothenburg Protocol is a multi-pollutant protocol to reduce acidification, eutrophication and ground-level ozone by setting emissions ceilings for sulfur dioxide, nitrogen oxides, volatile organic compounds and ammonia, which are to be met by 2020. Revised in 2012, the protocol requires national parties to jointly reduce emissions of NH_3, in the case of the EU-28 by 6 % between 2005 and 2020 (Reis et al., 2012). Under the revised NECD (EU, 2016), the EU is also committed to reduction of 6 % for NH_3 (but by a later date of 2029), as well as an additional 13 % reduction in NH_3 emission beyond 2030 compared with a 2005 baseline.

Although this demonstrates that there is currently no strong commitment to reduce NH_3 emissions compared with SO_2 and NO_x , other supporting measures should also be noted including the Industrial Emissions Directive 2010/75/EU (IED), which requires pig and poultry farms (above stated size thresholds) to reduce emissions using Best Available Techniques. The IED applies to around 70 % of the European poultry industry and around 25 % of the pig industry (UNECE, 2010). In tandem, revised UNECE “Critical Levels” (CLe) of NH_3 concentrations to protect sensitive vegetation and ecosystems

were adopted in 2007 (UNECE, 2007). These set limits of NH_3 concentrations to 1 and 3 µg NH_3 m^{-3} annual mean for the protection of lichens– bryophytes and other vegetation, respectively (Cape et al., 2009b). The new CLes replaced the previous single value of 8 µg NH_3 m^{-3} (annual mean) and have since been adopted as part of the revised Gothenburg Protocol. Such CLes for NH_3 are widely exceeded, including over the areas designated as Special Areas of Conservation (SAC) under the Habitats Directive, indicating a significant threat to the Natura 2000 network established by that directive (Bleeker et al., 2009; Hallsworth et al., 2010; van Zanten et al., 2017).

Few countries have established systematic networks to measure NH_3 across their domains. In the Netherlands, a continuous wet annular denuder method (AMOR, replaced by the DOAS (differential optical absorption spectroscopy) device in 2015) has been used at eight stations in the Dutch National Air Quality Monitoring Network (Van Pul et al., 2004; van Zanten et al., 2017). The Ammonia in Nature (MAN) network established in 2005 in the Netherlands monitors NH_3 with passive diffusion tubes in Natura 2000 areas (Lolkema et al., 2015). In the USA, the Ambient Ammonia Monitoring Network (AMoN) has been using passive (Radiello) samplers at 50 sites since Oct 2010 (Puchalski et al., 2011). Hungary (Horvath et al., 2009), Belgium (den Bril et al., 2011), Switzerland (Thöni et al., 2004), West Africa (Senegal and Mali under the Pollution of African Capitals programme; Adon et al., 2016) and China (Xu et al., 2016) also have long-term NH_3 measurement campaigns (see review by Bleeker et al., 2009).

In the UK, the National Ammonia Monitoring Network (NAMN) was established in September 1996 with the aim of establishing long-term continuous monthly measurements of atmospheric NH_3 gas (Sutton et al., 2001a). Particulate NH_4^+ measurements were added in 1999, since this was expected to exhibit different spatial patterns and temporal trends to gaseous NH_3 (Sutton et al., 2001b). The NAMN thus provides a unique and important long-term record for examining responses to changing agricultural practice and allows assessment

of the compliance of NH_3 emissions with targets established by international policies on emissions abatement. Measurements of NH_3 and NH_4^+ in the NAMN also address spatial patterns, covering both source and sink areas to test performance of atmospheric transport models, to support estimation of dry deposition of NH_x, to improve estimation of the UK NH_x budget (Fowler et al., 1998; Smith et al., 2000; Sutton et al., 2001b) and to assist with the assessment of exceedance of critical loads and critical levels (UNECE, 2007).

This paper provides an analysis on the state of atmospheric concentrations of NH_3 and NH_4^+ in the UK from 1998 to 2014 and their spatial and temporal trends. Overall, 17 years of continuous long-term NH_3 measurement data and 16 years of continuous long-term NH_4^+ measurement data from the NAMN are analysed to assess trends in concentrations in relation to estimated changes in emissions. The long-term measurement dataset is also used to explore spatial and temporal patterns in NH_3 and NH_4^+ across the UK in relation to regional variability in emission source sectors.

2.3 Methods

2.3.1 Network structure and site requirements

The design strategy for NAMN was to sample at a large number of sites (> 70) using low-frequency (monthly) sampling for cost-efficient assessment of temporal patterns and long-term trends. The network covers a wide distribution of monitoring sites with measurements in both agricultural and semi-natural areas. Monitoring locations are sited away from point sources (> 150 m) such as farm buildings, which avoids overestimating NH_3 concentrations compared with the grid square, since the aim is to provide meso-scale and regional patterns. In addition, where sampling is carried out in woodland areas, it is made in clearings. It was also recognized that the location of the network sites needed to consider the extent of sub-grid variability and the representativeness of sampling points. Spatially detailed local-scale NH_3 monitoring was therefore also carried out at a sub-1 km level to assess the

extent to which a monitoring location is representative (Tang et al., 2001b). The NAMN started with 70 sites. Over time, new sites were added to fill gaps in the map, some sites were closed following reviews and some sites had to be relocated due to local reasons, for example land ownership changes or site re-development. The number of sites peaked at 93 in 2000, but since 2009 has been stable at 85 sites. The locations of the NAMN sites for NH_3 and NH_4^+ in 2012 are shown in Figs. 2.1a, b. The selection of NAMN sites to provide a representative concentration field across the UK was aided by the availability of an estimated UK NH_3 concentration field at a 5 km by 5 km grid resolution provided by the Fine Resolution Atmospheric Multi-pollutant Exchange (FRAME) model (Singles et al., 1998; Fournier et al., 2002).

A comparison of FRAME-modelled NH_3 concentrations for NAMN sites with FRAME-modelled concentrations for the whole of the UK shows that the network has a good representation in the middle air concentration classes of 0.5 – 1.5 µg m^{-3} (33 % of NAMN sites, compared with 29 % of all FRAME 5 km × 5 km grid squares) and 1.5 – 3 µg m^{-3} (32 % of NAMN sites, compared with 39 % of all FRAME 5 km × 5 km grid squares), but with an over-representation at high concentrations and under-representation at low concentrations (Fig. 2.1c).

Since air concentrations are more variable in high-concentration areas, a larger number of monitoring sites were located in these areas than in remote lowconcentration areas where air concentrations are more homogeneous. Similarly, the monitoring sites were strategically selected to cover source areas of expected high concentrations and variability on the basis of the FRAME model NH_3 concentration estimates (Figs. 2.1a, b), and this approach was expected to provide additional evidence to test the performance of atmospheric dispersion models (Fournier et al., 2005; Dore et al., 2015).

When compared with other atmospheric chemistry transport models, FRAME was found to correlate well with measured NH_3 concentrations (Dore et al. 2015). The NAMN sites were also similarly checked for representativeness of

particulate NH_4^+ by comparing FRAME modelled NH_4^+ concentrations at NAMN sites with modelled concentrations for the whole of the UK, which demonstrates a good representation across the range of expected concentrations (Fig. 2.1d).

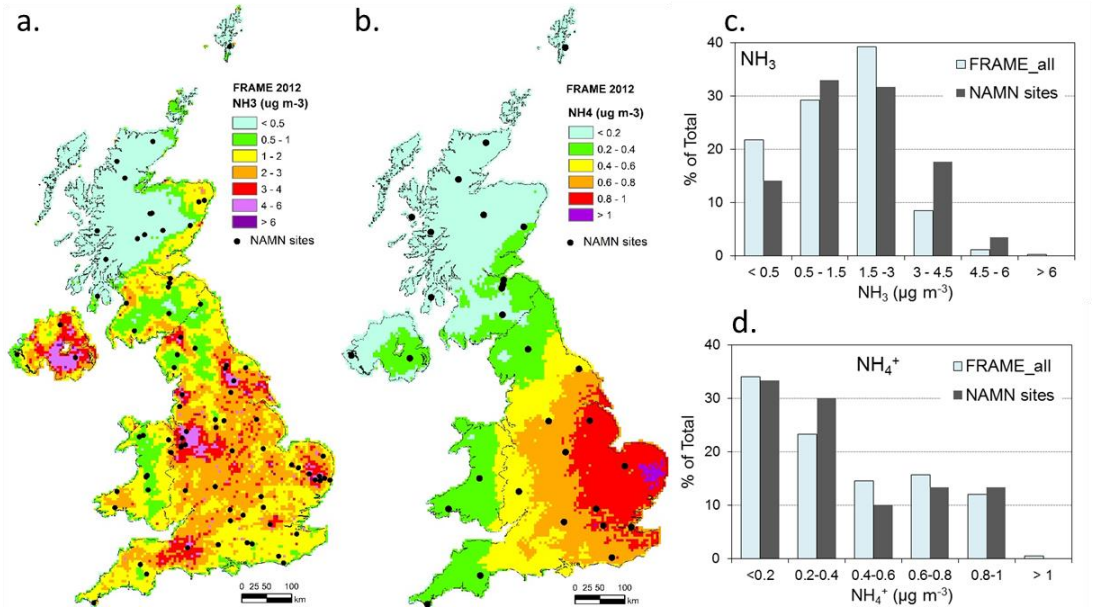

Figure 2.1. Maps of modelled annual mean concentrations of (a) NH_3 and (b) NH_4^+ at 5 km × 5 km grid resolution from the FRAME atmospheric transport model using 2012 UK emissions data, based on Dore et al. (2008), overlaid with the National Ammonia Monitoring Network (NAMN) measurement sites, and frequency distributions of the modelled concentrations of (c) NH_3 and (d) NH_4^+ for the FRAME 5 km grid squares containing a NAMN site (85 and 30 sites, respectively, in 2012) and for all model grid squares over the UK.

2.3.2 Atmospheric NH_3 and NH_4^+ measurements

Monthly time-integrated measurements of atmospheric NH_3 are made in the NAMN using a combination of passive samplers (Sutton et al., 2001a; Tang et al., 2001a) and an active diffusion denuder method referred to as the DEnuder for Long Term Atmospheric (DELTA) sampler (Sutton et al., 2001a, c). In terms of passive samplers, membrane diffusion tubes (3.5 cm long) with a limit of detection (LOD) around 1 µg NH_3 m^{-3} (Sutton et al., 2001a) were used in the first 4 years (September 1996–April 2000). These were replaced in May 2000 with the more sensitive Adapted Low-cost, Passive High Absorption (ALPHA, LOD = 0.03 µg NH_3 m^{-3}) diffusive samplers (Tang et al., 2001a; Tang and

Sutton, 2003), following a period of parallel testing (Sutton et al., 2001c). Particulate NH_4^+ measurement was added to the NAMN in 1999 at all DELTA sites (50) in the first 2 years (1999 and 2000). Following this initial period, the sampling density was reduced during early 2001 to 37 sites and has been stable at 30 sites since 2006. Although not presented in this paper, the DELTA samplers additionally provide concentrations of acid gases (HNO_3, SO_2, HCl) and aerosols (NO_3^-, SO_4^{2-}, Cl^-, Na^+, Ca^{2+}, Mg^{2+}) for the UK Acid Gases and Aerosols Monitoring Network (AGANet) at a subset of NAMN DELTA sites (Tang et al., 2015; Conolly et al., 2016). Measurement data from the AGANet (Tang et al., 2017) are used to aid interpretation of NH_3 and NH_4^+ results in Sect. 2.4.5.6.

2.3.2.1 DELTA method

The DELTA method uses a small pump to sample air (0.2 to 0.4 L min^{-1}) in combination with a high-sensitivity gas meter to record sampled volume (Sutton et al., 2001c). Two citric acid coated denuders (10 cm long borosilicate glass tubes) in series are used to collect NH_3 gas and to check the collection efficiency. A collection efficiency correction is applied to the measurement (Sutton et al., 2001d). The corrected air concentration is determined as (Eq. 1):

$$\chi_a\,(\text{corrected}) = \chi_a\,(\text{Denuder 1}) * \frac{1}{1-\left[\frac{\chi_a(\text{Denuder 2})}{\chi_a(\text{Denuder 1})}\right]} \qquad (1)$$

Typically, denuder collection efficiency is better than 90 % (Conolly et al., 2016). At 90 % collection efficiency, the correction represents 1 % of the corrected air concentration. Individual measurements with collection efficiency < 75 % (correction amounts to 11 % of the total at 75 %) are flagged as valid, but less certain (Tang and Sutton, 2003). Where less than 60 % of the total capture is recorded in the first denuder, the correction factor amounts to greater than 50 % and is not applied. The air concentration of (χ_a) of NH_3 is then determined as the sum of NH_3 in denuders 1 and 2:

$$\chi_a = \chi_a\,(\text{Denuder 1}) + \chi_a\,(\text{Denuder 2}) \qquad (2)$$

At sites where particulate NH_4^+ is also sampled, a 25 mm filter pack with a citric acid impregnated cellulose filter is added after the denuders to capture the NH_4^+ The calculated air concentrations (Y_a) of NH_4^+ is corrected for incomplete capture of NH_3 by the double denuder. The corrected air concentration of NH_4^+ is determined as:

$$Y_a\ (\text{corrected } NH_4^+) = Y_a\ (NH_4^+) - [((\chi_a\ (\text{corrected } NH_3) - [(\chi_a\ (\text{Denuder 1 } NH_3) + \chi_a\ (\text{Denuder 2 } NH_3)])^* (18/17)] \quad (3)$$

For NH_4^+ sampling, loss of NH_3 due to volatilization of NH_4^+ from the acid impregnated filter has been investigated, by adding a third citric acid coated denuder after the filter pack, which was found to be negligible. At DELTA sites where additional simultaneous sampling of acid gases and particulate phase components are made for AGANet, ion balance checks between anions and cations in the particulate phase are performed to provide an indication of the quality of the particulate measurements. For the acid and base particulate components, close coupling is expected between NH_4^+ and the sum of NO_3^- and SO_4^{2-}, as NH_3 is neutralized by HNO_3 and H_2SO_4 to form NH_4NO_3 and $(NH_4)_2SO_4$, respectively (Conolly et al., 2016).

At the Bush OTC site in Scotland (UK-AIR ID = UKA00128), duplicate DELTA measurements are made to assess the reproducibility of the method. For continuous monthly measurements between 1999 and 2014, the R^2 between the duplicate systems was 0.96 for both NH_3 and NH_4^+ (Supp. Fig. S2.1).

2.3.2.2 Passive methods

The NH_3 membrane diffusion tubes deployed in the NAMN from 1996 to 2000 are hollow cylindrical tubes (FEP, 3.5 cm long). A cap at the top end holds in place two stainless steel grids coated with sulfuric acid. The lower air-inlet end of the tube is capped with a gas-permeable membrane (Sutton et al., 2001a; Tang et al., 2001a; Thijsse, 1996). In comparison, the ALPHA passive sampler is a badge-type highsensitivity sampler with an uptake rate that is ~ 20 times faster than the diffusion tube. It consists of a cylindrical lowdensity

polyethylene body. An internal ridge supports a cellulose filter coated with citric acid, which is held in place with a polyethylene ring. The open end is capped with a PTFE membrane, providing a diffusion path length of 6 mm between the membrane and absorbent surface (Tang et al., 2001a).

Triplicate passive samplers are deployed for every measurement in the NAMN. Where the % coefficient of variation (CV) of the triplicate samplers is greater than 30 % for the diffusion tubes or greater than 15 % for the ALPHA samplers, the sample run is classed as failing the quality control test. Large discrepancies are most likely due to contamination of samples, and data from contaminated samples are excluded from the assessment in this paper.

The passive methods are calibrated against the DELTA method in the NAMN by ongoing comparison at several sites representing a wide range of ambient NH_3 concentrations (see Sect. 2.3.2.4). Since 2009, the number of inter-comparison sites has been nine. These are Auchencorth (UKA00451), Bush OTC (UKA00128), Glensaugh (UKA00348), Lagganlia (UKA00290), Llynclys Common (UKA00270), Moorhouse (UKA00357), Rothamsted (UKA00275), Sourhope (UKA00347) and Stoke Ferry (UKA00317). The intercomparison is used to establish a regression between the active and passive methods, with the DELTA samplers as the reference system, since the air volume sampled is accurately measured with high-sensitivity gas meters.

The calibration is necessary to account for the fact that the sampling path length in the passive samplers is longer than the distance between the membrane and adsorbent, due to the additional resistance to molecular diffusion imposed by the turbulence damping membrane at the inlet and the presence of a laminar boundary layer of air on the outside of the sampler (Tang et al., 2001a). In addition, parallel measurements were made at a high NH_3 concentration farm site (1998 – 2007) to extend the calibration range, and to ascertain linearity of response to high concentrations. To ensure that no bias is introduced in the sampling and to maintain the validity of long-term trends,

the calibration is evaluated on an annual basis (Tang and Sutton, 2003; Conolly et al., 2016).

For the period up to 2000 wwhen the diffusion tubes were implemented in the NAMN, their calibration (at 10 µg m^{-3}) amounts to an average of 1.5 % compared with the DELTA system. The mean ALPHA sampler calibration (at 10 µg m^{-3}), compared with the DELTA system, amounts to a correction of 10 % (ALP1: prototype 1, 1998– 2000), 15 % (ALP2: injection mould 1, 2001–2005), 17 % (ALP3: injection mould 2, 2006), 34 % (ALP4: injection mould 2 + new membrane, 2007–2008) and 40 % (ALP5: injection mould 2 + new membrane + new lab/instrument FloRRia, 2010–2014), respectively.

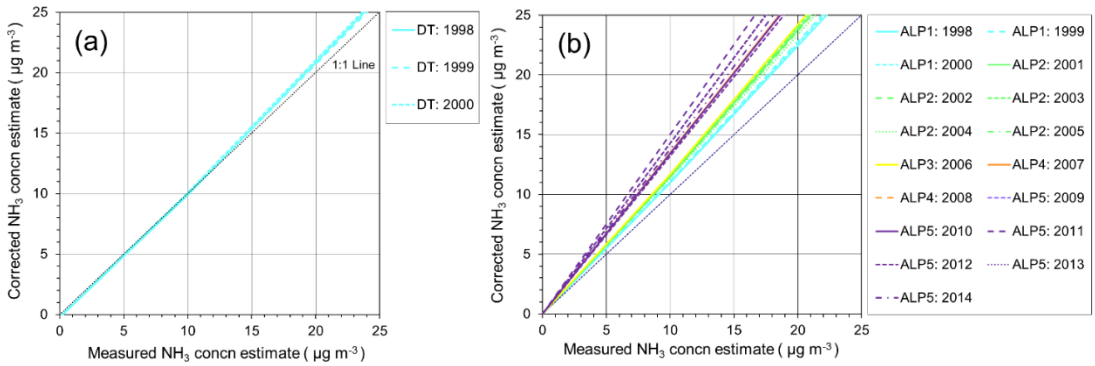

Figure 2.2. Comparison of annual empirical calibration curves for the passive samplers against the reference estimates from DELTA sampling at more than 9 sites in the UK National Ammonia Monitoring Network (NAMN). (a) DT, diffusion tubes. (b) ALP, ALPHA samplers; ALP1 is prototype 1 (1998–2000), ALP2 (2001–2005) and ALP3–ALP5 were manufactured from injection moulds 1 and 2, respectively. ALP4 and ALP5 have new inlet PTFE membrane (Swiftlab 07-OPM-027, 305 µm, regular polypropylene grid support material) that replaced the previous TE38 PTFE membrane (265 µm, randomly arranged polypropylene support material). ALP5: at new laboratory with analysis on FloRRia (previously on AMFIA).

The new PTFE membrane (5 µm pore size) is supported on a regular polypropylene grid and is thicker (305 µm) than the earlier PTFE membrane (also 5 µm pore size, but 265 µm thickness) used, which was supported instead on a randomly arranged polypropylene support material. The difference in calibration was therefore due to the extra resistance to gas diffusion imposed by the new thicker membrane. The annual calibration of the

methods shows both high precision and constancy between years (Fig. 2.2), which is important to support the detection of temporal trends in NH_3 concentrations. There is no systematic trend over time in either of the passive method calibrations.

The comparison of monthly measurement data between the DELTA and calibrated passive measurements demonstrated a close agreement (Fig. 2.3). The correlation (R^2) between DELTA and calibrated diffusion tubes was 0.91 (Fig. 2.3a), while the correlation between DELTA and calibrated ALPHA samplers was 0.92 (Fig. 2.3b). From the calibrated results, the intercept for the diffusion tubes was 0.10 µg NH_3 m^{-3}, while that for the ALPHA samplers was 0.03 µg NH_3 m^{-3}, demonstrating the improvement in sensitivity with the ALPHA samplers compared with the diffusion tubes (Fig. 2.3). In the present case the value of the intercepts, even for diffusion tubes, is much less than typical NH_3 air concentrations (see Sect. 2.4.1). However, this cannot be assumed to be the case in other implementations of the same methods.

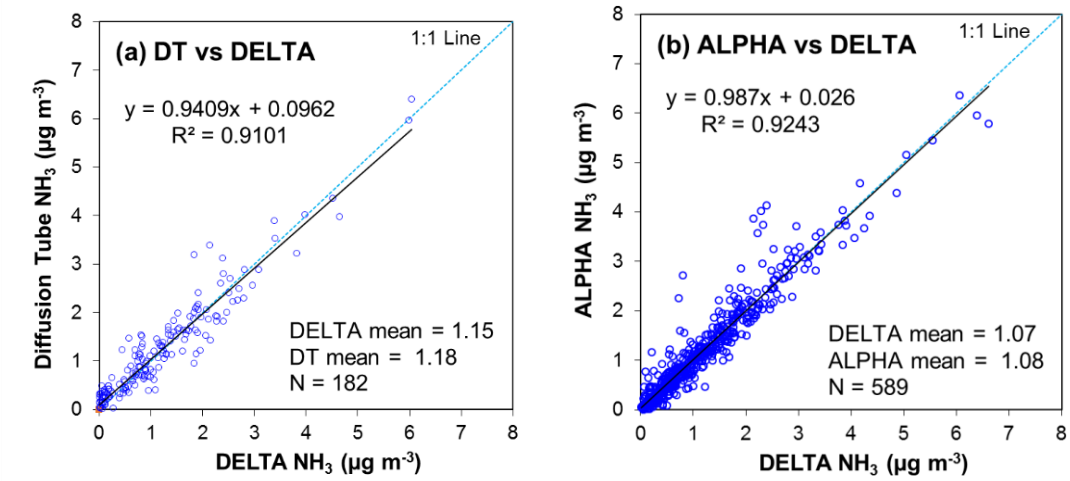

Figure 2.3. Regression of passive samplers vs. DELTA measurements at more than 9 sites in the UK National Ammonia Monitoring Network (NAMN), showing results for (a) diffusion tubes (DT), used during the early years of the network (1998–2000), and (b) for ALPHA samplers (results shown are for 2009–2014 where all analyses were carried out at a new laboratory). All passive data shown are the monthly measured concentrations for each site using the calibrated data for the respective passive methods.

Experience from other studies using the lower sensitivity diffusion tubes indicates a tendency to overestimate NH_3 concentrations under clean conditions (RGAR, 1990; Thijsse et al., 1996; Tang et al., 2001a; Lolkema et al., 2015). This observation points to the need for any application of NH_3 passive sampling for ambient monitoring to be accompanied by testing and calibration against a verified active sampling method. In independent assessments, for example in the USA (Puchalski et al., 2011), the ALPHA samplers performed well against a reference annular denuder method with a median relative percent difference of −2.4 %.

2.3.2.3 Chemical analysis

NH_3 gas captured on the acid coating of the denuder (DELTA), grid (diffusion tubes) or filter paper (ALPHA), and particulate NH_4^+ captured on the DELTA aerosol filter, are extracted into deionized water and analysed for NH_4^+ on an ammonia flow injection analysis system. The analytical instrument has changed over the network's operational period from the AMFIA (ECN, NL) to the FloRRIA (Mechatronics, NL), an updated model based on AMFIA (Conolly et al., 2016). The principles of operation of both instruments are the same and are based on selective diffusion of NH_4^+ across a PTFE membrane at c. pH 13 into a counter-flow of deionized water, allowing selective detection of NH_4^+ by conductivity (Wyers et al., 1993). The extracted samples were analysed for NH_4^+ against a series of NH_4^+ standards and quality controls. Parallel analysis of laboratory and field blank (unexposed) samples were used to determine the amounts of NH_4^+ derived from NH_3 and NH_4^+ in the atmosphere during transport and storage. The limit of detection (LOD) calculation of the ALPHA and DELTA methodologies are determined as 3 times the standard deviations of the laboratory blanks. For the DELTA method, the LODs were 0.01 µg m^{-3} for gaseous NH_3 and 0.02 µg m^{-3} for particulate NH_4^+. For the ALPHA method, the LOD was determined as 0.03 µg m^{-3}.

2.3.2.4 Data quality control

Measurement data are checked and screened, based on the quality management system applied in the UK air monitoring networks (Tang and Sutton, 2003). Data quality is assessed against the following set quality control criteria: (a) DELTA system: monitoring of the air flow rate and the use of two denuders in every sample to assess capture efficiency for NH_3, and (b) passive samplers: use of triplicate samplers for monitoring NH_3 concentrations at every site, to allow an assessment of sampling precision, and (c) ongoing calibration of passive samplers against the DELTA. Data flags are applied to the dataset; a full list of these is available from the EMEP website (http://www.nilu.no/projects/ccc/flags/index. html). Following the quality control checks and data flagging on the collected dataset, the annually ratified data from the NAMN are made publicly available on the Department for Environment, Food and Rural Affairs (Defra) UK-AIR website (https://uk-air.defra.gov.uk/; Tang et al., 2017) and are also in the process of being made available on the EMEP website (http://ebas.nilu.no/).

An inter-comparison of NH_3 measurements by the RIVM AMOR system (hourly, Wyers et al., 1993) and the DELTA sampling system (monthly) have been carried out at the Zegweld site (ID 633) in the Dutch National Air Quality Monitoring Network (van Zanten et al., 2017) since July 2003. Since September 2012, ALPHA measurements have also been included. To compare results, monthly mean concentrations were derived from the average of hourly AMOR data for the corresponding DELTA and ALPHA monthly sampling periods with good agreement (Supp. Fig. S2.2).

2.3.3 Trend analyses

Statistical trend analysis was conducted on the long-term dataset from the UK NAMN to identify trends (univariate monotonic, see e.g. Hirsch et al., 1991), estimate the rate of change and to address the question of whether trends in NH_3 and NH_4^+ concentrations (if any) are consistent with the changes in estimated UK annual NH_3 emissions (data downloaded from:

http://naei.beis.gov.uk/data/ data-selector-results?q=101505). The dataset is sufficiently long term (i.e. gaseous NH_3: 17 years and particulate NH_4^+: 16 years) and collected by consistent methods to allow for effective statistical trend analyses to be carried out. Trend analyses were carried out using (i) linear regression (LR), (ii) the Mann–Kendall (MK) test (Gilbert, 1987) on annually averaged and monthly mean data, and (iii) the seasonal Mann–Kendall (SMK) test (Hirsch et al., 1982) on monthly data only. MK tests were performed using the "Kendall" package (McLeod, 2015) in the R software. Computation of the Sen slope and confidence interval (for non-seasonal Sen slope only) of the linear trend were performed using the R "Trend" package (Pohlert, 2016). Since concentrations of NH_3 show strong seasonality, the SMK test was applied to identify the months that are driving the long-term trends in data. The SMK test (Hirsch et al., 1982) takes into account a 12-month seasonality in the time series data by computing the MK test on each of monthly "seasons" separately, and then combining the results. So for monthly "seasons", January data are compared only with January, February only with February, etc. No comparisons are made across season boundaries.

The Sen slope is the fitted median slope of a linear regression joining all pairs of observations. For the SMK, an estimate of the seasonal Sen trend slope over time is computed as the median of all slopes between data pairs within the same season (i.e. January compared only with January etc.). Therefore, no cross-season slopes contribute to the overall estimate of the SMK trend slope. Parametric LR analysis are simple and straightforward to use and interpret monotonic trend assessment in environmental data (e.g. Kindzierski et al., 2009; Meals et al., 2011), but they require assumptions about normality of data and homogeneity of variance of data. The MK approach on the other hand is widely used in environmental time series assessments, e.g. long-term trends in precipitation (Serrano et al., 1999) and long-term trends in European air quality (Colette et al., 2016; Torseth et al., 2012). The main advantages, as discussed in the literature, of the MK approach over linear regression for trend assessments are that (i) it does not require normally distributed data, (ii) it is

not affected by outliers, and (iii) it removes the effect of temporal auto-correlation in the data. However, linear trend assessment has been used in UK air quality monitoring network reports (e.g. Conolly et al., 2016). Therefore, both approaches were used in this paper, primarily as a quality assurance check.

2.4 Results and discussion

In order to summarize and discuss the NAMN dataset, the spatial patterns in the measurements of NH_3 and NH_4^+ are considered in Sect. 2.4.1 (comparison with emission estimates) and Sect. 2.4.2 (comparison with modelled concentration estimates). Seasonal patterns are discussed in Sect. 2.4.3, and long-term trends across the UK in Sect. 2.4.4.

2.4.1 Spatial variability in NH_3 and NH_4^+ concentrations in relation to estimated emissions

As a primary pollutant emitted from ground-level sources, NH_3 exhibits high spatial variability in concentrations (Sutton et al., 2001b; Hellsten et al., 2008; Vogt et al., 2013), confirmed by NH_3 data from the NAMN (e.g. range of 0.06–8.8 µg m^{-3} annual mean in 2005) (Fig. 2.4a). The observed variability is consistent with the large regional variability in NH_3 emissions and sources (Figs. 2.4c, d). With agriculture being the main source of NH_3 emissions, Fig. 2.4a shows the largest concentrations of measured NH_3 in parts of the UK with the highest livestock emissions, such as eastern England (East Anglia), northwest England (Eden Valley, Cumbria) and the border area between England and Wales (Shropshire) (Fig. 2.4d). By contrast, the lowest NH_3 measured concentrations are found in the northwest Scottish Highlands (< 0.2 µg m^{-3}), which is consistent with the emissions map (Fig. 2.4c). The 2005 data show exceedance of the Critical Levels for annual mean NH_3 concentrations of 1 and 3 µg NH_3 m^{-3} for the protection of lichens–bryophytes and vegetation, respectively (UNECE, 2007) at many of the sites (53 % > 1 and 13 % > 3 µg

NH_3 m^{-3}). In 2014, exceedance of the 1 and 3 µg NH_3 m^{-3} CLe increased to 60 and 16 %, respectively. The widespread exceedance of the CLe for NH_3 concentrations across the UK thus represents an ongoing threat to the integrity of sites designated under the Habitats Directive, as well as nationally designated Sites of Special Scientific Interest (SSSI) and other sensitive habitats.

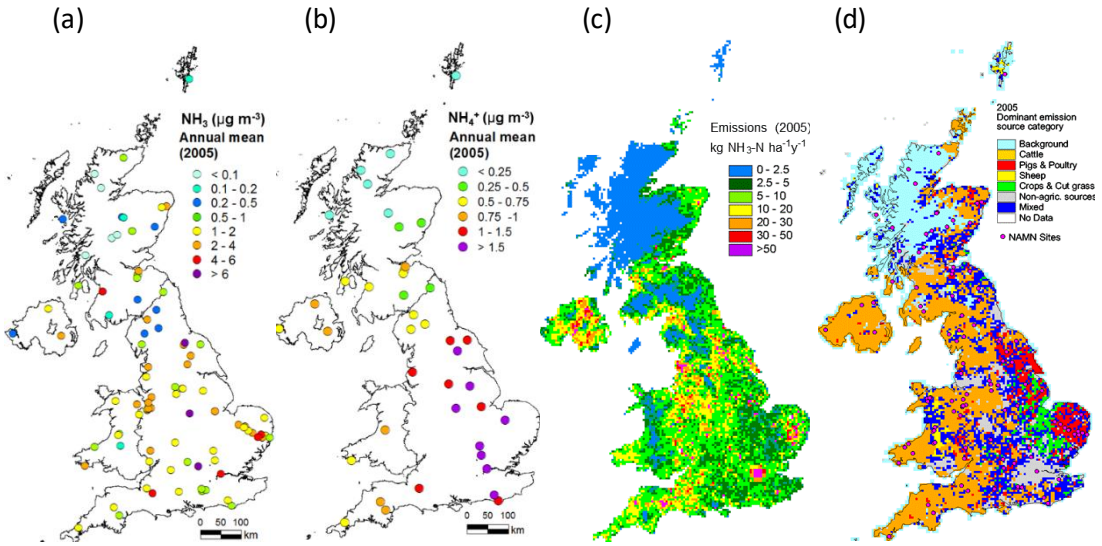

Figure 2.4. Measured annual mean concentrations from the UK National Ammonia Monitoring Network (NAMN) for 2005 for (a) NH_3 and (b) particulate NH_4^+, and maps at 5 km by 5 km grid resolution for 2005 of (c) the estimated annual NH_3 emissions (Dragosits et al., 2005) and (d) the dominant NH_3 emission source category (based on Hellsten et al., 2008), indicating the relationships between measured air concentrations and spatial variability in NH_3 emission sources. The measurements show a broad pattern of small air concentrations across NW Scotland. Conversely, the largest concentrations occur in areas with intensive cattle, pig and poultry farming with high NH_3 emissions e.g. East Anglia in SE England.

Concentrations of NH_4^+ are less spatially heterogeneous than those of NH_3, based on data from 30 sites (e.g. range of 0.14 to 1.8 µg m^{-3} annual mean in 2005) with a more coherent pattern of variation across the country, reflecting regional differences in NH_3 concentrations (Fig. 2.4b). Thus there is a general decreasing gradient from the southeast to the northwest of the UK, due to both NH_3 sources in England and import of particulate matter from Europe (Vieno et al., 2014; Dore et al., 2015). The limited variation across the UK for the annual average NH_4^+ concentrations can be attributed to the atmospheric

formation process (providing a diffuse source) and its longer atmospheric lifetime.

A similar picture is reported by the Dutch National Air Quality Monitoring Network (van Zanten et al., 2017), with large spatial variability of NH_3 concentrations (2 – 20 µg NH_3 m^{-3}) across the country and a more homogeneous distribution of particulate NH_4^+ (1 – 2 µg NH_4^+ m^{-3} in 2014), although the number of Dutch monitoring sites reported there is much smaller, with only eight stations providing continuous measurements. Both NH_3 and NH_4^+ concentrations were correlated with emission density, but the correlation was smaller for NH_4^+ than for NH_3 because of the larger contribution to NH_4^+ concentrations from long-range transport in the Netherlands.

The UK NH_3 emissions inventory is calculated and spatially distributed annually. Agricultural sources at a 5 km by 5 km grid resolution are combined with a large number of non-agricultural sources (Sutton et al., 2000; Tsagatakis et al., 2016) at a 1 or 5 km resolution to produce the annual NH_3 emissions data, and maps at a 1 km by 1 km grid resolution are reported by the official UK National Atmospheric Emissions Inventory (NAEI; http://naei.defra.gov.uk/data/mapping). In the UK, agriculture accounts for > 80 % of total NH_3 emissions and is estimated by the National Ammonia Reduction Strategy Evaluation System (NARSES) model (Webb & Misselbrook 2004; Misselbrook et al., 2015). For the agricultural NH_3 emission maps, parish statistics on livestock numbers and crop areas are combined with satellitebased land cover data to model emissions at a 1 km resolution, using the AENEID model (Dragosits et al., 1998; Hellsten et al., 2007). For reasons of data confidentiality, the 1 km data need to be aggregated to produce annual agricultural NH_3 emissions maps at a 5 km by 5 km grid resolution. National emission estimates for NH_3 are submitted to both the European Commission under the NECD (2001/81/EC) and the United Nations Economic Commission for Europe (UN/ECE) under the Convention on LongRange Transboundary Air Pollution (CLRTAP).

The AENEID approach (Dragosits et al., 1998) can further be used to classify each 5 km by 5 km grid square in the UK into dominant NH_3 emission source categories (Fig. 2.4d), following the method of Hellsten et al. (2008), where grid squares with > 45 % from a given category are referred to as dominated by that source. The seven categories are: cattle, pigs & poultry (combined for data disclosivity reasons), sheep, fertilizer application to crops and grassland, non-agricultural sources, as well as a mixed category where no single source dominates, and background. Background grid squares are defined by very low NH_3 emissions of < 1 kg N ha^{-1} yr^{-1}

Using the dominant emission sources map, each site in the NAMN is classified to one of the seven categories just described. This provides information of the main emission source type expected in the 5 km by 5 km grid square containing the monitoring site and is useful for assessing whether the network has a good representation of key emission source categories (Supp. Figs. S2.3a, b). Over the period since the NAMN was established, from 1996 to present, there have been substantial changes in emissions estimated for the different source sectors. For analysis in this paper, the dominant sources map for 2005 emission year was used as representing the mid-point of the data series (1998 – 2014) and compared with the classification from other years for consistency. This categorization of sites is used further in the interpretation of the monitored NH_3 and NH_4^+ concentrations and their longterm trends in the next sections.

2.4.2 Spatial variability in NH_3 and NH_4^+ concentrations in relation to modelled concentrations

The comparison of NAMN NH_3 and NH_4^+ measurements with modelled NH_3 concentrations from the FRAME model in this paper is made for an example year of 2012. This updates an earlier inter-comparison assessment carried out by Dore et al. (2007) for the year 2002, In the comparison of the FRAME model estimates (based on 2012 UK AENEID NH_3 emission data) with the NAMN

measurement results for 2012 (Fig. 2.5), the network annual mean concentrations for each site are compared against the model estimate for the 5 km grid square in which it occurs. Each point is also colourcoded according to the estimated dominant NH_3 emission source category for the 5 km by 5 km grid square, following the methodology described in a similar comparison from Sutton et al. (2001b) for the year 2000.

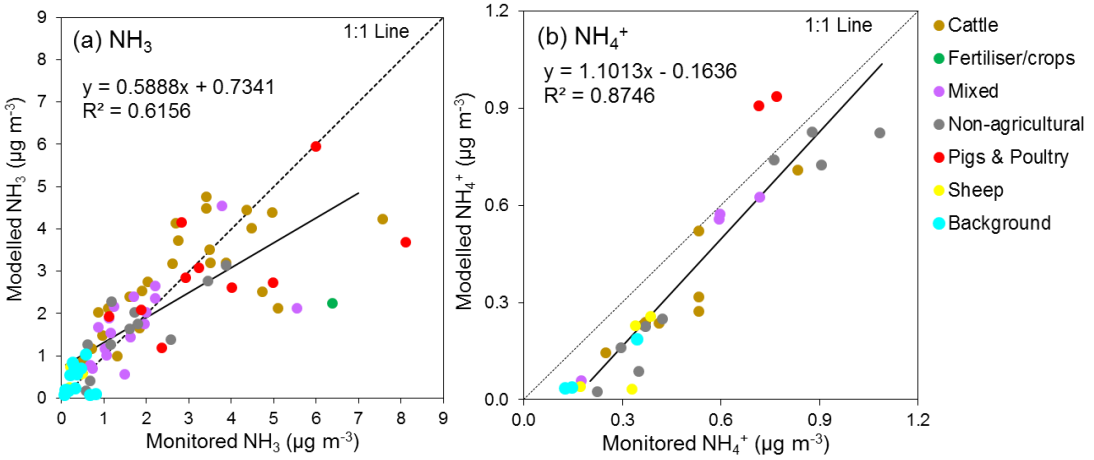

Figure 2.5. Comparison of 2012 annual mean concentrations of (a) NH_3 and (b) NH_4^+ modelled using the FRAME atmospheric model with 2012 measurements from the UK National Ammonia Monitoring Network (NAMN) for all sites according to dominant emission source classification.

For NH_3, both the model estimates and the measurement agree that background and sheep sites are characterised by small NH_3 concentrations (< 1 µg NH_3 m^{-3} annual mean), while agricultural areas, particularly areas with intensive pig and poultry areas, are associated with large NH_3 concentrations (up to 8 µg NH_3 m^{-3} annual mean). Overall, the comparison suggests a fairly good fit with regard to both the magnitude and spatial variability of NH_3 concentrations at a national scale (n = 85), with an R^2 value of 0.6 (Fig. 2.5a). UK NH_3 emissions with a 5 km × 5 km grid-square resolution is used as input in the FRAME model and the accuracy of the emissions data is critical to the model performance. The broad agreement between measurement and FRAME estimates broadly support the predictions of the FRAME model,

lending support to the AENEID model outputs. There is, however, significant scatter in the comparison, with some systematic differences in the comparison of FRAME and the measurements depending on the air concentration and dominant source.

NH_3 is known to exhibit large sub-grid variability (e.g. Dragosits et al., 2002), influenced by its proximity to emission source strength and type. In the vicinity of emission sources, NH_3 concentrations generally decay exponentially with distance away from source due to dispersion and dilution (e.g. Pitcairn et al., 1998). As it is a highly reactive gas, a significant fraction of the NH_3 emitted is also rapidly deposited within a 1 km radius of the source, so that concentrations reach background concentrations at distances of about 1 – 2 km from source (Fowler et al., 1998). This effect is particularly important in areas with high local variability in NH_3 emissions, such as intensive agricultural areas. The observed scatter in the comparison may therefore be due to the spatial location of the sampling site relative to the distribution of sources. For example, at many of the sites where the model overestimates concentrations, the measurements are in fact made in nature reserves or in clearings inside forests. The monitoring sites in these sink areas are typically well away from local sources and that would on average be more distant from sources than assumed in the FRAME 5 km average estimates, thereby underestimating concentrations. Conversely, some of the outliers where measurements are larger than the model predictions show indications of being affected by nearby emission sources, as was established by investigations during site visits. This effect is particularly important in areas with high local variability in NH_3 emissions, such as intensive agricultural areas, and illustrates the importance of having a large number of sites for comparison.

Figure 2.6 considers measured NH_3 concentrations at a subset of sites (44 out of the full 85 sites) that are located away from nearby local sources, in forest or semi-natural areas, following the site classification and assessment by Hallsworth et al. (2010). For this restricted set of sites, $R^2 = 0.76$ for 2012, which is higher than the correlation for the overall UK network. The

improvement in correlation between measured and modelled NH_3 concentrations for this subset of sites can be explained by the monitoring locations typically being further away from sources, so that uncertainties in local emission estimates are to some extent averaged out. This observation is also consistent with the findings of Vieno et al. (2009).

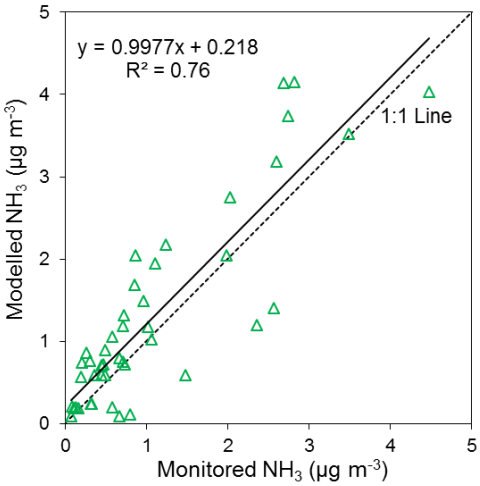

Figure 2.6. Comparison of 2012 annual mean concentrations of NH_3 from output of the FRAME atmospheric model with measurements from the UK National Ammonia Monitoring Network (NAMN) for a subset of sites classified as located in semi-natural or forest locations.

In contrast to NH_3, the correlation between NAMN measurements and FRAME model output is stronger for particulate NH_4^+ concentrations (R^2 = 0.87). However, measured concentrations are generally larger than the modelled ones (slope 1.1, intercept −0.16 µg m^{-3}; Fig. 2.5b). One reason for the better agreement for NH_4^+ is the more slowly changing spatial patterns in concentrations, which are not expected to vary on a finer scale than the model's 5 km by 5 km grid, improving the representativeness of site-based measurements. The 2012 comparison shown here updates an earlier intercomparison assessment carried out by Dore et al. (2007) for the year 2002 and demonstrates that the FRAME model is performing well in describing the spatial distribution of NH_4^+. However, for the 2012 inter-comparison, the FRAME model appears to underestimate NH_4^+ at sites with concentrations

<0.6 µg NH_4^+ m^{-3}, with better agreement at concentrations above 0.6 µg NH_4^+ m^{-3}. This suggests either too low a formation rate for NH_4^+ in the model at cleaner sites, or too high a removal rate for NH_4^+, or a combination of both. The presence of higher measured NH_4^+ concentrations in remote areas than shown by the model may also indicate that NH_4^+ has a longer residence time than treated in the model. Similar regressions between NAMN and FRAME NH_4^+ aerosol concentrations were observed for other years. For example, for 2008 the FRAME model underestimated NH_4^+ at concentrations < 0.7 µg NH_4^+ m^{-3} (slope 1.2, intercept −0.26 μg^{-3}; R^2 = 0.89, range = 0.2 − 1.4 µg m^{-3}). Changes in the chemical climate, such as reduced emissions of SO_2 in the UK, are postulated to affect conversion rates of NH_3 into NH_4^+, as well as the dry deposition rates, leading to more NH_3 remaining in the atmosphere (van Zanten et al., 2017). This is discussed further in Sect. 2.4.5.6.

2.4.3 Seasonal variability in measured UK NH_3 and NH_4^+ concentrations

A comprehensive account of the seasonal variability of NH_3 and NH_4^+ for different regions across the UK is provided by the NAMN. In Fig. 2.7, the average seasonal cycles of grouped sites from four different emission source categories are compared for NH_3 and NH_4^+.

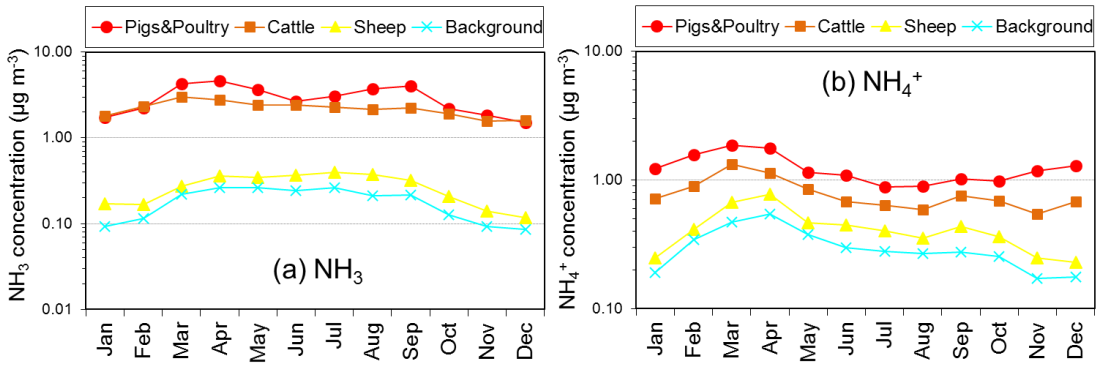

Figure 2.7. Seasonal trends in (a) NH_3 (mean monthly data for 1998–2014) and (b) NH_4^+ (mean monthly data for 1999–2014) concentrations of sites in the UK National Ammonia Monitoring Network (NAMN) classified according to four key emission source categories: cattle, sheep, pigs & poultry and background (based on 2005 dominant emission source classification). The concentrations are plotted on a log scale for better visualization of the low-concentration background and sheep profiles.

In addition to substantial differences in the overall magnitude of NH_3 concentrations, where the largest concentrations in the network are found at sites dominated by pig and poultry farming, followed by areas where cattle farming predominates, it is clear that the seasonal patterns of NH_3 also vary depending on the dominant source type (Fig. 2.7a). For background sites (defined as located in grid squares with NH_3 emissions < 1 kg N ha^{-1} yr^{-1}), a clear summer maximum in NH_3 concentrations can be observed, with minimum concentrations occurring in winter. The summer peak is probably related to increased land surface NH_3 emissions in warm, dry summer conditions, both from the presence of low-density grazing livestock and wildlife. It is also related to surface factors such as the compensation point for vegetation, which is defined as the concentration below which growing plants start to emit NH_3 into the atmosphere (Sutton et al., 1995). The interaction between atmospheric NH_3 concentrations and vegetation is complex, leading to both emission and deposition fluxes, depending on relative differences in concentrations.

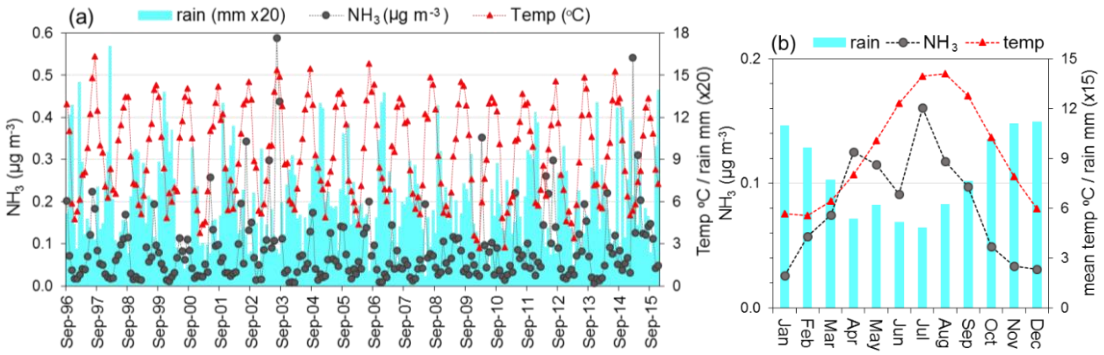

Figure 2.8. (a) Long-term trends in measured monthly-mean NH_3 concentrations at the remote background Inverpolly site in NW Scotland (UKA00457), demonstrating strong intra- and inter-annual variability, from the UK National Ammonia Monitoring Network (NAMN). Also plotted for comparison are monthly rainfall and temperature data from the nearby Aultbea meteorological station (ID no. 52; Met Office, 2016). (b) Comparison of seasonal trends in NH_3 concentrations with temperature and rainfall at Inverpolly. Data shown are averaged over the period 1996–2015. Peak concentrations of NH_3 can be seen to coincide with summer maxima in the temperature profile, while the lowest concentrations occur in winter when the temperature is lowest and also when rainfall is generally highest.

However, it is well established that warm, dry conditions promote NH_3 emission from vegetation (e.g. Massad et al., 2010; Flechard et al., 2013). It is therefore possible that bi-directional exchange with vegetation is at least partly controlling NH_3 concentrations at remote sites distant from intensive livestock farming.

The possibility for such interactions can be considered further using the example of Inverpolly (UKA00457), a remote background site in the NW Scottish Highlands. This site shows a very clear seasonal cycle with peak concentrations in July when warmer, drier conditions prevail, while lowest concentrations occur during the cooler and wetter winter months (Figs. 2.8a, b). A smaller peak in NH_3 can also be seen annually in April, which indicates potential longer-range influences of manure spreading in spring, even at this remote location (Fig. 2.8b). Although there is substantial scatter, Fig. 2.9 shows that there is significant correlation between monthly NH_3 concentrations and both temperature (R^2 = 0.33, n = 231, p < 0.05) and precipitation (R^2 = 0.19, n = 231, p < 0.05). The influence of temperature and rainfall on NH_3 emission and concentrations is well characterized (e.g. see Sutton et al., 2013; van Zanten et al., 2017).

For sites dominated by emissions from sheep farming, the seasonal profile in NH_3 concentrations is similar to that for background sites, although the summer maximum in NH_3 is larger than background sites, because grazing emissions are larger (Hellsten et al., 2008). It is notable that the peak NH_3 concentration occurs later in the year for background areas (July–September) than for sheep areas (June–August). This may be related to the seasonal presence of lambs, which are often only present for the first part of the summer. In areas with more intensive livestock farming, where emissions come from either cattle or from pig and poultry farming, the largest concentrations are observed in spring and autumn, corresponding to periods of manure application to land. The spring peak in March is larger than the autumn peak in September, which coincides with the main period for manure application being in spring, before the sowing of arable crops or early on in the grass-

growing period (Hellsten et al., 2007). Ammonia concentrations in these areas are also larger in summer than winter, due to warmer conditions promoting volatilization. Interestingly, the dip in concentrations in June matches a period when crops will be actively growing with possible uptake and removal of NH_3 from the atmosphere. Vegetation can be a source or a sink of atmospheric NH_3 and uptake of NH_3 can occur when the relative concentration of NH_3 in the atmosphere is higher than inside the plant stoma (e.g. Sutton et al.,1995; Massad et al., 2010; Flechard et al., 2013).

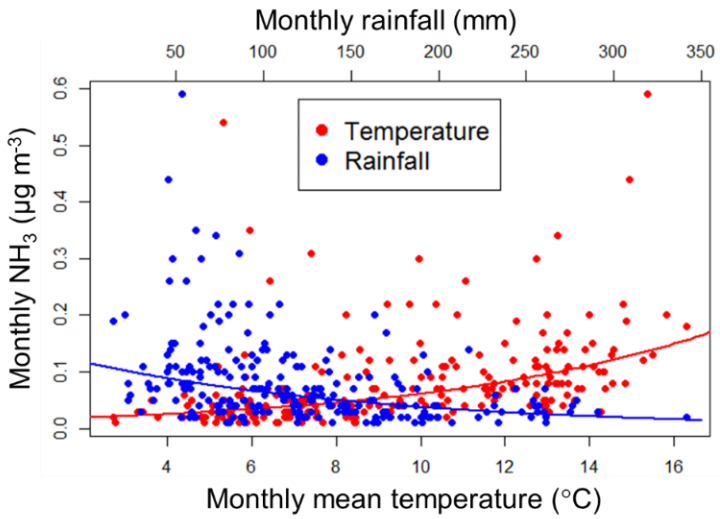

Figure 2.9. Relationships between measured monthly-mean NH_3 concentrations from the UK National Ammonia Monitoring Network (NAMN) and mean monthly temperature and rainfall at Inverpolly (UKA00457). NH_3 was negatively correlated with rainfall (blue line: $Log(NH_3) = -0.0059 \times Log(rain) - 2.1612$, $R^2 = 0.19$, $n = 231$, $p < 0.05$) and positively correlated with temperature (red line: $Log(NH_3) = 0.1482\ Log(temp) - 4.2708$, $R^2 = 0.33$, $n = 231$, $p < 0.05$). Rain and temperature data are from the nearby Aultbea meteorological station (ID no. 52; Met Office, 2016).

For particulate NH_4^+, as expected for a secondary pollutant, concentrations are more decoupled from the dominant NH_3 source sectors in the vicinity of a site. Although the formation of particulate NH_4^+ primarily depends on the occurrence of NH_3 in the atmosphere, synoptic meteorology and long-range transboundary transport from continental Europe are important drivers influencing the seasonal variations of NH_4^+ across the UK, due to its longer

lifetime (Vieno et al., 2014, 2016). The seasonal trends in particulate NH_4^+ are seen to be broadly similar for the four different emission source sectors (Fig. 2.7b), with the magnitude of the NH_4^+ concentrations reflecting NH_3 concentrations at a regional level. In the atmosphere, particulate NH_4^+ are primarily in the form of $(NH_4)_2SO_4$ and NH_4NO_3, formed when the acid gases HNO_3 and H_2SO_4 in the atmosphere are neutralized by NH_3 (Putaud et al., 2010). NH_3 preferentially neutralizes H_2SO_4 due to its low saturation vapour pressure (forming NH_4HSO_4 then $(NH_4)_2SO_4$, while NH_4NO_3 is formed when abundant NH_3 is available, In contrast to $(NH_4)_2SO_4$, NH_4NO_3 is a semi-volatile component (Stelson and Seinfeld, 1982).

Long-term data from the UK Acid Gases and Aerosols Monitoring Network (AGANet; Conolly et al., 2016) show a change in the particulate phase of NH_4^+ from $(NH_4)_2SO_4$ to NH_4NO_3, with particulate nitrate concentrations exceeding that of particulate sulfate approximately 3-fold (on a molar basis) (Fig. 2.18a). This suggests that the thermodynamic equilibrium between the gas phase NH_3 and HNO_3 and the aerosol phase NH_4NO_3 will have a much greater effect on the seasonal concentrations of NH_4^+ than $(NH_4)_2SO_4$. The formation and dissociation of NH_4NO_3 depend strongly on ambient temperature and humidity (Stelson and Seinfeld, 1982). Warm, dry weather in summer promotes dissociation, decreasing particulate phase NH_4NO_3 relative to gas phase NH_3 and HNO_3.

During the winter months, low temperature and high humidity favour the formation of NH_4NO_3 from the gas phase NH_3 and HNO_3. By contrast, the spring peak in NH_4^+ concentrations may be attributed to photochemical processes (elevated ozone) leading to enhanced formation of HNO_3 during this period (Pope et al., 2016) and also to import of particulate NO_3^- through long-range transboundary transport, e.g. from continental Europe, as discussed in Vieno et al. (2014). Nevertheless, it is notable that the winter minima for NH_4^+ aerosol concentrations at sheep and background sites are more pronounced than for pig-, poultry- and cattle-dominated sites. This may be a result of a combination of smaller NH_3 emissions in winter in these areas (as indicated by

Fig. 2.7a) and differences in long-range transport to the more remote areas in winter conditions. Overall, the seasonal distributions show that NH_3 concentrations are mostly governed by local emission sources and by changes in environmental conditions, with warm, dry weather favouring increased volatilization. By contrast, particulate NH_4^+ concentrations are largely determined by more distant sources through long-range transport and synoptic meteorology.

2.4.4 Long-term trends in estimated UK NH_3 emissions

UK NH_3 emissions are estimated to have fallen by 16 % between 1998 and 2014, from 336 to 281 kt (Fig. 2.10a) (http: //naei.defra.gov.uk/). The most significant cause of the estimated reductions has been decreasing cattle, pig and poultry numbers in the UK over this period. Between 2013 and 2014, the decreasing trend in UK NH_3 emissions was however reversed with an increase of 3.3 % from 272 to 281 kt NH_3 due to an increase in emissions from the agricultural sector from 224 kt in 2013 to 234 kt in 2014. This is attributed to an increase in dairy cow numbers (and dairy cow N excretion) and increase in fertilizer N use (particularly urea, which is associated with a higher emission factor than other fertilizer types used in the UK) (Misselbrook et al., 2015; http://naei.defra.gov.uk/).

Although the UK met the 2010 emission ceiling target of 297 kt NH_3 emission per year set out under the Gothenburg Protocol and NEC Directive, it is committed to a further emission reduction by 2020 of 8 % from the 2005 total under the 2012 revised Gothenburg Protocol, and by 17 % after 2030 under the revised 2016 NEC Directive (EU, 2016). The revised 2020 target of 282 kt NH_3 (8 % reduction of the baseline figure of 307 kt NH_3 emissions total in 2005) may require emission strategies to be implemented, rather than relying on decreasing livestock populations as during the recent decades.

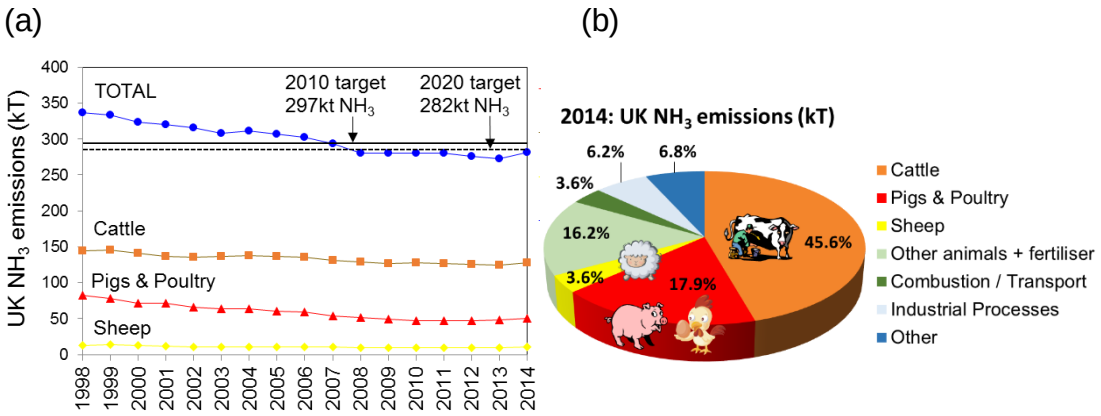

Figure 2.10. (a) Trends between 1998 and 2014 in the UK National Atmospheric Emission Inventory (NAEI) for total UK NH_3 emissions and selected sub-sources: cattle, pigs & poultry and sheep. The 2010 NH_3 national emissions ceiling target of 297 kt (Gothenburg protocol and NECD) and the 2020 target of 282 kt (revised Gothenburg protocol) are also shown for comparison. (b) UK NH_3 emission sources in 2014. Data from http://naei.defra.gov.uk/ and Misselbrook et al. (2015).

Agricultural emissions are by far the largest NH_3 sources in the UK's emission inventory, accounting for 86 and 83 % of the total NH_3 emissions in 1998 and 2014, respectively. The primary source of agricultural emissions is livestock manure management, in particular from cattle which contribute approximately 46 % of the total agricultural emissions, followed by pigs & poultry contributing another 18 % in 2014 (Defra, 2015; Misselbrook et al., 2015) (Fig. 2.10b). Over the period 1998 to 2014, NH_3 emissions from cattle are estimated to have decreased by 11 % (from 144 to 128 kt), with emissions estimated to have remained relatively stable since 2008, followed by a modest 2 % increase between 2013 and 2014 from 125 to 128 kt (Figs. 2.10a, 2.16). Emissions from pigs & poultry showed a large downward trend between 1998 and 2014, with a decrease of 39 % (from 82.7 to 50.3 kt) (Figs. 2.10a, 2.16), although the decreasing trend was reversed between 2012 and 2014, with an increase of 6 % from 46.7 to 50.3 kt. The sheep sector is a minor source, contributing 3.6 % to the total agricultural emissions. NH_3 emissions from this sector are estimated to have decreased by 24 % in 2014 relative to 1998 (from 13.3 to 10.1 kt).

2.4.5 Long-term trends in measured NH_3 concentrations

The UK NAMN dataset was analysed to compare levels and trends against the NH_3 emission inventory. To avoid bias due to changes in the number and locations of sites over the duration of the network, sites with incomplete data runs over selected periods for analysis are excluded. Based on these exclusion criteria, the number of sites with complete data runs was 59 for the period 1998 to 2014, 66 sites for 1999 to 2014, and 75 sites for the period 2000 to 2014. To ensure consistency in the trend analysis, several combinations of the available data were used:

1a. 1998–2014 (59 sites): annually averaged data
1b. 1998–2014 (59 sites): monthly mean data
2a. 1999–2014 (66 sites): annually averaged data
2b. 1999–2014 (66 sites): monthly mean data
3a. 2000–2014 (75 sites): annually averaged data
3b. 2000–2014 (75 sites): monthly mean data.

A visualization of the time series according to dataset 1a is summarized in Fig. 2.11. This shows the mean UK monitored annual NH_3 concentrations of 59 sites with complete data runs from 1998 (first complete year of monitoring) to 2014, summarized in a box plot, together with annual mean UK rainfall and temperature data and compared with NH_3 emissions trends over the same period. The interquartile ranges and the spread of the NH_3 concentrations can be seen to be variable from year to year, demonstrating both substantial inter- and intra-annual variability.

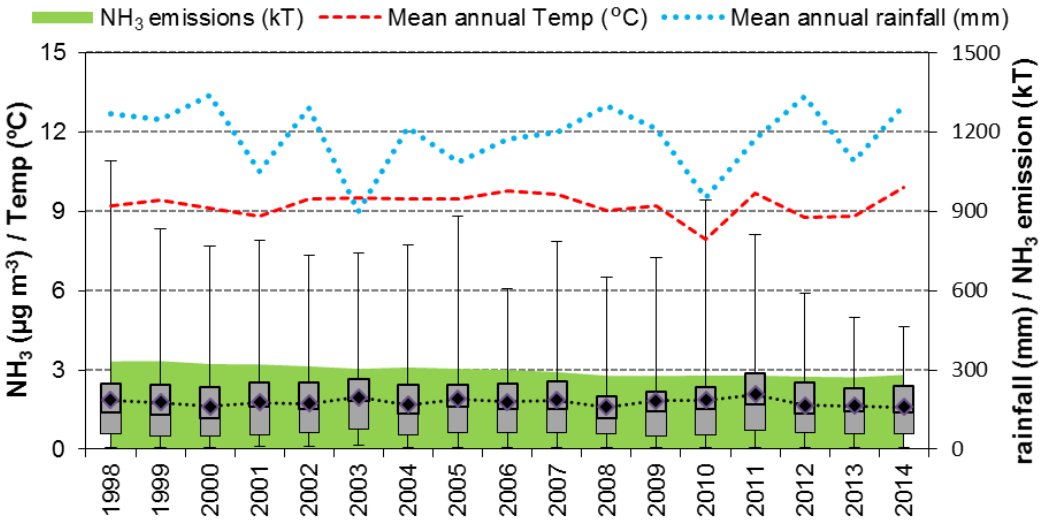

Figure 2.11. Changes in annual mean atmospheric NH_3 concentrations averaged over all sites in the National Ammonia Monitoring Network (NAMN) operational between 1998 and 2014 (59 sites). The diamonds show the mean NH_3 concentration, with the grey box indicating the median and interquartile range, while the error bars show the range (minimum and maximum) of measured mean concentrations. Annual mean UK meteorological data (source http://www.metoffice.gov.uk/) are also plotted for comparison over the same period. 2010 was an unusual year, characterized by a considerably lower than average mean annual temperature of 7.9 ºC due to an exceptionally cold winter, with December 2010 recorded as the coldest for over 100 years (cf. mean = 9.2 ºC for 1998 to 2014) and lower than average rainfall of 950 mm (*cf*. mean = 1190 mm for 1998 to 2014).

2.4.5.1 Mann–Kendall non-parametric time series analysis

To detect trends and to indicate the significance level of the trends in the long-term NAMN data, the non-parametric MK approach was used combined with the Sen slope method for estimating the trend and confidence interval of the linear trend (see Sect. 2.3.3). The classic MK test was used on the annually averaged data (datasets 1a, 2a, 3a), while both the classic MK and SMK tests were applied to the monthly averaged data (datasets 1b, 2b, 3b).

Results of the MK tests are summarized in Table 2.1. For each time series, the median annual trend (in units of µg NH_3^{-1} yr^{-1}) is estimated from the Sen slope and intercept of the MK linear trend. To assess the relative change over time, the % relative median change was calculated from the estimated NH_3 concentration at the start (y_0) and at the end (y_i) of the selected time period

($100 \times [(y_i - y_0)/y_0]$) computed from the Sen slope and intercept. This approach was adopted instead of a direct comparison of actual observed NH_3 concentrations at the start (y_0) and at the end (y_i) of the time series, since there is substantial inter-annual variability in the data (Figs. 2.10a, 2.16). Using the estimated concentrations at the start and end from the fitted Sen slope allows using a reference that is less sensitive to inter-annual variability than the actual observed concentrations.

Table 2.1. Summary of Mann–Kendall (MK) and seasonal Mann–Kendall (SMK) time series trend analysis on NH_3 data (annually averaged datasets 1a, 2a, 3a and monthly mean datasets 1b, 2b, 3b) from the UK National Ammonia Monitoring Network (NAMN). The following are shown: the p-value, median annual trend (Sen's slope, in µg NH_3 yr^{-1}) and the relative median change over the selected time period (in %). For the MK tests, the 95 % confidence interval (CI) for the trend and relative change are also estimated. For comparison, the reduction in estimated UK NH_3 emissions over the periods 1998–2014, 1999–2014 and 2000–2014 are 16.3, 15.6 and 13.1 % respectively.

Dataset	Time series	[a]Number of sites	*p-value*	Significant trend (p<0.05)	[b]Median annual trend & [95% CI] (µg NH_3 y^{-1})	[c]*R*elative median change over the period & [95% CI] (%)
1a: annual (MK)	1998-2014	59	0.46	no	-0.0071 [-0.0200, 0.0125]	-6.3 [-16, 12]
1b: monthly (MK)	1998-2014	59	0.22	no	-0.0096 [-0.0264, 0.0060]	-8.2 [-21, 5.5]
1b: monthly (SMK)	1998-2014	59	0.10	no	-0.0100	-5.8
2a: annual (MK)	1999-2014	66	1.00	no	0.0000 [-0.0227, 0.0200]	0.0 [-16, 16]
2b: monthly (MK)	1999-2014	66	0.51	no	-0.0060 [-0.0252, 0.0132]	-4.5 [-18, 11]
2b: monthly (SMK)	1999-2014	66	0.25	no	-0.0073	-4.2
3a: annual (MK)	2000-2014	75	1.00	no	0.0000 [-0.0283, 0.0175]	0.0 [-19, 14]
3b: monthly (MK)	2000-2014	75	0.43	no	-0.0072 [-0.0264, 0.0120]	-5.3 [-18, 9.5]
3b: monthly (SMK)	2000-2014	75	0.15	no	-0.0079	-4.5

[a]Number of sites providing complete data runs over the time period.
[b]Median annual trend = fitted Sen's slope of Mann-Kendall linear trend (unit = µg NH_3 y^{-1})
[c]Relative median change calculated based on the NH_3 concentration at the start (y_0) and at the end (y_i) of time series computed from the Sen's slope and intercept (=100*[(y_i-y_0) /y_0]).

For the annually averaged NH_3 concentrations across the UK, dataset 1a (1998–2014, 59 sites) show a small, but non-significant decreasing trend (relative median change = −6.3 %), while datasets 2a (1999–2014, 66 sites) and 3a (2000–2014, 75 sites) show no discernible trends (median relative change = 0.0 % for both) (Table 2.1). Results from the analysis of monthly data from all three different data groupings (1b, 2b, 3b) (relative median change −4.2 to −8.2 %) are similar to results for dataset 1a, based on analysis of annual data (Table 2.1). In the SMK tests on monthly data, two monthly "seasons" (January and April) in dataset 1b (1998–2014, 59 sites) are significant ($p < 0.05$), with a third monthly "season" (August) near-significant at $p = 0.06$. For datasets 2b (1999–2014, 66 sites) and 3b (2000–2014, 75 sites), August is the only monthly "season" in either time series to be close to significance at $p = 0.06$. Trends in individual monthly "seasons" are therefore weak and results between the MK and seasonal MK tests on monthly data are similar (Table 2.1).

2.4.5.2 Linear regression parametric time series analysis

The parametric linear regression time series trend analysis was also performed on the different data groupings. Results of the linear regression tests are summarized in Table 2.2, and a comparison of trends from the MK with the linear regression approach is provided in Fig. 2.12 for annual datasets 1a, 2a, 3a, and Fig. 2.13 for monthly datasets 1b, 2b, 3b. A similar approach to the MK was taken to assess the relative change, by calculating the % relative change from the estimated NH_3 concentration at the start (y_0) and at the end (y_i) of the time series ($100 \times [(y_i - y_0)/y_0]$) computed from the linear regression slope and intercept. The different data groupings all show small, but non-significant decreasing trends (relative change = −2.4 to −5.3 %), similar to the trends and % relative median change from the MK and SMK analysis (Figs. 2.12, 2.13). This suggests that the errors in the NAMN data are normally distributed and that no or few outliers are present, since the results from the non-parametric MK tests are very similar to the parametric least squares linear regression.

Table 2.2. Summary of linear regression time series trend analysis on NH_3 data (annually averaged datasets 1a, 2a, 3a and monthly mean datasets 1b, 2b, 3b) from the UK National Ammonia Monitoring Network (NAMN). The following are shown: the *p*-value, annual trend (fitted slope, in µg NH_3 yr^{-1}), R^2, and the relative change over the selected time period (in %). For comparison, the reduction in estimated UK NH_3 emissions over the periods 1998–2014, 1999–2014 and 2000–2014 are 16.3, 15.6 and 13.1 % respectively.

Dataset	Time series	[a]Number of sites	*p-value*	Significant trend (p<0.05)	[b]Annual Trend (µg NH_3 y^{-1})	R^2	[c]Relative change over the period (%)
1a: annual	1998-2014	59	0.62	no	-0.0035	0.0167	-3.1
1b: monthly	1998-2014	59	0.45	no	-0.0062	0.0028	-5.3
2a: annual	1999-2014	66	0.65	no	-0.0040	0.0154	-3.0
2b: monthly	1999-2014	66	0.74	no	-0.0031	0.0006	-2.4
3a: annual	2000-2014	75	0.69	no	-0.0038	0.0130	-2.8
3b: monthly	2000-2014	75	0.56	no	-0.0057	0.0019	-4.2

[a]Number of sites providing complete data runs over the time period.
[b]Annual trend = fitted slope of linear regression (unit = µg NH_3 y^{-1})
[c]Relative change calculated based on the estimated annual NH_3 concentration at the start (y_0) and at the end (y_i) of time series (=100[(y_i-y_0) /y_0]) computed from the slope and intercept (=100*[(y_i-y_0) /y_0]).*

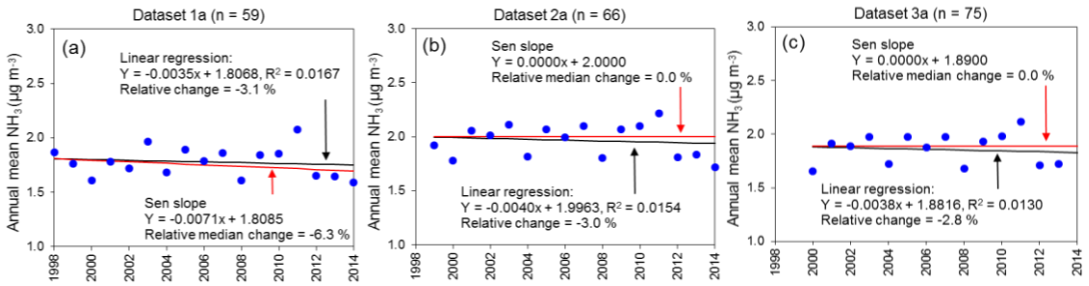

Figure 2.12. Time series trend analysis by non-parametric Mann–Kendall Sen slope vs. parametric linear regression on annually averaged NH_3 concentrations from the UK National Ammonia Monitoring Network (NAMN) for (a) dataset 1a (1998 to 2014, n = 59), (b) dataset 2a (1999 to 2014, n = 66) and (c) dataset 3a (2000 to 2014, n = 75). Individual data points are annually averaged NH_3 concentrations.

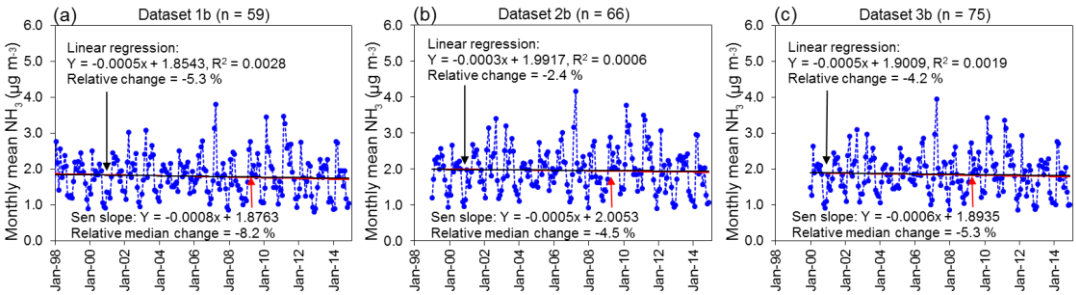

Figure 2.13. Time series trend analysis by non-parametric Mann–Kendall Sen slope vs. parametric linear regression on monthly mean NH_3 concentrations from the UK National Ammonia Monitoring Network (NAMN) for (a) dataset 1b (1998–2014, n = 59), (b) dataset 2b (1999– 2014, n = 66) and (c) dataset 3b (2000–2014, n = 75). Individual data points are monthly mean NH_3 concentrations.

2.4.5.3 Trends in NH_3 concentrations vs. trends in NH_3 emissions

Overall, the long-term NH_3 concentration data from the UK NAMN suggests evidence of a small, but non-significant decreasing trend (Figs. 2.12, 2.13). The level of reduction observed in the datasets is however less than the 16.3, 15.6 and 13.1 % reduction in estimated UK NH_3 emissions over the periods 1998–2014, 1999–2014 and 2000–2014, respectively (Tables 2.1, 2,2). Inventories have inherent uncertainties such as uncertainties in activity data and emission factors, or may be missing emission sources. In terms of measurement data, it has already been shown in Sects. 2.4.1 and 2.4.3 that the annually averaged data mask considerable spatial and seasonal variability in NH_3 concentrations. Drivers contributing to this variability include the influence of climate on emissions, variations in management practice for a particular emission source, and influence of local emission sources and interactions on concentrations at a site. In addition, once emissions have taken place, the resulting atmospheric NH_3 concentrations are influenced by local deposition, which is in turn affected by receptor surfaces and by concentrations of interacting chemical species that affect atmospheric lifetime and transport distance of NH_3 and physical dispersion (e.g. Bleeker et al., 2009; Sutton et al., 2013). In the following sections, we consider the possibility of interactions with climate, emission source type and chemical interactions as this may affect long-term trends in NH_3 concentrations.

2.4.5.4 Influence of climate

UK temperature and rainfall varied from year to year over the period 1998 to 2014 (Fig. 2.11), with no clear relationship with NH_3 easily visible in the graph. Plotting the annual mean NH_3 concentrations against the average temperature and rainfall however does show indicatively that elevated annual mean NH_3 concentrations are observed in warmer years, and reduced annual mean NH_3 concentrations are observed in wetter years (Supp. Fig. S2.4). This analysis for the full network is therefore consistent with the observation at a remote site (Inverpolly, Fig. 2.9). The thermodynamic equilibrium shifts NH_3 from the

aqueous (or particulate) phase to the gas phase with increased temperature, hence emissions from animal manures, soils and vegetation increase with increasing temperature (Asman et al., 1998; Sutton et al., 1993). Conversely, increases in precipitation decrease NH_3 emissions because rain events dilute the available NH_3 pool, while having the potential to wash urea and NH_x in solution from the surface. As NH_3 is soluble and washed out of the atmosphere by rainfall, this should also contribute to reduced NH_3 concentrations during wet periods.

An exception to this relationship can occur where N is excreted as uric acid from birds (e.g. poultry). In this case, sufficient water is needed to allow hydrolysis to form NH_3 (Riddick et al., 2014). In this situation, the arrival of rain promoted uric acid hydrolysis from seabird guano surfaces, which was limited in the absence of soil moisture. It is possible that this interaction could lead to NH_3 emissions from field spreading of poultry litter to be larger in wetter years. In a recent trend analysis of NH_3 concentrations from the Dutch Air Quality Monitoring Network, an attempt was also made to correct for meteorological (temperature and rainfall) influences for the eight monitoring stations, which broadly produced similar results with slightly enhanced statistical significance for the trends (van Zanten et al., 2017).

2.4.5.5 Influence of local emission sources

The inter- and intra-annual variability is also expected to be linked to influences from local emission source and activities. It has already been shown in Sect. 2.4.1 that the concentrations of NH_3 in air are greatest in parts of the country with a large presence of livestock farming, particularly in areas of pig, poultry and cattle farming. Using the classification of NAMN sites according to dominant emission source sectors described in Sect. 2.4.1, the long-term change in NH_3 concentrations at sites grouped into four different emission source sectors (background, sheep, cattle, and pigs & poultry) are compared in Fig. 2.14 (annual mean data) and Fig. 2.15 (monthly mean data). Results of the MK time series trend analysis are summarized in Table 2.3 and results of

linear regression analysis are summarized in Table 2.4. A comparison of trends in measured NH_3 concentrations with trends in NH_3 emissions for the different source types then provided indicative evidence to support and inform the national emission inventory compilation. In Fig. 2.16, the relative changes in UK emissions between 1998 and 2014 are compared with relative changes in mean measured NH_3 concentrations for all NAMN sites, and for grouped sites classified as dominated by cattle, pigs & poultry, and sheep.

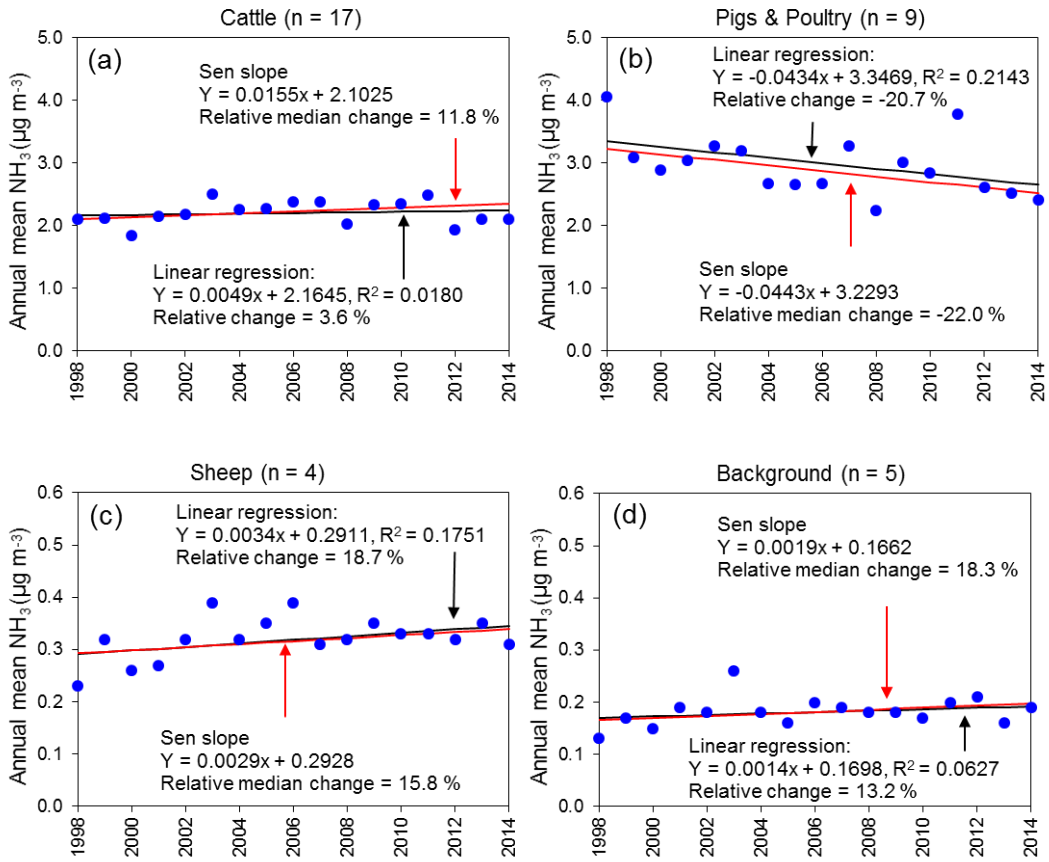

Figure 2.14. Time series trend analysis by non-parametric Mann–Kendall Sen slope vs. parametric linear regression on annually averaged NH_3 concentrations from the UK National Ammonia Monitoring Network (NAMN) for sites in 5 km grid squares classed as dominated by (a) cattle (> 45 % of total NH_3 emissions from this category in a grid square); (b) pigs & poultry (> 45 % of total NH_3 emissions from this category in a grid square); (c) sheep (> 45 % of total NH_3 emissions from sheep in a grid square); (d) NAMN sites in grid squares classed as background (defined as grid squares with average NH_3 emissions < 1 kg N ha^{-1} yr^{-1}). Individual data points are annually averaged NH_3 concentrations.

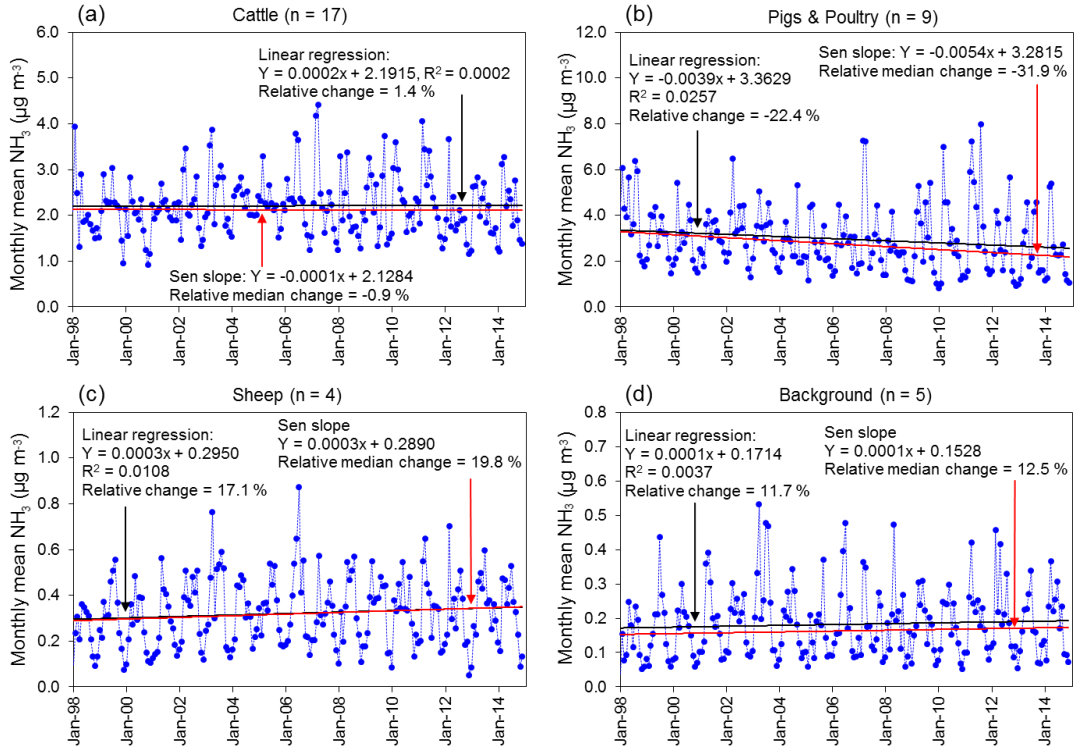

Figure 2.15. Time series trend analysis by non-parametric Mann–Kendall Sen slope vs. parametric least squares linear regression on annually averaged NH_3 concentrations from the UK National Ammonia Monitoring Network (NAMN) for sites in 5 km grid squares classed as dominated by (a) cattle (> 45 % of total NH_3 emissions from this category in a grid square); (b) pigs & poultry (> 45 % of total NH_3 emissions from this category in a grid square); (c) sheep (> 45 % of total NH_3 emissions from sheep in a grid square); (d) NAMN sites in grid squares classed as background (defined as grid squares with average NH_3 emissions < 1 kg N ha^{-1} yr^{-1}). Individual data points are monthly mean NH_3 concentrations.

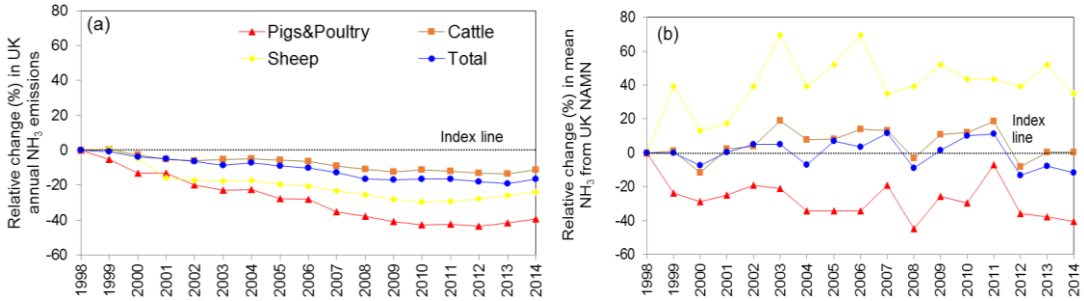

Figure 2.16. (a) Relative trends between 1998 and 2014 in NH_3 emissions from the UK National Atmospheric Emission Inventory (NAEI) for total emissions (all NH_3 sources) and emissions from cattle, pigs & poultry, and sheep separately (data from http://naei.defra.gov.uk/ and Misselbrook et al., 2015). (b) Relative trends between 1998 and 2014 in measured annual mean NH_3 concentrations (µg NH_3 m^{-3}) for all UK National Ammonia Monitoring Network (NAMN) sites, and for grouped sites classified as dominated by cattle, pigs & poultry, and sheep. Both figures are plotted with the same scale to allow direct comparison of the relative magnitudes in trends.

Table 2.3. Summary of Mann–Kendall (MK) and seasonal Mann–Kendall (SMK) time series trend analysis on grouped NH_3 concentration data (annually averaged and monthly mean data) from the UK National Ammonia Monitoring Network (NAMN) for four different emission source sectors. The following are shown: the p-value, median annual trend (Sen slope, in µg NH_3 yr^{-1}) and the relative median change over the selected time period (in %). For the MK tests, the 95 % confidence interval (CI) for the trend and relative change are also estimated.

Source sector	Time series (1998-2014)	[a]Number of sites	*p-value*	Significant trend (p<0.05)	[b]Median annual trend & [95% CI] (µg NH_3 y^{-1})	[c]Relative median change over the period & [95% CI] (%)
Cattle	Annual (MK)	17	0.46	no	0.0155 [-0.0150, 0.0300]	12 [-10, 24]
Cattle	Monthly (MK)	17	0.90	no	-0.0012 [-0.0192, 0.0168]	-0.9 [-14, 13]
Cattle	Monthly (SMK)	17	0.51	no	0.0043	3.9
Pigs&Poultry	Annual (MK)	9	0.02	yes	-0.0043 [-0.1008,-0.0071]	-22 [-42, -3.9]
Pigs&Poultry	Monthly (MK)	9	< 0.001	yes	-0.0648 [-0.0984,-0.0300]	-32 [-46, -16]
Pigs&Poultry	Monthly (SMK)	9	< 0.001	yes	-0.0588	-11
Sheep	Annual (MK)	4	0.17	no	0.0029 [0.0000, 0.0069]	16 [0.0, 46]
Sheep	Monthly (MK)	4	0.10	no	0.0036 [0.0000, 0.0072]	20 [0.0, 45]
Sheep	Monthly (SMK)	4	< 0.01	yes	0.0033	210
Background	Annual (MK)	5	0.20	no	0.0019 [-0.0012, 0.0038]	18 [-10, 41]
Background	Monthly (MK)	5	0.23	no	0.0012 [-0.0012, 0.0036]	13 [-11, 42]
Background	Monthly (SMK)	5	0.05	yes	0.0012	49

[a]Number of sites providing complete data runs over the period 1998 to 2014.
[b]Median annual trend = fitted Sen's slope of Mann-Kendall linear trend (unit = µg NH_3 y^{-1})
[c]Relative median change calculated based on the annual NH_3 concentration at the start (y_0) and at the end (y_i) of time series computed from the Sen's slope and intercept (=100[(y_i-y_0) /y_0]).*

Cattle sites: Bickerton Hill (UKA00297), Brown Moss (UKA00369), Castle Cary (UKA00328), Cwmystwyth (UKA00325), Fenn's Moss (UKA00291), High Muffles (UKA00169), Hillsborough (UKA00293), Little Budworth (UKA00298), Llynclys Common (UKA00270), Lough Navar (UKA00166), Myerscough (UKA00356), Northallerton (UKA00316), North Wyke (UKA00269), Penallt (UKA00324), Wardlow Hay Cop (UKA00119), Wem Moss (UKA00299), Yarner Wood (UKA00168).

Pig & Poultry sites: Bedlingfield (UKA00334), Dennington (UKA00331), Dunwich Heath (UKA00308), Fressingfield (UKA00335), Mere Sands Wood (UKA00280), Redgrave + Lopham (UKA00311), Sibton (UKA00012), Stoke Ferry (UKA00317), Stanford (UKA00476).

Sheep sites: Glensaugh (UKA00348; 2005 classification = background, but 1km radius is predominantly sheep from local landuse information), Moorhouse (UKA00357) and Sourhope (UKA00347) (2015 classification = cattle, but 1km radius around site is sheep from local landuse information), (Shetland UKA00486).

Background sites: Allt a Mharcaidh (UKA00086), Dumfries (UKA00368), Eskdalemuir (UKA00130), Inverpolly (UKA00457), Strathvaich (UKA00162).

Table 2.4. Summary of linear regression time series trend analysis on grouped NH_3 concentration data (annually averaged data and also monthly mean data) from the UK National Ammonia Monitoring Network (NAMN) for four different emission source sectors. The following are shown: the *p*-value, annual trend (fitted slope, in µg NH_3 yr^{-1}), R^2, and the relative change over the selected time period (in %).

Source sector	Time series (1998-2014)	[a]Number of sites	*p-value*	Significant trend (p<0.05)	[b]Annual Trend (µg NH_3 y^{-1})	R^2	[b] Relative change over the period [%]
Cattle	annual	17	0.61	no	0.0049	0.0180	3.6
Cattle	monthly	17	0.84	no	0.0019	0.0002	1.4
Pigs&Poultry	annual	9	0.06	no	-0.0434	0.2143	-21
Pigs&Poultry	monthly	9	0.02	yes	-0.0466	0.0257	-22
Sheep	annual	4	0.09	no	0.0034	0.1751	19
Sheep	monthly	4	0.14	no	0.0032	0.0108	17
Background	annual	5	0.33	no	0.0014	0.0627	13
Background	monthly	5	0.39	no	0.0013	0.0037	12

[a]Number of sites providing complete data runs over the specified time period in analysis
[b]Annual trend = fitted slope of linear regression (unit = µg NH_3 y^{-1})
[c]Relative change calculated based on the estimated annual NH_3 concentration at the start (y_0) and at the end (y_i) of time series (=100[(y_i-y_0) /y_0]) computed from the slope and intercept (=100*[(y_i-y_0) /y_0]).*

Cattle sites: Bickerton Hill (UKA00297), Brown Moss (UKA00369), Castle Cary (UKA00328), Cwmystwyth (UKA00325), Fenn's Moss (UKA00291), High Muffles (UKA00169), Hillsborough (UKA00293), Little Budworth (UKA00298), Llynclys Common (UKA00270), Lough Navar (UKA00166), Myerscough (UKA00356), Northallerton (UKA00316), North Wyke (UKA00269), Penallt (UKA00324), Wardlow Hay Cop (UKA00119), Wem Moss (UKA00299), Yarner Wood (UKA00168).

Pig & Poultry sites: Bedlingfield (UKA00334), Dennington (UKA00331), Dunwich Heath (UKA00308), Fressingfield (UKA00335), Mere Sands Wood (UKA00280), Redgrave + Lopham (UKA00311), Sibton (UKA00012), Stoke Ferry (UKA00317), Stanford (UKA00476).

Sheep sites: Glensaugh (UKA00348; 2005 classification = background, but 1km radius is predominantly sheep from local landuse information), Moorhouse (UKA00357) and Sourhope (UKA00347) (2015 classification = cattle, but 1km radius around site is sheep from local landuse information), (Shetland UKA00486).

Background sites: Allt a Mharcaidh (UKA00086), Dumfries (UKA00368), Eskdalemuir (UKA00130), Inverpolly (UKA00457), Strathvaich (UKA00162).

For the 17 sites in cattle-dominated areas, there is an increasing, but non-significant trend. Overall, based on MK analysis of annual data, the relative change from 1998 to 2014 is a 12 % increase (Table 2.3, Fig. 2.14), compared with a smaller increase of 4 % from linear regression (Table 2.4, Fig. 2.14). With the monthly data, there is no discernible trend (−0.9 % (MK); 1.4 % (LR)). In the seasonal MK test on monthly data (% relative median change = 3.9 %), no monthly "seasons" are significant, with only January approaching significance at p = 0.07. The near-significant trend for January is likely to be due to unusually high NH_3 concentrations recorded in January at some sites

in the first few months of the time series, attributed to manure spreading activities taking place in the winter months when the ground was frozen (confirmed by local observations), in direct contravention of good farming practice.

Although the long-term trend in monitored NH_3 concentrations at sites classified as dominated by cattle emissions shows a non-discernible or small increasing trend (nonsignificant), the opposite is happening with UK cattle NH_3 emissions, which declined by an estimated 11 % over the same period (Fig. 2.16, Table 2.5). In principle, a signal (changes in atmospheric NH_3 concentrations) related to substantial livestock changes associated with the 2000 outbreak of foot and mouth disease might have been expected. However, this outbreak was actually rather localized in northwest England and southwest England, and was followed by substantial restocking from 2001 (Sutton et al., 2006) and there was no detectable signal of foot and mouth disease in the average for cattle-dominated areas.

By contrast, in pig- and poultry-dominated areas (nine sites) there is a decreasing trend with significant reduction in measured NH_3 concentrations between 1998 and 2014 (−22 % (MK), $p = 0.02$, Table 2.3; −21 % (LR), $p = 0.06$, Table 2.4) from analysis of annual data (Fig. 2.14). For the monthly data, the overall change based on linear regression is also a 22 % decrease ($p = 0.02$) (Table 2.4, Fig. 2.15), compared with a larger level of decrease based on MK analysis (−32 %, $p = 0.01$) (Table 2.3, Fig. 2.15). The SMK test also shows a significant decreasing trend (−11 %, overall $p < 0.001$), with 6 of the 12 monthly “seasons” showing significant trends (February, June, November, December: $p < 0.05$, October: $p < 0.01$, January: $p < 0.001$). A decrease in emissions from pig and poultry of 39 % between 1998 and 2014 (Fig. 2.16, Table 2.5) is therefore broadly supported, although not matched by a similar decrease in measured NH_3 concentrations.

For sheep-dominated sites (four sites), there is an increasing trend in NH_3 (MK: +16 %, p = 0.17, Table 2.3; LR: 20 %, p = 0.09, Table 2.4) between 1998 and 2014 in the annual data (Fig. 2.14). The monthly data also show a similar upward trend (Fig. 2.14) with relative change in concentrations of +19 % based on MK (p = 0.10) (Table 2.3) and +17 % based on LR (p = 0.14) (Table 2.4). The increasing trend at sheep sites is therefore in contrast to the estimated 24 % decrease in NH_3 emissions from this sector since 1998 (Fig. 2.16, Table 2.5). For the SMK test, no individual monthly "seasons" were significant, although three of the monthly "seasons" approached the significance level (April, December: p = 0.08, October: p = 0.09). Overall, the increasing trend from the SMK test is significant at $p < 0.01$. While the Sen trend slope from both MK and SMK tests were comparable, at 0.0036 and 0.0033 µg NH_3 yr^{-1}, respectively, the % relative median change results computed from them are very different (MK = 16 % *cf.* SMK = 210 %), because the intercepts of the fitted Sen trend slopes are different (MK = 0.289 µg NH_3 m^{-3} *cf*. SMK = −0.0267 µg NH_3 m^{-3}). Caution therefore needs to be exercised when interpreting the % relative change results, especially at sites with low NH_3 concentrations, which must be examined together with the fitted trends.

Table 2.5. Comparison of % change in estimated UK NH_3 emissions reported by the National Atmospheric Emission Inventory (NAEI) (data from: http://naei.defra.gov.uk/) with % change between 1998 and 2014 in annually averaged NH_3 concentration data from the UK National Ammonia Monitoring Network (NAMN) for all NAMN sites (dataset 1a) and for grouped sites in four different emission source sectors.

Comparison period: 1998 - 2014	All sites (dataset 1a: n = 59)	Cattle (n=17)	Pigs & Poultry (n=9)	Sheep (n=4)	Background (n=5)
UK NH_3 emissions: % change relative to 1998	-16	-11	-39	-24	no data
UK NAMN NH_3: % relative median change estimated from MK Sen's slope and intercept	-6.3 (see Table 2.1)	12 (see Table 2.3)	-22* (see Table 2.3)	15 (see Table 2.3)	17 (see Table 2.3)
UK NAMN NH_3: % relative change estimated from linear regression slope and intercept	-3.1 (see Table 2.2)	3.6 (see Table 2.4)	-21$^{\Delta}$ (see Table 2.4)	19 (see Table 2.4)	13 (see table 2.4)

Significance: *p < 0.05, **p <0.01, ***p<0.001, $^{\Delta}$p = 0.06.

At background sites (five sites where total NH_3 emissions for the respective 5 km grid squares are estimated at < 1 kg N ha^{-1} yr^{-1}), NH_3 concentrations also appear to have increased (non-significant). Based on the MK analysis for the period 1998 to 2014, NH_3 concentrations increased overall by 18 and 13 % from the analysis of annual and monthly data, respectively (Table 2.3). Results from linear regression were similar, with an overall increase of 13 and 12 % from analysis of the annual and monthly data, respectively (Table 2.4). Similar to sheep sites, the % relative median change estimated from the seasonal MK Sen slope and intercept (+49 %) is larger than from the classic MK Sen slope (+13 %) due to differences in the intercepts of the fitted trend lines (MK = 0.1528 µg NH_3 m^{-3} *cf*. SMK = 0.0388 µg NH_3 m^{-3}) since the trend slopes are the same (0.0012 µg NH_3 yr^{-1}). Overall, the SMK test shows a significant increasing trend in the monthly data (p = 0.05). No individual monthly "seasons" were significant, with March, April and November monthly "seasons" approaching the significance level (p = 0.09).

As with the annual UK-wide long-term datasets (Sect. 2.4.5), it is useful to consider the significance of the NH_3 trends for the groupings of sites according to dominant emission source sectors. Tables 2.3 and 2.4 show that neither the annual nor the monthly time series showed a significant change in NH_3 concentrations for the cattle dominated sites. In the case of pig- and poultry-dominated sites, the decrease in measured NH_3 concentrations was significant for both the annual and monthly datasets. For sheep-dominated and backgrounds sites, the estimated increase in NH_3 concentrations was not significant based on the MK and linear regression tests on the annual and monthly data, but was significant based on the SMK test of the monthly data. Overall, these statistics confirm significant differences between NH_3 trends for sites dominated by different source types, with concentrations decreasing at pig- and poultry-dominated sites, concentrations increasing at sheep-dominated and background sites, and no significant trend at cattle-dominated sites (Table 2.5).

2.4.5.6 Changing chemical climate and effects on long-term trends in NH_3 and NH_4^+

Other pollutants that affect NH_3 concentrations in the atmosphere include SO_2 and NO_x emissions, which determine rates of secondary inorganic aerosol formation and therefore the lifetime of NH_3 in the atmosphere. UK emissions of SO_2 are estimated to have declined significantly by 81 % from 1.6 million tonnes in 1998 to 0.3 million tonnes in 2014 (Defra, 2015). Similarly, NO_x emissions over the same period are estimated to have fallen by 50 % from 2 million tonnes to 1 million tonnes (Defra, 2015). The reaction of NH_3 with H_2SO_4 to form $(NH_4)_2SO_4$ is effectively irreversible (in the absence of in-cloud reprocessing), whereas an equilibrium exists between gaseous NH_3 and particulate NH_4NO_3 and NH_4Cl components which are appreciably volatile at ambient temperatures. A change in the particulate phase from $(NH_4)_2SO_4$ to NH_4NO_3 suggests that NH_3 will remain longer in the atmosphere, since NH_4NO_3 is volatile and releases NH_3 in warm weather.

Elsewhere, a mismatch between reported trends in emissions and measurement data have similarly been investigated. The question of the "Ammonia Gap" in the Netherlands was debated over a number of years. There, the estimated reduction in emissions due to mitigation measures was not matched by expected decreases in measured NH_3 concentrations in air and/or NH_4^+ in precipitation (Erisman et al., 2001; Bleeker et al., 2009; van Zanten et al., 2017). Similarly in Hungary, monitored NH_3 concentrations from long-term measurements did not match the estimated reduction in NH_3 emissions following the decline in agricultural livestock population and fertilizer usage after political changes in 1989 (Horvath and Sutton, 1998). This was subsequently attributed to a reduction in SO_2 emissions over the same period, increasing the atmospheric lifetime of NH_3 (Horvath et al., 2009).

Dry deposition of SO_2 and NH_3 are enhanced in the presence of both gases, an interaction referred to as "co-deposition" (Fowler et al., 2001). The acid-base neutralization by each of the gases provides an efficient sink for dry deposition on leaf surfaces, and deposition enhancement for each gas

depends on the relative air concentrations of NH_3 and SO_2. For SO_2, the dry deposition process has been shown to be strongly influenced by ambient concentrations of NH_3 because the surface resistance is regulated mainly by uptake in moisture on foliar surfaces, which, in turn, is strongly influenced by the presence of NH_3. The large reduction in SO_2 emissions and ambient concentrations, compared with the relative stagnation in NH_3 emissions and concentrations over the same period, has meant that the SO_2 / NH_3 ratio has decreased dramatically. This has led to a systematic decrease in canopy resistance to uptake of SO_2 on surfaces, increasing dry deposition of SO_2 in the UK (ROTAP 2012). The underlying cause of the decrease in surface resistance is that the ambient NH_3 is sufficient to neutralize acidity from the solution and oxidation of deposited SO_2, maintaining large rates of deposition.

Similar interactions are seen to be occurring in the UK based on the NAMN data, where the concurrent reduction in SO_2 and NO_x emissions over the same period (Figure 2.18b) should theoretically lead to a longer atmospheric lifetime of NH_3, thereby increasing NH_3 concentrations in the UK, especially in remote areas. The interpretation of the NH_3 and NH_4^+ measurement data can further be aided by comparison with particulate nitrate (NO_3^-) and sulfate (SO_4^{2-}) data from the UK AGANet that are made concurrently with the NAMN NH_3 and NH_4^+ measurements at 30 sites (see Sect. 2.3.2). There is close agreement between the aerosol components, with a near 1:1 relationship between NH_4^+ and the sum of NO_3^- and SO_4^{2-}, lending support that particulate NH_4^+ in the UK is mainly derived from NH_3 and acidic gases such as SO_2 and NO_x to form $(NH_4)_2SO_4$ and NH_4NO_3, respectively (Conolly et al., 2016). For particulate NH_4^+, it has already been shown in Sect. 2.4.3 that this regional species has less of a relationship to the dominant NH_3 source sectors; trend analysis was therefore undertaken using all NH_4^+ site data combined. As with the NH_3 time series analysis, sites with incomplete data runs for particulate NH_4^+ due to reduced density of NH_4^+ measurements and site changes occurring from the period 2001–2006 were excluded (see Sect. 2.3.2.1).

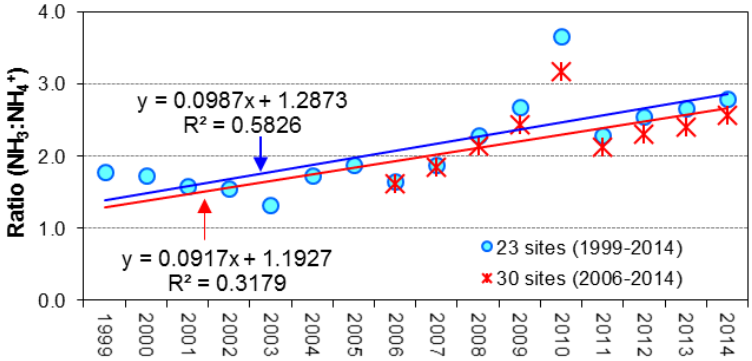

Figure 2.17. Long-term trends in ratio of NH_3:NH_4^+, indicating an increase in this ratio with time. The comparisons shown is for datasets i) 23 sites with complete NH_4^+ time series from 1999 to 2014, and ii) 30 sites with complete NH_4^+ time series from 2006 to 2014.

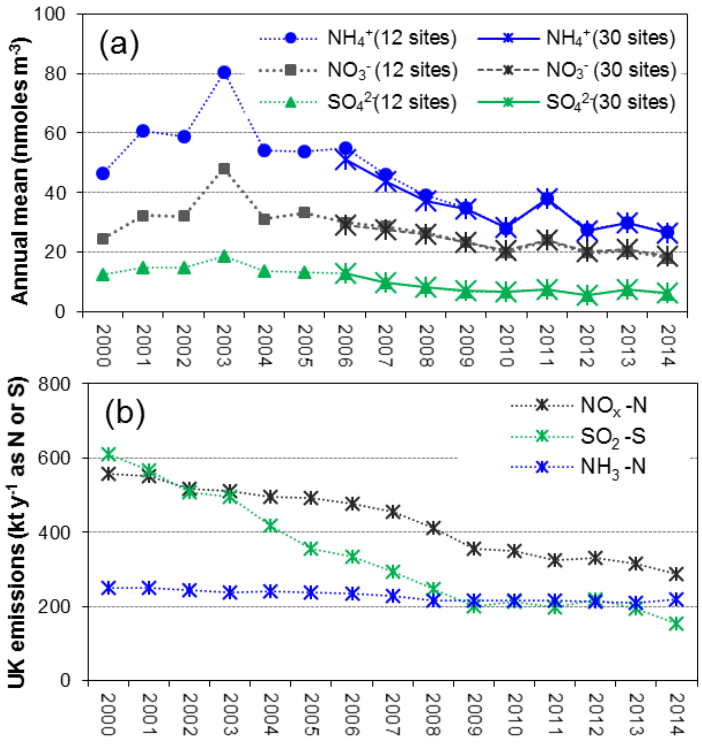

Figure 2.18. (a) Long-term trends in particulate NH_4^+ from the UK National Ammonia Monitoring Network (NAMN) compared with particulate NO_3^- and SO_4^{2-} concentrations from the UK Acid Gases and Aerosols Monitoring Network (AGANet; Conolly et al., 2016) measured at the same time. Each data point represents the averaged monthly measurements from all AGANet sites (increased from 12 to 30 sites since January 2006) and also the original l2 AGANet sites in the network (1999 data were excluded as measurements started in September 1999). (b) Trends in total UK emissions of NH_3, NO_x and SO_2 over the same period (2000–2014). Data from the National Atmospheric Emission Inventory (NAEI, http://naei.defra.gov.uk/).

Table 2.6. Comparison of % change in UK NH_3, SO_2 and NO_x emissions reported by the National Atmospheric Emission Inventory (NAEI) (data from: http://naei.defra.gov.uk/) with % change in annually averaged NH_4^+ and NH_3 concentration data from the UK National Ammonia Monitoring Network (NAMN) for sites with complete data runs of both NH_4^+ and NH_3 over the specified time periods.

	NH_4^+ (23 sites) (1999-2014)	NH_3 (23 sites) (1999-2014)	NH_4^+ (30 sites) (2006-2014)	NH_3 (30 sites) (2006-2014)
UK emissions: % change over the time period	-16 (NH_3), -75 (SO_2), -53 (NO_x)		-7 (NH_3), -54 (SO_2), -39 (NO_x)	
UK NAMN: % relative median change estimated from MK Sen's slope and intercept	-47**	3.0	-44**	-17
UK NAMN: % relative change estimated from linear regression slope and intercept	-49**	3.0	-43**	-18^{Δ}

Significance: *$p < 0.05$, **p <0.01, ***p<0.001, $^{\Delta}p = 0.06$.

Table 2.7. Comparison of % change in UK NH_3, SO_2 and NO_x emissions reported by the National Atmospheric Emission Inventory (NAEI) (data from: http://naei.defra.gov.uk/) with % change in annually averaged NH_4^+ concentration data from the UK National Ammonia Monitoring Network (NAMN) and SO_4^{2-} and NO_3^- concentration data from the UK Acid Gases and Aerosols Monitoring Network (AGANet) for sites with complete concurrent data runs over the specified time periods.

	NH_4^+ (12 sites) (2000-2014)	$SO4^{2-}$ (12 sites) (2000-2014)	NO_3^- (12 sites) (2000-2014)	NH_4^+ (30 sites) (2006-2014)	$SO4^{2-}$ (30 sites) (2006-2014)	NO_3^- (30 sites) (2006-2014)
UK emissions: % change over the time period	-16 (NH_3)	-75 (SO_2)	-53 (NO_x)	-7 (NH_3)	-54 (SO_2)	-39 (NO_x)
UK NAMN: % relative median change estimated from MK Sen's slope and intercept	-56**	-63***	-46***	-44**	-45*	-35**
UK NAMN: % relative change estimated from linear regression slope and intercept	-58**	-65***	-45**	-43**	-46**	-33***

Significance: *$p < 0.05$, **p <0.01, ***p<0.001.

Two data series for NAMN NH_4^+ data were selected for analysis: (i) 23 sites with complete NH_4^+ time series from 1999 to 2014, and (ii) 30 sites with complete NH_4^+ time series from 2006 to 2014. Both time series show a large significant downward trend in NH_4^+ ($p < 0.01$) (Table 2.6, Supp. Fig. S2.4). Overall, MK and LR tests show a significant decrease in NH_4^+ concentrations by 47 and 49 %, respectively, between 1999 and 2014 and by 44 and 43 %, respectively, between 2006 and 2014 (Table 2.6, Supp. Fig. S2.5). By contrast, concurrent NH_3 data from the same sites over the same time periods showed a much smaller, non-significant downward trend between 2006 and 2014 (−17 %, MK; −18 %, LR), and no discernible trend between 1999 and 2014 (+3 %, MK and LR) (Table 2.6). This reduction in particulate NH_4^+ can be seen to be closely associated with parallel decreases in particulate SO_4^{2-} and NO_3^- concentrations from AGANet (Table 2.7, Figs. 2.18a, S2.6), which are themselves associated with reductions in SO_2 and NO_x emissions (Table 2.7, Fig. 2.18b).

The comparisons above therefore suggest that reductions in SO_2 and NO_x emissions over the period have led to a lower formation of particulate NH_4^+ in the atmosphere. Further evidence in support of this is indicated by plotting the ratio of NH_3 / NH_4^+ (Fig. 2.17), which has increased from 1.8 in 1999 to 2.8 in 2014. This demonstrates how a larger fraction of the reduced N is staying in the gas phase as NH_3, increasing its atmospheric residence time and maintaining NH_3 concentrations at a higher level than solely based on NH_3 emission trends. Although the overall changes in NH_3 concentrations in the UK dataset are small and in many cases not significant for particular data groupings, they are consistent with similar phenomena observed in Hungary, the Netherlands and Denmark (Horvath et al., 2009; Erisman et al., 2001; Sutton et al., 2003; Bleeker et al., 2009).

2.5 Conclusion

Spatial and temporal trends in NH_3 are found to be related to variability in emission source types across the UK and also to be influenced by changes in environmental conditions. Extensive spatial heterogeneity in NH_3 concentrations was observed, with lowest annual mean concentrations at remote sites (< 0.2 µg m^{-3}) and highest in the areas with intensive agriculture (up to 22 µg m^{-3}). NH_4^+ concentrations show less spatial variability (e.g. range of 0.14 to 1.8 µg m^{-3} annual mean in 2005) with a general decreasing gradient from the southeast to the northwest of the UK, due to both regional differences in NH_3 concentrations and import of particulate matter into southeast England from Europe.

Peak NH_3 concentrations are observed in summer at background sites (defined by 5 km grid average NH_3 emissions <1 kg N ha^{-1} y^{-1}) and in areas dominated by sheep farming, driven by increased volatilization of NH_3 in warmer summer temperatures. In areas where cattle, pig and poultry farming is dominant, the largest NH_3 concentrations are in spring and autumn, matching periods of manure application to fields. By contrast, peak concentrations of NH_4^+ aerosol occur in spring from long-range transboundary sources. The spatial and seasonal patterns established for sites influenced by different emission source sectors are important for providing a foundation to understanding NH_3 exchange processes, impacts and the UK NH_3 budget and to inform abatement strategies.

Official published estimates of UK NH_3 emissions are estimated to have declined by 16.3 % between 1998 and 2014. The long-term NH_3 concentration data from the UK NAMN suggests evidence of a smaller, but non-significant decreasing trend (–6.3 % (MK); –3.1 % (LR)), based on analysis of annually averaged data (n = 59) over the same period (Table 2.2). Analysis of annually averaged data for different groupings of the NAMN dataset for the time periods 1999-2014 (n = 66) and 2000-2014 (n = 75) also gave similar results. In each case, the level of reduction observed in the datasets (1999-2014: 0.0 % (MK)

vs –3.0 % (LR); 2000-2014: 0.0 % (MK) *vs* –2.8 % (LR)) is less than the 15.6 % and 13.1 % reduction in estimated UK NH_3 emissions over the periods 1999-2014 and 2000-2014, respectively (Table 2.2).

In areas with intensive pig and poultry farming, there is a significant downward trend in NH_3 concentrations from the analysis of annually averaged data (–22 % (MK), $p = 0.02$; –21 % (LR), $p = 0.06$) that is consistent with, but not as large as the decrease in estimated NH_3 emissions from this sector over the same period (–39 %) (Table 2.5). By contrast, in cattle-dominated areas, there is evidence of a small increasing, but non-significant trend in NH_3 concentrations (+12 % (MK); +3.6 % (LR): annually averaged data), despite the decline in NH_3 emissions from this sector since 1998 (–11%) (Table 2.5). At background and sheep dominated sites, NH_3 concentrations increased (non-significant) over the monitoring period (Table 2.5). These increases in NH_3 concentrations at background (+17 % (MK); +13 % (LR): annually averaged data) and sheep dominated sites (+15 % (MK); +19 % (LR): annually averaged data) are consistent with decreasing SO_2 emissions (and to a lesser extent NO_x emissions) associated with a change in the PM from $(NH_4)_2SO_4$ to NH_4NO_3, the latter being volatile and releasing NH_3 in warm weather.

Particulate NH_4^+ represents a secondary pollutant formed from NH_3 and oxidation products of acidic gases such as SO_2 and NO_x. As the emissions of these acidic gases have reduced over the past years, the ratio between NH_3 and NH_4^+ has increased from 1.8 to 2.8 between 1999 and 2014. These changes are consistent with observed decreases in particulate SO_4^{2-} and NO_3^- concentrations that are associated with decline in SO_2 and NO_x emissions over the same period. This effect appears to be of sufficient magnitude to explain the lack of overall decrease in NH_3 concentrations, where the decrease in NH_4^+ is larger than for NH_3 at corresponding sites. Overall, UK annual particulate NH_4^+ concentrations decreased by –47 % (MK) and –49 % (LR) for period 1999-2014, associated with a slower formation of particulate NH_4^+ in the atmosphere from gas-phase NH_3. The findings are consistent with a parallel

change in partitioning from particulate NH_4^+ to gaseous NH_3 as also detected in Hungary, the Netherlands and Denmark.

Until now, only a modest commitment has been agreed to reduce European NH_3 emissions. By contrast, SO_2 and NO_x emissions have decreased over Europe over the past decades, and are projected to decrease further under the revised Gothenburg Protocol and revised NECD. As a result, the importance of NH_3 relative to oxidised N and SO_2 emissions is expected to continue to increase over the next decades, playing a significant role in the formation of fine PM and contributing to ecosystem effects through N deposition. With longer atmospheric lifetimes of gaseous NH_3 and little commitment to reduce emissions, combined with climate warming effects tending to increase NH_3 emissions, there is a substantial risk that exceedance of the NH_3 critical levels may increase in the future, exacerbating the threat to the most sensitive semi-natural habitats. The growing relative importance of reduced nitrogen to total acidic and total nitrogen deposition indicates that future strategies to tackle acidification and eutrophication will need to include measures to abate emissions of NH_3.

Acknowledgements

This work was carried out with funding from the Department for Environment, Food and Rural Affairs (Defra) and the devolved administrations, and from supporting NERC UKCEH programmes. The assistance and contributions from the large network of NAMN and AGANet site operators, former NAMN network managers (Ben Miners, Antje Branding), the Centralised Analytical Chemistry Facility at Lancaster, and in particular Heather Carter, Darren Sleep and Philip Rowland, colleagues at UKCEH Edinburgh (Sarah Leeson, Matt Jones, Chris Andrews, Margaret Anderson, David Leaver), colleagues at RIVM who operate Zegfeld station and Ricardo Energy and Environment (Martin Davies, Tim Bevington, Ben Davies) are also gratefully acknowledged.

References

Adon, M., Yoboue, V., Galy-Lacaux, C., Liousse, C., Diop, B., Doumbia, E. T., Gardrat, E., Ndiaye, S. A., and Jarnot, C.: Measurements of NO_2, SO_2, NH_3, HNO_3 and O_3 in West African urban environments, Atmos. Environ., 135, 31–40, doi:10.1016/j.atmosenv.2016.03.050, 2016.

Asman, W. A. H., Sutton, M. A., and Schjorring, J. K.: Ammonia: emission, atmospheric transport and deposition, New Phytol., 139, 27–48, doi:10.1046/j.1469-8137.1998.00180.x, 1998.

AQEG: Linking Emission Inventories and Ambient Measurements, AIR QUALITY EXPERT GROUP report prepared for: Department for Environment, Food and Rural Affairs, Scottish Executive, Welsh Government, and Department of the Environment in Northern Ireland, available at: http://uk-air.defra.gov.uk (last access: 10 January 2017), 2015.

Bleeker, A., Sutton, M. A., Acherman, B., Alebic-Juretic, A., Aneja, V. P., Ellermann, T., Erisman, J. W., Fowler, D., Fagerli, H., Gauger, T., Harlen, K. S., Hole, L. R., Horvath, L., Mitosinkova, M., Smith, R. I., Tang, Y. S., and van Pul, A.: Linking Ammonia Emission Trends to Measured Concentrations and Deposition of Reduced Nitrogen at Different Scales, Atmospheric Ammonia: Detecting Emission Changes and Environmental Impacts, edited by: Sutton, M. A., Reis, S., and Baker, S. M. H., 123–180, 2009.

Brunekreef, B., Harrison, R. M., Künzli, N., Querol, X., Sutton, M. A., Heederik, D. J. J., and Sigsgaard, T.: Reducing the health effect of particles from agriculture, The Lancet Respiratory Medicine, 3, 831–832, doi:10.1016/s2213- 2600(15)00413-0, 2015.

Colette, A., Aas, W., Banin, L., Braban, C. F., Ferm, M., Ortiz, A., Ilyin, I., Mar, K., Pandolfi, M., Putaud, J. P., and Shatalov, V.: Air pollution trends in the EMEP region between 1990 and 2012, Joint Report of the EMEP Task Force on Measurements and Modelling (TFMM), Chemical Co-ordinating Centre (CCC), Meteorological Synthesizing Centre-East (MSC-E), Meteorological Synthesizing Centre-West (MSC-W), EMEP/CCC-Report 1/2016, 2016.

Cape, J. N., van der Eerden, L. J., Sheppard, L. J., Leith, I. D., and Sutton, M. A.: Evidence for changing the critical level for ammonia, Environ. Poll., 157, 1033–1037, doi:10.1016/j.envpol.2008.09.049, 2009a.

Cape, J. N., van der Eerden, L. J., Sheppard, L. J., Leith, I. D., and Sutton, M. A.: Reassessment of Critical Levels for Atmospheric Ammonia, Atmospheric Ammonia, edited by: Sutton, M.A., Reis, S., and Baker, S.M. H., 15–40, 2009b.

Conolly, C., Davies, M., Knight, D., Vincent, K., Sanocka, A., Lingard, J., Richie, S., Donovan, B., Collings, A., Braban, C., Tang, Y. S., Stephens, A., Twigg, M., Jones, M., Simmons, I., Coyle, C., Kentisbeer, J., Leeson, S., van Dijk, N., Nemitz, E., Langford, B., Bealey, W., Leaver, D., Poskitt, J., Carter, H., Thacker, S., Patel, M., Keenan, P., Pereira, G., Lawlor, A., Warwick, A., Farrand, P., and Sutton, M. A.: UK Eutrophying and Acidifying Atmospheric Pollutants (UKEAP) Annual Report 2015, 2016. Defra: Defra National Statistics Release: Emissions of air pollutants in the UK, 1970 to 2014, Statistical release: 17 December 2015, 2015.

den Bril, B. V., Meremans, D., and Roekens, E.: A Monitoring Network on Acidification in Flanders, Belgium, Scientific World J., 11, 2358–2363, doi:10.1100/2011/897308, 2011.

Dore, A. J., Vieno, M., Tang, Y. S., Dragosits, U., Dosio, A., Weston, K. J., and Sutton, M. A.: Modelling the atmospheric transport and deposition of sulphur and nitrogen over the United Kingdom and assessment of the influence of SO_2 emissions from international shipping, Atmos. Environ., 41, 2355–2367, doi:10.1016/j.atmosenv.2006.11.013, 2007.

Dore, A. J., Theobald, M. R., Kryza, M., Vieno, M., Tang, S. Y., and Sutton, M. A.: Modelling the deposition of reduced nitrogen at different scales in the United Kingdom, in: Air Pollution Modelling and Its Application XIXXIX, edited by: Borrego, C., and Miranda, A. I., Nato Science for Peace and Security Series C, Environmental Security, 127–135, 2008.

Dore, A. J., Carslaw, D. C., Braban, C., Cain, M., Chemel, C., Conolly, C., Derwent, R. G., Griffiths, S. J., Hall, J., Hayman, G., Lawrence, S., Metcalfe, S. E., Redington, A., Simpson, D., Sutton, M. A., Sutton, P., Tang, Y. S., Vieno, M., Werner, M., and Whyatt, J. D.: Evaluation of the performance of different atmospheric chemical transport models and inter-comparison of nitrogen and sulphur deposition estimates for the UK, Atmos. Environ., 119, 131–143, doi:10.1016/j.atmosenv2015.08.008, 2015.

Dragosits, U. and Sutton, M. A.: Maps of Ammonia emissions from agriculture, waste, nature and other miscellaneous sources for the NAEI 2003, Report to AEAT/DEFRA, 2005.

Dragosits, U., Sutton, M. A., Place, C. J., and Bayley, A. A.: Modelling the spatial distribution of agricultural ammonia emissions in the UK, Nitrogen, the Confer-N-S, edited by: VanderHoek, K. W., Erisman, J. W., Smeulders, S., Wisniewski, J. R., and Wisniewski, J., 195–203, 1998.

Dragosits, U., Theobald, M. R., Place, C. J., Lord, E., Webb, J., Hill, J., ApSimon, H. M., and Sutton, M. A.: Ammonia emission, deposition and impact assessment at the field scale: a case study of sub-grid spatial variability, Environ. Poll., 117, 147–158, doi:10.1016/s0269-7491(01) 00147-6, 2002.

Erisman, J. W., Mosquera, J., and Hensen, A.: Two options to explain the ammonia gap in The Netherlands, Environ. Sci. Policy, 4, 97–105, doi:10.1016/S1462-9011(00)00115-5, 2001.

EEA: European Union emission inventory report 1990–2014 under the UNECE Convention on Long-range Transboundary Air Pollution (LRTAP) European Environment Agency Report No 16/2016, doi:10.2800/628267, 2016.

EU: Directive (EU) 2016/2284 of the European Parliament and of the Council of 14 December 2016 on the reduction of national emissions of certain atmospheric pollutants, amending Directive 2003/35/EC and repealing Directive 2001/81/EC, 2016.

Eurostat: Agriculture, forestry and fishery statistics, Publications Office of the European Union, Luxembourg, 2016.

Flechard, C. R., Massad, R. S., Loubet, B., Personne, E., Simpson, D., Bash, J. O., Cooter, E. J., Nemitz, E., and Sutton, M. A.: Advances in understanding, models

and parameterizations of biosphere-atmosphere ammonia exchange, Biogeosciences, 10, 5183–5225, doi:10.5194/bg-10-5183-2013, 2013.

Fournier, N., Pais, V.A., Sutton, M. A., Weston, K. J., Dragosits, U., Tang, S. Y., and Aherne, J.: Parallelisation and application of a multi-layer atmospheric transport model to quantify dispersion and deposition of ammonia over the British Isles, Environ. Poll., 116, 95–107, doi:10.1016/s0269- 7491(01)00146-4, 2002.

Fournier, N., Tang, Y. S., Dragosits, U., De Kluizenaar, Y., and Sutton, M. A.: Regional atmospheric budgets of reduced nitrogen over the British Isles assessed using a multi-layer atmospheric transport model, Water Air Soil Poll., 162, 331–351, doi:10.1007/s11270-005-7249-0, 2005.

Fowler, D., Sutton, M. A., Smith, R. I., Pitcairn, C. E. R., Coyle, M., Campbell, G., and Stedman, J.: Regional mass budgets of oxidized and reduced nitrogen and their relative contribution to the nitrogen inputs of sensitive ecosystems, Nitrogen, the ConferN-S, edited by: VanderHoek, K. W., Erisman, J. W., Smeulders, S., Wisniewski, J. R., and Wisniewski, J., 337–342, 1998.

Fowler, D., Sutton, M. A., Flechard, C., Cape, J. N., Storeton-West, R., Coyle, M., and Smith, R. I.: The control of SO_2 dry deposition on to natural surfaces by NH_3 and its effects on regional deposition, WASP., 1, 39–48, 2001.

Fowler, D., Pilegaard, K., Sutton, M. A., Ambus, P., Raivonen, M., Duyzer, J., Simpson, D., Fagerli, H., Fuzzi, S., Schjoerring, J. K., Granier, C., Neftel, A., Isaksen, I. S. A., Laj, P., Maione, M., Monks, P. S., Burkhardt, J., Daemmgen, U., Neirynck, J., Personne, E., Wichink-Kruit, R., Butterbach-Bahl, K., Flechard, C., Tuovinen, J. P., Coyle, M., Gerosa, G., Loubet, B., Altimir, N., Gruenhage, L., Ammann, C., Cieslik, S., Paoletti, E., Mikkelsen, T.N., Ro-Poulsen, H., Cellier, P., Cape, J. N., Horváth, L., Loreto, F., Niinemets, Ü., Palmer, P. I., Rinne, J., Misztal, P., Nemitz, E., Nilsson, D., Pryor, S., Gallagher, M. W., Vesala, T., Skiba, U., Brüggemann, N., Zechmeister-Boltenstern, S., Williams, J., O'Dowd, C., Facchini, M. C., de Leeuw, G., Flossman, A., Chaumerliac, N., and Erisman, J. W.: Atmospheric composition change: Ecosystems–Atmosphere interactions, Atmos. Environ., 43, 5193–5267, doi:10.1016/j.atmosenv.2009.07.068, 2009.

Fowler, D., Dise, N., and Sheppard, L.: Committee on air pollution effects research: 40 years of UK air pollution, Environ. Poll., 208, 876–878, doi:10.1016/j.envpol.2015.09.014, 2016.

Gilbert, R. O.: Statistical methods for environmental pollution monitoring, New York, John Wiley & Sons, 1987.

Hallsworth, S., Dore, A.J., Bealey, W.I., Dragosits, U., Vieno, M., Hellsten, S., Tang, Y.S., and Sutton, M.A.: The role of indicator choice in quantifying the threat of atmospheric ammonia to the "Natura 2000" network, Environ. Sci. Policy, 13, 671–687, doi:10.1016/j.envsci.2010.09.010, 2010.

Hellsten, S., Dragosits, U., Place, C. J., Misselbrook, T. H., Tang, Y. S., and Sutton, M. A.: Modelling Seasonal Dynamics from Temporal Variation in Agricultural Practices in the UK Ammonia Emission Inventory, Water Air Soil Poll., 7, 3–13, doi:10.1007/s11267-006-9087-5, 2007.

Hellsten, S., Dragosits, U., Place, C. J., Vieno, M., Dore, A. J., Misselbrook, T. H., Tang, Y. S., and Sutton, M.A.: Modelling the spatial distribution of ammonia emissions in the UK, Environ. Poll., 154, 370–379, doi:10.1016/j.envpol .2008.02.017, 2008.

Hirsch, R. M., and Slack, J. R.: A Nonparametric Trend Test for Seasonal Data With Serial Dependence, Water Resour. Res., 20, 727–732, doi:10.1029/WR020i006p00727, 1984.

Horvath, L. and Sutton, M. A.: Long-term record of ammonia and ammonium concentrations at K-Puszta, Hungary, Atmos. Environ., 32, 339–344, doi:10.1016/s1352- 2310(97)00046-0, 1998.

Horvath, L., Fagerli, H., and Sutton, M. A.: Long-Term Record (1981–2005) of Ammonia and Ammonium Concentrations at K-Puszta Hungary and the Effect of Sulphur Dioxide Emission Change on Measured and Modelled Concentrations, Atmospheric Ammonia, edited by: Sutton, M. A., Reis, S., and Baker, S. M. H., 181–185, 2009.

Kim, K.-H., Kabir, E., and Kabir, S.: A review on the human health impact of airborne particulate matter, Environ. Int., 74, 136–143, doi:10.1016/j.envint.2014.10.005, 2015.

Lolkema, D. E., Noordijk, H., Stolk, A. P., Hoogerbrugge, R., van Zanten, M. C., and van Pul, W. A. J.: The measuring ammonia in nature (MAN) network in the Netherlands, Biogeosciences, 12, 5133–5142, doi:10.5194/bg-12-5133-2015, 2015.

Massad, R. S., Nemitz, E., and Sutton, M. A.: Review and parameterisation of bi-directional ammonia exchange between vegetation and the atmosphere, Atmos. Chem. Phys., 10, 10359–10386, doi:10.5194/acp-10-10359-2010, 2010.

Met Office: UK Daily Temperature and rainfall Data, Part of the Met Office Integrated Data Archive System (MIDAS), NCAS British Atmospheric Data Centre, 15/12/16, 2016.

McLeod, A. I.: Package “Kendall”, version 2.2, Kendall rank correlation and Mann-Kendall trend test, https://cran.r-project. org/web/packages/Kendall/ Kendall.pdf (last access: 17 February 2017), 2015.

Misselbrook, T. H., Gilhespy, S. L., Cardenas, L. M., Williams, J., and Dragosits, U.: Inventory of Ammonia Emissions from UK Agriculture – 2014. DEFRA Contract SCF0102, 2015.

Pitcairn, C. E. R., Leith, I. D., Sheppard, L. J., Sutton, M. A., Fowler, D., Munro, R. C., Tang, S., and Wilson, D.: The relationship between nitrogen deposition, species composition and foliar nitrogen concentrations in woodland flora in the vicinity of livestock farms, Environ. Poll., 102, 41–48, doi:10.1016/s0269-7491(98)80013-4, 1998.

Pohlert, T.: Package “Trend”, version 0.2.0: Non-Parametric Trend Tests and Change-Point Detection, https://cran.r-project.org/ web/packages/trend/ trend.pdf (last access: 17 February 2017), 2016.

Pope, R. J., Butt, E. W., Chipperfield, M. P., Doherty, R. M., Fenech, S., Schmidt, A., Arnold, S. R., and Savage, N. H.: The impact of synoptic weather on UK surface ozone and implications for premature mortality, Environ. Res. Lett., 11, 1–10, doi:10.1088/1748-9326/11/12/124004, 2016.

Puchalski, M. A., Sather, M. E., Walker, J. T., Lehmann, C. M. B., Gay, D. A., Mathew, J., and Robarge, W. P.: Passive ammonia monitoring in the United States: Comparing three different sampling devices, J. Environ. Monitor., 13, 3156–3167, doi:10.1039/c1em10553a, 2011.

Putaud, J. P., Van Dingenen, R., Alastuey, A., Bauer, H., Birmili, W., Cyrys, J., Flentje, H., Fuzzi, S., Gehrig, R., Hansson, H. C. and Harrison, R. M.: A European aerosol phenomenology–3: Physical and chemical characteristics of particulate matter from 60 rural, urban, and kerbside sites across Europe, Atmos. Environ., 44, 1308–1320, doi:10.1016 /j.atmosenv.2009.12.011, 2010.

Reis, S., Grennfelt, P., Klimont, Z., Amann, M., ApSimon, H., Hettelingh, J.-P., Holland, M., LeGall, A.-C., Maas, R., Posch, M., Spranger, T., Sutton, M. A., and Williams, M.: From Acid Rain to Climate Change, Science, 338, 1153–1154, doi:10.1126/science.1226514, 2012.

Riddick, S. N., Blackall, T. D., Dragosits, U., Daunt, F., Braban, C. F., Tang, Y. S., MacFarlane, W., Taylor, S., Wanless, S., and Sutton, M. A.: Measurement of ammonia emissions from tropical seabird colonies, Atmos. Environ., 89, 35–42, doi:10.1016/j.atmosenv.2014.02.012, 2014.

Serrano, A., Mateos, V. L., and Garcia, J. A.: Trend analysis of monthly precipitation over the iberian peninsula for the period 1921–1995, Phys. Chem. Earth Pt. B, 24, 85–90, doi:10.1016/S1464-1909(98)00016-1, 1999.

Sheppard, L. J., Leith, I. D., Mizunuma, T., Cape, J. N., Crossley, A., Leeson, S., Sutton, M. A., Dijk, N., and Fowler, D.: Dry deposition of ammonia gas drives species change faster than wet deposition of ammonium ions: evidence from a longterm field manipulation, Glob. Change Biol., 17, 3589–3607, doi:10.1111/j.1365-2486.2011.02478.x, 2011.

Singles, R., Sutton, M. A., and Weston, K. J.: A multi-layer model to describe the atmospheric transport and deposition of ammonia in Great Britain, Atmos. Environ., 32, 393–399, doi:10.1016/s1352-2310(97)83467-x, 1998.

Smith, R. I., Fowler, D., Sutton, M. A., Flechard, C., and Coyle, M.: Regional estimation of pollutant gas dry deposition in the UK: model description, sensitivity analyses and outputs, Atmos. Environ., 34, 3757–3777, doi:10.1016/s1352-2310(99)00517-8, 2000.

Stelson, A. W. and Seinfeld, J. H.: Relative humidity and temperature dependence of the ammonium nitrate dissociation constant, Atmos. Environ., 16, 983–992, doi:10.1016/0004- 6981(82)90184-6, 1982.

Sutton, M. A. and Fowler, D.: Introduction: fluxes and impacts of atmospheric ammonia on national, landscape and farm scales, Environ. Poll., 119, 7–8, doi:10.1016/s0269- 7491(01)00145-2, 2002.

Sutton, M. A., Pitcairn, C. E. R., and Fowler, D.: The Exchange of Ammonia Between the Atmosphere and Plant Communities, Adv. Ecol. Res., 24, 301–393, doi:10.1016/S0065- 2504(08)60045-8, 1993.

Sutton, M. A., Fowler, D., Burkhardt, J. K., and Milford, C.: Vegetation atmosphere exchange of ammonia: Canopy cycling and the impacts of elevated nitrogen inputs, Water Air Soil Poll., 85, 2057–2063, doi:10.1007/bf01186137, 1995.

Sutton, M. A., Milford, C., Dragosits, U., Place, C. J., Singles, R. J., Smith, R. I., Pitcairn, C. E. R., Fowler, D., Hill, J., ApSimon, H. M., Ross, C., Hill, R., Jarvis, S. C., Pain, B. F., Phillips, V. C., Harrison, R., Moss, D., Webb, J., Espenhahn, S. E., Lee, D. S., Hornung, M., Ullyett, J., Bull, K. R., Emmett, B. A., Lowe, J., and Wyers, G. P.: Dispersion, deposition and impacts of atmospheric ammonia: quantifying

local budgets and spatial variability, Environ. Poll., 102, 349–361, doi:10.1016/s0269-7491(98)80054-7, 1998.

Sutton, M. A., Dragosits, U., Tang, Y. S., and Fowler, D.: Ammonia emissions from non-agricultural sources in the UK, Atmos. Environ., 34, 855–869, doi:10.1016/S1352- 2310(99)00362-3, 2000.

Sutton, M. A., Miners, B., Tang, Y. S., Milford, C., Wyers, G. P., Duyzer, J. H., and Fowler, D.: Comparison of low cost measurement techniques for long-term monitoring of atmospheric ammonia, J. Environ. Monitor., 3, 446–453, doi:10.1039/b102303a, 2001a.

Sutton, M. A., Tang, Y. S., Dragosits, U., Fournier, N., Dore, A.J., Smith, R. I., Weston, K. J., and Fowler, D.: A spatial analysis of atmospheric ammonia and ammonium in the UK, Scientific World J., 2, 275–286, 1 Supplement, doi:10.1100/tsw.2001.313, 2001b.

Sutton, M. A., Tang, Y. S., Miners, B., and Fowler, D.: A new diffusion denuder system for long-term, regional monitoring of atmospheric ammonia and ammonium, Water, Air and Soil Pollution, Focus, 1, Part 5/6, 145–156, doi:10.1023/A:1013138601753, 2001c.

Sutton, M. A., Asman, W. A. H., Ellermann, T., Van Jaarsveld, J. A., Acker, K., Aneja, V., Duyzer, J., Horvath, L., Paramonov, S., Mitosinkova, M., Tang, Y. S., Achermann, B., Gauger, T., Bartniki, J., Neftel, A., and Erisman, J. W.: Establishing the link between ammonia emission control and measurements of reduced nitrogen concentrations and deposition, Environ. Monit. Assess., 82, 149–185, doi:10.1023/a:1021834132138, 2003.

Sutton, M. A., Dragosits, U., Simmons, I., Tang, Y. S., Hellsten, S., Love, L., Vieno, M., Skiba, U., di Marco, C., Storeton-West, R. L., Fowler, D., Williams, J., North, P., Hobbs, P., and Misselbrook, T.: Monitoring and modelling trace-gas change's following the 2001 outbreak of Foot and Mouth Disease to reduce the uncertainties in agricultural emissions abatement, Environ. Sci. Policy, 9, 407–422, doi:10.1016/j.envsci .2006.04.001, 2006.

Sutton, M. A., Reis, S., Riddick, S. N., Dragosits, U., Nemitz, E., Theobald, M. R., Tang, Y. S., Braban, C. F., Vieno, M., Dore, A. J., Mitchell, R. F., Wanless, S., Daunt, F., Fowler, D., Blackall, T. D., Milford, C., Flechard, C. R., Loubet, B., Massad, R., Cellier, P., Personne, E., Coheur, P. F., Clarisse, L., Van Damme, M., Ngadi, Y., Clerbaux, C., Skjoth, C. A., Geels, C., Hertel, O., Kruit, R. J. W., Pinder, R. W., Bash, J. O., Walker, J. T., Simpson, D., Horvath, L., Misselbrook, T. H., Bleeker, A., Dentener, F., and de Vries, W.: Towards a climate-dependent paradigm of ammonia emission and deposition, Philos. T. R. Soc. B-Biological, 368, 1–13, doi:10.1098/rstb.2013.0166, 2013.

Tang, Y. S., Cape, J. N., and Sutton, M. A.: Development and types of passive samplers for monitoring atmospheric NO_2 and NH_3 concentrations, Scientific World J., 1, 513–529, doi:10.1100/tsw.2001.82, 2001a.

Tang, Y. S., Dragosits, U., Theobald, M. R., Fowler, D., and Sutton, M. A.: Sub-grid variability in ammonia concentrations and dry deposition in an upland landscape, in: Air surface exchange of gases and particles: Poster proceedings, edited by: Fowler, D., Pitcairn, C. E. R., Douglas, L., and Erisman, J. W., 48–57, 2001b.

Tang, Y. S. and Sutton, M. A.: Quality management in the UK national ammonia monitoring network, in: Proceedings of the International Conference: QA/QC in the

field of emission and air quality measurements: harmonization, standardization and accreditation, held in Prague, 21–23 May 2003, edited by: Borowiak, A., Hafkenscheid, T., Saunders, A., and Woods, P., European Commission, Ispra, Italy, 297–307, 2003.

Tang, Y. S., Cape, J. N., Braban, C. F., Twigg, M. M., Poskitt, J., Jones, M. R., Rowland, P., Bentley, P., Hockenhull, K., Woods, C., Leaver, D., Simmons, I., van Dijk, N., Nemitz, E., and Sutton, M. A.: Development of a new model DELTA sampler and assessment of potential sampling artefacts in the UKEAP AGANet DELTA system: summary and technical report, London, Defra, CEH Project no. C04544, C04845, 2015.

Tang, Y. S., Poskitt, J., Cape, J. N., Nemitz, E., Bealey,W. J., Leaver, D., Simmons, I., Wood, C., Pereira, G., Sutton, M. A., Davies, M., Conolly, C., Donovan, B., and Braban, C. F.: UK Eutrophying and Acidifying Atmospheric Pollutant project's National Ammonia Monitoring Network, NAMN, Data funded by Defra and the Devolved Administrations and published under the Open Government Licence v1.0, https://uk-air.defra.gov.uk/networks/ network-info?view=nh3, last access: 10 January 2017a.

Tang, Y. S., Poskitt, J., Cape, J. N., Nemitz, E., Bealey,W. J., Leaver, D., Beith, S., Thacker, S., Simmons, I., Letho, K., Wood, C., Pereira, G., Sutton, M. A., Davies, M., Conolly, C., Donovan, B., and Braban, C. F.: UK Eutrophying and Acidifying Atmospheric Pollutant project's Acid Gases and Aerosol Network, AGANet (Data funded by Defra and the Devolved Administrations and published under the Open Government Licence v1.0, https://uk-air.defra.gov.uk/networks/network-info?view=aganet), last access: 10 January 2017b.

Thijsse, T. R., Wyers, G. P., Duyzer, J. H., Verhagen, H. L. M., Wayers, A., and Mols, J. J.: Measurement of ammonia with diffusion tube samplers, Atmos. Environ., 32, 333–337, doi:10.1016/S1352-2310(97)00278-1, 1996.

Thöni, L., Brang, P., Braun, S., Seitler, E., and Rihm, B.: Ammonia Monitoring in Switzerland with Passive Samplers: Patterns, Determinants and Comparison with Modelled Concentrations, Environ. Monitor. Assess., 98, 93–107, doi:10.1023/B:EMAS.0000038181.99603.6e, 2004.

Tørseth, K., Aas, W., Breivik, K., Fjæraa, A. M., Fiebig, M., Hjellbrekke, A. G., Lund Myhre, C., Solberg, S., and Yttri, K. E.: Introduction to the European Monitoring and Evaluation Programme (EMEP) and observed atmospheric composition change during 1972–2009, Atmos. Chem. Phys., 12, 5447–5481, doi:10.5194/acp-12-5447-2012, 2012.

Tsagatakis, I., Brace, S., Jephcote, C., Passant, N., Pearson, B., Kiff, B., and Fraser, A.: UK Emission Mapping Methodology – A report of the National Atmospheric Emission Inventory 2014, Ricardo/ED59800104 – Issue Number 1, 2016.

UNECE: Edinburgh workshop on atmospheric ammonia: Detecting emission changes and environmental impacts (4–6 December 2006), Report by the organizers with the assistance of the secretariat. Report to: the Executive Body for the Convention on Long-Range Transboundary Air Pollution, the Working Group on Strategies and Review; the Working Group on Effects, the Steering Body to the Cooperative Programme for Monitoring and Evaluation of the Long-range Transmission of Air Pollutants in Europe (EMEP), 2007.

UNECE: Options for revising the Gothenburg Protocol, Reactive Nitrogen, Report by the Co-chairs of the Task Force on Reactive Nitrogen, Working Group on Strategies and Review, ECE/EB.AIR/WG.5/2010/4, Geneva, 2010.

Van Pul, A., Van Jaarsveld, H., Van Der Meulen, T., and Velders, G.: Ammonia concentrations in the Netherlands: Spatially detailed measurements and model calculations, Atmos. Environ., 38, 4045–4055, doi:10.1016/j.atmosenv.2004 .03.051, 2004.

van Zanten, M. C., Wichink Kruit, R. J., Hoogerbrugge, R., Van der Swaluw, E., and van Pul, W. A. J.: Trends in ammonia measurements in the Netherlands over the period 1993–2014, Atmos. Environ., 148, 352–360, doi:10.1016/j.atmosenv .2016.11.007, 2017.

Vieno, M., Dore, A. J., Wind, P., Marco, C. D., Nemitz, E., Phillips, G., Tarrasón, L., and Sutton, M. A.: Application of the EMEP Unified Model to the UK with a Horizontal Resolution of 5 × 5 km2 , in: Atmospheric Ammonia: Detecting emission changes and environmental impacts, edited by: Sutton, M.A., Reis, S., and Baker, S.M.H., Springer Netherlands, Dordrecht, 367–372, 2009.

Vieno, M., Heal, M. R., Hallsworth, S., Famulari, D., Doherty, R. M., Dore, A. J., Tang, Y. S., Braban, C. F., Leaver, D., Sutton, M. A., and Reis, S.: The role of long-range transport and domestic emissions in determining atmospheric secondary inorganic particle concentrations across the UK, Atmos. Chem. Phys., 14, 8435–8447, doi:10.5194/acp-14-8435-2014, 2014.

Vogt, E., Dragosits, U., Braban, C. F., Theobald, M. R., Dore, A. J., van Dijk, N., Tang, Y. S., McDonald, C., Murray, S., Rees, R. M., and Sutton, M. A.: Heterogeneity of atmospheric ammonia at the landscape scale and consequences for environmental impact assessment, Environ. Poll., 179, 120–131, doi:10.1016/ j.envpol.2013.04.014, 2013.

Webb, J. and Misselbrook, T. H.: A mass-flow model of ammonia emissions from UK livestock production, Atmos. Environ., 38, 2163–2176, doi:10.1016/j.atmosenv .2004.01.023, 2004.

Wichink, Kruit, R. J., Schaap, M., Sauter, F. J., van Zanten, M. C., and van Pul, W. A. J.: Modeling the distribution of ammonia across Europe including bi-directional surface–atmosphere exchange, Biogeosciences, 9, 5261–5277, doi:10.5194/bg-9-5261-2012, 2012.

Wyers, G. P., Otjes, R. P., and Slanina, J.: A continuous-flow denuder for the measurement of ambient concentrations and surface-exchange fluxes of ammonia, Atmos. Environ. Pt. A, 27, 2085–2090, doi:10.1016/0960-1686(93)90280-C, 1993.

Xu, W., Wu, Q., Liu, X., Tang, A., Dore, A. J., and Heal, M.R.: Characteristics of ammonia, acid gases, and $PM_{2.5}$ for three typical land-use types in the North China Plain, Environ. Sci. Poll. Res., 23, 1158–1172, doi:10.1007/s11356-015-5648- 3, 2016.

Chapter 3 Acid gases and aerosol measurements in the UK (1999 – 2015): regional distribution and trends

This chapter is based on the research paper published in *`Atmospheric Chemistry and Physics' (Tang, Y. S., Braban, C. F., Dragosits, U., Simmons, I., Leaver, D., van Dijk, N., Poskitt, J., Thacker, S., Patel, M., Carter, H., Pereira, M. G., Keenan, P. O., Lawlor, A., Connolly, C., Vincent, K., Heal, M. R. and Sutton, M. A.: Acid gases and aerosol measurements in the UK (1999–2015): regional distributions and trends. Atmos. Chem. Phys., 18 (22), 16293-16324, https://doi.org/10.5194/acp-18-16293-2018, 2018).*

Author contributions:

As network manager for the AGANet (1999 – 2016), I coordinated the establishment of the network and measurement with the support of a large network of local site operators (monthly exchange of air samples), chemical laboratories (Harwell Scientific (now Scientific Analysis Laboratories Ltd) 1999 – 2009 and UKCEH Lancaster from 2009), and UKCEH / Ricardo EE field teams (site and equipment maintenance). Mark Sutton conceived the AGANet and together we developed the acid gas and aerosol measurements with the DELTA®. Ulli Dragosits assisted with the DELTA® vs Annular Denuder System comparisons, network establishment and provided GIS advice. Ivan Simmons helped with building DELTA® systems and setting up sites when the network expanded from 12 to 30 sites and servicing equipment. David Leaver designed the CEH AAGA database for processing the AGANet data. Several of the authors contributed to measurements, network operations and equipment/site maintenance. Christine Braban is project coordinator for UKEAP, of which NAMN and AGANet are component networks. Keith Vincent provided support

in data submission to the UK-AIR website. I prepared network samples up to 2009, performed the data collection, data data analysis (including statistics) and wrote the manuscript,with input from all co-authors. Mark Sutton and Mat Heal provided valuable advice on the interpretation of results.and feedback on the manuscript.

3.1 Abstract

The UK Acid Gases and Aerosol Monitoring Network (AGANet) was established in 1999 (12 sites, increased to 30 sites from 2006), to provide long-term national monitoring of acid gases (HNO_3, SO_2, HCl) and aerosol components (NO_3^-, SO_4^{2-}, Cl^-, Na^+, Ca^{2+}, Mg^{2+}). An extension of a low-cost denuder-filter pack system (DELTA) that is used to measure NH_3 and NH_4^+ in the UK National Ammonia Monitoring Network (NAMN) provides additional monthly speciated measurements for the AGANet. A comparison of the monthly DELTA measurement with averaged daily results from an annular denuder system showed close agreement, while the sum of HNO_3 and NO_3^- and the sum of NH_3 and NH_4^+ from the DELTA are also consistent with previous filter pack determination of total inorganic nitrogen and total inorganic ammonium, respectively. With the exception of SO_2 and SO_4^{2-}, the AGANet provides for the first time the UK concentration fields and seasonal cycles for each of the other measured species. The largest concentrations of HNO_3, SO_2, and aerosol NO_3^- and SO_4^{2-} are found in south and east England and smallest in western Scotland and Northern Ireland, whereas HCl are highest in the southeast, southwest and central England, that may be attributed to dual contribution from anthropogenic (coal combustion) and marine sources (reaction of sea salt with acid gases to form HCl). Na^+ and Cl^- are spatially correlated, with largest concentrations at coastal sites, reflecting a contribution from sea salt. Temporally, peak concentrations in HNO_3 occurred in late winter and early spring attributed to photochemical processes. NO_3^- and SO_4^{2-} have

.

a spring maxima that coincides with the peak in concentrations of NH_3 and NH_4^+, and are therefore likely attributable to formation of NH_4NO_3 and $(NH_4)_2SO_4$ from reaction with higher concentrations of NH_3 in spring. By contrast, peak concentrations of SO_2, Na^+ and Cl^- during winter are consistent with combustion sources for SO_2 and marine sources in winter for sea salt aerosol.

Key pollutant events were captured by the AGANet. In 2003, a spring episode with elevated concentrations of HNO_3 and NO_3^- was driven by meteorology and transboundary transport of NH_4NO_3 from Europe. A second, but smaller episode occurred in September 2014, with elevated concentrations of SO_2, HNO_3, SO_4^{2-}, NO_3^- and NH_4^+ that was shown to be from the Icelandic Holuhraun volcanic eruptions. Since 1999, AGANet has shown substantial decrease in SO_2 concentrations relative to HNO_3 and NH_3, consistent with estimated decline in UK emissions. At the same time, large reductions and changes in the aerosol components provides evidence of a shift in the particulate phase from $(NH_4)_2SO_4$ to NH_4NO_3.

The potential for NH_4NO_3 to release NH_3 and HNO_3 in warm weather, together with the surfeit of NH_3 also means that a larger fraction of the reduced and oxidised N is remaining in the gas phase as NH_3 and HNO_3 as indicated by the increasing trend in ratios of NH_3:NH_4^+ and HNO_3:NO_3^- over the 16 year period. Due to different removal rates of the component species by wet and dry deposition, this change is expected to affect spatial patterns of pollutant deposition with consequences for sensitive habitats with exceedance of critical loads of acidity and eutrophication. The changes are also relevant for human health effects assessment, particularly in urban areas as NH_4NO_3 constitutes a significant fraction of fine particulate matter (< 2.5 μm) that are linked to increased mortality from respiratory and cardiopulmonary diseases.

3.2 Introduction

Monitoring the atmospheric concentrations of acid gases and their aerosol reaction products is important for assessing their effects on human health, ecosystems, long-range transboundary transport and global radiative balance. Concentration data are necessary for quantifying long-term trends and spatial patterns, understanding gas–aerosol phase interactions, and estimating the contributions of different pollutants to dry deposition fluxes (ROTAP, 2012; AQEG, 2013a; Colette et al., 2016), as well as to provide data for testing the performance of atmospheric models (e.g. Chemel et al., 2010; Vieno et al., 2014, 2016).

Acid gases in the atmosphere include sulfur dioxide (SO_2), nitrogen oxides (NO_x), nitric acid (HNO_3), hydrochloric acid (HCl) and nitrous acid (HONO). Secondary inorganic aerosols (SIA) include sulfate (SO_4^{2-}), nitrate (NO_3^-), chloride (Cl^-) and nitrite (NO_2^-) that are formed from reactions of SO_2 and NO_x (and HNO_3, a secondary product of NO_x) with ammonia (NH_3) in the atmosphere. These aerosols make an important contribution to concentrations of particulate matter (PM) in the UK (15 %– 50 % of the mass of atmospheric PM) and constitute a significant fraction of fine particles that are less than 2.5 µm in diameter ($PM_{2.5}$) implicated in harming human health (AQEG, 2012, 2013b). In addition, base cations in aerosol are also of interest to estimate the extent to which acidity is neutralized and to estimate the contribution of marine influences (ROTAP, 2012; Werner et al., 2011).

Anthropogenic emissions of SO_2, NO_x , HCl, and NH_3 in the UK declined by 81 %, 51 %, 87 %, and 13 %, respectively, over the period 1999 to 2015 (NAEI, 2018). Despite the success in mitigating SO_2 emissions however, sulfur still remains a pollutant of national importance, because reduction in sulfur deposition in remote sensitive areas have been more modest than close to major sources (ROTAP, 2012). HCl was also recently identified as another important acidifying pollutant for sensitive habitats (Evans et al., 2011). Emissions of HCl (from coal burning in power stations) have however declined

to very low levels (from 74 kt in 1999 to 9 kt in 2015), although it could still pose a threat to habitats close to these sources. For NO_x, the more modest decrease in emissions reflects difficulties in their abatement, while for NH_3, the decrease to date is largely a result of changes in animal numbers (NAEI, 2018).

With the decline in SO_2 emissions and deposition, the large number of reactive nitrogen compounds in the atmo sphere are assuming greater importance owing to the complexities of the global N cycle and associated challenges in their abatement. These include the gas phase components NH_3, with over 80 % estimated from agricultural emissions (EEA, 2017) and nitrogen oxides (NO, NO_2) from combustion, the secondary gas phase reaction products HNO_3, HONO and PAN (peroxyacetyl nitrate), and particulate phase components ($(NH_4)_2SO_4$, NH_4HSO_4, and NH_4NO_3) formed by the reaction between NH_3 and acid gases (AQEG, 2012). Ammonia and the N-containing aerosols are known to cause nitrogen enrichment and eutrophication, as well as contributing to acidification processes (Sutton et al., 2011). Oxidized nitrogen species (NO_x) are precursors to ground-level O_3 formation, while the production of acids (HNO_3, HONO) and PAN in the atmosphere affects air quality and is damaging both to human health and to vegetation (Cowling et al., 1998; Bobbink et al., 2010).

In Europe, air pollution policies regarding acidification and nitrogen eutrophication apply the “critical loads approach” (Bull, 1995; Gregor et al., 2001), which requires that atmospheric deposition inputs be mapped at an appropriate scale for the assessment of effects. In parallel, the “critical levels” of concentrations addresses the direct impacts of concentrations of nitrogen components in the atmosphere (Bull, 1991; Gregor et al., 2001; Cape et al., 2009). Quantifying the dry deposition of reactive nitrogen compounds is a major challenge and a key source of uncertainty for effects assessment (Dentener et al., 2006; Flechard et al., 2011; Schrader et al., 2018; Sutton et al., 2007). While deposition may be estimated using atmospheric transport and chemistry models (e.g. Dore et al., 2015; Flechard et al., 2011; Smith et al.,

2000), air concentration data at sufficient spatial resolution are needed, both to assess the atmospheric models and provide input data for estimating deposition using inferential models.

In light of policies to reduce atmospheric emissions, e.g. the amended 2012 Gothenburg Protocol (UNECE, 2018) and the revised National Emissions Ceilings Directive (NECD, EU Directive 2016/2284) (EU, 2016), it is important to assess long-term trends in the measured pollutants, since this provides the only independent means to assess the effectiveness of any abatement policies. Both these international agreements set emissions reduction commitments for SO_2, NO_x and NH_3, of 59 %, 42 %, and 6 %, respectively, by 2020 (with 2005 as base year) and includes $PM_{2.5}$ for the very first time. Under the 2016 NECD, further reduction commitments of 79 % (SO_2), 63 % (NO_x), and 19 % (NH_3) are also set for the EU 28 countries from 2030. Since emissions of these gases come from different sources, emissions controls require very different strategies, making it important to monitor and assess the relative concentrations and deposition of nitrogen and sulfur components.

The spatial and temporal patterns of gases and particulate phases of these pollutants differ substantially. Although it is widely acknowledged that speciation between reactive gas and aerosol measurement is critical, there are few national long-term monitoring programmes dedicated to measuring their concentrations and dry depositions separately at high spatial resolution (Tørseth et al., 2012). Across Europe, the European Monitoring and Evaluation Programme (EMEP, 2014) continues to recommend using a daily filter pack sampling method to measure oxidized nitrogen (total inorganic nitrate, TIN) and reduced nitrogen (total inorganic ammonia, TIA) (Tørseth et al., 2012; Colette et al., 2016). The filter pack method is generally considered as robust for measuring SO_2 and SO_4^{2-} concentrations (EMEP, 2014; Hayman et al., 2006; Sickles et al., 1999). However, many papers have shown that there are potential artefacts in filter-pack sampling for HNO_3 and HCl, due to interactions with NH_3 and the volatility of NH_4NO_3 and NH_4Cl aerosol (Pio, 1992; Sickles et al., 1999; Cheng et al., 2012). Results from EMEP filter pack measurements

are therefore reported as TIN and TIA, due to phase uncertainties in the method (Tørseth et al., 2012). This has been complemented by daily measurements of HNO_3 and NO_3^- using annular denuders (Allegrini et al., 1987; EMEP, 2014) that are made at a restricted number of sites because of the resources required. In North America, filter pack sampling is also used in weekly measurements of sulfur and nitrogen species in the CASTnet (Clean Air Status Trends Network) national monitoring network of 95 sites across the contiguous USA, Canada, and Alaska (https://www.epa.gov/castnet, last access: 25 October 2018). At a small number of CASTnet sites, hourly measurements of water-soluble gases and aerosols are made with the Monitor for AeRosols and GAses in ambient air (MARGA) system (Rumsey and Walker, 2016).

High time-resolution measure ements of gases and aerosols are useful at selected locations for detailed analysis and model testing, but the high costs and resources required for these measurements make them unsuitable for the assessment of long-term trends at many sites, particularly where spatial patterns are required. To achieve this, a larger number of sites operated at lower time-resolution is needed. In the UK, the Eutrophying and Acidifying Atmospheric Pollutants (UKEAP) network provides long-term measurements for the UK rural atmospheric concentrations and deposition of air pollutants that contribute to acidification and eutrophication processes (Conolly et al., 2016). UKEAP is comprised of two EMEP supersites and four component networks: precipitation network (Precip-net), NO_2 diffusion tube network (NO_2-net), National Ammonia Monitoring Network (NAMN), and the Acid Gases and Aerosol Network (AGANet). At the two EMEP supersites (Auchencorth and Harwell – relocated to Chilbolton in 2016), semi-continuous hourly speciated measurements of reactive gases and aerosols are made with the MARGA system (Twigg et al., 2016). These measurements are contributing to the validation and improvement of atmospheric models, such as FRAME (Dore et al., 2015) and EMEP4UK (Vieno et al., 2014, 2016) that are used to de velop and provide the evidence base for air quality policies, both nationally and

internationally. The long-term dataset of monthly speciated measurements from the AGANet (1999–2015) are analysed in this paper to provide a comprehensive assessment of the spatial, temporal, and long-term trends in atmospheric concentrations of the acid gases HNO_3, SO_2, HCl and related aerosol components NO_3^-, SO_4^{2-} and Cl^- (and also base cations Na^+, Ca^{2+}, and Mg^{2+}) across the UK, together with an assessment of the DELTA denuder-filter pack sampling method (Sutton et al., 2001b; Tang et al., 2009) as compared with other sampling techniques. To aid interpretation of the relative changes and trends in the acid gases and aerosols, NH_3 and particulate NH_4^+ data from the NAMN (Tang et al., 2018) are included, since atmospheric NH_3 is a major interacting precursor gas in neutralization reactions with the acid gases.

3.3 Methods

3.3.1 Acid Gases and Aerosol monitoring Network (AGANet)

The UK Acid Gases and Aerosol Network (AGANet), known previously as the nitric acid monitoring network, was started in September 1999 under the Acid Deposition Monitoring Network (ADMN, Hayman et al., 2007) to deliver for the very first time, long-term monthly speciated measurement data on gaseous HNO_3 and particulate NO_3^- across the UK. Other acid gases (SO_2, HCl) and aerosols (SO_4^{2-}, Cl^-, plus base cations Na^+, Ca^{2+}, Mg^{2+}) are also measured and reported.

AGANet and NAMN are closely integrated, with AGANet established at a subset of NAMN sites to provide additional speciated measurements of the acid gases and aerosol components. To improve on national coverage, the number of sites in AGANet was increased in 2006 from 12 to 30 (Fig. 3.1, Table 3.1). At the same time, the Rural Sulfur Dioxide Monitoring Program ceased, replaced by SO_2 and SO_4^{2-} measurements made under the expanded AGANet (Hayman et al., 2007).

Table 3.1. List of sites in the UK Acid Gas and Aerosol Network (AGANet) with details of locations, start dates and UK-AIR ID (https://uk-air.defra.gov.uk/networks/network-info?view=aganet).

Site Name	UK-AIR ID	Latitude	Longitude	Start
Barcombe Mills	UKA00069	50.9191	0.0486	Apr '00
Bush OTC	UKA00128	55.8623	-3.2058	Sep '99
Cwmystwyth	UKA00325	52.3524	-3.8053	Sep '99
Eskdalemuir	UKA00130	55.3153	-3.2061	Sep '99
Glensaugh	UKA00348	56.9072	-2.5594	Sep '99
High Muffles	UKA00169	54.3349	-0.8086	Sep '99
Lough Navar	UKA00166	54.4395	-7.9003	Oct '99
Rothamsted	UKA00275	51.8065	-0.3604	Sep '99
Stoke Ferry	UKA00317	52.5599	0.5061	Sep '99
Strathvaich	UKA00162	57.7345	-4.7766	Sep '99
Sutton Bonington	UKA00312	52.8366	-1.2512	Sep '99
Yarner Wood	UKA00168	50.5976	-3.7165	Sep '99
New sites added from January 2006				
Auchencorth Moss	UKA00451	55.7922	-3.2429	Jan '06
Caenby	UKA00492	53.3979	-0.5074	Feb '06
Carradale	UKA00389	55.5825	-5.4962	Jan '06
Detling	UKA00481	51.3079	0.5827	Feb '06
Edinburgh St Leonards	UKA00454	55.9456	-3.1822	Jan '06
Goonhilly	UKA00056	50.0506	-5.1815	Jan '06
Halladale	UKA00314	58.4124	-3.8758	Jan '06
Harwell	UKA00047	51.5711	-1.3253	May '06
Hillsborough	UKA00293	54.4525	-6.0833	Jan '06
Ladybower	UKA00171	53.4034	-1.7520	Feb '06
Lagganlia	UKA00290	57.1110	-3.8921	Jan '06
Lerwick	UKA00486	60.1392	-1.1853	Jan '06
London Cromwell Road 2	UKA00370	51.4955	-0.1787	Jan '06
Moorhouse	UKA00357	54.6901	-2.3769	Jan '06
Narberth	UKA00323	51.7818	-4.6915	Mar '06
Plas Y Brenin	UKA00493	53.1018	-3.9179	May '06
Rosemaund	UKA00491	52.1214	-2.6363	Jan '06
Rum	UKA00276	57.0100	-6.2718	Feb '06

A broad spatial coverage of the UK is provided by the AGANet sites, with a focus on sites providing parallel information on other air pollutants (e.g. collocation with the Automatic Urban and Rural Network that provides compliance monitoring against the Ambient Air Quality Directives (https://uk-air.defra.gov.uk/networks/, last access: 25 October 2018) and ecosystem assessments (e.g. Environmental Change Network, http://www.ecn.ac.uk/, last access: 25 October 2018) (Monteith et al., 2016). NAMN for measurement

of NH_3 gas and aerosol NH_4^+ (Sutton et al., 2001a, b; Tang et al., 2018) is extended to provide additional simultaneous monthly time-integrated average concentrations of acid gases (HNO_3, SO_2, HCl) and particulate phase NO_3^-, SO_4^{2-}, Cl^-, Na^+, Ca^{2+}, and Mg^{2+} for the AGANet (Conolly et al., 2016; Tang et al., 2015).

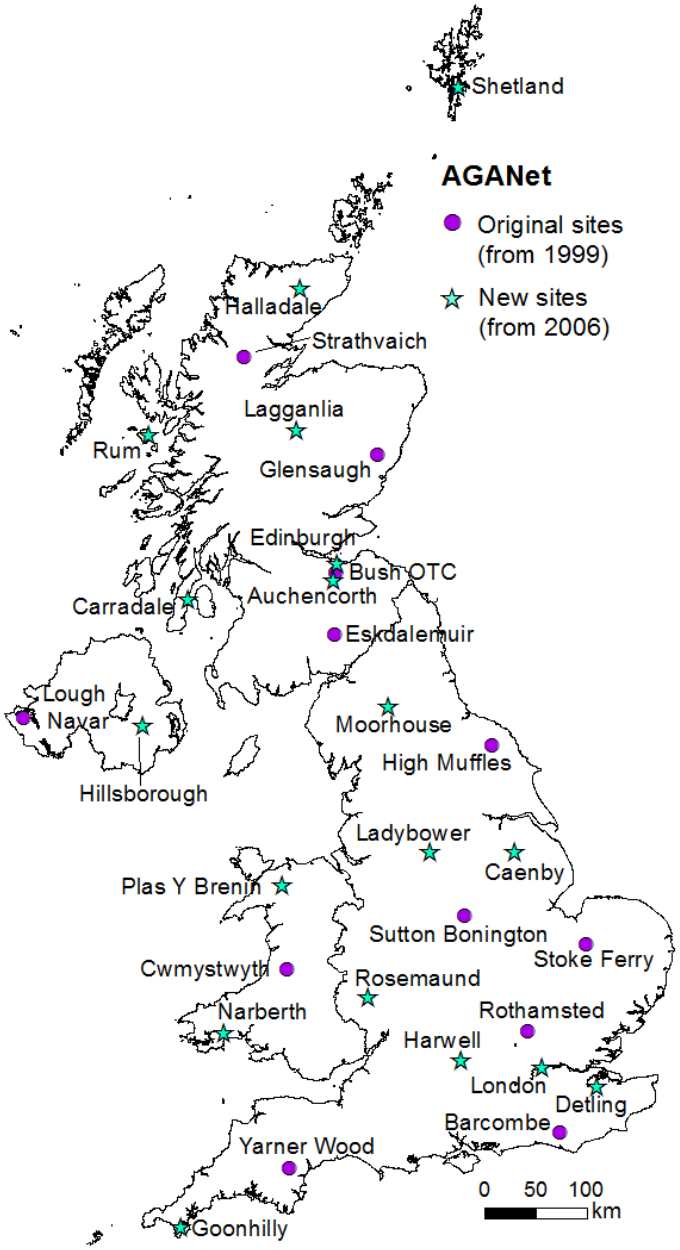

Figure 3.1. Site map of the UK Acid Gases and Aerosol Network (AGANet). The AGANet was established in September 1999 with 12 sites and expanded to 30 sites from January 2006 to improve national coverage. These sites also provide measurements of NH_3 and NH_4^+ for the UK National Ammonia Monitoring Network (NAMN, Tang et al., 2018).

3.3.2 Extended DELTA methodology for sampling acid gases and aerosol in AGANet

A low-cost manual denuder-filter pack method, DELTA (DEnuder for Long-Term Air sampling) implemented in the NAMN for measurement of NH_3 gas and aerosol NH_4^+ (Sutton et al., 2001a, b; Tang et al., 2018) is extended to provide additional simultaneous monthly time-integrated average concentrations of acid gases (HNO_3, SO_2, HCl) and particulate phase NO_3^-, SO_4^{2-}, Cl^-, Na^+, Ca^{2+}, and Mg^{2+} for the AGANet (Conolly et al., 2016; Tang et al., 2015).

AGANet has also been applied in an extensive European-scale network of 58 sites to deliver 4 years of atmospheric concentrations and deposition data for reactive trace gas and aerosols from 2006 to 2009 (Tang et al., 2009; Flechard et al., 2011). Detailed descriptions of the DELTA method are provided by Sutton et al. (2001b) and by Tang et al. (2009, 2015). In brief, a small air pump is used to provide low sampling rates of 0.2–0.4 L min^{-1}, and air volumes are measured by a highsensitivity diaphragm gas meter. By sampling air slowly, the method is optimized for monthly measurements, with sufficient sensitivity to resolve low concentrations at clean back Fig. 3.1. Site map of the UK Acid Gases and Aerosol Network (AGANet). The AGANet was established in September 1999 with 12 sites and expanded to 30 sites from January 2006 to improve national coverage. These sites also provide measurements of NH_3 and NH_4^+ for the UK National Ammonia Monitoring Network (NAMN, Tang et al., 2018).

An extended denuder-filter pack sampling train is used to provide speciated sampling of reactive gases and aerosols (Supp. Fig. S3.1) (Tang et al., 2009, 2015). A Teflon inlet (2.8 cm long) at the front end ensures development of a laminar air stream (Supp. Table S3.3), followed by a first pair of K_2CO_3 and glycerol coated denuders to collect HNO_3, SO_2, and HCl, a second pair of citric acid coated denuders to collect NH_3 and a 2-stage filter pack at the end to collect aerosol components. Stage 1 of the filter pack is a cellulose filter impregnated with K_2CO_3 and glycerol to collect NO_3^-, SO_4^{2-}, Cl^-, Na^+, Ca^{2+},

Mg^{2+}, with evolved aerosol NH_4^+ from this filter collected on the stage 2 citric acid impregnated filter. The separation of gases and aerosol is achieved by higher diffusivities of re active gases to the denuder walls where they react with the chemical coating and are retained, whereas aerosol components pass through and are retained by post-denuder filters (Ferm, 1979). In this approach, potential artefacts caused by phase interactions associated with filter packs and bubblers are avoided (e.g. Sickles et al., 1999). A particle size cutoff of around 4.5 µm was estimated for the DELTA air inlet (Tang et al., 2015). The DELTA will therefore also sample fine mode aerosols in the $PM_{2.5}$ fraction, as well as some of the coarse mode aerosols < $PM_{4.5}$.

Na_2CO_3 is reported to be an effective sorbent for acid gases, allowing simultaneous collection of HNO_3, SO_2, and HCl on denuders (e.g. Ferm, 1986), but since the measurement of aerosol Na^+ is also of key interest in AGANet, a K_2CO_3 coating is used instead to eliminate possible Na^+ contamination from Na_2CO_3. Glycerol is added to increase adhesion, stabilize the base coating (Ferm, 1986; Finn et al., 2001) and to minimize potential oxidation of nitrite that is also collected on the denuder to nitrate in the presence of atmospheric oxidants such as ozone (Allegrini et al., 1987; Perrino et al., 1990). The lengths of denuders (borosilicate glass tubes 10 and 15 cm long to capture > 95 % of NH_3 and acid gases, respectively) in the sampling train was calculated according to the procedures described by Sutton et al. (2001b), based on the calculations derived by Gormley and Kennedy (1948) and Ferm (1979); see Supp. Table S3.3. All sites were set up as “outdoor” systems sampling directly from the atmosphere, avoiding potential adsorption losses (in particular HNO_3, which is highly surface active) and artefacts in air inlet lines. The sampling train is installed inside a simple watertight housing (Supp. Fig. S1), which is mounted on a steel post in the desired location. A low density polyethylene funnel (89 mm aperture) is placed at the inlet as a rain shelter, and sampling height is approx. 1.5 m.

3.3.3 Chemical analysis

K_2CO_3 / glycerol-coated denuders and aerosol filters are extracted into 5 mL of deionized H_2O for analysis. Anions (NO_3^-, SO_4^{2-}, and Cl^-) in the denuder and filter extracts are analysed by ion chromatography (IC). Base cations Na^+, Mg^{2+} and Ca^{2+} from the filter extracts were analysed by IC between 1999–June 2008 and by inductively coupled plasma-optical emission spectroscopy (ICP-OES/ICP-AES) from July 2008. Citric acid coated denuders and filter papers are also extracted into deionized H_2O (3 and 4 mL, respectively), with analysis of NH_4^+ performed on a high sensitivity ammonia flow injection analysis system, as described in Tang et al. (2018).

Up to June 2009, analyses were carried out at Harwell Laboratory (Hayman et al., 2007) and from July 2009 at CEH Lancaster (Conolly et al., 2016). The limit of detection (LOD) for the DELTA method for the different components are calculated by analysing a series of laboratory blanks. The mean and standard deviation of the results are calculated and the LOD is calculated as 3 times the standard deviation divided by 15 m^3, the typical volume of air sampled over a month by the DELTA system. Details of changes in laboratory, analytical methods, and LODs for the gases and aerosols are summarized in Supp. Tables S3.1 and S3.2, respectively

3.3.4 Calculation of air concentrations

The air concentration (χa) of a gas or aerosol is calculated according to Eq. 1 (see Sutton et al., 2001b, Tang et al., 2018):

$$\chi a = \frac{Q}{V} \qquad (1)$$

where

Q = amount of a gas or aerosol collected on a denuder or aerosol filter, and
V = volume of air sampled (from gas meter, typically 15 m^3 in a month)

The denuder capture efficiency for each of the gas is calculated by comparing the concentrations of the individual gases in the denuder pairs (Eq. 2) and are applied in an infinite series correction on the raw data to provide corrected air concentrations ($\chi_{a\,(corrected)}$) according to Eq. 3 (see Sutton et al., 2001b; Tang et al., 2018):

$$\text{Denuder capture efficiency (\% CE)} = 100 \text{ x } \frac{\text{Denuder 1}}{(\text{Denuder 1+ Denuder 2})} \qquad (2)$$

$$\chi_a\,(\text{corrected}) = \chi_a\,(\text{Denuder 1}) \times \frac{1}{1-\left[\frac{\chi_a(\text{Denuder 2})}{\chi_a(\text{Denuder 1})}\right]} \qquad (3)$$

where

Q is the amount of a gas or aerosol collected on a denuder or aerosol filter

V is the volume of air sampled (from gas meter, typically 15 m³ in a month).

Sutton et al. (2001b) and Tang et al. (2003) have shown that this procedure provides an important quality control, flagging up occurrences of poorly coated denuders and/or sampling issues. With denuder capture efficiency better than 90 %, the correction represents < 1 % of the corrected air concentration of the gas. Below 60 %, the correction is large (> 50 %) and is not applied, and the air concentration is then calculated as the sum of concentrations of the denuder pair. The amount of correction for gas not captured that is added to the corrected gas concentration, is subtracted from the estimated aerosol concentrations of matching anions and cations (see Tang et al., 2018).

3.3.5 Data quality control

The following data quality checks are applied to the network data, as part of the network quality management system (Tang and Sutton, 2003; Conolly et al., 2016).

i. Air flow rate (0.2 – 0.4 L min^{-1}) – where this is below the expected range for a sampling period, the data are flagged as valid but failing the QC standard.

ii. Denuder capture efficiency – where this is less than 75 % for a sample, the data are flagged as valid but less certain.

iii. Ion balance checks – close agreement expected between NH_4^+ and the sum of NO_3^- and 2 × SO_4^{2-}, as NH_3 is neutralized by HNO_3 and H_2SO_4 to form NH_4NO_3 and $(NH_4)_2SO_4$, respectively (Conolly et al., 2016), and for Na^+ and Cl^-, as these are marine (sea salt) in origin.

iv. Screening the whole dataset for sampling anomalies and outliers, e.g. due to contamination or other issues.

3.3.6 HNO_3 measurement artefact and correction

Tang et al. (2009, 2015) have identified that HNO_3 concentrations (NO_3^- on denuders assumed to be from HNO_3) may be overestimated on carbonate coated denuders, due to partial co-collection of other oxidized nitrogen components such as nitrous acid (HONO). In the case of HONO, this collects on the denuder carbonate coating as nitrite (NO_2^-), but oxidizes to nitrate (NO_3^-) in the presence of oxidants such as ozone (Bytnerowicz et al., 2005) which can result in a positive interference in HNO_3 determination (Tang et al., 2009, 2015). Other oxidized nitrogen species present in the atmosphere such as peroxyacetyl nitrate (PAN) and nitrogen oxides (NO_x) can also potentially contribute to a further small interference (Allegrini et al., 1987; Bai et al., 2003). Based on the tests of Tang et al. (2015), raw HNO_3 data are corrected with an empirical factor of 0.45 which is estimated to be uncertain by ± 30 %. Apart

from where stated, all HNO_3 data reported in this study have the 0.45 correction factor applied.

3.3.7 Time series trend analyses

Statistical trend analyses using both parametric linear regression (LR) and non-parametric Mann–Kendall (MK) (Gilbert, 1987; Chatfield, 2016) tests were performed on annually averaged data from AGANet, and on a subset of annually averaged data from NAMN made at the same AGANet sites. The datasets are considered sufficiently long-term (> 10 years) and produced by a consistent method for effective statistical trend analyses. Both the LR and MK approaches are widely adopted for trend analyses in long-term atmospheric data (e.g. Meals et al., 2011; Colette et al., 2016; Jones and Harrison, 2011; Marchetto et al., 2013; Hayman et al., 2007; Conolly et al., 2016), and were used in a recent trend assessment of atmospheric NH_3 and NH_4^+ data (1998–2014) from the NAMN (Tang et al., 2018).

As described in Tang et al. (2018), LR tests were performed using R, and MK tests used the R "Kendall" package (McLeod, 2015), with estimation of the MK Sen's slope (fitted median slope of a linear regression joining all pairs of observations) and confidence interval of the fitted trend using the R "Trend" package (Pohlert, 2016). Results from both tests provides an indication of uncertainty associated with the choice of approach. Since there was no difference between either tests, MK results only are presented and discussed in the paper. A comparison of trend analyses from both approaches is, however provided in supplementary materials (Supp. Figs. S3.6 and S3.7 and Supp. Tables S3.4–S3.6).

3.4 Results and Discussion

3.4.1 Performance of the DELTA method

This section presents the performance of the DELTA measurements, including a comparison with other air sampling methods and networks. Replicated sampling with the DELTA method were also made to assess measurement reproducibility and this is shown for example for the Bush OTC site in Scotland (UKA00128). A comparison of the parallel measurements (Fig. 3.2) showed good reproducibility in the method, with close agreement for all components (e.g. mean difference of < ± 3 % for all components and ± 6 % for HCl).

3.4.1.1 Comparison with daily annular denuder measurements

An assessment of the DELTA method for NH_3 has previously been reported by Sutton et al. (2001b). Following the extension to additionally sample acid gases and aerosols, the modified system was compared with independent daily measurements from an annular denuder system (ADS). The ADS (ChemspecTM model 2500 air sampling system, R&P Co. Inc.) was operated at Barcombe Mills in southern England (UKA00069) alongside the AGANet DELTA monthly measurements for a period of 18 months. Due to significant instrument and local site issues resulting in low data capture with the ADS, only 11 months of data were available for intercomparison. The sampling train used in the ADS consisted of 2 K_2CO_3 / glycerol-coated annular denuders (same coating as AGANet DELTA), 2 citric acid-coated annular denuders; a cyclone with 2.5 µm cut-off, followed by a 2 - stage filter pack containing a 2 µm PALL Zefluor teflon mem brane (collection of NO_3^-, SO_4^{2-}, Cl^-, Na^+, Mg^{2+}, Ca^{2+}) and a 1 µm PALL Nylasorb nylon membrane (collection of evolved NO_3^-), with a sampling rate of 10 L min^{-1}. To compare against the monthly DELTA measurements, daily ADS values were averaged to the corresponding monthly periods, with results summarized in Fig. 3.3.

(a) Gases (HNO_3, SO_2, HCl, NH_3)

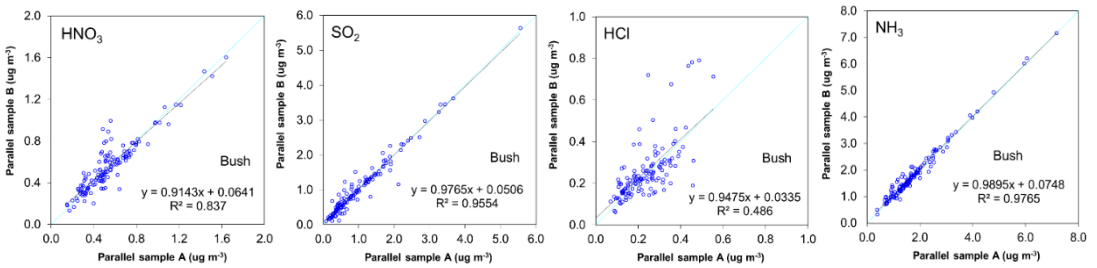

(b) Particulate (NO_3^-, SO_4^{2-}, Cl^-, NH_4^+)

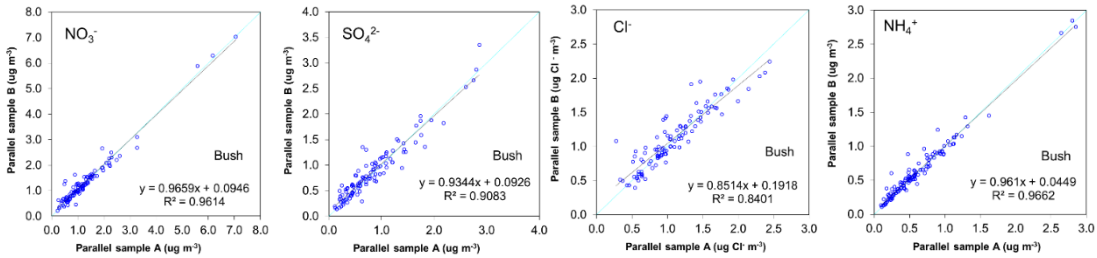

(c) Summary of regression analysis

	Gases				Particulates			
	HNO_3	SO_2	HCl	NH_3	NO_3^-	SO_4^{2-}	Cl^-	NH_4^+
R^2	0.837***	0.955***	0.486***	0.976***	0.961***	0.908***	0.840***	0.966***
slope	0.914*	0.976^{ns}	0.947^{ns}	0.989^{ns}	0.966 ^{ns}	0.934*	0.851***	0.961*
intercept	0.064**	0.051*	0.033^{ns}	0.075**	0.095**	0.093**	0.192***	0.045***
No. observations (*n*)	130	130	128	140	108	108	104	119
mean A (µg m^{-3})	0.54	1.02	0.23	1.75	1.29	0.84	1.09	0.61
mean B (µg m^{-3})	0.56	1.05	0.25	1.80	1.34	0.87	1.12	0.63

Significance level (slope different from 1, intercept = 0): * $p < 0.05$, ** $p < 0.01$, *** $p < 0.001$. *ns* = not significant ($p > 0.05$)

Figure 3.2. Comparisons of parallel measurement of monthly (a) atmospheric reactive gases (HNO_3, SO_2, HCl and NH_3) and (b) particulate (NO_3^-, SO_4^{2-}, Cl^- and NH_4^+) concentrations from duplicate DELTA sampling at the UK Acid Gas and Aerosol Monitoring Network (AGANet) and National Ammonia Monitoring Network (NAMN) site Bush OTC (UKA00128) in Southern Scotland for the period 1999 to2015. (c) A summary of the regression analyses. Each point represents a comparison between the paired monthly DELTA measurements.

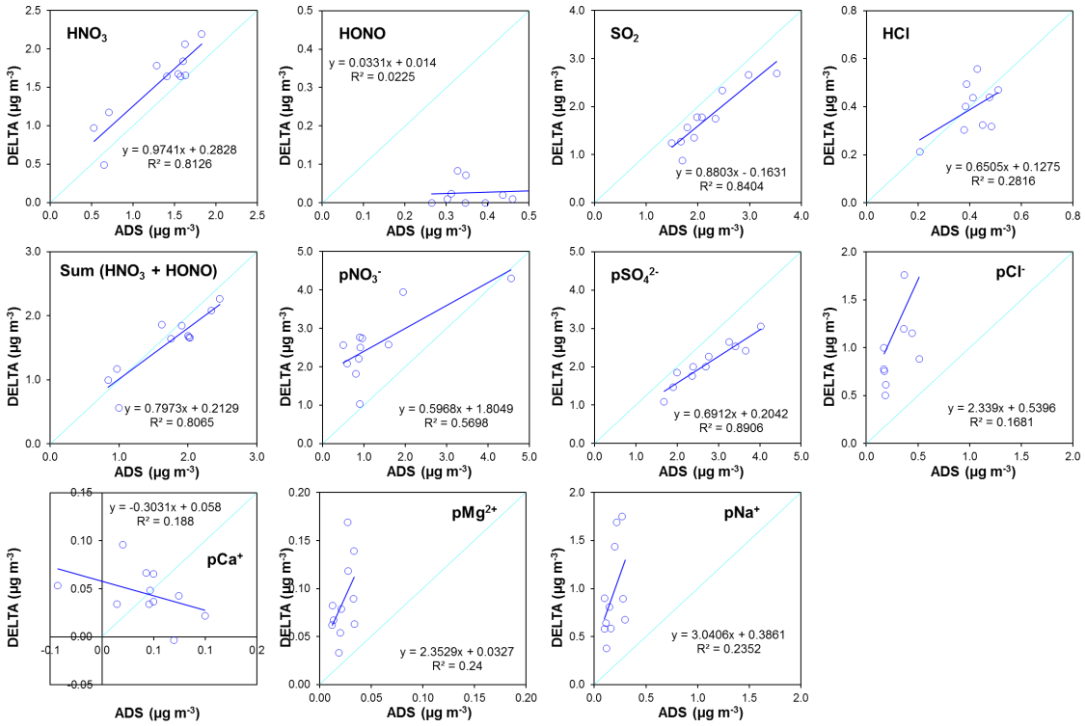

	Gases					Particulates					
	HNO_3	(HNO_3+HONO)	HONO	SO_2	HCl	NO_3^-	SO_4^{2-}	Cl^-	Na^+	Ca^{2+}	Mg^{2+}
Linearregression: R^2	0.81***	0.81***	0.02^{ns}	0.84***	0.28^{ns}	0.57**	0.89***	0.17^{ns}	0.81***	0.19^{ns}	0.24^{ns}
slope	0.97^{ns}	0.80^{ns}	0.03***	0.88^{ns}	0.65^{ns}	0.57*	0.69**	2.34^{ns}	0.97^{ns}	-0.30	2.35
intercept	0.28^{ns}		0.01^{ns}	-0.16^{ns}	0.13^{ns}	1.81***	0.20^{ns}	0.54^{ns}	0.28^{ns}	0.06***	0.03^{ns}
Observations: *n*	11	11	11	11	10	11	11	11	11	11	11
mean DELTA (µg m^{-3})	1.56	1.58	0.03	1.75	0.40	2.59	2.10	1.24	1.56	0.05	0.09
mean ADS (µg m^{-3})	1.31	1.72	0.41	2.18	0.41	1.32	2.74	0.30	1.31	0.04	0.02

Significance level (slope different from 1, intercept = 0): * $p < 0.05$, ** $p < 0.01$, *** $p < 0.001$. *ns* = not significant ($p > 0.05$)

Figure 3.3. Comparison of HNO_3, HONO, sum (HNO_3+HONO), SO_2, HCl and aerosol NO_3^-, SO_4^{2-}, Cl^-, Na^+, Ca^{2+}, Mg^{2+} concentrations by the Acid Gases and Aerosol Network (AGANet) DELTA method with available measurements from the co-located ChemSpec Daily Annular Denuder system (ADS) at Barcombe Mills (UKA00069). Mean concentrations were derived from the average of daily ADS data for the corresponding DELTA sampling periods (monthly). HNO_3 values shown for DELTA and ADS are as calculated from the amount of NO_3^- collected on the denuders and have not been adjusted by a bias correction factor (see Sect. 4.3.2.3). A summary of the regression analyses is provided in the table below the graphs.

In the measurement of gases, HNO_3 determination on DELTA (mean = 1.56 HNO_3 µg m^{-3}, n = 11) was on average 23 % higher than the ADS (mean = 1.31 HNO_3 µg m^{-3}, n = 11). Since both methods used the same carbonate coating on the denuders to sample acid gases, the HNO_3 data here have not been corrected with the empirical factor described in Sect. 3.3.6. Nitrous acid (HONO) was found to be close to or below limit of detections for most of the DELTA measurements (mean = of 0.03 µg HONO m^{-3}), compared with a significantly higher concentration (mean = 0.41 HONO µg m^{-3}) from the ADS. Since the sampling period of the ADS is daily, any HONO collected as nitrite on the ADS is likely to remain as nitrite and not oxidized to nitrate.

The very low HONO (nitrite on the denuders assumed to be from HONO) concentrations from the DELTA supports the hypothesis of the retention of HONO that is subsequently oxidized to nitrate, resulting in an artefact in HNO_3 determination (Possanzini et al., 1983; Allegrini et al., 1987; Tang et al., 2015). Further corroboration is provided by the improved agreement between both methods (line of fit closer to the 1:1 line) when comparing the sum of HNO_3 and HONO (Fig. 3.3). Agreement between the DELTA and ADS was within 19 % for SO_2 (mean DELTA = 1.75 µg m^{-3} *cf.* mean ADS = 2.18 µg m^{-3}) and 4 % for HCl (mean DELTA = 0.40 µg m^{-3} *cf.* mean ADS = 0.41 µg m^{-3}). Given the limited data available, it is not clear why SO_2 measured on the ADS is higher than the DELTA, since there was good agreement for HCl.

For the particle-phase components, NO_3^- measured by the DELTA method (mean = 2.59 µg NO_3^- m^{-3}) was on average 2-fold higher than the ADS method (mean = 1.32 µg NO_3^- m^{-3}), whereas SO_4^{2-} by the DELTA method was on average 23 % lower (DELTA = 2.10 vs. ADS = 2.74 µg SO_4^{2-} m^{-3}) (Fig. 3.3). NO_3^- and SO_4^{2-} are both present as fine mode (< 1 µm) NH_4NO_3 and $(NH_4)_2SO_4$ (Putaud et al., 2010). Some NO_3^- can also be present in the coarse mode (> 2.5 µm), likely as calcium nitrate ($Ca(NO_3)_2$) from a reaction between gas-phase HNO_3 (or its precursors) and soil dust particles (Putaud et al., 2010), while some of the SO_4^{2-} will be coarse mode sea salt SO_4^{2-} (see Sect. 3.4.5). A particle size cut-off of 4.5 µm was estimated for the DELTA air inlet) (Tang

et al., 2015), so the DELTA will also sample a small amount of coarse mode aerosols. An ion balance check of the ratio of µeq. NH_4^+ to sum µeq. (NO_3^- + SO_4^{2-}) yielded a near unity value, confirming that NO_3^- and SO_4^{2-} collected by the DELTA aerosol filter are mainly fine mode NH_4NO_3 and $(NH_4)_2SO_4$. In comparison, the ADS has a 2.5 µm cyclone in front of the aerosol filters to collect aerosols < 2.5 µm on the aerosol filters. NH_4^+ was unfortunately not analysed in these tests, which would have allowed a similar ion balance check. Na^+ and Cl^- concentrations on the DELTA were also on average 331 % and 444 % higher than on the ADS and the ion balance check of the ratio of Na^+: Cl^- was unity for both methods. In the absence of analytical errors, loss of NO_3^-, Na^+ and Cl^- on the surface of the cyclone, coupled to a small fraction of the aerosols > 2.5 µm that is collected (but not analysed) in the cyclone, could partly account for the observed lower concentrations of the aerosol components. Since Ca^{2+} and Mg^{2+} concentrations by both methods were at or below detection limits, comparisons of these are not meaningful and have not been made.

3.4.1.2 Comparisons with filter pack measurements: HNO_3/NO_3^- and NH_3/NH_4^+

The EMEP network (http://www.emep.int/, last access: 17 March 2017) measures atmospheric concentrations and depositions of a wide range of pollutants at rural background sites across Europe (Aas, 2014; Tørseth et al., 2012). A daily filter pack method continues to be implemented at 39 sites across Europe for assessment of oxidized and reduced nitrogen species, with results reported as total inorganic nitrate (TIN: HNO_3 + NO_3^-) and total inorganic ammonia (TIA: NH_3 + NH_4^+) (Colette et al., 2016; Tørseth et al., 2012), as these are considered more reliable than reporting for the gas and aerosol components separately.

At the UK Eskdalemuir site (EMEP station code GB0002R; UKAIR ID UKA00130), a Scottish rural background site on the border between Scotland and England, daily filter pack measurements of TIN and TIA were made as part of the EMEP network from 1989 to 2000 (EMEP, 2017a). Following installation of the DELTA system in September 1999, both methods were operated in parallel for 14 months at Eskdalemuir, allowing a comparison to be made of TIN and TIA from both systems. Comparison results are shown in Fig. 3.4 of parallel data from the AGANet (sum of HNO_3 and NO_3^-) and NAMN (sum of NH_3 and NH_4^+), demonstrating close agreement between the two independent measurements.

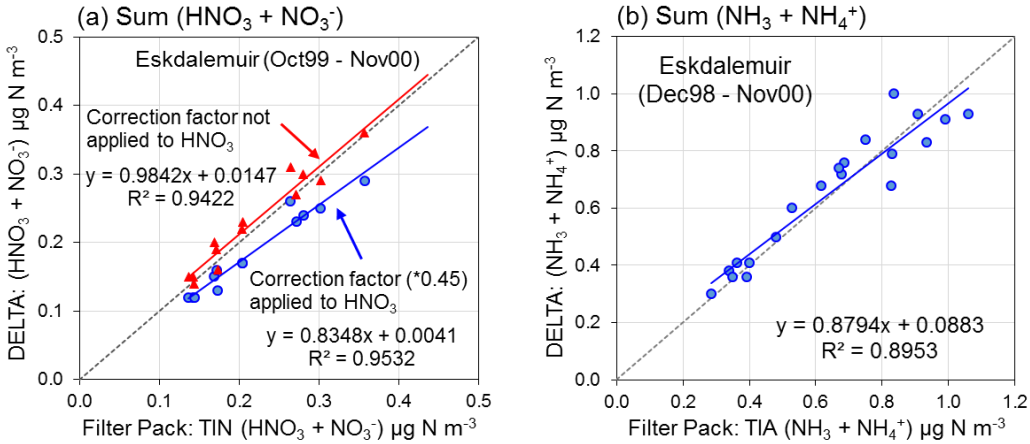

	DELTA TIN	EMEP TIN	DELTA TIN (corrected HNO_3)	EMEP TIN	DELTA TIA	EMEP TIA
Linear regression: R^2	0.942***		0.953***		0.895***	
slope	0.984^{ns}		0.835*		0.879^{ns}	
intercept	0.015^{ns}		0.004^{ns}		0.088^{ns}	
mean (µg N m^{-3})	0.23	0.22	0.19	0.22	0.58	0.54
No. of observations (*n*)	13	13	13	13	13	13

Significance level (slope different from 1, intercept = 0): * $p < 0.05$, ** $p < 0.01$, *** $p < 0.001$. *ns* = not significant ($p > 0.05$)

Figure 3.4. Comparison of (a) total inorganic nitrate, TIN (sum of HNO_3+NO_3^-) and (b) total inorganic ammonium, TIA (sum of NH_3+NH_4^+) concentrations at the Eskdalemuir monitoring station (EMEP station code = GB0002R; UK-AIR ID = UKA00130) measured under the EMEP program with concentrations of the corresponding gas and aerosol from the UK Acid Gases and Aerosol (AGANet, HNO_3 and NO_3^-) and UK National Ammonia Monitoring Network (NAMN, NH_3 and NH_4^+). EMEP values (EMEP, 2017a) are means of daily measurements for TIN and TIA by the EMEP filter pack method, matched to the AGANet and NAMN sampling periods (monthly). Filter pack measurements at Eskdalemuir terminated in December 2000. A summary of the regression analyses is provided in the table below the graphs.

The EMEP values shown are daily measurements of TIN and TIA averaged to corresponding monthly means for comparison with the DELTA data. For TIN, the regression between EMEP TIN and AGANet (sum of uncorrected HNO_3 and NO_3^-) is close to unity (slope = 0.98, R^2 = 0.94), which provided independent verification and support of the DELTA HNO_3 measurements at the start of the network. After applying a bias adjustment factor of 0.45 to the HNO_3 data (see Sect. 3.3.6), the AGANet values (sum of corrected HNO_3 and NO_3^-) are smaller than the EMEP TIN (slope = 0.835, R^2 = 0.95). It is possible however, that the filter pack method may also be subject to similar artefacts in HNO_3 determination due to co-collection of other oxidized nitrogen species (Tang et al., 2015).

3.4.1.3 Comparisons with bubbler and filter pack measurements: SO_2 and SO_4^{2-}

Independent measurements of SO_2 and SO_4^{2-} with a daily bubbler and filter pack method, respectively, are also available for comparison with the DELTA method at the Eskdalemuir site. Daily SO_2 data with a bubbler method (Hayman, 2005) from December 1977 to December 2001 and daily SO_4^{2-} data with an EMEP filter pack method from December 1977 to April 2009 (Hayman, 2006) were downloaded from the EMEP website (EMEP, 2017b). A close agreement is found between the bubbler and DELTA method for SO_2 (slope = 0.86, R^2 = 0.82), while there is more scatter between the filter pack and DELTA method for SO_4^{2-} (slope = 0.67, R^2 = 0.66) (Fig. 3.5). Concentrations of SO_2 for the 26 month overlap period were comparable (mean of bubbler method = 0.40 µg S m^{-3} *cf* mean of DELTA method = 0.44 µg S m^{-3}), whereas the filter pack SO_4^{2-} concentration (mean = 0.44 µg S m^{-3}, *n* = 87) is larger than the corresponding monthly DELTA measurement (mean = 0.28 µg S m^{-3}, *n* = 87) (Fig. 3.5). An earlier detailed assessment of the DELTA system against filter pack with a focus on SO_2 and SO_4^{2-} in 1999 by Hayman et al. (2006) had shown close agreement between the methods. It is therefore unclear why the DELTA gives a reading lower than the filter pack SO_4^{2-} at Eskdalemuir in this

assessment, since the dataset was a continuation of the original inter-comparison. Possible explanations include uncertainties associated with limit of detection of the daily filter pack method at the very low concentrations encountered at this site, or the sampling of coarser particles by this method (due to high flow rate and open-face sampling) with higher concentrations of sea salt sulfate. The DELTA methodology was unchanged for the duration of the AGANet dataset (1999–2015) in this manuscript, which allows a consistent assessment of overall trends in the SO_4^{2-} data.

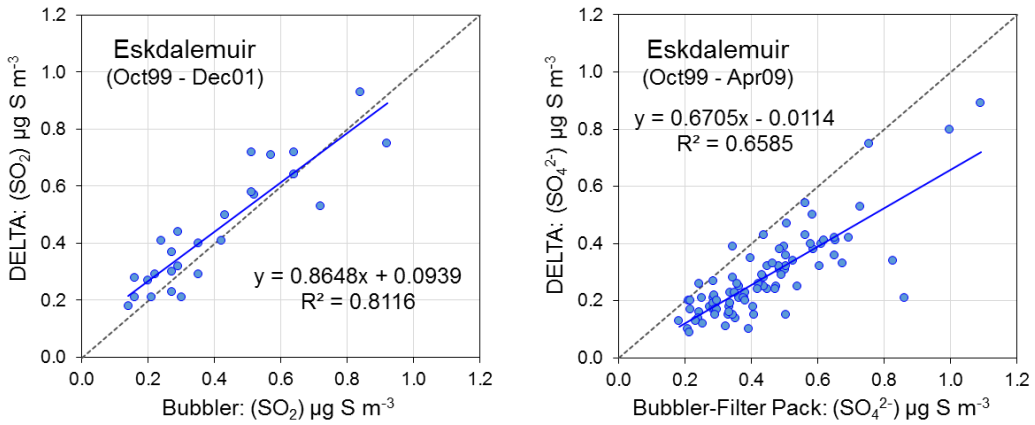

	AGANet DELTA: SO_2	Bubbler: SO_2	AGANet DELTA: SO_4^{2-}	Filter Pack: SO_4^{2-}
Linear regression: R^2	0.812***		0.658***	
slope	0.865^{ns}		0.670***	
intercept	0.094*		0.011^{ns}	
mean (µg S m^{-3})	0.44	0.40	0.28	0.44
No. of observations (*n*)	26	26	87	87

Significance level (slope different from 1, intercept = 0): * $p < 0.05$, ** $p < 0.01$, *** $p < 0.001$. *ns* = not significant ($p > 0.05$)

Figure 3.5. Comparison of gaseous SO_2 and particulate SO_4^{2-} concentrations at the Eskdalemuir monitoring station (EMEP station code = GB0002R; UK-AIR ID = UKA00130) measured under the Acid Deposition Monitoring Program (ADMN, Hayman et al., 2007) with the corresponding gas and aerosol from the UK Acid Gases and Aerosol network (AGANet). ADMN values (EMEP, 2017b) are means of daily measurements for SO_2 by the bubbler method and SO_4^{2-} by the EMEP filter pack method (Hayman et al., 2007), matched to the AGANet sampling periods (monthly). Bubbler and filter pack measurements at Eskdalemuir terminated in December 2001 and April 2009, respectively. A summary of the regression analyses is provided in the table below the graphs.

3.4.2 AGANet data

Annual data from the AGANet (and also from the NAMN) are submitted to the Department for Environment, Food & Rural Affairs (Defra) UK-AIR database (https://ukair.defra.gov.uk/, last access: 17 March 2017), in a format consistent with other UK Authority air quality networks and relevant reporting requirements. Every concentration value is labelled with a validity flag and an EMEP flag (see http://www.nilu.no/projects/ccc/flags/index.html, last access: 23 March 2017). Ratified calendar year data are published from around June the year following collection. Currently, work is also in progress for the data to be made available from the EMEP database (http://ebas.nilu.no/, last access: 23 March 2017). All data used in this paper (up to 2015), except where specified, are accessed from the UKAIR website (Tang et al., 2017a, b).

3.4.3 Uncertainties in HNO_3 determination

HNO_3 data were corrected for sampling artefacts in the DELTA method with an empirical correction factor of 0.45 (see Sect. 3.3.6). Interferences in HNO_3 determination arise through the simultaneous collection of reactive oxidized nitrogen species on the K_2CO_3 coating that forms nitrate ions in the aqueous extracts of exposed denuders. Potential interfering species include HONO, NO_2, N_2O_5 and PAN, as well as other inorganic and organic nitrogen species. HONO is most likely to contribute to the interference, since it is collected effectively on a carbonate coating and concentrations of HONO have been reported to be comparable to, and in some places exceed HNO_3 in the UK (e.g. Kitto and Harrison, 1992; Conolly et al., 2016). Interference from NO_2 on the other hand should be small, since the reactivity of a carbonate coating surface towards NO_2 is low (Allegrini et al., 1987), with capture of NO_2 on carbonate ranging from 0.5 % to 5 % (Allegrini et al., 1987; Fitz, 2002) and their concentrations are also small at rural AGANet sites (< 10 µg NO_2 m^{-3}; Conolly et al., 2016). Tests by Steinle (2009) on the DELTA K_2CO_3 / glycerol coated denuders also confirmed low capture (*ca.* 3 %) of NO_2.

The correction factor was derived from two years of field intercomparison measurements at five sites across a range of pollutant concentrations across the UK, from a clean rural background site in southern Scotland (Auchencorth) to a polluted urban site (London, Cromwell road) in southern England (Tang et al., 2015). It is recognized that the correction factor to derive the "real HNO_3" signal from the carbonate coated denuders will also be dependent on the relative concentrations of HNO_3 to interfering species present in the atmosphere and likely to be both site and season specific. The 2 years of data indeed show this variability between sites and between seasons. Given the complexities of atmospheric chemistry of the large family of oxidized nitrogen species, further work is clearly needed to understand what the carbonate denuders are measuring, before an improved correction algorithm for the HNO_3 data can be developed with any confidence.

The empirical 0.45 HNO_3 correction factor is therefore at present a best estimate across a range of pollutant concentrations and seasons encountered in the UK, based on available test data from 5 sites. At the cleanest rural sites (e.g. Eskdalemuir), where a much smaller HONO and NO_2 interference of the DELTA HNO_3 signal is expected, the HNO_3 concentrations may be under-estimated after correction. This may partly explain the slope deviating from unity in the comparison of corrected DELTA TIN with EMEP filter pack TIN data (slope = 0.835, R^2 = 0.95) at Eskdalemuir (see Sect. 3.4.1.2). Conversely, at more polluted sites such as London that are affected by a larger interference from HONO and NO_2, the HNO_3 determination may be over-estimated after correction. Apart from two urban sites (London and Edinburgh), all other sites in the AGANet are rural, located away from traffic, and the 0.45 correction factor should be more representative.

Since January 2016, the DELTA denuder sample train configuration in AGANet was changed to two NaCl coated denuders (selective for HNO_3, e.g. Allegrini et al., 1987), with a third K_2CO_3 / glycerol coated denuder to collect SO_2. At three sites (Auchencorth, Bush OTC and Stoke Ferry), parallel measurements of the old configuration (two K_2CO_3 / glycerol coated denuders)

and new configuration (two NaCl coated denuders + K_2CO_3 / glycerol coated denuder) were conducted over 12 months in 2016. In the new configuration, nitrates measured on the NaCl denuders are reported as HNO_3, whereas nitrate on the K_2CO_3 denuder are assumed to come from other oxidized nitrogen species and are not reported. Comparing the sum of nitrate concentrations from the new (2× NaCl + 1× K_2CO_3) with the old (2× K_2CO_3) configurations indicated matching capture of total nitrate by the two parallel systems (new / old nitrate ratio = 0.95). A comparison of nitrate concentrations on the 2× NaCl denuders only (new configuration) with the 2× K_2CO_3 denuders (old configuration) yielded an average ratio of 0.42, lending further support to the 0.45 empirical factor. Additionally, the new sample train configuration is providing an extensive dataset which will allow the magnitude of HNO_3 interference at each site to be quantified, by comparing the amount of nitrate measured on the 2× NaCl and K_2CO_3 coated denuders.

Initial analysis of 2016 data (unpublished data) showed that the mean ratio of nitrate on NaCl : K_2CO_3 of all sites was 0.44, ranging from 0.31 (Bush OTC) to 0.59 (Moorhouse). Seasonally, the average monthly ratio (taken as the mean across all sites for each month) was lowest in winter (0.25 in December and 0.27 in January) and highest between May to June (0.59, 0.56 and 0.57). It may therefore be possible to derive an improved correction algorithm that is both site and season specific, and work is ongoing to make this assessment. A detailed assessment of sampling artefacts and uncertainties in the DELTA method and the effects of a method change in the AGANet forms the subject of a next paper that is currently in preparation.

3.4.4 Spatial patterns in relation to pollutant sources and transport

In Fig. 3.6, the spatial patterns for each of the gas and aerosol components measured are shown in the annual maps for the example year 2013. A gradient in the concentrations of acid gases HNO_3 and SO_2, and related aerosols NO_3^- and SO_4^{2-} can be seen across the UK, highest in the south and east (combustion or vehicular sources and long-range transboundary pollutant transport from Europe) and lowest in the north and west of the UK (fewer sources, furthest from influence of Europe). The ranges in site-annual mean concentrations (µg molecule m^{-3}) in 2013 for the gases were as follows: HNO_3: 0.12–1.2; HCl: 0.15–0.52; SO_2: 0.10 – 1.08, while those for aerosol were as follows: NO_3^- : 0.33– 3.1; Cl^-: 0.54–3.3; SO_4^{2-}: 0.35–1.2; Na^+: 0.35–1.8; Ca^{2+}: < lod–0.11; Mg^{2+}: 0.03–0.19.

The largest HNO_3 concentrations were measured at the London Cromwell site (2013 site annual mean = 1.3 µg HNO_3 m^{-3} *cf*. 2013 mean of 30 sites = 0.40 µg HNO_3 m^{-3}). London and Edinburgh are the only two urban sites in the AGANet, with the other 28 sites all in rural environments. HNO_3 concentrations in Edinburgh, the capital of Scotland with a population that is 18 times smaller than London (0.5 million *vs*. 8.8 million), is about 2 times lower than London, but larger than the national average (2013 annual mean = 0.58 µg HNO_3 m^{-3}).

For SO_2, the highest concentrations were recorded at Sutton Bonington due to close proximity to the 2000 MW capacity coal-fired Ratcliffe-on-Soar power station (2 km North). A peak monthly concentration of 10.9 µg SO_2 m^{-3} was recorded in May 2000 at this site, with an annual mean concentration of 5.9 µg SO_2 m^{-3} for that year that was also 3 times higher than the national average (mean of 12 sites = 1.9 SO_2 m^{-3} *cf*. mean of 11 sites (excl. Sutton Bonington = 1.5 SO_2 m). At remote sites further away from sources, concentrations of HNO_3 and SO_2 are smaller, e.g. Lough Navar in Northern Ireland (2013 annual mean: 0.15 µg HNO_3 m^{-3} and 0.21 µg SO_2 m^{-3}) and Strathvaich Dam in north-western Scotland (2013 annual mean = 0.17 µg HNO_3 m^{-3} and 0.18 µg SO_2

m^{-3}). NO_3^- and SO_4^{2-} as secondary aerosols have longer residence times in the atmosphere and are expected to be more spatially homogeneous than their precursor gases. The spatial distribution in concentrations of particulate NO_3^- (0.33–3.1 µg m^{-3}) and SO_4^{2-} (0.35–1.2 µg m^{-3}) are however similar to that of HNO_3 (0.12–1.3 µg m^{-3}) and SO_2 (0.10–1.1 µg m^{-3}), with no clear differences in the main regional patterns from only 30 sites.

HCl is mostly emitted from coal combustion and the highest concentrations are in the source areas in the southeast and south-west, and also in central England (north of Ratcliffe-on-Soar power station). There is also a marine source for HCl formed by the reaction of sea salt with HNO_3 and H_2SO_4 (Roth and Okada, 1998; Ianniello et al., 2011) that may contribute to additional enhancement of local to regional HCl concentrations. The spatial distributions of Cl^- and Na^+ were similar, with largest concentrations at the coastal sites Goonhilly in south-western England and Lerwick in the Shetland Isles, highlighting the importance of marine sources to the sea salt (NaCl) aerosol. Further away from the coast and influence of marine aerosol, the smallest concentrations of Cl^- and Na^+ are measured in the west of the country (Lough Navar in Northern Ireland and Cwmystwyth in mid-Wales) and most of Scotland (with the exception of Shetland). Mg^{2+} is also seen to show a similar spatial distribution to Na^+ and Cl^-, which suggests that it may be in the form of $MgCl_2$, although the range of concentrations at sites are small (0.03–0.19 µg m^{-3}). There is however no clear spatial pattern for Ca^{2+}, but since concentrations are mostly at or below LOD, any assessment of this component is highly uncertain.

In the case of NH_3, the extensive spatial heterogeneity seen is related to large variation in emission sources at ground level across the UK (Tang et al., 2018). Aerosol NH_4^+, as expected for a secondary component, show a less variable concentration field. The spatial distribution of NH_4^+ is similar to SO_4^{2-} and NO_3^- over the UK (Fig. 3.6), due to the close coupling between species from the formation of particle phase $(NH_4)_2SO_4$ and NH_4NO_3 (see next section).

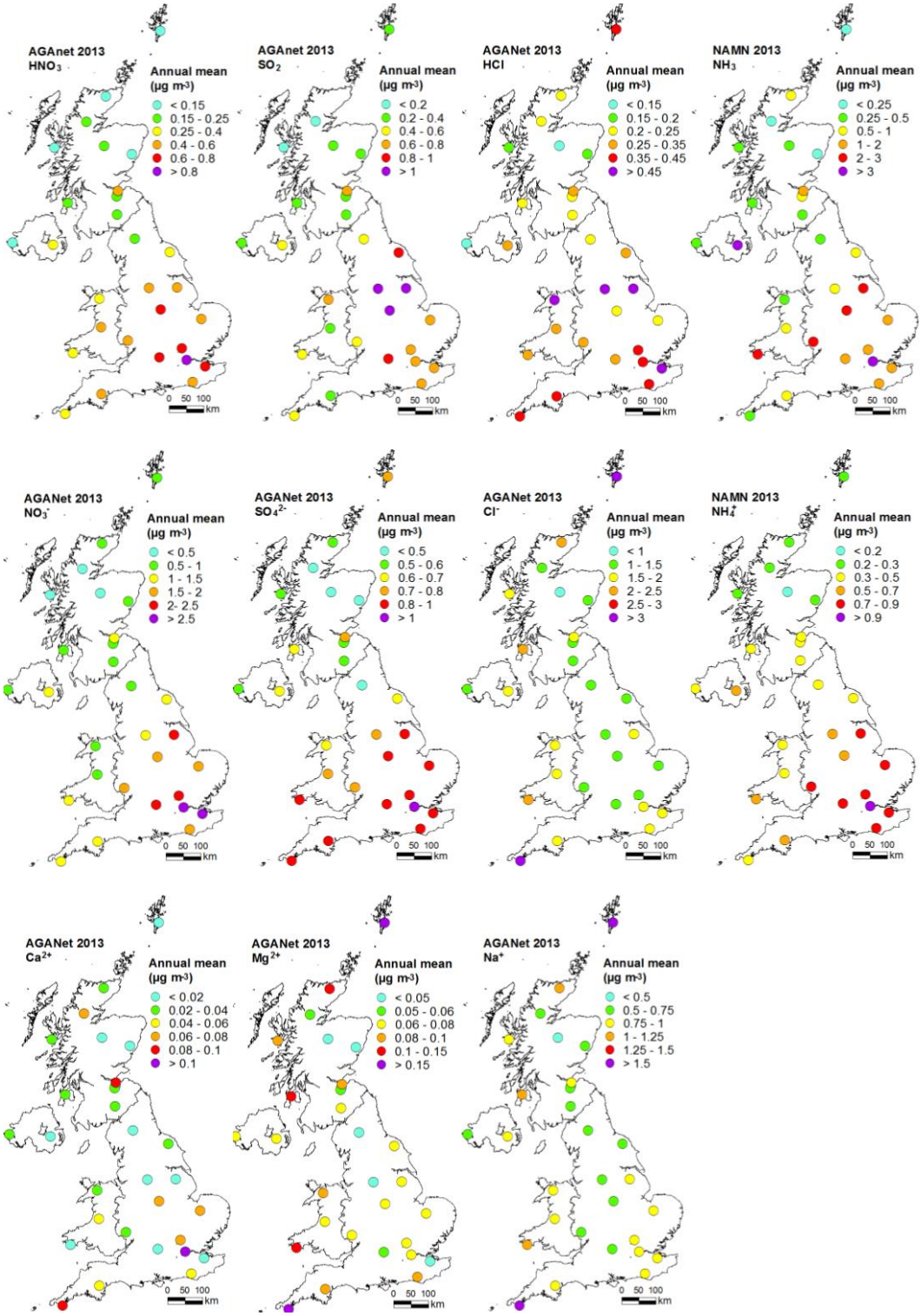

Figure 3.6. Annual mean monitored acid gas (HNO_3, SO_2, HCl) and aerosol (NO_3^-, SO_4^{2-}, Cl^-, Na^+, Ca^{2+}, Mg^{2+}) concentrations from the UK Acid Gas and Aerosol Monitoring Network (AGANet) across the UK from annual averaged monthly measurements made in 2013. NH_3 and NH_4^+ measured at the same time from the UK National Ammonia Monitoring Network (NAMN, Tang et al., 2018) are also shown alongside for comparison.

3.4.5 Correlations between gas and aerosol species

Correlations plots between the gas and aerosol phases of the different components are shown in Fig. 3.7, with a summary of the regression results provided in Table 3.2. The comparison of gas phase concentrations show that gaseous NH_3 is poorly correlated with either SO_2 or HNO_3, as might be expected since the emission sources of these pollutants are different.

(a) **Gaseous components**

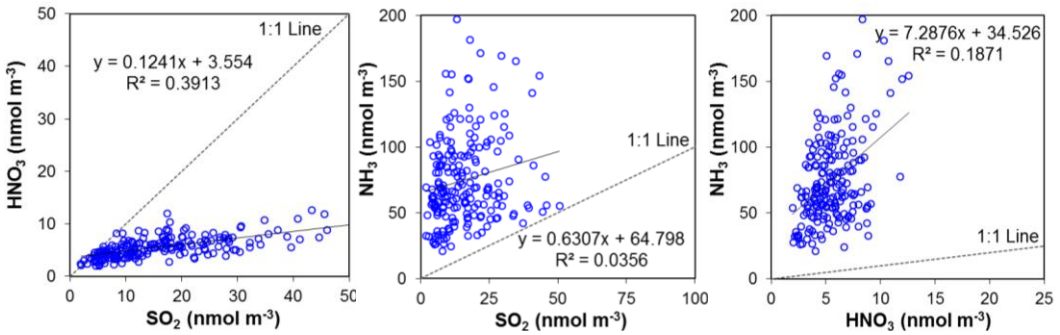

(b) Particulate components

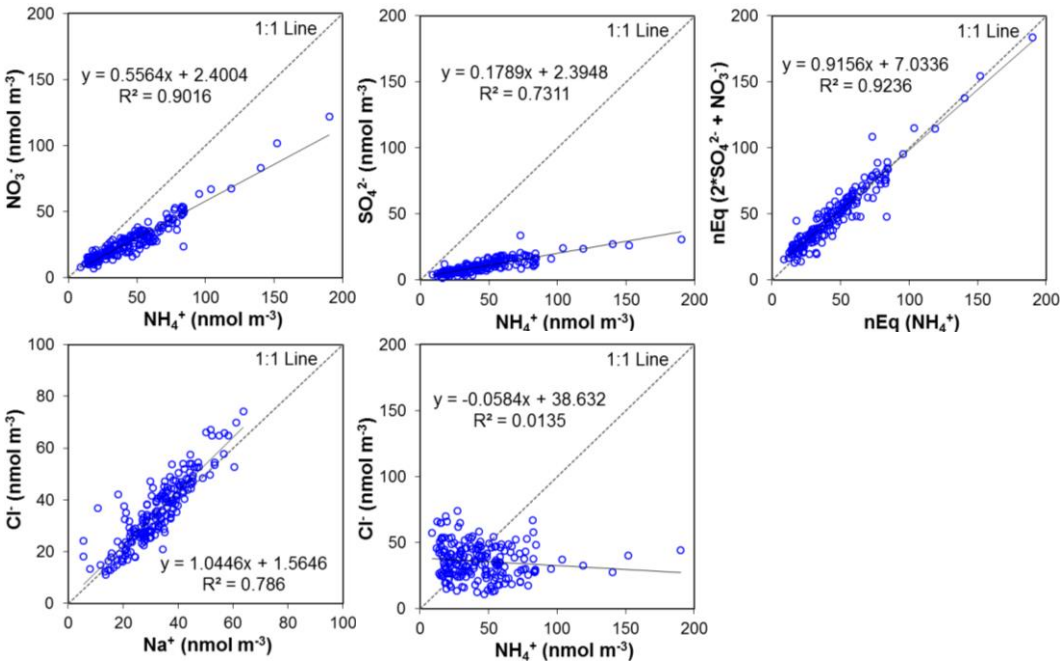

Figure 3.7. Scatter plots between concentrations of (a) gaseous species HNO_3, SO_2, and NH_3, and (b) particulate species NO_3^-, SO_4^{2-}, NH_4^+, Cl^-, and Na^+ from mean monthly measurements (1999–2015) from the 12 sites in the UK Acid Gas and Aerosol Monitoring Network (AGANet) that were operational over the whole period. NH_3 and NH_4^+ data are from the UK National Ammonia Monitoring Network (NAMN, Tang et al., 2018) made at the same time. Each data point represents a single monthly DELTA measurement.

Table 3.2. Correlation coefficients (R^2) for different species across the 30 measurement sites

	HNO_3	HCl	SO_2	NO_3^-	Cl^-	SO_4^{2-}	NH_4^+	Na^+
HNO_3	1.00	0.25***	0.39***	0.45***	0.07***	0.54***	0.49***	0.02*
HCl	-	1.00	0.21***	0.14***	0.01^{ns}	0.24***	0.19***	0.04**
SO_2	-	-	1.00	0.30***	0.00^{ns}	0.47***	0.37***	0.01^{ns}
NO_3^-	-	-	-	1.00	0.00^{ns}	0.61***	0.90***	0.02^{ns}
Cl^-	-	-	-	-	1.00	0.04**	0.01^{ns}	0.79***
SO_4^{2-}	-	-	-	-	-	1.00	0.73***	0.00^{ns}
NH_4^+	-	-	-	-	-	-	1.00	0.00^{ns}
Na^+	-	-	-	-	-	-	-	1.00

*Significance level: * $p < 0.05$, ** $p < 0.01$, *** $p < 0.001$. ns = not significant ($p > 0.05$)*

In the case of the acid gases however, the significant correlations between HNO_3 : SO_2 ($R^2 = 0.35$), HNO_3 : HCl ($R^2 = 0.25$), and SO_2 : HCl ($R^2 = 0.21$) may be related to similarity in the regional distribution of their emissions. These comparisons show that there is on average 5 times more NH_3 than SO_2 and 13 times more NH_3 than HNO_3 at the AGANet sites (on a molar basis), and that SO_2 concentration is nearly 3 times larger than HNO_3 (on a molar basis).

In the aerosol components, there is very high correlation between NO_3^-, SO_4^{2-}, and NH_4^+, and between Na^+ and Cl^-, but no discernible relationship between NH_4^+ and Cl^- (Fig. 3.7). The near 1 : 1 relationship in the scatter plot of the sum of NO_3^- and SO_4^{2-} (neq m^{-3}) vs. NH_4^+ (neq m^{-3}) (slope = 0.91, $R^2 = 0.93$), in the absence of any correlation between NH_4^+ and Cl^-, suggests that H_2SO_4 and HNO_3 in the atmosphere are fully neutralized by NH_3 to form $(NH_4)_2SO_4$, NH_4HSO_4 and NH_4NO_3 (Aneja et al., 2001). For Cl^-, the high correlation with Na^+ (slope = 1.04, $R^2 = 0.8$) lends support that the Cl^- measured in the DELTA are derived mainly from sea salt (NaCl). Similar to the relative concentrations of gases, NH_4^+ concentrations (on a molar basis) are larger than SO_4^{2-} and NO_3^-, but NO_3^- is in molar excess over SO_4^{2-}. The correlations between NH_4^+ and sum ($NO_3^- + 2\times SO_4^{2-}$), and for Na^+ and Cl^- forms the basis of ion balance checks in data quality assessment, and shows that robust data are obtained.

Seasalt aerosol, derived from sea spray, has essentially the same composition as seawater (Keene et al., 1986). The marine aerosol comprises two distinct aerosol types: (1) primary sea salt aerosol produced by the mechanical disruption of the ocean surface and (2) secondary aerosol, primarily in the form of non-sea salt (nss) sulfate and organic species, formed by gas-to-particle conversion processes such as binary homogeneous nucleation, heterogeneous nucleation and condensation (O'Dowd and Leeuw, 2007). It has been shown that the ratio of the mass concentrations of SO_4^{2-} and Cl^- to the reference Na^+ species in seawater may be used to estimate mass concentrations of non-sea salt SO_4^{2-} (nss_SO_4) and non-sea salt Cl^- (nss_Cl) in aerosol, according to Eqs. 4 and 5, respectively (Keene et al., 1986; O'Dowd and de Leeuw, 2007).

$$[nss\_SO_4] = [SO_4^{2-}] - (0.25 \times [Na^+]) \quad (4)$$

$$[nss\_Cl] = [Cl^-] - (1.80 \times [Na^+]) \quad (5)$$

Applying Eq. 4 to the SO_4^{2-} data in Fig. 3.7, nss_SO_4 is estimated to comprise on average 25 % (range = 3 % – 83 %, n = 187) of the measured total SO_4^{2-} aerosol. Regression of nss_SO_4 *vs*. NH_4^+ (slope = 0.18, intercept = 0.47, R^2 = 0.71) (Supp. Fig. S3.3) was not significantly different from the regression of total SO_4^{2-} vs. NH_4^+ (slope = 0.18, intercept = 2.4, R^2 = 0.73) (Fig. 3.7). Sources of nss_SO_4 are (i) biological oxidation of dimethylsulfide and (ii) oxidation of SO_2 (O'Dowd and de Leeuw, 2007). This analysis demonstrates that sea salt SO_4^{2-} aerosol makes up a significant and variable fraction of the total SO_4^{2-} measured, consistent with observations of the contribution by sea salt SO_4^{2-} to the total SO_4^{2-} in precipitation in the UK (ROTAP, 2012). The improved intercept from the nss_SO_4 regression (Supp. Fig. S3.3) suggests that nss_SO_4 are mainly associated with NH_4^+.

Estimated nss_Cl concentrations according to Eq. 4 was however negligible (mean = −0.09 µg m^{-3}, *n* = 188), compared to the total Cl^- (mean = 1.3 µg m^{-3}, *n* = 188). Studies have shown that part of the chloride of sea salt can be

substituted by SO_4^{2-} and NO_3^- through a reaction with H_2SO_4 and HNO_3, known as the Cl^- deficit (Ayers et al., 1999). The close coupling between Cl^- and Na^+ (near 1:1 relationship) presented here suggests that the measured Cl^- in the aerosol are mostly sea salt in origin, with no evidence of depletion of Cl^- from sea salt aerosols.

3.4.6 Seasonal variation in acid gases and aerosols

The average seasonal cycles for all gas and aerosol components derived from the mean of monthly data of all sites for the period 2000 to 2015 are compared in Fig. 3.8. Clear differences are observed in these seasonal cycles, influenced by local to regional emissions, climate, meteorology and photochemical processes.

HNO_3 is a secondary product of NO_x, but NO_x emissions are dominated by vehicular sources which are not expected to show large seasonal variations. Seasonal changes in chemistry and meteorology are therefore more likely to be a source of the observed variations in HNO_3 and NO_3^- (Fig. 3.8). A weak seasonal cycle is observed in HNO_3, with slightly higher concentrations in late winter and early spring that may be attributed to photochemical processes with elevated ozone in spring (AQEG, 2009) leading to formation of HNO_3 during this period (Pope et al., 2016). As discussed in Sect. 3.4.3, a constant correction factor was applied to all HNO_3 data, which does not take into account seasonal dependency. The concentrations in HNO_3 may therefore be over-estimated in winter (less HNO_3 formed from photochemical processes) and under-estimated in summer (larger HNO_3 concentrations due to increased $\cdot OH$ radicals for reaction with NO_2 to form HNO_3), masking the true extent in the seasonal profile.

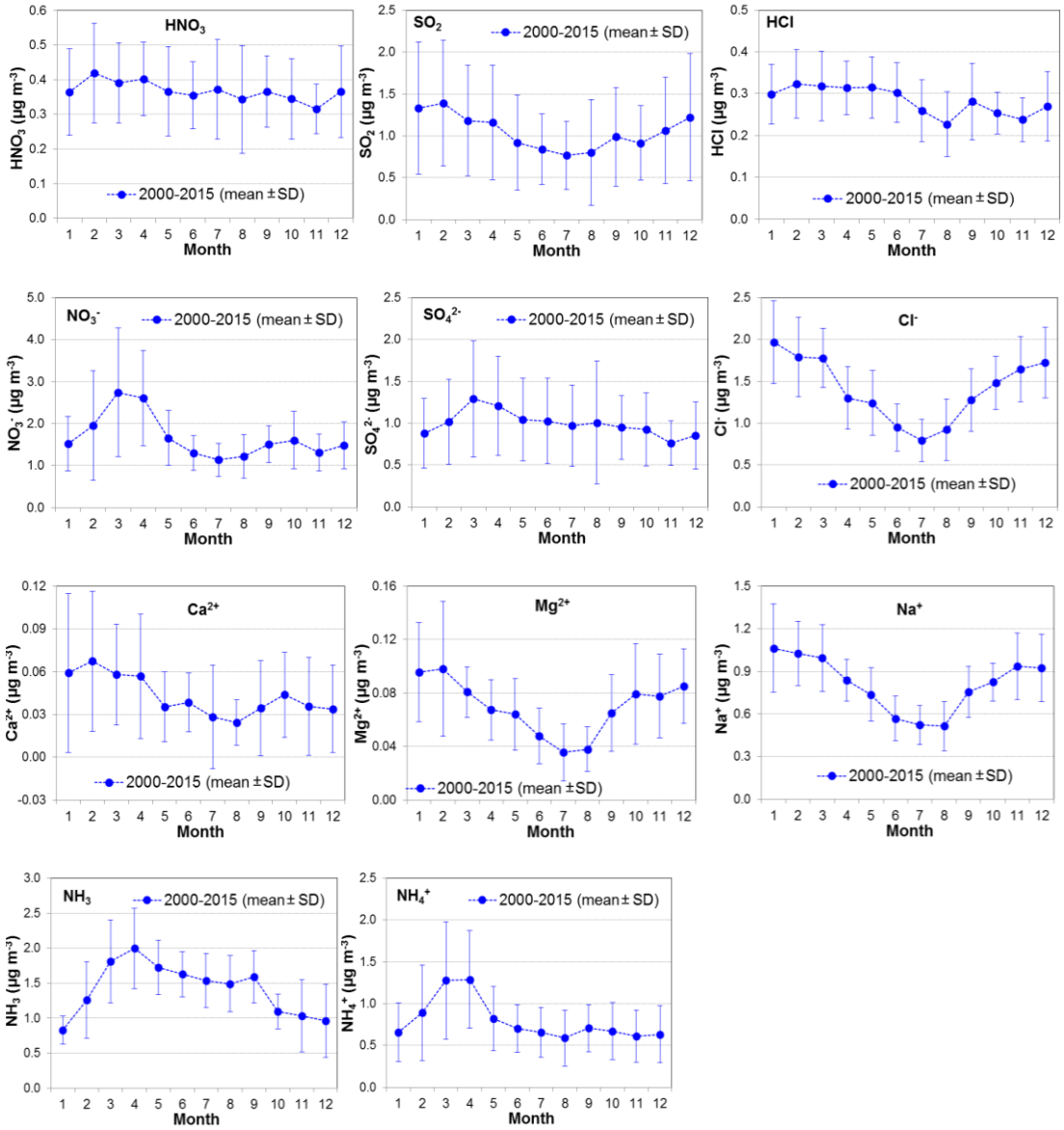

Figure 3.8. Average annual cycles for HNO_3, SO_2, HCl and aerosol NO_3^-, SO_4^{2-}, Cl^-, Na^+, Ca^{2+} and Mg^{2+} from the UK Acid Gases and Aerosol Monitoring Network (AGANet). The NH_3 and NH_4^+ concentrations measured at the same time in the UK National Ammonia Monitoring Network (NAMN, Tang et al., 2018) are also shown for comparison. Each data point in the graphs represents the mean ± SD of monthly measurements of all sites in the network.

In contrast, the seasonal cycle for particulate NO_3^- is more distinct with a large peak in concentrations that occur every spring, together with a second smaller peak in autumn (Fig. 3.8). NH_3, the main neutralizing gas in the atmosphere that reacts with HNO_3 to form NH_4NO_3, has a correspondingly large peak in concentration in spring, a second smaller peak in autumn, but with elevated concentrations in summer and lowest in winter (Fig. 3.8). Although particulate NO_3^- formation is dependent upon the availability of NH_3 for reaction with HNO_3, its concentration is also governed by the equilibrium that exists between gaseous HNO_3, NH_3, and particulate NH_4NO_3, the latter of which is appreciably volatile at ambient temperatures (Stelson and Seinfeld, 1982). Partitioning between the gas and aerosol phase is therefore also a key driver for their atmospheric residence times and concentrations. HNO_3 and NH_3 that are not removed by deposition may react together in the atmosphere to form NH_4NO_3 aerosol, when the concentration product $[NH_3],[HNO_3]$ exceeds equilibrium values. Since NH_4NO_3 is semi-volatile, any that is not dry or wet deposited can potentially dissociate to release NH_3 and HNO_3, effectively increasing their residence times in the atmosphere. The formation and dissociation in turn are strongly influenced by ambient temperature and humidity.

Warm, dry conditions in summer promote dissociation, increasing gas-phase HNO_3 relative to particulate-phase NH_4NO_3. This process accounts for the minima in NO_3^- concentrations (Fig. 3.8) and the highest ratio of HNO_3 to NO_3^- seen in July (Fig. 3.9). Cooler conditions in the spring and au tumn sees a larger fraction of the volatile NH_4NO_3 remaining in the aerosol phase. The largest peak in NO_3^- concentrations (Fig. 3.8) and the lowest HNO_3 : NO_3^- ratio in springtime (Fig. 3.9) is thus a combination of increased NO_3^- formation from reaction between higher concentrations of the precursor gases HNO_3 and NH_3, and increased partitioning to the aerosol phase in cooler, more humid climate. Import from long-range transboundary transport of particulate NO_3^-, e.g. from continental Europe into the UK, as discussed in Vieno et al. (2014, 2016) adds to the elevated NO_3^- concentrations. In winter, low temperature and high humidity also shifts the equilibrium to formation of NH_4NO_3 from the gas-phase

HNO_3 and NH_3. Since NH_3 concentrations are also lowest in winter, with less NH_3 available for reaction, NH_4NO_3 concentrations are correspondingly smaller in winter than in spring or autumn.

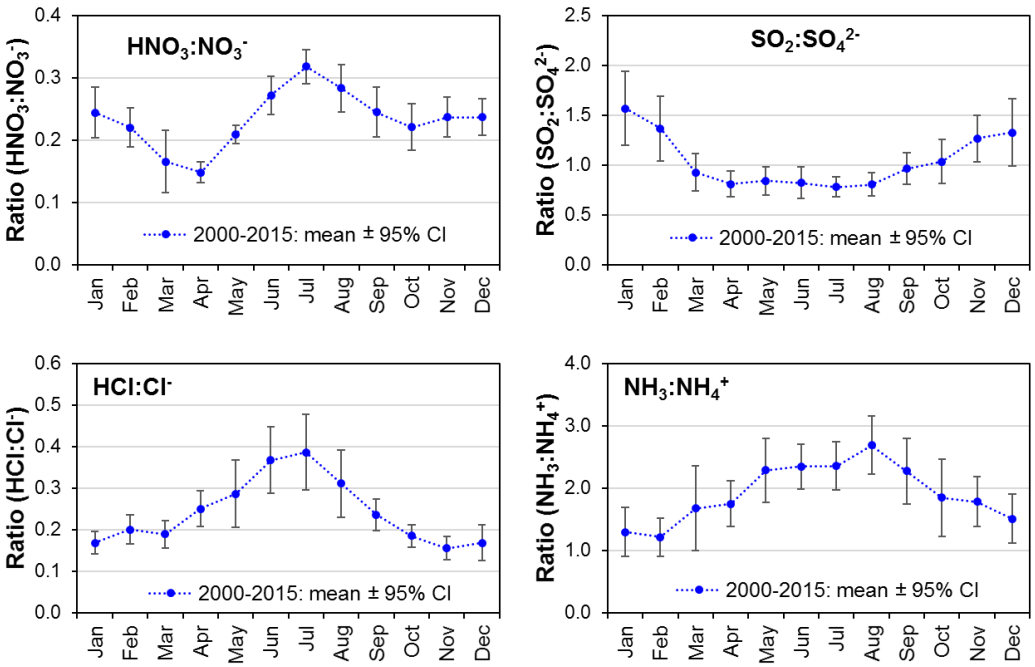

Figure 3.9. Average annual cycles in the ratios of gas:aerosol component concentrations. HNO_3, SO_2, HCl and aerosol NO_3^-, SO_4^{2-}, Cl^- data (annual mean, µg m^{-3}) are from the UK Acid Gases and Aerosol Monitoring Network (AGANet). NH_3 and NH_4^+ data (annual mean, µg m^{-3}) that are measured at the same time for the UK National Ammonia Monitoring Network (NAMN, Tang et al., 2018) are also shown for comparison. Each data point in the graphs represents the mean ± 95 % confidence interval (CI) of monthly measurements of 12 sites operational in the network over the period 2000 to 2015.

By contrast, SO_2 are highest in the winter, with concentrations exceeding summer values on average by a factor of 2 (Fig. 3.8). Higher emissions of SO_2 from combustion pro cesses (heating) during the winter months, coupled to stable atmospheric conditions resulting in build-up of concentrations at ground level contributes to the winter maximum. Since the reaction of SO_2 with NH_3 to form $(NH_4)_2SO_4$ is effectively irreversible (Bower et al., 1997), the ratio of the concentrations of SO_2 and SO_4^{2-} (Fig. 3.9) is largely governed by the availability of SO_2 and NH_3 to form $(NH_4)_2SO_4$. The temporal profile of SO_4^{2-}

has a peak in concentrations in spring, although not as pronounced as the NO_3^- peak (Fig. 3.8). This may be attributed to enhanced formation of $(NH_4)_2SO_4$, since peaks in concentrations of NH_3 and NH_4^+ also occur in spring (Fig. 3.8) and from the import of particulates from long range transboundary transport. Unlike SO_2, aerosol SO_4^{2-} concentrations are higher in summer than in winter, due to increased photochemical oxidation of SO_2 to H_2SO_4 and subsequent formation of sulfate aerosols in sunnier and warmer conditions (Mihalopoulos et al., 2007). In winter, lower SO_2 oxidation rates limits H_2SO_4 formation and therefore also the formation of $(NH_4)_2SO_4$.

Na^+ and Cl^- also have highest concentrations during winter, highlighting the importance of marine sources (more stormy weather) in winter for sea salt aerosol. The seasonal trends in Mg^{2+} are similar to Na^+, with maxima during winter and minima in summer (Fig. 3.8). While sea salt aerosols comprise mainly of NaCl, other chemical ions are also common in seawater, such as K^+, Mg^{2+}, Ca^{2+} and SO_4^{2-} (Keene et al., 1986). Some of the sea salt aerosol may therefore be in the form of $MgCl_2$. Magnesium is however also a crustal element, and so it is not as good as sodium as a tracer for sea salt. Similarly, calcium is also a rock-derived element and its presence in the atmosphere is thought to come from chemical weathering of carbonate minerals (Schmitt and Stille, 2005). The seasonal cycle of Ca^{2+} is similar to, but less pronounced than, Na^+ and Mg^{2+}. Measured concentrations of Ca^{2+} were mostly at or below the method LOD which makes interpretation uncertain, but the higher concentrations of Ca^{2+} in the winter months is likely to be both crustal dust and sea salt in origin.

Large inter- and intra-annual variability are also observed in the long-term mean monthly concentrations of gas and aerosol components, as illustrated in Fig. 3.10. In 2003, elevated concentrations of HNO_3 and NO_3^- (and also NH_4^+) were observed between February to April that were more pronounced than the normal peak in concentrations that occur in spring.

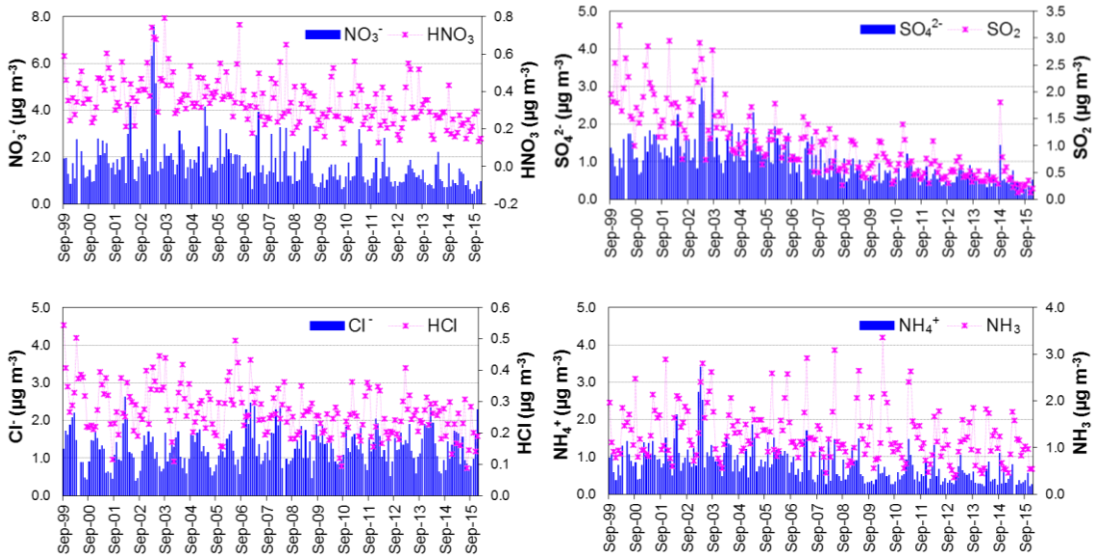

Figure 3.10. Monthly mean concentrations in gaseous HNO_3, SO_2, HCl and aerosol NO_3^-, SO_4^{2-}, Cl^- from the UK Acid Gases and Aerosol Monitoring Network (AGANet). Monthly mean concentrations of NH_3 and NH_4^+ that were measured at the same time in the UK National Ammonia Monitoring Network (NAMN, Tang et al., 2018) are also shown for comparison. Each data point in the graphs represents the mean of monthly measurements of 12 sites operational in the network over the period September 1999 to December 2015. The same plots for the full 30 site network from 2006 to 2015 are shown in Supp. Fig. S3.6.

The large spike in concentrations was of a sufficient magnitude to elevate the annual mean concentrations for 2003 of HNO_3 (0.54 µg m^{-3} *cf.* 0.39 and 0.36 µg m^{-3} for 2002 and 2004, respectively), particulate NO_3^- (2.98 µg m^{-3} *cf.* 1.99 and 1.93 µg m^{-3} for 2002 and 2004, respectively) and NH_4^+ (1.45 µg m^{-3} *cf.* 1.06 and 0.97 µg m^{-3} for 2002 and 2004, respectively). In comparison, a much smaller spike in elevated SO_4^{2-} concentrations resulted in a slight increase in annual average SO_4^{2-} (1.79 µg m^{-3} *cf.* 1.41 and 1.31 µg m^{-3} for 2002 and 2004, respectively) (Fig. 3.10). Meteorological back trajectory analysis of the period showed air masses coming across the UK from Europe, and the pollution episode was attributed to the formation and transport of NH_4NO_3 from Europe, since other gases (SO_2, HCl and NH_3) and particulate Cl^- were not affected (Vieno et al., 2014). At the same time, stable atmospheric conditions due to a persistent high-pressure system over the UK led to an accumulation of

pollutant concentrations from both local and import sources. A similar pollution episode, of a shorter duration, occurred in spring 2014. At the time, the observed elevated PM was blamed on a Saharan dust plume, but which in fact was then shown to be from long-range transport of NH_4NO_3 (Vieno et al., 2016). Although the 2014 episode was not sufficiently large to be captured in the monthly AGANet data, it reaffirms the substantial contribution of long-range transport into the UK of NH_4NO_3, with precursor gas emissions from outside of the UK presenting a major driver (Vieno et al., 2016).

A second, but smaller pollutant episode that was captured by the AGANet occurred in September 2014, with elevated concentrations of SO_2, HNO_3, SO_4^{2-}, NO_3^-, and NH_4^+ that came from the Icelandic Holuhraun volcanic eruptions (Twigg et al., 2016). The elevated SO_2 concentration in September 2014 led to a modest increase in annual concentrations in SO_2 for 2014 (0.58 µg m^{-3}, *cf*. annual mean = 0.54 and 0.27 µg m^{-3} for 2013 and 2015, respectively). For the other components (HNO_3, particulate SO_4^{2-}, NO_3^- and NH_4^+), the spikes in concentrations were smaller than for SO_2 and did not noticeably elevate their annual mean concentrations for that year. These pollution events together illustrate very clearly how short pollutant episodes can have a major influence on the measured annual concentrations in the UK, and that changes in meteorological conditions, coupled with long-range transboundary import can have a large effect on the UK concentration field.

3.4.7 Long-term trends at Eskdalemuir

At the Eskdalemuir rural background site, EMEP filter pack data in TIN (sum of HNO_3 and NO_3^-) and TIA (sum of NH_3 and NH_4^+) are available since 1989 (Sect. 3.4.1.2). In Fig. 3.11, the EMEP filter pack TIN and TIA time series (April 1989 to December 2000) is extended with AGANet (HNO_3 and NO_3^-) and NAMN (NH_3 and NH_4^+) DELTA data (September 1999 to December 2015), with an overlapping period of 14 months. The combined time series shows that the annual concentrations of TIN has halved in 26 years between 1990 to

2015, from 0.36 to 0.16 µg N m^{-3}, compared with a 3-fold reduction in NO_x emissions (from 928 to 302 kt NO_2−N) (NAEI, 2018) over the same period. For TIA, the 52 % decrease between 1990 to 2015 (from 0.93 to 0.45 µg N m^{-3}) is larger than the corresponding 13 % reduction in NH_3 emissions (from 265 to 231 kt NH_3−N) (NAEI, 2018). Speciated NH_3 and NH_4^+ data from NAMN over the period 2000 – 2015 shows that the decrease in TIA is mainly driven by NH_4^+, which decreased by 59 % between 2000 (annual mean = 0.62 µg NH_4^+ m^{-3}) and 2015 (annual mean = 0.25 µg NH_4^+ m^{-3}), compared with no change in NH_3 (annual mean 0.32 µg NH_3 m^{-3} in 2000, unchanged in 2015). This is consistent with findings by Tang et al. (2018) that contrary to the reported decrease in UK NH_3 emissions, NH_3 concentrations at background sites (defined by 5 km grid average NH_3 emissions < 1 kg N ha^{-1} yr^{-1}) are showing an indicative increasing trend, while at the same time, a large downward trend in particulate NH_4^+ is observed. Together, the AGAnet and NAMN are thus providing an important long-term dataset that distinguishes between the gas and aerosol phase, allowing gas–aerosol phase interactions to be explored.

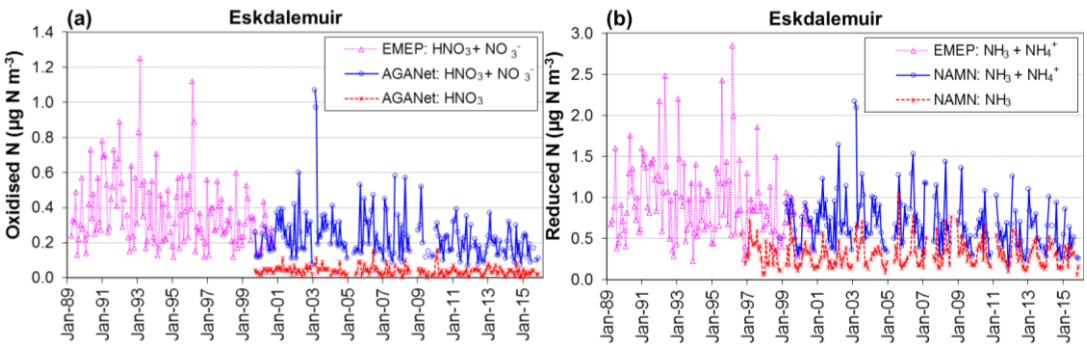

Figure 3.11. Long-term time series of (a) oxidized nitrogen (HNO_3 and NO_3^-) and (b) reduced nitrogen (NH_3 and NH_4^+) concentrations at Eskdalemuir (EMEP station code = GB0002R; UK-AIR ID = UKA00130). EMEP values (EMEP, 2017a) are monthly means of daily measurements for total inorganic nitrogen, TIN (sum of HNO_3 and NO_3^-) and total inorganic nitrogen, TIA (sum of NH_3 and NH_4^+) by the EMEP filter pack method (April 1989–November 2000), matched to the AGANet and NAMN sampling periods (monthly) where the measurements overlap. The AGANet and NAMN data are for gaseous HNO_3 and NH_3 and for the sum of (HNO_3 + NO_3^-) and sum of (NH_3 + NH_4^+), respectively, by the DELTA method. The AGANet HNO_3 values shown here includes the bias correction (Sect. 3.3.6).

An extended time series illustrating the continued decline in SO_2 and SO_4^{2-} has also been constructed by combining historic SO_2 and SO_4^{2-} measurement data at the Eskdalemuir site going back to December 1977 (see Sect. 3.4.1.3) with AGANet SO_2 and SO_4^{2-} data (September 1999 to December 2015) (Fig. 3.12). A substantial decline in SO_2 is observed, falling by 98 % from 4.5 µg S m^{-3} in 1978 to 0.07 µg S m^{-3} in 2015, in good agreement with similarly large reduction in UK SO_2 emissions over the same period of 95 % (from 2570 to 126 kt SO_2−S) (NAEI, 2018). The decrease in SO_4^{2-} is of a smaller magnitude, declining by 88 % from an annual mean concentration of 0.89 µg S m^{-3} in 1978 to 0.11 µg S m^{-3} in 2015, highlighting the non-linearity in relationship between the atmospheric gas and aerosol phase of sulfur at this background site.

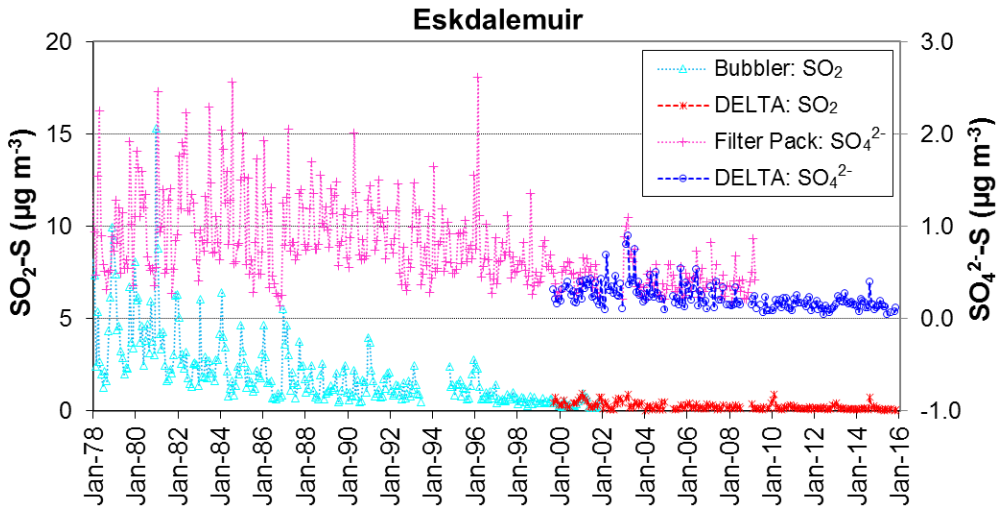

Figure 3.12. Long-term time series of SO_2 (December 1977–July 1993) and SO_4^{2-} (December 1977–December 2001) concentrations measured in the UK Acid Deposition Monitoring Network (ADMN) (Hayman et al., 2007) and the AGANet DELTA measurements (October 1999–December 2015) at the Eskdalemuir monitoring station (EMEP station code = GB0002R; UKAIR ID = UKA00130). ADMN values (EMEP, 2017b) are monthly means of daily measurements for SO_2 and SO_4^{2-} by a daily bubbler and filter pack method, respectively, matched to the AGANet sampling periods (monthly) where the measurements overlap.

3.4.8 Assessment of trends in relation to UK emissions

The long-term time series in annually averaged concentrations of the gas and aerosol components are compared in Figs 3.13a and b, respectively. Since there was a change in the number of sites during the operation of the AGANet, annually averaged data from the original 12 sites for the period 2000–2015 (1999 data excluded since AGANet started in September 1999) and from the full network (30 sites) for the period 2006–2015 are plotted alongside each other for comparison. From 2006–2015, the decreasing trends for all gas and aerosol components from the expanded 30 sites are seen to be similar to those from the original 12 sites. The annual mean concentrations in gas and aerosol components derived from the expanded 30 sites (2006–2015) or from the original 12 sites over the same period are also in general comparable (Table 3.3).

Table 3.3. Comparison of mean concentrations from the original 12 Acid gases and Aerosol Network (AGANet) sites *vs* the expanded 30 AGANet sites for the different gas and aerosol components. NH_3 and NH_4^+ measured at the same time in the UK National Ammonia Monitoring Network (NAMN, Tang et al., 2018) are also included for comparison. Each data point are the mean ± SD of annual mean concentrations over the period 2006 to 2015.

	Mean concentration (2006 – 2015), µg m^{-3}										
	HNO_3	**SO_2**	**HCl**	**NO_3^-**	**SO_4^{2-}**	**Cl^-**	**Na^+**	**Ca^{2+}**	**Mg^{2+}**	**NH_3**	**NH_4^+**
12 sites (mean±SD)	0.31± *0.06*	0.66 ± *0.24*	0.25 ± *0.04*	1.40 ± *0.31*	0.73 ± *0.25*	1.33 ± *0.09*	0.75 ± *0.07*	0.04 ± *0.03*	0.06 ± *0.01*	1.18 ± *0.16*	0.62 ± *0.18*
30 sites (mean±SD)	0.34 ± *0.06*	0.70 ± *0.25*	0.28 ± *0.04*	1.41 ± *0.26*	0.74 ± *0.23*	1.54 ± *0.09*	0.84 ± *0.08*	0.04 ± *0.02*	0.07 ± *0.01*	1.40 ± *0.16*	0.61 ± *0.16*

The exceptions are Na^+ and Cl^- that have higher mean concentrations from the 30 sites than the original 12 sites (Table 3.3), due to the addition of two coastal sites (Shetland and Rum), with larger contribution from sea salt. Larger HNO_3 concentrations are due to two urban sites, London and Edinburgh (higher NO_x emissions from vehicular traffic). The addition of three sites in high NH_3 emission (agricultural) areas (Rosemaund in England, Narberth in Wales and Hillsborough in Northern Ireland) also elevated measured annual mean NH_3 concentrations. The comparisons here thus illustrate very clearly the need

to consider the effect of site changes in a national network and the importance of maintaining consistency and site continuity for assessing long-term trends.

In the gas phase, SO_2 decreased 7-fold from an annual mean concentration of 1.9 µg SO_2 m^{-3} in 2000 to 0.25 µg SO_2 m^{-3} in 2015 (n = 12), compared with more modest reductions in HNO_3 (from 0.35 to 0.21 µg HNO_3 m^{-3}), NH_3 (from 1.4 to 1.0 µg NH_3 m^{-3}) and HCl (from 0.31 to 0.20 µg HCl m^{-3}) over the same period (Fig. 3.13a). Particulate SO_4^{2-}, NO_3^-, and NH_4^+ also decreased in concentrations with time, but unlike their gas phase precursors, the trends of these aerosol components track each other closely, differing only in the magnitude of concentrations (Fig. 3.13b), illustrating very clearly the close coupling between these components. On the other hand, the absence of a trend in the particulate Cl^- is likely to reflect the sea salt origin of Cl^- which is not expected to vary over time.

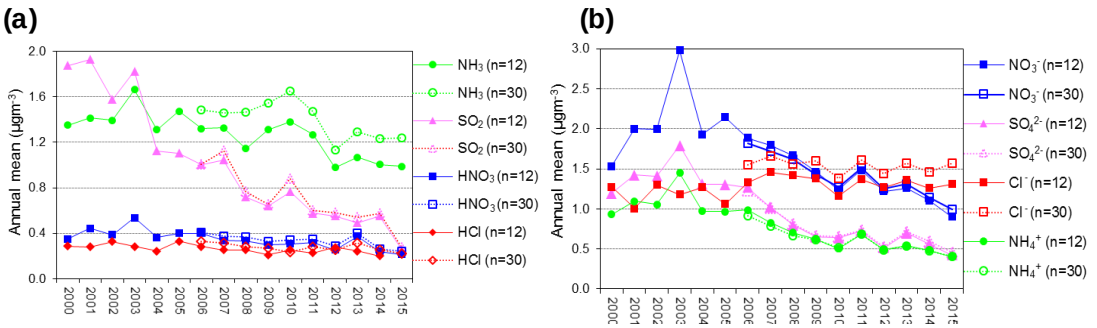

Figure 3.13. Long-term trends in (a) acid gases and (b) aerosol concentrations (µg molecule m^{-3}) from the UK Acid Gases and Aerosol Network (AGANet). Each data point represents the annually averaged measurements from either the original 12 AGANet sites for the 16 year period from 2000 to 2015 or the expanded 30 AGANet sites for the 10-year period from 2006 to 2015. NH_3 and particulate NH_4^+ measured at the same time in the UK National Ammonia Monitoring Network (NAMN, Tang et al., 2018) are also included for comparison.

Important changes in the chemical climate is captured by the parallel monitoring of acid gases and aerosols in AGANet and of NH_3, NH_4^+ in NAMN. It is clear from the long-term data that there is substantial intra- (Fig. 3.10) and inter-annual variability in the annual mean concentrations of both the gas and aerosol phases (Fig. 3.13), in particular the spike in concentrations in 2003 (see Sect. 3.4.6) that buckles the trend. An interpretation of the direct

relationship between emissions and concentrations in the atmosphere is therefore not straight forward, as the concentrations are also influenced by other factors such as variations in meteorological conditions and long-range transboundary import into the UK.

In Fig. 3.14, the relative trends in UK NO_x, SO_2, HCl and NH_3 emissions (NAEI, 2018) are compared with the annually averaged gas and particulate concentrations measured in the AGANet and NAMN for (i) original 12 sites for the 16 year period from 2000 to 2015, (ii) original 12 sites for the 15 year period from 2001 to 2015 (because annual mean concentrations in 2000 for all components were smaller than in 2001–2006), and (iii) expanded 30 sites and also original 12 sites for the 10 year period from 2006 to 2015. All data were normalized to 0 for the start years in each of the comparison.

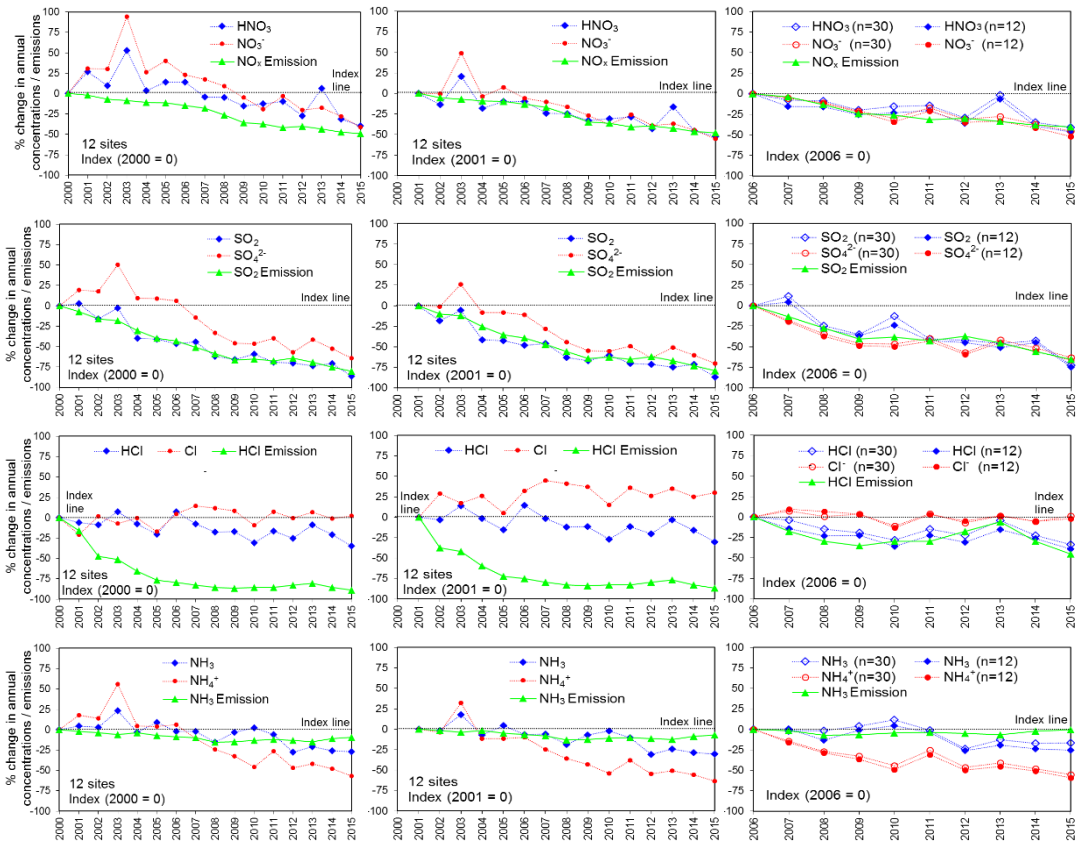

Figure 3.14. Relative trends in UK emissions (NAEI, 2018) and in annually averaged gas and particulate concentrations from the UK AGANet and UK National Ammonia Monitoring Network (NAMN, Tang et al., 2018) for (a) the original 12 sites for the 16 year period from 2000 to 2015, and (b) expanded 30 sites compared with the original 12 sites for the 10 year period from 2006 to 2015.

The long-term trends in HNO_3, SO_2, HCl and particulate NO_3^-, SO_4^{2-}, Cl^-, based on MK statistical trend analysis (Sect. 3.3.7) of annual mean measurement data are compared in Fig. 3.15 and summarized in Table 3.4 for the two time series: (i) the original 12 AGANet sites for the 16 year period from 2000 to 2015, and (ii) the expanded 30 AGANet sites for the 10 year period from 2006 to 2015. This approach avoids introducing bias as a result of changes in the sites and ensures site continuity for the long-term trend assessment. NH_3 and NH_4^+ concentrations from the NAMN that were measured at the same time at the AGANet sites were included for comparison and to aid interpretation of the acid gas and aerosol data.

To quantify changes in measured concentrations over time, annual trends (e.g. µg HNO_3 m^{-3} yr^{-1}) are estimated from the regression results of the MK tests. This is considered as providing a more reliable estimate of trend than comparing measured annual concentrations at the beginning and end of the time series, which is subject to bias due to substantial variability in annual concentrations between years (Tang et al., 2018). Changes in measured concentrations over time (MK percentage median change) in the time series are estimated from the MK Sen's slope and intercept (Eq. 6). MK annual trends and percentage median change are summarized in Fig. 3.15 and Table 3.4.

$$\% \text{ median change } = 100.\frac{[Yi-Yo)}{Yo} \qquad (6)$$

where (y_0) and (y_i) are estimated annual mean concentrations at the start and end of the selected time period, estimated from the slope and intercept of the LR or MK tests.

Table 3.4. Summary of Mann–Kendall (MK) time series trend analysis on annually averaged gas and aerosol concentrations from the UK Acid Gases and Aerosol Monitoring Network (AGANet) for (i) 12 sites that were operational over the period 2000 to 2015 and (ii) 30 sites that were operational over the period 2006 to 2015. NH_3 and NH_4^+ concentrations data measured at the same time from the UK National Ammonia Monitoring Network (NAMN, Tang et al., 2018) are also included for comparison. The 95 % confidence interval (CI) for the median trend and relative median change (%) are also estimated.

Annual mean data (µg m^{-3})	Mann-Kendall (MK): 12 sites (2000 - 2015)		Mann-Kendall (MK): 30 sites (2006 – 2015)	
	[a]Median annual trend & [95% CI] (µg y^{-1})	[b]Relative median change & [95% CI] (%)	[a]Median annual trend & [95% CI] (µg y^{-1})	[b]Relative median change & [95% CI] (%)
HNO_3	-0.0135** [-0.0067, -0.0180]	-45** [-26, -55]	-0.0167* [-0.0075, -0.0200]	-36* [-18, -41]
SO_2	-0.1010*** [-0.0729, -0.1255]	-81*** [-72, -91]	-0.0717** [-0.0300, -0.0108]	-60** [-33, -73]
HCl	-0.0057** [-0.0020, -0.0100]	-28** [-11, -42]	-0.0088* [0.0000, -0.0200]	-24* [0.0, -47]
NH_3	-0.0300** [-0.0125, -0.0433]	-30*** [-13, -39]	-0.0312^{ns} [0.0033, -0.0625]	-18^{ns} [+2.0, -31]
NO_3^-	-0.0810*** [-0.0520, -0.1125]	-52*** [-37, -63]	-0.0900** [-0.0580, -0.1300]	-43** [-30, -56]
SO_4^{2-}	-0.0750*** [-0.0450, -0.-0988]	-69*** [-52, -82]	-0.0675** [-0.0233, -0.1167]	-54** [-25, -78]
NSS_ SO_4^{2-}	-0.0733*** [-0.0500, -0.-1012]	-78*** [-64, -92]	-0.0575** [-0.0167, -0.1033]	-62** [-25, -86]
Cl^-	0.0079^{ns} [-0088, 0.0236]	9.6^{ns} [-9.5, 33]	-0.0075^{ns} [+0.0167, -0.0300]	-4.2^{ns} [+10, -16]
NH_4^+	-0.0500*** [-0.0375, -0.0675]	-62*** [-51, -74]	-0.0480** [0.0267, -0.0700]	-49** [-33, -64]

Significance level: * $p < 0.05$, ** $p < 0.01$, *** $p < 0.001$, ^{ns} non-significant ($p > 0.05$)
[a]Median annual trend = fitted Sen's slope of Mann-Kendall linear trend (unit = µg y^{-1})
[b]Relative median change estimated from the annual concentration at the start (y_0) and at the end (y_i) of time series computed from the Sen's slope and intercept (=100*[(y_i-y_0) /y_0])

Statistical trend analysis of monthly mean measurement data in the gas and aerosol components are also shown for comparison in Supp. Fig. S3.3 (mean monthly data of 12 sites for period 2000–2015) and Supp. Fig. S3.4 (mean monthly data of 12 sites for period 2006–2015). MK annual trends and percentage median change, based on the monthly data (Supp. Tables S3.7, S3.8) were similar to the annual test results (Table 3.4). While not discussed further here, since assessment of long-term trends in this paper focuses on trends in annual mean concentrations for comparison with trends in estimated annual emissions, the monthly plots serves to illustrate the large intra-annual variability of concentrations in gases and aerosols.

3.4.8.1 Trends in HNO_3 and NO_3^- *vs* NO_x emissions

The overall downward trends in HNO_3 and NO_3^- are seen to be broadly consistent with the −49 % fall in estimated NO_x emissions (NAEI, 2018) over the 16 year period between 2000 and 2015 (Fig. 3.14). Reductions in combustion (power stations and industrial) and vehicular sources (fitting of catalytic converters), coupled to tighter regulations are major contributory factors to the decrease in UK NO_x emissions. The rate of reduction however stagnated in the period 2009 and 2012 (improvement in emissions abatement offset by proportionate increase from diesel combustion and increase in vehicle numbers), followed by a 16 % decrease between 2012 and 2015 due to the closure of a number of coal-fired power stations.

It is notable that the first 6 years (2000–2006) of HNO_3 and NO_3^- annual data show substantial variability between years and in particular is dominated by the large 2003 peak in concentrations (see Sect. 3.4.6). This highlights the sensitivity of the trend assessment to the selection of a reference start for the time series, since the annual mean concentrations of both HNO_3 and NO_3^- in 2000 are in fact smaller than concentrations in the following 6 years. Re-analysis of the same annual data normalized against 2001 instead of 2000 takes the relative trend lines for HNO_3 and NO_3^- much closer to the relative trend line in NO_x emissions. In the later period between 2006 and 2015, the relative trend lines in HNO_3 and NO_3^- derived from the mean of either 12 or 30 sites were not significantly different, and the relative trend lines in emission and concentrations followed each other closely (Fig. 3.14).

Results of MK tests showed that the reductions in annual HNO_3 concentrations are statistically significant for both time series (Fig. 3.15; Table 3.4). The MK percentage median change in annual mean HNO_3 was −45 % (2000– 2015, n = 12) and −36 % (2006–2015, n = 30), consistent with the −49 % and −40 % fall in estimated NO_x emissions over the corresponding periods (Table 3.5). The decrease in HNO_3 is accompanied by a larger decrease in particulate NO_3^- (2000–2015: MK = −52 % (n = 12), 2006–2015: MK = −43 % (n = 30)) (Table

3.4) and an indicative small increasing trend is observed in the ratio of HNO_3 to NO_3^- with time (Fig. 3.16), hinting at an increased partitioning to the gas phase. Since HNO_3 is one of the major oxidation products of NO_x, through reaction with $OH\cdot$ or heterogeneous conversion of N_2O_5, it provides an important measure of the fraction of NO_x emissions that is oxidized and signals any long-term changes in the atmospheric processing timescales of NO_x over the country. NO_2 is measured at 24 rural sites across the UK in the UKEAP NO_2-net, with 11 sites collocated with the AGANet (Conolly et al., 2016). The long-term time series in the data also showed a matching decreasing trend in network averaged NO_2 concentrations with NO_x emissions between 2000 and 2015, with annual mean NO_2 concentrations across the network falling 2-fold to 4 µg NO_2 m^{-3} in 2015 (Conolly et al., 2016). Despite the uncertainty in corrected HNO_3 data (Sect. 3.4.3), the encouraging agreement between trends in HNO_3 and NO_2 concentrations and NO_x emissions lends support to a linear response in HNO_3 concentrations to reductions in NO_x emissions.

3.4.8.2 Trends in SO_2 and SO_4^{2-} *vs* SO_2 emissions

Unlike NO_x, there has been a more significant decline in SO_2, both in emissions and measured concentrations during this period (Fig. 3.14). Between 2000 and 2009, SO_2 emissions fell substantially by 66 % from 1286 to 432 kt SO_2. The reduction reflects mitigation measures introduced since the 1980s (fitting of flue gas desulfurization to coal fired power stations) to control S pollution, reductions in energy production and manufacturing and the switch from coal to gas at the same time. Similar to trends in NO_x emission, the decreasing trend in SO_2 emissions plateaued between 2009 and 2012 and then decreased again by a further 45 % between 2012 and 2015 following the closure of a number of coal-fired power stations, as well as conversion of some coal-fired stations to burn biomass.

Table 3.5. Comparison of percentage change in estimated UK NO_x, SO_2, and NH_3 emissions reported by the National Atmospheric Emission Inventory (NAEI, 2018) with % change between 2000 and 2015 (12 sites with complete time series) and between 2006 and 2015 (30 sites with complete time series) in annually averaged HNO_3/NO_3^- and SO_2/SO_4^{2-} concentrations from the UK Acid Gas and Aerosol Monitoring Network (AGANet), and annually averaged NH_3/NH_4^+ concentrations from the UK National Ammonia Monitoring Network (NAMN, Tang et al., 2018).

Components	2000 – 2015 (12 sites)		2006 – 2015 (30 sites)	
	UK emissions[b] % change	**MK Sen Slope** % relative median change[a]	**UK emissions**[c] % change	**MK Sen slope** % relative median change[a]
Gas HNO_3	-49 (NO_x)	-45**	-40 (NO_x)	-36*
Particulate NO_3^-		-52***		-43**
Gas SO_2	-80 (SO_2)	-81***	-65 (SO_2)	-60***
Particulate SO_4^{2-}		-69***		-54**
NSS_ SO_4^{2-}		-78***		-62**
Gas HCl	-87 (HCl)	-28^{ns}	-45 (HCl)	-24^{ns}
Particulate Cl^-		$+10^{ns}$		-4^{ns}
Gas NH_3	-9 (NH_3)	-30***	-0.7 (NH_3)	-18^{ns}
Particulate NH_4^+		-62***		-49**

Significance level: * $p < 0.05$, ** $p < 0.01$, *** $p < 0.001$, ^{ns} non-significant ($p > 0.05$)
[a]Relative median change calculated based on the estimated annual concentration at the start (y_0) and at the end (y_i) of time series computed from the Sen's slope and intercept ($=100*[(y_i-y_0)/y_0]$)
[b]UK emissions data from NAEI (http://naei.beis.gov.uk/data/, accessed 17/09/18)

Over the same period, the network annual mean concentration decreased from 1.9 µg SO_2 m^{-3} in 2000 to 0.25 µg SO_2 m^{-3} in 2015 (mean of 12 sites), continuing the long-term decline in SO_2 concentrations observed at the background Eskdalemuir site (Sect. 3.4.1.3) and across the UK (ROTAP, 2012). The relative trends in SO_2 emissions and concentrations tracked each other closely for all the time periods considered and it is clear that these decreases are highly correlated (Fig. 3.14). In the case of particulate SO_4^{2-} however, there is an apparent "gap" between emissions and concentrations in the trend normalized against the year 2000. Like NO_3^-, re-analysis of the same annual data normalized against 2001, instead of 2000, takes the relative trend line for SO_4^{2-} closer to the trend lines in both SO_2 emissions and concentrations (Fig. 3.14), thus again highlighting the potential bias in the use of a measured value at a specific time point in trend assessments when there is substantial inter-annual variability in the data.

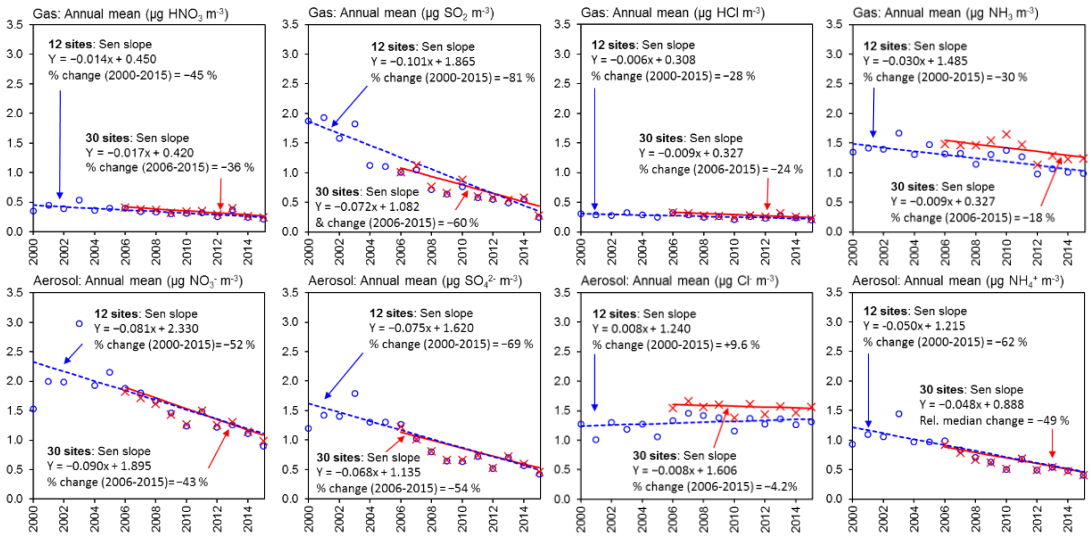

Figure 3.15. Time series trend analysis by non-parametric Mann-Kendall Sen slope on annually averaged gas and aerosol concentration data from the UK Acid Gases and Aerosol Monitoring Network (AGANet) of (i) 12 sites with complete time series over the period 2000 to 2015 and (ii) expanded 30 sites with complete times series over the period 2006-2015. NH_3 and NH_4^+ concentrations data measured at the same time in the UK National Ammonia Monitoring Network (NAMN, Tang et al.,2018) are also included for comparison.

From the MK trend analysis, the decrease in annual mean SO_2 concentrations of −81 % (2000–2015, *n* = 12), and −60 % (2006–2015, *n* = 30) (Fig. 3.15, Table 3.4) are consistent with the substantial reduction of −80 % and −64 % in SO_2 emissions over the two overlapping periods, respectively (Table 3.5). The decrease in both emissions and concentrations SO_2 is also almost twice as large as HNO_3 (Table 3.5), illustrating the greater success in mitigating sulfur than nitrogen and the increasing dominance of N components in the atmosphere compared with S, with larger decline in SO_2 than NO_x.

At the same time, the reduction in SO_2 emission and measured concentration is accompanied by a smaller negative trend in particulate SO_4^{2-} (2000–2015: −69 % MK; 2006– 2015: −54 % MK) (Table 3.5), with concentrations falling 3-fold from an annual mean of 1.2 µg SO_4^{2-} m^{-3} in 2000 to 0.42 µg SO_4^{2-} m^{-3} in 2015. The smaller decrease in particulate SO_4^{2-} compared with its gaseous precursor, SO_2, is similar to that observed at Eskdalemuir (Sect. 3.4.1.3). A similar picture is also seen in Europe, where atmospheric concentrations of

gas phase SO_2 decreased by about 92 % compared with a smaller reduction of 65 % in particulate SO_4^{2-} in response to sulfur emissions abatement over the 1990 – 2012 period in the EMEP region (EMEP, 2016). The ratio of SO_2 : SO_4^{2-} is also seen to show a decreasing trend over time (Fig. 3.16), with the largest change occurring between 2000 and 2006 that matches the period of largest decline in SO_2 emissions.

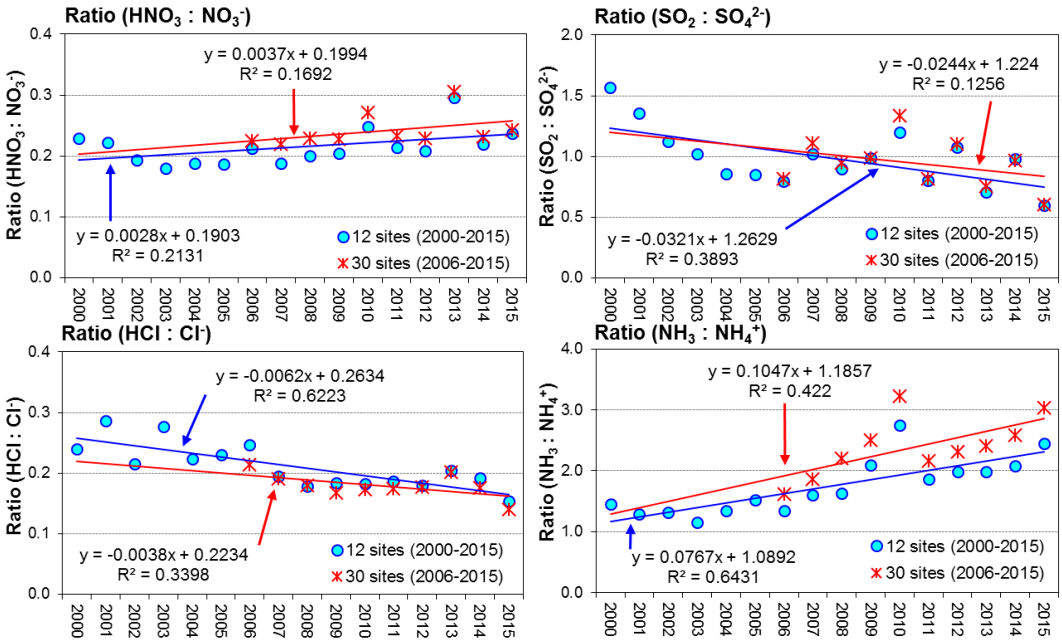

Figure 3.16. Long-term trends in the gas:aerosol ratio, from a comparison of the annual mean concentrations of 12 sites with complete time series from 2000 to 2015, and 30 sites with complete time series from 2006 to 2015, showing indicative differences in direction of trends in this ratio with time.

Sea salt SO_4^{2-} (ss_SO_4) aerosol, as discussed in Sect. 3.4.5, makes up a significant fraction of the total SO_4^{2-}. It is possible that the smaller reduction in particulate SO_4^{2-}, compared with SO_2, may be explained by an underlying increase in the relative proportion of ss_SO_4 to total SO_4^{2-}. To assess the contribution of ss_SO_4 to the observed trends in total SO_4^{2-}, ss_SO_4 concentrations (estimated according to Eq. 4 described in Sect. 3.4.5) and nss_SO_4 (= total SO_4^{2-} − ss_SO_4) are compared with the long-term trends in

total SO_4^{2-} in Fig. 3.17. Overall, there is no apparent trend in the long-term annual mean ss_SO_4 data, with concentrations in range of 0.16 to 0.21 µg SO_4^{2-}. Since ss_SO_4 is derived from an empirical relationship with Na^+ (Sect. 3.4.5), the long-term trend data for Na^+ is also included in the analysis (Fig. 3.17). Similar to ss_SO_4, there is no overall trend in the Na^+ data, with small inter-annual variability and annual mean concentrations in the range of 0.65–0.85 µg Na^+ m^{-3}. ss_SO_4 made up just 10 % of the total SO_4^{2-} in 2000, but by 2015, this had increased to just over 50 % due to the decrease in nss_SO_4 over that time. MK analysis of the nss_SO_4 (Table 3.4) showed decrease in concentrations of −78 % (2000– 2015) and −62 % (2006–2015), similar to that observed in SO_2 (−81 %: 2000–2015 and −60 %: 2006–2015), indicating a closer relationship between nss_SO_4 and SO_2 than between total SO_4^{2-} and SO_2.

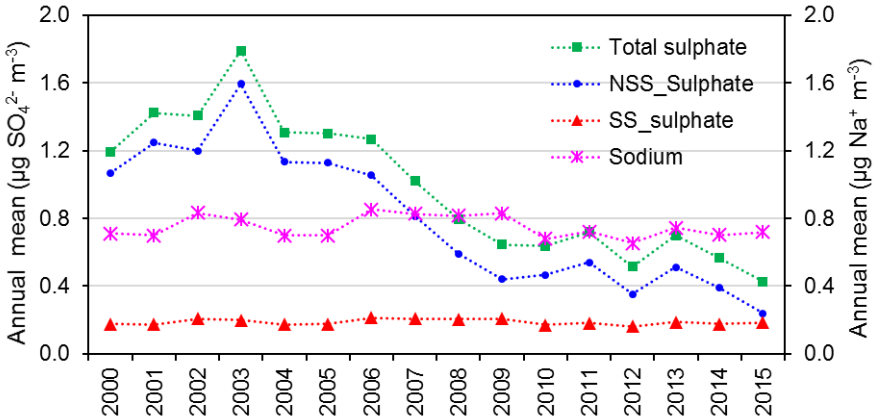

Figure 3.17. Comparison of long-term trends in annual mean concentrations of total sulfate (as determined from the amount of sulfate collected on the AGANet aerosol filter), nss_sulfate (estimated from the empirical relationship: [nss_SO_4] = [SO_4^{2-}] − (0.25 × [Na+]), ss_sulfate (Total − nss) and sodium. Each data point represents the annually averaged mean concentration of 12 sites for the 16 year period from 2000 to 2015.

3.4.8.3 Trends in HCl and Cl^- *vs* HCl emissions

HCl emissions in the UK also decreased substantially by 89 % between 2000 and 2015, from 82 to 9 kt in 2015 (NAEI, 2018), contrasting with a smaller, but non-significant decreasing trend in HCl concentrations (Figs. 3.14, 3.15, Table 3.5). The annual mean monitored concentrations in HCl over this period decreased from 0.30 µg HCl m^{-3} in 2000 to 0.19 µg HCl m^{-3} in 2015. Most of the reduction in HCl emissions occurred before 2006 (−79 %, from 82 kt in 2000 to 17 kt in 2006), with emissions plateauing since 2006 (NAEI, 2018) (Fig. 3.14). A corresponding decrease is not seen in the HCl measurement data, where concentrations remained fairly stable at between 0.31 µg m^{-3} HCl in 2000 to 0.33 µg m^{-3} HCl in 2006. Since 2006 however, the relative change in HCl emissions is closely tracked by changes in concentrations of both the annual mean data from the original 12 sites and from the expanded 30 sites in the AGANet, with the small peak in HCl emissions in 2013 also captured in the annual mean data. This part of the time series therefore clearly shows a direct relationship between emissions and concentrations.

So why is the most significant fall in HCl emissions between 2000 and 2006 not captured by the network? HCl is mainly released as point sources. Coal burning, particularly from coal-fired power stations, is responsible for the majority of UK emissions: 92 % in 1990 and 76 % in 2015, and reductions in HCl emissions in the UK inventory are largely as a result of declining coal use and the installation of emissions abatement measures at coal-fired power stations (implemented since 1993) aimed at reducing S that also coincidentally reduced HCl emissions. It may be that a network of only 12 sites in the early periods failed to capture peak emissions and changes in source areas. While there is an indicative, but non-significant decreasing trend in HCl (2000–2015: MK = −28 %, 2006–2015: MK = −24 %), no detectable trend in particulate Cl^- can be seen (Table 3.4). Since Cl^- is mainly associated with Na^+ (sea salt) in the AGANet measurements (Sect. 3.4.5), the absence of a trend in Cl^- (Fig. 3.15) and Na^+ (Sect. 3.4.8.3, Fig. 3.17) provides evidence of a constant background in sea salt in the UK atmosphere.

3.4.9 Trends in NH_3 and NH_4^+ *vs* NH_3 emissions

In comparison to the acid gases, there is a more modest decrease of −9 % in NH_3 emissions, from 254 kt NH_3 in 2000 to 231 kt NH_3 in 2015 (NAEI, 2018). This is smaller than the decrease seen in the annually averaged NH_3 concentrations at the 12 AGANet sites (2000–2015: −30 % MK) over the same period (Figs. 3.14, 3.15, Table 3.5). A recent assessment by Tang et al. (2018) showed that NH_3 trends are highly dependent on site selection and categorization of sites in the analysis. A more comprehensive analysis of a larger number of sites shows smaller reductions over time, whereas a significant decreasing trend in NH_3 concentrations was observed in the grouped analysis of sites in areas classed as dominated by pig and poultry emissions, contrasting with an upward (non-significant) trend for sites in cattle-dominated areas. Therefore there is a large degree of uncertainty in interpreting the trends in NH_3 concentrations from a subset of just 12 sites, since NH_3 emissions are dominated by agricultural emissions (> 80 %) that vary hugely on a local to regional scale across the UK.

At the same time, there is a larger decrease in particulate NH_4^+ concentrations (−62 % MK), contrasting with the smaller decrease in NH_3 concentrations over the period 2010–2015 (−30 % MK) (Table 3.4), with the NH_3 : NH_4^+ ratio also increasing with time (Fig. 3.16). This provides evidence for a shift in partitioning from the particulate phase NH_4^+ to the gaseous phase NH_3 in the UK data, discussed in Tang et al. (2018). The change in partitioning from particulate NH_4^+ to gaseous NH_3 is also occurring in other parts of Europe, where decreases in NH_3 concentrations have been smaller than emission trends would suggest, due to large decreases in SO_2 emissions (Bleeker et al., 2009; Horvath et al., 2009).

3.4.9.1 Changes in UK chemical climate

Atmospheric SO_2 concentrations in the UK has declined to very low levels over the 16 years of measurements in AGANet, with annual mean concentrations in 2015 (0.25 µg SO_2 m^{-3}, n = 12) approaching that of the other acid gases HNO_3 (0.21 µg HNO_3 m^{-3}, n = 12) and HCl (0.20 µg HCl m^{-3}, n = 12). NH_3 measured at the same time at the AGANet sites also decreased, but to a smaller extent, to a mean concentration of 1.0 µg NH_3 m^{-3} (n = 12) in 2015. The changes in measured concentrations of SO_2, HNO_3, HCl and NH_3 are consistent with the estimated decrease in emissions of SO_2, NO_x, HCl, and NH_3 since 2000. SO_2 is therefore no longer the dominant acid gas, with HNO_3 and HCl together contributing a larger fraction of the total acidity in the UK atmosphere.

Past studies have shown that the increasing ratio of NH_3 to SO_2 in the atmosphere leads to increased dry deposition of SO_2, accelerating the decrease in atmospheric SO_2 concentrations than would be achieved by emissions reduction alone (Fowler et al., 2001, 2009; ROTAP 2012). The dry deposition of SO_2 and NH_3, by uptake of the gases in a liquid film on leave surfaces, are known to be enhanced when both gases are present in a process termed “co-deposition” (Fowler et al., 2001). Where ambient NH_3 concentrations exceed that of SO_2, there is enough NH_3 to neutralize acidity in the liquid film and oxidize deposited SO_2, and maintain large rates of deposition of SO_2. With changes in the relative concentrations of acid gases in the UK and across Europe however, the deposition rates will increasingly be controlled by the NH_3 / combined acidity (sum of SO_2, HNO_3 and HCl) molar ratio, rather than based on SO_2 alone (Fowler et al., 2009).

To look at the UK situation, an analysis of the molar ratios of NH_3 to acid gases is presented in Fig. 3.18a. The molar ratio of NH_3 to acid gases (sum of SO_2, HNO_3 and HCl) increased with time, from 1.9 in 2000 to 4.7 in 2015, confirming that NH_3 is increasingly in molar excess over atmospheric acidity. The ratio of annual mean concentrations of NH_3 (80 nmol m^{-3}) to SO_2 (29 nmol m^{-3}) was

2.7 in 2000. By 2015, this ratio had increased to 15 (annual mean concentrations of NH_3 = 58 nmol m^{-3} *cf.* SO_2 = 4 nmol m^{-3}). Molar concentrations of HNO_3 (4 nmol m^{-3}) and HCl (6 nmol m^{-3}) were comparable to SO_2 in 2015, highlighting the increasing importance of HNO_3 and HCl in contributing to atmospheric acidity. A larger decrease in SO_2 (−81 %) than particulate sulfate (−69 %) in the AGANet data (Table 3.4) would appear at first to suggest that the large NH_3:SO_2 ratio is contributing to a more rapid decrease in SO_2 concentrations. However, when the sea salt fraction of SO_4^{2-} is removed from the sulfate trend (Sect. 3.4.8.2), the decrease in nss_SO4 (−78 %) is similar to SO_2 (−81 %) (Table 3.4). Since the decreasing trend in the ratio of SO_2 to SO_4^{2-} also appeared to stabilize after 2006 (Sect. 3.4.8.2), this would suggest that maximum deposition rates for SO_2 may have been reached with the smaller SO_2 concentrations since 2006.

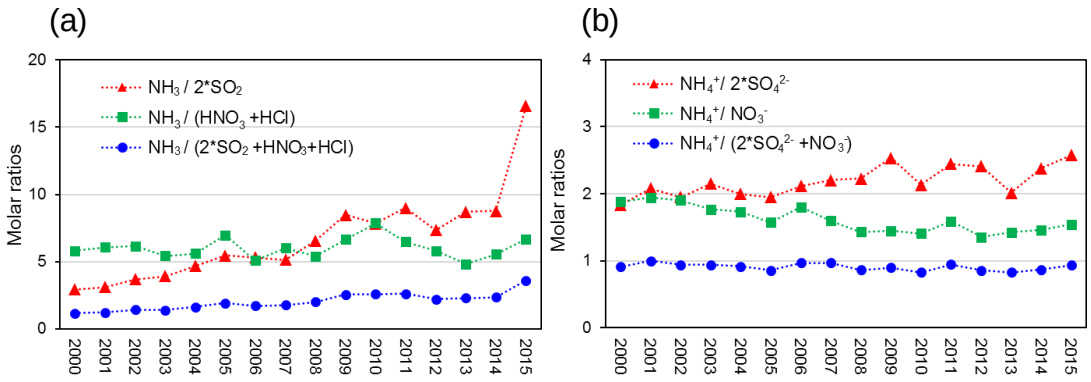

Figure 3.18. Long-term changes between 2000 and 2015 in (a) molar ratio of NH_3 to acid gases (SO_2, HNO_3, and HCl) and (b) molar ratio of particulate NH_4^+ to acid aerosols (SO_4^{2-} and NO_3^-) from measurements made at 12 sites in AGANet.

The substantial decrease in UK SO_2 emissions and concentrations, while UK NO_x emissions and concentrations remain relatively high in comparison, set against a much smaller decrease in NH_3 emissions and concentrations since 2000 is leading to changes in the respective particulate SO_4^{2-}, NO_3^- and NH_4^+ concentrations. Since the affinity of H_2SO_4 (oxidation product of SO_2) for NH_3 is much larger than that of HNO_3 and HCl, available NH_3 is first taken up by H_2SO_4 to form ammonium sulfate compounds (NH_4HSO_4 and $(NH_4)_2SO_4$), with any excess NH_3 then available to react with HNO_3 and HCl to form NH_4NO_3 and NH_4Cl. Analysis of the different particulate components in Sect. 3.4.5 showed that the ammonium aerosols are mainly made up of $(NH_4)_2SO_4$ and NH_4NO_3. With the large reduction in SO_2, more NH_3 is available to react with HNO_3 to form NH_4NO_3 and concentrations of NH_4^+ and NO_3^- are now observed to be in molar excess over SO_4^{2-}, providing evidence of a change in the particulate phase from $(NH_4)_2SO_4$ to NH_4NO_3 (Fig. 3.18b).

A change to an NH_4NO_3 rich atmosphere and the potential for NH_4NO_3 to release NH_3 and HNO_3 in warm weather, together with the surfeit of NH_3 also means that a larger fraction of the reduced and oxidized N is remaining in the gas phase as NH_3 and HNO_3. An increased partitioning to the gas phase may account for the larger decrease in particulate NH_4^+ (MK −62 % between 2000 and 2015, n = 12) and NO_3^- (MK −52 % between 2000 and 2015, n = 12) than NH_3 (MK −30 % between 2000 and 2015, n = 12), HNO_3 (MK −45 % between 2000 and 2015, n = 12) (Table 3.4) and the increase in gas to aerosol ratios (NH_3 : NH_4^+ and HNO_3 : NO_3^-) over the 16 year period (Fig. 3.16). A higher concentration of the gas-phase NH_3 and HNO_3 may therefore be maintained in the atmosphere than expected on the basis of the emissions trends in NH_3 and NO_x. Given the larger deposition velocities of NH_3 and HNO_3 compared to aerosols, more of the NH_3 and HNO_3 emitted will have the potential to deposit more locally with a smaller footprint within the UK.

Currently, the critical loads of acidity (sulfur and nitrogen) are exceeded by 44 % of the area of sensitive habitats in the UK (based on mean deposition data for 2012– 2014), whereas the figure for exceedance of eutrophication (nutrient nitrogen) is even larger, at 62 % (based on deposition data for 2012–2014) (Hall and Smith, 2016). Air quality policies have been very successful in abating SO_2 emissions (−80 %: 2000–2015) and moderately successful with NO_x emissions (−58 %: 2000–2015), with both on course to meet the emission reduction targets set out under the 2012 Gothenburg protocol and 2016 NECD. Difficulties in abating NH_3 is reflected in the smaller reduction in NH_3 emissions (−9 %: 2000–2015), with emissions increasing, rather than decreasing since 2013 and it is likely that abatement measures may be required to meet emission reduction targets. In recognizing the need to tackle the ammonia problem, the Code of Good Agricultural Practice (COGAP) was published under the UK government's Clean Air Strategy (launched in July 2018) as a step towards reducing NH_3 emissions from agriculture.

Based on the current emission trends and evidence from AGANet and NAMN long-term measurements, atmospheric N deposition from oxidized N (NO_x, HNO_3 and NO_3^-) and from reduced N (NH_3, NH_4^+) are likely to continue to exceed critical loads of N deposition over large areas of sensitive habitats, with implications for UK's commitment to maintain or restore natural habitats (e.g. Natura 2000 sites; Hallsworth et al., 2010) to a favourable conservation status under the EU Habitats Directive (Council Directive 92/43/EEC) and ecosystem monitoring under Article 9 and Annex V of Directive 2016/2284 (NECD). The changes are also relevant for human health effects assessment, since NH_4NO_3 and $(NH_4)_2SO_4$ are mainly in the fine mode and constitute a significant fraction of $PM_{2.5}$ that are associated with acute and chronic human health problems. The change in partitioning from $(NH_4)_2SO_4$ to NH_4NO_3, coupled to import of NH_4NO_3 from long-range transport (driven by emissions of NH_3 and NO_x from outside the UK) poses policy challenges in protection of human health from effects of air pollution particularly in urban areas where concentrations of the $PM_{2.5}$ precursor gases NO_x, SO_2 and NH_3 are higher.

3.5 Conclusions

The UK Acid Gases and Aerosol network (AGANet) is delivering, uniquely, a comprehensive UK long-term dataset of speciated acid gases (HNO_3, SO_2, HCl) and aerosol components (NO_3^-, SO_4^{2-}, Cl^-, Na^+, Ca^{2+}, Mg^{2+}) and also of NH_3 and NH_4^+ measured within the National Ammonia Monitoring Network (NAMN). Speciated measurements are made with an established low-cost DELTA denuder-filter pack methodology, allowing assessment of atmospheric chemical composition and gas-aerosol phase interactions. Other manual denuder-filter implementations designed for high time-resolution measurements are useful at selected locations for detailed analysis and model testing, but they are resource intensive and expensive. The DELTA monthly measurements on the other hand are cost-efficient for estimating annual mean concentrations, providing sufficient resolution for analysis of temporal trends and which can be operated at a large number of sites in the network to provide long-term trends and temporal/spatial patterns.

Large regional patterns in concentrations are observed, with the largest concentrations of HNO_3, SO_2, and aerosol NO_3^- and SO_4^{2-} in south and east England, attributed to anthropogenic (combustion, vehicular) and long-range transboundary sources from Europe, and smallest in western Scotland and Northern Ireland. HCl concentrations are also largest in the southeast, southwest and central England, attributed to dual contribution from anthropogenic (coal combustion) and marine sources (reaction of sea salt with HNO_3 and H_2SO_4 to form HCl). For Cl^-, this has a similar spatial distribution as Na^+, with highest concentrations of at coastal sites, reflecting their origin from marine sources (sea salt).

Distinctive temporal trends are established for the different components, with the seasonal variability influenced by local to regional emissions, climate, meteorology and photochemistry. A weak seasonal cycle is observed in HNO_3, with slightly higher concentrations in late winter and early spring, due to formation from photochemical production processes. Particulate NO_3^- and

SO_4^{2-} have highest concentrations in spring, coinciding with the peak in concentrations of NH_3 and NH_4^+, and are therefore likely to be attributed to formation of NH_4NO_3 and $(NH_4)_2SO_4$ from reaction with a surplus of higher concentrations of NH_3 at that time of year. Conversely, peak concentrations of SO_2, Na^+ and Cl^- occur during winter, likely from combustion processes (heating) for SO_2 and marine sources in winter (more stormy weather) for sea salt generation. Magnesium is a crustal elements, but which is also present in sea salt aerosols. The seasonal trend in Mg^{2+} is similar to Na^+, with maxima during winter and minima in summer; therefore some of the sea salt aerosol may be in the form of $MgCl_2$.

Enhancement of local to regional concentrations of reactive gases and aerosols in the UK from long-range transboundary transport of pollutants into the UK is highlighted by two pollution events, captured in the long-term AGANet monthly measurements. In 2003, a spring episode with elevated concentrations of HNO_3 and NO_3^- was driven by meteorology, with easterly winds transporting NH_4NO_3 formed in Europe into the UK and a high pressure system over the UK (Feb-April) that led to a build-up of NH_4NO_3 and HNO_3 concentrations from both local and transboundary sources. A second, but smaller episode of elevated concentrations of SO_2 and HNO_3, as well as of particulate SO_4^2, NO_3^- and NH_4^+, in September 2014 was shown to be from transport of pollutant plume from the Icelandic Holuhraun volcanic eruptions at that time.

After more than 16 years of operation, the AGANet is also capturing important long-term changes in the concentrations and partitioning between gas and aerosol of the N and S components in the atmosphere. A significant decrease of –81 % (MK) in annual mean concentrations of SO_2 between 2000 and 2015 was in agreement with the estimated –80 % reduction in SO_2 emissions, but larger than the accompanying decline in particulate SO_4^{2-} (–69 % MK). A more modest reduction in HNO_3 (–45 % MK) and particulate NO_3^- (–52 % MK) are consistent with the estimated 58 % decline in NO_x emissions over this same period. The decrease in particulate NH_4^+ (–62 % MK) is larger than the

precursor gas NH_3 (2000 – 2015 = –30 % MK / LR) and larger than the estimated decline in estimated NH_3 emissions of 9 %. However, it should be noted that NH_3 trends are highly dependent on site selection according to an earlier assessment made on a more comprehensive dataset from the UK NAMN.

The substantial decrease in UK SO_2 emissions and concentrations, while UK NO_x emissions and concentrations (HNO_3) remain relatively high in comparison, set against a much smaller decrease in NH_3 emissions and concentrations since 2000 is leaving more NH_3 available to react with HNO_3 to form the semi-volatile particulate NH_4NO_3. Particulate NH_4^+ and NO_3^- are now in molar excess over SO_4^{2-}, providing evidence of a shift in the particulate phase from $(NH_4)_2SO_4$ to NH_4NO_3. A change to an NH_4NO_3 rich atmosphere and the potential for NH_4NO_3 to release NH_3 and HNO_3 in warm weather, together with the surfeit of NH_3 also means that a larger fraction of the reduced and oxidised N is remaining in the gas phase as NH_3 and HNO_3. The change in partitioning from particulate NH_4^+ to gaseous NH_3 is also occurring in other parts of Europe, where decreases in NH_3 concentrations have been smaller then emission trends would suggest, due to successful mitigation in SO_2 emissions. Higher concentrations of the NH_3 and HNO_3 in the atmosphere will deposit more locally, exacerbating the effects of local N deposition loads over large areas of sensitive habitats, with implications for UK's commitment to maintain or restore natural habitats (e.g. Natura 2000 sites) to a favourable conservation status under the EU Habitats Directive (Council Directive 92/43/EEC) and ecosystem monitoring under Article 9 and Annex V of Directive 2016/2284 (NECD). The changes are also important in terms of human effects assessment since NH_4NO_3 constitute a significant fraction of $PM_{2.5}$ that are implicated in acute and chronic human health effects and linked to increased mortality from respiratory and cardiopulmonary diseases.

Acknowledgements

The UK AGANet and NAMN are funded by the Department for Environment, Food and Rural Affairs (Defra) and the devolved administrations, under the UK Acid Deposition Monitoring Network (ADMN: 1999 - 2008), UK Eutrophying and Acidifying Atmospheric Pollutants network (UKEAP: 2009 - present) and from supporting NERC CEH programmes. The authors gratefully acknowledge assistance and contributions from the following: the large numbers of dedicated local site operators without whom the monitoring work would not be possible, site owners for provision of facilities, Harwell Scientifics Laboratory (now Environmental Scientifics Group (ESG) Ltd) for provision of chemical analysis for the AGANet between 1999 to 2009, the Centralised Analytical Chemistry facility in Lancaster (in particular Heather Carter, Darren Sleep and Philip Rowland) for sample preparation and chemical analysis since 2009, and colleagues at both CEH Edinburgh (Robert Storeton-West, Linda Love, Sarah Leeson, Matt Jones, Chris Andrews, Amy Stephens, Margaret Anderson, Ian D. Leith) and Ricardo Energy & Environment field team (Martin Davies, Tim Bevington, Ben Davies, Chris Colbeck) for assisting in site / equipment maintenance and data collection.

References

Aas, W., Carou, S., Alebic-Juretic, A., Aneja, V. P., Balasubramanian, R., Berge, H., Cape, J. N., Delon, C., Denmead, O. T., Dennis, R. L., Dentener, F., Dore, A. J., Du, E., Forti, M. C., GalyLacaux, C., Geupel, M., Haeuber, R., Iacoban, C., Komarov, A. S., Kubin, E., Kulshrestha, U. C., Lamb, B., Liu, X., Patra, D. D., Pienaar, J. J., Pinho, P., Rao, P. S. P., Shen, J., Sutton, M. A., Theobald, M. R., Vadrevu, K. P., and Vet, R.: Progress in nitrogen deposition monitoring and modelling, in: Nitrogen deposition, critical loads and biodiversity, edited by: Sutton, M. A., Mason, K. E., Sheppard, L. J., Sverdrup, H., Haeuber, R., and Hicks, W. K., Dordrecht, Springer, 455–463, 2014.

Allegrini, I., De Santis, F., Di Palo, V., Febo, A., Perrino, C., Possanzini, M., and Liberti, A.: Annular denuder method for sampling reactive gases and aerosols in the atmosphere, Sci. Total Environ., 67, 1–16, doi:10.1016/0048-9697(87)90062-3, 1987.

Aneja, V. P., Roelle, P.A., Murray, G. C., Southerland, J., Erisman, J. W., Fowler, D., Asman, W. A. H., and Patni N.: Atmospheric nitrogen compounds II: emissions, transport, transformation, deposition and assessment, Atmos. Environ., 35, 1903–1911, 2001.

Ayers, G. P., Gillett, R. W., Cainey, J. M., and Dick, A. L.: Chloride and Bromide Loss from Sea salt Particles in Southern Ocean Air, J. Atmos. Chem., 33, 299–319, doi:10.1023/A:1006120205159, 1999.

AQEG: Ozone in the United Kingdom, Air Quality Expert Group report, Department for Environment, Food and Rural Affairs, Scottish Executive, Welsh Government, Department of the Environment in Northern Ireland, available at: https://uk-

air.defra. gov.uk/assets/documents/reports/ aqeg/aqeg-ozone-report.pdf (last access: 25 March 2017), 2009.

AQEG: Fine Particulate Matter ($PM_{2.5}$) in the United Kingdom, Air Quality Expert Group report, Department for Environment, Food and Rural Affairs, Scottish Executive, Welsh Government, Department of the Environment in Northern Ireland, available at: https://uk-air.defra.gov.uk/assets/ documents/reports/cat11/ 1212141150_AQEG_Fine_Particulate_Matter_in_the_UK.pdf (last access: 25 March 2017), 2012.

AQEG: Linking Emission Inventories and Ambient Measurements, Air Quality Expert Group report, Department for Environment, Food and Rural Affairs, Scottish Executive, Welsh Government, Department of the Environment in Northern Ireland, available at: https://uk-air.defra.gov.uk/assets/documents/reports/ cat11/1508060906_DEF-PB14106_Linking_Emissions_ Inventories_And_Ambie nt_Measurements _Final.pdf (last access: 25 March 2017), 2013a.

AQEG: Mitigation of United Kingdom $PM_{2.5}$ Concentrations, Air Quality Expert Group report, Department for Environment, Food and Rural Affairs, Scottish Executive, Welsh Government, Department of the Environment in Northern Ireland, available at: https://uk-air.defra.gov.uk/assets/documents/reports/ cat11/ 1508060903 _DEF-PB14161_Mitigation_of_UK_PM25.pdf (last access: 25 March 2017), 2013b.

Bai, H., Chungsying, L., Chang, K.-F., and Fang, G.-C.: Sources of sampling error for field measurement of nitric acid gas by a denuder system, Atmos. Environ., 37, 941–947, doi:10.1016/S1352-2310(02)00972-x, 2003

Bleeker, A., Sutton, M. A., Acherman, B., Alebic-Juretic, A., Aneja, V. P., Ellermann, T., Erisman, J. W., Fowler, D., Fagerli, H., Gauger, T., Harlen, K. S., Hole, L. R., Horvath, L., Mitosinkova, M., Smith, R. I., Tang, Y. S., and van Pul, A.: Linking Ammonia Emission Trends to Measured Concentrations and Deposition of Reduced Nitrogen at Different Scales, in: Atmospheric Ammonia – Detecting Emission Changes and Environmental Impacts, edited by: Sutton, M. A., Reis, S., and Baker, S. M. H., Springer Netherlands, 123–180, 2009.

Bobbink, R., Hicks, K., Galloway, J., Spranger, T., Alkemade, R., Ashmore, M., Bustamante, M., Cinderby, S., Davidson, E., Dentener, F., Emmett, B., Erisman, J.-W., Fenn, M., Gilliam, F., Nordin, A., Pardo, L., and De Vries, W.: Global assessment of nitrogen deposition effects on terrestrial plant diversity: a synthesis, Ecol. Appl., 20, 30–59, doi:10.1890/08-1140.1, 2010.

Bower, K. N., Choularton, T. W., Gallagher, M. W., Colvile, R. N., Wells, M., Beswick, K. M., Wiedensohler, A., Hansson, H.-C., Svenningsson, B., Swietlicki, E., Wendisch, M., Berner, A., Kruisz, C., Laj, P., Facchini, M. C., Fuzzi, S., Bizjak, M., Dollard, G., Jones, B., Acker, K., Wieprecht, W., Preiss, M., Sutton, M. A., Hargreaves, K. J., Storeton-West, R. L., Cape, J. N., and Arends, B. G.: Observations and modelling of the processing of aerosol by a hill cap cloud, Atmos. Environ., 31, 2527–2544, doi:10.1016/S1352-2310(96)00317-2, 1997.

Bull, K. R.: The critical loads/levels approach to gaseous pollutant emission control, Environ. Poll., 69, 105–123, doi:10.1016/0269-7491(91)90137-L, 1991.

Bull, K. R.: Critical loads — Possibilities and constraints, Water Air Soil Poll., 85, 201–212, doi:10.1007/bf00483701, 1995.

Bytnerowicz, A., Sanz, M. J., Arbaugh, M. J., Padgett, P. E., Jones, D. P., and Davila, A.: Passive sampler for monitoring ambient nitric acid (HNO_3) and nitrous acid (HNO_2) concentrations, Atmos. Environ., 39, 2655–2660, doi:10.1016/ j.atmosenv.2005.01.018, 2005.

Cape, J. N., van der Eerden, L. J., Sheppard, L. J., Leith, I. D., and Sutton, M. A.: Evidence for changing the Critical Level for ammonia, Environ. Poll., 157, 1033–1037, doi:10.1016/j.envpol.2008.09.049, 2009.

Chatfield, C.: The analysis of time series: an introduction, CRC press, 2016.

Chemel, C., Sokhi, R. S., Yu, Y., Hayman, G. D., Vincent, K. J., Fore, A. J., Tang, Y. S., Prain, H. D., and Fisher, B. E. A.: Evaluation of a CMAQ simulation at high resolution over the UK for the calendar year 2003, Atmos. Environ., 44, 2927–2939, doi:10.1016/j.atmosenv.2010.03.029, 2010.

Cheng, Y., Duan, F.-K., He, K.-B., Du, Z.-Y., Zheng, M., and Ma, Y.-L.: Sampling artifacts of organic and inorganic aerosol: Implications for the speciation measurement of particulate matter, Atmos. Environ., 55, 229–233, doi:10.1016/j.atmosenv.2012.03.032, 2012.

Colette, A., Aas, W., Banin, L., Braban, C. F., Ferm, M., González Ortiz, A., Ilyin, I., Mar, K., Pandolfi, M., Putaud, J.-P., Shatalov, V., Solberg, S., Spindler, G., Tarasova, O., Vana, M., Adani, M., Almodovar, P., Berton, E., Bessagnet, B., Bohlin-Nizzetto, P., Boruvkova, J., Breivik, K., Briganti, G., Cappelletti, A., Cuvelier, K., Derwent, R., D'Isidoro, M., Fagerli, H., Funk, C., Garcia Vivanco, M., González Ortiz, A., Haeuber, R., Hueglin, C., Jenkins, S., Kerr, J., de Leeuw, F., Lynch, J., Manders, A., Mircea, M., Pay, M. T., Pritula, D., Putaud, J.-P., Querol, X., Raffort, V., Reiss, I., Roustan, Y., Sauvage, S., Scavo, K., Simpson, D., Smith, R. I., Tang, Y. S., Theobald, M., Tørseth, K., Tsyro, S., van Pul, A., Vidic, S., Wallasch, M., and Wind, P.: Air pollution trends in the EMEP region between 1990 and 2012, EMEP/CCC-Report 1/2016, Joint Report of the EMEP Task Force on Measurements and Modelling (TFMM), Chemical Coordinating Centre (CCC), Meteorological Synthesizing CentreEast (MSC-E), Meteorological Synthesizing Centre-West (MSCW), available at: http://hdl.handle.net/11250/2393346 (last access: 25 March 2017), 2016.

Conolly, C., Davies, M., Knight, D., Vincent, K., Sanocka, A., Lingard, J., Richie, S., Donovan, B., Collings, A., Braban, C., Tang, Y. S., Stephens, A., Twigg, M., Jones, M., Simmons, I., Coyle, C., Kentisbeer, J., Leeson, S., van Dijk, N., Nemitz, E., Langford, B., Bealey, W., Leaver, D., Poskitt, J., Carter, H., Thacker, S., Patel, M., Keenan, P., Pereira, G., Lawlor, A., Warwick, A., Farrand, P., and Sutton, M. A.: UK Eutrophying and Acidifying Atmospheric Pollutants (UKEAP) Annual Report 2015, UK Department for Environment, Food & Rural Affairs, 2016.

Cowling, E. B., Erisman, J. W., Smeulders, S. M., Holman, S. C., and Nicholson, B. M.: Optimizing air quality management in Europe and North America: Justification for integrated management of both oxidized and reduced forms of nitrogen, Environ. Poll., 102, 599–608, doi:10.1016/S0269-7491(98)80088-2, 1998.

Dentener, F., Drevet, J., Lamarque, J. F., Bey, I., Eickhout, B., Fiore, A. M., Hauglustaine, D., Horowitz, L. W., Krol, M., Kulshrestha, U. C., Lawrence, M., Galy-Lacaux, C., Rast, S., Shindell, D., Stevenson, D., Van Noije, T., Atherton, C., Bell, N., Bergman, D., Butler, T., Cofala, J., Collins, B., Doherty, R., Ellingsen, K., Galloway, J., Gauss, M., Montanaro, V., Müller, J. F., Pitari, G., Rodriguez, J., Sanderson, M., Solmon, F., Strahan, S., Schultz, M., Sudo, K., Szopa, S., and

Wild, O.: Nitrogen and sulfur deposition on regional and global scales: A multimodel evaluation, Global Biogeochem. Cy., 20, GB4003, doi:10.1029/2005 GB002672, 2006.

Dore, A. J., Carslaw, D. C., Braban, C., Cain, M., Chemel, C., Conolly, C., Derwent, R. G., Griffiths, S. J., Hall, J., Hayman, G., Lawrence, S., Metcalfe, S. E., Redington, A., Simpson, D., Sutton, M. A., Sutton, P., Tang, Y. S., Vieno, M., Werner, M., and Whyatt, J. D.: Evaluation of the performance of different atmospheric chemical transport models and inter-comparison of nitrogen and sulphur deposition estimates for the UK, Atmos. Environ., 119, 131–143, doi:10.1016/j.atmosenv 2015.08.008, 2015.

EEA: Air quality in Europe 2017, Report No 13/2017, available at: https://www.eea.europa.eu/publications/ air-quality-in-europe-2017, last access: 22 March 2017. EMEP: EMEP Manual for Sampling and Analysis, available at: www.nilu.no/projects/ccc/manual/ (last access: 17 March 2017), 2014. EMEP: Daily filter pack data of ammonia and ammonium (TIA) and nitric acid and nitrate (TIN) for the Eskdalemuir EMEP site, available at: http://ebas.nilu.no/, last access: 17 March 2017a. EMEP: SO_2 and SO_4^{2-} data by daily bubbler and filter pack method for the Eskdalemuir EMEP site, available at: http://ebas.nilu.no/, last access: 17 March 2017b.

EU: Directive (EU) 2016/2284 of the European Parliament and of the Council of 14 December 2016 on the reduction of national emissions of certain atmospheric pollutants, amending Directive 2003/35/EC and repealing Directive 2001/81/EC, 2016.

Evans, C. D., Monteith, D. T., Fowler, F., Cape, J. N., and Brayshaw, S.: Hydrochloric Acid: An overlooked driver of environmental change, Environ. Sci. Technol., 45, 1887–894, doi:10.1021/es103574u, 2011.

Ferm, M.: Method for determination of atmospheric ammonia, Atmos. Environ., 13, 1385–1393, doi:10.1016/0004- 6981(79)90107-0, 1979.

Ferm, M.: A Na_2CO_3-coated denuder and filter for determination of gaseous HNO_3 and particulate NO_3^- in the atmosphere, Atmos. Environ., 20, 1193–1201, doi:10.1016/0004- 6981(86)90153-8, 1986.

Finn, D., Rumburg, B., Claiborn, C., Bamesberger, L., and Siems, W. F.: Sampling artifacts from the use of denuder tubes with glycerol based coatings in the measurement of atmospheric particulate matter, Environ. Sci. Technol., 35, 40–44, doi:10.1021/es001325i, 2001.

Fitz, D. R.: Evaluation of Diffusion Denuder Coatings for Removing Acid Gases from Ambient Air, Final Report, U.S. Environmental Protection Agency, Riverside, 2002.

Flechard, C. R., Nemitz, E., Smith, R. I., Fowler, D., Vermeulen, A. T., Bleeker, A., Erisman, J. W., Simpson, D., Zhang, L., Tang, Y. S., and Sutton, M. A.: Dry deposition of reactive nitrogen to European ecosystems: a comparison of inferential models across the NitroEurope network, Atmos. Chem. Phys., 11, 2703–2728, doi:10.5194/acp-11-2703-2011, 2011.

Fowler, D., Sutton, M. A., Flechard, C., Cape, J. N., StoretonWest, R., Coyle, M., and Smith, R. I.: The control of SO_2 dry deposition on to natural surfaces by NH3 and its effects on regional deposition, Water Air Soil Poll., 1, 39–48, doi:10.1023/A:1013161912231, 2001.

Fowler, D., Pilegaard, K., Sutton, M. A., Ambus, P., Raivonen, M., Duyzer, J., Simpson, D., Fagerli, H., Fuzzi, S., Schjoerring, J. M., Granier, C., Neftel, A., Isaksen, I. S. A., Laj, P., Maione, M., Monks, P. S., Burkhardt, J., Daemmgen, U., Neirynck, J., Personne, E., Wichink-Kruit, R., Butterbach-Bahl, K., Flechard, C., Tuovinen, J. P., Coyle, M., Gerosa, G., Loubet, B., Altimir, N., Gruenhage, L., Ammann, C., Cieslik, S., Paoletti, E., Mikkelsen, T. N., Ro-Poulsen, H., Cellier, P., Cape, J.N., Horváth, L., Loreto, F., Niinemets, Ü., Palmer, P. I., Rinne, J., Misztal, P., Nemitz, E., Nilsson, D., Pryor, S., Gallagher, M. W., Vesala, T., Skiba, U., Brüggemann, N., Zechmeister-Boltenstern, S., Williams, J., O'Dowd, C., Facchini, M.C., de Leeuw, G., Flossman, A., Chaumerliac, N., and Erisman, J. W.: Atmospheric composition change: Ecosystems– Atmosphere interactions, Atmos. Environ., 43, 5193–5267, doi:10.1016/j.atmosenv.2009.07.068, 2009.

Gilbert, R. O.: Statistical methods for environmental pollution monitoring, New York, John Wiley & Sons, 1987.

Gormley, P. and Kennedy, M.: Diffusion from a stream flowing through a cylindrical tube, P. Roy. Irish Acad. A, 52, 163–169, 1948.

Gregor, H.-D., Nagel, H.-D., and Posch, M.: The UN/ECE International Programme on Mapping Critical Loads and Levels, Water Air Soil Poll., 1, 5–19, doi:10.1023/a:1011503115918, 2001.

Hall, J. and Smith, R.: Trends in critical load exceedances in the UK – CEH Report to Defra, prepared under contract AQ0826, version 02/06/16, 35 pp., available at: http://www.cldm.ceh.ac.uk/sites/cldm.ceh.ac.uk/files/TrendsReport_June2015_WEB.pdf (last access: 25 January 2018), 2016.

Hallsworth, S., Dore, A. J., Bealey, W. J., Dragosits, U., Vieno, M., Hellsten, S., Tang, Y. S., and Sutton, M. A.: The role of indicator choice in quantifying the threat of atmospheric ammonia to the "Natura 2000" network, Environ. Sci. Policy, 13, 671–687, doi:10.1016/j.envsci.2010.09.010, 2010.

Hayman, G., Vincent, K. J., Lawrence, H., Smith, M., Davies, M., Sutton, M., Tang, Y. S., Dragosits, U., Love, L., Fowler, D., Kendall, M., and Page, H.: Management and Operation of the UK Acid Deposition Monitoring Network: Data Summary for 2004, Department for Environment, Food and Rural Affairs, the Scottish Executive, the Welsh Assembly Government, Department of the Environment Northern Ireland, AEAT/ENV/R/2093 Issue 1, AEA Technology plc, The Gemini Building, Fermi Avenue, Harwell, 2005.

Hayman, G., Lawrence, H., Vincent, K., Smith, M., Davies, M., Colbeck, C., Hasler, S., Baker, S., Stedman, J., Sansom, L., Page, H., and Kendall, M.: Rural Sulphur Dioxide Monitoring in the UK: Data Summary 2001–2005, Report ref: ED48204, AEAT/ENV/R/2292 Issue 1, 2006.

Hayman, G. D., Vincent, K., Lawrence, H., Smith, M., Colbeck, C., Davies, M., Sutton, M. A., Tang, Y. S., Dragosits, U., Love, L., Fowler, D., Kendall, M., and Page, H.: Management and Operation of the UK Acid Deposition Monitoring Network: Data Summary for 2005, AEA Energy & Environment Report AEAT/ENV/R/2342 Issue 1, AEA Technology plc, The Gemini Building, Fermi Avenue, Harwell, 2007.

Horvath, L., Fagerli, H., and Sutton, M. A.: Long-Term Record (1981–2005) of Ammonia and Ammonium Concentrations at K-Puszta Hungary and the Effect of Sulphur Dioxide Emission Change on Measured and Modelled Concentrations,

Atmospheric Ammonia, edited by: Sutton, M. A., Reis, S., and Baker, S. M. H., Springer, Heidelberg Germany, 181–185, 2009.

Ianniello, A., Spataro, F., Esposito, G., Allegrini, I., Hu, M., and Zhu, T.: Chemical characteristics of inorganic ammonium salts in PM2.5 in the atmosphere of Beijing (China), Atmos. Chem. Phys., 11, 10803–10822, doi:10.5194/acp-11-10803-2011, 2011.

Jones, A. M. and Harrison, R. M.: Temporal trends in sulphate concentrations at European sites and relationships to sulphur dioxide, Atmos. Environ., 45, 873–882, doi:10.1016/j.atmosenv.2010.11.020, 2011.

Keene, W. C., Pszenny, A. A. P., Galloway, J. N., and Hawley, M. E.: Sea salt corrections and interpretation of constitutent ratios in marine precipitation, J. Geophys. Res., 91, 6647–6658, doi:10.1029/JD091iD06p06647, 1986.

Kitto, A.-M. N. and Harrison, R. M.: Nitrous and nitric acid measurements at sites in South-East England, Atmos. Environ., 26, 235–241, doi:10.1016/0960-1686(92)90305-5, 1992.

Marchetto, A., Rogora, M., and Arisci, S.: Trend analysis of atmospheric deposition data: A comparison of statistical approaches, Atmos. Environ., 64, 95–102, doi:10.1016/j.atmosenv.2012.08.020, 2013.

Meals, D. W., Spooner, J., Dressing, S. A., and Harcum, J. B.: Statistical analysis for monotonic trends, TechNotes 6, National Nonpoint Source Monitoring Program, U.S. Environmental Protection Agency, 23 pp., available at: https://www.epa.gov/sites/production/files/2016-05/documents/tech_notes_6_dec2013_trend.pdf (last access: 20 March 2017), 2011.

McLeod, A. I.: Package “Kendall”, version 2.2, Kendall rank correlation and Mann-Kendall trend test, available at: https://cran. r-project.org/web/packages/Kendall/Kendall.pdf (last access: 17 February 2017), 2015.

Mihalopoulos, N., Kerminen, V. M., Kanakidou, M., Berresheim, H., and Sciare, J.: Formation of particulate sulfur species (sulfate and methanesulfonate) during summer over the Eastern Mediterranean: A modelling approach, Atmos. Environ., 41, 6860–6871, doi:10.1016/j.atmosenv.2007.04.039, 2007.

Monteith, D., Henrys, P., Banin, L., Smith, R., Morecroft, M., Scott, T., Andrews, C., Beaumont, D., Benham, S., Bowmaker, V., Corbett, S., Dick, J., Dodd, B., Dodd, N., McKenna, C., McMillan, S., Pallett, D., Pereira, M. G., Poskitt, J., Rennie, S., Rose, R., Schäfer, S., Sherrin, L., Tang, S., Turner, A., and Watson, H.: Trends and variability in weather and atmospheric deposition at UK Environmental Change Network sites (1993–2012), Ecol. Indic., 68, 21–35, doi:10.1016/j.ecolind.2016.01.061, 2016.

NAEI: UK emissions data selector, National Atmospheric Emissions Inventory, available at: http://naei.beis.gov.uk/data/ data-selector-results?q=101505)? , last access: 19 September 2018.

O’Dowd, C. D., and de Leeuw, G.: Marine aerosol production: a review of the current knowledge, Phil. Trans. R. Soc. A, 365, 1753–1774, doi:10.1098/rsta.2007.2043, 2007.

Perrino, C., De Santis, F., and Febo, A.: Criteria for the choice of a denuder sampling technique devoted to the measurement of atmospheric nirous and nitric acids, Atmos. Environ., 24, 617–626, doi:10.1016/0960-1686(90)90017-H, 1990.

Pio, C.: Measurement of ammonia an ammonium in the atmosphere by denuder and filter pack methods, Evaluation of the Rome Field Intercomparison Exercise, Development of Analytical Techniques for Atmospheric Pollutants, Air Pollution Research Report, 41, 239–252, 1992.

Pohlert, T.: Package "Trend", version 0.2.0: Non-Parametric Trend Tests and Change-Point Detection, available at: https://cran. r-project.org/web/packages/trend/trend.pdf (last access: 10 October 2018), 2016.

Pope, R. J., Butt, E. W., Chipperfield, M. P., Doherty, R. M., Fenech, S., Schmidt, A., Arnold, S. R., and Savage, N. H.: The impact of synoptic weather on UK surface ozone and implications for premature mortality, Environ. Res. Lett., 11, 124004, doi:10.1088/1748-9326/11/12/124004, 2016.

Possanzini, M., Febo, A., and Liberti, A.: New design of a highperformance denuder for the sampling of atmospheric pollutants, Atmos. Environ., 17, 2605–2610, doi:10.1016/0004- 6981(83)90089-6, 1983.

Putaud, J. P., Van Dingenen, R., Alastuey, A., Bauer, H., Birmili, W., Cyrys, J., Flentje, H., Fuzzi, S., Gehrig, R., Hansson, H. C., and Harrison, R. M.: A European aerosol phenomenology–3: Physical and chemical characteristics of particulate matter from 60 rural, urban, and kerbside sites across Europe, Atmos. Environ., 44, 1308–1320, doi:10.1016/j.atmosenv.2009.12.011, 2010.

ROTAP: Review of Transboundary Air Pollution: Acidification, Eutrophication, Ground Level Ozone and Heavy Metals in the UK, Contract Report to the Department for Environment, Food and Rural Affairs, Centre for Ecology & Hydrology, available at: http://www.rotap.ceh.ac.uk/ (last access: 30 March 2018), 2012.

Roth, B. and Okada, K.: On the modification of sea-salt particles in the coastal atmosphere, Atmos. Environ., 32, 1555–1569, 1998.

Rumsey, I.C. and Walker, J.T.: Application of an online ionchromatography-based instrument for gradient flux measurements of speciated nitrogen and sulfur, Atmos. Meas. Tech., 9, 2581–2592, doi:10.5194/amt-9-2581-2016, 2016.

Schmitt, A.-D. and Stille, P.: The source of calcium in wet atmospheric deposits: Ca-Sr isotope evidence, Geochim. Cosmochim. Ac., 69, 3463–3468, doi:10.1016/j.gca.2004.11.010, 2005.

Schrader, F., Schaap, M., Zöll, U., Kranenburg, R., and Brümmer, C.: The hidden cost of using low resolution concentration data in the estimation of NH_3 dry deposition fluxes, Sci. Rep., 8, 969, doi:10.1038/s41598-017-18021-6, 2018.

Sickles, I.J.E., Hodson, L.L., and Vorburger, L.M.: Evaluation of the filter pack for long-duration sampling of ambient air, Atmos. Environ., 33, 2187–2202, doi:10.1016/S1352- 2310(98)00425-7, 1999.

Smith, R.I., Fowler, D., Sutton, M.A., Flechard, C., and Coyle, M.: Regional estimation of pollutant gas dry deposition in the UK: model description, sensitivity analyses and outputs, Atmos. Environ., 34, 3757–3777, doi:10.1016/s1352-2310(99)00517-8, 2000.

Steinle, S.: Report on work placement at the Centre for Ecology and Hydrology (CEH), Edinburgh, 01/09/2008–28/02/2009, 2009. Stelson, A. W. and Seinfeld, J. H.: Relative humidity and temperature dependence of the ammonium nitrate dissociation constant, Atmos. Environ., 16, 983–992, doi:10.1016/0004-6981(82)90184-6, 1982.

Sutton, M. A., Tang, Y. S., Dragosits, U., Fournier, N., Dore, A. J., Smith, R. I., Weston, K. J., and Fowler, D.: A spatial analysis of atmospheric ammonia and ammonium in the UK, Sci. World J., 28, 275–286, doi:10.1100/tsw.2001.313, 2001a.

Sutton, M. A., Tang, Y. S., Miners, B., and Fowler, D.: A new diffusion denuder system for long-term, regional monitoring of atmo spheric ammonia and ammonium, Water Air Soil Poll., 1, 145– 156, doi:10.1023/A:101313 8601753, 2001b.

Sutton, M. A., Nemitz, E., Erisman, J. W., Beier, C., Bahl, K. B., Cellier, P., de Vries, W., Cotrufo, F., Skiba, U., Di Marco, C., Jones, S., Laville, P., Soussana, J. F., Loubet, B., Twigg, M., Famulari, D., Whitehead, J., Gallagher, M. W., Neftel, A., Flechard, C. R., Herrmann, B., Calanca, P. L., Schjoerring, J. K., Daemmgen, U., Horvath, L., Tang, Y. S., Emmett, B. A., Tietema, A., Penuelas, J., Kesik, M., Brueggemann, N., Pilegaard, K., Vesala, T., Campbell, C. L., Olesen, J. E., Dragosits, U., Theobald, M. R., Levy, P., Mobbs, D. C., Milne, R., Viovy, N., Vuichard, N., Smith, J. U., Smith, P., Bergamaschi, P., Fowler, D., and Reis, S.: Challenges in quantifying biosphere-atmosphere exchange of nitrogen species, Environ. Poll., 150, 125–139, doi:10.1016/j.envpol.2007.04.014, 2007.

Sutton, M. A., Oenema, O., Erisman, J. W., Leip, A., van Grinsven, H., and Winiwarter. W.: Too much of a good thing, Nature, 472, 159–161, doi:10.1038/472159a, 2011.

Tang, Y. S. and Sutton, M. A.: Quality management in the UK national ammonia monitoring network, in: Proceedings of the International Conference: QA/QC in the field of emission and air quality measurements: harmonization, standardization and accreditation, Prague, 21–23 May 2003, edited by: Borowiak, A., Hafkenscheid, T., Saunders, A., and Woods, P., European Commission, Ispra, Italy, 297–307, 2003.

Tang, Y. S., Simmons, I., van Dijk, N., Di Marco, C., Nemitz, E., Dammgen, U., Gilke, K., Djuricic, V., Vidic, S., Gliha, Z., Borovecki, D., Mitosinkova, M., Hanssen, J. E., Uggerud, T. H., Sanz, M. J., Sanz, P., Chorda, J. V., Flechard, C. R., Fauvel, Y., Ferm, M., Perrino, C., and Sutton, M. A.: European scale application of atmospheric reactive nitrogen measurements in a low-cost approach to infer dry deposition fluxes, Agr. Ecosyst. Environ., 133, 183–195, doi:10.1016/ j.agee.2009.04.027, 2009.

Tang, Y. S., Cape, J. N., Braban, C. F., Twigg, M. M., Poskitt, J., Jones, M. R., Rowland, P., Bentley, P., Hockenhull, K., Woods, C., Leaver, D., Simmons, I., van Dijk, N., Nemitz, E., and Sutton, M. A.: Development of a new model DELTA sampler and assessment of potential sampling artefacts in the UKEAP AGANet DELTA system: summary and technical report, London, Defra, CEH Project no. C04544, C04845, available at: https://uk-air. defra.gov.uk/library/reports?report_ id=861 (last access: 20 October 2018), 2015.

Tang, Y. S., Braban, C. F., Dragosits, U., Dore, A. J., Simmons, I., van Dijk, N., Poskitt, J., Dos Santos Pereira, G., Keenan, P. O., Conolly, C., Vincent, K., Smith, R. I., Heal, M. R., and Sutton, M. A.: Drivers for spatial, temporal and long-term trends in atmospheric ammonia and ammonium in the UK, Atmos. Chem. Phys., 18, 705–733, doi:10.5194/acp-18-705- 2018, 2018.

Tang, Y. S., Poskitt, J., Cape, J. N., Nemitz, E., Bealey, W.J., Leaver, D., Beith, S., Thacker, S., Simmons, I., Letho, K., Wood, C., Pereira, G., Sutton, M. A., Davies, M., Conolly, C., Donovan, B., and Braban, C. F.: UK Eutrophying and Acidifying Atmospheric Pollutant project's Acid Gas and Aerosol Network (Data funded by Defra and the Devolved Administrations and published under the Open

Government Licence v1.0, AGANet, available at: http://uk-air.defra.gov.uk/networks/network-info?view= ukeap, last access: 23 March 2017a.

Tang, Y. S., Poskitt, J., Cape, J. N., Nemitz, E., Bealey, W. J., Leaver, D., Simmons, I., Wood, C., Pereira, G., Sutton, M. A., Davies, M., Conolly, C., Donovan, B., and Braban, C. F.: UK Eutrophying and Acidifying Atmospheric Pollutant project's National Ammonia Monitoring Network (Data funded by Defra and the Devolved Administrations and published under the Open Government Licence v1.0), NAMN, available at: https://uk-air.defra. gov.uk/networks/network-info?view=nh3, last access: 23 March 2017b.

Tørseth, K., Aas, W., Breivik, K., Fjæraa, A. M., Fiebig, M., Hjellbrekke, A. G., Lund Myhre, C., Solberg, S., and Yttri, K. E.: Introduction to the European Monitoring and Evaluation Programme (EMEP) and observed atmospheric composition change during 1972–2009, Atmos. Chem. Phys., 12, 5447–5481, doi:10.5194/acp-12-5447-2012, 2012.

Twigg, M. M., Ilyinskaya, E., Beccaceci, S., Green, D. C., Jones, M. R., Langford, B., Leeson, S. R., Lingard, J. J. N., Pereira, G. M., Carter, H., Poskitt, J., Richter, A., Ritchie, S., Simmons, I., Smith, R. I., Tang, Y. S., Van Dijk, N., Vincent, K., Nemitz, E., Vieno, M., and Braban, C. F.: Impacts of the 2014– 2015 Holuhraun eruption on the UK atmosphere, Atmos. Chem. Phys., 16, 11415–11431, doi:10.5194/acp-16-11415- 2016, 2016.

UNECE: Protocol to Abate Acidification, Eutrophication and Ground-level Ozone, the 1999 Gothenburg Protocol to Abate Acidification, Eutrophication and Ground-level Ozone, available at: http://www.unece.org/env/lrtap /multi_h1.html, last access: March 2018.

Vieno, M., Heal, M. R., Hallsworth, S., Famulari, D., Doherty, R. M., Dore, A. J., Tang, Y. S., Braban, C. F., Leaver, D., Sutton, M. A., and Reis, S.: The role of long-range transport and domestic emissions in determining atmospheric secondary inorganic particle concentrations across the UK, Atmos. Chem. Phys., 14, 8435–8447, doi:10.5194/acp-14-8435-2014, 2014.

Vieno, M., Heal, M. R., Twigg, M. M., MacKenzie, I. A., Braban, C. F., Lingard, J. N. N., Ritchie, S., Beck, R. C., Móring, A., Ots, R., Di Marco, C. F., Nemitz, E., Sutton M. A., and Reis, S.: The UK particulate matter air pollution episode of March–April 2014: more than Saharan dust, Environ. Res. Lett., 11, 044004, doi:10.1088/1748-9326/11/4/044004, 2016.

Werner, M., Kryza, M., Dore, A. J., Blas, M., Hallsworth, S., Vieno, M., Tang, Y. S., and Smith, R. I.: Modelling of marine base cation emissions, concentrations and deposition in the UK, Atmos. Chem. Phys., 11, 1023–1037, doi:10.5194/acp11-1023-2011, 2011.

Chapter 4 Pan-European rural atmospheric monitoring network shows dominance of NH_3 gas and NH_4NO_3 aerosol in inorganic pollution load

This chapter is based on the research paper submitted to `Atmospheric Chemistry and Physics' (*Tang, Y. S., Flechard, C. R., Dämmgen, U., Vidic, S., Djuricic, V., Mitosinkova, M., Uggerud, H. T., Sanz, M. J., Simmons, I., Dragosits, U., Nemitz, E., Twigg, M., van Dijk, N., Fauvel, Y., Sanz, F., Ferm, M., Perrino, C., Catrambone, M., Braban, C. F., Leaver, D., Cape, J. N., Heal, M. R., and Sutton, M. A.: Pan-European rural atmospheric monitoring network shows dominance of NH_3 gas and NH_4NO_3 aerosol in inorganic pollution load, Atmos. Chem. Phys. Discuss., https://doi.org/10.5194/acp-2020-275, in review, 2020.*

Author contributions:

I coordinated the establishment of the network, measurement and collection of data with the support of several European laboratories. A large number of research institutes provided monitoring sites and local support for installation of equipment and carrying out the monthly exchange of air samples. Mark Sutton conceived the NEU project and the DELTA® network. Ivan Simmons helped with designing and building the low-voltage DELTA® equipment. Eiko Nemitz helped with network logistics and provided science advice. Netty van Dijk helped with running proficiency testing schemes and inter-comparisons. Ulli Dragosits provided GIS support and science advice. Cinzia Perrino, Maria Sanz and Ulrich Dämmgen facilitated and hosted the DELTA® inter-comparisons at their field sites. Ulrich Dämmgen also sourced Rotenkamp bulk collectors for the project. Neil Cape provided advice on bulk wet deposition measurements and calculations. Chris Flechard, Ulrich Dämmgen, Sonja Vidic, Marta Mitosinkova, Hilde Uggerud and Maria Sanz led the chemical laboratories that shared the DELTA® and wet deposition measurements. David

Leaver developed the NEU database and provided support in data submission. Several of the authors contributed to measurements, network operations and equipment/site maintenance. I performed all the data collection, data analysis (including statistics) and wrote the manuscript, with input from all co-authors. Mark Sutton, Mat Heal, Chris Flechard, Ulrich Dämmgen, Martin Ferm and Neil Cape provided valuable advice on the interpretation of results and feedback on the manuscript.

4.1 Abstract

A comprehensive European dataset on monthly atmospheric NH_3, acid gases (HNO_3, SO_2, HCl) and aerosols (NH_4^+, NO_3^-, SO_4^{2-}, Cl^-, Na^+, Ca^{2+}, Mg^{2+}) is presented and analyzed. Speciated measurements were made with a low-volume denuder and filter pack method (DELTA®) as part of the EU NitroEurope (NEU) integrated project. Altogether, there were 64 sites in 20 countries (2006-2010), coordinated between 7 European laboratories. Bulk wet deposition measurements were carried out at 16 co-located sites (2008-2010). Inter-comparisons of chemical analysis and DELTA® measurements allowed an assessment of comparability between laboratories.

The form and concentrations of the different gas and aerosol components measured varied between individual sites and grouped sites according to country, European regions and 4 main ecosystem types (crops, grassland, forests and semi-natural). Smallest concentrations (with the exception of SO_4^{2-} and Na^+) were in Northern Europe (Scandinavia), with broad elevations of all components across other regions. SO_2 concentrations were highest in Central and Eastern Europe with larger SO_2 emissions, but particulate SO_4^{2-} concentrations were more homogeneous between regions. Gas-phase NH_3 was the most abundant single measured component at the majority of sites with the the largest variability in concentrations across the network.

The largest concentrations of NH_3, NH_4^+ and NO_3^- were at cropland sites in intensively managed agricultural areas (e.g. Borgo Cioffi in Italy), and smallest at remote semi-natural and forest sites (e.g. Lompolojänkkä, Finland), highlighting the potential for NH_3 to drive the formation of both NH_4^+ and NO_3^- aerosol. In the aerosol phase, NH_4^+ was highly correlated with both NO_3^- and SO_4^{2-}, with a near 1:1 relationship between the equivalent concentrations of NH_4^+ and sum (NO_3^- + SO_4^{2-}), of which around 60% was as NH_4NO_3.

Distinct seasonality were also observed in the data, influenced by changes in emissions, chemical interactions and the influence of meteorology on partitioning between the main inorganic gases and aerosol species. Springtime maxima in NH_3 were attributed to the main period of manure spreading, while the peak in summer and trough in winter were linked to the influence of temperature and rainfall on emissions, deposition and gas-aerosol phase equilibrium. Seasonality in SO_2 were mainly driven by emissions (combustion), with concentrations peaking in winter, except in Southern Europe where the peak occurred in summer. Particulate SO_4^{2-} showed large peaks in concentrations in summer in Southern and Eastern Europe, contrasting with much smaller peaks occurring in early spring in other regions. The peaks in particulate SO_4^{2-} coincided with peaks in NH_3 concentrations, attributed to the formation of the stable $(NH_4)_2SO_4^{2-}$.

HNO_3 concentrations were more complex, related to traffic and industrial emissions, photochemistry and HNO_3:NH_4NO_3 partitioning. While HNO_3 concentrations were seen to peak in the summer in Eastern and Southern Europe (increased photochemistry), the absence of a spring peak in HNO_3 in all regions may be explained by the depletion of HNO_3 through reaction with surplus NH_3 to form the semi-volatile aerosol NH_4NO_3. Cooler, wetter conditions in early spring favour the formation and persistence of NH_4NO_3 in the aerosol phase, consistent with the higher springtime concentrations of NH_4^+ and NO_3^-. The seasonal profile of NO_3^- was mirrored by NH_4^+, illustrating the influence of gas:aerosol partitioning of NH_4NO_3 in the seasonality of these components.

Gas-phase NH_3 and aerosol NH_4NO_3 were the dominant species in the total inorganic gas and aerosol species measured in the NEU network. With the current and projected trends in SO_2, NO_x and NH_3 emissions, concentrations of NH_3 and NH_4NO_3 can be expected to continue to dominate the inorganic pollution load over the next decades, especially NH_3 which is linked to substantial exceedances of ecological thresholds across Europe. The shift from $(NH_4)_2SO_4$ to an atmosphere more abundant in NH_4NO_3 is expected to maintain a larger fraction of reactive N in the gas phase by partitioning to NH_3 and HNO_3 in warm weather, while NH_4NO_3 continues to contribute to exceedances of air quality limits for $PM_{2.5}$.

4.2 Introduction

Air quality policies and research on atmospheric sulfur (S) and nitrogen (N) pollutant impacts on ecosystem and human health have focused on the emissions, concentrations and depositions of sulfur dioxide (SO_2), nitrogen oxides (NO_x), ammonia (NH_3) and their secondary inorganic aerosols (SIAs: ammonium sulfate, $(NH_4)_2SO_4$; ammonium nitrate, NH_4NO_3) (ROTAP, 2012; EMEP, 2019). The aerosols, formed through neutralisation reactions between the alkaline NH_3 gas and acids generated in the atmosphere by the oxidation of SO_2 and NO_x (Huntzicker et al., 1980; AQEG, 2012) are a major component of fine particulate matter ($PM_{2.5}$) (AQEG, 2012; Vieno et al., 2016a) and precipitation (ROTAP, 2012; EMEP, 2019).

The negative effects of these pollutants on sensitive ecosystems are mainly through acidification (excess acidity) and eutrophication (excess nutrient N) processes that can lead to a loss of key species and decline in biodiversity (e.g. Hallsworth et al., 2010; Stevens et al., 2010). They are also implicated in radiative forcing, and influence climate change through inputs of nitrogen that can alter the carbon cycle (Reis et al., 2012; Sutton et al., 2013; Zaehle & Dalmonech, 2011).

A number of EU policy measures (e.g. 2008/50/EC Ambient Air Quality Directive, EC, 2008; 2016/2284/EU National Emissions Ceilings Directive NECD, EU, 2016) and wider international agreements (e.g. Gothenburg protocol; UNECE, 2012) are targeted at abating the emissions and environmental impacts of SO_2, NO_x and NH_3. The largest emissions reductions have been achieved for SO_2, which decreased by 82 % across the EEA-33 since 1990, to 4743 kt SO_2 in 2017 (EEA, 2019). Reductions in NO_x emissions have been more modest, at 45 % over the same period, with emissions in 2017 of 8563 kt NO_x exceeding those of SO_2. By contrast, the reductions in NH_3 emissions (of which over 90% come from agriculture) have been more modest, decreasing by only 18 %. Here, the decrease was largely driven by reductions in fertiliser use and livestock numbers, in particular from eastern European

countries, rather than through implementation of any abatement or mitigation measures. More worryingly, the decreasing trend has reversed in recent years, with emissions increasing by 5 % since 2010, to 4788 kt NH_3 in 2017 (EEA, 2019).

In recent assessments, critical loads of acidity were exceeded in about 5 % of the ecosystem area across Europe in 2017 (EMEP, 2018). While the substantial decline in SO_2 emissions has allowed the recovery of ecosystems from acid rain, NH_3 from agriculture and NO_x from transport are increasingly contributing to a larger fraction of the acidity load. Although NH_3 is not an acid gas, nitrification of NH_3 and ammonium (NH_4^+) releases hydrogen ions (H^+) that acidify soils and freshwater. The deposition of reactive N (N_r, including oxidised N: NO_x, HNO_3, NO_3^- and reduced N: NH_3, NH_4^+) and their contribution to eutrophication effects have also been identified by the EEA as the most important impact of air pollutants on ecosystems and biodiversity (EEA, 2019). The deposition of N_r throughout Europe remains substantially larger than the level needed to protect ecosystems, with critical loads thresholds for eutrophication from N exceeded in around 62 % of the EU-28 ecosystem area and in almost all countries in Europe in 2017 (EMEP, 2018).

Following emission, atmospheric transport and fate of the gases are controlled by the following processes: short range dispersion and deposition, chemical reaction and formation of NH_4^+ aerosols, and the long-range transport and deposition of the aerosols (Sutton et al., 1998; ROTAP, 2012). Atmospheric S and N_r inputs from the atmosphere to the biosphere occur though i) dry deposition of gases and aerosols, ii) wet deposition in rain and snow, and iii) occult deposition in fog and cloud (Smith et al., 2000; ROTAP, 2012). The deposition processes contribute very different fractions of the total S or N_r input and different chemical forms of the pollutants at different spatial scales. NH_3 is a highly reactive, water-soluble gas and deposits much faster than NO_x (which is not very water soluble and has low deposition velocity). Dry N deposition by NH_3 therefore contributes a significant fraction of the total N deposition to receptors close to source areas and will often exert the larger ecological

impacts, compared with other N pollutants (Cape et al., 2004; Sutton et al., 1998, 2007). Numerous studies have shown that N_r deposition in the vicinity of NH_3 sources is dominated by dry NH_3-N deposition (e.g. Pitcairn et al., 1998; Sheppard et al., 2011), with removal of NH_3 close to a source controlled by physical, chemical and ecophysiological processes (Flechard et al., 2011; Sutton et al., 2007, 2013). Unlike NO_x, HNO_3 (from oxidation of NO_x) is very water-soluble, while NO_3^- particles can act as cloud condensation nuclei (CCN) so that they are both scavenged quickly and removed efficiently by precipitation. Since NO_x is inefficiently removed by precipitation, wet deposition of NO_x near a source is small and only becomes important after NO_x has been converted to HNO_3 and NO_3^-.

Because of the large numbers of atmospheric N species and their complex atmospheric chemistry, quantifying the deposition of N_r is hugely complex and is a key source of uncertainty for ecosystems effects assessment (Bobbink et al., 2010; Fowler et al., 2007; Schrader et al., 2018; Sutton et al., 2007). Input by dry deposition can be estimated using a combination of measured and/or modelled concentration fields with high-resolution inferential models (e.g. Smith et al., 2000; Flechard et al., 2011), or by making direct flux measurements (e.g. Fowler et al., 2001; Nemitz et al., 2008). Although it is possible to measure N_r deposition directly (e.g. Skiba et al., 2009), the flux measurement techniques are complex and resource intensive, unsuited to routine measurements at a large number of sites. The 'inferential' modelling approach provides a direct estimation of deposition from N_r measurements by applying a land-use dependent deposition velocity (V_d) to measured concentrations (Dore et al., 2015; Flechard et al., 2011; Simpson et al., 2006; Smith et al., 2000).

At present, there are limited atmospheric measurements that speciate the gas and aerosol phase components at multiple sites over several years. On a European scale, atmospheric measurements of sulfur (SO_2, particulate SO_4^{2-}) and nitrogen (NH_3, HNO_3, particulate NH_4^+, NO_3^-) have been made by a daily filter pack method across the European Monitoring and Evaluation Program

(EMEP) networks since 1985, providing data for evaluating wet and dry deposition models (EMEP, 2016; Torseth et al., 2012). The method, however, does not distinguish between the gas and aerosol phase N species. Consequently, these data are reported as total inorganic ammonium (TIA = sum of NH_3 and NH_4^+) and total inorganic nitrate (TIN = sum HNO_3 and NO_3^-), limiting the usefulness of the data. Speciated measurements by an expensive and labour-intensive daily annular denuder method are also made (Torseth et al., 2012), but are necessarily restricted to a small number of sites, due to the high costs associated with this type of measurement. There are also networks with a focus on specific N components, for example, the national NH_3 monitoring networks in the Netherlands (LML, van Zanten et al., 2017) and in the UK (National Ammonia Monitoring Network, NAMN; Tang et al., 2018a), or compliance monitoring across Europe in the case of SO_2 and NO_x. The UK is unique in having an extensive set of speciated gas and aerosol monitoring data from the Acid Gas and Aerosol Network (AGANet), with measurements from 1999 to the present (Tang et al., 2018b).

In this context, there is an ongoing need for cost-effective, easy-to-operate, time-integrated atmospheric measurement for the respective gas and aerosol phases at sufficient spatial scales. Such data would help to, 1) improve estimates of N deposition, 2) contribute to development and validation of long-range transport models, e.g. EMEP (Simpson et al., 2006) and EMEP4UK (Vieno et al., 2014, 2016), 3) interpret interactions between the gas and aerosol phases, and 4) interpret ecological responses to nitrogen (e.g. ecosystem biodiversity or net carbon exchange). To contribute to this goal, a '3-level' measurement strategy in the EU Framework Programme 6 Integrated Project "NitroEurope" (NEU, www.nitroeurope.ceh.ac.uk) between 2006 and 2010 delivered a comprehensive integrated assessment of the nitrogen cycle, budgets and fluxes for a range of European terrestrial ecosystems (Sutton et al., 2007; Skiba et al., 2009). At the most intensive level (Level 3), state of art instrumentation for high resolution, continuous measurements at a small number of 13 'flux super sites' provided detailed understanding on atmospheric

and chemical processes (Skiba et al., 2009). By contrast, manual methods with a low temporal frequency (monthly) at the basic level (Level 1) provided measurements of N_r components at a large number of sites (> 50 sites) in a cost-efficient way in a pan-European network (Tang et al., 2009). Key species of interest included NH_3, HNO_3 and ammonium aerosols ($(NH_4)_2SO_4$, NH_4NO_3).

In this paper, we present and discuss four years of monthly reactive gas (NH_3, HNO_3, HCl) and aerosol (NH_4^+, NO_3^-, SO_4^{2-}, Cl^-, Na^+, Ca^{2+}, Mg^{2+}) measurements from the Level 1 network set up under the NEU integrated project, complemented by two years of bulk wet deposition data made at a subset of the network sites (Fig. 4.1). A harmonised measurement approach with a simple, cost-efficient time-integrated method, applied with high spatial coverage allowed a comprehensive assessment across Europe. Measurements across the network were coordinated between multiple European laboratories. The measurement approach and the operations of the networks, including the implementation of annual inter-comparisons to assess comparability between the laboratories, are described. The data are discussed in terms of spatial and temporal variation in concentrations, relative contribution of the inorganic nitrogen and sulfur components to the inorganic pollution load, and changes in atmospheric concentrations of acid gases and their interactions with NH_3 gas and NH_4^+ aerosol.

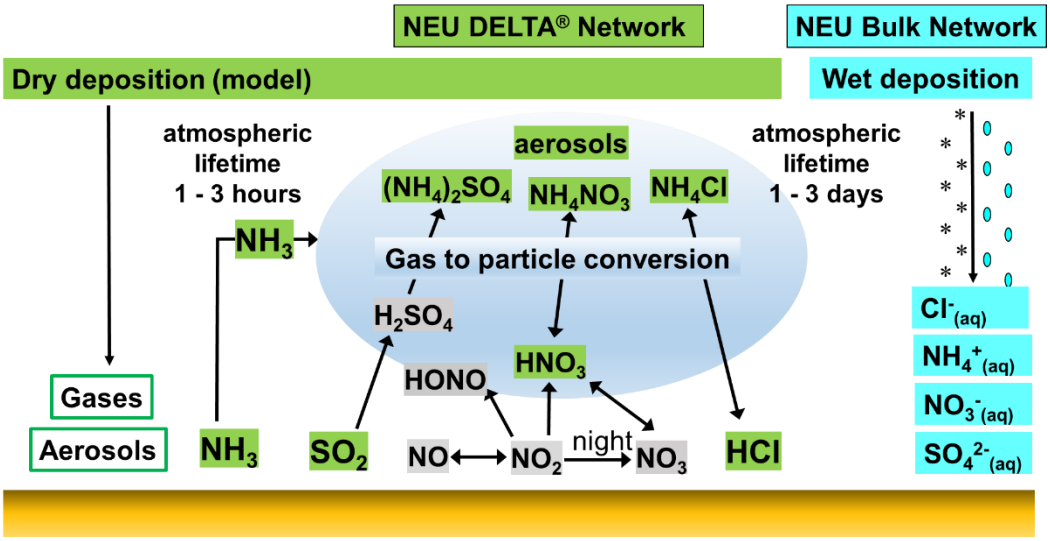

Figure 4.1. Reaction scheme for the formation of ammonium aerosols from interaction of NH_3 with acid gases HNO_3, SO_2 and HCl, showing the components (green) that were measured in NitroEurope (NEU) DELTA® network. Dry deposition of the gas and aerosol components was estimated by inferential modelling (Flechard et al., 2011), while wet deposition (blue) was measured in the NEU bulk wet deposition network at a subset of the DELTA® sites.

4.3 Methods

4.3.1 NEU Level 1 DELTA® network

The NitroEurope (NEU) Level 1 network was operated between November 2006 and December 2010 to deliver the core measurements of reactive nitrogen gases (NH_3, HNO_3) and aerosols (NH_4^+, NO_3^-) for the project (Fig. 4.1). A low-volume denuder-filter pack method, the 'DEnuder for Long-Term Atmospheric sampling' system (DELTA®, Sutton et al., 2001a; Tang et al., 2009, 2018b) with time-integrated monthly sampling was used, which made implementation at a large number of sites possible. Other acid gases (SO_2, HCl) and aerosols (SO_4^{2-}, Cl^-, Na^+, Ca^{2+}, Mg^{2+}) were also collected at the same time and measured by the DELTA® method. DELTA® measurements were co-located with all NEU Level 3 sites with advanced flux measurements (Skiba et al., 2009), and with the network of main CarboEurope-IP CO_2 flux monitoring

sites (www.carboeurope.eu) (Flechard et al., 2011, 2020). Two of the UK sites in the NEU DELTA® network are existing UK NAMN (Tang et al., 2018a) and AGANet sites (Tang et al., 2018b). These are Auchencorth Moss (UK-Amo) and Bush (UK-EBu) located in Southern Scotland. Monthly gas and aerosol data at the two sites, made as part of the UK national networks, were included in the NEU network. NEU network N_r data were used, together with a range of dry deposition models, to model dry deposition fluxes (Flechard et al., 2011) and to assess the influence of N_r on the C cycle, potential C sequestration and the greenhouse gas balance of ecosystems using CO_2 exchange data from the co-located CarboEurope sites (Flechard et al., 2020). Other measurements made at the Level 1 sites included estimation of wet deposition fluxes (Sect. 4.3.3) and also soil and plant bioassays (Schaufler et al., 2010).

Altogether, the DELTA® network covered a wide distribution of sites across 20 countries and 4 major ecosystem types: crops, grassland, semi-natural and forests. These sites can be described as 'rural', and were chosen to provide a regionally representative estimate of air composition. The network site map is shown in Fig. 4.2, with site details given in Supp. Table S4.1. Further information on the network sites are also provided in Flechard et al. (2011). Network establishment started in November 2006, with 57 sites operational from March 2007 onwards. Over the course of the network, some sites closed or were relocated due to infrastructure changes and new sites were also added. A total of 64 sites provided measurements at the end of the project, with 45 of the sites operational the entire time. In addition, replicated DELTA® measurements were made at 4 sites:

1) Auchencorth Moss parallel (P) (UK-AMoP; NH_3/NH_4^+ measured only)
2) Easter Bush parallel (P) (UK-EBuP; same method as main site),
3) SK04 parallel (P) (SK04P; same method as main site).
4) Fougéres parallel (P) (FR-FgsP: different sample train with 2 x NaCl coated denuders instead of 2 x K_2CO_3/Glycerol coated denuders to capture HNO_3; see Sect. 4.3.2.3) from February to December 2010 only.

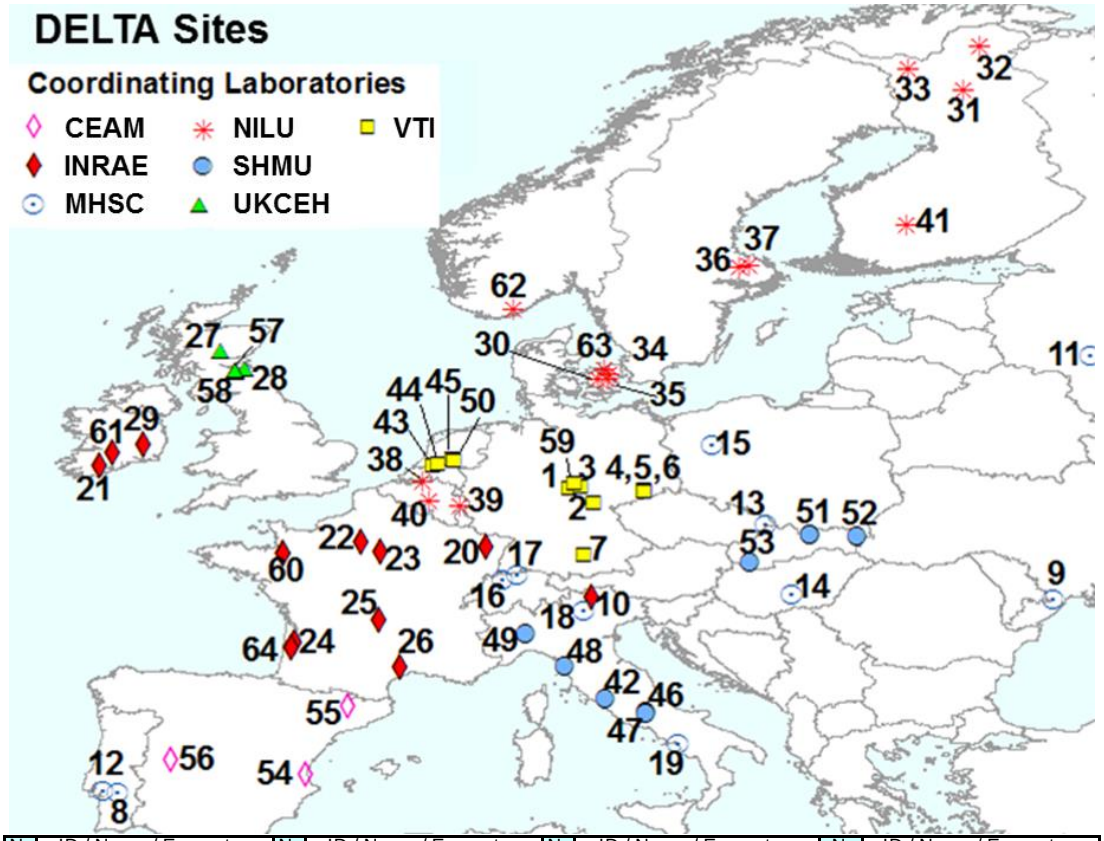

Nr	ID / Name / Ecosystem			Nr	ID / Name / Ecosystem			Nr	ID / Name / Ecosystem			Nr	ID / Name / Ecosystem		
1	DE-Hai	Hainich	F	18	IT-MB	Monte Bondone	SN	35	DK-Ris	Risby holm	C	51P	SK-04P	Stara Lesna	G
2	DE-Wet	Wetzstein	F	19	IT-BCi	Borgo Cioffi	C	36	SE-Nor	Norunda	F	52	SK-06	Starina	G
3	DE-Geb	Gebesee	C	20	FR-Hes	Hesse	F	37	SE-Sky	Skyttorp	F	53	SK-07	Topolniky	G
4	DE-Tha	Tharandt	F	21	IE-Dri	Dripsey	G	38	BE-Bra	Braschaat	F	54	ES-ES1	El Saler	F
5	DE-Gri	Grillenburg	G	22	FR-Gri	Grignon	C	39	BE-Vie	Vielsalm	F	55	ES-VDA	Vall de Alinà	SN
6	DE-Kli	Klingenberg	C	23	FR-Fon	Fontainebleau	F	40	BE-Lon	Lonzee	C	56	ES-LMa	Las Majadas	F
7	DE-Hoe	Höglwald	F	24	FR-LBr	Le Bray	F	41	FI-Hyy	Hyytiälä	F	57	UK-AMo	Auchencorth	SN
8	PT-Mi1	Mitra	F	25	FR-Lq2	Laqueuille	G	42	IT-Ro2	Roccarespampani	F	57P	UK-AMoP	Auchencorth	SN
9	U-Pet	Petrodolinskoye	C	26	FR-Pue	Puechabon	F	43	NL-Ca1	Cabauw	G	58	UK-Bu	Easter Bush	G
10	IT-Ren	Renon	F	27	UK-Gr	Griffin	F	44	NL-Hor	Horstermeer	SN	58P	UK-BuP	Easter Bush	G
11	RU-Fyo	Fyodorovskoe bog	F	28	UK-ES	East Saltoun	C	45	NL-Spe	Speulder	F	59	DE-Meh	Mehrstedt	F
12	PT-Esp	Espirra	F	29	IE-Ca2	Carlow	G	46	IT-Amp	Amplero	SN	60	FR-Fgs	Fougéres	F
13	CZ-BK1	BKFORES	F	30	DK-Sor	Soroe	F	47	IT-Col	Collelongo	F	60P	FR-FgsP	Fougéres	F
14	HU-Bug	Bugac	SN	31	FI-Sod	Sodankylä	F	48	IT-SRo	San Rossore	F	61	IE-Sol	Solohead	G
15	PL-Pol	Polwet	SN	32	FI-Kaa	Kaamanen	SN	49	IT-PoV	Po Valley Pavia	C	62	NO-Bir	Birkenes	F
16	CH-Oe1	Oensingen	G	33	FI-Lom	Lompolojänkkä	SN	50	NL-Loo	Loobos	F	63	DK-Brj	Brandbjerg	SN
17	CH-Lae	Laegern	F	34	DK-Lva	Rimi	G	51	SK-04	Stara Lesna	G	64	FR-Bil	Bilos	F

Figure 4.2. NitroEurope (NEU) DELTA® network sites operated between 2006 and 2010. The colour of the symbols indicates the responsible laboratories: CEAM (The Mediterranean Center for Environmental Studies), vTI (von Thunen Institut), INRAE (French National Research Institute for Agriculture, Food and Environment), MHSC (Meteorological and Hydrological Service of Croatia), UKCEH (UK Centre for Ecology & Hydrology), NILU (Norwegian Institute for Air Research), SHMU (Slovak Hydrometeorological Institute). Ecosystem types are C: Crops, G: Grassland, F: Forests and SN: short Semi-Natural (includes moorland, peatland, shrubland and unimproved/upland grassland). Replicated (P = parallel) DELTA measurements are made at 4 sites: SK04/SK04P; UK-AMo/UK-AMoP (NH_3/NH_4^+ only), UK-Bu/UK-BuP and FR-Fgs/FR-FgsP (NaCl coated denuders instead of K_2CO_3/glycerol in sample train).

4.3.1.1 Coordinating laboratories

A team of seven European laboratories shared responsibility for running the network. Measurement was on a monthly timescale, with each laboratory preparing and analysing the monthly samples with documented analytical methods for between 5 and 16 DELTA sites (Fig. 4.2). The use of a harmonised DELTA® methodology, coupled to defined quality protocols (Tang et al., 2009) ensured comparability of data between the laboratories (see later in Sect. 4.4.1 and Sect. 4.4.2). A network of local site operators representing the science teams of each site performed the monthly sample changes and posted the exposed samples back to their designated laboratories for analysis. Air concentration data were submitted by the laboratories for their respective sites in a standard reporting template to UKCEH. Following data checks against defined quality protocols (Tang et al., 2009), the finalised dataset was uploaded to the NEU database (www.nitroeurope.ceh.ac.uk). Establishment of the network, including the first year of measurement results on N_r components are reported in Tang et al. (2009). Information on co-located measurements and agricultural activities at each of the sites were also collected and are accessible from the NEU website (www.nitroeurope.ceh.ac.uk).

4.3.2 DELTA® methodology

The DELTA® method used in the NEU Level 1 network is based on the system developed for the UK Acid Gas and Aerosol monitoring network (AGANet, Tang et al., 2018b). Full details of the DELTA® method and air concentration calculations in the NEU network are provided by Tang et al. (2009, 2018b). The method uses a small 6 V air pump to deliver low air sampling rates of between 0.2 to 0.4 L min^{-1}, a high sensitivity gas meter to record the typically monthly volume of air collected and a DELTA® denuder-filter pack sample train to collect separately the gas and aerosol phase components. The sample train is made up of two pairs of base and acid impregnated denuders (15 cm and 10 cm long) to collect acid gases and NH_3, respectively, under laminar

conditions. A 2-stage filter pack with base and acid coated cellulose filters collects the aerosol components downstream of the denuders. The base coating used was K_2CO_3/glycerol which is effective for the simultaneous collection of HNO_3, SO_2 and HCl (Ferm, 1986), while the acid coating was either citric acid for temperate climates or phosphorous acid for Mediterranean climates (Allegrini et al., 1987; Ferm, 1979; Perrino et al., 1999; Fitz, 2002). In this way, artefacts between gas and aerosol phase concentrations are minimized (Ferm et al., 1979; Sutton et al., 2001a). The DELTA® air inlet has a particle cut-off of ~ 4.5 µm which means fine mode aerosols in the $PM_{2.5}$ fraction and some of the coarse mode aerosols < $PM_{4.5}$ will be collected (Tang et al., 2015).

A low voltage version of the AGANet DELTA® system was built centrally by UKCEH and sent to each of the European sites where they were installed by local site contacts. These systems operated on either 6 V (off mains power with a transformer) or 12 V from batteries (wind and solar powered). Air sampling was direct from the atmosphere without any inlet lines or filters to avoid potential loss of components, in particular HNO_3 that is very “sticky”, to surfaces. Sampling height was 1.5 m above ground/vegetation in open areas. In forested areas, the DELTA® equipment was set up either in large clearings, or on towers at 2 – 3 m above the canopy (see Flechard et al., 2011).

4.3.2.1 Calculation of gas and aerosol concentrations

Atmospheric gas and aerosol concentrations in the DELTA® method are calculated from the amount of inorganic ions (NH_4^+, NO_3^-, SO_4^{2-}, Cl^-, and base cations) in the denuder/aerosol aqueous extracts and the volume of air sampled (from gas meter readings), which is typically 15 m^3 for a monthly sample. The volume of deionised water used to extract acid coated denuders and aerosols filters are 3 mL and 4 mL, respectively. For the base coated denuders and aerosol filters, the extract volume in both cases is 5 mL An example is shown here for calculating the atmospheric concentrations of NH_3

(gas) (Eq. 1) and NH_4^+ (aerosol) (Eq. 2) from the aqueous extracts, based on an air volume of 15 m^3 collected in a typical month.

$$\text{Gas } NH_3\ (\mu g\ m^{-3}) = \frac{NH_4^+\ (mg\ L^{-1})\ [\text{sample}-\text{blank}]\ x\ 3\ mL\ x\ (\frac{17}{18})}{15\ m^3} \quad [1]$$

$$\text{Particle } NH_4^+ (\mu g\ m^{-3}) = \frac{NH_4^+\ (mg\ L^{-1})\ [\text{sample}-\text{blank}]\ x\ 4\ mL}{15\ m^3} \quad [2]$$

Pairs of base and acid coated denuders are used to collect the acid gases and alkaline NH_3 gas, respectively. This allows denuder collection efficiency of, for example, NH_3 (Eq. 3) to be assessed as part of the data quality assessment process. An imperfect acid coating on the denuders for example can lead to lower capture efficiencies (Sutton et al., 2001a; Tang et al., 2003).

$$\text{Denuder collection efficiency, } NH_3\ (\%) = 100\ x\ \frac{NH_3\ (\text{Denuder 1})}{NH_3\ (\text{Denuder 1}+\text{Denuder 2})} \quad [3]$$

A correction, based on the collection efficiency, is applied to provide a corrected air concentration (χ_a (corrected), Eq. 4) (Sutton et al., 2001a; Tang et al., 2018a, 2018b). With a collection efficiency of 95 %, the correction amounts to 0.3 % of the corrected air concentration. For an efficiency below 60 %, the correction amounts to more than 50 % and is not applied. The air concentration of (χ_a) of NH_3 is then determined as the sum of NH_3 in denuders 1 and 2 (Tang et al., 2018a). By applying the infinite series correction, the assumption is that any NH_3 (and other gases) that is not captured by the denuders will be collected on the downstream aerosol filter. To avoid double counting, the estimated amount of 'NH_3 breakthrough' is subtracted from the NH_4^+ concentrations on the aerosol filter.

$$\chi_a\ (\text{corrected}) = \chi_a\ (\text{Denuder 1}) * \frac{1}{1-\left[\frac{\chi_a(\text{Denuder 2})}{\chi_a(\text{Denuder 1})}\right]} \quad [4]$$

4.3.2.2 Estimating sea salt and non-sea salt SO_4^{2-}

Sea salt SO_4^{2-} ($ss\text{-}SO_4^{2-}$) in aerosol was estimated according to Eq. 5, based on the ratio of the mass concentrations of SO_4^{2-} to the reference Na^+ species in seawater (Keene et al., 1986; O'Dowd and de Leeuw, 2007).

$$[ss\text{-}SO_4^{2-}]\ (\mu g\ ss\text{-}SO_4^{2-}\ m^{-3}) = 0.25 \times [Na^+]\ (\mu g\ Na^+\ m^{-3}) \quad [5]$$

Non-sea salt SO_4^{2-} ($nss\text{-}SO_4^{2-}$) was then derived as the difference between total measured SO_4^{2-} and $ss\text{-}SO_4^{2-}$ (Eq. 6).

$$[nss\text{-}SO_4^{2-}]\ (\mu g\ nss\text{-}SO_4^{2-}\ m^{-3}) = [Total\ SO_4^{2-}]\ (\mu g\ SO_4^{2-}\ m^{-3}) - [ss\_SO_4^{2-}]\ (\mu g\ ss\text{-}SO_4^{2-}\ m^{-3}) \quad [6]$$

4.3.2.3 Artefact in HNO_3 determination

Results from the first DELTA® inter-comparison in the NEU network (Tang et al., 2009) (see also Sect. 4.3.5) and further work by Tang et al. (2015, 2018b) have shown that HNO_3 concentrations may be overestimated on the carbonate coated denuders used, due to co-collection of other oxidized nitrogen components, most likely from nitrous acid (HONO). In the UK AGANet, HNO_3 data are corrected with an empirical factor of 0.45 derived by Tang et al. (2015). Since the correction factor for HNO_3 is uncertain (estimated to be ± 30 %) and derived for UK conditions, no attempt has been made to correct the HNO_3 data from the NEU network. The DELTA® method remained unchanged throughout the entire network operation and provided a consistent set of measurements by the same protocol. The caveat is that the HNO_3 data presented in this paper also includes an unknown fraction of oxidized N, most probably HONO, and therefore represents an upper limit in the determination of HNO_3. Contribution from NO_2 is likely to be small, since this is collected with a low efficiency on carbonate coated denuders (Bai et al., 2003; Tang et al., 2015) and the network sites are rural, where NO_x concentrations are expected to be in the low ppbs. At the French Fougéres parallel site (FR-FgsP), NaCl coated denuders were used to measure HNO_3, to compare with results from K_2CO_3/glycerol coated denuders at the main site (FR-Fgs) (see Sect. 4.3.1).

4.3.3 NEU Bulk wet deposition network

The NEU bulk wet deposition network (Fig. 4.3, Supp. Table S4.2) was established to provide wet deposition data on NH_4^+ and NO_3^-. It was set up two years after the establishment of the NEU DELTA® network, with sites located at a subset of DELTA® sites that did not already have on-site wet deposition measurements. Sampling commenced at some sites in January 2008, with 14 sites operational from March 2008. Site changes also occurred during the operation of this network, again with some site closures and new site additions over time. In total, 12 sites provided 2 years of monthly data, with a further 6 sites providing 1 year of monthly data between 2008 to October 2010 when measurements ended.

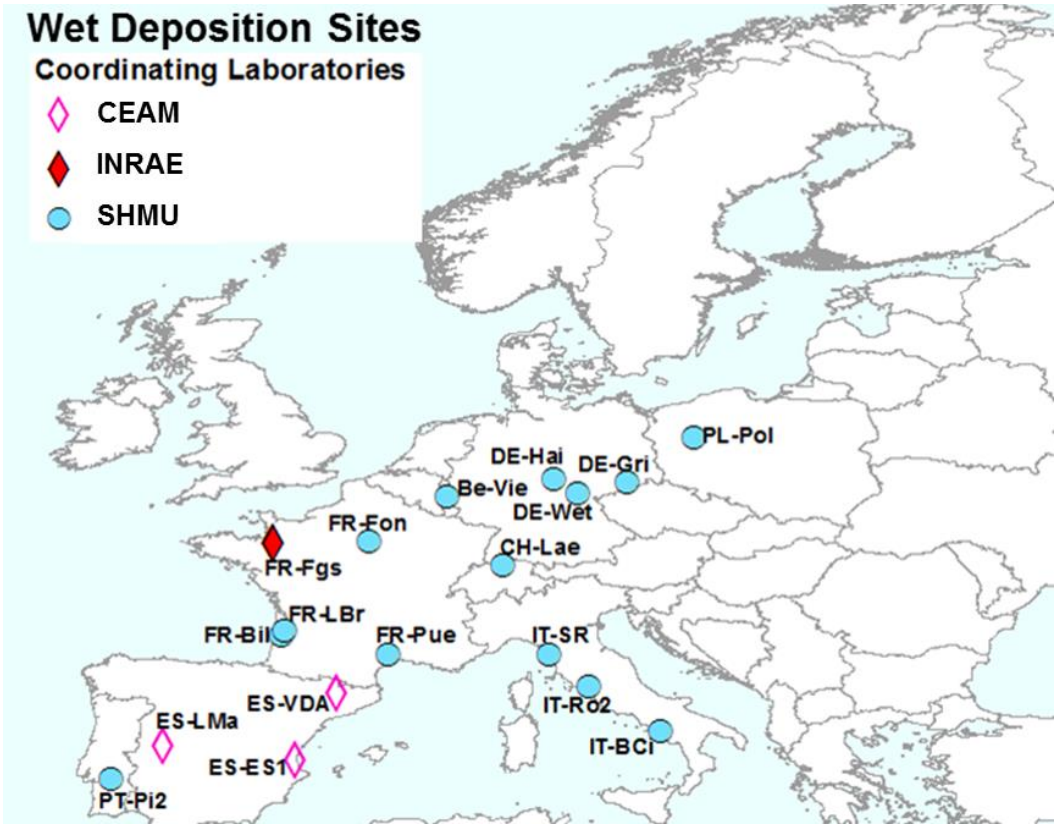

Figure 4.3. NitroEurope (NEU) Bulk wet deposition network sites operated between 2008 and 2010. The colour of the symbols indicates the responsible laboratories: CEAM (The Mediterranean Center for Environmental Studies), INRAE (French National Research Institute for Agriculture, Food and Environment), and SHMU (Slovak Hydrometeorological Institute).

The type of bulk precipitation collector used was a Rotenkamp sampler (Dämmgen et al., 2005), mounted 1.5 m above ground, or in the case of forest sites, either in clearings or above the canopy. Each unit has two collectors providing replicated samples, comprising of a pyrex glass funnel (aperture area = 84.9 cm^2) with vertical sides, connected directly to a 3 L collection bottle (material = low density polyethylene) which was changed monthly. Thymol (5-methyl-2-(1-methylethyl)phenol) (150 mg) was added as a biocide (Cape et al., 2012) to a clean, dry pre-weighed bottle at the start of each collection period. This provided a minimum thymol concentration of 50 mg L^{-1} for a full bottle to preserve the sample against biological degradation of labile nitrogen compounds during the month-long sampling.

Three European laboratories shared management and chemical analysis for the network (Fig. 4.3). The laboratories were CEAM (all 3 Spanish sites), INRAE (French Renon site) and SHMU, designated the main laboratory responsible for all other sites. A full suite of precipitation chemistry analyses were carried out that included: pH, conductivity, NH_4^+, NO_3^-, SO_4^{2-}, PO_4^{3-}, Cl^-, Na^+, K^+, Ca^{2+} and Mg^{2+}. Rain volumes and precipitation chemistry data were submitted in a standard template to UKCEH for checking and then uploaded to the NEU database (www.nitroeurope.ceh.ac.uk). Samples with high P (> 1 µg L^{-1} PO_4^{3-}), high K^+ and/or NH_4^+ values that are indicative of bird contamination were rejected. Annual wet deposition (e.g. kg N ha^{-1} yr^{-1}) were estimated from the product of the species concentrations and rain volume. Determinations of organic N were also carried out on some of the rain samples in a separate investigation reported by Cape et al. (2012).

4.3.4 Laboratory inter-comparisons: chemical analysis

All laboratories in the DELTA® and bulk wet deposition networks participated in water chemistry proficiency testing (PT) schemes in their own countries, as well as the EMEP (once annual, http://www.emep.int) and/or WMO-GAW (twice annual, http://www.qasac-americas.org/lab_ic.html) laboratory inter-

comparison schemes. PT samples for analysis are synthetic precipitation samples for determination of pH, conductivity and all the major inorganic ions at trace levels. In addition, UKCEH also organised an annual PT scheme for the duration of the project (NEU-PT) to compare laboratory performance in the analysis of inorganic ions at higher concentrations relevant for DELTA® measurements. This comprised the distribution of reference solutions containing known concentrations of ions that were analysed by the laboratories as part of their routine analytical procedures.

4.3.5 Laboratory inter-comparisons: DELTA measurements

Prior to the NEU DELTA® network establishment, a workshop was held to provide training to participating laboratories on sample preparation and analysis. This was followed by a 4-month inter-comparison exercise (July to October 2006) between six laboratories at four test sites (Montelibretti, Italy; Braunschweig, Germany; Paterna, Spain, and Auchencorth, UK). Results of the inter-comparison on N_r components were reported by Tang et al. (2009), which demonstrated good agreement under contrasting climatic conditions and atmospheric concentrations of the N_r gases and aerosols. The first DELTA® inter-comparison allowed the new laboratories to gain experience in making measurements, and was an extremely useful exercise to check how the whole system works, starting with coating of denuders and filters and DELTA® train preparation, sample exchange *via* post, sample handling and inter-comparing laboratory analytical performance. Further DELTA® inter-comparisons between laboratories were conducted each year for the duration of the project, details of which are summarised in Table 4.1. At each test site, DELTA® systems were randomly assigned to each of the participating laboratories. All laboratories provided DELTA® sampling trains for each of the inter-comparison sites and carried out chemical analysis on the returned exposed samples. Measurement results were returned in a standard template to UKCEH, the central coordinating laboratory for collation and analysis.

Table 4.1. Details of annual NitroEurope (NEU) DELTA® field inter-comparisons conducted between 2006 and 2010.

Inter-comparison period	Test sites	Participating laboratories	Number of monthly measurement periods
2006 (Jul – Oct)	Auchencorth, UK Braunschweig, Germany Montelibretti, Italy Paterna, Spain	6	4
2007 (Jul – Aug)	Auchencorth, UK Montelibretti, Italy	6	2
2008 (Apr – May)	Auchencorth, UK Braunschweig, Germany	7 (INRAE = new laboratory)	2
2009 (Nov – Dec)	Auchencorth, UK Montelibretti, Italy	7 (INRAE = new laboratory)	2

4.3.6 European emissions data

National emissions data:

With the exception of Russia and Ukraine, official reported national emissions data on SO_2, NO_x and NH_3 are available for all other 18 countries in the NEU network from the European Environment Agency (EEA) website (EEA, 2020). Emissions data for the period 2007 to 2010 were extracted and the emission densities of each gas (tonnes (t) km^{-2} yr^{-1}) in each country was derived by dividing the 4-year averaged total emissions by the land area (km^2).

Gridded emissions data:

Gridded emissions data (at 0.1º x 0.1º resolution) for SO_2, NO_x and NH_3 are available from the EMEP emissions database (EMEP, 2020). The 0.1º x 0.1º gridded data for the period 2007 to 2010 were downloaded and were used to:

- Estimate national total emissions (sum of all grid squares in each country) and 4-year averaged emission densities (t km^{-2} yr^{-1}) for Russia and Ukraine. As a check, total emissions for the other 18 countries were also calculated by this method and were the same as the national emission totals reported by the EEA (EEA, 2019).
- Extract gas emissions for individual grids (0.1º x 0.1º) that contains a NEU DELTA® site.

- Extract gas emissions for groups of 4 grids (each = 0.1º x 0.1º) that surrounds a NEU site and derive grid-averaged emissions.

4.3.7 National air quality network data from the Netherlands and UK

4.3.7.1 Dutch LML network data

Atmospheric NH_3 has been monitored at 8 sites in the Dutch national air quality monitoring network (LML, Landelijk Meetnet Luchtkwaliteitl) since 1993 (van Zanten et al., 2017). The low density, high time-resolution LML network is complemented by a high density monthly diffusion tube network, the Measuring Ammonia in Nature (MAN) network (http://man.rivm.nl) (Lolkema et al., 2015). The MAN network has 136 monitoring locations sited within nature reserves that includes 60 Natura 2000 sites, with concentrations ranging between 1.0 and 14 µg m^{-3} (Lolkema et al., 2015). The focus of the MAN network is to provide site-based NH_3 concentrations for the nature conservation sites, rather than a representative spatial concentration field for the country. Hourly NH_3 and SO_2 data which were also available from the 8 sites in the LML network were downloaded from the RIVM website (http://www.lml.rivm.nl/gevalideerd/index.php). The 4-year averaged NH_3 and SO_2 concentrations for the period 2007 to 2010 were calculated and used to complement measurement data from the 4 Dutch sites in the NEU DELTA® network.

4.3.7.2 UK NAMN and AGANet data

Atmospheric NH_3, acid gases and aerosols are measured in the UK NAMN (since 1996) and AGANet (since 1999) (Tang et al., 2018a, 2018b). The UK approach is a high density network with low time-resolution (monthly) measurements, combining an implementation of the DELTA® method used in the present NEU DELTA® network and a passive ALPHA® method (Tang et al., 2001) to increase network coverage in NH_3 measurements (Sutton et al.,

2001b; Tang et al., 2018a). Monthly and annual data for the overlapping period of the project were extracted from the UK-AIR website (https://uk-air.defra.gov.uk/) and nested with the NEU network data for analysis in this paper.

4.4 Results and Discussion

4.4.1 Laboratory inter-comparison results: chemical analysis

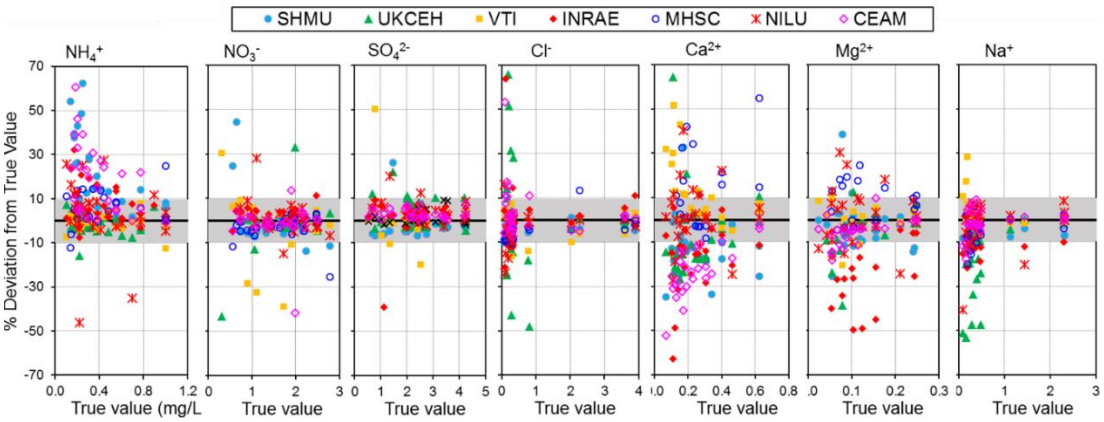

Component	Reference solute concentration (mg L^{-1})	[1]Equivalent gas concentration ($\mu g\ m^{-3}$)		[2]Equivalent aerosol concentration ($\mu g\ m^{-3}$)		% of reported results within ± 10% of true value. Mean of all labs (range = min, max)	*n*
NH_4^+	0.1 - 0.9	NH_3	0.02 - 0.17	NH_4^+	0.03 - 0.24	68% (39 – 97 %)	191
	1		0.19		0.27	90% (67 – 100 %)	16
NO_3^-	0.3 - 0.98	HNO_3	0.06 - 0.2	NO_3^-	0.08 - 0.26	85% (78 – 93%)	197
	1 - 3		0.2 - 0.6		0.27 - 0.80	88% (81 – 96%)	152
SO_4^{2-}	0.5 - 0.8	SO_2	0.07 - 0.11	SO_4^{2-}	0.13 - 0.21	91% (83 – 100 %)	199
	1 - 22		0.13 - 2.9		0.27 - 5.9	93% (85 – 100%)	178
Cl^-	0.07 - 0.8	HCl	0.01 - 0.16	Cl^-	0.02 - 0.21	76% (48 – 93%)	187
	1 - 10		0.27 - 4.5		0.27 - 5.9	96% (83 – 100%)	45
Ca^{2+}	0.07 - 0.6			Ca^{2+}	0.02 - 0.16	36% (12 – 59%)	176
	1 - 24				0.27 - 6.4	80% (0 = 100 %)	10
Mg^{2+}	0.05 - 0.25			Mg^{2+}	0.01 - 0.07	59% (22 – 75%)	160
	1 - 5				0.27 - 1.3	90% (50 – 100%)	10
Na^+	0.08 - 0.5			Na^+	0.02 - 0.13	72% (46 – 85%)	170
	1 - 52				0.27 - 14	89% (60 – 100%)	48

[1]Equivalent gas concentrations, based on denuder extraction volumes of 3 mL (NH_3) and 5 mL (HNO_3, SO_2, HCl) and air volume of 15 m^3 (typical volume of air sampled by DELTA® system over a month).
[2]Equivalent aerosol concentrations, based on aerosol filter extraction volume of 4 mL (NH_4^+) and 5 mL (NO_3^-, SO_4^{2-}, Cl^-, Na^+, Ca^{2+} and Mg^{2+}) and air volume of 15 m^3 (typical volume of air sampled by DELTA® system over a month).

Figure 4.4. Summary of reported results from all laboratories in wet chemistry proficiency testing (PT) schemes for chemical analysis of aqueous inorganic ions (2006 – 2010: EMEP, WMO-GAW and NitroEurope), expressed as a percentage deviation from the true value (PT reference solutions). The grey shaded areas in the graphs show values that are within ± 10 % of true value.

Figure 4.4 compares the percentage deviation of results from reference solution concentrations ('true value') reported by the laboratories for different chemical components in the EMEP, WMO-GAW and NEU proficiency testing (PT) schemes, combined from 2006 to 2010. Each data point is colour-coded in the graphs according to the laboratory providing the measurements.

Altogether, results from the combined PT schemes produced >100 observations for each reported chemical component over the 4 year period. The performances of laboratories in Fig. 4.4 can be summarised in terms of the percentage of reported results agreeing within 10 % of the true values (see summary table below Fig. 4.4), where the true values represent the nominal concentrations in the aqueous test solutions. The best agreements was for SO_4^{2-} and NO_3^-, with an average of 92 % and 87 % of all reported results agreeing within 10 % of the true value across the concentration range covered in the PT schemes. In the case of NH_4^+, while an average of 90 % of reported results were within 10% of the reference at 1 mg L^{-1} NH_4^+, laboratory performance was poorer (68 % agreeing within 10 %) at lower concentrations (0.1 – 0.9 mg L^{-1}).

Poorer performance at the low concentrations was largely due to two laboratories (CEAM and SHMU) with > 50 % of their results reading high. For Na^+ and Cl^-, the percentages of results agreeing within 10 % of the reference were 81 % and 86 %, respectively, across the full range of PT concentrations. At concentrations above 1 mg L^{-1}, the agreement improved and increased to 89 % for Na^+ and 96% for Cl^-. A larger spread around the reference values were provided for the base cations Ca^{2+} and Mg^{2+} at low concentrations (< 1 mg L^{-1}). The percentage of results passing at low concentrations below 1 mg L^{-1} was 36 % (Ca^{2+}) and 59 % (Mg^{2+}), increasing to 80 % (Ca^{2+}) and 90 % (Mg^{2+}) above 1 mg L^{-1}. The larger scatter at low concentrations is likely due to uncertainty in the chemical analysis at or close to the method limit of detection, and reflects challenges of measuring base cations, in particular Ca^{2+} as this is very 'sticky' and adsorbs/desorbs from surfaces leading to analytical artefacts.

To show what the PT reference solution concentrations would correspond to if they were a denuder and/or aerosol extract, equivalent gas (Eq. 1) and/or aerosol concentrations (Eq. 2) (Sect. 4.3.2.1) are calculated for each of the ions and provided in the summary table in Fig. 4.4. A 0.5 mg L^{-1} NH_4^+ solution, for example, is equivalent to an atmospheric concentration of 0.09 µg NH_3 m^{-3} (gas), or 0.13 µg NH_4^+ m^{-3} (aerosol) for a monthly sample.

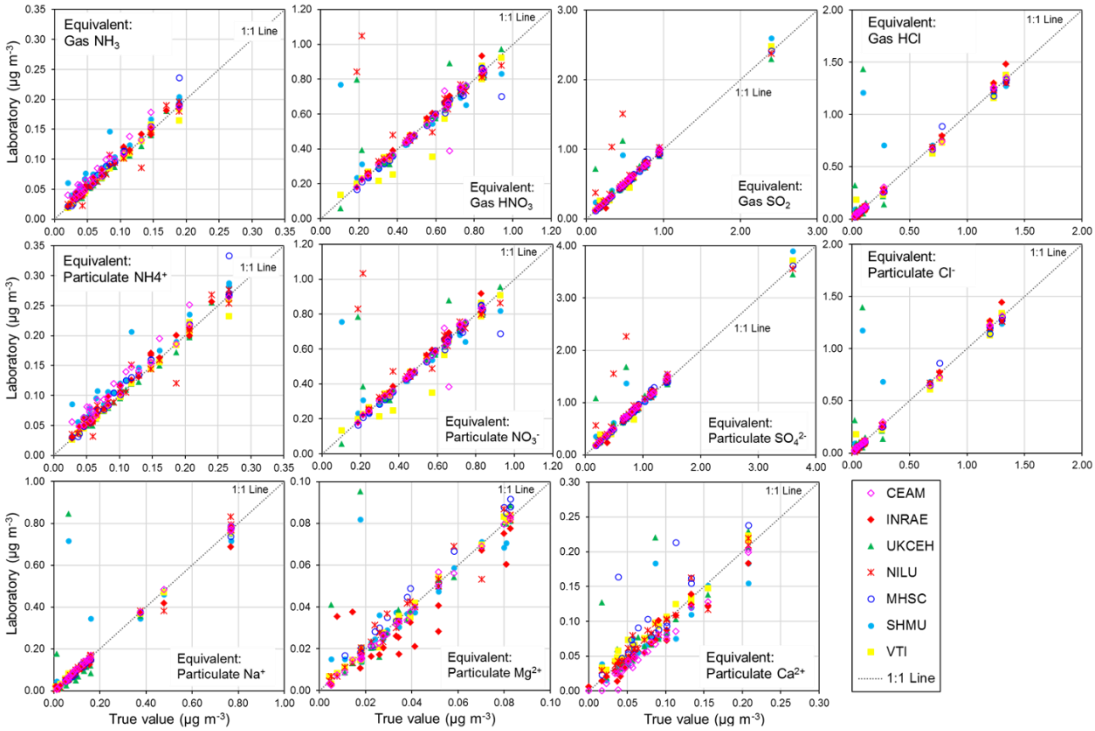

Figure 4.5. Scatter plots comparing all NEU laboratory reported results from wet chemistry proficiency testing (PT) schemes (2006 – 2010: EMEP, WMO-GAW and NitroEurope) *vs* true values (PT reference solutions). All aqueous ion concentrations (mg L^{-1}) from Fig. 4.4 are converted to equivalent gas and aerosols concentrations (µg m^{-3}) for the comparisons.

In Fig. 4.5, scatter plots are shown comparing all NEU laboratory reported results with PT reference, where all ion concentrations (mg L^{-1}) from Fig. 4.4 have been converted to equivalent gas and aerosol concentrations (µg m^{-3}), based on a typical volume of 15 m^3 over a month. With the exception of a small number of outliers, most data points are close to the 1:1 line with laboratory

results agreeing within ± 0.05 µg m^{-3} in equivalent gas and/or aerosol concentrations. These are low ambient concentrations and show that the measurement uncertainty in the analysis of very low concentrations in the PT schemes will be small for the majority of sites in the network, where concentrations were found to be much higher (see Fig. 4.6).

4.4.2 Laboratory inter-comparison results: DELTA® measurements

Results from 4 years of annual DELTA® field inter-comparisons (2006 – 2009), for all field sites, are combined and summarised in Fig. 4.6. The gas and aerosol concentrations measured and reported by each of the laboratories are compared with the median estimate of all laboratories in each of the scatter plots, with the colour of the symbols identifying the laboratory providing the measurements. Regression results (slope and R^2) in the table below the plots provide the main features of the inter-comparison. The slope is equivalent to the mean ratio of each laboratory against the median value, where values close to unity indicate closer agreement to the median value. Overall, the scatter plots show good agreement between the laboratories, with some laboratories showing very close agreement to the median estimates, and more scatter observed from the others.

The occurrence of outliers in some of the individual monthly values indicates that caution needs to be exercised in the interpretation of these data points in the inter-comparison. To average out the influence of a few individual outliers, the mean concentrations from each of the seven laboratories for each of the four field sites were calculated and compared with averaged median estimates of all laboratories for each site.

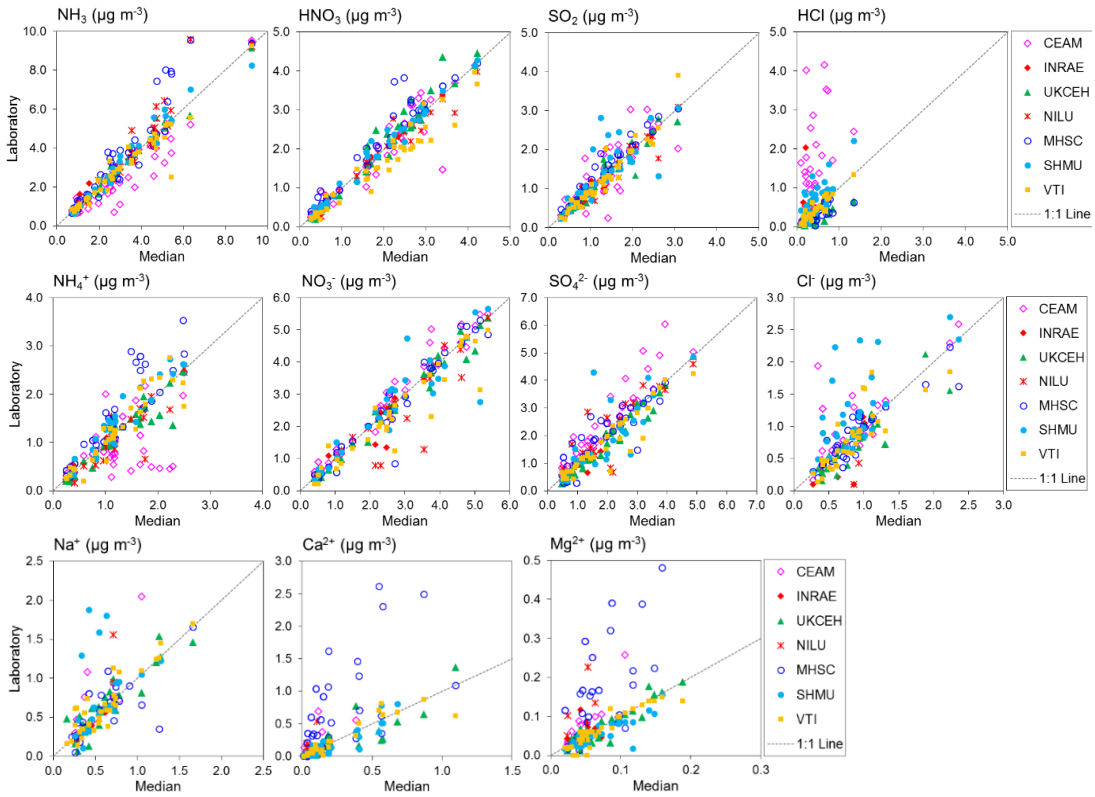

Lab	Gas: NH_3			Gas: HNO_3			Gas: SO_2			Gas: HCl		
	R^2	slope	*n*	R^2	slope	*n*	R^2	slope	*n*	R^2	slope	*n*
CEAM	0.87	0.89	41	0.80	0.90	39	0.66	0.94	41	0.16	1.77	41
INRAE	0.99	1.00	8	0.99	0.99	8	0.88	1.25	7	0.02	1.73	8
UKCEH	0.99	1.00	42	0.96	1.10	42	0.92	0.96	42	0.43	0.52	42
NILU	0.92	1.17	30	0.96	0.93	30	0.91	0.95	30	0.08	0.70	4
MHSC	0.87	1.21	41	0.93	1.08	37	0.92	1.01	38	0.58	0.58	39
SHMU	0.96	1.0	38	0.98	1.0	37	0.62	0.88	39	0.62	1.37	39
VTI	0.92	0.91	42	0.94	0.88	42	0.91	1.08	42	0.87	0.96	42
Lab	Particle: NH_4^+			Particle: NO_3^-			Particle: SO_4^{2-}			Particle: Cl^-		
	R^2	slope	*n*	R^2	slope	*n*	R^2	slope	*n*	R^2	slope	*n*
CEAM	0.22	0.42	41	0.96	1.03	41	0.89	1.20	41	0.54	1.01	40
INRAE	0.98	0.93	8	0.72	0.82	8	0.75	0.75	8	0.70	1.31	8
UKCEH	0.90	0.93	43	0.98	0.98	39	0.96	0.99	38	0.77	0.87	37
NILU	0.80	0.94	26	0.82	0.92	27	0.76	0.91	27	-	2.61	2
MHSC	0.80	1.26	40	0.93	1.02	41	0.78	0.89	39	0.80	0.85	39
SHMU	0.91	1.09	39	0.85	0.92	39	0.59	0.90	39	0.38	0.85	39
VTI	0.87	1.02	41	0.91	0.91	40	0.88	0.88	41	0.68	0.91	41
Lab	Particle: Na^+			Particle: Ca^{2+}			Particle: Mg^{2+}					
	R^2	slope	*n*	R^2	slope	*n*	R^2	slope	*n*			
CEAM	0.53	1.40	12	0.52	1.60	11	0.66	1.86	12			
INRAE	0.99	0.99	8	0.39	0.57	8	0.04	0.33	8			
UKCEH	0.82	0.95	38	0.77	0.92	38	0.86	1.05	40			
NILU	0.84	2.24	4	0.75	4.72	4	0.48	2.56	4			
MHSC	0.49	0.88	34	0.42	1.74	40	0.49	2.42	39			
SHMU	1.0	0.78	27	0.82	1.01	39	0.70	0.74	39			
VTI	0.82	1.0	41	0.75	0.88	37	0.84	0.95	41			

Figure 4.6. Scatter plots comparing atmospheric gas (NH_3, HNO_3, SO_2 and HCl) and aerosol (NH_4^+, NO_3^-, SO_4^{2-}, Cl^-, Na^+, Ca^{2+}, Mg^{2+}) concentrations measured by each of the NEU laboratories with the median estimate of all laboratories. Data from all field inter-comparisons (2006 – 2009) for all test sites (Auchencorth-UK, Braunschweig-Gemany, Montelibretti-Italy and Paterna-Spain) are combined in the analysis. A summary of the regression results is shown in the table below the graphs. Note (i) there are fewer data points for INRAE because they joined the NEU network later in 2007 and participated in the 2008 and 2009 inter-comaprisons only, (ii) low number of observations in some cases were due to some laboratories not reporting all parameters. NILU: HCl, Cl^-, Na^+, Ca^{2+} and Mg^{2+} reported for 2008 inter-comparisons only; CEAM: Na^+, Ca^{2+}, Mg^{2+} reported for 2007-2009 inter-comparisons only.

Table 4.2. Inter-comparison of results from 7 European laboratories at 4 different field test sites for all years (2006 – 2010). The results shown are the mean concentrations from each laboratory for each site and the averaged median estimates derived from all laboratories for each site

Site	Median (all years)	CEAM	% diff	CEH	% diff	MHSC	% diff	NILU	% diff	SHMU	% diff	VTI	% diff	*Median (2008/09)	*INRAE	*% diff
NH_3																
Auchencorth	1.42	1.23	-13	1.39	-2	1.51	6	1.60	13	1.48	4	1.38	-2	1.06	1.17	10
Braunschweig	4.32	3.61	-16	4.34	0	4.62	7	4.87	13	4.27	-1	4.41	2	6.40	6.64	4
Montelibretti	2.46	1.66	-33	2.44	-1	2.89	18	2.77	12	2.63	7	2.34	-5	1.91	1.91	0
Paterna	5.21	4.39	-16	5.27	1	7.00	34	6.22	19	5.55	7	4.57	-12			
NH_4^+																
Auchencorth	0.73	0.69	-6	0.64	-13	0.92	26	0.73	0	0.96	31	0.74	2	0.58	0.60	2
Braunschweig	1.55	1.54	-1	1.61	4	2.15	39	1.18	-24	1.64	6	1.45	-6	1.38	1.31	-5
Montelibretti	0.95	0.87	-9	0.86	-9	1.21	27	0.72	-24	1.13	19	0.93	-3	0.96	0.96	0
Paterna	1.80	0.50	-72	1.56	-13	2.12	18	1.64	-9	2.04	13	2.26	25			
HNO_3																
Auchencorth	0.57	0.57	-1	0.53	-7	0.69	21	0.62	9	0.59	3	0.49	-15	0.55	0.59	7
Braunschweig	2.36	1.79	-24	2.82	19	2.67	13	2.43	3	2.48	5	2.09	-11	2.85	2.85	0
Montelibretti	2.64	2.53	-4	2.74	4	3.08	17	2.60	-2	2.77	5	2.31	-13	1.70	1.70	0
Paterna	2.67	2.82	6	2.73	2	3.18	19	2.61	-2	2.40	-10	2.05	-23			
NO_3^-																
Auchencorth	1.21	1.24	3	1.18	-2	1.16	-4	1.27	4	1.20	-1	1.18	-3	1.26	1.14	-9
Braunschweig	3.26	3.70	14	3.43	5	3.33	2	2.28	-30	3.09	-5	2.36	-28	2.92	2.94	1
Montelibretti	1.81	2.00	10	1.84	1	1.57	-13	1.28	-29	1.91	5	1.56	-14	2.11	2.11	0
Paterna	4.52	4.73	5	4.34	-4	4.60	2	4.34	-4	4.57	1	4.32	-4			
SO_2																
Auchencorth	0.95	0.91	-4	0.88	-7	0.99	4	1.10	15	0.91	-4	1.05	10	0.93	1.21	30
Braunschweig	1.49	1.33	-11	1.49	0	1.65	10	1.32	-12	1.41	-5	1.45	-3	1.05	1.17	11
Montelibretti	1.12	1.29	15	1.15	2	1.48	31	0.94	-16	1.45	29	0.99	-12	0.54	0.54	0
Paterna	1.96	2.07	6	1.96	0	2.04	4	1.93	-2	1.99	2	1.78	-9			
SO_4^{2-}																
Auchencorth	1.04	1.21	17	0.80	-23	1.14	10	1.66	60	1.23	19	0.97	-7	0.82	0.58	-29
Braunschweig	2.04	2.67	31	2.12	4	2.35	15	1.58	-22	1.72	-16	1.51	-26	1.61	1.37	-15
Montelibretti	1.55	1.89	22	1.35	-13	1.61	4	1.49	-4	1.79	16	1.43	-8	0.83	0.83	0
Paterna	3.28	4.19	28	3.06	-7	3.06	-7	3.68	12	3.01	-8	3.21	-2			
HCl																
Auchencorth	0.20	1.01	396	0.19	-9	0.15	-28	0.21	4	0.33	62	0.19	-6	0.22	0.74	244
Braunschweig	0.39	1.35	247	0.22	-43	0.16	-59	0.08	-78	0.63	62	0.35	-9	0.16	0.10	-37
Montelibretti	0.40	1.01	151	0.33	-18	0.40	-1	-	-	0.58	45	0.36	-11	0.54	0.54	0
Paterna	0.73	1.77	141	0.42	-42	0.47	-36	-	-	1.32	80	0.81	10			
Cl^-																
Auchencorth	0.84	0.93	10	0.73	-13	0.86	3	0.26	-69	1.17	39	0.85	1	0.95	0.81	-15
Braunschweig	0.52	0.78	51	0.35	-32	0.57	10	-	-	0.81	56	0.36	-30	0.33	0.21	-39
Montelibretti	0.85	0.94	11	0.76	-11	0.84	-1	-	-	1.19	41	0.86	1	0.66	0.66	0
Paterna	1.37	1.74	27	1.11	-19	1.31	-5	-	-	2.10	54	1.06	-23			
Na^+																
Auchencorth	0.53	0.79	47	0.55	2	0.60	13	1.25	134	0.68	28	0.56	5	0.65	0.57	-11
Braunschweig	0.37	0.38	4	0.21	-43	0.37	1	0.24	-34	0.85	131	0.37	1	0.27	0.19	-29
Montelibretti	0.59	0.99	67	0.62	4	0.70	18	-	-	0.84	42	0.59	-1	0.51	0.51	0
Paterna	0.94	-	-	1.01	7	0.71	-25	-	-	0.94	-1	0.95	1			
Ca^{2+}																
Auchencorth	0.06	0.06	-5	0.06	-11	0.32	415	0.15	137	0.05	-27	0.06	-12	0.03	0.04	38
Braunschweig	0.16	0.07	-57	0.14	-15	0.61	272	0.36	122	0.09	-47	0.11	-34	0.07	0.08	15
Montelibretti	0.16	0.54	241	0.16	-1	0.45	183	-	-	0.15	-4	0.16	2	0.08	0.08	0
Paterna	0.64	-	-	0.53	-17	1.69	163	-	-	0.49	-24	0.57	-12			
Mg^{2+}																
Auchencorth	0.05	0.07	27	0.05	-3	0.14	172	0.18	251	0.05	-6	0.05	-8	0.05	0.09	65
Braunschweig	0.05	0.03	-33	0.04	-26	0.10	114	0.08	61	0.03	-35	0.02	-56	0.02	0.04	77
Montelibretti	0.06	0.13	113	0.06	-2	0.18	185	-	-	0.05	-13	0.06	2	0.04	0.04	0
Paterna	0.13	-	-	0.13	-4	0.33	147	-	-	0.10	-24	0.13	-2			

A summary of the mean concentrations and the percentage difference from median is presented in Table 4.2. Since the INRAE laboratory did not join the NEU network until 2008, averaged median values from the 2008 and 2009 inter-comparisons are used to compare with the INRAE results, included in the table for clarity. The mean concentrations between laboratories are broadly comparable. Each of the laboratories were also able to resolve the main differences in mean concentrations at the four field sites, ranging from the smallest concentrations at Auchencorth (e.g. median = 1.4 µg NH_3 m^{-3}) to higher concentrations representing a more polluted site at Paterna (e.g. median = 5.2 µg NH_3 m^{-3}) for the test periods (Table 4.2). Larger differences for HCl, Ca^{2+} and Mg^{2+} are due to clear outliers from one or two laboratories at the very low concentrations of these species encountered and may be related to measurement uncertainties at the low air concentrations. The comparability between laboratories for each of the components is next considered in turn.

4.4.2.1 Inter-comparisons: NH_3, NH_4^+, HNO_3, NO_3^-

The best agreement between laboratories was for the N_r gases (NH_3, HNO_3) and aerosol species (NH_4^+, NO_3^-), with slopes within ± 10 % of the median values and $R^2 > 0.9$ in the regression analysis from five of the laboratories (Fig. 4.6, Table 4.2). This is important since N_r species were the primary focus for the NEU DELTA® network. Slightly poorer agreement for NH_3 and NH_4^+ were provided by CEAM and MHSC laboratories, with data points both above and below the 1:1 line (Fig. 4.6). The outliers above the 1:1 line from MHSC were from the 2006 inter-comparison exercise. Removal of these 2006 outliers improved the MHSC regression slope for NH_3 from 1.21 ($R^2 = 0.87$, $n = 41$) to 0.99 ($R^2 = 0.99$, $n = 10$) (Supp. Fig. S4.1). While this seems to suggest that the performance of MHSC for NH_3 improved following the first inter-comparison exercise, the regression slope for aerosol NH_4^+ increased instead from a slope of 1.26 ($R^2 = 0.83$, $n = 41$) to 1.48 ($R^2 = 0.93$, $n = 10$), suggesting an over-estimation of NH_4^+ concentrations (Supp. Fig. S4.1). A possible cause may be the quality and/or variability in the aerosol filter blank values for NH_4^+, as laboratory blanks are subtracted from exposed samples to estimate aerosol

NH_4^+ concentrations. Laboratory blank results were however not reported to allow this assessment. Another possibility is a breakthrough of NH_3 from the acid coated denuders onto the aerosol filters. The denuder collection efficiency of NH_3 gas (Eq. 3, Sect. 4.3.2.1) reported by MHSC was on average 88 % for all years and 91 % where 2006 data have been excluded (Supp. Table S4.3). This is comparable with the mean collection efficiencies of all laboratories (91 and 90 %) (Supp. Table S4.3), which makes NH_3 breakthrough an unlikely explanation for the higher readings. The assessment of NH_4^+ is however more uncertain from the reduced number of data points (n = 10).

For the CEAM laboratory, reported NH_3 concentrations were on average 16 % lower (n = 41) than the median, with a slope of 0.89 (R^2 = 0.87) and particulate NH_4^+ were on average 13 % lower (n = 41) than the median, with a slope of 0.42 (R^2 = 0.22) (Fig. 4.6). A need to improve the NH_4^+ analysis (Indophenol colorimetric assay) in the acid coated denuders and aerosol filters by the CEAM laboratory was identified from the 2006 inter-comparison (Tang et al., 2009). The Indophenol method for aqueous NH_4^+ determination is pH sensitive. Calibration solutions and quality control checks for the colorimetric assays are made up in deionised water (pH 7), whereas the aqueous extracts from the DELTA® acid coated denuders and cellulose filters are acidic (pH ~3). Determination of NH_4^+ in the denuder extracts may therefore be under-estimated if the pH of the indophenol reaction has not been adjusted for the increased acidity in the sample extracts.

When the 2006 data are excluded from the regression analysis, the slopes for NH_3 and NH_4^+ increased to 1.02 (R^2 = 0.94, n = 12) and 0.98 (R^2 = 0.51, n = 12), respectively (Supp. Fig. S4.1). The improved agreement with other laboratories after the 2006 inter-comparison suggests that the method under-read was largely resolved, reflected in an improvement in the slope. Despite some uncertainties in the NH_3/NH_4^+ measurements, the laboratories were able to clearly resolve the main differences in mean concentrations at the four different field sites in all years (Table 4.2). The results presented here for CEAM and MHSC highlight the importance of the initial inter-comparison

exercise in identifying and resolving sampling and analytical issues at the start of the project.

4.4.2.2 Inter-comparisons: SO_2, SO_4^{2-}

Six laboratories provided slopes within 12 % of the median values in the regression analysis for SO_2 (Fig. 4.6). The smaller R^2 values were from two laboratories (CEAM and SHMU, $R^2 < 0.7$), with data points both above and below the 1:1 line. For INRAE, the larger slope of 1.6 ($R^2 = 9$) was due to a single high SO_2 reading reported for Auchencorth of 2.0 µg SO_2 m^{-3}, compared with the median of 1.4 µg SO_2 m^{-3}. When the mean SO_2 concentrations measured by INRAE are compared with the median, the difference was on average 13 %, providing acceptable agreement, which suggests that the high reading may just be an outlier. There was more scatter in the inter-comparison for SO_4^{2-}, although the majority of points are still close to the 1:1 line (Fig. 4.6). Six laboratories provided slopes within 12 % of the median values in the regression analysis also for SO_4^{2-}. The regression slope from CEAM for SO_4^{2-} was 1.2 ($R^2 = 0.9$) which is still within 20% of the median. The SO_2 and SO_4^{2-} measurements were broadly comparable between the laboratories, with mean concentrations agreeing on average within 6 % of the median (Table 4.2).

4.4.2.3 Inter-comparisons: HCl, Cl^-

The HCl inter-comparison show clear outliers from the CEAM laboratory, with concentrations that were on average up to 2 times higher than other laboratories (slope = 1.8). For example, a mean concentration of 1.8 µg HCl m^{-3} was reported by CEAM for Paterna, compared with a median of 0.7 µg HCl m^{-3}. Apart from CEAM, the mean concentrations of HCl reported by the other laboratories were generally comparable (Table 4.2). The larger % differences between the measured mean and median at each site reflect the challenges of measuring the very low concentrations of HCl at these sites of < 0.5 µg HCl m^{-3} (slightly higher at Paterna). HCl results were reported by NILU for the 2008 inter-comparison exercise only, limiting the number of measurements (n = 4) available for comparison.

The comparison for Cl^- showed better agreement of the CEAM laboratory results with other laboratories, in both the inter-comparison of individual monthly values (Fig. 4.6) and the mean concentrations (Table 4.2). Like HCl, larger % differences between the measured concentrations and median at each site may be attributed to higher measurement uncertainties at the low concentrations of Cl^-. For NILU, there were only 2 data points for Cl^- from the Auchencorth site in the 2008 inter-comparison. Overall, the inter-comparison for HCl and Cl^- showed that the laboratories were able to resolve the main differences in mean concentrations at the different sites even at the low concentrations encountered.

4.4.2.4 Inter-comparisons: Base cations (Na^+, Ca^{2+}, Mg^{2+})

Measurements of Ca^{2+} and Mg^{2+} were the most uncertain, with the largest scatter in the inter-comparisons (Fig. 4.6). Despite the trace levels of these base cations at all field sites, 4 laboratories (INRAE, UKCEH, SHMU, VTI) provided data close to the 1:1 line, demonstrating close agreement between these laboratories. The clear outliers above the 1:1 line are from CEAM, MHSC and NILU, with slopes > 2. While MHSC over-read Ca^{2+} and Mg^{2+}, their results for Na^+ were in better agreement with other laboratories, with a slope of 0.9 (R^2 = 0.5) (Fig. 4.6). There was a lot of scatter in the data however, with outlier points both above and below the 1:1 line, suggesting measurement uncertainties in their base cation measurements.

For NILU, the only base cation results reported by the laboratory were for the 2008 DELTA® inter-comparisons at Auchencorth and Braunschweig. This accounts for the low number of data points (n = 4) from the NILU laboratory. The median concentrations of Ca^{2+} and Mg^{2+} at both field sites were very low (< 0.1 µg m^{-3}), which makes comparison with the few data reported from NILU highly uncertain. Like NILU, CEAM also did not report base cations results for all of the DELTA® inter-comparison. Base cation results provided by CEAM were for 2007 – 2009 only.

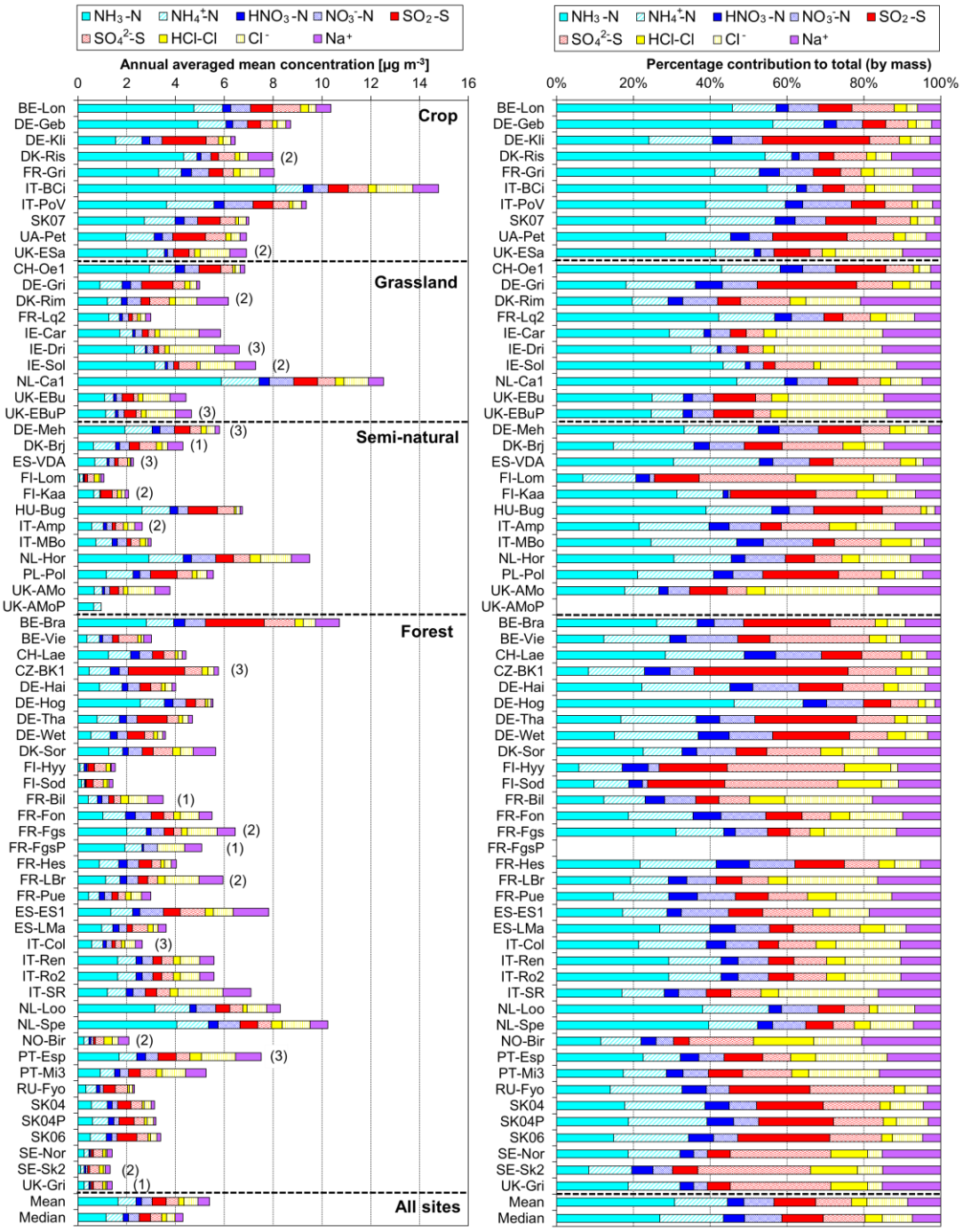

Figure 4.7. (LEFT) Annual averaged gas and aerosol concentrations (2007 – 2010) of sites in the NEU DELTA® network, grouped according to ecosystem types: crops (n = 10), grassland (n = 9 + 1 parallel), semi-natural (n = 11 + 1 parallel) and forests (n = 34 + 2 parallel). (RIGHT) Percentage composition of gas and aerosol components measured at NEU DELTA® network sites (n = 64 + 4 parallel sites) (mean of all annual mean concentrations from 2007 to 2010). Years with < 7 months of data, including 2006, are excluded. Where the number of years contributing to the annual average is < 4, the number is shown in brackets beside the site data. Ca^{2+} and Mg^{2+} data are not included as these were mostly at or below limit of detection. Replicated DELTA measurements are made at 4 sites: FR-Fgs/FR-FgsP (NaCl instead of K_2CO_3/glycerol coated denuders - HCl not measured), SK04/SK04P; UK-Ebu/UK-EbuP and UK-AMo/UK-AMoP (NH_3/NH_4^+ only).

4.4.3 Variation in annual mean gas and aerosol concentrations and composition

4.4.3.1 Comparisons according to ecosystem types

Annual averaged concentrations of gases and aerosols measured in the NEU DELTA® network are presented in Fig. 4.7, with sites grouped according to each of four major ecosystem types: crops, grassland, forests and semi-natural. These are the classifications used in dry deposition models, where ecosystem-specific deposition velocities (V_d) are combined with measurement data to produce estimates of N_r dry deposition (Flechard et al., 2011). In some models such as the Concentration Based Estimates of Deposition (CBED) model (Smith et al., 2000; Flechard et al., 2011), a canopy compensation point and the bi-directional exchange of NH_3 between vegetation-type and the atmosphere are also considered (e.g. Sutton et al., 1995; Massad et al., 2010; Flechard et al., 2011).

A total of 64 sites from 20 different countries, including replicated measurements at 4 of the sites, are compared in Fig. 4.7. Not all of the sites were however operational all of the time or at the same time. Changes in the numbers and locations of sites occurred over the duration of the network, for example, due to site closures, relocations and/or new site additions. The annual averaged concentrations plotted for each site are the mean of all available annual means. Where the annual averaged concentration is derived from less than 4 full years of data, the number of years providing the mean is shown, in brackets, next to the site data in the graph.

To avoid bias in the calculation of annual means, due to seasonality in the data (see later in Sect. 4.4.5), years with incomplete data coverage (< 7 months of data in any year) were excluded. Applying these data exclusions, the number of sites that provided annual data was 55 sites for 2007, 57 sites for 2008, 54 sites for 2009 and 55 sites for 2010. The number of sites that provided annual data for each year over the entire period was 45 sites.

Sites with parallel (P) DELTA® measurements were Auchencorth Moss (UK-AMoP), Easter Bush (UK-EBuP), Fougéres (FR-FgsP) and SK04P (EMEP site in Slovakia) (Fig. 4.7). Overall, good reproducibility in DELTA® measurements was demonstrated by the parallel measurements. At the Auchencorth Moss parallel site (UK-AMoP), NH_3 and NH_4^+ only were measured, and agreement for these 2 components were on average within 5 % at the low concentrations measured at this site (annual mean: 0.5 – 0.9 µg NH_3 m^{-3} and 0.3 – 0.5 µg NH_4^+ m^{-3}). Parallel measurements at Easter Bush (UK-EBuP) stopped in March 2010. With the exception of Ca^{2+} and Mg^{2+}, the comparison of annual mean data from the replicated measurements for 2007 to 2009 provided excellent agreement of 2 % (Na^+) to 13 % (SO_4^{2-}) at Easter Bush.

At Fougéres, HNO_3 concentration measured on K_2CO_3/Glycerol coated denuders (FR-Fgs) was about 2-fold higher than on NaCl coated denuders in the parallel DELTA® system (FR-FgsP), consistent with over-estimation of HNO_3 (on average 45 %) on carbonate coated denuders (see Sect. 4.3.2.3). The disadvantage of a NaCl coating, however, is that it can only collect HNO_3 and not the other acid gases. A third carbonate denuder is necessary in the sample train to collect and measure HNO_3, since SO_2 is only partially captured and HCl cannot be measured on NaCl denuders (Tang et al., 2015, 2018b). This explains the smaller SO_2 concentrations reported by the FR-FgsP site, with break-through of SO_2 (inefficiently captured by NaCl denuders) onto the aerosol filters resulting in larger particulate SO_4^{2-} concentrations than the Fr-Fgs site.

For the SK04 site, measurement reproducibility for the 4 years of parallel data for N and S component was good, with agreement ranging from 0.4 % (NH_4^+) to 15 % (SO_4^{2-}). HCl and Na^+ and determinations were however more uncertain with differences of 21 and 28%, respectively. It has to be noted, however, that the concentrations of the two components were very low, at < 0.2 µg HCl m^{-3} and < 0.4 µg Na^+ m^{-3}. The differences in concentrations are therefore actually within ± 0.1 µg m^{-3} for HCl and within ± 0.2 µg m^{-3} for Na^+.

A key feature in Fig. 4.7 is the dominance of N over S species at most sites, when expressed as µg m^{-3} of the element. The mean percentage contribution of sum N_r (NH_3-N, HNO_3-N, NH_4^+-N, NO_3^--N) concentrations to the total mass of gas and aerosol species measured is 52 % (range = 24 – 80%), twice as much as from sum S (SO_2-S and SO_4^{2-}-S; mean = 23 %, range = 7 – 53%) (Fig. 4.8). This is consistent with more substantial reductions in SO_2 emissions (−72%) than achieved with NO_x (−43%) or NH_3 (−18%) in Europe between 1991 – 2010 (EEA, 2019). The differences in atmospheric composition of S and N species in the present assessment therefore reflected changes in emissions of the precursor gases, and are also in agreement with a recent assessment of air quality trends showing important changes in S and N composition in air and rain across the EMEP networks (EMEP, 2016).

Most of the N_r concentrations at each site in turn are dominated by reduced N (NH_3-N, NH_4^+-N), rather than by oxidised N species (HNO_3-N, NO_3^--N). Of the sum N_r concentrations measured, 60 – 97 % (mean = 76%, *n* = 66) were reduced N (N_{red}) (Fig. 4.8). Even more strikingly, NH_3 (NH_3-N) was by far the single most dominant component at the majority of sites, contributing on average 42% (range = 24 – 56 %, *n* = 10) at cropland sites and 20 % (6 – 46%, *n* = 35) of the total gas/aerosol concentrations at forest sites (Fig. 4.8).

This illustrates very clearly the importance of NH_3 and by association agricultural emissions in contributing to NH_3-N concentrations and deposition in Europe, with 92 % of total NH_3 emissions in Europe estimated to come from agriculture (EEA, 2019). The reaction of NH_3 with the acid gases HNO_3 and SO_2 forms NH_4^+-containing particulate matter (PM) that are primarily NH_4NO_3 and $(NH_4)_2SO_4$ (Fig. 4.1) (see Sect. 4.4.4). Together, particulate NH_4^+-N, NO_3^--N and SO_4^{2-}-S made up on average 28% (17 – 40 %, *n* = 10) of the total gas/aerosol concentrations measured at cropland sites (Fig. 4.8). At semi-natural and forest sites however, that number was even bigger at 33% (20 – 40%, *n* = 11) and 37 % (24 – 57%, *n* = 35), respectively (Fig. 4.8).

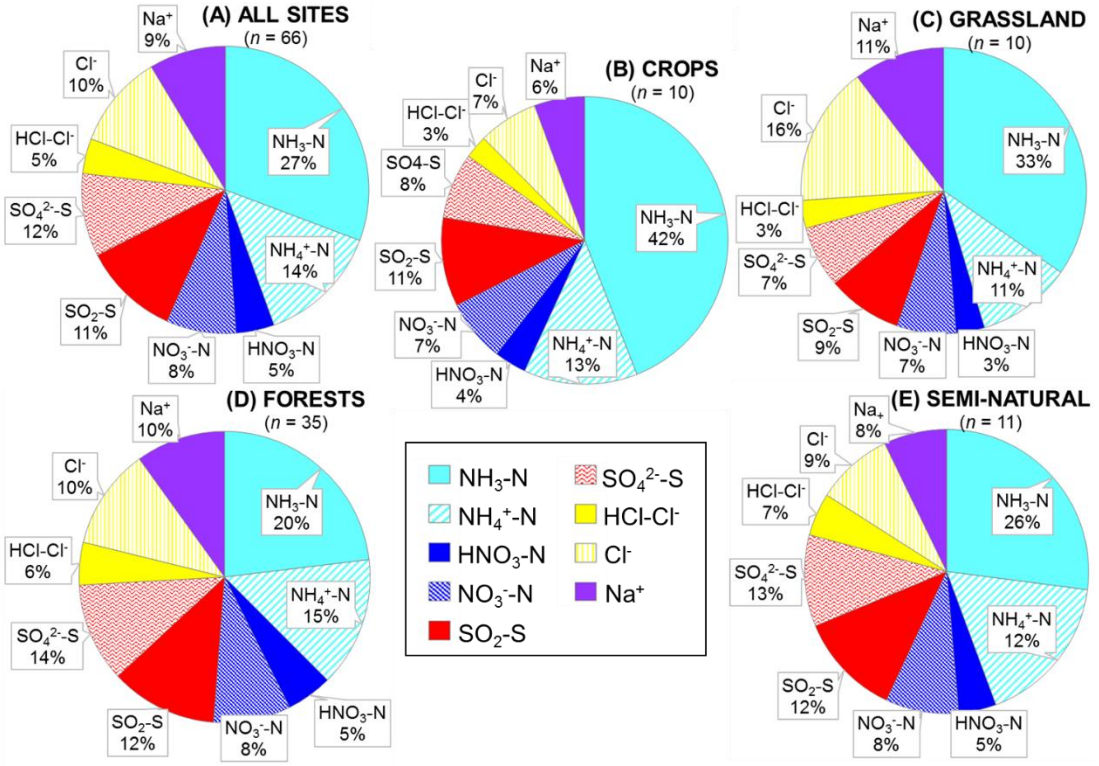

Annual mean (µg m^{-3})	Percentage contribution to total gas and aerosol measured (by mass)														
	(A) ALL SITES (*n* = 66) %			(B) CROPS (*n* = 10) %			(C) GRASSLAND (*n* = 10) %			(D) FORESTS (*n* = 35) %			(E) SEMI-NATURAL (*n* = 11) %		
	mean	min	max	mean	min	max	mean	min	max	mean	min	max	mean	min	max
NH_3-N	27	6	56	42	24	56	33	18	47	20	6	46	26	7	39
NH_4^+-N	14	6	23	13	7	21	11	6	18	15	9	23	12	6	20
HNO_3-N	5	1	9	4	2	5	3	1	7	5	3	9	5	1	8
NO_3^--N	8	0	15	7	4	13	7	3	9	8	1	13	8	0	15
SO_2-S	11	3	40	11	4	28	9	3	26	12	4	40	12	6	20
SO_4^{2-}-S	12	3	31	8	3	12	7	4	13	14	5	31	13	5	26
HCl-Cl$^-$	5	1	21	3	1	3	3	1	5	6	2	16	7	1	21
Cl$^-$	10	2	29	7	3	17	16	3	28	10	2	26	9	2	29
Na$^+$	9	1	21	6	2	13	11	3	21	10	1	21	8	1	17
Total	*100*				*100*							*100*	*100*		
Sum N_r	54	24	80	66	54	80	54	41	73	49	24	80	51	24	67
Sum N_{red}	41	17	70	55	41	70	44	29	59	35	17	64	38	19	56
Sum N_{ox}	13	2	24	11	5	17	10	5	16	13	5	20	13	2	24
Sum S	23	7	53	18	11	36	16	7	35	26	11	53	25	15	38
Sum (NH_4^+-N + NO_3-N + SO_4^{2-}-S)	34	15	57	28	17	40	25	15	36	37	24	57	33	20	40
	Percentage contribution: by groups of components measured (by mass)														
N_{red} / N_r	76	60	97	84	76	91	81	69	91	72	62	82	75	60	97
NaCl / total aerosol	20	4	45	12	6	27	27	6	43	20	4	42	17	4	45

Figure 4.8. (TOP) Pie charts showing the mean atmospheric composition of gas and aerosol components from annual averaged concentrations (µg m^{-3}) measured at NEU DELTA® sites, for A) All sites (n = 66) and sites grouped according to ecosytem types, B) Crops (n = 10), C) Grassland (n = 10), D) Forests (n = 35) and E) Semi-natural (n = 11). UK-AmoP (parallel DELTA® at Auchencorth: NH_3/NH_4^+ only) and FR-FgsP (parallel DELTA® at Fougéres: different sample train) were excluded in this analysis. (BOTTOM) Summary statistics on percentage composition by mass (µg m^{-3} element) measured. Sum N_r = sum (NH_3-N + NH_4^+-N + HNO_3-N + NO_3^--N), Sum S = sum (SO_2-S + SO_4^{2-}-S), N_{red} = sum reduced N (NH_3-N + NH_4^+-N), N_{ox} = sum oxidised N (HNO_3-N + NO_3^--N).

Secondary NH_4^+ particles are mainly in the 'fine' mode with diameters of less than 2.5 µm ($PM_{2.5}$) and estimated to contribute between 10 to 50 % of ambient $PM_{2.5}$ mass concentration in some parts of Europe (Putaud et al., 2010, Schwartz et al., 2016). An assessment by Hendriks et al. (2013) found that secondary NH_4^+ contributed 10 – 20% of the $PM_{2.5}$ mass in densely populated areas in Europe and even higher contributions in areas with intensive livestock farming. Concentrations of $PM_{2.5}$ continue to exceed the EU limit values of 25 µg m^{-3} annual mean in large parts of Europe in 2017 (EEA, 2019). Particulate NH_4^+ data presented from the DELTA® network therefore highlights the potential contribution of NH_3 of agricultural origin to fine NH_4^+ aerosols in $PM_{2.5}$. The formation and transport of these secondary aerosols poses a serious risk to human health, since $PM_{2.5}$ are linked with increased mortality from respiratory and cardiopulmonary diseases (AQEG, 2012).

A considerable fraction of the aerosol components measured was made up of sea salt (Na^+ and Cl^-), with contributions from sum (Na^+ and Cl^-) ranging from 4 % of the total aerosol loading at the inland Höglwald site in Germany (DE-Hog) to 43 % at Dripsey (IE-Dri), a coastal site in Ireland (Fig. 4.7). With the reduction in European emissions and concentrations of the gases SO_2, NO_x and NH_3 for formation of NH_4^+-containing aerosols, sea salt is therefore assuming a proportionate increase of the aerosol composition, consistent with observations from a recent European assessment of composition and trends in long-term EMEP measurements (EMEP, 2016). The concentrations of Ca^{2+} and Mg^{2+} were very low across the network, with values (mean of all sites = < 0.1 µg m^{-3}) that were at or below method limit of detection (LOD = ~ 0.1 µg m^{-3}). These data are also considered to be under-estimated due to the DELTA particle sampling cut-off (~ $PM_{4.5}$) and they were excluded from further assessment in this paper.

4.4.3.2 Comparisons with national gas emissions

In Fig. 4.9, the annual averaged gas and aerosol concentrations of grouped sites from each country are plotted with the corresponding national emission densities derived for NH_3, NO_x and SO_2. The emissions data in the graphs are the 4-year averages for the period 2007 to 2010, expressed as emissions per unit area of the country per year (t km^{-2} yr^{-1}) (see Sect. 4.3.6) and ranked in order of increasing emission densities. The error bars, where shown, is the range (min and max) of annual averaged concentrations of sites in each country. Where error bars are not visible, this indicates either that the country has measurement from just one site, or the range of concentrations measured are very close to the average.

From the visual comparisons, national mean measured concentrations in each country appear to scale reasonably well with the ranked emission densities. This is supported by further regression analyses which showed significant correlation between annual averaged concentrations of NH_3, NO_x and SO_2 with emission densities of NH_3 ($R^2 = 0.49$, $p < 0.001$, Fig. 4.10A1), NO_x ($R^2 = 0.20$, $p < 0.05$, Fig. 4.10A2) and SO_2 ($R^2 = 0.65$, $p < 0.001$, Fig. 4.10A3), respectively (Table 4.3). The particulate components NH_4^+ and NO_3^- were also correlated with both precursor gases NH_3 and HNO_3 (Table 4.3). By contrast, there was no relationship between SO_4^{2-} with any of the three gases, possibly because of contributions to SO_4^{2-} from long-range transport. All regression plots of concentrations against emission densities, including summary statistics are provided in Supp. Fig. S4.2.

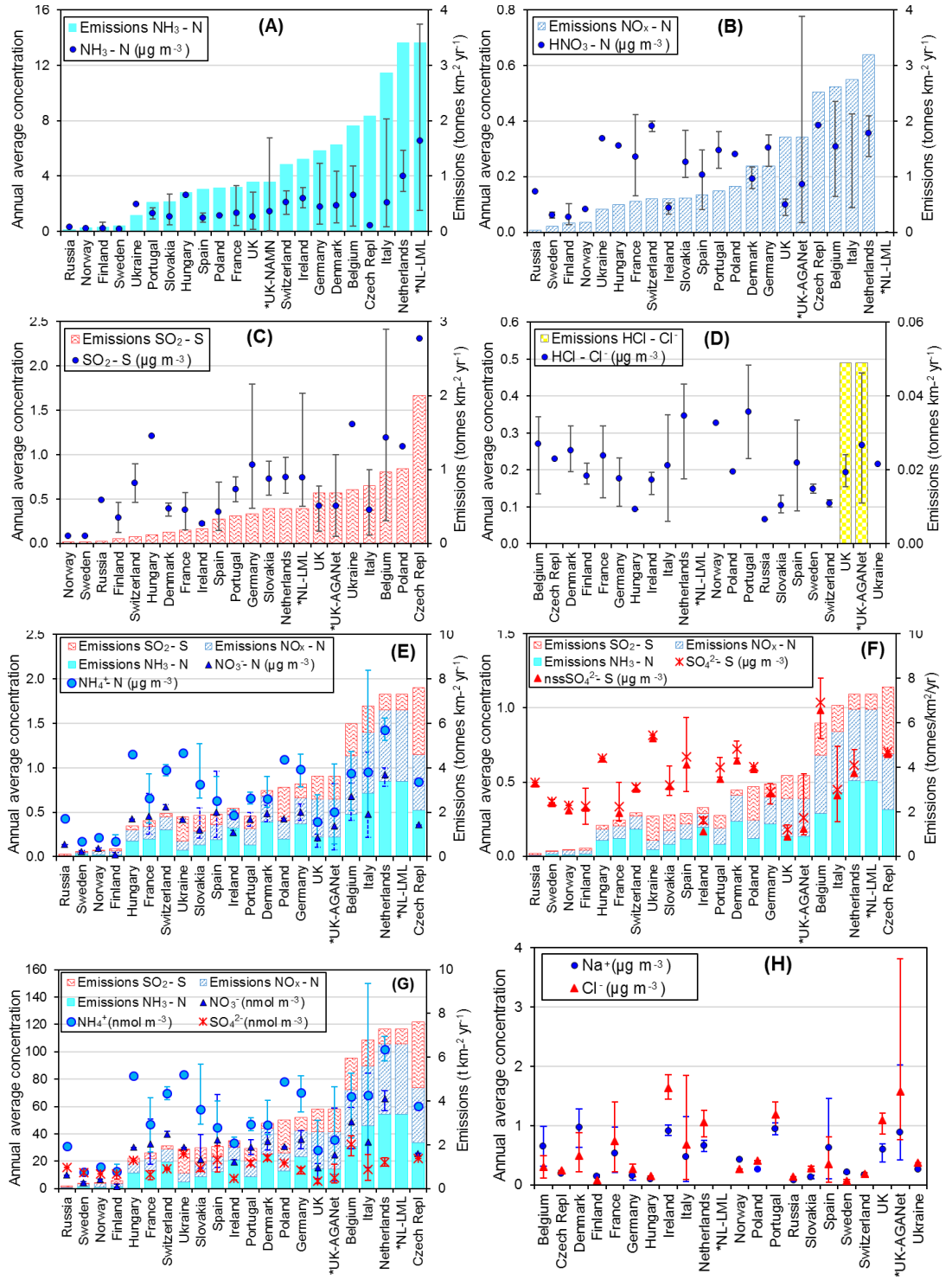

Figure 4.9. Comparisons of annual averaged gas and aerosol concentrations (2007 – 2010) of sites in the NEU DELTA® network, grouped by countries, with the respective 4-year averaged annual emission densities of gases (NH_3, NO_x and SO_2) over the same period. Monitoring data from 3 national monitoring networks: *UK NAMN (NH_3 from 72 sites and NH_4^+ from 30 sites; Tang et al., 2018a), *UK AGANet (raw uncorrected HNO_3, SO_2, HCl, NO_3^-, SO_4^{2-}, Cl^-, Na^+ from 30 sites; Tang et al. 2018b) and *NL-LML (NH_3 and SO_2 from 8 sites; van Zanten et al. 2017) are also included to illustrate the wider range of concentrations from larger numbers of sites. Error bars show the minimum and maximum concentrations measured in each country in the network

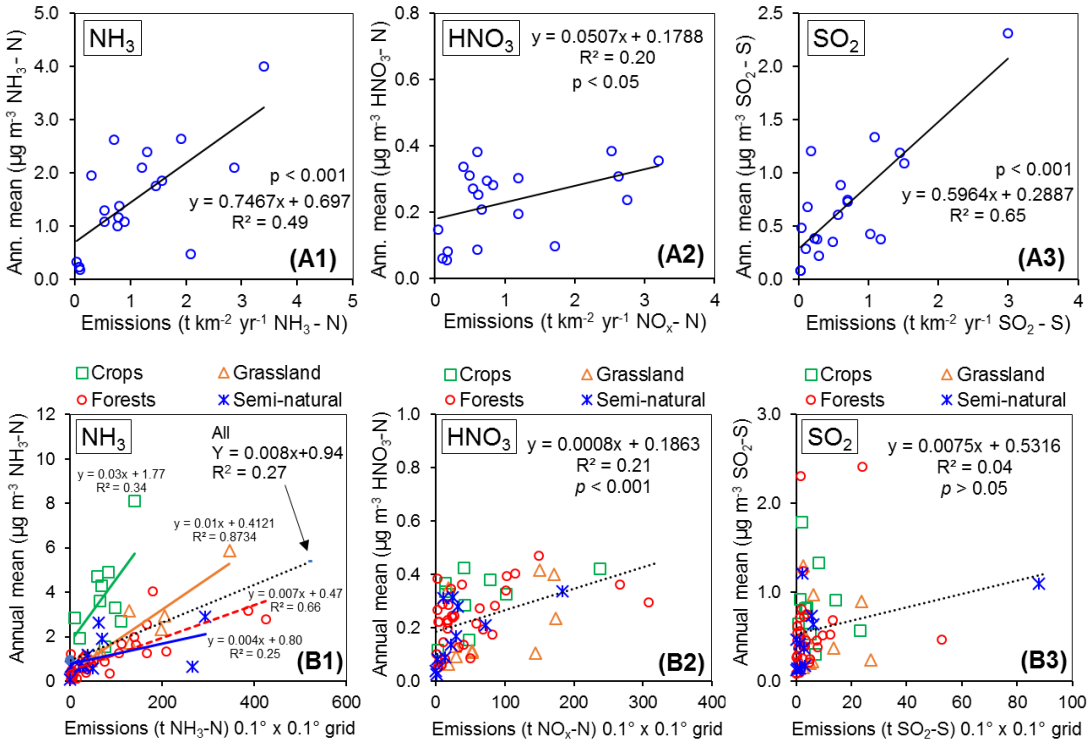

Figure 4.10. (A) Regression plots of national annual averaged gas (NH_3, HNO_3, SO_2) concentrations (2007 – 2010) vs 4-year national averaged emission densities of respective gases (NH_3, NO_x and SO_2: tonnes km^{-2} yr^{-1}) from each country over the same period (n = 20). (B) Regression plots of annual averaged gas (NH_3, HNO_3, SO_2) concentrations (2007 – 2010) at each site in the NEU DELTA® network vs 4-year averaged total emissions of gases (NH_3, NO_x and SO_2: tonnes yr^{-1}) from single EMEP grids (0.1º x 0.1º) in which each site is located (n = 66). Coloured symbols indicate the ecosystem classification of each site (Crops, n = 10; Grassland, n = 10; Forests, n = 35 and Semi-natural, n = 11).

Table 4.3. Summary statistics of regression analyses between national annual averaged gas (NH_3, HNO_3, SO_2) and aerosol (NH_4^+, NO_3^-, SO_4^{2-}) concentrations, and national emission densities (4-year average for period 2007 to 2010, expressed as emissions per unit area of the country per year) for each of the 20 countries in the NEU DELTA® network.

National annual average (n = 20)	National emission densities (20 countries)								
	NH_3 (tonnes N km^{-2} yr^{-1})			NO_x (tonnes N km^{-2} yr^{-1})			SO_2 (tonnes S km^{-2} yr^{-1})		
($\mu g\ m^{-3}$)	slope	intercept	R^2	slope	intercept	R^2	slope	intercept	R^2
Gas NH_3 - N	0.75	0.70	0.49***	0.57	0.90	0.30*	0.05	1.46	0.00^{ns}
Gas HNO_3 - N	0.06	0.17	0.24*	0.05	0.18	0.20*	0.08	0.18	0.25*
Gas SO_2 - S	0.17	0.52	0.24^{ns}	0.22	0.46	0.16^{ns}	0.60	0.29	0.65***
Aerosol NH_4^+ - N	0.23	0.50	0.36**	0.19	0.54	0.27*	0.20	0.61	0.16^{ns}
Aerosol NO_3^- - N	0.18	0.20	0.57***	0.15	0.23	0.44**	0.08	0.33	0.07^{ns}
Aerosol SO_4^{2-} - S	0.06	0.47	0.07^{ns}	0.07	0.45	0.12^{ns}	0.12	0.44	0.18^{ns}

4.4.3.3 Comparisons with gridded emissions

The comparisons in Sect. 4.4.3.2 used national emission totals, where emissions have been summed and averaged across very large and heterogeneous areas in each country. Another approach is to compare the individual site mean data with gridded emissions from individual 0.1° x 0.1° EMEP grids in which the NEU sites are located (see Sect. 4.3.6). This also provided significant correlations for NH_3 ($p < 0.001$, $n = 66$, Fig. 4.10B1) and HNO_3 *vs* NO_x ($p < 0.05$, Fig. 4.10B2), but not for SO_2 (Fig. 4.10B3, Supp. Fig. S4.3). Some interesting features also emerged in the NH_3 comparisons, with clustering of data according to ecosystem types (Fig. 4.10B1). The cropland sites have highest NH_3 concentrations compared with gridded emissions (slope = 0.03, $R^2 = 0.34$, $p = 0.08$, $n = 10$), followed by grassland sites (slope = 0.01, $R^2 = 0.87$, $p < 0.001$, $n = 10$) (Fig. 4.10B1, Supp. Fig. S4.3). Forest (slope = 0.007, $R^2 = 0.87$, $p < 0.001$, $n = 35$) and semi-natural sites (slope = 0.004, $R^2 = 0.25$, $p = 0.11$, $n = 11$) are similar, with smaller NH_3 concentrations compared with their gridded emissions.

Since NH_3 is spatially heterogeneous even at a local sub-grid scale (e.g. Dragosits et al., 2002), the smaller concentrations at semi-natural and forest sites in grids with large emissions indicates these sites may be located further away from sources in the grid (Tang et al., 2018a; van Zanten et al., 2017). Dry deposition of NH_3 is also largest to forests and semi-natural areas (larger V_d than to crops/grass ecosystem types, e.g. Smith et al., 2000; Flechard et al., 2011), which could also contribute to the smaller concentrations at higher emissions. Relationship between emissions and concentrations in the atmosphere is however complex, influenced by other factors such as chemical interactions, variations in meteorological conditions and long-range transboundary import.

The lack of correlation between SO_2 concentrations and gridded emissions (Fig. 4.10B3) suggests that a 0.1° x 0.1° grid may be too local a spatial scale for an emission-concentration comparison for SO_2, as SO_2 is likely to be highly

localised with emissions occurring from a smaller number of large point sources at an elevated height. Indeed, emissions in neighbouring grids surrounding each site are highly variable. For example, the 4-year averaged SO_2 emissions in the 4 EMEP grids around the Italian San Rossore site (IT-SRo) varied between 0.47 to 610 kt SO_2 yr^{-1}. Further analysis was also carried out comparing site mean concentrations against the averaged emissions of an extended number of EMEP grids (4 x grids) (Supp. Fig. S4.4). Since the analysis provided similar results to the comparisons with individual gridded emissions, they are not included for further discussions in this paper. All regression plots and summary statistics for both comparisons (gridded emissions from single grids or from average of 4 grids) are provided in Supp. Figs S4.3 and S4.4.

4.4.3.4 Spatial variability across geographical regions

The form and concentrations of the different gas and aerosol components measured also varied according to geographic regions across Europe (Fig. 4.11). Smallest concentrations (with the exception of SO_4^{2-} and Na^+) were in Northern Europe (Scandinavia), with broad elevations across other regions. Gas-phase NH_3 and particulate NH_4^+ were the dominant species in all regions (Fig. 4.11). NH_3 showed the widest range of concentrations, with largest concentrations in Western Europe (mean = 2.4 NH_3 m^{-3}, range = 0.2 – 7.1 µg NH_3 m^{-3}, *n* = 26 in 4 countries).

By contrast, HNO_3 and SO_2 concentrations were largest in high NO_x and SO_2 emitting countries in Central and Eastern Europe (Sect. 4.4.3.3). Particulate SO_4^{2-} concentrations were however more homogeneous between regions, which may be attributed to atmospheric dispersion and long-range transboundary transport of this stable aerosol between countries in Europe (Szigeti et al., 2015; Schwarz et al., 2016). In the aerosol components, the spatial correlations between NO_3^-, NH_4^+ and NH_3 illustrates the potential for NH_3 emissions to drive the formation and thus regional variations in NH_4^+ and NO_3^- aerosol. Particulate SO_4^{2-} concentrations in Northern Europe

(Scandinavia) were similar to other countries, despite having the smallest SO_2 and NH_3 emissions and concentrations (Fig. 4.9). By comparison, the smaller particulate NH_4^+ and NO_3^- concentrations in Northern Europe are consistent with smallest emissions (NH_3 and NO_x) and concentrations of NH_3 and HNO_3 (Fig. 4.9). As discussed later in Sect. 4.4.4, the larger SO_4^{2-} concentrations reported in Northern Europe were flagged up as anomalous from ion balance checks (ratio of NH_4^+:sum anions).

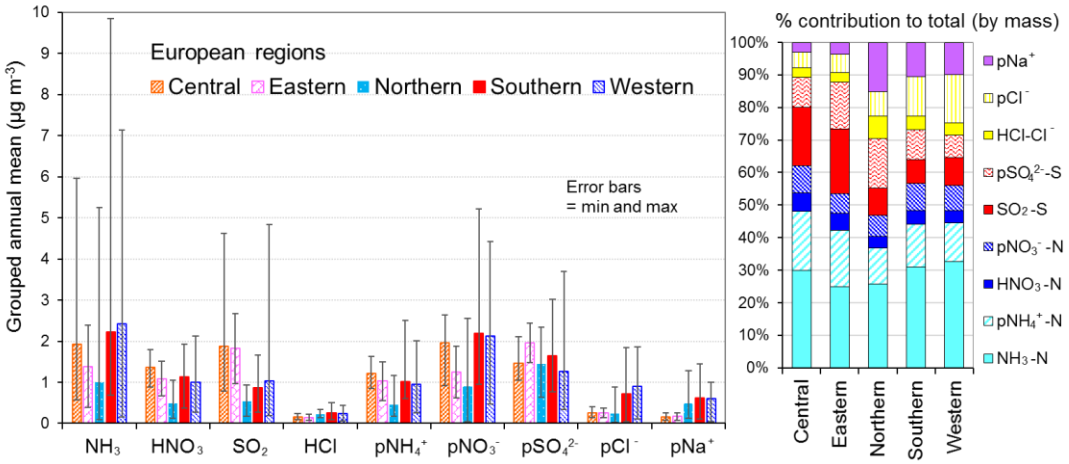

Figure 4.11. (LEFT) Spatial variation in annual averaged gas and aerosol concentrations (2007 to 2010) measured in the NEU DELTA® network across Europe, grouped according to geographical distribution of the monitoring sites: Central (n = 17), Eastern (n = 2), Northern (n = 11), Southern (n = 12) and Western (n = 26). p in front of component name denotes particulate. (RIGHT) Percentage composition of gas and aerosol components according to European regions.

4.4.3.5 Comparisons by grouped components

In the following sections, variations in concentrations of the different gas and aerosol components according to ecosystem types (crops, grassland, forests and semi-natural) and in relation to emissions (NH_3, NO_x and SO_2) are further discussed. For ease of interpretation, components are grouped as follows: reduced N (NH_3, NH_4^+), oxidised N (HNO_3, NO_3^-), S (SO_2, SO_4^{2-}), HCl, Na^+ and Cl^-.

Reduced N (NH_3 and NH_4^+)

Broad differences in NH_3 concentrations are observed between the grouped sites, with the largest concentrations at cropland sites, as expected, as these are intensively managed agricultural areas dominated by NH_3 emissions (Fig. 4.7). Borgo Cioffi (IT-BCi) in an intensive buffalo farming region of Southern Italy provided the highest 4-year average of 8.1 µg NH_3-N m^{-3} (*cf.* group mean = 3.8 µg NH_3-N m^{-3}, *n* = 10) (Table 4.4, Supp. Table S4.4). Next highest in this group are the German Gebesse (DE-Geb) and the Belgian Lonzee (BE-Lon) sites with 4-year average concentrations of 4.9 and 4.8 µg NH_3-N m^{-3}, respectively (Supp. Table S4.4). At Gebesse, a decrease in NH_3 concentrations was observed over the 4 year period, falling almost 2-fold from an annual mean of 8.8 µg NH_3-N in 2007 to 4.8 µg NH_3-N in 2010 (Supp. Table S4.4). Annual mean concentrations in 2008 (2.9 µg NH_3-N m^{-3}) and 2009 (3.2 µg NH_3-N m^{-3}) were similar, but smaller than in 2010.

Table 4.4. Annual averaged concentrations of gas and aerosol concentrations, measured at all sites and at grouped sites classified according to each of 4 ecosystem types in the NEU DELTA® network.

NEU Network	Annual averaged concentrations (µg m^{-3}) (2007 – 2010)								
	NH_3-N	NH_4^+-N	HNO_3-N	pNO_3^--N	SO_2-S	pSO_4^{2-}-S	HCl-Cl^-	Cl^-	Na^+
All sites (*n* = 66)	1.63	0.73	0.23	0.42	0.58	0.48	0.22	0.57	0.46
Crops (*n* = 10)	3.81	1.11	0.32	0.61	0.87	0.63	0.24	0.58	0.49
Grassland (*n* = 10)	2.16	0.67	0.20	0.42	0.53	0.38	0.21	0.98	0.64
Forest (*n* = 35)	1.04	0.65	0.23	0.39	0.54	0.48	0.22	0.52	0.45
Semi-natural (*n* = 11)	1.11	0.70	0.18	0.35	0.50	0.43	0.22	0.37	0.30

This illustrates the large inter-annual variability in concentrations that can occur even over a short time period. Variability between years may reflect changes in meteorological conditions on emissions from potential sources, with for example warmer, drier years increasing emissions and concentrations, contrasting with lower emissions and concentrations from the same source in a colder and wetter year. Episodic pollution events can also have a large

influence on the annual mean concentration, rather than the direct effects of changes in anthropogenic emissions over this short time scale. This suggests that for compliance assessment, an average over several years would provide a more robust basis than individual years. The assessment of trends also needs a longer time series of at least 10 years (Tang et al., 2018a, 2018b; Torseth et al., 2012; van Zanten et al., 2017).

Grassland sites, with NH_3 emissions from grazing and fertilisers, provided the next highest concentrations, with annual averaged concentrations of 2.2 µg NH_3-N m^{-3} from the 10 sites in this group (Table 4.4). Cabauw in the Netherlands (NL-Cab) in this group was the second highest NH_3 concentration site in the DELTA® network, after Borgo Cioffi (IT-BCi), with a 4-year annual averaged concentration of 5.9 µg NH_3-N m^{-3} (Supp. Table S4.4). Unlike the Gebesse site (DE-Geb), annual NH_3 concentrations were consistent between years at Cabauw, ranging from annual mean of 6.3 µg NH_3-N m^{-3} in 2017 to 5.8 µg NH_3-N m^{-3} in 2010 (Supp. Table S4.4).

At the clean end of the NH_3 gradient are semi-natural and forest sites. The smallest concentrations were found at remote background sites in Russia (Fyodorovskoe bog, RU-Fyo) and the Scandinavian countries, in Finland (Lompolojänkkä FI-Lom, Hyytiälä FI-Hyy, Sodankylä FI-Sod), Norway (Birkenes, NO-Bir) and Sweden (Norunda SE-Nor, Skyytopr SE-Sky), where NH_3 concentration at each site was < 0.3 NH_3-N m^{-3} (Fig. 4.7, Supp. Table S4.4). By contrast, the semi-natural Horstermeer (NL-Hor) and forest sites Speulder (NL-Spe) and Loobos (NL-Loo) in the Netherlands gave concentrations that were ten-fold higher (2.9 - 4.1 µg NH_3-N m^{-3}) (Fig. 4.7, Supp. Table S4.4). This is consistent with much higher NH_3 emission density in the Netherlands (4-year average = 3.4 kt NH_3-N km^{-2} yr^{-1}) (Fig. 4.9).

With the exception of the Czech Republic, the annual averaged NH_3 concentrations scaled reasonably well with the 4-year averaged mean NH_3 emission density in each country (Figs 4.9, 4.10A1, 4.10B1) (see also Sect. 4.4.3.2 and Sect. 4.4.3.3). In the Czech Republic, measurement was made at

a single site, BKFores (CZ-BK1), located at a remote forest location. The 4-year averaged emissions in the EMEP grid (0.1° x 0.1°) containing the site is very small, at 2 t NH_3-N yr^{-1}, compared with an average of 68 t NH_3-N yr^{-1} (range = < 0.01 to 567 t NH_3-N yr^{-1}) across the Czech Republic. The low emissions, combined with the small concentrations measured at BKFores (0.5 µg NH_3-N m^{-3}), suggests it is highly likely to represent concentrations at the low end of the range of NH_3 concentrations that might be expected to be encountered in the Czech Republic. By comparison, Belgium has a similar emission density as the Czech Republic, but the mean concentrations from 3 sites (2.6 µg NH_3-N m^{-3}) encompassed sites located in cropland areas (Lonzee BE-Lon, 4.7 µg NH_3-N m^{-3}) and forest sites (Braschaat BE-Bra, 2.8 µg NH_3-N m^{-3}, and Vielsalm BE-Vie, 0.4 µg NH_3-N m^{-3}) (Supp. Table S4.4).

The markedly high concentrations of NH_3 across the NEU network indicates that emission and deposition of NH_3 would be a major contributor to the effects of N_r on sensitive habitats. In comparing the annual averaged NH_3 concentration with the revised UNECE 'Critical Levels' of NH_3 concentrations (Cape et al., 2009), the lower limit of 1 µg NH_3 m^{-3} annual mean for the protection of lichens-bryophytes were exceeded in 63 % of sites (40 sites in 15 countries) (Supp. Table S4.5). Even the higher 3 µg NH_3 m^{-3} annual mean for the protection of vegetation was still exceeded at 27 % of sites (17 sites in 10 countries) (Supp. Table S4.5). Most notably, all 4 sites from the Netherlands were in exceedance of both the 1 and the 3 µg NH_3 m^{-3} thresholds.

The large concentrations in the Netherlands highlights the high levels of NH_3 that semi-natural and forest areas are exposed to within an intensive agricultural landscape, where 117 out of the 166 Natura 2000 areas were reported to be sensitive to nitrogen input (Lolkema et al., 2015). A recent assessment estimated that critical loads for eutrophication were exceeded in virtually all European countries and over about 62 % of the European ecosystem area in 2016 (EMEP, 2018). In particular, the highest exceedances occurred in the Po Valley (Italy), the Dutch-German-Danish border areas and north-western Spain where the highest NH_3 concentrations have been

measured in this network. Since NH_3 is preferentially deposited to semi-natural and forests (high V_d to these ecosystem types, Sutton et al., 1995), then NH_3 will dominate dry NH_3-N dry deposition and exert the larger ecological impact. In Flechard et al. (2011), dry NH_3-N deposition from the first 2 years of NH_3 measurement in the NEU DELTA® network was estimated to contribute between 25 and 50% of total dry N deposition in forests, according to models. The fraction is larger in short semi-natural vegetation, since V_d for NH_4^+ and NO_3^- is smaller in short vegetation than to forests (Flechard et al., 2011).

Comparison with NH_3 data from the Dutch LML network

The 4-year averaged NH_3 concentrations from the Dutch LML air quality network (see Sect. 4.3.7.1) for the period 2007 to 2010 are plotted alongside the NH_3 measurements made at the 4 Dutch sites in the DELTA® network (Fig. 4.9A). The 4-year averaged concentrations from the 8 LML sites were between 1.5 to 15 µg NH_3-N m^{-3}, highlighting the high concentrations and spatial variability in concentrations in the Netherlands. The mean NH_3 concentrations measured at the 4 Dutch sites in the DELTA® network of 2.9 µg NH_3-N m^{-3} (Horstermeer, NL-Hors; semi-natural) to 5.9 µg NH_3-N m^{-3} (Cabauw, NL-Cab; grassland) were within the range of concentrations measured in the Dutch LML network.

Comparison with NH_3 data from the UK NAMN network

The 4-year averaged NH_3 concentrations calculated from the 72 sites in the NAMN (see Sect. 4.3.7.2) for the period 2007 to 2010 were smaller than the Dutch LML network, ranging from 0.05 to 6.7 µg NH_3-N m^{-3} that are consistent with smaller NH_3 emission from the UK (Fig. 4.9A). In a joint collaboration between the UK and Dutch networks, inter-comparison of NH_3 measurements by the DELTA® method (monthly) with the Dutch network AMOR wet chemistry system (hourly, van Zanten et al., 2017) were carried out at the Zegweld site (ID 633) in the Dutch LML network (van Zanten et al., 2017) between 2003 and 2015. Good agreement was provided lending support for comparability between the independent measurements, reported in Tang et al. (2018a).

Particulate NH_4^+

Particulate NH_4^+ concentrations across the 64 sites were more homogeneous than NH_3, varying over a narrower range between 0.13 µg NH_4^+-N m^{-3} at Sodankylä (Finland, FI-Sod) and 2.1 µg NH_4^+-N m^{-3} at Borgo Cioffi (Italy, IT-BCi) (Fig. 4.7, Supp. Table S4.6). By comparison, the difference in NH_3 between the smallest (0.07 µg NH_3-N m^{-3} at Lompolojänkkä, Finland, FI-Lom) and largest (8.1 µg NH_3-N m^{-3} at Borgo Cioffi, Italy, IT-BCi) concentrations varied by a factor of 110 (Fig. 4.7, Supp. Table S4.4). Secondary aerosols have longer atmospheric lifetimes and will therefore vary spatially much less than their precursor gas concentrations. While the concentrations of NH_3 vary at a local to regional level owing to large numbers of sources at ground level, and high deposition in the landscape, NH_4^+ is less influenced by proximity to NH_3 emission sources and varies in concentration at regional scales (Sutton et al., 1998; Tang et al., 2018a).

In Fig. 4.9, annual averaged NH_4^+ concentrations (µg NH_4^+-N, Fig. 4.9E; nmol m^{-3} in Fig. 4.9G) are plotted with 4-year averaged emissions densities for NH_3, NO_x and SO_2 from each country, with the combined total emission densities shown in ranked order. Regression analyses showed NH_4^+ concentrations to be correlated with NH_3 emissions (R^2 = 0.36, p < 0.01, n = 20) and NO_x emissions (R^2 = 0.27, p = 0.02, n = 20), but not with SO_2 emissions (Table 4.3, Supp. Fig. S4.2). The smallest NH_4^+ concentrations were in Sweden, Norway and Finland (annual average < 0.3 µg NH_4^+-N m^{-3}) with the lowest emissions of NH_3, NO_x and SO_2 and also the smallest concentrations of the precursors gases NH_3 (< 0.3 µg NH_3-N m^{-3}), HNO_3 (< 0.1 µg HNO_3-N m^{-3}) and SO_2 (< 0.3 µg SO_2-S m^{-3}).

The UK and Irish sites have the next smallest NH_4^+ concentrations of 0.4 and 0.5 µg NH_4^+-N m^{-3} (*cf.* mean of all countries = 0.74 µg NH_4^+-N m^{-3}). Particulate NH_4^+ data from the UK NAMN (Tang et al., 2018a) are also included for comparison. The 4-year average concentrations from the 30 sites (0.5 µg NH_4^+-N m^{-3}, range = 0.14 to 1.0 µg NH_4^+-N m^{-3}) are comparable with the mean

of 0.40 µg NH_4^+-N m^{-3} (range = 0.2 to 0.9 µg NH_4^+-N m^{-3}) from just 4 sites in the NEU network. A combination of lower emissions of precursor gases (Fig. 4.9) and being further away from the influence of long-range transport of NH_4^+ aerosols from the higher emission countries on mainland Europe may be contributing factors to the small NH_4^+ concentrations measured in the UK and Ireland.

The largest national mean concentration of particulate NH_4^+ (1.4 µg NH_4^+-N m^{-3}) was measured in the Netherlands, which also has highest NH_3 and NO_x emissions (Fig. 4.9E). Indeed, the NH_4^+ was matched by large NO_3^- concentration (0.9 µg HNO_3-N m^{-3}) (Fig. 4.9E), lending support to the contribution of NH_4NO_3 to the NH_4^+ and NO_3^- load, together with contribution from $(NH_4)_2SO_4$ (0.6 µg SO_4^{2-}-S) (Fig. 4.9F). The particulate NH_4^+ concentrations measured in Italy (mean = 1.0 µg NH_4^+-N m^{-3}) (Fig. 4.9E), which includes the site in the Po Valley (IT-PoV) with a mean concentration of 1.9 µg NH_4^+-N m^{-3} (Supp. Table S4.6), is comparable with an assessment of $PM_{2.5}$ composition at 4 sites in the Po Valley (Ricciardelli et al., 2017).

Oxidised N (HNO_3 and NO_3^-)

The percentage mass contribution of oxidised N (sum of HNO_3 and NO_3^-, µg N m^{-3}) to the total gas and aerosol species measured was on average 13 % (range = 2 – 24 %) (Fig. 4.8). This compares with 41 % (range = 17 – 70 %) from reduced N (sum NH_3 and NH_4^+, µg N m^{-3}), and 23 % (range = 7 – 53 %) from sulfur (sum of SO_2 and SO_4^{2-}, µg S m^{-3}) (Fig. 4.8). DELTA® measurements of HNO_3 also include contributions from co-collected oxidised N species such as HONO (see Sect. 4.3.2.3) and are therefore an upper estimate, that may in some cases be twice as large as the actual HNO_3 concentration, based on observations in the UK (Tang et al 2018b; correction factor of 0.45) and from the parallel DELTA® measurements made at Fougéres (FR-FgsP). At this site, HNO_3 measurement with NaCl coated denuders provided an annual mean concentration of 0.08 µg HNO_3-N m^{-3}, compared with 0.19 µg HNO_3-N m^{-3} measured on carbonate coated denuders from the main site (FR-Fgs) (Supp.

Table S4.7). With this caveat in mind, uncorrected annual mean HNO_3 concentrations were in the range of 0.03 µg HNO_3-N at Kaamenan (Finland, FI-Kaa) to 0.47 µg HNO_3-N at Braschaat (Belgium, BE-Bra) (Supp. Table S4.7).

In Fig. 4.9B, HNO_3 concentrations are compared with NO_x emissions, the precursor gas for secondary formation of HNO_3. Russia has the lowest NO_x emission densities (0.04 t NO_x-N yr^{-1}), but HNO_3 from the single site (0.15 µg HNO_3-N m^{-3}) is larger than the smallest concentrations measured in Finland, Norway and Sweden (annual average < 0.1 µg HNO_3-N m^{-3}). HNO_3 concentrations in the UK and Ireland are marginally higher than the Scandinavian countries. Here, the annual averaged concentrations of HNO_3 are similar (0.10 *vs* 0.09 µg m^{-3}) (Supp. Table S4.7), despite NO_x emissions density (t km^{-2} yr^{-1}) in the UK being 3 times larger than in Ireland (Fig. 4.9B). HNO_3 concentrations on the European continent were generally higher (0.3 – 0.6 µg HNO_3-N m^{-3}). Overall, a weak, but significant correlation was observed between concentrations of HNO_3 and NO_x emission densities across the 20 countries (R^2 = 0.2, p < 0.05) (Fig. 4.10A2, Table 4.3, Supp. Fig. S4.2).

In the UK, HNO_3 data are also available on a wider spatial scale from the AGANet (Tang et al., 2018b, Sect. 4.3.7.2). The 4-year average concentrations of HNO_3 from 30 sites in the AGANet are plotted alongside the NEU HNO_3 data from the 4 UK sites in its network in Fig. 4.9B. The UK HNO_3 data on the UK-AIR database (https://uk-air.defra.gov.uk/) have been corrected for HONO interference with a 0.45 correction factor (see Tang et al. 2018b). For consistency in Fig. 4.9B, the UK raw uncorrected HNO_3 data are used for the present comparison. The 30-site mean (0.17 µg HNO_3-N m^{-3}) was higher than from just 4 UK sites in the NEU network (0.10 µg HNO_3 m^{-3}). The range of concentrations were also wider, from 0.03 µg HNO_3 m^{-3} at a remote background site in Northern Ireland to 0.77 µg HNO_3 m^{-3} at a central London urban site, where interference from HONO and NO_x in HNO_3 determination is likely to be larger (Tang et al., 2015; 2018b).

Like particulate NH_4^+, NO_3^- concentrations are also correlated with emission densities of NH_3 (R^2 = 0.57, p < 0.001, n = 20) and NO_x (slope = 0.15, R^2 = 0.44, p <0.01, n = 20), but not with SO_2 (Table 4.3, Supp. Fig. S4.2). Smallest NO_3^- concentrations were again in Sweden, Norway and Finland with low NH_3 and NO_x emissions and also smallest concentrations of HNO_3, SO_2 and NH_4^+ in the network (Fig. 4.9). Largest NO_3^- concentrations was measured in the Netherlands with a mean of 0.92 µg NO_3^--N m^{-3}, compared with a network average of 0.39 µg NO_3^--N m^{-3} (Fig. 4.9E, Supp. Table S4.8). The higher NO_3^- concentrations correlated well with the high NH_3, HNO_3 and NH_4^+ concentrations in the Netherlands (Fig. 4.9). This suggests that concentrations of NO_3^- are linked to local formation of NH_4NO_3, which is dependent on concentrations of NH_3 and HNO_3, and also to the influence of meteorology on transport of NH_4NO_3 between countries on mainland Europe and export out of Europe. Countries in Scandinavia such as Sweden, Norway and Finland and in the British Isles are furthest from the influence of long-range transboundary transport from Europe, with concentrations of NH_4NO_3 that are smaller than on the continent.

Sulfur (SO_2 and SO_4^{2-})

Annual averaged SO_2 concentrations measured across the network were between 0.9 and 2.3 µg SO_2-S m^{-3} (Fig. 4.9C, Supp. Table S4.9). This corroborates observations from monitoring made in the EMEP networks of large reductions in ambient concentrations and deposition of sulfur species during the last decades (EMEP, 2016), reflecting successes of air quality policies across Europe in achieving substantial reductions in SO_2 emissions, which decreased by 74 % between 1990 and 2010. Annual mean SO_2 concentrations of 0.03 to 5.5 µg SO_2-S m^{-3} were reported from the EMEP network from 58 rural background sites across Europe over the period of 2007 – 2010, with largest SO_2 concentrations from North Macedonia and Serbia (EMEP, 2016). Since the highest emitting countries in European countries were not included in the DELTA® network, the SO_2 concentrations provided by

the DELTA® network are smaller, but are within the range reported by EMEP (EMEP, 2016).

SO_2 concentrations were also correlated with SO_2 emission density ($R^2 = 0.65$, $p < 0.001$, $n = 20$) in each country (Fig. 10A3, Table 4.3). The smallest and largest SO_2 annual average concentrations corresponded with the lowest emissions in Norway and highest in the Czech Republic (Fig. 4.9C). By contrast, SO_2 concentrations from the single measurement site Bugac in Hungary (HU-Bug) are much higher than expected on the basis of SO_2 emission density estimated for the country. Gridded emissions for the single grid (0.1° x 0.1°) containing the semi-natural Bugac site are all at the low end of the range of gridded emissions across Hungary for SO_2, NO_x and NH_3:

- SO_2-S: t yr^{-1} = 2.1 (range = < 0.1 to 5144)
- NO_x-N: t yr^{-1} = 11 (range = < 0.1 to 3230)
- NH_3-N: t yr^{-1} = 63 (range = < 0.1 to 589)

Although the Bugac site is located in a grid with low emissions of all the gases, the higher SO_2 (1.2 µg S m^{-3}), together with elevated NH_3 (2.6 µg N m^{-3}) and HNO_3 (0.3 µg N m^{-3}) concentrations measured at this site suggests that it is likely to be affected by proximity to sources. This contrasts with the BKFores site in the Czech Republic (CZ-BK1) which had smaller NH_3 concentrations due to its location away from sources.

Following emission, SO_2 disperses and undergoes chemical oxidation in the atmosphere to form SO_4^{2-} both in the gas phase and in cloud and rain droplets (Baek et al., 2004; Jones and Harrison, 2011). Particulate SO_4^{2-} produced is generally associated with NH_4^+ and NO_3^- (see Sect. 4.4.4). The regional pattern of SO_4^{2-} was similar to, and correlated well with, particulate NH_4^+ and NO_3^- (Fig. 4.9G), suggesting well-mixed air on the continent, since $(NH_4)_2SO_4$ is stable and long-lived. Countries in the British Isles (UK and Ireland) and in Scandinavia (Sweden, Norway, Finland) have smaller concentrations of SO_4^{2-} (Supp. Table S4.10). They are located far enough away from sources and

activities on continental Europe such that they are less influenced by the emissions from central Europe.

As discussed earlier, particulate NH_4^+ and NO_3^- concentrations were smallest in the Scandinavian countries, which corresponded with low emission densities of the precursor gases NH_3 and NO_x. By analogy, since these countries also have the lowest emission densities of SO_2 (Fig. 4.9C), then particulate SO_4^{2-} concentrations would be expected to be similarly low. Particulate SO_4^{2-} in Finland and Norway (mean = 0.34 µg SO_4^{2-}-S m^{-3}) and Sweden (mean = 0.37 µg SO_4^{2-}-S m^{-3}) were however comparable with concentrations on mainland Europe (range = 0.33 to 1.0 µg SO_4^{2-}-S m^{-3}) and larger than the UK (0.18 µg SO_4^{2-}-S m^{-3}) and Ireland (0.24 µg SO_4^{2-}-S m^{-3}) (Fig. 4.9F). An ion balance check on the ratio of equivalent concentrations of NH_4^+ to the sum of NO_3^- and SO_4^{2-} (see next Sect. 4.4.4) was less than 0.5. Since NH_4^+ is a counter-ion to NO_3^- and SO_4^{2-} formation, the imbalance suggests that SO_4^{2-} concentrations may be over-estimated at the sites in Sweden, Norway and Finland.

HCl, Cl^- and Na^+

The average concentrations of HCl across the network were of low magnitude, with limited variability, ranging from 0.07 in Russia to 0.36 µg HCl-Cl^- m^{-3} in Portugal (Fig. 4.9D). At a site level, HCl concentrations varied between 0.06 at Renon (Italy, IT-Ren – inland location) to 0.48 µg HCl-Cl^- m^{-3} at Espirra (Portugal, PT-Esp – coastal location) (Supp. Table S4.11). In the UK AGANet network, the highest concentrations of HCl were found in the source areas in SE and SW of England, and also in central England, north of a large coal-fired power station (Tang et al., 2018b).

HCl emissions and concentrations in the atmosphere are mostly derived from combustion of fossil fuels (coal and oil), biomass burning and from the burning of municipal and domestic waste in municipal incinerators (Roth and Okada 1998; McCulloch et al., 2011; Ianniello et al., 2011). Several manufacturing processes, including cement production also emits HCl (McCulloch et al.,

2011). At coastal sites, HCl released from the reaction of sea salt with HNO_3 and H_2SO_4 can be a significant source (Roth and Okada 1998; Keene et al., 1999; McCulloch et al., 2011; Ianniello et al., 2011). UK is the only country with available HCl emission estimates (https://naei.beis.gov.uk/data/). Emissions of HCl in the UK (mainly from coal burning in power stations) have declined to very low levels, from 74 kt in 1999 to 5.7 kt in 2015. The 4-year averaged emission density for HCl for the period 2007 to 2010 was just 0.05 tonnes HCl-Cl^- km^{-2} yr^{-1}, although HCl emissions could still pose a threat to sensitive habitats close to sources (Evans et al., 2011). The low HCl concentrations measured in the network would suggest that the shift in Europe's energy system from coal to other sources has contributed to low HCl emissions (UK) and concentrations (observed across the network).

Particulate Cl^- on the other hand is predominantly marine in origin, with sea salt (NaCl) as the most significant source (Keene et al. 1999). Molar concentrations of Cl^- and Na^+ are seen to be similar in most countries, demonstrating close coupling between the two components (Fig. 4.9H). Largest concentrations of Na^+ and Cl^- occurred at coastal countries such as the UK, Ireland, Netherlands and Portugal, with the highest of country-averaged annual concentrations of 1.6 µg Cl^- m^{-3} and 0.9 µg Na^+ m^{-3} from Ireland (Supp. Tables S4.12 and S4.13). Data from the 30 sites in the UK AGANet network showed a wider range of Cl^- and Na^+ concentrations (Fig. 4.9H), with the highest 4-year annual averaged concentrations of 3.8 µg Cl^- m^{-3} and 2.0 µg Na^+ m^{-3} from the coastal Lerwick monitoring site on the east coast of the Shetland Islands, exposed to the North Atlantic.

Further away from the coastal influence of marine aerosol, the smallest concentrations of Cl^- and Na^+ were measured in land-locked countries such as Germany (mean of all sites = 0.27 µg Cl^- m^{-3} and 0.15 µg Na^+ m^{-3}). Concentrations in Hungary, Poland, the Czech Republic and Russia were also low, but inferences about these countries are necessarily limited by measurements at a single site in each of these countries. At coastal sites in Norway (NO-Bir) and Sweden (SE-Nor and SE-Sk2), the very low particulate

Cl^- concentrations (< 0.1 - 0.3 µg m^{-3}), and high Na:Cl molar ratios (3 – 5) are anomalous. It is possible for sea salt to be depleted in Cl^- (through the loss of HCl gas) by the reaction of NaCl particles with atmospheric acids (Finalyson-Pitts and Pitts, 1999; Keene et al., 1999), leading to high Na:Cl ratios for sea salts transported over long distances. The coastal locations of these sites (Fig. 4.2) suggests that they are more likely to be influenced by freshly generated marine aerosols (*cf.* coastal sites in UK and Ireland), and larger concentrations of sea salt (Na^+ and Cl^-) and a 1:1 relationship between Na^+ and Cl^- are expected. The Cl^- concentrations are likely to be under-estimated at these sites (see Sect. 4.4.2.3) and further discussed in the next section (Sect. 4.4.4).

Table 4.5. Regression correlations (R^2) between the mean molar concentrations (nmol m^{-3}) of gas and aerosol components at sites (*n* = 66) in the NEU DELTA® network.

	HNO_3	HCl	SO_2	NH_3	NO_3^-	Cl^-	2 x SO_4^{2-}	2 x nss-SO_4^{2-}	NH_4^+	Na^+
HNO_3	1									
HCl	0.13**	1								
SO_2	0.46***	0.05^{ns}	1							
NH_3	0.28***	0.11**	0.08*	1						
NO_3^-	0.66***	0.21**	0.19***	0.43***	1					
Cl^-	0.00^{ns}	0.22***	0.01^{ns}	0.11**	0.06*	1				
2 x SO_4^{2-}	0.34***	0.24***	0.33***	0.18***	0.39***	0.01^{ns}	1			
2 x nss-SO_4^{2-}	0.35***	0.17***	0.36***	0.15**	0.35***	0.04^{ns}	0.98***	1		
NH_4^+	0.72***	0.06^{ns}	0.34***	0.43***	0.75***	0.00^{ns}	0.28***	0.30***	1	
Na^+	0.00^{ns}	0.42***	0.00^{ns}	0.10**	0.13**	0.65***	0.09*	0.03^{ns}	0.00^{ns}	1

Significance level: * p < 0.05, ** p < 0.01, *** p < 0.001, *ns* = non-significant (p > 0.05)

4.4.4 Correlations between gas and aerosol components

Regression analyses was carried out between the mean molar equivalent concentrations of all inorganic gas and aerosol components measured at each site (*n* = 66; Fr-FgsP and UK-AmoP excluded) in the NEU network, with summary statistics provided in Table 4.5. With the exception of SO_2 *vs* HCl (R^2 = 0.05, *p* > 0.05), the gases were positively correlated with each other, possibly due to similarities in the regional distribution of their emissions and concentrations. Comparing the mean molar concentrations of NH_3 with SO_2

and HNO_3 showed that NH_3 was on average 6-fold and 7-fold higher, respectively, whereas molar concentrations of SO_2 and HNO_3 were similar (Table 4.6, Fig. 4.12A). The molar ratio of NH_3 to the sum of all acid gases (SO_2, HNO_3 and HCl) was on average 3 (Table 4.6, Fig. 4.12A), confirming that there is a surplus of the alkaline NH_3 gas to neutralise the atmospheric acids in the atmosphere, similar to that observed in the UK (Tang et al., 2018b). With the more substantial decline in emissions of SO_2, compared with a more modest reduction in NO_x, the concentrations of SO_2 are at a level where it is no longer the dominant acid gas, such that HNO_3 and HCl are together contributing a larger fraction of the total acidity in the atmosphere in the present assessment.

Table 4.6. Mean molar concentrations of gases and NH_3:acid gas ratios measured at sites (*n* = 66) in the NEU DELTA® network.

All NEU sites	Molar concentrations (nmol m^{-3})					Ratios		
	NH_3	HNO_3	SO_2	HCl	sum acids	NH_3 : HNO_3	NH_3 : SO_2	NH_3 : sum acids
mean	115	16.5	18.3	6.4	41.1	7.5	7.7	2.9
min	5.4	2.0	2.5	1.6	10.9	0.8	0.5	0.3
max	566	33.8	78.2	13.4	122	34	33	13
SD	108	8.4	14.7	2.8	22.4	7.2	6.6	2.6
n	66	66	66	66	66	66	66	66

In the aerosol phase, NH_4^+ correlated well with NO_3^- ($R^2 = 0.75$, $p < 0.001$, Fig. 4.13A) and SO_4^{2-} ($R^2 = 0.75$, $p < 0.001$, Fig. 4.13B) (Tables 4.5 and 4.7), but not with Cl^- (Table 4.5). Regression of the molar equivalent concentrations of the sum of NO_3^- and SO_4^{2-} against NH_4^+ show points close to the 1:1 line (slope = 0.84) and significant correlation ($R^2 = 0.64$, $p < 0.001$), which demonstrates the close coupling between the base NH_4^+ and the acid $NO_3^- + SO_4^{2-}$ aerosols (Fig. 4.13C, Table 4.7). The reaction of NH_3 with H_2SO_4 is irreversible (i.e. 'one-way') under atmospheric conditions (Baek et al., 2004; Finlayson-Pitts and Pitts, 1999; Jones and Harrison, 2011; Huntzicker et al., 1980), whereas any NH_4NO_3 or NH_4Cl that are formed can dissociate to release NH_3 which can then be 'removed' by reaction with H_2SO_4. The lack of correlation between

NH_4^+ and Cl^- (R^2 = 0.00, Table 4.5) in the analysis suggests that NH_4^+ is mainly associated with NO_3^- and SO_4^{2-}.

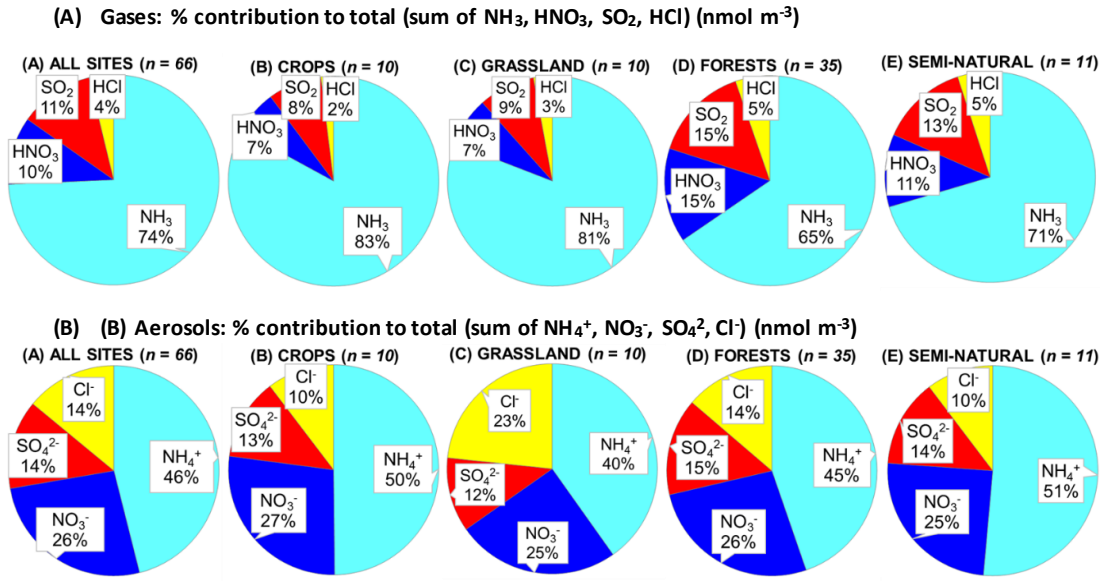

Figure 4.12. Pie charts of mean relative proportions of (TOP) Gases: NH_3, HNO_3, SO_2, HCl, and (BOTTOM) Aerosols: NH_4^+, NO_3^-, SO_4^{2-}, Cl^-. Data are annual averaged concentrations (nmol m^{-3}) measured at NEU DELTA® sites, for (A) All sites (*n* = 66) and sites grouped according to ecosystem types,(B) Crops (*n* = 10), C) Grassland (*n* = 10), D) Forests (*n* = 35) and E) Semi-natural (*n* = 11). UK-AmoP (parallel DELTA® at Auchencorth: NH_3/NH_4^+ only) and FR-FgsP (parallel DELTA® at Fougéres: different sample train) were excluded in this analysis

Table 4.7. Linear regressions between the mean molar equivalent concentrations of aerosol components (neq m^{-3}) at sites (*n* = 66) in the NEU DELTA® network.

Linear Regression	Mean molar equivalent concentrations (neq m^{-3})						
	NH_4^+ *vs* NO_3^-	NH_4^+ *vs* SO_4^{2-}	NH_4^+ *vs* sum (NO_3^- + SO_4^{2-})	Na^+ *vs* nss-SO_4^{2-}	NH_4^+ *vs* sum (NO_3^- + nss-SO_4^{2-})	Na^+ vs Cl^- (all data)	Na^+ *vs* Cl^- (outliers excluded)
R^2	0.75***	0.28***	0.64***	0.30***	0.67***	0.65***	0.95***
slope	0.57***	0.27***	0.84^{ns}	0.27***	0.84*	0.75***	1.01^{ns}
intercept	0.01^{ns}	16.1***	16.1**	13.6***	13.6**	1.56^{ns}	-0.05^{ns}
No. of sites: *n*	66	66	66	66	66	66	50

*Significance level: * p < 0.05, ** p < 0.01, *** p < 0.001, ns = non-significant (p > 0.05)*

Particulate Cl^- was correlated with Na^+ (R^2 = 0.65, p < 0.001) (Fig. 4.13F, Tables 4.5, 4.7), consistent with observations that NaCl in atmospheric aerosols are mainly sea salt in origin (O'Dowd and de Leeuw, 2007; Tang et al., 2018b). Like the precursor gases, the molar concentrations of particulate NH_4^+ are larger than either NO_3^- or SO_4^{2-} (Fig. 4.12B, Table 4.8).

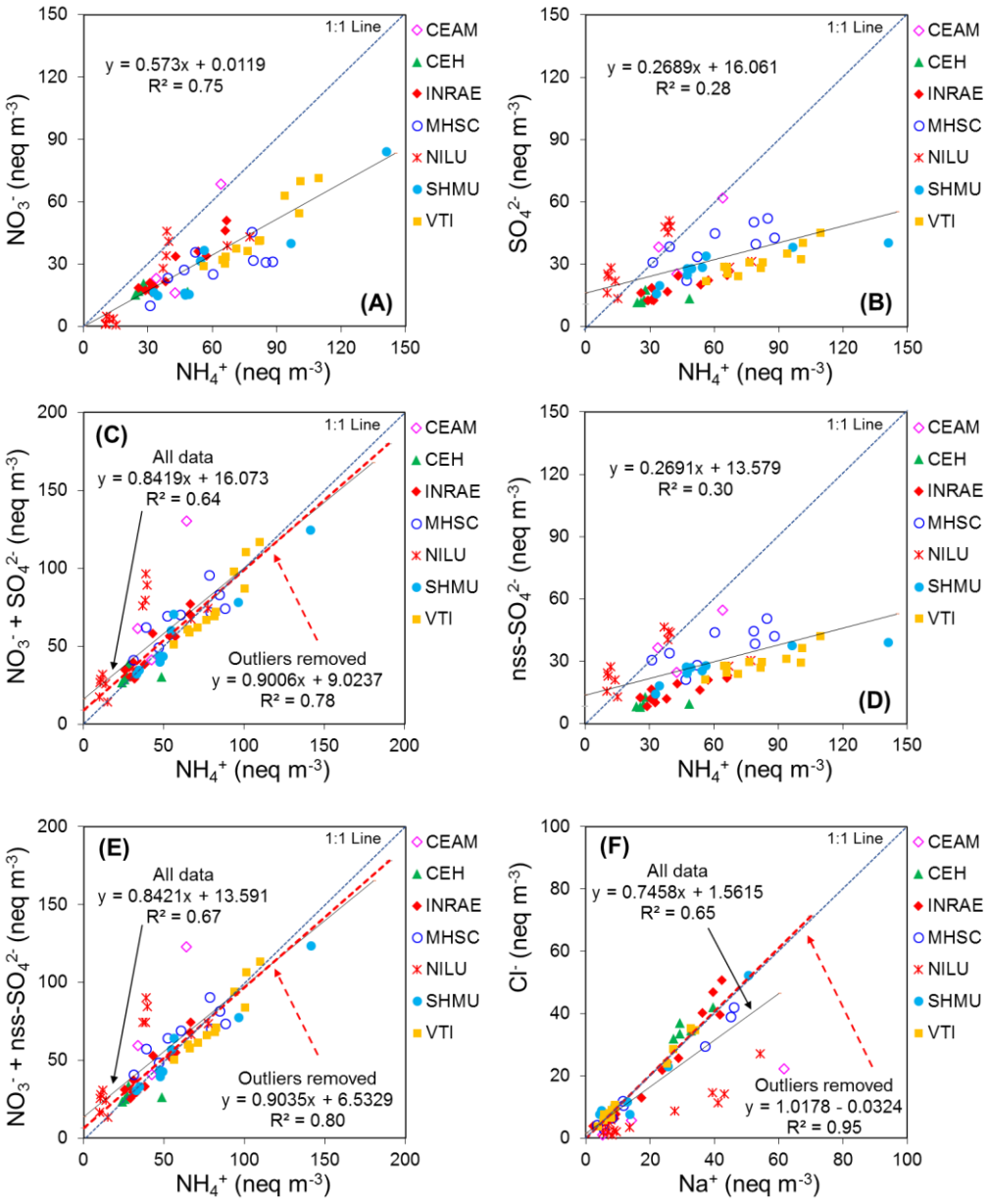

Figure 4.13. Regression plots between mean molar equivalent concentrations of (A) NH_4^+ and NO_3^-, (B) NH_4^+ and SO_4^{2-}, (C) NH_4^+ and sum (NO_3^- + SO_4^{2-}), (D) NH_4^+ and nss-SO_4^{2-}, (E) NH_4^+ and sum (NO_3^- + nss-SO_4^{2-}) and (F) Na^+ and Cl^-, measured in the NEU DELTA® network. Each data point represents the mean of all monthly measurements at each site, with different coloured symbols for each laboratory making the measurements. Outliers: where equivalent concentrations of NH_4^+:sum (anions) < 0.5 and Na:Cl > 2.

Particulate NO_3^- concentrations were on average 2-fold higher than particulate SO_4^{2-} (on a molar basis), so that there was twice as much NH_4NO_3 (Fig. 4.13A) as $(NH_4)_2SO_4$ (Fig. 4.13B). The shift in PM composition from $(NH_4)_2SO_4$ to NH_4NO_3 across Europe is well documented (Bleeker et al., 2009; Fowler et al., 2009; Tang et al. 2018b; Torseth et al., 2017).

Table 4.8. Mean molar concentrations of aerosols and ratios measured at sites (*n* = 66) in the NEU DELTA® network.

All NEU sites	Molar concentrations (nmol m^{-3})				Ratios			
	NH_4^+	NO_3^-	SO_4^{2-}	nss-SO_4^{2-}	NH_4^+ : NO_3^-	NH_4^+ : 2xSO_4^{2-}	NH_4^+ : 2xnss-SO_4^{2-}	NH_4^+ : (NO_3^- + 2xSO_4^{2-})
mean	52.8	30.2	15.1	13.9	2.4	1.8	2.1	0.9
min	10.1	0.7	5.8	4	0.9	0.4	0.4	0.4
max	141	84.3	38.4	35.8	21	3.6	5.1	1.6
SD	27.6	18.2	7.0	6.8	2.7	0.8	0.9	0.3
n	66	66	66	66	66	66	66	66

Non-sea salt SO_4^{2-} (nss-SO_4^{2-}) was also estimated from the SO_4^{2-} and Na^+ data (see Sect. 4.3.2.1). The nss-SO_4^{2-} is estimated to comprise on average 25 % (range = 3 – 83 %, *n* = 187) of the measured total SO_4^{2-} aerosol (Table 4.8). This demonstrates that sea salt SO_4^{2-} (ss-SO_4^{2-}) aerosol makes up a large and variable fraction of the total SO_4^{2-} measured, consistent with observations of the contribution by ss-SO_4^{2-} to the total SO_4^{2-} in precipitation (ROTAP, 2012). Regression of nss-SO_4^{2-} *vs* NH_4^+ (slope = 0.27, R^2 = 0.30) was not significantly different from the regression of SO_4^{2-} *vs* NH_4^+ (slope = 0.27, R^2 = 0.28) (Table 4.5). This suggests that NH_4^+ is mainly associated with the nss-SO_4^{2-}.

Correlation between NH_4^+ and the sum of anions ($NO_3^- + SO_4^{2-}$) is an important point of discussion (Table 4.7), as the ion balance serves as a quality check for the aerosol measurement. Due to some outliers in the comparison, the correlation between NH_4^+ and SO_4^{2-} (R^2 = 0.28, Fig. 4.13B) is weaker than between NH_4^+ and NO_3^- (R^2 = 0.75, Fig. 4.13C, Table 4.7). The outliers were

measurements made by NILU and CEAM, although these vary according to monitoring locations. The NILU laboratory made DELTA® measurements for 16 sites in 6 different countries (Belgium, Denmark, Finland, Norway, Sweden and Switzerland). At 3 sites (Kaamanen FI-Kaa, Laegern CH-Lae, Oensingen CH-Oe1), the ion balance of equivalent concentrations of NH_4^+:sum (NO_3^- + SO_4^{2-}) was 1.0, whereas the ratios at the other 13 sites were between 0.4 and 0.7. The CEAM laboratory made measurements for all 3 sites in Spain. For CEAM, the ion balance ratio at Vall de Aliñá (ES-VDA) was 1, whereas the other 2 sites had ratios of 0.5 and 0.6.

Removal of the outlier NILU (7 out of 16) and CEAM (1 out of 3) data points with ion balance ratio < 0.5 improved both the slope (new slope = 0.90) and correlation (new R^2 = 0.78) (Fig. 4.13C). This indicates either an over-read of the anions (NO_3^-, SO_4^{2-}) or under-read of NH_4^+ concentrations by the two laboratories at some sites. Results reported by NILU in the DELTA® field inter-comparisons (Sect. 4.4.2) showed that, with the exception of a few high NH_4^+ and NO_3^- readings, there was on average no overall bias in the NH_4^+, NO_3^- or SO_4^{2-} measurements by the NILU laboratory that could account for the high SO_4^{2-} outliers in the regression (Fig. 4.13B). The ion balance checks suggest possible over-read and increased uncertainty in the SO_4^{2-} measurements for 7 sites: Hyytiälä (FI-Hyy), Sodankylä (FI-Sod), Rimi (DK-Rim), Risbyholm (DK-Ris), Soroe (DK-Sor), Skyttorp (SE-Sk2) and Vielsalm (BE-Vie). For the CEAM lab, the uncertainty in SO_4^{2-} measurements affected 2 sites, El Saler (ES-Els) and Las Majadas (ES-Lam) (see also Sect. 4.4.3.4).

The regression of Na^+ and Cl^- also showed the majority of data points close to the 1:1 line, but with a small group of outliers below the 1:1 line from the CEAM and NILU laboratories (Fig. 4.13F). Both laboratories performed well in laboratory PT schemes (Sect. 4.4.1), with more than 80% of reported data agreeing within ± 10% of reference values in both Na^+ and Cl^-, with no bias in the analytical method. The outliers in the ion balance therefore suggests some problems with Na^+ and Cl^- determination on the DELTA® aerosol filters. Na^+ and Cl^- data for some of the field DELTA® inter-comparisons were omitted from

submissions by CEAM and NILU, and submitted data were in poor agreement with other laboratories (Sect. 4.4.2). Further regression analyses were carried out on individual monthly data, with sites grouped according to measurements made by each of the seven laboratories (Supp. Fig. S4.5). Regressions for CEAM and NILU show the vast majority of data points below the 1:1 line, indicating a systematic under-estimation of particulate Cl^- concentrations. The other 5 laboratories (INRAE, MHSC, SHMU, UKCEH and VTI) all have data points close to the 1:1 line, with larger scatter both above and below the 1:1 line at lower concentrations. In Fig. 4.13F, a new regression line has therefore also been fitted where outlier data with Na:Cl ratios > 2 from NILU (13 out of 16 sites) and CEAM (all 3 sites) have been removed. Exclusion of the outlier data points provided a regression line that is not significant different from unity (slope = 1.02), with a R^2 value of 0.95 ($p < 0.001$). The near 1:1 relationship between particulate Na^+ and Cl^- is consistent with their origin from sea salt (NaCl).

The ion balance checks, together with the regular PT exercises and field inter-comparisons therefore provided the platform against which to assess data quality and comparability of measurements between laboratories. This shows that overall, with the exception of a few identified outlier measurements, the laboratories are performing well and providing good agreement.

4.4.5 Seasonal variability in gases and aerosol

The time series of monthly averaged concentrations for the period 2006 to 2010 have been plotted to examine seasonality in the different gas and aerosol components according to ecosystem types (crops, grassland, semi-natural and forests) (Fig. 4.14) and geographical regions (Fig. 4.15). Distinct seasonality were observed in the data, influenced by seasonal changes in emissions, chemical interactions and the influence of meteorology on partitioning between the main inorganic gases and aerosol species.

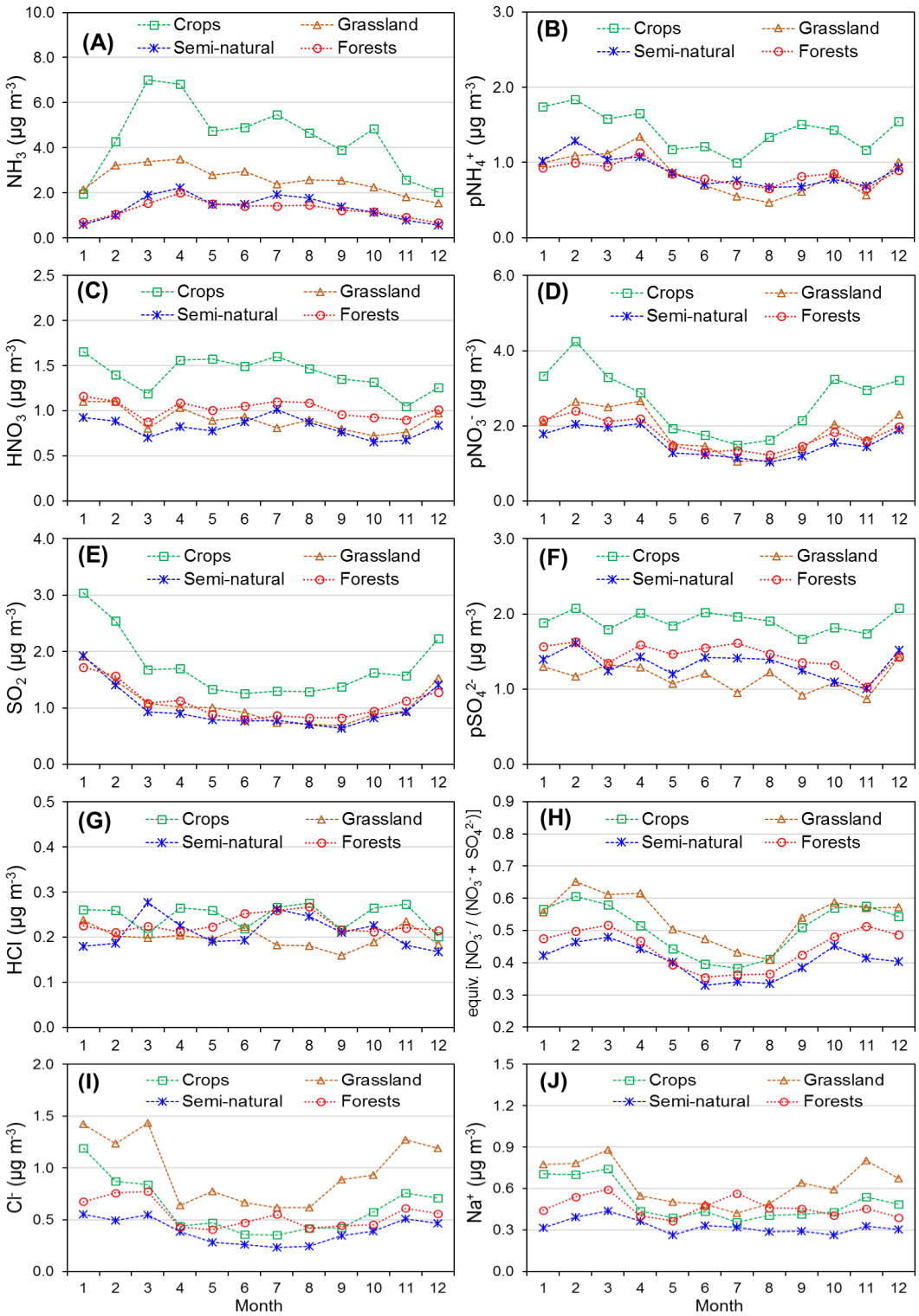

Figure 4.14. Seasonal variability in atmospheric gas (A) NH_3, (C) HNO_3, (E) SO_2, (G) HCl) and aerosol concentrations (B) pNH_4^+, (D) pNO_3^-, (F) pSO_4^{2-}, (I) pCl^-, (J) pNa^+ (p in front of component name denotes particulate). Each data point is the monthly averaged concentrations of grouped sites for the period 2006 to 2010, classified according to four ecosystem types: crops (*n* = 10), grassland (*n* = 10), semi-natural (*n* = 11) and forests (*n* = 35). Graph (H) shows the monthly mean ratio of molar equivalent (equiv.) concentrations of NO_3^- to sum (NO_3^- + SO_4^{2-}). Month 1 = January and Month 12 = December.

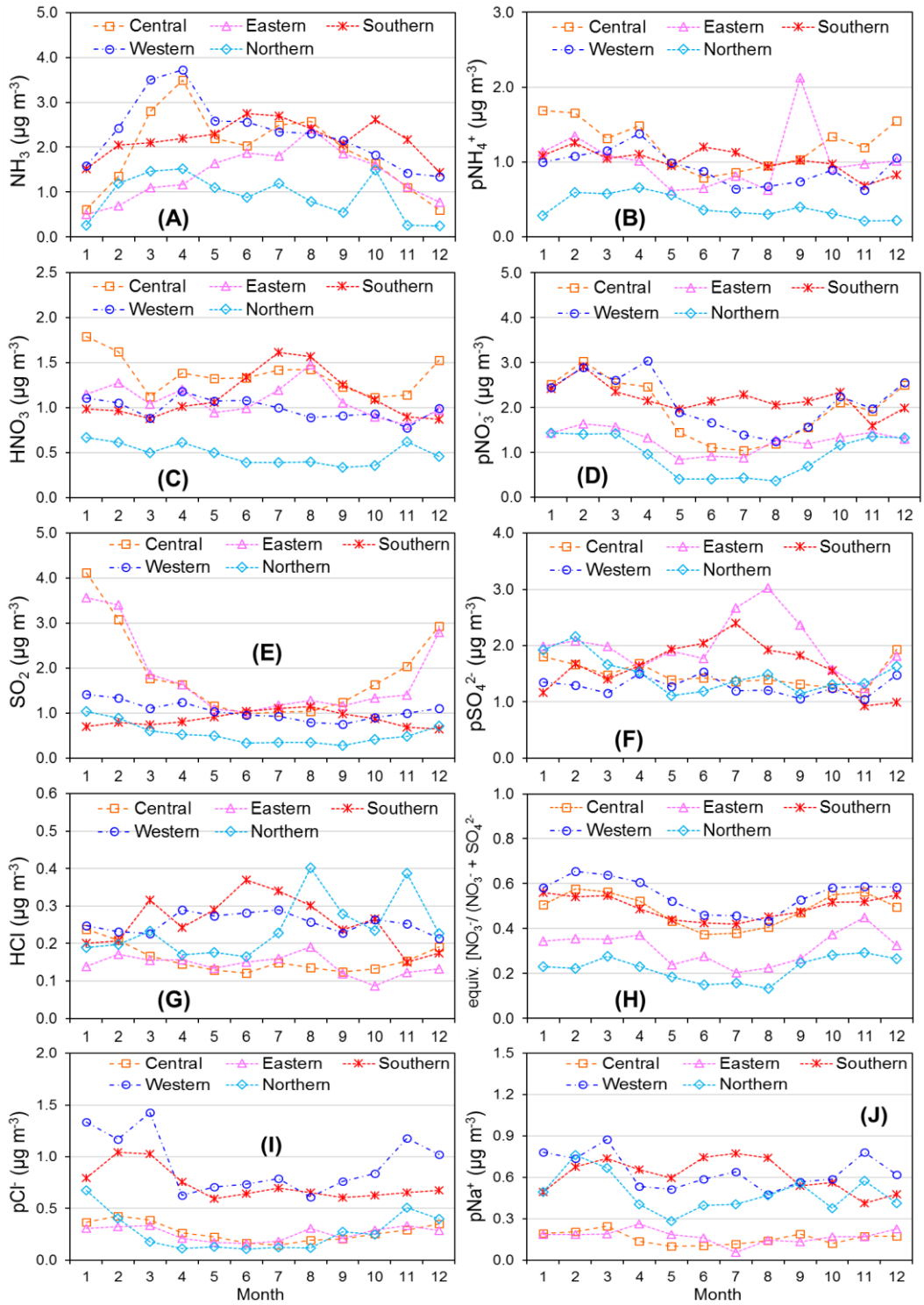

Figure 4.15. Seasonal variability at sites grouped according to European regions in atmospheric gas (A) NH_3, (C) HNO_3, (E) SO_2, (G) HCl) and aerosol concentrations (B) pNH_4^+, (D) pNO_3^-, (F) pSO_4^{2-}, (I) pCl^-, (J) pNa^+ (p in front of component name denotes particulate). Each data point is the monthly averaged concentrations of grouped sites for the period 2006 to 2010, classified according to five European regions: Central (n = 17), Eastern (n = 2), Northern (n = 11), Southern (n = 12) and Western (n = 26). Graph (H) shows the monthly mean ratio of molar equivalent (equiv.) concentrations of NO_3^- to sum (NO_3^- + SO_4^{2-}). Month 1 = January and Month 12 = December.

4.4.5.1 NH_3

Distinctive and contrasting features in the seasonal cycle are observed, with largest concentrations at cropland sites and smallest at semi-natural and forest sites (Fig. 4.14A). Similar to that observed in the annual mean concentrations (Figs 4.9, 4.11), the monthly concentrations are also smallest in Northern Europe and largest in Western Europe (Fig. 4.15A).

Semi-natural sites:

There are two distinct peaks in the seasonal cycle of grouped semi-natural sites, in April (mean = 2.2 µg NH_3 m^{-3}, *n* = 12) and in July (mean = 1.9 µg NH_3 m^{-3}, *n* = 12) (Fig. 4.14A). Since these sites are located away from agricultural sources, the seasonality in NH_3 concentrations is mostly governed by changes in environmental conditions and regional changes in NH_3 emissions. The differences in concentrations between the summer and winter at these sites was by a factor of 3, with smallest concentrations in wintertime (Dec and Jan) when low temperatures and wetter conditions decrease NH_3 emissions from regional agricultural sources, while favouring a thermodynamic shift from gaseous NH_3 to the aerosol NH_4^+ phase. Conversely, warm, dry conditions in summer increases surface volatilization of NH_3 from low density grazing livestock and wild animals, and favour a thermodynamic shift to the gaseous (NH_3) phase, producing the summer peak. Vegetation is another potential source at these background sites under the right conditions (Flechard et al., 2013; Massad et al., 2010).

A complex interaction between atmospheric NH_3 concentrations and vegetation can lead to both emission and deposition fluxes known as “bi-directional exchange”, dependent on relative differences in concentrations. This process is controlled by the so-called ‘compensation point’, defined as the concentration below which growing plants start to emit NH_3 into the atmosphere (Flechard et al., 1999; Massad et al., 2010; Sutton et al., 1995). At sites distant from intensive farming and emissions, the bi-directional exchange with vegetation will partly control NH_3 concentrations. Inclusion of

bi-directional exchange in dispersion modelling of NH_3, by incorporating a 'canopy compensation point' is shown to improve model results for NH_3 concentrations in remote areas (e.g. Flechard et al., 1999, 2011; Massad et al., 2010; Smith et al., 2000;). The larger peak in April at these sites on the other hand suggests the influence of emissions from agricultural sources, e.g. from land spreading of manures.

Forest sites:

The average seasonal cycle from the forest sites is similar to that of the semi-natural sites, but diverged over the summer months (Fig. 4.14A). Here, the seasonal profile is characterised by the absence of any peaks in summer, with concentrations plateauing between May and August. Studies have shown that atmospherically deposited N is taken up by forest canopies, since growth in forest ecosystems is commonly limited by the availability of N (Sievering et al., 2007) and tree canopies are a potential sink for atmospheric NH_3 (Fowler et al., 1989; Theobald et al., 2001). The capture and uptake of NH_3 during the growing seasons over the summer period could therefore account for the absence of a summer peak in NH_3 concentrations at forest monitoring sites, although a similar effect would also be expected for semi-natural sites.

Cropland sites:

Fertilizers and arable crops are significant sources of NH_3 emissions and concentrations in an intensive agricultural landscape. Sites in this group showed considerably higher monthly mean monitored NH_3 concentrations than the other groups (Fig. 4.14A). A more complex seasonal pattern can be seen, with three peaks in NH_3 concentrations. Concentrations here are also lowest in the winter, although the wintertime concentrations are 3 times larger than semi-natural and forest sites, reflecting the elevated regional background in NH_3 concentrations located within agricultural landscapes. This rises rapidly with improving weather conditions and peaks in the spring to coincide with the main period for manure spreading and fertiliser application before the sowing of arable crops (Hellsten et al., 2007). The distinct springtime maxima in NH_3

also reflects implementation of the Nitrates Directive (91/676/EEC), which prohibits manure spreading in winter. In summer, the second peak in NH_3 concentrations may be associated with increased land surface emissions promoted by warm, dry conditions, and possibly from the application of fertilisers. The smaller autumn peak is also expected to be related to seasonal farming activities/manure spreading. The key drivers for seasonal variability in NH_3 concentrations at crops sites are therefore a combination of seasonal changes in agricultural practices (e.g. timing of fertiliser/manure applications) and climate that will affect emissions, concentrations, transport and deposition of NH_3.

Grassland sites:

An additional major source of NH_3 in this group of sites is expected to come from grazing emissions and housed livestock (e.g. cattle). Concentrations in this group of sites were generally 2 - 3 times larger than semi-natural sites (Fig. 4.14A), attributed to the increased emissions and concentrations from livestock (Hellsten et al., 2007). The spring peak is related to the practice of fertiliser and manure being spread on grazing fields to aid spring grass growth, which will be cut for hay and silage later in the year. NH_3 concentrations in June and July are smaller than in spring or late summer, possibly because grass will be actively growing with possible uptake and removal of NH_3 from the atmosphere. The concentrations are also larger in summer than winter, with warmer conditions promoting NH_3 volatilization and thermodynamic shift to the gas phase.

European regions:

The seasonal profiles of NH_3 for Central and Western European regions were similar, characterised by a large peak in spring that is likely to be agriculture–related (Fig. 4.15A), as observed at cropland sites (Fig. 4.14A). While the peak concentrations in both regions are of comparable magnitude (Central = 2.6 µg NH_3 m^{-3}, Western = 2.8 µg NH_3 m^{-3}), winter concentrations in Central Europe (0.6 µg NH_3 m^{-3}) were three times smaller than the West (1.5 µg NH_3 m^{-3}). This

may be related to either lower regional background in NH_3 concentrations and/or suppressed emissions in colder temperature of Central Europe in winter. By contrast, Eastern and Southern European regions have a broad peak in summer, although the Eastern region also has a second peak in October (likely agriculture related). Smallest concentrations were found in Northern Europe with the lowest NH_3 emissions (Fig. 4.9). The three peaks in the profile shows elevated concentrations in summer driven by warming temperatures, with the spring and autumn peaks attributed to influence from NH_3 emissions from agricultural sources.

4.4.5.2 HNO_3

The seasonal distribution in HNO_3 is similar between the different ecosystem groups, varying only in magnitude of concentrations (Fig. 4.14C) and reflects the secondary nature of this component that is formed from oxidation of NO_x (Fahey et al., 1986; ROTAP, 2012). HNO_3 concentrations in the crops group are up to 2 times larger than the grassland group, while the smallest concentrations are in the semi-natural group. This is likely related to proximity of sites in the different groups to combustion sources. A weak seasonal cycle is seen in the secondary HNO_3 air pollutant in all cases, with slightly higher concentrations in late winter, spring and summer and smallest in March and November. The reaction of NO_2 with the OH radical is an important source of HNO_3 during daytime, whereas N_2O_5 hydrolysis is considered an important source of HNO_3 at night time (Chang et al., 2011). Larger HNO_3 concentrations in summer are therefore from increased OH radicals for reaction with NO_2 to form HNO_3. Similarly, higher concentrations of ozone in spring in Europe (EMEP, 2016) can potentially increase HNO_3 concentrations in springtime. Conversely, HNO_3 concentrations are lower in winter when oxidative capacity is less.

Seasonal variability in HNO_3 will also be influenced by gas-aerosol phase equilibrium. In the atmosphere, HNO_3 reacts reversibly with NH_3 forming the semi-volatile NH_4NO_3 aerosol if the necessary concentration product

[HNO_3].[NH_3] is exceeded (Baek et al., 2004; Jones and Harrison et al., 2011). Because of this process, the prime influences upon HNO_3 concentrations at sites where NH_4NO_3 is formed are expected to be ambient temperature, relative humidity and NH_3 concentrations that affect the partitioning between the gas and aerosol phase (Allen et al., 1989; Stelson and Seinfeld, 1982). The availability of surplus NH_3 in spring (Sect. 4.4.5.1) would tend to reduce HNO_3 and increase NH_4NO_3 formation, which is reflected in the reduced HNO_3 concentrations observed in March when NH_3 is at a maximum. In summer, warmer, drier conditions promotes volatilisation of the NH_4NO_3 aerosol, increasing the gas phase concentrations of HNO_3 and NH_3 relative to the aerosol phase. Seasonality in HNO_3 is therefore complex, related to traffic and industrial emissions, photochemistry and HNO_3:NH_4NO_3 partitioning.

An analysis of the same data grouped according to geographical regions revealed distinctive cycles in HNO_3 in Eastern and Southern Europe (Fig. 4.15C). These two regions showed highest concentrations in summer and smallest in winter, consistent with enhanced photochemistry in warmer, sunnier climates and thermodynamic equilibrium favouring gas phase-HNO_3 (Fig. 4.15C). Summertime peak concentrations in NH_3 were also observed in these 2 regions (Fig. 4.15A). In comparison, the seasonal profiles of HNO_3 in other regions were similar to that described for different ecosystem types (Fig. 4.14C).

4.4.5.3 SO_2

Seasonality in SO_2 show concentrations peaking in winter at most sites (Fig. 4.14E), except in Southern Europe where the peak appeared in summer (Fig. 4.15E). Increased SO_2 emissions from combustion processes (heating) in the winter months, coupled to stable atmospheric conditions can result in build-up of concentrations at ground level, thereby contributing to the peak wintertime concentrations. The largest winter concentrations in Central and Eastern regions exceeded summer values on average by a factor of 4, compared with smaller differences in other regions (Fig. 4.15E). Enhanced oxidation

processes in summer also tend to further reduce concentrations of SO_2 through the oxidation of SO_2 to H_2SO_4 (Saxena and Seigneur, 1987; Sickles and Shadwick, 2007; Paulot et al., 2017). In Southern Europe, the seasonal cycle have winter minima and summer maxima instead, likely from increased combustion sources to meet energy demands for air-conditioning over the hot summer months. It was shown earlier in Sect. 4.4.4 that SO_2 was spatially correlated to HNO_3; differences in relative concentrations between the different ecosystem groups (Fig. 4.14E) is thus also likely related to relative distance from emission sources.

4.4.5.4 NH_4^+, NO_3^- and SO_4^{2-}

The seasonal profiles of particulate NH_4^+ (Figs. 4.14B, 4.15B) were mirrored by particulate NO_3^- (Figs. 4.14D, 4.15D) in all groups, demonstrating temporal, as well as regional (see Sect. 4.4.3.5) correlation between these two components. Since NH_4NO_3 is more abundant than $(NH_4)_2SO_4$, the seasonality of NH_4^+ is likely to be influenced more by the temperature and humidity dependence of the semi-volatile NH_4NO_3, than by the stable $(NH_4)_2SO_4$. In summer, warmer and drier conditions promotes the dissociation of NH_4NO_3, decreasing particulate phase NH_4NO_3 relative to gas phase NH_3 and HNO_3. This process accounts for the summertime minima in NH_4^+ (Figs. 4.14B and 4.15B) and NO_3^- (Figs. 4.14D and 4.15D). Conversely, cooler temperatures and higher humidity conditions in winter, spring and autumn shift the equilibrium to the aerosol phase, with observed peaks in concentrations of NH_4^+ and NO_3^-.

Since NH_3 concentrations are also generally higher in spring than in autumn (Figs. 4.14A, 4.15A), the increased availability of NH_3 in this period contributes towards the higher concentrations of NH_4NO_3 in spring than in autumn. In winter, the combination of NH_4NO_3 remaining in the aerosol phase, combined with the stable conditions that can often develop, maintains high concentrations of NH_4^+ and NO_3^- in the atmosphere. The peak in NO_3^- in Southern Europe was in February only, compared with broader peaks (Feb-

April) in other regions (Fig. 4.15D) which may reflect differences in climatic conditions. In Figs. 4.14H and 4.15H, the ratio of the molar equivalent concentrations of NO_3^- to sum (NO_3^- + SO_4^{2-}) are plotted. The ratios were highest in spring and autumn, and smallest in summer, lending support to the importance of NH_4NO_3 in controlling the seasonality of NH_4^+.

In the seasonal profiles for particulate SO_4^{2-}, clear summer maxima and winter minima were provided by sites in Southern and Eastern Europe (Fig. 4.15F). The peaks occurred at different times, in July (Southern Europe) and in August (Eastern Europe) (Fig. 4.15F) and coincided with the timing of corresponding peaks in NH_3 concentrations (Fig. 4.15A), illustrating the importance of NH_3 in driving the formation of the stable $(NH_4)_2SO_4$. Since $(NH_4)_2SO_4$ is formed through the preferential and irreversible reaction between the precursor gases (Bower et al., 1997), particulate SO_4^{2-} concentrations will be governed by the availability of NH_3 and H_2SO_4 (from oxidation of SO_2).

As discussed earlier, SO_2 concentrations in Southern Europe have a different seasonal cycle from other regions, with higher concentrations in summer than in the winter months (Fig. 4.15E). Although the seasonal cycle for Eastern Europe showed smallest SO_2 concentrations in the summer, the summer minima here (mean = 1.3 µg SO_2 m^{-3}) are in fact larger than the summer peak in Southern Europe (mean = 1.1 µg SO_2 m^{-3}) and concentrations in other regions (0.4 - 1.0 µg SO_2 m^{-3}). Enhanced summertime concentrations in HNO_3 were observed in these two regions (Fig. 4.15B) which also suggests potentially increased oxidative capacity for more of the SO_2 to be converted H_2SO_4 (Sect. 4.4.5.3). The ready availability of both SO_2 (and conversion to H_2SO_4) and NH_3 (Fig. 4.15A) in Southern and Eastern regions in this period thus coincide to produce the summer peak in particulate SO_4^{2-}.

In other regions (Central, Northern, Western), formation of $(NH_4)_2SO_4$ will be limited by the availability of SO_2 which is lowest in summer (Fig. 4.15E). Conversely, SO_2 concentrations is highest in winter (Fig. 4.15E), but lower oxidative capacity at this time of year limits formation of H_2SO_4. Since NH_3

concentrations are also smallest in winter (Fig. 4.15A), formation of $(NH_4)_2SO_4$ is also limited in winter. This accounts for the higher concentrations of particulate SO_4^{2-} concentrations in winter and in early spring in these regions (Fig. 4.15F).

4.4.5.5 HCl, Cl^- and Na^+

The concentrations of HCl measured at all sites, in all groups, were very small, with monthly mean concentrations varying between 0.1 and 0.3 µg HCl m^{-3} (Figs. 4.14G, 4.15G). There is no discernible seasonality in the data, which suggests either sites in the network are not affected by any large sources of HCl, or that small differences between months are not detectable due to measurement uncertainties at the very low concentrations (method limit of detection ~ 0.1 µg HCl m^{-3} for monthly sampling). By contrast, Cl^- (Figs. 4.14I, 4.15I) has a distinctive seasonal cycle with higher concentrations in the winter months than summer, similar to that of Na^+ (Figs. 4.14J, 4.15J). The temporal correlation in the data therefore lends further support that Na^+ and Cl^- in the measurements are mainly sea salt (see also spatial correlation in Sect. 4.4.4). The highest concentrations of Na^+ and Cl^- during winter months would be consistent with increased generation and transport of sea salt generated by more stormy weather from marine sources during those periods (O'Dowd and de Leeuw, 2007).

4.4.6 Bulk wet deposition measurements

Annual mean wet deposition of chemical species measured at the NEU bulk sampling sites was estimated by combining measured concentrations with annual precipitation. Site changes also occurred during the operation of the bulk wet deposition network, with some sites closed and new sites added. At Mitra (PT-Mi3), contamination of the rain samples from bird strikes resulted in the rejection of a large proportion of the monthly data and this site was excluded from the data analysis. In total, 12 sites provided 2 years of monthly

data, with a further 5 sites providing 1 year of monthly data over the period 2008 to 2010. Due to differences in start and end dates for bulk measurements between the sites, the annual mean data derived are for 12 month periods or 2 x 12 month periods, and not from calendar years.

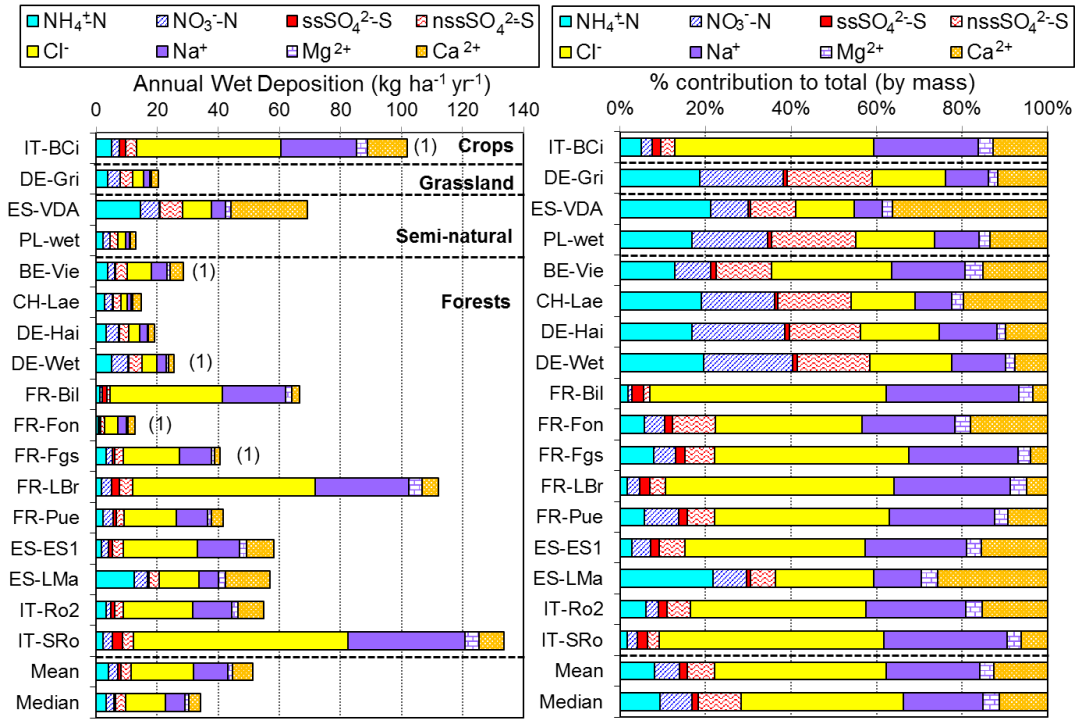

Figure 4.16. (LEFT) Annual wet deposition of inorganic components (kg ha^{-1} yr^{-1}) estimated from Rotenkamp bulk precipitation collectors in the NEU bulk wet deposition network. (RIGHT) Percentage contribution of inorganic components to total (by mass) measured at 17 sites from 2008 to 2010. The data shown are 2-year averaged deposition, made between 2008 and 2010, except at 5 sites with 1 year of measurement only, as indicated in the graph in brackets.

Annual mean wet deposition data for the 17 sites from 6 countries (Belgium, France, Germany, Italy, Poland, Spain and Switzerland) are summarised in Fig. 4.16. Using Na^+ as a tracer for sea-salt (Keene et al,. 1986), nss-SO_4^{2-} concentrations were also estimated from the total SO_4^{2-} (see Sect. 4.3.2.2) and are included for comparison. Since the measurements were made at a limited number of sites across Europe, there is insufficient information to make

inferences about spatial differences in concentrations. Detailed assessments of extensive precipitation chemistry across Europe are made elsewhere, for example from the EMEP wet deposition networks (EMEP, 2016; Torseth et al., 2012). What the NEU bulk network data clearly shows is that N_r components in rain also exceed that of S (Fig. 4.16), as was observed in the atmospheric data. The mean proportional contribution of total N (NH_4^+ and NO_3^-) to the sum total of all wet deposited species measured (by mass) was 19% (range = 3 – 39%), compared with a smaller 9 % (range = 1 – 19%) contribution from nss-SO_4^{2-} (Supp. Table S4.14). Wet deposited N (NH_4^+ and NO_3^-) was on average 2 times higher than nss-SO_4^{2-}, similar to that seen in the relative proportion of total N_r (sum of NH_3, NH_4^+, HNO_3, NO_3^-) to total S (sum of SO_2, SO_4^{2-}) in the atmospheric data (Sect. 4.4.3.5). Similar to the atmospheric data (Sect. 4.4.3.5), a considerable fraction of the wet deposited components was made up of sea salt (Na^+ and Cl^-), with the sum of Na^+ and Cl^- contributing on average 50% of the total wet deposited components (range = 20 – 84 %, *n* = 17). Contributions by the other base cations Ca^{2+} and Mg^{2+} gave a further 20 % (range = 8 – 41 %, *n* = 17) (Supp. Table S4.14).

The intention of the bulk network at the outset was to provide wet deposition data at DELTA® sites that do not already have such measurements on site. The wet deposition data on NH_4^+ and NO_3^-, combined with a wider precipitation chemistry dataset (e.g. from EMEP and other national precipitation networks) was used to estimate total N_r deposition to a site (Flechard et al., 2011; 2020). Together, the dry (DELTA® network) and wet N_r estimates (NEU bulk network, combined with data from other national precipitation chemistry networks) are used to compare with EMEP models and to examine the interactions between N_r supply and greenhouse gas exchange at the NEU DELTA® sites, presented in a separate paper by Flechard et al. (2020).

4.5 Implications for a chemical climate dominated by NH_3 and NH_4NO_3 in Europe

International agreements such as the UNECE Convention on Long-Range Transboundary Air Pollution (CLRTAP 1999 Gothenburg Protocol, amended in 2012) (UNECE, 2018), NEC Directive 2016/2284 (revised also in 2012) (EU, 2016) and Ambient Air Quality Directives (EU Directive 2008/50/EC) (EC, 2008) have achieved reductions in emissions of SO_2 and NO_x, but with limited ambition in NH_3. The amended NEC Directive (2016/2284) sets further emission reduction commitments for SO_2, NO_x, NH_3, as well as primary fine particulate matter ($PM_{2.5}$), for the years 2020 to 2029 with 2005 as the base year and additional reductions beyond 2030. Provisions for ecosystem monitoring under Article 9 and Annex V of Directive 2016/2284 (EU, 2016) also require member states to monitor (Article 9) and report (Article 10.4) the negative impacts of NH_3, SO_2 and NO_x on ecosystems from national networks that are representative of the Member State's freshwater, natural and semi-natural habitats and forest ecosystem types.

In 2017, the European Commission published tighter new standards for large combustion plants, including many large coal-fired power stations, giving them four years to meet the standards, detailed in the Decision (EU) 2017/1442 under Directive 2010/75/EU (EC, 2017). Tighter rules are set for emissions of NO_x, SO_2 and PM and concentrations of these are expected to continue to fall in future years. Measurements in the network have shown that the concentrations of SO_2 have declined to a level where it is no longer the dominant acid gas, such that HNO_3 and HCl are together contributing an equal or larger fraction of the total acidity in the atmosphere in the present assessment (Fig. 4.12A). However, SO_2 (by mass) has a higher acidification potential (1 kg SO_2 = 1.00 kg eq. SO_2 than NO_x (1 kg NO_2 = 0.70 kg eq. SO_2 (see Hauschild and Wenzel, 1998), so SO_2 will remain important in contributing to exceedances of critical loads for acidification, estimated to be exceeded in 5 % of the European ecosystem area in 2015 (EEA, 2019).

Emissions of NH_3 in Europe have increased by about 3% from the agricultural sector between 2013 - 2016 (EEA, 2018) and abatement measures are likely to be needed to meet emission targets set for NH_3 (Sutton and Howard, 2018). Thresholds for atmospheric concentrations and deposition of N_r components to semi-natural habitats were exceeded in 63% of the EU-28 ecosystem area in 2016 (EMEP, 2018). In deposition models, oxidised nitrogen species currently included are HNO_3, NO_2 and aerosol nitrate (NO_3^-), with deposition velocities dependent on meteorology and vegetation characteristics (e.g. Flechard et al., 2011). NH_3 is the most important individual term in the calculation of total N dry deposition, along with NH_4^+ and HNO_3 dry deposition and wet deposited NH_4^+ and NO_3^-. Although NO_2 (not measured in NEU DELTA® network) will also provide a relevant contribution to dry N deposition, it will (especially for rural semi-natural and forest ecosystems) be smaller than for NH_3, based on rather small deposition velocities for NO_2 (Smith et al., 2000).

The annually averaged data also show exceedance of the Critical Levels for annual mean NH_3 concentrations of 1 and 3 µg NH_3 m^{-3} for the protection of lichens-bryophytes (including ecosystems where they are important for integrity) and other vegetation, respectively, at many of the sites (62 % > 1 µg NH_3 m^{-3} and 27 % > 3 µg NH_3 m^{-3}) (Supp. Table S4.5). The widespread exceedance of the Critical Levels for NH_3 concentrations across Europe represents an ongoing threat to the integrity of sites designated under the EU Habitats Directive (EU, 1992). In tandem, the growing relative importance of NH_3 and NH_4^+ to total acidic and total nitrogen deposition indicates that strategies to tackle acidification and eutrophication will also need to include measures to abate emissions of NH_3.

The agricultural sector makes up 92% of the total estimated NH_3 emission in Europe (EEA, 2019), with 80 % of that generated by less than 10 % of the farms, so that the largest emission reduction potential could be attained by targeting the small number of industrial-scale farms (Maas and Greenfelt, 2016). A modelling study by Backes et al. (2016) suggested a halving of NH_3

emissions could deliver a 24% reduction in total $PM_{2.5}$ concentrations in northwest Europe, driven mainly by reduced formation of NH_4NO_3 and that targeting emission reductions during winter had a larger effect than at other times of the year. In recognising the need to tackle NH_3, the UNECE has published a guidance document and code of good agricultural practice (COGAP) for reducing NH_3 emissions (Bittman et al., 2014), which has also been adopted in the EC NECD and by the UK government in its Clean Air Strategy (Defra, 2019).

4.6 Conclusion

The NitroEurope DELTA® network has provided for the first time a comprehensive quality-assured multi-annual dataset on reactive gases (NH_3, HNO_3, SO_2, HCl) and aerosols (NH_4^+, NO_3^-, SO_4^{2-}, Cl^-) across the major gradients of pollution, ecosystem type and climatic zones of Europe. The harmonised measurement approach of monthly time-integrated monitoring with a simple low-cost DELTA® method represented an effective use of resources, making it possible to operate a network with a common measurement method across multiple laboratories at a large number of sites. At the same time, the concurrent measurement of the gas and aerosol components permitted an assessment of the atmospheric composition, spatial and seasonal characteristics in the gas and aerosol phase of these components. The dataset has also been used to develop estimates of site-based N_r dry deposition fluxes across Europe, including supporting the development and validation of long-range transport models. Combined with estimates of wet deposition (NEU bulk wet deposition network and data by other networks) to these sites, an assessment of the interactions between N supply and greenhouse gas exchange was addressed in a separate paper by Flechard et al. (2020), using N_r and CO_2 flux data from the co-location of the NEU DELTA® with CarboEurope Integrated Project sites.

Two key features have emerged in the data. The first is the dominance of NH_3 as the largest single component at the majority of sites, with molar concentrations exceeding those of HNO_3 and SO_2, combined. Changes in the relative concentrations of these gases across Europe suggests that the deposition rates of SO_2 and NH_3 will increasingly be controlled by the molar ratio of NH_3 to combined acidity (sum of SO_2, HNO_3 and HCl) and deposition models should take these changes into account. As expected, the largest NH_3 concentrations were measured at cropland sites, in intensively managed agricultural areas dominated by NH_3 emissions. The smallest concentrations were at remote semi-natural and forest sites, although concentrations in the Netherlands, Italy and Germany were up to 45 times larger than similarly classed sites in Finland, Norway and Sweden (< 0.6 µg NH_3-N m^{-3}), illustrating the high NH_3 concentrations that sensitive habitats are exposed to in intensive agricultural landscapes in Europe.

Temporally, peak concentrations in NH_3 for crops and grassland sites occurred in spring, reflecting the implementation of the EU Nitrates Directive that prohibits winter manure spreading. The spring agriculture-related peak was seen even at semi-natural and forest sites, highlighting the influence of NH_3 emissions at sites that are more distant from sources. Summer peaks, promoted by increased volatilisation of NH_3, but also by gas-aerosol phase thermodynamics under warmer, drier conditions were seen in all ecosystem groups, except at forest sites. The seasonality in the NH_3 concentrations captured for the different groups is important, both for identifying periods when abatement might be targeted and for model development.

Seasonality in the other gas and aerosol components is also driven by changes in emission sources, chemical interactions and by changes in environmental conditions influencing partitioning between the precursor gases (SO_2, HNO_3, NH_3) and secondary aerosols (SO_4^{2-}, NO_3^-, NH_4^+). Seasonal cycles in SO_2 were mainly driven by emissions (combustion), with concentrations peaking in winter, except in Southern Europe where the peak occurred in summer. HNO_3 concentrations were more complex, as affected by photochemistry,

meteorology and by gas-aerosol phase equilibrium. Southern and eastern European regions provided the clearest seasonal cycle for HNO_3, with highest concentrations in summer and smallest in winter, attributed to increased photochemistry in the summer months in hotter climates. In comparison, a weaker seasonal cycle is seen in other regions, with marginally elevated concentrations in late winter, spring and summer and smallest in March and November. Increased ozone in spring is likely to enhance oxidation of NO_x to HNO_3 for forming the semi-volatile NH_4NO_3 by reaction with a surplus of NH_3. Cooler, wetter conditions in spring also favour the formation of NH_4NO_3 and more of the NH_4NO_3 remains in the aerosol or condensed phase. This accounts for the higher concentrations of NH_4^+ and NO_3^- in spring and the absence of a HNO_3 peak at this time of year. Conversely, increased partitioning to the gas phase in summer decreases NH_4NO_3 concentrations relative to gas phase NH_3 and HNO_3.

Particulate SO_4^{2-} showed large peaks in concentrations in summer in Southern and also Eastern Europe, contrasting with much smaller peaks occurring in early spring in other regions. The peaks in particulate SO_4^{2-} coincided with peaks in NH_3 concentrations, illustrating the importance of NH_3 in driving the formation of $(NH_4)_2SO_4$. Since NH_4NO_3 is more abundant than $(NH_4)_2SO_4$, the seasonality of NH_4^+ is likely to be influenced more by the temperature and humidity dependence of the semi-volatile NH_4NO_3, than by the stable $(NH_4)_2SO_4$. This is supported by similarity in the seasonal profiles of NH_4^+ and NO_3^- at all sites, demonstrating temporal, as well as regional correlation between these two components.

The second key feature is the dominance of NH_4NO_3 over $(NH_4)_2SO_4$, with on average twice as much NO_3^- as SO_4^{2-} (on a molar basis). A change to an atmosphere that is more abundant in NH_4NO_3 will likely increase the atmospheric lifetimes and extend the footprint of the NH_3 and HNO_3 gases, due to the potential for the semi-volatile NH_4NO_3 to act as a reservoir and release NH_3 and HNO_3 in warm weather. The potential increase in atmospheric lifetime of NH_3 suggests that a larger fraction of the reduced and oxidised N

will remain in the gas phase as NH_3, resulting in a non-linearity in relationship between emissions and concentrations of NH_3. Ammonia is an important term in the calculation of total N dry deposition and a significant contributor to the exceedances of thresholds for atmospheric concentrations and deposition of N_r components to sensitive habitats across much of Europe. In the DELTA® network, the Critical Levels of 1 and 3 µg NH_3 m^{-3} for the protection of lichens-bryophytes and vegetation were exceeded at 62 % and 27 % of the sites, respectively. The importance of NH_3 is therefore expected to further increase relative to oxidised N, as NO_x emissions continue to decrease.

Acknowledgements

Research work under the NitroEurope (NEU) Integrated Project was funded by the European Commission under the EU FP6 Grant 17841: The nitrogen cycle and its influence on the European greenhouse gas balance (NitroEurope) (http://www.nitroeurope.ceh.ac.uk/), together with supporting funds from NERC CEH programmes. Atmospheric measurements in the UK National Ammonia Monitoring Network (NAMN) and Acid Gas and Aerosol Monitoring Network (AGANet) are funded by the UK Department for Environment, Food and Rural Affairs (Defra) and devolved administrations. The Mediterranean Center for Environmental Studies (CEAM) is partly supported by Generalitat Valenciana, Bancaja, and the Programm CONSOLIDER-INGENIO 2010 (GRACCIE). The authors gratefully acknowledge support and contributions by: 1) the large network of dedicated local site contacts, field teams and host organisations at NEU DELTA® and bulk wet deposition sites, 2) all chemical laboratory personnel involved in the sample preparations and chemical analyses from the chemical laboratories, 3) RIVM for hosting the DELTA-AMOR inter-comparsions at Vredepeel, and 4) Jan Vonk at RIVM for providing links to access NH_3 and SO_2 data from the Dutch national network LML (Landelijk Meetnet Luchtkwaliteitl).

References

Allen, A. G., Harrison, R. M., and Erisman, J. W.: Field measurements of the dissociation of ammonium nitrate and ammonium chloride aerosols, Atmos. Environ. (1967), 23(7), 1591–1599. doi:10.1016/0004-6981(89)90418-6, 1989.

Allegrini, I., De Santis, F., Di Palo, V., Febo, A., Perrino, C., Possanzini, M., and Liberti, A.: Annular denuder method for sampling reactive gases and aerosols in the atmosphere, Sci. Total Environ., 67, 1-16, doi:10.1016/0048-9697(87)90062-3, 1987.

AQEG: Fine Particulate Matter ($PM_{2.5}$) in the United Kingdom, Air Quality Expert Group report prepared for Department for Environment, Food and Rural Affairs; Scottish Executive; Welsh Government; and Department of the Environment in Northern Ireland. http://uk-air.defra.gov.uk, 2012.

Backes, A. M., Aulinger, A., Bieser, J., Matthias, V., and Quante, M.: Ammonia emissions in Europe, part II: How ammonia emission abatement strategies affect secondary aerosols, Atmos. Environ., 126, 153-161, doi:10.1016/j.atmosenv. 2015.11.039, 2016.

Baek, B. H., Aneja, V. P., and Tong, Q.: Chemical coupling between ammonia, acid gases, and fine particles, Environ. Poll., 129(1), 89-98, doi:10.1016/j.envpol. 2003.09.022, 2004.

Bai, H., Chungsying, L., Chang, K -F., and Fang, G -C.: Sources of sampling error for field measurement of nitric acid gas by a denuder system, Atmos. Environ., 37: 941-947, doi:10.1016/S1352-2310(02)00972-x, 2003

Bittman, S., Dedina, M., Howard C. M., Oenema, O., Sutton, M. A., (eds): Options for Ammonia Mitigation: Guidance from the UNECE Task Force on Reactive Nitrogen, Centre for Ecology and Hydrology, Edinburgh, UK, 2014.

Bleeker, A., Sutton, M. A., Acherman, B., Alebic-Juretic, A., Aneja, V. P., Ellermann, T., Erisman, J. W., Fowler, D., Fagerli, H., Gauger, T., Harlen, K. S., Hole, L. R., Horvath, L., Mitosinkova, M., Smith, R. I., Tang, Y. S., and van Pul, A.: Linking Ammonia Emission Trends to Measured Concentrations and Deposition of Reduced Nitrogen at Different Scales, Atmospheric Ammonia: Detecting Emission Changes and Environmental Impacts, edited by: Sutton, M. A., Reis, S., and Baker, S. M. H., 123-180 pp., 2009.

Bobbink, R., Hicks, K., Galloway, J., Spranger, T., Alkemade, R., Ashmore, M., Bustamante, M., Cinderby, S., Davidson, E., Dentener, F., Emmett, B., Erisman, J., Fenn, M., Gilliam, F., Nordin, A., Pardo, L., and De Vries, W.: Global assessment of nitrogen deposition effects on terrestrial plant diversity: a synthesis, Ecol. App., 20: 30-59, doi:10.1890/08-1140.1, 2010.

Bower K. N., Choularton T. W., Gallagher M. W., Colvile R. N., Wells M., Beswick K. M., Wiedensohler A., Hansson H.-C., Svenningsson B., Swietlicki E., Wendisch M., Berner A., Kruisz C., Laj P., Facchini M. C., Fuzzi S., Bizjak M., Dollard G., Jones B., Acker K., Wieprecht W., Preiss M., Sutton M. A., Hargreaves K. J., Storeton-West R. L., Cape J. N., and Arends, B. G.: Observations and modelling of the processing of aerosol by a hill cap cloud, Atmos. Environ., 31, 2527–2544, doi:10.1016/S1352-2310(96)00317-2, 1997.

Cape J. N., Tang Y. S., van Dijk N., Love L., Sutton M. A., and Palmer S. C. F.: Concentrations of ammonia and nitrogen dioxide at roadside verges and their contribution to nitrogen deposition, Environ. Poll., 132, 469-478, doi:10.1016/j.envpol.2004.05.009, 2004.

Cape, J. N., van der Eerden, L. J., Sheppard, L .J., Leith, I. D., and Sutton, M. A.: Evidence for changing the critical level for ammonia, Environ. Poll., 157, 1033-1037, doi:10.1016/j.envpol.2008.09.049, 2009.

Cape, J. N., Tang, Y. S., Gonzalez-Benıtez, J. M., Mitosinkova, M., Makkonen, U., Jocher, M., and Stolk, A.: Organic nitrogen in precipitation across Europe, Biogeosciences, 9 (11), 4401-4409, doi:10.5194/bg-9-4401-2012, 2012.

Chang, W. L., Bhave, P. V., Brown, S. S., Riemer, N., Stutz, J., and Dabdub, D.: Heterogeneous Atmospheric Chemistry, Ambient Measurements, and Model Calculations of N_2O_5: A Review, Aerosol Sci. Technol., 45:6, 665-695, doi:10.1080/02786826. 2010.551672, 2011.

Dämmgen, U., Erisman, J. W., Cape, J. N., Grűnhage, L., and Fowler, D.: Practical considerations for addressing uncertainties in monitoring bulk deposition, Environ. Poll., 134, 535–548, doi:10.1016/j.envpol.2004.08.013, 2005.

Defra, Clean Air Strategy 2019, https://www.gov.uk/government/publications/ clean-air-strategy-2019, Published 14 January 2019.

Dore, A. J., Carslaw, D. C., Braban, C., Cain, M., Chemel, C., Conolly, C., Derwent, R. G., Griffiths, S.J., Hall, J., Hayman, G., Lawrence, S., Metcalfe, S. E., Redington, A., Simpson, D., Sutton, M. A., Sutton, P., Tang, Y. S., Vieno, M., Werner, M., and Whyatt, J. D.: Evaluation of the performance of different atmospheric chemical transport models and inter-comparison of nitrogen and sulphur deposition estimates for the UK, Atmos. Environ., 119, 131-143, doi:10.1016/ j.atmosenv.2015.08.008, 2015.

Dutkiewicz, V. A., Das, M., and Husain, L.: The relationship between regional SO_2 emissions and the downwind aerosol sulphate concentrations in the north eastern US, Atmos. Environ., 34, 1821-1832, doi:10.1016/S1352-2310(99)00334-9, 2000.

EC: Habitats Directive (EU) Council Directive 92/43/EEC of 21 May 1992 on the conservation of natural habitats and of wild fauna and flora, 1992.

EC: Directive (EU) 2008/50/EC of the European Parliament and of the Council of 21 May 2008 on ambient air quality and cleaner air for Europe, 2008.

EC: Decision (EU) 2017/1442 Commission Implementing Decision (EU) 2017/1442 of 31 July 2017 establishing best available techniques (BAT) conclusions, under Directive 2010/75/EU of the European Parliament and of the Council, for large combustion plants (notified under document C(2017) 5225), 2017.

EEA: European Union emission inventory report 1990-2017 under the UNECE Convention on Long-range Transboundary Air Pollution (LRTAP), EEA Report No 6/2018, European Environment Agency, https://www.eea.europa.eu/publications/ european-union-emissions-inventory-report-1, 2018.

EEA: European Union emission inventory report 1990-2017 under the UNECE Convention on Long-range Transboundary Air Pollution (LRTAP), EEA Report No 8/2019, European Environment Agency, https://www.eea.europa.eu/publications/ european-union-emissions-inventory-report-2017, accessed 09 December 2019.

EEA: Datasource: https://www.eea.europa.eu/data-and-maps/dashboards/air-pollutant-emissions-data-viewer-2, accessed 15 January 2020.

EMEP: Air pollution trends in the EMEP region between 1990 and 2012, CCC-Report 1/2016, http://www.ivl.se/download/18.7e136029152c7d48c202d81/1466685735821/C206.pdf), 2016.

EMEP: Transboundary particulate matter, photooxidants, acidifying and eutrophying components, EMEP Status Report 1/2018, http://emep.int/publ/reports/2018/EMEP_Status_Report_1_2018.pdf, 2018.

EMEP: Transboundary particulate matter, photooxidants, acidifying and eutrophying components, EMEP Status Report 1/2019, http://www.diva-portal.org/smash/record.jsf?pid=diva2%3A1371039&dswid=-7800, 2019.

EMEP: Datasource: EMEP/CEIP 2019, distributed emission data as used in EMEP models, accessed 15 January 2020.

EU: Directive (EU) 2016/2284 of the European Parliament and of the Council of 14 December 2016 on the reduction of national emissions of certain atmospheric pollutants, amending Directive 2003/35/EC and repealing Directive 2001/81/EC, 2016.

Evans, C. D., Monteith, D. T., Fowler, D., Cape, J. N., and Brayshaw, S.: Hydrochloric Acid: An Overlooked Driver of Environmental Change, Env. Sci. Technol., 45 (5), 1887-1894, doi:10.1021/es103574u , 2011.

Fahey, D. W., Hübler, G., Parrish, D. D., Williams, E. J., Norton, R. B., Ridley, B. A., Singh, H. B., Liu, S. C., and Fehsenfeld, F. C.: Reactive nitrogen species in the troposphere: Measurements of NO, NO_2, HNO_3, particulate nitrate, peroxyacetyl nitrate (PAN), O_3, and total reactive odd nitrogen (NO_y) at Niwot Ridge, Colorado, Journal Geophysical Research, 91(D9), 9781–9793, doi:10.1029/JD091iD09p09781, 1986.

Ferm, M.: Method for determination of atmospheric ammonia, Atmos. Environ., 13, 1385-1393, doi:10.1016/0004-6981(79)90107-0, 1979.

Ferm, M.: A Na_2CO_3-coated denuder and filter for determination of gaseous HNO_3 and particulate NO_3^- in the atmosphere, Atmos. Environ. (1967), 20 (6), 1193-1201, doi: 10.1016/0004-6981(86)90153-8, 1986.

Finlayson-Pitts, B. J. and Pitts, J. N.: Chemistry of the upper and lower atmosphere: theory, experiments, and applications, Academic Press, San Diego, CA, USA, 969 pp., 1999.

Fitz, D. R.: Evaluation of Diffusion Denuder Coatings for Removing Acid Gases from Ambient Air. Final Report, U.S. Environmental Protection Agency. Riverside, 2002.

Flechard, C. R., Fowler, D., Sutton, M. A., and Cape, J. N.: A dynamic chemical model of bi-directional ammonia exchange between semi-natural vegetation and the atmosphere, Q. J. Roy. Meteor. Soc., 125, 2611–2641, doi:10.1002/qj.49712555914, 1999.

Flechard, C. R., Nemitz, E., Smith, R.I., Fowler, D., Vermeulen, A.T., Bleeker, A., Erisman, J.W., Simpson, D., Zhang, L., Tang, Y.S., and Sutton, M.A.: Dry deposition of reactive nitrogen to European ecosystems: a comparison of inferential models across the NitroEurope network, Atmos. Chem. Phys., 11, 2703–2728, doi:10.5194/acp-11-2703-2011, 2011.

Flechard, C. R., Massad, R. S., Loubet, B., Personne, E., Simpson, D., Bash, J. O., Cooter, E. J., Nemitz, E., and Sutton, M. A.: Advances in understanding, models and parameterizations of biosphere-atmosphere ammonia exchange, Biogeosciences, 10, 5183-5225, 10.5194/bg-10-5183-2013, 2013.

Flechard, C. R., Ibrom, A., de Vries, W., Simpson, D., Loustau, D., Legout, A., Zechmeister-Boltenstern, S., Kitzler, B., Schjørring, J. K., Frumau, A., Siemens, J., Mitosinkova, M., Sanz, F., Tang, Y. S., van Oijen, M., Cameron, D., Fauvel, Y., Hamon, Y., Neirynck, J., Butterbach-Bahl, K., Kiese, R., Dise, N. B., Skiba, U., Nemitz, E., and Sutton, M. A.: Carbon / nitrogen interactions in European forests and semi-natural vegetation. Part I: Fluxes and budgets of carbon, nitrogen and greenhouse gases from ecosystem monitoring and modelling, Biogesciences, 17(6), 1583-1620, doi:10.5194/bg-17-1583-2020, 2020.

Fowler, D., Cape, N., and Unsworth, M. H.: Deposition of atmospheric pollutants on forests, Philosophical Transactions of the Royal Society of London. B, Biological Sciences, 324 (1223), doi:10.1098/rstb.1989.0047, 1989.

Fowler, D., Coyle, M., Flechard, C., Hargreaves1, K., Nemitz, E., Storeton-West, R., Sutton, M., and Erisman, J. W.: Advances in micrometeorological methods for the measurement and interpretation of gas and particle nitrogen fluxes, Plant and Soil, 228: 117-129, doi:10.1023/A:1004871511282, 2001.

Fowler, D., and Reis, S.: Challenges in quantifying biosphere-atmosphere exchange of nitrogen species, Environ. Poll., 150, 125-139, doi:10.1016/j.envpol. 2007.04.014, 2007.

Fowler, D., Pilegaard, K., Sutton, M. A., Ambus, P., Raivonen, M., Duyzer, J., Simpson, D., Fagerli, H., Fuzzi, S., Schjoerring, J.K., Granier, C., Neftel, A., Isaksen, I. S. A., Laj, P., Maione, M., Monks, P. S., Burkhardt, J., Daemmgen, U., Neirynck, J., Personne, E., Wichink-Kruit, R., Butterbach-Bahl, K., Flechard, C., Tuovinen, J. P., Coyle, M., Gerosa, G., Loubet, B., Altimir, N., Gruenhage, L., Ammann, C., Cieslik, S., Paoletti, E., Mikkelsen, T.N, Ro-Poulsen, H., Cellier, P., Cape, J. N., Horváth, L., Loreto, F., Niinemets, Ü., Palmer, P. I., Rinne, J., Misztal, P., Nemitz, E., Nilsson, D., Pryor, S., Gallagher, M. W., Vesala, T., Skiba, U., Brüggemann, N., Zechmeister-Boltenstern, S., Williams, J., O'Dowd, C., Facchini, M. C., de Leeuw, G., Flossman, A., Chaumerliac, N., and Erisman, J. W.: Atmospheric composition change: Ecosystems–Atmosphere interactions, Atmos. Environ., 43(33), 5193-5267, doi:10.1016/j.atmosenv.2009.07.068, 2009.

Hallsworth S., Dore A. J., Bealey W. J., Dragosits U., Vieno M., Hellsten S., Tang Y. S., and Sutton M. A.: The role of indicator choice in quantifying the threat of atmospheric ammonia to the 'Natura 2000' network. Env. Sci. Policy, 13, 671-687, doi:10.1016/j.envsci. 2010.09.010, 2010.

Hauschild, M. and Wenzel, H.: Acidification as a criterion in the environmental assessment of products in Environmental assessment of products. Volume 2 Scientific background (eds.) Hauschild, M. & Wenzel, H. London: Chapman & Hall, 1988.

Hellsten, S., Dragosits, U., Place, C. J., Misselbrook, T. H., Tang, Y. S., and Sutton, M. A.: Modelling Seasonal Dynamics from Temporal Variation in Agricultural Practices in the UK Ammonia Emission Inventory, WASP: Focus, 7, 3-13, doi:10.1007/s11267-006-9087-5, 2007.

Hendriks, C., Kranenburg, R., Kuenen, J., van Gijlswijk, Kruit, R. W., Segers, A., van der Gon, H. D., and Schaap, M.: The origin of ambient particulate matter concentrations in the Netherlands, Atmos. Environ., 69, 289-303, doi:10.1016/j.atmosenv.2012.12.017, 2013.

Huntzicker, J. J., Robert A. Cary, R. A., and Ling, C -S.: Neutralization of sulfuric acid aerosol by ammonia. Env. Sci. Technol., 14 (7), 819-824, doi:10.1021/ es60167a009, 1980.

Ianniello, A., Spataro, F., Esposito, G., Allegrini, I., Hu, M., and Zhu, T.: Chemical characteristics of inorganic ammonium salts in PM2.5 in the atmosphere of Beijing (China), Atmos. Chem. Phys., 11, 10803–10822, doi:10.5194/acp-11-10803-2011, 2011.

Jones, A. M. and Harrison, R. M.: Temporal trends in sulphate concentrations at European sites and relationships to sulphur dioxide, Atmos. Environ., 45, 873-882, doi:10.1016/j.atmosenv.2010.11.020, 2011.

Keene, W. C., Pszenny, A. A. P., Galloway, J. N., and Hawley, M. E.: Sea salt corrections and interpretation of constitutent ratios in marine precipitation. J. Geophys. Res. 91(D6), 6647-6658, doi:10.1029/JD091iD06p06647, 1986.

Keene, W. C., Aslam M., Khalil, K., Erickson D. J., McCulloch, A., Graedel, T. E., Lobert, J. M., Aucott, M. L., Gong, S. L., Harper, D. B., Kleiman, G., Midgley, P., Moore, R. M., Seuzaret, C., Sturges, W. T., Benkovitz, C. M., Koropalov, V., Barrie, L.A., and Li, Y. F.: Composite global emissions of reactive chlorine from anthropogenic and natural sources: Reactive Chlorine Emissions Inventory, J. Geophys. Res., 104 (D7), 8429– 8440, doi:10.1029/1998JD100084, 1999.

Lolkema, D. E., Noordijk, H., Stolk, A. P., Hoogerbrugge, R., van Zanten, M. C., and van Pul, W. A. J.: The Measuring Ammonia in Nature (MAN) network in the Netherlands, Biogeosciences, 12, 5133–5142, doi:10.5194/bg-12-5133-2015, 2015.

Maas, R. and Grennfelt, P. (eds), Towards cleaner air, Scientific Assessment Report 2016, EMEP Steering Body and Working Group on Effects of the Convention on Long-Range Transboundary Air Pollution, Oslo, 2016.

Massad, R. S., Nemitz, E., and Sutton, M. A.: Review and parameterisation of bi-directional ammonia exchange between vegetation and the atmosphere, Atmos. Chem. Phys., 10, 10359–10386, doi:10.5194/acp-10-10359-2010, 2010.

McCulloch, A., Aucott, M. L., Benkovitz, C. M., Graedel, T. E., Kleiman, G., Midgley, P. M., and Li, Y. F.: Global emissions of hydrogen chloride and chloromethane from coal combustion, incineration and industrial activities: Reactive Chlorine Emissions Inventory, J. Geophys. Res., 104(D7), 8391– 8403, doi:10.1029/ 1999JD900025, 1999.

Mihalopoulos, N., Kerminen, V. M., Kanakidou, M., Berresheim, H., and Sciare. J.: Formation of particulate sulfur species (sulfate and methanesulfonate) during summer over the Eastern Mediterranean: A modelling approach. Atmos. Environ., 41(32), 6860-6871, doi:10.1016/j.atmosenv.2007.04.039, 2007.

O'Dowd, C. D. and de Leeuw, G.: Marine aerosol production: a review of the current knowledge, Phil. Trans. R. Soc. A, 365, 1753-1774, doi: 10.1098/rsta.2007.2043, 2007.

Nemitz, E., Jimenez, J. L., Huffman, J.A., Ulbrich, I. M., Canagaratna, M. R., Worsnop, D. R., and Guenther, A. B.: An Eddy-Covariance System for the Measurement of Surface/Atmosphere Exchange Fluxes of Submicron Aerosol Chemical Species—First Application Above an Urban Area, Aerosol Sci. Technol., 42:8, 636-657, doi:10.1080/02786820802227352, 2008.

Paulot, F., Fan, S., and Horowitz. L. W.: Contrasting seasonal responses of sulfate aerosols to declining SO_2 emissions in the Eastern U.S.: Implications for the efficacy of SO_2 emission controls, Geophys. Res. Lett., 44, 455–464, doi:10.1002/2016GL070695, 2017.

Perrino, C., De Santis, F., and Febo, A.: Criteria for the choice of a denuder sampling technique devoted to the measurement of atmospheric nitrous and nitric acids, Atmos. Environ.. Part A. General Topics, 24, 617-626, doi:10.1016/0960-1686(90)90017-H, 1990.

Pitcairn, C. E. R., Leith, I. D., Sheppard, L. J., Sutton, M. A., Fowler, D., Munro, R. C., Tang, S., and Wilson, D.: The relationship between nitrogen deposition, species composition and foliar nitrogen concentrations in woodland flora in the vicinity of livestock farms, Environ. Poll., 102, 41-48, doi:10.1016/s0269-7491(98)80013-4, 1998.

Putaud, J. P., Van Dingenen, R., Alastuey, A., Bauer, H., Birmili, W., Cyrys, J., Flentje, H., Fuzzi, S., Gehrig, R., Hansson, H. C., Harrison, R. M., Herrmann, H., Hitzenberger, R., Hüglin, C., Jones, A. M., Kasper-Giebl, A., Kiss, G., Kousa, A., Kuhlbusch, T. A. J., Löschau, G., Maenhaut, W., Molnar, A., Moreno, T., Pekkanen, J., Perrino, C., Pitz, M., Puxbaum, H., Querol, X., Rodriguez, S., Salma, I., Schwarz, J., Smolik, J., Schneider, J., Spindler, G., ten Brink, H., Tursic, J., Viana, M., Wiedensohler, A., and Raes, F.: A European aerosol phenomenology III: Physical and chemical characteristics of particulate matter from 60 rural, urban, and kerbside sites across Europe, Atmos. Environ., 44(10), 1-13, doi:10.1016/j.atmosenv.2009.12.011, 2010.

Reis, S., Grennfelt, P., Klimont, Z., Amann, M., ApSimon, H., Hettelingh, J.-P., Holland, M., LeGall, A.-C., Maas, R., Posch, M., Spranger, T., Sutton, M. A., and Williams, M.: From acid rain to climate change, Science, 338, 1153–1154, doi:10.1126/science.1226514, 2012.

Ricciardelli, I., Bacco, D., Rinaldi, M., Bonafè, G., Scotto, F., Trentini, A., Bertacci, G., Ugolini, P., Zigola, C., Rovere, F., Maccone, C., Pironi, C., and Poluzzi, V.: A three-year investigation of daily PM2.5 main chemical components in four sites: the routine measurement program of the Supersito Project (Po Valley, Italy), Atmos. Environ., 152, 418-430, doi:10.1016/j.atmosenv.2016.12.052, 2017.

ROTAP: Review of Transboundary Air Pollution: Acidification, Eutrophication, Ground Level Ozone and Heavy Metals in the UK. Contract Report to the Department for Environment, Food and Rural Affairs. Centre for Ecology & Hydrology, http://www.rotap.ceh.ac.uk/, 2012.

Roth, B. and Okada, K.: On the modification of sea-salt particles in the coastal atmosphere, Atmos. Environ., 32(9), 1555-1569, doi:10.1016/S1352-2310(97)00378-6, 1998.

Saxena, P. and Seigneur, C.: On the oxidation of SO_2 to sulfate in atmospheric aerosols, Atmos. Environ. (1967), 21(4), 807-812, doi:10.1016/0004-6981(87)90077-1, 1987

Schaufler, G., Kitzler, B., Schindlbacher, A., Skiba, U., Sutton, M. A., and Zechmeister-Boltenstern, S.: Greenhouse gas emissions from European soils under different land use: effects of soil moisture and temperature, Eur. J. Soil Sci., doi:10.1111/j.1365-2389.2010.01277.x, 2010.

Schrader, F., Schaap, M., Zöll, U., Kranenburg, R., and Brümmer, C.: The hidden cost of using low resolution concentration data in the estimation of NH_3 dry deposition fluxes, Nature Sci. Reports, 8:969, doi:10.1038/s41598-017-18021-6, 2018

Schwarz, J., Cusack, M., Karban, J., Chalupníčková, E., Havránek, V., Smolík, J., and Ždímal, V.: $PM_{2.5}$ chemical composition at a rural background site in Central Europe, including correlation and air mass back trajectory analysis, Atmos. Res., 176–177, 108-120, doi:10.1016/j.atmosres.2016.02.017, 2016.

Sheppard, L. J., Leith, I. D., Mizunuma, T., Cape, J. N, Crossley, A., Leeson, S., Sutton, M. A., van, Dijk, N. and Fowler, D.: Dry deposition of ammonia gas drives species change faster than wet deposition of ammonium ions: evidence from a long-term field manipulation, Global Change Biol., 17, 3589-3607, doi:10.1111/j.1365-2486.2011.02478.x, 2011.

Sickles, J. E. and Shadwick, D. S.: Seasonal and regional air quality and atmospheric deposition in the eastern United States, J. Geophys. Res., 112, D17302, doi:10.1029/2006JD008356, 2007.

Sievering, H., Tomaszewski, T., and Torizzo, J.: Canopy uptake of atmospheric N deposition at a conifer forest: part I -canopy N budget, photosynthetic efficiency and net ecosystem exchange, Tellus B: Chem. Phys. Meteo., 59:3, 483-492, doi:10.1111/j.1600-0889.2007.00264.x, 2007.

Simpson, D., Butterbach-Bahl, K., Fagerli, H., Kesik, M., Skiba, U., and Tang, Y. Deposition and emissions of reactive nitrogen over European forests: A modelling study. Atmos. Environ., 40, 5712-5726, doi:10.1016/j.atmosenv.2006.04.063, 2006.

Skiba, U., Drewer, J., Tang, Y. S., van Dijk, N., Helfter, C., Nemitz, E., Famulari, D., Cape, J. N., Jones, S. K., Twigg, M., Pihlatie, M., Vesala, T., Larsen, K. S., Carter, M. S., Ambus, P., Ibrom, A., Beier, C., Hensen, A., Frumau, A., Erisman, J. W., Brűggemann, N., Gasche, R., Butterbach-Bahl, K., Neftel, A., Spirig, C., Horvath, L., Freibauer, A., Cellier, P., Laville, P., Loubet, B., Magliulo, E., Bertolini, T., Seufert, G., Andersson, M., Manca, G., Laurila, T., Aurela, M., Lohila, A., Zechmeister-Boltenstern, S., Kitzler, B., Schaufler, G., Siemens, J., Kindler, R., Flechard, C., and Sutton, M. A.: Biosphere-atmosphere exchange of reactive nitrogen and greenhouse gases at the NitroEurope core flux measurement sites: Measurement strategy and first data sets, Agric. Ecosys. Environ., 133 (3-4), 139–149, doi:10.1016/j.agee.2009.05.018, 2009.

Smith, R. I., Fowler, D., Sutton, M. A., Flechard, C., and Coyle, M.: Regional estimation of pollutant gas dry deposition in the UK: model description, sensitivity analyses and outputs, Atmos. Environ., 34, 3757-3777, doi:10.1016/s1352-2310(99)00517-8, 2000.

Stelson, A. W., and Seinfeld, J. H.: Relative humidity and temperature dependence of the ammonium nitrate dissociation constant, Atmos. Environ. (1967), 16, 983-992, doi:10.1016/0004-6981(82)90184-6, 1982.

Stevens, C. J., Thompson, K., Grime, J. P., Long, C. J., and Gowing, D. J. G.: Contribution of acidification and eutrophication to declines in species richness of

calcifuge grasslands along a gradient of atmospheric nitrogen deposition, Funct. Ecol., 24, 478-484, doi:10.1111/j.1365-2435.2009.01663.x, 2010

Sutton, M. A., Tang, Y. S., Miners, B., and Fowler, D.: A new diffusion denuder system for long-term, regional monitoring of atmospheric ammonia and ammonium, WASP: Focus 1: 145. doi:10.1023/A:1013138601753, 2001.

Sutton, M. A., Fowler, D., Burkhardt, J. K., and Milford, C.: Vegetation atmosphere exchange of ammonia: Canopy cycling and the impacts of elevated nitrogen inputs, WASP, 85, 2057-2063, doi:10.1007/bf01186137, 1995.

Sutton, M. A., Milford, C., Dragosits, U., Place, C. J., Singles, R. J., Smith, R. I., Pitcairn, C. E. R., Fowler, D., Hill, J., ApSimon, H. M., Ross, C., Hill, R., Jarvis, S. C., Pain, B F., Phillips, V. C., Harrison, R., Moss, D., Webb, J., Espenhahn, S. E., Lee, D. S., Hornung, M., Ullyett, J., Bull, K. R., Emmett, B. A., Lowe, J., and Wyers, G. P.: Dispersion, deposition and impacts of atmospheric ammonia: quantifying local budgets and spatial variability, Environ. Poll., 102, 349-361, doi:10.1016/s0269-7491(98)80054-7, 1998.

Sutton, M. A., Nemitz, E., Erisman, J. W., Beier, C., Bahl, K. B., Cellier, P., de Vries, W., Cotrufo, F., Skiba, U., Di Marco, C., Jones, S., Laville, P., Soussana, J. F., Loubet, B., Twigg, M., Famulari, D., Whitehead, J., Gallagher, M. W., Neftel, A., Flechard, C. R., Herrmann, B., Calanca, P. L., Schjoerring, J.K., Daemmgen, U., Horvath, L., Tang, Y. S., Emmett, B. A., Tietema, A., Penuelas, J., Kesik, M., Brueggemann, N., Pilegaard, K., Vesala, T., Campbell, C. L., Olesen, J. E., Dragosits, U., Theobald, M. R., Levy, P., Mobbs, D. C., Milne, R., Viovy, N., Vuichard, N., Smith, J. U., Smith, P., Bergamaschi, P., Fowler, D. and Reis, S.: Challenges in quantifying biosphere-atmosphere exchange of nitrogen species, Environ. Poll., 150, 125-139, doi:10.1016/j.envpol.2007.04.014, 2007.

Sutton, M. A., Reis, S., Riddick, S. N., Dragosits, U., Nemitz, E., Theobald, M. R., Tang, Y. S., Braban, C. F.. Vieno, M., Dore, A. J., Mitchell, R. F., Wanless, S., Daunt, F., Fowler, D., Blackall, T. D., Milford, C., Flechard, C. R., Loubet, B., Massad, R., Cellier, P., Personne, E., Coheur, P., Clarisse, L., Van Damme, M., Ngadi, Y., Clerbaux, C., Skjoth, C., Geels, C., Hertel, O., Kruit, R. J. W., Pinder, R. W., Bash, J. O., Walker, J. T., Simpson, D., Horvath, L., Misselbrook, T. H., Bleeker, A., Dentener, F., and de Vries, W.: Towards a climate-dependent paradigm of ammonia emission and deposition [in special issue: The global nitrogen cycle in the twenty-first century] Phil. Trans. Royal Soc., (B), 368 (1621), 20130166. 13 pp, doi:10.1098/rstb.2013.0166, 2013.

Sutton, M. A., and Howard, C.: Satellite pinpoints ammonia sources globally, Nature, 564, 49-50, doi: 10.1038/d41586-018-07584-7, 2018.

Szigeti, T., Mihucz, V. G., Óvári, M., Baysal, A., Atılgan, S., Akman, S., and Záray, G.: Chemical characterization of PM2.5 fractions of urban aerosol collected in Budapest and Istanbul, Microchem. J., 107, 86-94, doi:10.1016/j.microc. 2012.05.029, 2013.

Szigeti, T., Óvári, M., Dunster, C., Kelly, F.J., Lucarelli, F., and Záray, G.: Changes in chemical composition and oxidative potential of urban PM2.5 between 2010 and 2013 in Hungary, Sci. Total Environ., 518–519, 534-544, doi:10.1016/j.scitotenv.2015.03.025, 2015.

Tang, Y. S., Cape, J. N., and Sutton, M. A.: Development and types of passive samplers for monitoring atmospheric NO_2 and NH_3 concentrations, ScientificWorldJournal, 1, 513-529, doi:10.1100/tsw.2001.82, 2001.

Tang, Y. S., and Sutton, M. A.: Quality management in the UK national ammonia monitoring network. In: Proceedings of the International Conference: QA/QC in the field of emission and air quality measurements: harmonization, standardization and accreditation, held in Prague, 21-23 May 2003 (eds. Borowiak A., Hafkenscheid T., Saunders A. and Woods P.). European Commission, Ispra, Italy, 297-307, 2003.

Tang, Y. S., Simmons, I., van Dijk, N., Di Marco, C., Nemitz, E., Dämmgen, U., Gilke, K., Djuricic, V., Vidic, S., Gliha, Z., Borovecki, D., Mitosinkova, M., Hanssen, J. E., Uggerud, T, H., Sanz, M. J., Sanz, P., Chorda, J. V., Flechard, C. R., Fauvel, Y., Ferm, M., Perrino, C., and Sutton, M. A.: European scale application of atmospheric reactive nitrogen measurements in a low-cost approach to infer dry deposition fluxes, Agric. Ecosys. Environ., 133, 183–195, doi:10.1016/j.agee.2009.04.027, 2009.

Tang, Y. S., Cape, J. N., Braban, C. F., Twigg, M. M., Poskitt, J., Jones, M. R., Rowland, P., Bentley, P., Hockenhull, K., Woods, C., Leaver, D., Simmons, I., van Dijk, N., Nemitz, E., and Sutton, M. A.: Development of a new model DELTA sampler and assessment of potential sampling artefacts in the UKEAP AGANet DELTA system: summary and technical report. London, Defra. (CEH Project no. C04544, C04845), https://uk-air.defra.gov.uk/library/reports?report_id=861, 2015.

Tang, Y. S., Braban, C. F., Dragosits, U., Dore, A. J., Simmons, I., van Dijk, N., Poskitt, J., Pereira, M. G., Keenan, P. O., Conolly, C., Vincent, K., Smith, R. I., Heal, M. R., and Sutton, M. A.: Drivers for spatial, temporal and long-term trends in atmospheric ammonia and ammonium in the UK, Atmos. Chem. Phys., 18, 705-733, doi:10.5194/acp-18-705-2018, 2018a.

Tang, Y. S., Braban, C. F., Dragosits, U., Simmons, I., Leaver, D., van Dijk, N., Poskitt, J., Thacker, S., Patel, M., Carter, H., Pereira, M. G., Keenan, P. O., Lawlor, A., Connolly, C., Vincent, K., Heal, M. R. and Sutton, M. A.: Acid gases and aerosol measurements in the UK (1999–2015): regional distributions and trends, Atmos. Chem. Phys., 18, 16293-16324, doi:10.5194/acp-18-16293-2018, 2018b.

Theobald, M. R., Milford, C., Hargreaves, K. J., Sheppard, L. J., Nemitz, E., Tang, Y. S., Phillips, V. R., Sneath, R., McCartney, L., Harvey, F. J., Leith, I. D., Cape, J. N., Fowler, D., and Sutton, M. A.: Potential for Ammonia Recapture by Farm Woodlands: Design and Application of a New Experimental Facility, ScientificWorldJournal, 1, Article ID 956452, doi:10.1100/tsw.2001.338, 2001.

Tørseth, K., Aas, W., Breivik, K., Fjæraa, A. M., Fiebig, M., Hjellbrekke, A. G., Lund Myhre, C., Solberg, S., and Yttri, K. E.: Introduction to the European Monitoring and Evaluation Programme (EMEP) and observed atmospheric composition change during 1972-2009, Atmos. Chem. Phys., 12, 5447-5481, doi:10.5194/acp-12-5447-2012, 2012.

UNECE: 1999 Protocol to Abate Acidification, Eutrophication and Ground-level Ozone to the Convention on Long range Transboundary Air Pollution, as amended on 4 May 2012, 2012.

van Zanten, M. C., Wichink Kruit, R. J., Hoogerbrugge, R., Van der Swaluw, E., and van Pul, W. A. J.: Trends in ammonia measurements in the Netherlands over the

period 1993–2014, Atmos. Environ., 148, 352-360, doi:10.1016/ j.atmosenv. 2016.11.007, 2017.

Vieno, M., Heal, M. R., Hallsworth, S., Famulari, D., Doherty, R. M., Dore, A. J., Tang, Y. S., Braban, C. F., Leaver, D., Sutton, M. A., and Reis, S.: The role of long-range transport and domestic emissions in determining atmospheric secondary inorganic particle concentrations across the UK, Atmos. Chem. Phys., 14, 8435-8447, doi:/10.5194/acp-14-8435-2014, 2014.

Vieno, M., Heal, M. R., Williams, M. L., Carnell, E. J., Stedman, J. R. and Reis, S.: Sensitivities of UK $PM_{2.5}$ concentrations to emissions reductions, Atmos. Chem. Phys., 16, 265–276, doi:10.5194/acp-16-265-2016, 2016a.

Vieno, M., Heal, M. R., Twigg, M. M., MacKenzie, I. A., Braban, C. F., Lingard, J. N. N., Ritchie, S., Beck, R. C., Móring, A., Ots, R., Di Marco, C. F., Nemitz, E., Sutton, M. A., and Reis S.: The UK particulate matter air pollution episode of March–April 2014: more than Saharan dust. Env. Res. Lett., 11, 044004, doi:10.1088/1748-9326/11/4/044004, 2016b.

Zaehle, S. and Dalmonech, D.: Carbon–nitrogen interactions on land at global scales: current understanding in modelling climate biosphere feedbacks, Current Opinion in Environmental Sustainability, 3(5), 311-320, doi:10.1016/j.cosust.2011.08.008, 2011.

Chapter 5 Conclusions and future work

Simple, low-cost, low-time-resolution air sampling methods (ALPHA® and DELTA®) have been developed, suitable for monitoring ambient concentrations of NH_3, acid gases and aerosols. The low-cost of these methods made it possible to deploy large numbers of them for measurement, while the simplicity of deployment allowed a network to be operated with the support of locally-based site operators to perform monthly changeover of samples. This permitted the application of standardised methods and quality protocols at multiple sites in cost-efficient monitoring strategies, designed to measure temporal, spatial and long-term trends in the respective air pollutants.

The application of the ALPHA® and DELTA® methods provided quality assured, concurrent data of the gas and aerosol phase pollutants in two integrated long-term UK national networks (Chapters 2 and 3) and a pan-European project (Chapter 4) for the first time. These measurements have also contributed to increasing the availability of long-term observational data made with comparable protocols that are relevant for air quality and climate research on the regional to international scales. This chapter presents a summary of the monitoring and assessment, with a discussion on policy implications from the measurement data and recommendations for future research to address questions raised and identified by the work carried out in the thesis.

5.1 ALPHA® passive NH_3 gas sampling method

The ALPHA® sampler (Sect. 1.4.1.1) is a high sensitivity passive sampler (LOD = 0.03 µg NH_3 m^{-3} for monthly monitoring) developed for monitoring ambient concentrations of atmospheric NH_3. Its development was motivated by the need for a passive sampler with the required sensitivity to measure across the

range of ambient concentrations of NH_3 expected across the UK, from very low concentrations at clean background sites (< 0.1 µg NH_3 m^{-3}), to more polluted sites in source regions (> 10 µg NH_3 m^{-3}). The ALPHA® method replaced the less sensitive Gradko membrane diffusion tubes (LOD = 1 - 2 µg NH_3 m^{-3} for monthly monitoring) early on in the UK NAMN (Chapter 2). In a recent inter-comparison exercise, the ALPHA® sampler outperformed other types of NH_3 passive samplers (Martin et al., 2019). The ALPHA® approach is widely used, with applications ranging from site-based effects assessment (e.g. Sheppard et al., 2011), landscape studies (e.g. Vogt et al., 2013), and in estimating emissions from sources (e.g. Bell et al., 2018; Riddick et al., 2018; Loubet et al., 2018).

5.2 DELTA® active gas and aerosol sampling method

The DELTA® system (Sect. 1.4.1.4) was developed for monthly measurement of NH_3 in the UK NAMN, and then extended to also measure particulate NH_4^+ (Chapter 2). In recognising the need to measure interacting pollutants, the method was further extended to provide additional sampling of acid gases and aerosols in the UK AGANet (Chapter 3) and the NitroEurope network (Chapter 4). Since this method requires power to run the small air pumps, deployment are necessarily restricted to sites with access to power, or where a wind-solar powered system can be set up safely. The DELTA® also served as a reference method to calibrate the ALPHA® sampler uptake rate. Like the ALPHA®, the DELTA® was designed with simplicity of use in mind. Specialist training is not required and the monthly exchange of samples is also carried out with a network of local site operators, some of whom are interested members of the public, keen to take part in the monitoring project.

5.3 Application of ALPHA® and DELTA® approach in monitoring NH_3 and NH_4^+ in the UK NAMN

The implementation of the DELTA® approach to measure NH_3 and NH_4^+, complemented by ALPHA® monitoring sites allowed high density monitoring for NH_3, which in particular is of high spatial variability. A long-term dataset of monthly atmospheric NH_3 gas (1998-2014, > 70 sites) and monthly particulate NH_4^+ (1999-2014, > 23 sites) was collected and used to assess spatial, seasonal and long-term variability in concentrations across the UK.

Spatial: The high spatial coverage allowed assessment of NH_3 and NH_4^+ concentrations at regional to national scales and (FRAME) model verification, in support of the UK government's "evidence-based" policy. Data showed widespread exceedance of the UNECE Critical Levels of NH_3 concentrations across the UK.

Temporal: Drivers for seasonality included variations in emission sources, climate and long-range transboundary sources. Distinct seasonal profiles were established for different dominant emission source sectors (e.g. background, sheep, cattle, pigs & poultry). This information is important for developing strategies for emissions abatement and model development / verification.

Long-term trends: Trends in NH_3 varied between sites grouped according to dominant emission source sectors. For example, a significant decreasing trend was observed at sites classed as dominated by emissions from pigs and poultry, contrasting with an upward, but non-significant trend for sites in cattle emission areas. This is important for examining responses to changing agricultural practice and allowing assessment of the compliance of NH_3 emissions with targets established by international policies on emissions abatement. Particulate NH_4^+showed larger reductions over time than NH_3. The findings are consistent with a change in partitioning from particulate NH_4^+ to gaseous NH_3, such that more of the NH_3 emitted is staying in the gas phase, with associated implications for the role of NH_3 as a precursor to PM formation and increased risk to sensitive habitats.

As emissions of SO_2 and NO_x continues to fall, NH_3 emissions in the UK have instead been rising since 2013. Emissions of NH_3 in 2017 had increased by 9.6 %, back to to the emission of 2005 (283 kt yr^{-1} NH_3). The agricultural sector remains the biggest contributor to NH_3 pollution, accounting for 87 % of all UK NH_3 emissions in 2017. Under the revised Gothenburg Protocol and NECD, the UK is required to reduce NH_3 emissions by 8 % compared with 2005 emissions by 2020. With the current trend, intervention may be necessary for the UK to meet its target. The need to abate NH_3 in farming was acknowledged for the first time in the UK Government's 25 year environment plan, published in January 2018 (Defra, 2018). In parallel, a national code of good agricultural practice (COGAP) was drawn up in the Clean Air Strategy (Defra, 2019) which makes recommendations for reducing NH_3 emissions from farming by requiring adoption of low emissions farming techniques. Continuation of the present monitoring of NH_3 and NH_4^+ in the UK NAMN will be key to providing the evidence for detecting any changes in concentrations and in supporting development of effective mitigation measures.

5.4 Extension of DELTA approach to measure NH_3, acid gases and aerosols in two integrated UK networks

The close integration between the UK NAMN and UK AGANet demonstrated the versatility and cost-effectiveness of the DELTA® system. Implementation of the DELTA® method provided the simultaneous determination of NH_3/NH_4^+ for the NAMN and acidic gases/aerosols, including base cations for the UK AGANet. Data on HNO_3 and HCl was provided for the first time, representing a big step forward in addressing the lack of previous data.

Spatial: The AGANet delivered for the first time a comprehensive dataset for the acid gases HNO_3 and particulate NO_3^- concentrations, which was used to estimate the contribution of these species to the N budget in the UK. Atmopsheric data on HCl and Cl^- were also provided for the first time. This is

important, since HCl, like SO_2, contributes to input of excess acidity to sensitive habitats (Evans et al., 2011). At the same time, the concurrent measurements of SO_2 gas and particulate SO_4^{2-} are used to map S deposition and effects. Sulfur measurements by AGANet replaced measurements of these components that were made under previous UK rural SO_2 monitoring programmes (Hayman et al., 2007), providing cost-efficiency savings for UK air monitoring efforts.

Temporal: Distinctive temporal trends were established for the different components, with seasonality in the gases and aerosols influenced by local to regional emissions, photochemistry, meteorology and gas:aerosol phase equilibrium. This information is important in the development of regional models for the treatment of seasonality.

Long-term trends: Changes in UK chemical climate were captured, consistent with emission trends in the different gases (NH_3, SO_2, NO_x, HCl). A decrease in SO_2/SO_4^{2-} ratio over time was attributed to increased deposition of SO_2, due to the substantial decline in SO_2 emissions, similar to that reported across Europe. With the substantial decline in SO_2 and SO_4^{2-}, the data provide evidence of a shift in relative abundance in the particulate phase from $(NH_4)_2SO_4$ to NH_4NO_3, with indications that atmospheric lifetime of HNO_3 and NH_3 has increased.

Contribution from long-range transport: Pollutant episodes captured by the AGANet shows import of NH_4NO_3 and $(NH_4)_2SO_4$ into the UK from long-range transboundary transport, and the importance of this source in the UK N and S budgets.

Atmospheric concentrations of NH_3 and NH_4NO_3 exceeded SO_2 and $(NH_4)_2SO_4$ in the gas and aerosol phase at the rural monitoring sites in the networks. The current and projected trends in the emissions of the gases SO_2, NO_x and NH_3 suggests that NH_3 and NH_4NO_3 can be expected to continue to

dominate the inorganic pollution load in the UK, if substantial reductions in NH_3 emissions and, in particular, from the agricultural sector are not achieved. Continuation of the integrated monitoring of NH_3 and the interacting acid gases and particles in the UK NAMN and AGANet provides underpinning data for monitoring and understanding any changes in concentrations of the different chemical forms of the pollutants and in the different fractions of the total sulfur or nitrogen input to receptors.

Data from the AGANet supports visions laid out in the UK Government's 25 Year Plan to improve the Environment (Defra, 2018) and in the new Clean Air Strategy (Defra, 2019). The data are used in the Department for Environment, Food and Rural Affairs (Defra) national Pollution Climate Mapping (PCM) models to produce background pollution maps at 1 x 1 km resolution each year (https://uk-air.defra.gov.uk/data/pcm-data). These maps feed into air quality assessments, reported to the European Commission in accordance with European Directives (e.g. reporting of SO_2, NO_x and $PM_{2.5}$ / PM_{10}; EU Directive (2008/50/EC) and also to OSPAR (OSlo Convention 1972 & PARis Convention 1974; EC, 1992), to address all sources of pollution which might affect the quality of the North East Atlantic. The integrated dataset also provides a baseline against which any changes and potential recovery in ecosystem response to emissions reductions under the NECD (2016/2284) may be assessed, as required under Article 9 of the NECD (EU, 2016).

5.5 Application of UK DELTA® monitoring approach to European scale

The DELTA® approach and strategy established in the UK networks was extended to a pan-European network. By sharing the method and protocol with several European laboratories, and piggy-backing onto established infrastructure (CarboEurope network + EMEP field sites), it has proven possible to establish a large-scale network within a relatively short time-scale and with low costs. Key elements were a standard, harmonised methodology

and the implementation of quality protocols that included regular laboratory inter-comparisons, allowing comparability between laboratories to be made.

This activity has contributed to an increase in the availability of speciated data for research and for evaluation of regional models. The dominance of NH_3 in the gas phase and the shift from $(NH_4)_2SO_4$ to an atmosphere rich in NH_4NO_3 was demonstrated across Europe. This has highlighted the importance of monitoring the contribution of NH_3 to the exceedance of critical levels (concentrations) and critical loads (deposition) for nitrogen. By measuring the acid gases and related aerosols, information about the chemical climate and partitioning between the gas and aerosol phase was captured, which allowed an assessment of the interactions between the component phases.

From the extensive measurements in the UK and across Europe, it is clear that high levels of NH_3 pollution remain an ongoing concern. At the same time, the shift to larger concentrations of the semi-volatile NH_4NO_3 than the stable $(NH_4)_2SO_4$ have the potential to maintain a larger fraction of the pollutants in the gas phase by the re-volatilisation of NH_4NO_3 in warm weather. This has the effect of potentially extending the lifetime, and geographical footprint of the impacts from NH_3 and HNO_3. Indications from the current and projected trends in the emissions of the gases SO_2, NO_x and NH_3, are that NH_3 and NH_4NO_3 will continue to dominate the inorganic pollution load over the next decades, contributing to ecosystem effects through acid and N deposition and to harmful effects on human health in the formation of fine PM.

Although the DELTA® approach is included in the EMEP Level 1 measurement strategy in the EMEP manual (EMEP, 2014), it has to date not been implemented across its networks. There is therefore a need for a monitoring network with sufficient coverage across Europe that provides long-term speciated data, to contribute to model validation and to address uncertainties in deposition modelling, in particular of N species (EMEP, 2019). A target of > 125 sites (at a minimum site density of 1 site per 50,000 km^2) had been suggested by Torseth and Hov (2003) as a reasonable number of sites to map

the concentration fields across Europe. The EMEP daily filter-pack network continues to provide a large set of total nitrate and ammonium data, but which are not very helpful for understanding changes in the gas and aerosol phase N. Since the daily filter-pack approach is resource intensive and does not deliver required speciation, it would be better to redirect the measurement effort using a DELTA® approach. As demonstrated by the NEU network, it is possible to coordinate a network of that size across Europe with the participation of multiple laboratories, as is currently done with the daily filter-pack network.

The Clean Air Programme for Europe sets targets of a 35 % reduction of the ecosystem area subjected to eutrophication by 2030, compared with 2005, and also targets for reduction of health impact across Europe. An implementation of the DELTA® approach across Europe would provide cost-efficient monitoring of the gas and aerosol phase pollutants for which reduction commitments are set out in Annex II to the NECD (SO_2, NO_x, NH_3 and $PM_{2.5}$). There is currently a lack of NH_3 and speciated monitoring of the aerosol composition across the EU. Monitoring of NH_3 and the interacting acid gases and aerosols are needed to assess contributions of NH_3 to $PM_{2.5}$ and also to provide a baseline against which any changes and potential recovery in ecosystem response to changes in emissions (see next Sect. 5.6).

5.6 Linking air pollution to negative impacts on ecosystems and human health

The critical levels and critical loads approach are policy tools that are widely adopted to assess the risk of change to ecosystems resulting from air pollution impacts (Hall et al., 2018; Hallsworth et al., 2010). Ammonia data from UK NAMN are used with the Fine Resolution Atmospheric Multi-pollutant Exchange (FRAME) model (Singles et al., 1998) for calculating NH_3 concentrations in the UK at 5 km and 1 km resolution, used to assess critical level exceedance (Hall et al., 2018).

Measurement data on the inorganic gases (NH_3, HNO_3, SO_2) and aerosols (NH_4^+, NO_3^-, SO_4^{2-}) from the UK NAMN and AGANet national networks, combined with NO_2 and wet deposition data (from other UK networks) are used to produce maps of acidity and pollutant (N and S) deposition across the UK at a 5 km grid resolution. The maps are then compared with critical loads mapped over the estimated main distribution of different habitat types at a 1 km grid resolution to calculate critical loads exceedance (Hall et al., 2018; ROTAP, 2012). This is a key element in assessing UK habitats that are at risk from acidification and eutrophication, used to assess the conservation status at protected sites (SSSIs, SACs, SPAs, RAMSAR sites), required under the EU Habitats Directive (1992).

The revised NECD also requires Member States to monitor (Article 9) and report (Article 10.4) the negative impacts of air pollution (acidifying and eutrophying pollutants, ozone) on ecosystems from national networks that are representative of the Member State's freshwater, natural and semi-natural habitats and forest ecosystem types. Since NH_3 is also a precursor to the formation of PM (NH_4NO_3 and $(NH_4)_2SO_4$), the two UK networks are identified as providing the air quality evidence for contributing to the UK assessment.

5.7 Evidence for assessing effectiveness of current and future abatement policies

The growing relative importance of NH_3 and NH_4^+ to total acidic and total N deposition indicates that strategies to tackle acidification and eutrophication need to include measures to abate emissions of NH_3. Under the 2012 UNECE Gothenburg protocol, EU member states must jointly cut their emissions of NH_3 by 6 % between 2005 and 2020. As a precursor to PM, controlling NH_3 is also important to reducing particle concentrations of $PM_{2.5}$ and PM_{10}.

In recognising the need to reduce NH_3 emissions, in particular from the agricultural sector, which accounts for around 90% of emissions across

Europe, a guidance document and code of good agricultural practice for reducing NH_3 emissions was published by the UNECE (Bittman et al., 2014), which has also been adopted in the EC NECD. In parallel, the UK government also produced its first comprehensive clean air strategy with guidance and support for farmers to invest in infrastructure and equipment (e.g. low emission spreading and reducing urea fertiliser use) required to reduce emissions (Defra, 2019).

The control of NH_3 emissions is not straightforward. This is because NH_3 emissions are from diffuse sources over large areas, occurring mainly from ground level. The amount of NH_3 emitted is also influenced by environmental factors such as wind speed and temperature and different options are therefore needed to control emissions.

Long-term data from the networks are necessary, particularly with regards to changes in agricultural practices and abatement measures, and for testing atmospheric transport models. The seasonal patterns of NH_3 concentrations, shown in detail for the first time in this work, provide important insights into both the relationship to occurrence of emissions and possible abatement measures to target peak emission periods.

5.8 Future research

The research presented in this thesis has identified several topics for further considetation, in order to develop and extend the applications of the monitoring approaches reported.

5.8.1 Specificity of HNO_3 measurement on DELTA®

The K_2CO_3-glycerol coated denuders used in the DELTA® method have significant interferences in the determination of HNO_3 from oxidised N species that are also captured on the denuders as nitrate. The denuder configuration was subsequently changed from 2 x K_2CO_3-glycerol (2 denuders) to 2 x NaCl – K_2CO_3-glycerol (3 denuders) in series (Tang et al., 2015; Conolly et al., 2018). Of the many potential interfering species, HONO is thought to be the most likely, since HONO, like HNO_3, is captured with high efficiency on a carbonate coating. Oxidised N speciation therefore remains an important area for further research to understand which species are being captured on the denuders to allow optimisation of the denuder coating. Increasingly, research efforts are focussing on measuring HONO, but challenges remain in measuring HONO. It is therefore of interest and importance to also be able to measure HNO_3 and HONO at the same time, which will allow the contribution of HONO to the N budget to be quantified.

5.8.2 Development and validation of ALPHA® and DELTA® approach for different climates

A major new South Asian Nitrogen Hub (SANH) with a focus on N and sustainable development was formed in 2019, supported by the Global Challenges Research Fund (GCRF; https://gtr.ukri.org/projects?ref=NE%2FS009019%2F1). South Asia is a key global region for N pollution, linked to growing economies and increasing consumption of meat and dairy with associated rise in nitrogen-related problems. To improve measurement capabilities and data in South Asia, further work on the development and validation for the ALPHA® and DELTA® approach will be conducted to extend

application of the methods in different parts of the world under different climatic conditions. Key challenges are in optimising chemical coatings suitable for different climatic conditions and deriving uptake rates for the ALPHA® for those conditions.

5.8.3 Miniaturisation of DELTA® system

With technological advances and the need for novel deployment locations and off-grid measurements, the development of a next generation miniaturised DELTA® system (DELTA-Mi) with low unit costs will help expand the range of locations and applications of the DELTA®. There is also potential to extend the range of pollutants measured, by considering emerging pollutants that can be measured by the selective use of different chemical coating and denuder-filter pack sampling train configurations.

Miniaturisation – DELTA-Mi system:

Some investigative work was carried out into options to develop a miniaturised system, DELTA-Mi (Tang et al., 2018). The key requirements are that the new system should be compact, light-weight, low-voltage/low power-consumption and low-cost (< £2k) to maximise flexibility in deployment options and affordability.

A Mini-ANnular DEnuder (MANDE; 5 cm long) has been developed (Solera et al., 2017; Tang et al., 2018) that are amenable for developing much more compact sampling trains than using simple glass denuders (10 cm + 15 cm long in current DELTA® system). This will reduce costs of postal exchange between site and laboratory compared with the current sampling trains used in AGANet.

Further tests and validation of MANDE sampling trains in gas and aerosol measurements are however needed, e.g. intercomparisons *vs* conventional DELTA® sampling train. In the MANDE, the inner glass tube is attached to the outer glass tube with glass contacts at one end, which is necessary to fix the

tubes in place. The glass contacts can potentially capture aerosol species and tests are needed to check if this is an issue.

DELTA-Mi + air flow sensing

The current DELTA® system uses a diaphragm gas meter to record volume of air sampled. While the gas meter is low-cost (< £100) and robust, it is large and heavy and the gas meter readings has to be read and recorded by someone visiting the site. Replacement of the gas meter with a wireless flowmeter would allow miniaturisation of the DELTA® system. Establishment of flow sensing capabilities for the DELTA® air monitoring sites would also allow remote monitoring / linking of flow rates and metered volumes to a central database. Such a system can potentially minimise data loss and equipment down-time by online monitoring, so that site service visits can be arranged promptly. Sourcing a suitable wireless flowmeter with telemetry that is light-weight, low power-consumption and low-cost for incorporation into a DELTA-Mi sensor network has, however, proved to be particularly challenging. Off-the-shelf air-flow sensors of the sensitivity required for monitoring low flow rates are not yet available on the market, but may become available in the future.

5.8.4 Local assessment of NH_3 impacts on ecosystems

The primary focus of UK NAMN is providing ambient concentrations that are regionally representative. Numerous studies have shown that N deposition in the vicinity of NH_3 sources are dominated by dry NH_3-N deposition (e.g. Pitcairn et al., 1998; Sheppard et al., 2011). Where a sensitive receptor is in close proximity to a source (within 1 km), the concentration that the site is exposed to is likely to be higher.

While the N deposition maps are useful for critical loads assessment at a regional to national level, the resolution is not sufficient for assessment at a local level. This particularly applies to impacts assessment of NH_3, since this shows very high spatial variability and deposition at a local scale. Dry

deposition of NH_3 is generally largest in the high emission areas, where NH_3 concentrations are also greatest, and intensively fertilized areas may in fact act as a net source for NH_3 rather than a sink. Therefore, deposition will mainly occur to nearby unfertilised land with a small N content, and the amount of deposited N increases substantially close to the source. Semi-natural ecosystems and conservation areas (which are of low N status) near emission source are therefore particularly at risk. Also, while the centre of a large reserve may be less at risk than the overall national assessments suggests, smaller reserves and the edges of large reserves are much more at risk.

Monitoring efforts should therefore focus on quantifying the on-site NH_3 concentrations and site-specific contribution by NH_3-N dry deposition to the total N deposition to the sensitive receptor. N deposition from other reactive nitrogen species in the atmosphere that include dry deposited N from HNO_3, NO_2 and NH_4^+, and wet deposited N from NH_4^+ and NO_3^-, can be derived from national deposition maps that provide N deposition information at a 5 km grid level (ROTAP, 2012).

5.8.5 Low-cost NH_3 gas sensors

There is increasing interest and technological advances in (miniaturised) gas sensors for air monitoring, from environmental to medical applications. In particular, numerous sensors have come onto the market in recent years for monitoring NO_2 for air quality compliance assessment in cities. Of these, the AQMesh NO_2 gas sensor (https://www.aqmesh.com/) is widely deployed across the UK and US, although there remains large uncertainties regarding the quality of the measurements due to the lack of validation data.

Sensitive optical instruments for online monitoring of NH_3 are too large to be portable, and too expensive to be deployed at many sites. The ALPHA® and DELTA® are time-integrated air sampling methods requiring offline analysis. These types of manual air samplers can only provide time-integrated average concentrations over a prescribed sampling period (usually weekly to monthly).

Since chemical analyses are performed after sample collection, there is also an additional delay before air concentration data is finally available.

There are a small number of NH_3 sensors currently available on the market that measures in the ppm range for industrial measurements (e.g. leak detection in refrigeration systems), but not for air quality monitoring (low ppb levels). These include the Alphasense NH_3-A1 and NH_3-B1, and Industrial Scientific's personal single-gas detector GasBadge® Pro, Ventis™ Pro Series, and the MX6 iBrid, Radius™ BZ1 Area ammonia detectors (Tang et al., 2019).

A number of reviews on NH_3 sensors have been published (Kwak et al., 2019; Timmer et al., 2005; Yunusa et al., 2014), as well as numerous research papers on NH_3 sensor development work, although no-one has to date achieved detection better than ppm levels. A semiconductor type chemi-resistor sensor, based on conducting polymers as the sensing platform would meet the criteria for high specificity to NH_3 gas, high sensitivity (ppb detection limits for ambient air monitoring) and low-cost fabrication. Of the range of conducting polymers (e.g. polypyrrole, polyaniline), nanomolecules (e.g. graphene derivatives) or cellulose described in the literature, fluorographene (FG) (Tadi et al., 2014) look promising and research work is currently being conducted on FG sensor chips (Tang et al., 2019).

The 'holy grail' is for a miniaturised NH_3 gas sensor that is sensitive (measures down to low ppb levels) and selective (not subject to cross-interference from other gases and humidity). An NH_3 sensor with a similar level of selectivity, sensitivity and accuracy as the ALPHA® and DELTA® approaches will have the potential for deployment in a sensor network.

References

Bell, M. W., Tang, Y. S., Dragosits, U., Flechard, C. R., Ward, P., and Braban, C. F.: Ammonia emissions from an anaerobic digestion plant estimated using atmospheric measurements and dispersion modelling, Waste Management, 56, 113-124, doi:10.1016/j.wasman.2016.06.002,2, 2016.

Bittman, S., Dedina, M., Howard C. M., Oenema, O., and Sutton, M. A., (eds): Options for Ammonia Mitigation: Guidance from the UNECE Task Force on Reactive Nitrogen, Centre for Ecology and Hydrology, Edinburgh, UK, 2014.

Bobbink, R. and Hettelingh, J. P. (eds) Review and revision of empirical critical loads and dose response relationships. Coordination Centre for Effects, National Institute for Public Health and the Environment (RIVM). http://wge-cce.org, 2011.

Conolly, C., Davies, M., Knight, D., Vincent, K., Sanocka, A., Lingard, J., Richie, S., Donovan, B., Collings, A., Braban, C., Tang, Y. S., Stephens, A., Twigg, M., Jones, M., Simmons, I., Coyle, C., Kentisbeer, J., Leeson, S., van Dijk, N., Nemitz, E., Langford, B., Bealey, W., Leaver, D., Poskitt, J., Carter, H., Thacker, S., Patel, M., Keenan, P., Pereira, G., Lawlor, A., Warwick, A., Farrand, P. and Sutton, M. A.: UK Eutrophying and Acidifying Atmospheric Pollutants (UKEAP) Annual Report 2015, 2016.

Defra: A Green Future: Our 25 Year Plan to Improve the environment. www.gov.uk/government/publications, Published 11 January 2018, 2018.

Defra: Clean Air Strategy 2019, https://www.gov.uk/government/publications/ clean-air-strategy-2019, Published 14 January 2019, 2019.

EC: Habitats Directive, Council Directive 92/43/EEC of 21 May 1992 on the conservation of natural habitats and of wild fauna and flora, 1992.

EC: The OSPAR Convention (1992) for the Protection of the marine Environment of the North-East Atlantic, https://ec.europa.eu/environment/marine/international-cooperation/regional-sea-conventions/ospar/index_en.htm, 1992.

EMEP: EMEP Manual for Sampling and Analysis. Revised February 2014, www.nilu.no/projects/ccc/manual/, 2014.

EU: Directive (EU) 2016/2284 of the European Parliament and of the Council of 14 December 2016 on the reduction of national emissions of certain atmospheric pollutants, amending Directive 2003/35/EC and repealing Directive 2001/81/EC, 2016.

Evans, C. D., Monteith, D. T., Fowler, F., Cape, J. N and Brayshaw, S.: Hydrochloric Acid: An overlooked driver of environmental change, Environ. Sci. Technol., 2011 45 (5), 1887-1894, doi:10.1021/es103574u, 2011.

Hall, J., Smith, R., and Dore. T.: Trends Report 2017: Trends in critical load and critical level exceedances in the UK. Report to Defra under Contract AQ0843, CEH Bangor, August 2018, http://www.cldm.ceh.ac.uk, 2018.

Hallsworth S., Dore A. J., Bealey W. J., Dragosits U., Vieno M., Hellsten S., Tang Y. S., and Sutton M. A.: The role of indicator choice in quantifying the threat of atmospheric ammonia to the 'Natura 2000' network. Env. Sci. Policy, 13, 671-687, doi:10.1016/j.envsci. 2010.09.010, 2010.

Hayman, G. D., Vincent, K., Lawrence, H., Smith, M., Colbeck, C., Davies, M., Sutton, M. A., Tang, Y. S., Dragosits, U., Love, L., Fowler, D., Kendall, M., and Page, H.:

Management and Operation of the UK Acid Deposition Monitoring Network: Data Summary for 2005, AEA Energy & Environment Report AEAT/ENV/R/2342 Issue 1, AEA Technology plc, The Gemini Building, Fermi Avenue, Harwell, OX11 0QR., 2007.

Kwak, D., Lei, Y., and Maric, R.: Ammonia gas sensors: A comprehensive review, Talanta, 204, 713-730, doi:10.1016/j.talanta.2019.06.034, 2019.

Loubet, B., Carozzi, M., Voylokov, P., Cohan, J.-P., Trochard, R., and Génermont, S.: Evaluation of a new inference method for estimating ammonia volatilisation from multiple agronomic plots, Biogeosciences, 15, 3439–3460, doi:10.5194/bg-15-3439-2018, 2018.

Pitcairn, C. E. R., Leith, I. D., Sheppard, L. J., Sutton, M. A., Fowler, D., Munro, R. C., Tang, S., and Wilson, D.: The relationship between nitrogen deposition, species composition and foliar nitrogen concentrations in woodland flora in the vicinity of livestock farms, Environ. Poll., 102, 41-48, doi:10.1016/s0269-7491(98)80013-4, 1998.

Riddick, Stuart N., Dragosits, U., Blackall, T. D., Tomlinson, S. J., Daunt, F., Wanless, S., Hallsworth, S., Braban, C. F., Tang, Y. S., and Sutton, M. A.: Global assessment of the effect of climate change on ammonia emissions from seabirds, Atmos. Environ., 184. 212-223. doi:10.1016/j.atmosenv.2018.04.038, 2018

ROTAP: Review of Transboundary Air Pollution: Acidification, Eutrophication, Ground Level Ozone and Heavy Metals in the UK. Contract Report to the Department for Environment, Food and Rural Affairs. Centre for Ecology and Hydrology. www.rotap.ceh.ac.uk, 2012.

Sheppard, L. J., Leith, I. D., Mizunuma, T., Cape, J. N, Crossley, A., Leeson, S., Sutton, M. A., van, Dijk, N., and Fowler, D.: Dry deposition of ammonia gas drives species change faster than wet deposition of ammonium ions: evidence from a long-term field manipulation, Glob. Change Biol., 17, 3589-3607, doi:10.1111/j.1365-2486.2011.02478.x, 2011.

Singles, R., Sutton, M. A., & Weston, K. J.: A multi-layer model to describe the atmospheric transport and deposition of ammonia in Great Britain, Atmos. Environ., 32, 393-399, doi:10.1016/S1352-2310(97)83467-X, 1998.

Smith, R. I., Fowler, D., Sutton, M. A., Flechard, C., and Coyle, M.: Regional estimation of pollutant gas deposition in the UK: model description, sensitivity analyses and outputs. Atmos. Environ., 34, 3757-3777, doi:10.1016/S1352-2310(99)00517-8, 2000.

Solera García, M. A., Timmis, R. J., Van Dijk, N., Whyatt, J. D., Leith, I. D., Leeson, S. R., Braban, C. F., Sheppard, L. J., Sutton, M. A., and Tang, Y. S.: 2017 Directional passive ambient air monitoring of ammonia for fugitive source attribution; a field trial with wind tunnel characteristics. Atmos. Environ., 167. 576-585, doi:10.1016/j.atmosenv.2017.07.043

Tadi, K. K., Pal, S., and Narayanan, T. N.: Fluorographene based Ultrasensitive Ammonia Sensor. Sci. Rep. 6, 25221, doi:10.1038/srep25221, 2016.

Tang, Y. S., Cape, J. N., Braban, C. F., Twigg, M. M., Poskitt, J., Jones, M. R., Rowland, P., Bentley, P., Hockenhull, K., Woods, C., Leaver, D., Simmons, I., van Dijk, N., Nemitz, E., and Sutton, M. A.: Development of a new model DELTA sampler and assessment of potential sampling artefacts in the UKEAP AGANet

DELTA system: summary and technical report, London, Defra. (CEH Project no. C04544, C04845), https://uk-air.defra.gov.uk/library/reports? report_id=861, 2015.

Tang, Y. S., Stephens, A., Farrand, P., Warwick, A., Simmons, I., Jones, M., Poskitt, J., Keenan, P. O., Dos Santos, D. M. G., Sutton, M. A., and Braban C. F.: 2018. CEH DELTA-Mi System for sampling atmospheric gases and aerosols, 24pp, May 2018.

Tang, Y. S., Mullinger, N., Simmons, I., Stephens, A., Coyle, M., and Braban C. F.: Development of a high sensitivity ammonia sensor: Phase 1 feasibility study report (01/05/18 – 31/08/18), 41pp, September 2018.

Timmer, B., Olthuis, W., and Berg, A. van den.: Ammonia sensors and their applications—a review. Sensors and Actuators B: Chemical 107, 666–677, doi:10.1016/j.snb.2004.11.054, 2005.

Torseth, K. and Hov, O. (Eds) The EMEP monitoring strategy for 2004-2009. EMEP Report 9/2003, 2003.

Yunusa, Z., Hamidon, M. N., Kaiser, A., and Awang, Z.: Gas Sensors: A Review. Sensors & Transducers 168, 61–75, 2014.

Apendix 1: Supplementary Information for Chapter 2

This contains supplementary material for Chapter 2: Drivers for spatial, temporal and long-term trends in atmospheric ammonia and ammonium in the UK. Yuk S. Tang et al. Supplement of Atmos. Chem. Phys., 18, 705-733, 2018, https://doi.org/10.5194/acp-18-705-2018-supplement.

Supp. Figure S2.1: Comparisons of parallel measurement of monthly (a) NH_3 and (b) particulate NH_4^+ concentrations from duplicate DELTA sampling at the UK National Ammonia Monitoring Network (NAMN) site Bush OTC (UKA00128) for the period 1999 to 2014.

Supp. Figure S2.2: Comparison of the monthly NH_3 concentrations determined by: a) DELTA (mean of replicate results), and b) ALPHA methods with the AMOR results derived from the average of hourly AMOR data at the Zegfeld Dutch National Air Quality Monitoring Network site (ID 633) for the corresponding DELTA and ALPHA sampling periods (unpublished data).

Supp. Figure S2.3: Frequency distribution of sites in the UK National Ammonia Monitoring Network NAMN measuring (a) NH_3 (85 sites) and (b) NH_4^+ (30 sites), according to each of seven dominant NH_3 source sectors**Error! Reference source not found.** based on the network structure for 2005) compared with the dominant source classification for the whole land area of the UK.

Supp. Figure S4: (a) Relationships between UK mean annual measured NH_3 concentrations from 59 sites in the National Ammonia Monitoring Network (NAMN) and mean annual temperature and rainfall (data downloaded from http://www.metoffice.gov.uk/) for the period 1998 to 2014. NH_3 was negatively correlated with rainfall (blue line: $Log(NH_3) = -0.0003*Log(rain) + 0.9656$, $R^2 = 0.32$, $n = 17$, $p = 0.02$). For the relationship between NH_3 and temperature, although most of the data shows an increase in NH_3 with temperature, the correlation was not significant (red line: $Log(NH_3) = 0.0227*Log(temp) + 0.3618$, $R^2 = 0.02$, $n = 17$, $p = 0.59$). 2010 (data point marked on graph) was an unusual year with considerably lower annual mean temperature (7.9 °C) than normal (mean = 9.2 °C for period 1998 – 2014). This was due to exceptionally cold winter temperatures occurring in Jan, Feb, Nov and Dec 2010, with Dec 2010 being the coldest for over 100 years. While the mean temperature for 2010 was lower than usual, the mean annual NH_3 concentration for 2010 was in fact similar to other years, since the lowest NH_3 concentrations occurred in the winter months. (b) Relationships between UK mean monthly measured NH_3 concentrations from the NAMN and mean monthly temperature and rainfall from the same selection of sites for the period 1998 to 2014. NH_3 was negatively correlated with rainfall (blue line: $Log(NH_3) = -0.0057*Log(rain) + 1.0579$, $R_2 = 0.45$, $n = 204$, $p < 0.01$).) and positively correlated with temperature (red line: $Log(NH_3) = 0.0370*Log(rain) + 0.1580$, $R^2 = 0.24$, $n = 204$, $p < 0.01$).

Supp. Figure S5: Time series trend analysis by Mann-Kendall Sen's slope *vs* squares linear regression on annually averaged particulate NH_4^+ and gaseous NH_3 concentrations from the UK National Ammonia Monitoring Network (NAMN) for a) NH_4^+ (1999-2014, n=23), b) NH_4^+ (2006-2014, n= 30), c) NH_3 (1999-2014, n=23, same sites as a), and d) NH_3 (2006-2014, n=30, same sites as b). Individual data points are annually averaged concentrations.

Supp. Figure S6: Time series trend analysis by Mann-Kendall Sen's slope *vs* linear regression on annually averaged particulate NH_4^+ from the UK National Ammonia Monitoring Network (NAMN) and particulate NO_3^- and SO_4^{2-} from the UK Acid Gas and Aerosol Network (AGANet for time periods a) 2000 – 2014 (12 sites) and b) 2006 – 2014 (30 sites). Individual data points are annually averaged concentrations.

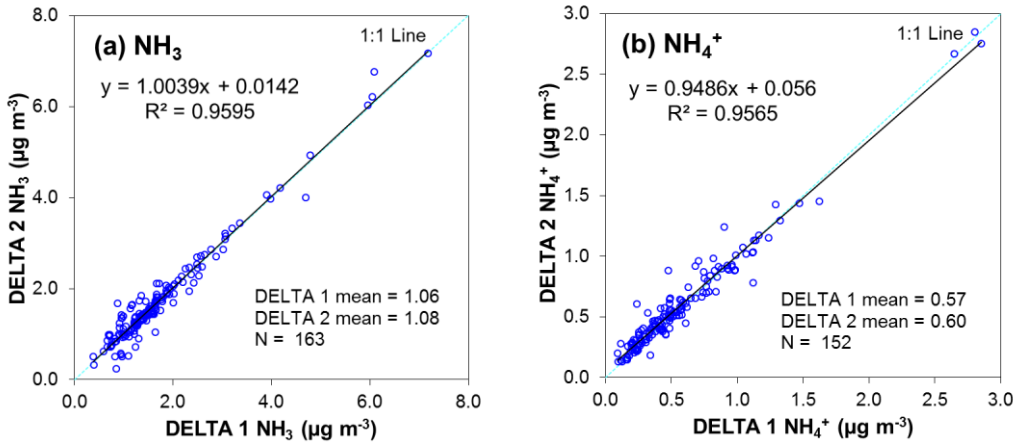

Supp. Figure S1: Comparisons of parallel measurement of monthly (a) NH_3 and (b) particulate NH_4^+ concentrations from duplicate DELTA sampling at the UK National Ammonia Monitoring Network (NAMN) site Bush OTC (UKA00128) for the period 1999 to 2014.

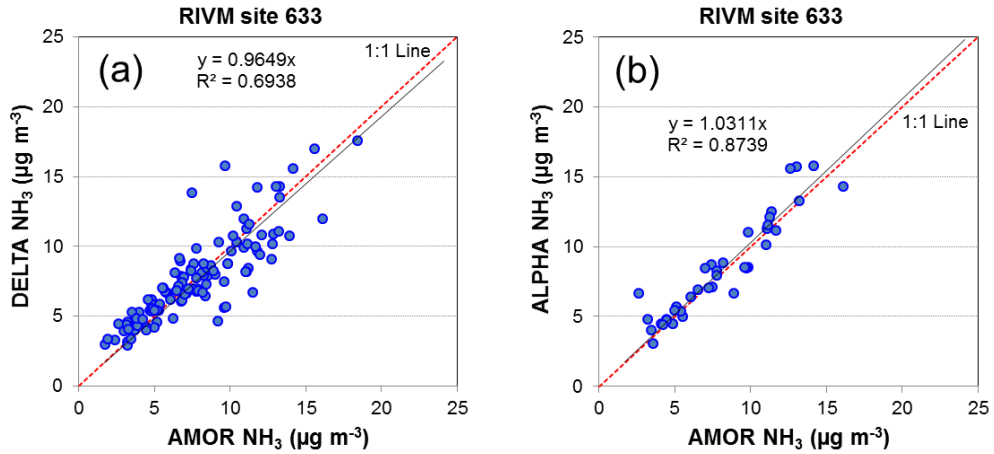

Supp. Figure S2: Comparison of the monthly NH_3 concentrations determined by: a) DELTA (mean of replicate results), and b) ALPHA methods with the AMOR results derived from the average of hourly AMOR data at the Zegfeld Dutch National Air Quality Monitoring Network site (ID 633) for the corresponding DELTA and ALPHA sampling periods (unpublished data).

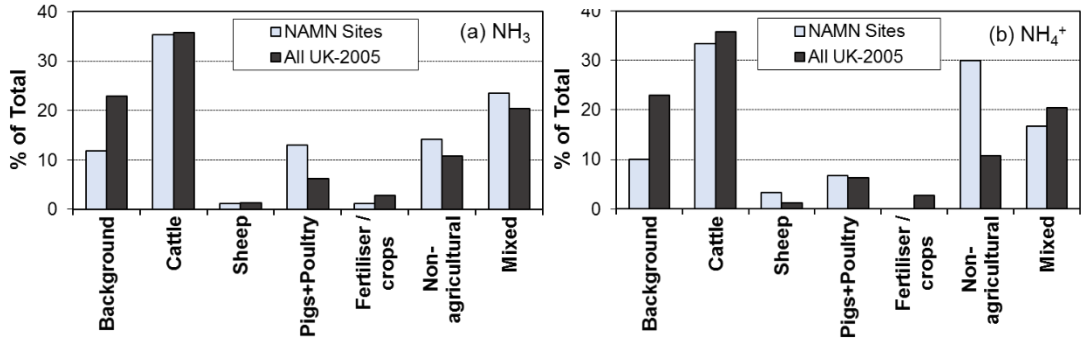

Supp. Figure S3: Frequency distribution of sites in the UK National Ammonia Monitoring Network NAMN measuring (a) NH_3 (85 sites) and (b) NH_4^+ (30 sites), according to each of seven dominant NH_3 source sectors (based on the network structure for 2005) compared with the dominant source classification for the whole land area of the UK.

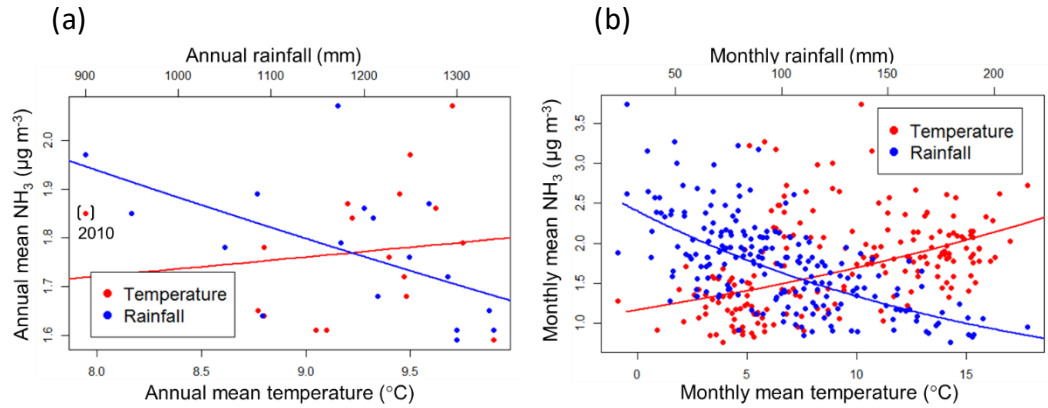

Supp. Figure S4: (a) Relationships between UK mean annual measured NH_3 concentrations from 59 sites in the National Ammonia Monitoring Network (NAMN) and mean annual temperature and rainfall (data downloaded from http://www.metoffice.gov.uk/) for the period 1998 to 2014. NH_3 was negatively correlated with rainfall (blue line: $Log(NH_3) = -0.0003*Log(rain) + 0.9656$, $R^2 = 0.32$, $n = 17$, $p = 0.02$). For the relationship between NH_3 and temperature, although most of the data shows an increase in NH_3 with temperature, the correlation was not significant (red line: $Log(NH_3) = 0.0227*Log(temp) + 0.3618$, $R^2 = 0.02$, $n = 17$, $p = 0.59$). 2010 (data point marked on graph) was an unusual year with considerably lower annual mean temperature (7.9 °C) than normal (mean = 9.2 °C for period 1998 – 2014). This was due to exceptionally cold winter temperatures occurring in Jan, Feb, Nov and Dec 2010, with Dec 2010 being the coldest for over 100 years. While the mean temperature for 2010 was lower than usual, the mean annual NH_3 concentration for 2010 was in fact similar to other years, since the lowest NH_3 concentrations occurred in the winter months. (b) Relationships between UK mean monthly measured NH_3 concentrations from the NAMN and mean monthly temperature and rainfall from the same selection of sites for the period 1998 to 2014. NH_3 was negatively correlated with rainfall (blue line: $Log(NH_3) = -0.0057*Log(rain) + 1.0579$, $R_2 = 0.45$, $n = 204$, $p < 0.01$).) and positively correlated with temperature (red line: $Log(NH_3) = 0.0370*Log(rain) + 0.1580$, $R^2 = 0.24$, $n = 204$, $p < 0.01$).

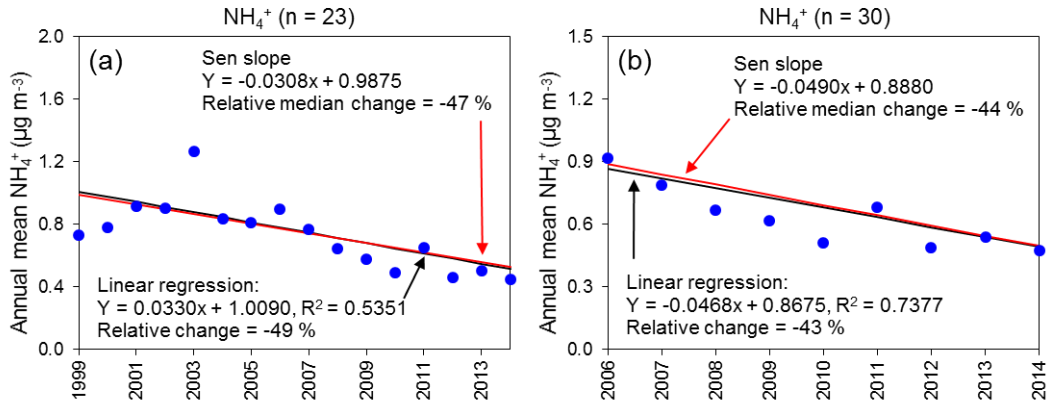

Supp. Figure S5: Time series trend analysis by Mann-Kendall Sen's slope *vs* squares linear regression on annually averaged particulate NH_4^+ and gaseous NH_3 concentrations from the UK National Ammonia Monitoring Network (NAMN) for a) NH_4^+ (1999-2014, n=23), b) NH_4^+ (2006-2014, n= 30), c) NH_3 (1999-2014, n=23, same sites as a), and d) NH_3 (2006-2014, n=30, same sites as b). Individual data points are annually averaged concentrations.

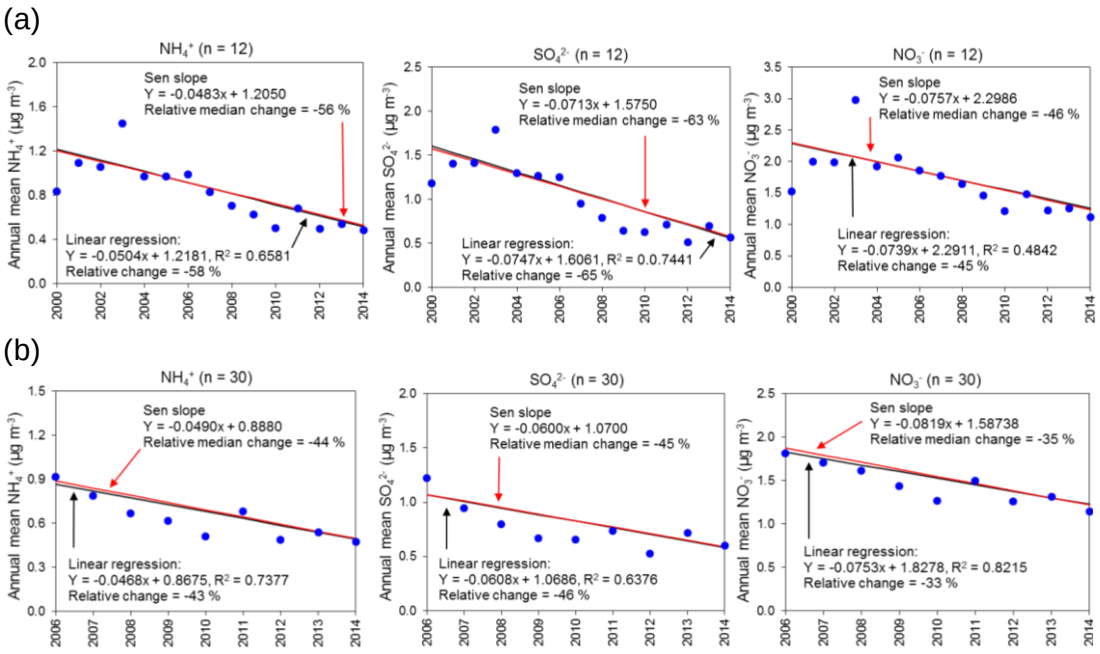

Supp. Figure S6: Time series trend analysis by Mann-Kendall Sen's slope *vs* linear regression on annually averaged particulate NH_4^+ from the UK National Ammonia Monitoring Network (NAMN) and particulate NO_3^- and SO_4^{2-} from the UK Acid Gas and Aerosol Network (AGANet for time periods a) 2000 – 2014 (12 sites) and b) 2006 – 2014 (30 sites). Individual data points are annually averaged concentrations.

Apendix 2: Supplementary Information for Chapter 3

This contains supplementary material for Chapter 3: Acid gases and aerosol measurements in the UK (1999 – 2015): regional distribution and trends.

Y. Sim Tang et al.

Supplement of Atmos. Chem. Phys., 18, 16293-16324, 2018,
https://doi.org/10.5194/acp-18-16293-2018-supplement.

List of Supplementary Figures:

Supp. Figure S3.1: Left: DEnuder for Long-Term Atmospheric sampling (DELTA) as applied for the monthly measurements of reactive gases and particulate matter composition in the UK Acid Gases and Aerosol Network (AGANet), with sampling train *in situ*. Right: sampling train consisting of 2 x 15 cm long K_2CO_3 + glycerol coated denuders (determination of HNO_3, SO_2, HCl), 2 x 10 cm long acid coated denuders (determination of NH_3), carbonate coated filter (determination of NO_3^-, SO_4^{2-}, Cl^-, Na^+, Ca^{2+}, Mg^{2+}) and acid coated filter (determination of evolved NH_4^+).

Supp. Figure S3.2: Scatter plots between concentrations of (a) non-sea salt sulphate (nss_SO4) vs NH_4^+, and (b) non-sea salt chloride (nss_Cl) *vs* Na^+ from mean monthly measurements (1999-2015) for the 12 sites in the UK Acid Gas and Aerosol Monitoring Network (AGANet) that were operational over the whole period. NH_3 and NH_4^+ data are from the UK National Ammonia Monitoring Network (NAMN, Tang et al., 2018) made at the same time.

Supp. Figure S3: Time series trend analysis by non-parametric Mann-Kendall Sen slope and by parametric linear regression on monthly mean gas and aerosol concentration data from the UK Acid Gases and Aerosol Monitoring Network (AGANet) for the 12 sites that were operational over the period 2000 to 2015. NH_3 and NH_4^+ concentrations data measured at the same time in the UK National Ammonia Monitoring Network (NAMN, Tang et al., 2018) are also included for comparison. Individual data points are monthly mean concentrations across 12 sites.

Supp. Figure S4: Time series trend analysis by non-parametric Mann-Kendall Sen slope and by parametric linear regression on monthly mean gas and aerosol concentration data from the UK Acid Gases and Aerosol Monitoring Network (AGANet) for the 30 sites that were operational over the period 2006 to 2015. NH_3 and NH_4^+ concentrations data measured at the same time in the UK National Ammonia Monitoring Network (NAMN, Tang et al., 2018) are also included for comparison. Individual data points are monthly mean concentrations across 30 sites.

Supp. Figure S5: Monthly mean concentrations in gaseous HNO_3, SO_2, HCl and aerosol NO_3^-, SO_4^{2-}, Cl^- from the UK Acid Gases and Aerosol Monitoring Network (AGANet) over the period 2006 - 2015. Monthly mean concentrations of NH_3 and NH_4^+ that were measured at the same time in the UK National Ammonia Monitoring Network (NAMN, Tang et al., 2018) are also shown for comparison. Each data point in the graphs represents the mean of monthly measurements of 30 sites operational in the network over the period 2006 to 2015

Supp. Figure S6: Time-series trend analysis by non-parametric Mann-Kendall Sen slope and by parametric linear regression on annually averaged gas and aerosol concentration data from the UK Acid Gases and Aerosol Monitoring Network (AGANet) of 12 sites that were operational over the period 2000 to 2015. NH_3 and NH_4^+ concentrations measured at the same time in the UK National Ammonia Monitoring Network (NAMN, Tang et al., 2018) are also included for comparison.

Supp. Figure S7: Time series trend analysis by non-parametric Mann-Kendall Sen slope and by parametric linear regression on annually averaged gas and aerosol concentration data from the UK Acid Gases and Aerosol Monitoring Network (AGANet) of 30 sites that were operational over the period 2006 to 2015. NH_3 and NH_4^+ concentrations data measured at the same time in the UK National Ammonia Monitoring Network (NAMN, Tang et al., 2018) are also included for comparison.

Supp. Figure S8: UK annual mean temperature and rainfall (data source: https://www.metoffice.gov.uk/climate/uk/summaries)

List of Supplementary Tables:

Supp. Table S1: Major ions measured in DELTA extracts and typical limits of detection (LOD).

Supp. Table S2: Major ions measured in aerosol filter extracts and typical limits of detection (LOD).

Supp. Table S3: Calculated lengths of chemically impregnated denuders (borosilicate glass tubes, 10 mm o.d, 0.65 mm i.d) to capture 95 % of gas of interest at a flow rate of 0.4 LPM under laminar flow.

Supp. Table S4: Summary of Mann-Kendall (MK) and Linear Regression (LR) time series trend analysis on annually averaged gas and aerosol concentrations from the UK Acid Gases and Aerosol Monitoring Network (AGANet) for the 12 sites that were operational over the period 2000 to 2015. NH_3 and NH_4^+ concentrations measured at the same time in the UK National Ammonia Monitoring Network (NAMN, Tang et al., 2018) are also included for comparison. For the MK tests, the 95% confidence interval (CI) for the median trend and relative change are also estimated.

Supp. Table S5: Summary of Mann-Kendall (MK) and Linear Regression (LR) time series trend analysis on annually averaged gas and aerosol concentrations from the UK Acid Gases and Aerosol Monitoring Network (AGANet) for the 30 sites that were operational over the period 2006 to 2015. NH_3 and NH_4^+ concentrations data measured at the same time from the UK National Ammonia Monitoring Network (NAMN, Tang et al., 2018) are also included for comparison. For the MK tests, the 95% confidence interval (CI) for the median trend and relative change are also estimated.

Supp. Table S6: Comparison of % change in estimated UK NO_x, SO_2 and NH_3 emissions reported by the National Atmospheric Emission Inventory (NAEI) (data from http://naei.defra.gov.uk/) with % change between 2000-2015 (12 sites with complete time series) and between 2006-2015 (30 sites with complete time series) in annually averaged HNO_3 / NO_3^- and SO_2 / SO_4^{2-} concentrations from the UK Acid Gas and Aerosol Monitoring Network (AGANet), and annually averaged NH_3 / NH_4^+ concentrations from the UK National Ammonia Monitoring Network (NAMN, Tang et al., 2018).

.

Supp. Table S7: Summary of Mann-Kendall (MK) and Linear Regression (LR) time series trend analysis on monthly mean gas and aerosol concentration data from the UK Acid Gases and Aerosol Monitoring Network (AGANet) for the 12 sites that were operational over the period 2000 to 2015. NH_3 and NH_4^+ concentrations measured at the same time in the UK National Ammonia Monitoring Network (NAMN, Tang et al., 2018) are also included for comparison. For the MK tests, the 95% confidence interval (CI) for the median trend and relative change are also estimated

Supp. Table S8: Summary of Mann-Kendall (MK) and Linear Regression (LR) time series trend analysis on monthly mean gas and aerosol concentration data from the UK Acid Gases and Aerosol Monitoring Network (AGANet) for the 30 sites that were operational over the period 2006 to 2015. NH_3 and NH_4^+ concentrations measured at the same time in the UK National Ammonia Monitoring Network (NAMN, Tang et al., 2018) are also included for comparison. For the MK tests, the 95% confidence interval (CI) for the median trend and relative change are also estimated.

Denuder theory

References

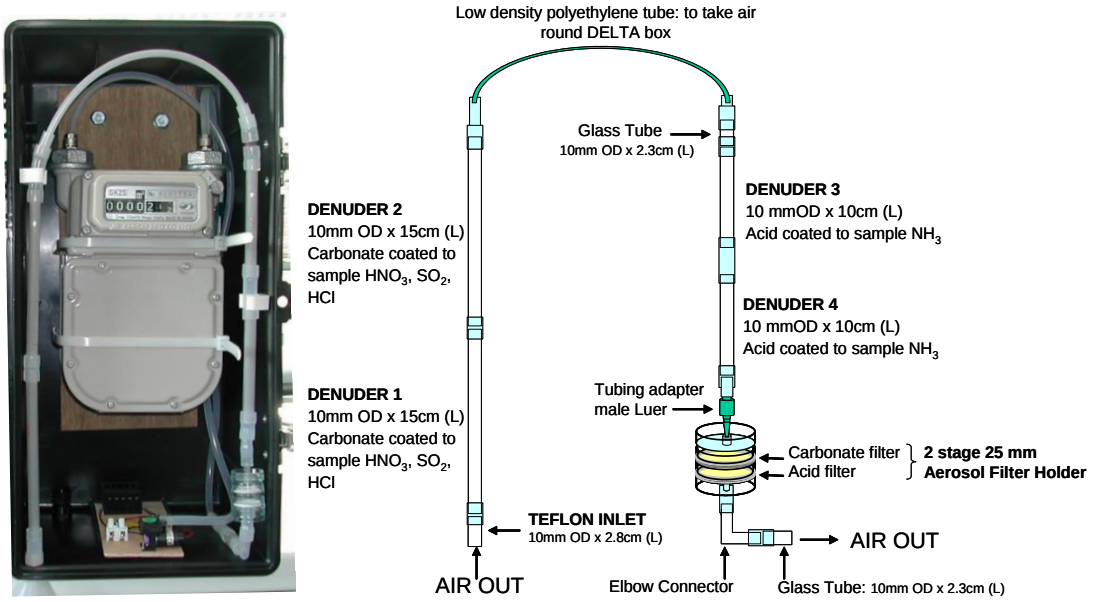

Supp. Figure S1: Left: DEnuder for Long-Term Atmospheric sampling (DELTA) as applied for the monthly measurements of reactive gases and particulate matter composition in the UK Acid Gases and Aerosol Network (AGANet), with sampling train *in situ*. Right: sampling train consisting of 2 x 15 cm long K_2CO_3 + glycerol coated denuders (determination of HNO_3, SO_2, HCl), 2 x 10 cm long acid coated denuders (determination of NH_3), carbonate coated filter (determination of NO_3^-, SO_4^{2-}, Cl^-, Na^+, Ca^{2+}, Mg^{2+}) and acid coated filter (determination of evolved NH_4^+).

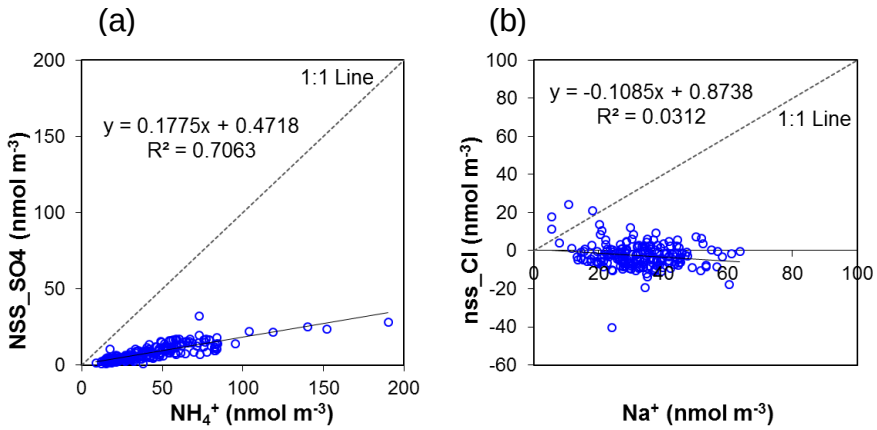

Supp. Figure S2: Scatter plots between concentrations of (a) non-sea salt sulphate (nss_SO4) vs NH_4^+, and (b) non-sea salt chloride (nss_Cl) *vs* Na^+ from mean monthly measurements (1999-2015) for the 12 sites in the UK Acid Gas and Aerosol Monitoring Network (AGANet) that were operational over the whole period. NH_3 and NH_4^+ data are from the UK National Ammonia Monitoring Network (NAMN, Tang et al., 2018) made at the same time.

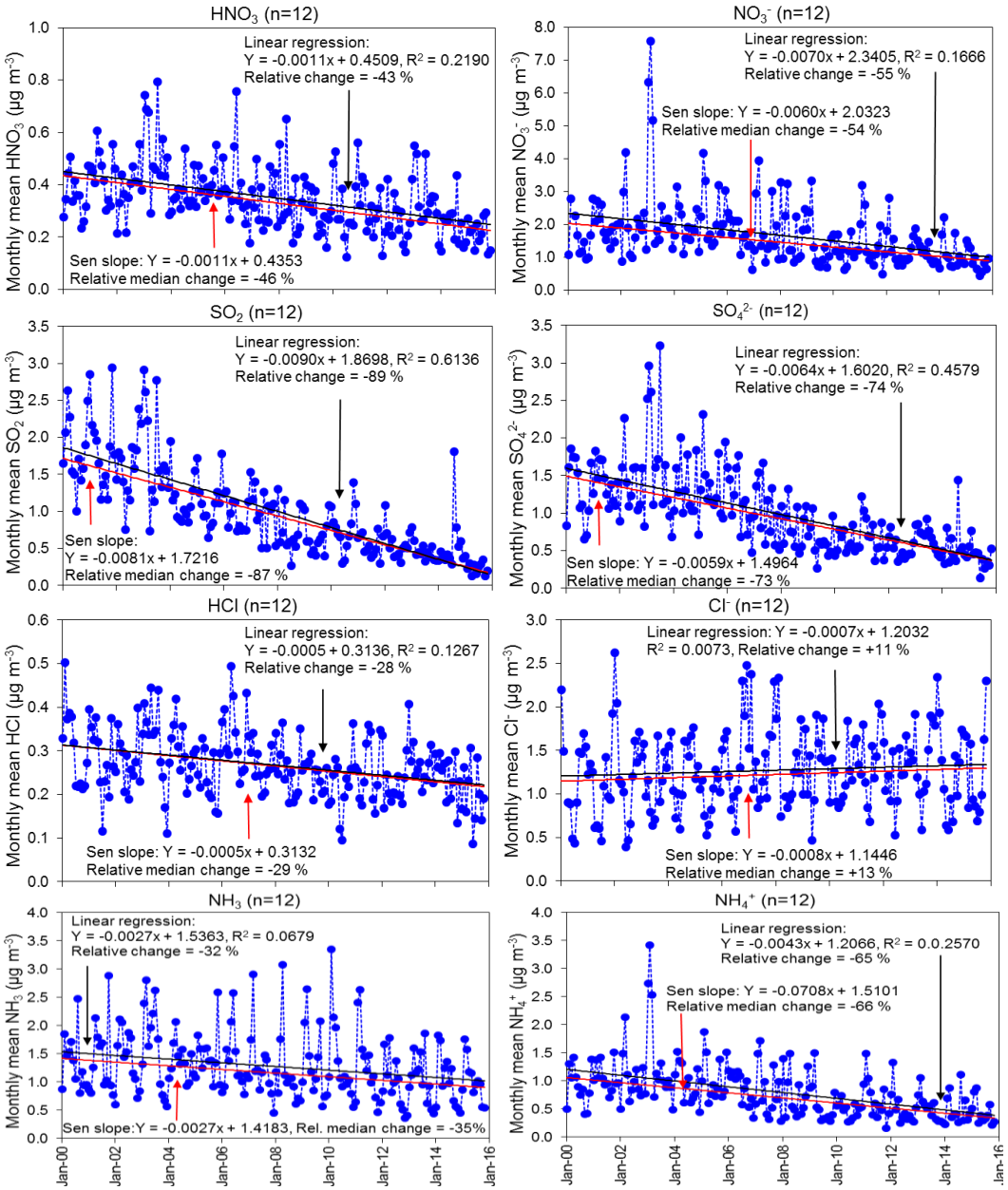

Supp. Figure S3: Time series trend analysis by non-parametric Mann-Kendall Sen slope and by parametric linear regression on monthly mean gas and aerosol concentration data from the UK Acid Gases and Aerosol Monitoring Network (AGANet) for the 12 sites that were operational over the period 2000 to 2015. NH_3 and NH_4^+ concentrations data measured at the same time in the UK National Ammonia Monitoring Network (NAMN, Tang et al., 2018) are also included for comparison. Individual data points are monthly mean concentrations across 12 sites.

[Appendix II]

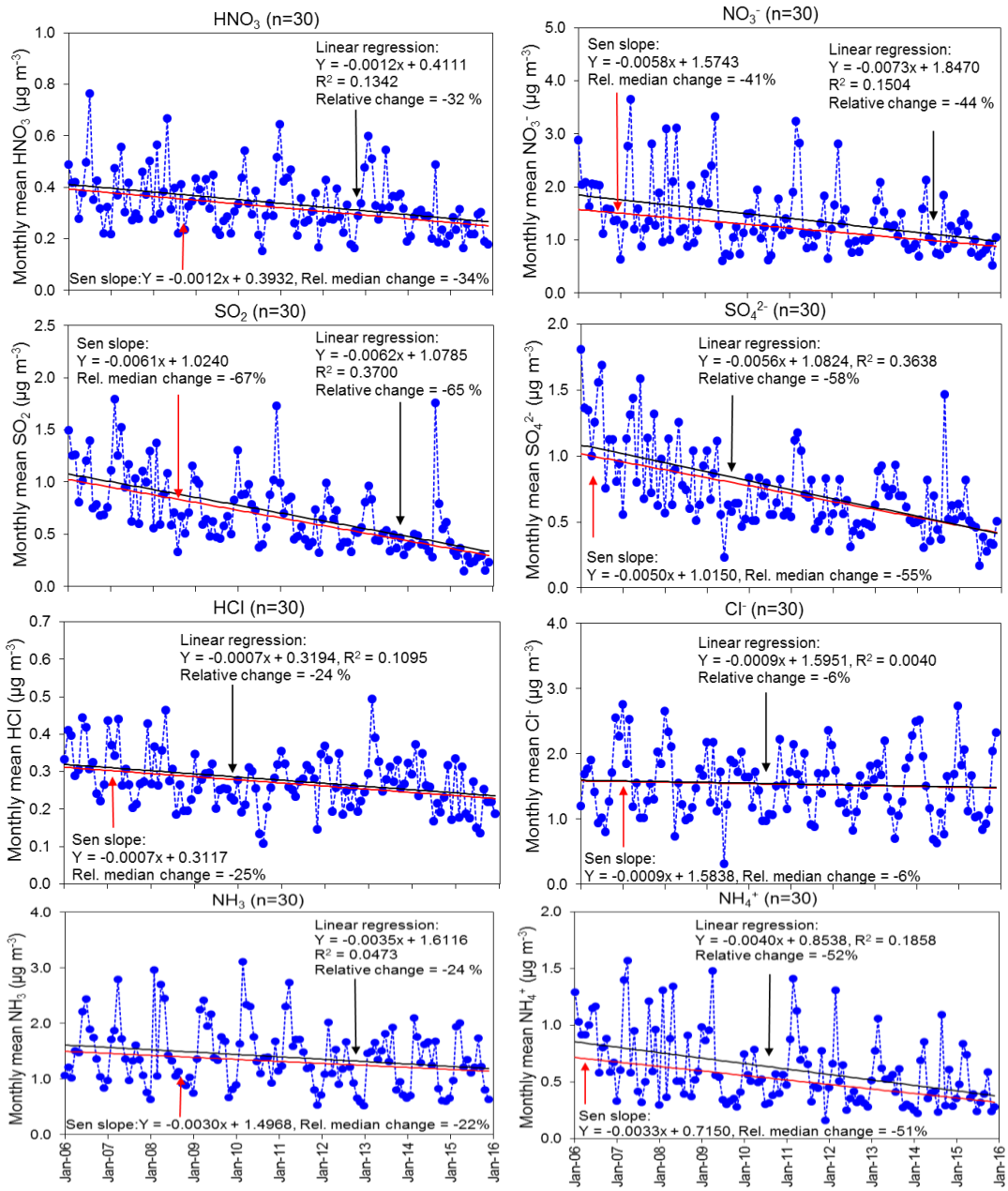

Supp. Figure S4: Time series trend analysis by non-parametric Mann-Kendall Sen slope and by parametric linear regression on monthly mean gas and aerosol concentration data from the UK Acid Gases and Aerosol Monitoring Network (AGANet) for the 30 sites that were operational over the period 2006 to 2015. NH_3 and NH_4^+ concentrations data measured at the same time in the UK National Ammonia Monitoring Network (NAMN, Tang et al., 2018) are also included for comparison. Individual data points are monthly mean concentrations across 30 sites.

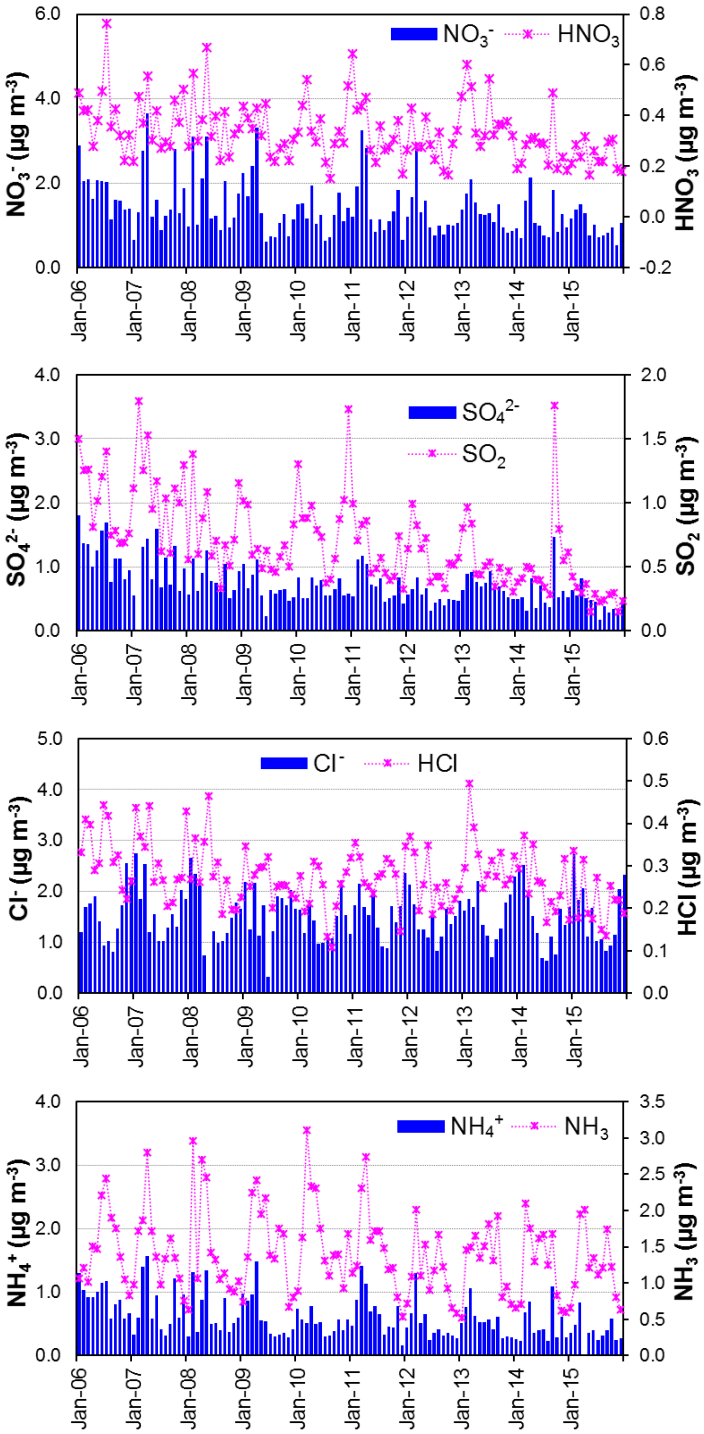

Supp. Figure S5: Monthly mean concentrations in gaseous HNO_3, SO_2, HCl and aerosol NO_3^-, SO_4^{2-}, Cl^- from the UK Acid Gases and Aerosol Monitoring Network (AGANet) over the period 2006 - 2015. Monthly mean concentrations of NH_3 and NH_4^+ that were measured at the same time in the UK National Ammonia Monitoring Network (NAMN, Tang et al., 2018) are also shown for comparison. Each data point in the graphs represents the mean of monthly measurements of 30 sites operational in the network over the period 2006 to 2015.

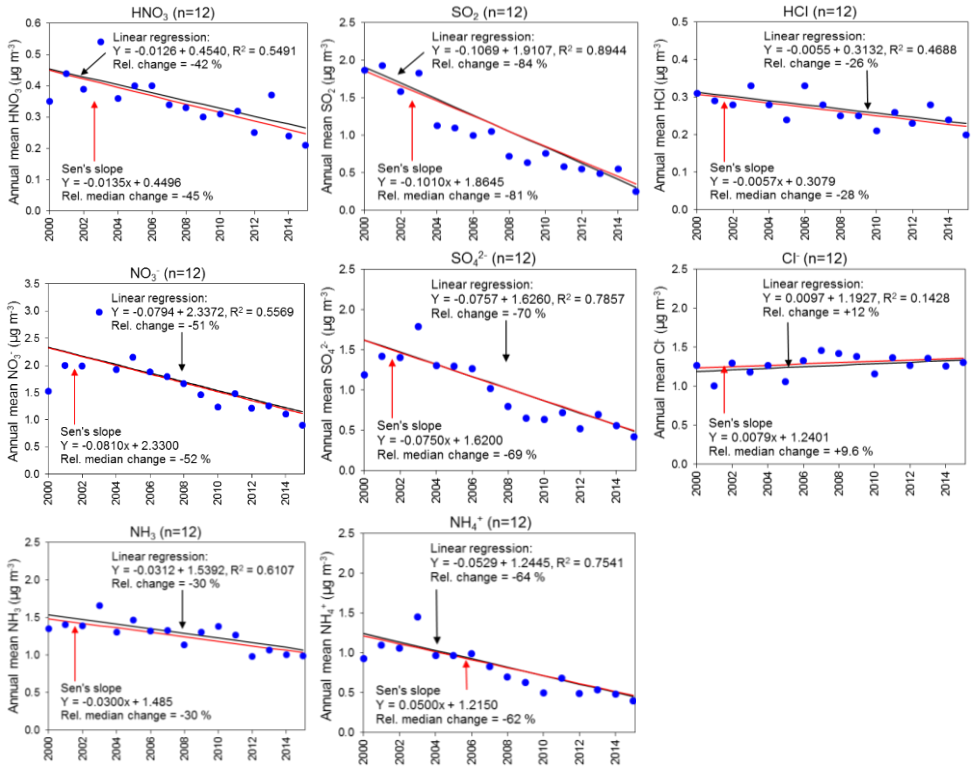

Supp. Figure S6: Time-series trend analysis by non-parametric Mann-Kendall Sen slope and by parametric linear regression on annually averaged gas and aerosol concentration data from the UK Acid Gases and Aerosol Monitoring Network (AGANet) of 12 sites that were operational over the period 2000 to 2015. NH_3 and NH_4^+ concentrations measured at the same time in the UK National Ammonia Monitoring Network (NAMN, Tang et al., 2018) are also included for comparison.

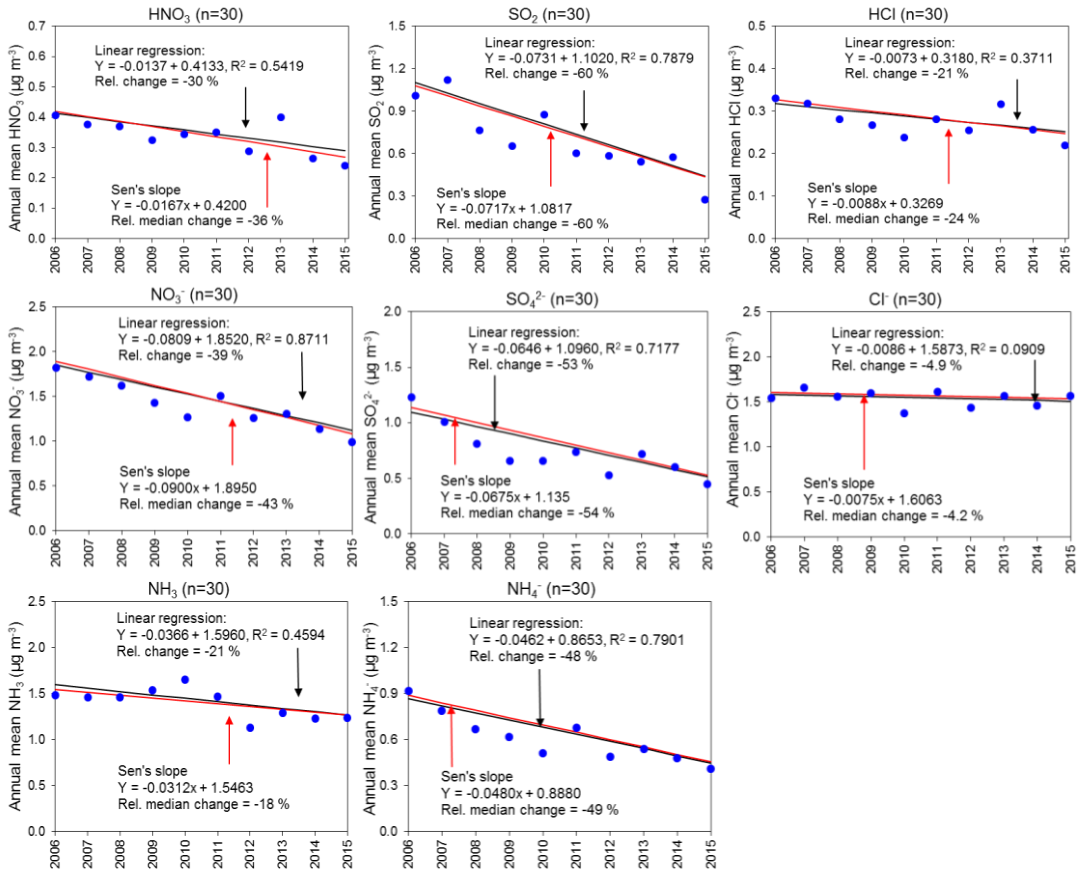

Supp. Figure S7: Time series trend analysis by non-parametric Mann-Kendall Sen slope and by parametric linear regression on annually averaged gas and aerosol concentration data from the UK Acid Gases and Aerosol Monitoring Network (AGANet) of 30 sites that were operational over the period 2006 to 2015. NH_3 and NH_4^+ concentrations data measured at the same time in the UK National Ammonia Monitoring Network (NAMN, Tang et al., 2018) are also included for comparison.

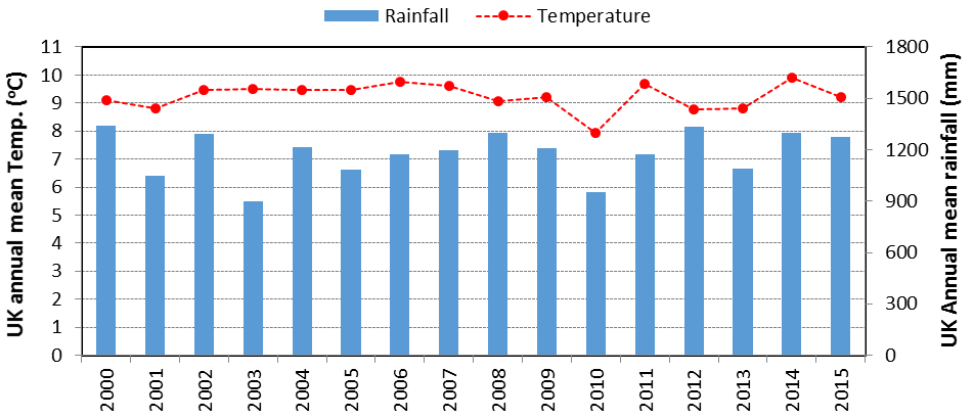

Supp. Figure S8: UK annual mean temperature and rainfall (data source: https://www.metoffice.gov.uk/climate/uk/summaries)

Supp. Table S1: Major ions measured in DELTA extracts and typical limits of detection (LOD).

Analytes (denuder aqueous extracts)	Harwell Laboratory (Sep99 – Jun09)		CEH Lancaster (from Jul09)	
	Analytical Method	Typical LOD (µg m^{-3})	Analytical Method	Typical LOD (µg m^{-3})
NO_3^-	IC	0.05 (HNO_3)	IC	0.05 (HNO_3)
NO_2^-	Colorimetry	0.05 (HONO)	IC	0.05 (HONO)
SO_4^{2-}	IC	0.05 (SO_2)	IC	0.05 (SO_2)
Cl^-	IC	0.05 (HCl)	IC	0.05 (HCl)

Supp. Table S2: Major ions measured in aerosol filter extracts and typical limits of detection (LOD).

Analytes (aerosol filter aqueous extracts)	Harwell Laboratory (Sep99 – Jun09)		CEH Lancaster (from Jul09)	
	Method	Typical LOD (µg m^{-3})	Method	Typical LOD (µg m^{-3})
NO_3^-	IC	0.05 (NO_3^-)	IC	0.06 (NO_3^-)
NO_2^-	Colorimetry	0.05 (NO_2^-)	IC	0.05 (NO_2^-)
SO_4^{2-}	IC	0.06 (SO_4^{2-})	IC	0.06 (SO_4^{2-})
Cl^-	IC	0.08 (Cl^-)	IC	0.16 (Cl^-)
Ca^{2+}	IC (Sep99-Jun08)	0.05	ICP-OES	0.09
Mg^{2+}	IC (Sep99-Jun08)	0.05	ICP-OES	0.05
Na^+	IC (Sep99-Jun08)	0.1	ICP-OES	0.16
Ca^{2+}	ICP-AES (Jul08-Jun09)	0.05		
Mg^{2+}	ICP-AES (Jul08-Jun09)	0.05		
Na^+	ICP-AES (Jul08-Jun09)	0.1		

Supp. Table S3: Calculated lengths of chemically impregnated denuders (borosilicate glass tubes, 10 mm o.d, 0.65 mm i.d) to capture 95 % of gas of interest at a flow rate of 0.4 LPM under laminar flow.

Reactive gas	HNO_3	SO_2	HCl	NH_3
Diffusion coefficient @ 10ºC	1.15 x 10^{-5} m^2 s^{-1} (Massman 1998)	1.22 x 10^{-5} m^2 s^{-1} (Durham & Stockburger 1986)	5.25 x 10^{-5} m^2 s^{-1} (Mumallah 1986)	2.01 x 10^{-5} m^2 s^{-1} (Hargreaves & Atkins, 1986)
L (cm): for 95 % capture efficiency at flow rate of 0.4 LPM	14	13	3	8

Note: 10 cm and 15 cm long denuders are used in the UK National Ammonia Monitoring Network (NAMN) and UK Acid Gases and Aerosol network (AGANet) to sample NH_3 and acid gases (HNO_3, SO_2, HCl), respectively.

Supp. Table S4: Summary of Mann-Kendall (MK) and Linear Regression (LR) time series trend analysis on annually averaged gas and aerosol concentrations from the UK Acid Gases and Aerosol Monitoring Network (AGANet) for the 12 sites that were operational over the period 2000 to 2015. NH_3 and NH_4^+ concentrations measured at the same time in the UK National Ammonia Monitoring Network (NAMN, Tang et al., 2018) are also included for comparison. For the MK tests, the 95% confidence interval (CI) for the median trend and relative change are also estimated.

2000 - 2015 (12 sites: annual data)	Mann-Kendall (MK)		Linear Regression (LR)		
	[a]Median annual trend & [95% CI] (µg y^{-1})	[b]Relative median change 2000-2015 & [95% CI] (%)	[c]Annual Trend (µg NH_3 y^{-1})	[d]Relative change 2000-2015 [%]	R^2
HNO_3	-0.0135 [-0.0067, -0.0180]	-45** [-26, -55]	-0.0126	-42**	0.549
SO_2	-0.1010 [-0.0729, -0.1250]	-81*** [-72, -91]	-0.1069	-84***	0.894
HCl	-0.0057 [-0.0020, -0.0100]	-28*** [-11, -42]	-0.0055	-26**	0.469
NH_3	-0.0300 [-0.0125, -0.0433]	-30** [-13, -39]	-0.0312	-30***	0.611
NO_3^-	-0.0810 [-0.0520, -0.1125]	-52** [-37, -63]	-0.0794	-51***	0.557
SO_4^{2-}	-0.0750 [-0.0450, -0.-0988]	-69** [-52, -82]	-0.0757	-70***	0.786
Cl^-	0.0079 [-0088, 0.0236]	9.6^{ns} [-9.5, 33]	0.0097	$+12^{ns}$	0.143
NH_4^+	-0.0500 [-0.0375, -0.0675]	-62** [-51, -74]	-0.0529	-64***	0.754

Significance level: * $p < 0.05$, ** $p < 0.01$, *** $p < 0.001$, ^{ns} non-significant ($p > 0.05$)
[a]Median annual trend = fitted Sen's slope of Mann-Kendall linear trend (unit = µg y^{-1})
[b]Relative median change calculated based on the estimated annual concentration at the start (y_0) and at the end (y_i) of time series computed from the Sen's slope and intercept (=100*[(yi-y_0) /y_0])
[c]Annual trend = fitted slope of linear regression (unit = µg NH_3 y^{-1})
[d]Relative change calculated based on the estimated annual concentration at the start (y_0) and at the end (y_i) of time series computed from the slope and intercept (=100*[(yi-y_0) /y_0])

Supp. Table S5: Summary of Mann-Kendall (MK) and Linear Regression (LR) time series trend analysis on annually averaged gas and aerosol concentrations from the UK Acid Gases and Aerosol Monitoring Network (AGANet) for the 30 sites that were operational over the period 2006 to 2015. NH_3 and NH_4^+ concentrations data measured at the same time from the UK National Ammonia Monitoring Network (NAMN, Tang et al., 2018) are also included for comparison. For the MK tests, the 95% confidence interval (CI) for the median trend and relative change are also estimated.

2006 - 2015 (30 sites: annual data)	Mann-Kendall (MK)		Linear Regression (LR)		
	[a]Median annual trend & [95% CI] (µg NH_3 y^{-1})	[b]Relative median change 2000-2015 & [95% CI] (%)	[c]Annual Trend (µg NH_3 y^{-1})	[d]Relative change 2000-2015 [%]	R^2
HNO_3	-0.0167 [-0.0075, -0.0200]	-36* [-18, -41]	-0.0137	-30*	0.542
SO_2	-0.0717 [-0.0300, -0.0108]	-60*** [-33, -73]	-0.0731	-60***	0.788
HCl	-0.0088 [0.0000, -0.0200]	-24* [0.0, -47]	-0.0073	-21^{ns}	0.371
NH_3	-0.0312 [0.0033, -0.0625]	-18^{ns} [+2.0, -31]	-0.0366	-21*	0.459
NO_3^-	-0.0900 [-0.0580, -0.1300]	-43*** [-30, -56]	-0.0809	-39***	0.871
SO_4^{2-}	-0.0675 [-0.0233, -0.1167]	-54** [-25, -78]	-0.0646	-53***	0.718
Cl^-	-0.0075 [+0.0167, -0.0300]	-4.2^{ns} [+12, -16]	-0.0086	-4.9^{ns}	0.091
NH_4^+	-0.0480 [0.0267, -0.0700]	-49** [-33, -64]	-0.0462	-48***	0.790

Significance level: * $p < 0.05$, ** $p < 0.01$, *** $p < 0.001$, ^{ns} non-significant ($p > 0.05$)
[a]Median annual trend = fitted Sen's slope of Mann-Kendall linear trend (unit = µg y^{-1})
[b]Relative median change calculated based on the estimated annual concentration at the start (y_0) and at the end (y_i) of time series computed from the Sen's slope and intercept (=100*[(yi-y_0) /y_0])
[c]Annual trend = fitted slope of linear regression (unit = µg NH_3 y^{-1})
[d]Relative change calculated based on the estimated annual concentration at the start (y_0) and at the end (y_i) of time series computed from the slope and intercept (=100*[(yi-y_0) /y_0])

Supp. Table S6: Comparison of % change in estimated UK NO_x, SO_2 and NH_3 emissions reported by the National Atmospheric Emission Inventory (NAEI) (data from http://naei.defra.gov.uk/) with % change between 2000-2015 (12 sites with complete time series) and between 2006-2015 (30 sites with complete time series) in annually averaged HNO_3 / NO_3^- and SO_2 / SO_4^{2-} concentrations from the UK Acid Gas and Aerosol Monitoring Network (AGANet), and annually averaged NH_3 / NH_4^+ concentrations from the UK National Ammonia Monitoring Network (NAMN, Tang et al., 2018).

Components	2000 – 2015 (12 sites)			2006 – 2015 (30 sites)		
	UK emissions % change	**MK Sen Slope** % relative median change[a]	**LR** % relative change[b]	**UK emissions** % change	**MK Sen slope** % relative median change[a]	**LR** % relative change[b]
Gas HNO_3	-58 (NO_x)	-45**	-42**	-41 (NO_x)	-36*	-43*
Particulate NO_3^-		-52***	-51***		-30**	-39***
Gas SO_2	-80 (SO_2)	-81***	-84***	-64 (SO_2)	-60***	-60***
Particulate SO_4^{2-}		-69***	-70***		-54**	-53***
Gas NH_3	-10 (NH_3)	-30**	-30***	-3.5 (NH_3)	-18^{ns}	-21*
Particulate NH_4^+		-62***	-64***		-49**	-48***

Significance level: * $p < 0.05$, ** $p < 0.01$, *** $p < 0.001$, ^{ns} non-significant ($p > 0.05$)

Supp. Table S7: Summary of Mann-Kendall (MK) and Linear Regression (LR) time series trend analysis on monthly mean gas and aerosol concentration data from the UK Acid Gases and Aerosol Monitoring Network (AGANet) for the 12 sites that were operational over the period 2000 to 2015. NH_3 and NH_4^+ concentrations measured at the same time in the UK National Ammonia Monitoring Network (NAMN, Tang et al., 2018) are also included for comparison. For the MK tests, the 95% confidence interval (CI) for the median trend and relative change are also estimated.

2000 - 2015 (12 sites: monthly data)	Mann-Kendall (MK)		Linear Regression (LR)		
	[a]Median annual trend & [95% CI] (µg NH_3 y^{-1})	[b]Relative median change 2000-2015 & [95% CI] (%)	[c]Annual Trend (µg NH_3 y^{-1})	[d]Relative change 2000-2015 [%]	R^2
HNO_3	-0.0132 [-0.0096, -0.0156]	-46*** [-36, -52]	-0.0128	-43***	0.219 .
SO_2	-0.0972 [-0.0864, -0.1080]	-87*** [-82, -90]	-0.1078	-89***	0.614
HCl	-0.0060 [-0.0036, -0.0084]	-29*** [-19, -40]	-0.0058	-28***	0.127
NH_3	-0.0324 [-0.0168, -0.0468]	-35*** [-20, -46]	-0.0325	-32***	0.068
NO_3^-	-0.0720 [-0.0528, -0.0900]	-54*** [-44, -63]	-0.0839	-55***	0.167
SO_4^{2-}	-0.0708 [-0.0600, -0.0804]	-73*** [-66, -77]	-0.0770	-74***	0.458
Cl^-	0.0096 [-0.0048, 0.0252]	+13^{ns} [-5.7, +36]	+0.0085	+11^{ns}	0.007
NH_4^+	-0.0456 [-0.0360, -0.0552]	-66*** [-57, -74]	-0.0516	-65***	0.257

Significance level: * $p < 0.05$, ** $p < 0.01$, *** $p < 0.001$, ^{ns} non-significant ($p > 0.05$)
[a]Median annual trend = fitted Sen's slope of Mann-Kendall linear trend (unit = µg y^{-1})
[b]Relative median change calculated based on the estimated annual concentration at the start (y_0) and at the end (y_i) of time series computed from the Sen's slope and intercept (=100*[(yi-y_0) /y_0])
[c]Annual trend = fitted slope of linear regression (unit = µg NH_3 y^{-1})
[d]Relative change calculated based on the estimated annual concentration at the start (y_0) and at the end (y_i) of time series computed from the slope and intercept (=100*[(yi-y_0) /y_0])

Supp. Table S8: Summary of Mann-Kendall (MK) and Linear Regression (LR) time series trend analysis on monthly mean gas and aerosol concentration data from the UK Acid Gases and Aerosol Monitoring Network (AGANet) for the 30 sites that were operational over the period 2006 to 2015. NH_3 and NH_4^+ concentrations measured at the same time in the UK National Ammonia Monitoring Network (NAMN, Tang et al., 2018) are also included for comparison. For the MK tests, the 95% confidence interval (CI) for the median trend and relative change are also estimated.

2006 - 2015 (30 sites: monthly data)	Mann-Kendall (MK)		Linear Regression (LR)		
	[a]Median annual trend & [95% CI] (µg NH_3 y^{-1})	[b]Relative median change 2006-2015 & [95% CI] (%)	[c]Annual Trend (µg NH_3 y^{-1})	[d]Relative change 2006-2015 [%]	R^2
HNO_3	-0.0144 [-0.0072, -0.0204]	-34*** [-18, -44]	-0.0146	-32***	0.134
SO_2	-0.0732 [-0.0564, -0.0924]	-67*** [-59, -74]	-0.0749	-65***	0.370
HCl	-0.0084 [-0.0036, -0.0120]	-25** [-11, -33]	-0.0084	-24***	0.109
NH_3	-0.0360 [-0.0036, -0.0696]	-22* [-26, -39]	-0.0425	-24*	0.047
NO_3^-	-0.0696 [-0.0408, -0.0101]	-41*** [-26, -54]	-0.0875	-44***	0.150
SO_4^{2-}	-0.0600 [-0.0432, -0.0768]	-55*** [-44, -64]	-0.0674	-58***	0.364
Cl^-	-0.0108 [-0.0228, -0.0432]	-6^{ns} [-14, +23]	-0.0111	-6^{ns}	0.004
NH_4^+	-0.0396 [-0.0024, -0.0588]	-51*** [-35, -64]	-0.0480	-52***	0.186

Significance level: * $p < 0.05$, ** $p < 0.01$, *** $p < 0.001$, ^{ns} non-significant ($p > 0.05$)
[a]Median annual trend = fitted Sen's slope of Mann-Kendall linear trend (unit = µg y^{-1})
[b]Relative median change calculated based on the estimated annual concentration at the start (y_0) and at the end (y_i) of time series computed from the Sen's slope and intercept (=100*[(yi-y_0) /y_0])
[c]Annual trend = fitted slope of linear regression (unit = µg NH_3 y^{-1})
[d]Relative change calculated based on the estimated annual concentration at the start (y_0) and at the end (y_i) of time series computed from the slope and intercept (=100*[(yi-y_0) /y_0])

[Appendix II]

Denuder theory:

The length of denuder required to obtain near complete capture of a reactive gas is a function of the diffusion rate of the reactive gas and the air sampling rate. For cylindrical tubes, with laminar flow and where the tube wall is a perfect sink for the gas of interest, Gormley & Kennedy (1949) and Ferm (1979) showed that the collection efficiency of a simple denuder for a reactive gas may be calculated using Eq. 1.

$$\eta = 1 - \frac{\beta_1}{\beta_0} = 1 - 0.819 \cdot e^{-14.6272\delta} + 0.0976 \cdot e^{-89.22\delta_r} + 0.01896 \cdot e^{-212\delta_r} \quad (1)$$

where

η is the collection efficiency of the denuder;
β_1 is the mass concentration of gas at the denuder outlet
β_0 is the mass concentration of gas at the denuder inlet

δ is described by Eq. 2:

$$\delta = \frac{\pi DL}{4\phi} \quad (2)$$

where

D is the molecular diffusion coefficient of reactive gas, in cm^2/s
L is effective length of the denuder, in cm
ϕ is the air flow rate through the denuder, in cm^3/s.

For collection efficiencies ≥ 95%, contributions from terms 2 and 3 in Eq. 1 are insignificant (< 0.3 %) and only the first term is significant. Eq. 1 may then be simplified to Eq. 3 and Eq. 4:

$$\eta = 1 - \frac{\beta_1}{\beta_0} = 1 - 0.819 \cdot e^{-14.6272\left(\frac{\pi DL}{4\phi}\right)} \quad (3)$$

$$\frac{\beta 1}{\beta o} = 0.819\, e^{-14.6272\ (\frac{\pi DL}{4\phi})} \quad , \frac{\beta 1}{\beta o} = 0.05 \text{ for 95 \% capture efficiency} \quad (4)$$

Laminar flow is achieved a short distance from the inlet. The minimum length of tube at inlet not coated with sorbent, L_{min} to fully develop laminar flow is given by Eq. 5.

$$L_{min} = 0.05.\mathrm{Re}.d \quad (5)$$

where

Re is the Reynolds number
d internal diameter of tube

An inlet length of 2.8 cm (uncoated Teflon tube: 10 mm o.d, 6.5 mm i.d) is used in the AGANet sampling train to develop laminar flow. Reynolds number must be <2000 for laminar flow. The Reynolds number for this is calculated to be 86 (at flow rate = 0.4 LPM and internal tube diameter = 6.5 mm).

References:

Durham, J.L., and Stockburger, L.: Nitric acid-air diffusion coefficient: Experimental determination. Atmospheric Environment, 20(3), 559-563, doi:10.1016/0004-6981(86)90098-3, 1986.

Ferm, M.: Method for determination of atmospheric ammonia. Atmospheric Environment, 13, 1385-1393, doi:10.1016/0004-6981(79)90107-0, 1979.

Gormley. P, and Kennedy, M.: Diffusion from a stream flowing through a cylindrical tube. Proc. Royal Irish Acad., 52, 163-169, 1949.

Hargreaves, K. J., and Atkins, D.H.F.: The measurement of ammonia in the outdoor environment using passive diffusion tube samplers. Report AERE-R-12568. Harwell Laboratory, Didcot, OXON, UK, 1987.

Massman, W.J.: A review of the molecular diffusivities of H_2O, CO_2, CH_4, CO, O_3, SO_2, NH_3, N_2O, NO, and NO_2 in air, O_2 and N_2 near STP. Atmospheric Environment 32(6), 1111-1127, doi:10.1016/S1352-2310(97)00391-9, 1998.

Mumallah, M.A.: Hydrochloric acid diffusion coefficients at acid-fracturing conditions, Journal of Petroleum Science and Engineering. 15. 361-374. doi:10.1016/0920-4105(95)00086-0, 1986.

Tang, Y. S., Braban, C. F., Dragosits, U., Dore, A. J., Simmons, I., van Dijk, N., Poskitt, J., Pereira, M. G., Keenan, P. O., Conolly, C., Vincent, K., Smith, R. I., Heal, M. R. and Sutton, M. A.: Drivers for spatial, temporal and long-term trends in atmospheric ammonia and ammonium in the UK, Atmospheric Chemistry and Physics, 18, 705-733, doi:10.5194/acp-18-705-2018, 2018.

Apendix 3: Supplementary Information for Chapter 4

This contains supplementary material for Chapter 4: Pan-European rural atmospheric monitoring network shows dominance of NH_3 gas and NH_4NO_3 aerosol in inorganic pollution load. Y. Sim Tang et al. Supplement of Atmos. Chem. Phys., https://www.atmos-chem-phys-discuss.net/acp-2020-275/.

.

List of Supplementary Figures:

Figure S4.1: Scatter plots comparing atmospheric gas (NH_3, HNO_3, SO_2 and HCl) and aerosol (NH_4^+, NO_3^-, SO_4^{2-}, Cl^-, Na^+, Ca^{2+}, Mg^{2+}) concentrations measured by each of the NEU laboratories with the median estimate of all laboratories for field inter-comparisons conducted between 2007 – 2009 only. Data from the 2006 inter-comparisons are excluded in this analysis, to compare with Figure 6 in main text which included all periods. A summary of the regression results is shown in the table below the graphs. Note (i) There are fewer data points for INRAE because they joined the NEU network later in 2007 and participated in the 2008 and 2009 inter-comaprisons only. (ii) Low number of observations in some cases were due to some laboratories not reporting all parameters. NILU: HCl, Cl^-, Na^+, Ca^{2+} and Mg^{2+} reported for 2008 inter-comparisons only.

Figure S4.2: (TOP) Scatter plots and (BOTTOM) summary statistics of regression analyses between national annual averaged gas (NH_3, HNO_3, SO_2) and aerosol (NH_4^+, NO_3^-, SO_4^{2-}) concentrations, and the national emission densities of NH_3-N (upper plots), NO_x-N (middle plots) and SO_2-S (lower plots) (expressed as emissions per unit area of the country per year, averaged over the 4-year period 2007 to 2010) for each of the 20 countries in the NEU DELTA® network.

Figure S4.3: (TOP) Scatter plots and (BOTTOM) summary statistics of regression analyses between annual averaged gas (NH_3, HNO_3, SO_2) and aerosol (NH_4^+, NO_3^-, SO_4^{2-}) concentrations at each NEU DELTA® site, and the emissions of NH_3-N (upper plots), NO_x-N (middle plots) and SO_2-S (lower plots) from individual EMEP grids (0.1º x 0.1º) containing the site (emissions expressed per EMEP grid, averaged over the 4-year period 2007 to 2010).

Figure S4.4: (TOP) Scatter plots and (BOTTOM) summary statistics of regression analyses between annual averaged gas (NH_3, HNO_3, SO_2) and aerosol (NH_4^+, NO_3^-, SO_4^{2-}) concentrations at each NEU DELTA® site, and the averaged emissions of 4 EMEP grids (each grid = 0.1º x 0.1º, emissions expressed per EMEP grid, averaged over the 4-year period 2007 to 2010) surrounding each site, of NH_3-N (upper plots), NO_x-N (middle plots) and SO_2-S (lower plots)

Figure S4.5: Regression plots between molar concentrations of Na^+ and Cl^-, with analysis grouped by sites with measurements made by each of the seven laboratories, NILU (*n* = 16), CEAM (*n* = 3), INRAE (*n* = 10), MHSC (*n* = 9), SHMU (*n* = 9), UKCEH (*n* = 5) and VTI (*n* = 12). In each case, the same plots are also shown on a log scale, to improve visualisation of data points at the lower concentrations. Each data point is the monthly measured concentration at individual sites.

[Appendix III]

List of Supplementary Tables:

Table S4.1: Details of all sites in the NEU DELTA® network.

Table S4.2: Details of sites in the NEU Wet Deposition Network.

Table S4.3: Summary statistics on denuder capture efficiencies for atmospheric NH_3 gas by the 7 laboratories from DELTA inter-comparisons conducted at 4 different field test sites for all years (2006 – 2010).

Table S4.4: Annual mean NH_3 gas concentrations measured in the NEU DELTA® network and summary statistics.

Table S4.5: Annual average NH_3 concentration measured in the NEU 1 DELTA® network and comparison with UNECE critical levels of NH_3 concentrations (annual mean), showing percentage exceedances for all sites and according to sites grouped by ecosystem type.

Table S4.6: Annual mean particulate NH_4^+ concentrations measured in the NEU DELTA® network and summary statistics.

Table S4.7: Annual mean HNO_3 gas concentrations measured in the NEU DELTA® network and summary statistics.

Table S4.8: Annual mean particulate NO_3^- concentrations measured in the NEU DELTA® network and summary statistics.

Table S4.9: Annual mean SO_2 gas concentrations measured in the NEU DELTA® network and summary statistics.

Table S4.10: Annual mean particulate SO_4^{2-} concentrations measured in the NEU DELTA® network and summary statistics.

Table S4.11: Annual mean HCl gas concentrations measured in the NEU DELTA® network and summary statistics.

Table S4.12: Annual mean particulate Cl^- concentrations measured in the NEU DELTA® network and summary statistics.

Table S4.13: Annual mean particulate Na^+ concentrations measured in the NEU DELTA® network and summary statistics.

Table S14: Annual wet deposition of inorganic components (kg ha^{-1} yr^{-1}) estimated from Rotenkamp bulk precipitation collectors in the NEU bulk wet deposition network and percentage composition by mass measured. The data shown are 2-year averaged deposition, made between 2008 and 2010, except at 5 sites with 1 year of measurement only (BE-Vie, FR-Fgs, FR-LBr, DE-Wet, IT-BCi).

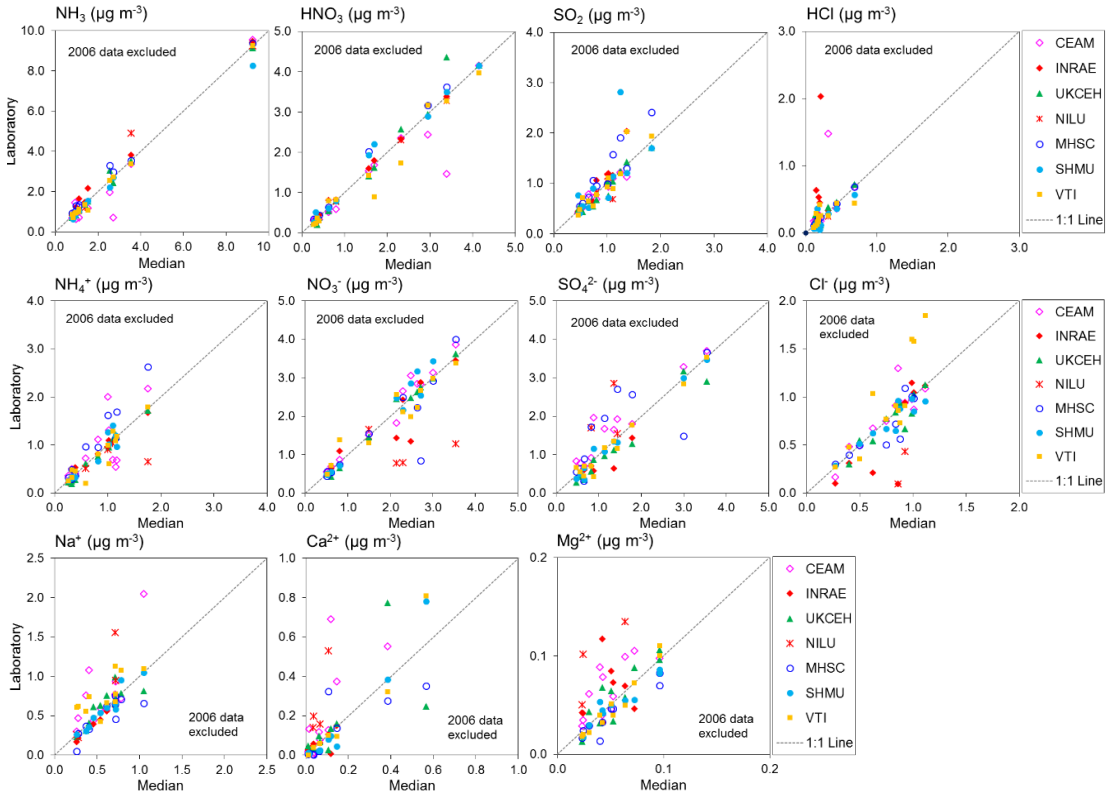

Lab	Gas: NH_3			Gas: HNO_3			Gas: SO_2			Gas: HCl		
	R^2	slope	*n*	R^2	slope	*n*	R^2	slope	*n*	R^2	slope	*n*
CEAM	0.94	1.02	12	0.83	0.81	12	0.90	0.85	11	0.88	0.92	11
INRAE	0.99	1.00	8	0.99	0.99	8	0.88	1.25	7	0.02	1.73	8
UKCEH	1.00	0.99	12	0.97	1.12	12	0.94	0.97	12	0.88	1.03	12
NILU	0.97	1.00	4	1.00	0.96	4	0.00	0.02	4	0.08	0.79	3
MHSC	0.99	0.99	10	0.99	1.16	9	0.86	1.33	10	0.99	1.02	10
SHMU	1.00	0.89	10	0.98	0.99	10	0.80	1.10	10	0.74	0.84	10
VTI	1.00	1.00	12	0.95	0.96	12	0.84	1.19	12	0.54	0.58	12

Lab	Particle: NH_4^+			Particle: NO_3^-			Particle: SO_4^{2-}			Particle: Cl^-		
	R^2	slope	*n*	R^2	slope	*n*	R^2	slope	*n*	R^2	slope	*n*
CEAM	0.51	0.97	12	0.97	1.08	12	0.91	0.96	12	0.78	1.03	12
INRAE	0.98	0.93	8	0.77	0.86	8	0.75	0.75	8	0.64	1.24	8
UKCEH	0.99	1.06	12	0.99	1.05	11	0.95	0.93	11	0.83	0.98	10
NILU	0.01*	0.06*	4	0.03	-0.08	4	0.90	1.63	3	-	-	2
MHSC	0.93	1.48	10	0.97	1.05	9	0.54	0.75	10	0.74	0.92	9
SHMU	0.88	1.08	10	0.96	1.14	10	0.98	1.00	10	0.86	0.83	10
VTI	0.86	0.99	12	0.91	0.86	11	0.97	0.99	12	0.73	1.62	12

Lab	Particle: Na^+			Particle: Ca^{2+}			Particle: Mg^{2+}		
	R^2	slope	*n*	R^2	slope	*n*	R^2	slope	*n*
CEAM	0.20	0.54	11	0.52	1.60	11	0.55	0.94	11
INRAE	0.99	0.99	8	0.39	0.57	8	0.04	0.33	8
UKCEH	0.67	0.84	11	0.47	0.85	11	0.82	1.09	12
NILU	0.84	2.24	4	0.78	4.85	4	0.47	2.49	4
MHSC	0.74	0.78	9	0.67	0.64	10	0.88	0.79	9
SHMU	0.91	1.05	10	0.95	1.33	10	0.90	0.78	10
VTI	0.51	0.70	11	0.93	1.31	8	0.96	1.18	11

*regression line excluding one outlier; $Y = 0.98x - 0.06$, $R^2 = 1.00$

Figure S4.1: Scatter plots comparing atmospheric gas (NH_3, HNO_3, SO_2 and HCl) and aerosol (NH_4^+, NO_3^-, SO_4^{2-}, Cl^-, Na^+, Ca^{2+}, Mg^{2+}) concentrations measured by each of the NEU laboratories with the median estimate of all laboratories for field inter-comparisons conducted between 2007 – 2009 only. Data from the 2006 inter-comparisons are excluded in this analysis, to compare with Figure 6 in main text which included all periods. A summary of the regression results is shown in the table below the graphs. Note (i) There are fewer data points for INRAE because they joined the NEU network later in 2007 and participated in the 2008 and 2009 inter-comaprisons only. (ii) Low number of observations in some cases were due to some laboratories not reporting all parameters. NILU: HCl, Cl^-, Na^+, Ca^{2+} and Mg^{2+} reported for 2008 inter-comparisons only.

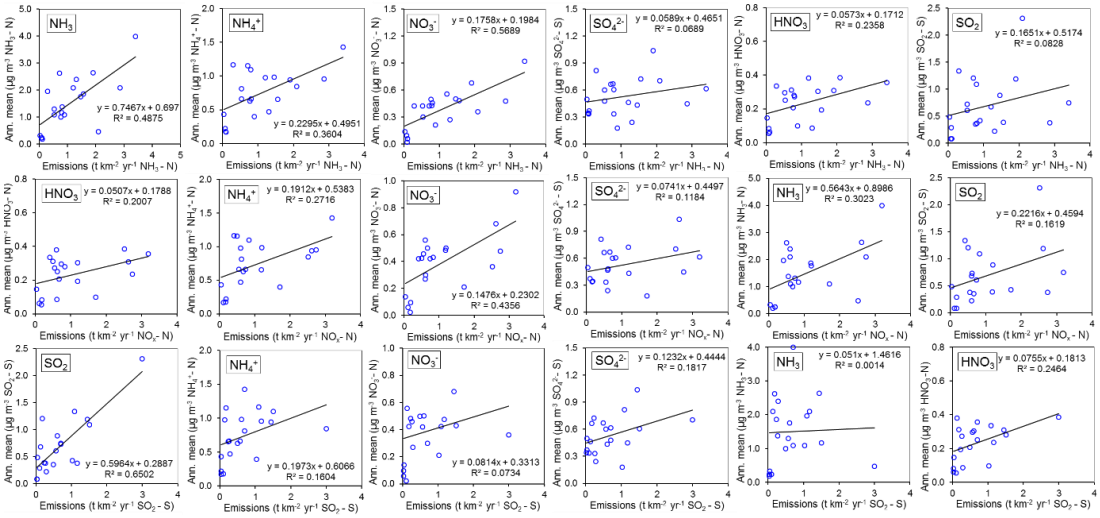

National annual average (n = 20)	4-year averaged national emission densities (2007 – 2010, 20 countries)								
	NH_3 (tonnes N km^{-2} yr^{-1})			NO_x (tonnes N km^{-2} yr^{-1})			SO_2 (tonnes S km^{-2} yr^{-1})		
(µg m^{-3})	slope	intercept	R^2	slope	intercept	R^2	slope	intercept	R^2
Gas NH_3 - N	0.75	0.70	0.49***	0.57	0.90	0.30*	0.05	1.46	0.00^{ns}
Gas HNO_3 - N	0.06	0.17	0.24*	0.05	0.18	0.20*	0.08	0.18	0.25*
Gas SO_2 - S	0.17	0.52	0.24^{ns}	0.22	0.46	0.16^{ns}	0.60	0.29	0.65***
Aerosol NH_4 - N	0.23	0.50	0.36**	0.19	0.54	0.27*	0.20	0.61	0.16^{ns}
Aerosol NO_3^- - N	0.18	0.20	0.57***	0.15	0.23	0.44**	0.08	0.33	0.07^{ns}
Aerosol SO_4^{2-} - S	0.06	0.47	0.07^{ns}	0.07	0.45	0.12^{ns}	0.12	0.44	0.18^{ns}

Figure S4.2: (TOP) Scatter plots and (BOTTOM) summary statistics of regression analyses between national annual averaged gas (NH_3, HNO_3, SO_2) and aerosol (NH_4^+, NO_3^-, SO_4^{2-}) concentrations, and the national emission densities of NH_3-N (upper plots), NO_x-N (middle plots) and SO_2-S (lower plots) (expressed as emissions per unit area of the country per year, averaged over the 4-year period 2007 to 2010) for each of the 20 countries in the NEU DELTA® network.

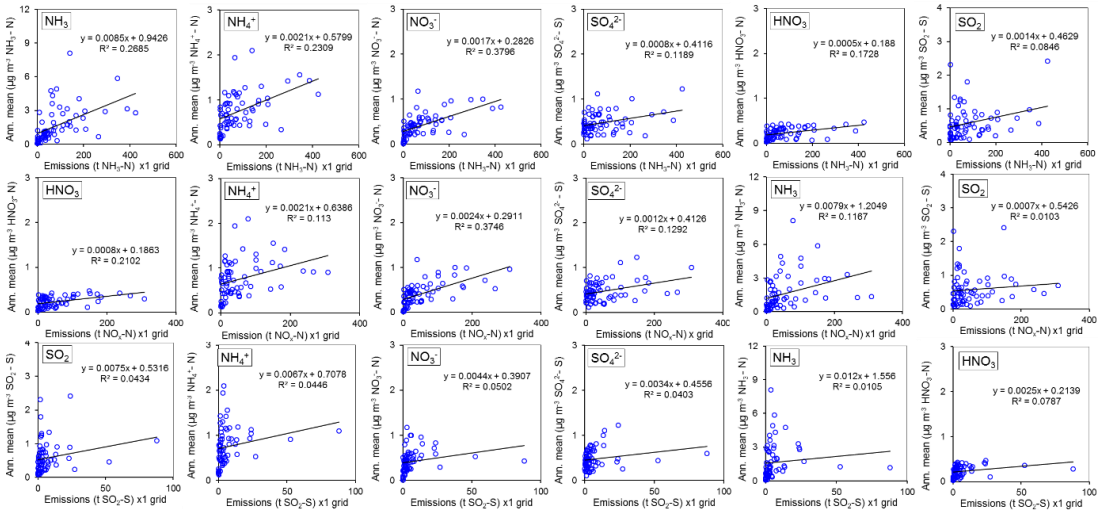

Site annual average (n = 66)	4-year averaged emissions (2007 – 2010) from single EMEP grid (0.1º x 0.1º) containing monitoring site								
	NH_3 (tonnes N yr^{-1})			NO_x (tonnes N yr^{-1})			SO_2 (tonnes yr^{-1})		
(µg m^{-3})	slope	intercept	R^2	slope	intercept	R^2	slope	intercept	R^2
Gas NH_3 - N	0.0085	0.94	0.27***	0.0079	1.2	0.12**	0.0120	1.56	0.01^{ns}
Gas HNO_3 - N	0.0005	0.19	0.17***	0.0008	0.19	0.21***	0.0025	0.21	0.08*
Gas SO_2 - S	0.0014	0.46	0.08*	0.0007	0.54	0.01^{ns}	0.0075	0.53	0.04^{ns}
Aerosol NH_4 - N^+	0.0021	0.58	0.23***	0.0021	0.64	0.11**	0.0067	0.71	0.04^{ns}
Aerosol NO_3^- - N	0.0017	0.28	0.38***	0.0024	0.29	0.37***	0.0044	0.39	0.05^{ns}
Aerosol SO_4^{2-} - S	0.0008	0.41	0.12**	0.0012	0.41	0.13**	0.0034	0.46	0.04^{ns}

Figure S4.3: (TOP) Scatter plots and (BOTTOM) summary statistics of regression analyses between annual averaged gas (NH_3, HNO_3, SO_2) and aerosol (NH_4^+, NO_3^-, SO_4^{2-}) concentrations at each NEU DELTA® site, and the emissions of NH_3-N (upper plots), NO_x-N (middle plots) and SO_2-S (lower plots) from individual EMEP grids (0.1º x 0.1º) containing the site (emissions expressed per EMEP grid, averaged over the 4-year period 2007 to 2010).

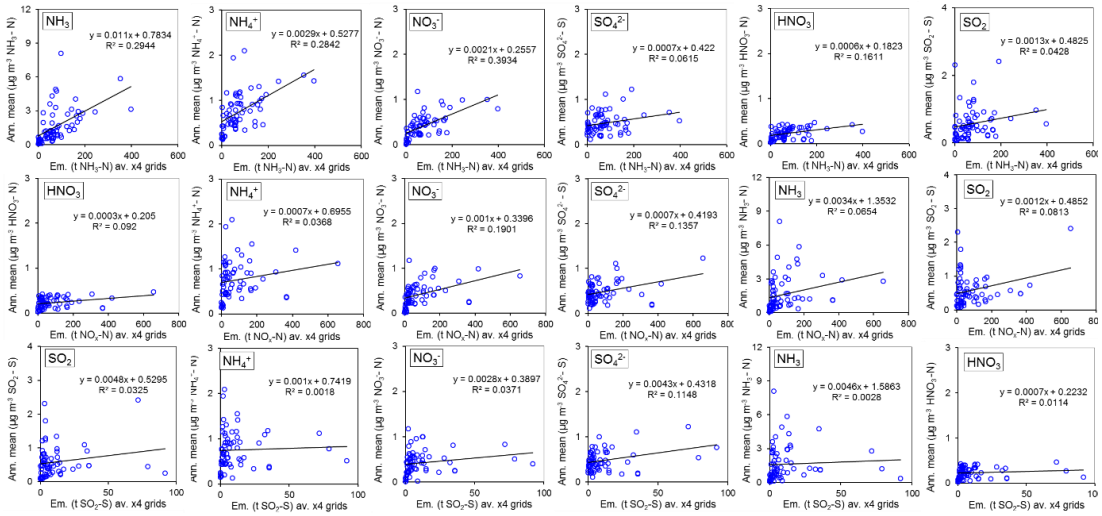

Site annual average (n = 66)	4-year averaged emissions (2007 – 2010) from 4 x EMEP grids (each = 0.1º x 0.1º) surrounding each site								
	NH_3 (tonnes N km^{-2} yr^{-1})			NO_x (tonnes N km^{-2} yr^{-1})			SO_2 (tonnes S km^{-2} yr^{-1})		
(µg m^{-3})	slope	intercept	R^2	slope	intercept	R^2	slope	intercept	R^2
Gas NH_3 - N	0.0110	0.78	0.29***	0.0034	1.35	0.07*	0.0046	1.59	0.00^{ns}
Gas HNO_3 - N	0.0006	0.18	0.16***	0.0003	0.21	0.09*	0.0007	0.22	0.01^{ns}
Gas SO_2 - S	0.0013	0.48	0.04^{ns}	0.0012	0.49	0.08*	0.0048	0.53	0.03^{ns}
Aerosol NH_4 - N^+	0.0029	0.53	0.28***	0.0007	0.70	0.04^{ns}	0.0010	0.74	0.00^{ns}
Aerosol NO_3^- - N	0.0021	0.26	0.39***	0.0010	0.34	0.19***	0.0028	0.39	0.04^{ns}
Aerosol SO_4^{2-} - S	0.0007	0.42	0.06*	0.0007	0.42	0.14**	0.0043	0.43	0.11**

Figure S4.4: (TOP) Scatter plots and (BOTTOM) summary statistics of regression analyses between annual averaged gas (NH_3, HNO_3, SO_2) and aerosol (NH_4^+, NO_3^-, SO_4^{2-}) concentrations at each NEU DELTA® site, and the averaged emissions of 4 EMEP grids (each grid = 0.1º x 0.1º, emissions expressed per EMEP grid, averaged over the 4-year period 2007 to 2010) surrounding each site, of NH_3-N (upper plots), NO_x-N (middle plots) and SO_2-S (lower plots)

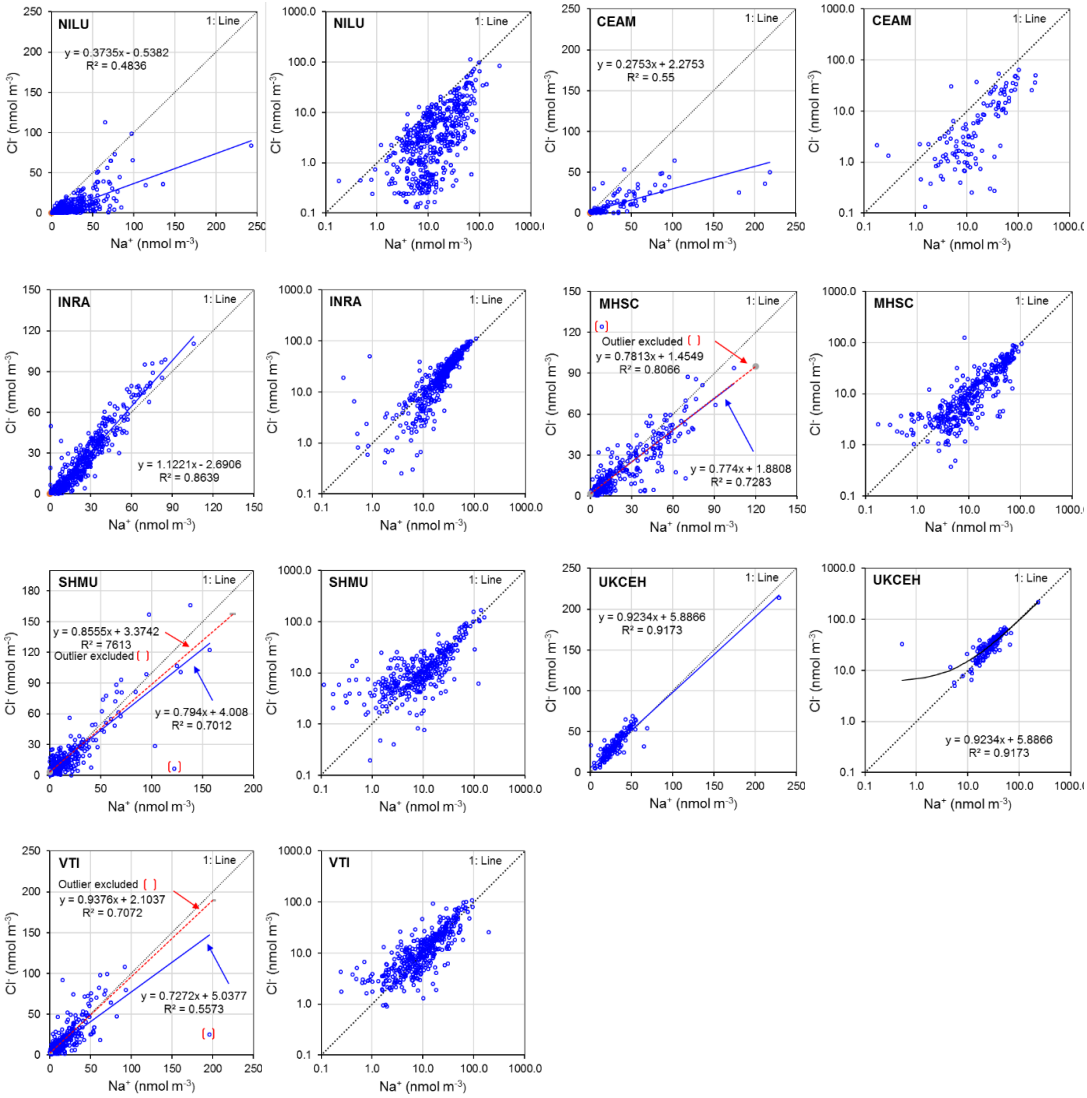

Figure S4.5: Regression plots between molar concentrations of Na^+ and Cl^-, with analysis grouped by sites with measurements made by each of the seven laboratories, NILU (*n* = 16), CEAM (*n* = 3), INRAE (*n* = 10), MHSC (*n* = 9), SHMU (*n* = 9), UKCEH (*n* = 5) and VTI (*n* = 12). In each case, the same plots are also shown on a log scale, to improve visualisation of data points at the lower concentrations. Each data point is the monthly measured concentration at individual sites.

Table S4.1: Details of all sites in the NEU DELTA® network.

Site no.	Site name	Site Code	Lat. (°N)	Long. (°E)	Ecosystem Type	Host organisation	START	END
1	Hainich	DE-Hai	51.0792	10.4519	Forests	Max-Planck-Institut für Biogeochemie	21/02/07	04/01/11
2	Wetzstein	DE-Wet	50.4533	11.4575	Forests		22/02/07	05/01/11
3	Gebesee	DE-Geb	51.1000	10.9142	Crops		21/02/07	05/01/11
4	Tharandt	DE-Tha	50.9636	13.5669	Forests	Technical University Dresden	07/02/07	28/12/10
5	Grillenburg	DE-Gri	50.9494	13.5125	Grassland		07/02/07	28/12/10
6	Klingenberg	DE-Kli	50.8931	13.5222	Crops		07/02/07	28/12/10
7	Hoglwald	DE-Hog	48.3000	11.1000	Forests	FZK/IMK-IFU	28/02/07	10/01/11
8	Mitra II	PT-Mi1	38.5406	-8.0000	Forests	Lisbon University	01/12/06	24/01/11
9	Petrodolinskoye	UA-Pet	46.5000	30.3000	Crops	Odessa National University	01/12/06	28/12/10
10	Renon	IT-Ren	46.5878	11.4347	Forests	Autonome Provinz Bozen	03/01/07	03/01/11
11	Fyodorovskoe bog	RU-Fyo	56.4617	32.9239	Forests	Russian Academy of Sciences	01/12/06	01/01/11
12	Espirra	PT-Esp	38.6392	-8.6017	Forests	Instituto Superior Technico Lisboa	09/01/07	04/01/11
13	BKFORES	CZ-BK1	49.5025	18.5383	Forests	Inst. Systems Biology & Ecology	08/11/06	04/01/11
14	Bugac	HU-Bug	46.6917	19.6017	Semi-nat	Hungarian Met.Service	13/11/06	05/01/11
15	POLWET	PL-Pol	52.7622	16.3094	Semi-nat	University of Poznan	10/11/06	03/01/11
16	Oensingen	CH-Oe1	47.2856	7.7319	Grassland	VTI (von Thunen Institut)	03/11/06	03/01/11
17	Laegern	CH-Lae	47.4778	8.3653	Forests	ETH	07/11/06	03/01/11
18	Monte Bondone	IT-MBo	46.0294	11.0828	Semi-nat	Centro di Ecologia Alpina	01/12/06	21/01/11
19	Piana del Sele (Borgo Cioffi)	IT-BCi	40.5236	14.9572	Crops	CNR ISAFom	05/12/06	03/01/11
20	Hesse	FR-Hes	48.6742	7.0656	Forests	INRAE7UHP	19/02/07	10/01/11
21	Dripsey	IE-Dri	51.9867	-8.7517	Grassland	University College Cork	01/12/06	03/06/10
22	Grignon	FR-Gri	48.8439	1.9522	Crops	INRAE7INAPG	29/11/06	20/01/11
23	Fontainebleau	FR-Fon	48.4761	2.7800	Forests	Université Paris-Sud	29/11/06	07/01/11
24	Le Bray	FR-LBr	44.7172	-0.7689	Forests	INRAE Bordeaux	14/12/06	24/01/09
25	Laqueuille	FR-Lq2	45.6392	2.7369	Grassland	INRAE	09/11/06	07/01/11
26	Puechabon	FR-Pue	43.7414	3.5958	Forests	Dream CEFE-CNR	27/10/06	28/12/10
27	Griffin	UK-Gri	56.6167	-3.8000	Forests	University of Edinburgh	06/12/06	19/11/08
28	East Saltoun	UK-ESa	55.9000	-2.8380	Crops		07/11/06	21/10/08
29	Carlow	IE-Ca2	52.8500	-6.9000	Grassland	Trinity College Dublin	01/11/06	05/01/11
30	Soroe	DK-Sor	55.4869	11.6458	Forests	RISOE	31/10/06	15/12/10
31	Sodankyla	FI-Sod	67.3617	26.6378	Forests	Finnish Meteorological Institute	27/11/06	17/01/11
32	Kaamanen	FI-Kaa	69.1407	27.2833	Semi-nat		02/01/09	02/10/09
33	Lompolojänkkä	FI-Lom	68.2144	24.3531	Semi-nat		04/11/06	29/11/06
34	Rimi	DK-Lva	55.6953	12.1178	Grassland	RISOE	30/10/06	11/03/09
35	Risbyholm	DK-Ris	55.5303	12.0972	Crops	Geografisk Institut	30/11/06	04/08/08
36	Norunda	SE-Nor	60.0833	17.4667	Forests	Dept Physical Geography & Ecosystems Analysis	14/11/06	10/12/10
37	Skyttorp	SE-Sk2	60.1294	17.8400	Forests		11/01/07	02/12/08
38	Braschaat	BE-Bra	51.3092	4.5206	Forests	University of Antwerpen	31/10/06	04/01/11
39	Vielsalm	BE-Vie	50.3053	5.9967	Forests	Faculté universitaire des Sciences agronomiques de Gembloux	09/11/06	03/02/11
40	Lonzee	BE-Lon	50.5519	4.7447	Crops		10/11/06	27/01/11
41	Hyytiälä	FI-Hyy	61.8475	24.2950	Forests	University of Helsinki	01/12/06	09/12/10
42	Roccarespampani	IT-Ro2	42.3900	11.9208	Forests	University of Tuscia	01/12/06	05/01/11
43	Cabauw	NL-Ca1	51.9708	4.9269	Grassland	ECN (Energy Research, Netherlands)	31/01/07	29/12/10
44	Horstermeer	NL-Hor	52.0289	5.0675	Semi-nat	Universiteit Amsterdam	13/03/07	04/01/11
45	Speulder	NL-Spe	52.2523	5.6905	Forests	ECN	09/11/06	29/11/10
46	Amplero	IT-Amp	41.9039	13.6050	Semi-nat	University of Tuscia	01/12/06	24/09/08
47	Collelongo	IT-Col	41.8494	13.5881	Forests		14/12/06	20/01/11
48	San Rossore	IT-SRo	43.7278	10.2844	Forests	DC-DG JRC (Joint Research Centre, Italy)	01/02/07	12/01/11
49	Po Valley Pavia	IT-PoV	45.0628	8.6683	Crops		12/12/06	12/01/11
50	Loobos	NL-Loo	52.1678	5.7439	Forests	Alterra	14/12/06	14/01/11
51	SK04 Stara Lesna	SK04	49.1500	20.2833	Grassland	SHMU (Slovak Hydrometeorological Institute)	08/11/06	04/01/11
51P	SK04 Stara Lesna Parallel	SK04P	49.1500	20.2833	Grassland		08/11/06	04/01/11
52	SK06 Starina	SK06	49.0500	22.2667	Grassland		08/11/06	04/01/11
53	SK07 Topolniky	SK07	47.9667	17.8667	Grassland		31/10/06	03/01/11
54	El Saler	ES-ES1	39.3458	-0.3186	Forests	CEAM Fundación Centro de Estudios Ambientales del Mediterráneo	14/03/07	12/01/11
55	Vall de Aliñá	ES-VDA	42.1519	1.4483	Semi-natural		01/03/07	15/01/11
56	Las Majadas del Tietar (Caceres)	ES-LMa	39.9414	-5.7733	Forests		13/03/07	20/01/11
57	Auchencorth	UK-AMo	55.7917	-3.2389	Semi-nat	UKCEH (UK Centre for Ecology & Hydrology)	01/11/06	05/01/11
57B	Auchencorth	UK-AMoP	55.7917	-3.2389	Semi-nat		01/11/06	05/01/11
58	Easter Bush	UK-EBu	55.8658	-3.2056	Grassland		01/11/06	05/01/11
58P	Easter Bush P	UK-EBu	55.8658	-3.2056	Grassland		01/11/06	01/03/10
59	Mehrstedt	DE-Meh	51.2761	10.6572	Forests	Max-Planck-Institut für Biogeochemie	13/08/07	05/01/11
60	Fougeres	FR-Fgs	48.3830	-1.1847	Forests	INRAE	05/08/08	05/01/11
60P	Fougeres Parallel	FR-FgsP	48.3830	-1.1847	Forests		10/02/10	05/01/11
61	Solohead	UK-Sol	52.5100	-8.2100	Forests		26/11/08	05/01/11
62	Birkenes	NO-Bir	58.3833	8.2500	Forests	Dept Physical Geography & Ecosystems Analysis	01/01/09	01/01/10
63	Brandbjerg	DK-Bra	55.8833	11.9667	Semi-nat	RISOE	08/04/09	13/12/10
64	Bilos	FR-Bil	44.5217	-0.8960	Forests	INRAE Bordeaux	01/10/09	12/01/11

Table S4.2: Details of sites in the NEU Wet Deposition Network.

Site no.	Site name	Site Code	Lat. (°N)	Long. (°E)	Ecosystem Type	Host organisation	START	END
1	Hainich	DE-Hai	51.0792	10.4519	Forests	Max-Planck-Institut für Biogeochemie	04/12/08	11/01/11
2	Wetzstein	DE-Wet	50.4533	11.4575	Forests		19/02/08	12/01/11
5	Grillenburg	DE-Gri	50.9494	13.5125	Grassland		02/12/08	28/12/10
8	Mitra II	PT-Mi1	38.5406	-8.0000	Forests	Lisbon University	08/02/08	09/03/10
15	POLWET	PL-wet	52.7622	16.3094	Semi-natural	University of Poznan	30/01/08	16/02/11
17	Laegern	CH-Lae	47.4778	8.3653	Forests	ETH	29/01/08	03/01/11
19	Piana del Sele (Borgo Cioffi)	IT-BCi	40.5236	14.9572	Crops	CNR ISAFom	28/10/08	23/04/10
23	Fontainebleau	FR-Fon	48.4761	2.7800	Forests	Université Paris-Sud	30/01/08	03/11/10
24	Le Bray	FR-LBr	44.7172	-0.7689	Forests	INRAE Bordeaux	01/02/08	05/01/09
26	Puechabon	FR-Pue	43.7414	3.5958	Forests	Dream CEFE-CNR	01/02/08	28/12/10
39	Vielsalm	BE-Vie	50.3053	5.9967	Forests	Faculté universitaire des Sciences agronomiques de Gembloux	30/01/08	03/02/11
42	Roccarespampani	IT-Ro2	42.3900	11.9208	Forests	University of Tuscia	03/09/08	05/01/11
48	San Rossore	IT-SR	43.7278	10.2844	Forests	DC-DG JRC	19/12/07	12/01/11
54	El Saler)	ES-ES1	39.3458	-0.3186	Forests	CEAM	18/12/07	01/12/09
55	Vall de Alinà	ES-VDA	42.1519	1.4483	Semi-natural		28/02/08	15/01/11
56	Las Majadas del Tietar (Caceres)	ES-LMa	39.9414	-5.7733	Forests		20/02/07	20/01/11
60	Fougeres	FR-Fgs	48.3830	-1.1847	Forests	INRAE	23/06/09	31/08/10
64	Bilos	FR-Bil	44.5217	-0.8960	Forests	INRAE Bordeaux	01/10/09	12/01/11

Table S4.3: Summary statistics on denuder capture efficiencies for atmospheric NH_3 gas by the 7 laboratories from DELTA inter-comparisons conducted at 4 different field test sites for all years (2006 – 2010).

	Denuder capture Efficiency (%) NH_3				Denuder capture Efficiency (%) NH_3			
	4 years (2006 - 2009)				3 years (2007 - 2009)			
	mean	min	max	N	mean	min	max	N
VTI	95	65	99	10	95	65	99	10
MHSC	88	67	100	41	91	77	99	12
UKCEH	90	58	99	42	91	58	99	13
CEAM	82	49	100	41	78	49	100	13
NILU	92	81	105	30	89	84	98	5
SHMU	93	47	100	38	87	47	96	11
INRAE	97	94	99	8	97	94	99	8
Mean all	91				90			

VTI: denuder capture efficiencies reported for 2008 and 2009 periods only. INRAE: 2009 period only.

Table S4.4: Annual mean NH_3 gas concentrations measured in the NEU DELTA® network and summary statistics.

Site	Ecosystem type	NH_3-N (µg m^{-3})				Summary statistics					Group Mean
		2007	2008	2009	2010	mean	min	max	sd	N	
UK-ESa	Crops	4.30	1.40	-	-	2.85	1.40	4.30	2.05	2	
DE-Geb	Crops	8.78	2.87	3.22	4.79	4.92	2.87	8.78	2.71	4	
FR-Gri	Crops	3.00	3.33	4.19	2.72	3.31	2.72	4.19	0.64	4	
DE-Kli	Crops	1.81	1.48	1.60	1.31	1.55	1.31	1.81	0.21	4	
BE-Lon	Crops	4.33	3.44	7.34	3.88	4.75	3.44	7.34	1.77	4	
UA-Pet	Crops	2.07	2.93	1.61	1.24	1.96	1.24	2.93	0.73	4	
IT-BCi	Crops	6.82	7.53	10.89	7.20	8.11	6.82	10.89	1.88	4	
IT-PoV	Crops	3.49	3.35	4.16	3.54	3.64	3.35	4.16	0.36	4	
DK-Ris	Crops	3.59	5.07	-	-	4.33	3.59	5.07	1.05	2	
SK07	Crops	2.73	3.98	1.99	2.16	2.72	1.99	3.98	0.90	4	**3.81**
FR-Bil	Forest	-	-	-	0.43	0.43	0.43	0.43	-	1	
NO-Bir	Forest	-	-	0.25	0.23	0.24	0.23	0.25	0.01	2	
CZ-BK1	Forest	0.46	0.55	-	0.41	0.47	0.41	0.55	0.07	3	
BE-Bra	Forest	2.75	2.68	3.20	2.57	2.80	2.57	3.20	0.28	4	
IT-Col	Forest	-	0.45	0.74	0.51	0.57	0.45	0.74	0.15	3	
ES-ES1	Forest	1.56	1.56	1.34	0.92	1.35	0.92	1.56	0.30	4	
PT-Esp	Forest	2.12	1.61	1.61	1.42	1.69	1.42	2.12	0.30	4	
FR-Fon	Forest	1.01	0.80	1.17	1.14	1.03	0.80	1.17	0.17	4	
FR-Fgs	Forest	-	-	2.00	2.01	2.01	2.00	2.01	0.01	2	
FR-FgsP	Forest	-	-	-	1.93	1.93	1.93	1.93	-	1	
RU-Fyo	Forest	0.26	0.29	0.42	0.32	0.32	0.26	0.42	0.07	4	
UK-Gri	Forest	0.13	-	-	-	0.13	0.13	0.13	-	1	
DE-Hai	Forest	0.74	0.67	1.07	1.07	0.89	0.67	1.07	0.21	4	
FR-Hes	Forest	1.02	0.77	0.91	0.81	0.88	0.77	1.02	0.11	4	
DE-Hog	Forest	2.31	2.28	3.18	2.47	2.56	2.28	3.18	0.42	4	
FI-Hyy	Forest	0.07	0.07	0.10	0.11	0.09	0.07	0.11	0.02	4	
CH-Lae	Forest	1.15	1.12	1.48	1.27	1.26	1.12	1.48	0.16	4	
ES-LMa	Forest	1.29	0.82	1.06	0.71	0.97	0.71	1.29	0.26	4	
FR-LBr	Forest	0.97	1.31	-	-	1.14	0.97	1.31	0.24	2	
NL-Loo	Forest	4.04	2.89	3.19	2.50	3.16	2.50	4.04	0.65	4	
PT-Mi1	Forest	0.94	0.94	0.86	-	0.91	0.86	0.94	0.05	3	
SE-Nor	Forest	0.09	0.25	0.44	0.27	0.26	0.09	0.44	0.14	4	
FR-Pue	Forest	0.48	0.38	0.47	0.43	0.44	0.38	0.48	0.05	4	
FR-Ren	Forest	0.28	0.25	0.51	0.28	0.33	0.25	0.51	0.12	4	
IT-Ro2	Forest	1.55	2.13	1.53	1.29	1.63	1.29	2.13	0.36	4	
IT-SRo	Forest	1.04	0.65	2.54	0.58	1.20	0.58	2.54	0.91	4	
SK04	Forest	0.61	0.52	0.56	0.54	0.56	0.52	0.61	0.04	4	
SK04P	Forest	0.60	0.62	0.62	0.54	0.60	0.54	0.62	0.04	4	
SK06	Forest	0.45	0.51	0.50	0.55	0.50	0.45	0.55	0.04	4	
SE-Sk2	Forest	0.15	0.08	-	-	0.12	0.08	0.15	0.05	2	
FI-Sod	Forest	0.19	0.05	0.13	0.17	0.14	0.05	0.19	0.06	4	
DK-Sor	Forest	1.26	1.28	1.28	1.27	1.27	1.26	1.28	0.01	4	
NL-Spe	Forest	3.72	4.08	4.46	3.96	4.06	3.72	4.46	0.31	4	
DE-Tha	Forest	0.53	0.70	0.96	0.96	0.79	0.53	0.96	0.21	4	
BE-Vie	Forest	0.29	0.37	0.35	0.46	0.37	0.29	0.46	0.07	4	
DE-Wet	Forest	0.31	0.50	0.60	0.76	0.54	0.31	0.76	0.19	4	**1.04**
UK-EBu	Grass	1.34	0.76	0.91	1.39	1.10	0.76	1.39	0.31	4	
UK-EBuP	Grass	1.35	0.98	1.11	-	1.15	0.98	1.35	0.19	3	
NL-Ca1	Grass	6.29	5.60	5.85	5.75	5.87	5.60	6.29	0.30	4	
IE-Car	Grass	1.69	1.44	1.52	2.22	1.72	1.44	2.22	0.35	4	
IE-Dri	Grass	2.28	1.78	2.88	-	2.31	1.78	2.88	0.55	3	
DE-Gri	Grass	0.93	0.79	0.89	1.00	0.90	0.79	1.00	0.09	4	
FR-Lq2	Grass	1.14	1.09	1.45	1.36	1.26	1.09	1.45	0.17	4	
CH-Oe1	Grass	3.20	2.17	3.62	2.76	2.94	2.17	3.62	0.62	4	
DK-Rim	Grass	1.22	1.21	-	-	1.22	1.21	1.22	0.01	2	
UK-Sol	Grass	-	-	2.37	3.94	3.16	2.37	3.94	1.11	2	**2.16**
IT-Amp	Semi-Nat	0.52	0.61	-	-	0.57	0.52	0.61	0.06	2	
UK-AMo	Semi-Nat	0.64	0.61	0.72	0.69	0.67	0.61	0.72	0.05	4	
UK-AMoP	Semi-Nat	0.61	0.61	0.69	0.69	0.65	0.61	0.69	0.05	4	
DK-Brj	Semi-Nat	-	-	-	0.64	0.64	0.64	0.64	-	1	
HU-Bug	Semi-Nat	2.36	2.18	3.07	2.88	2.62	2.18	3.07	0.42	4	
NL-Hor	Semi-Nat	2.52	2.47	2.85	3.77	2.90	2.47	3.77	0.60	4	
FI-Kaa	Semi-Nat	-	-	1.01	0.29	0.65	0.29	1.01	0.51	2	
FI-Lom	Semi-Nat	0.06	0.06	0.09	0.08	0.07	0.06	0.09	0.02	4	
DE-Meh	Semi-Nat	-	1.80	1.73	2.25	1.93	1.73	2.25	0.28	3	
IT-MBo	Semi-Nat	0.76	0.71	0.82	0.66	0.74	0.66	0.82	0.07	4	
PL-Pol	Semi-Nat	1.12	0.78	1.82	0.95	1.17	0.78	1.82	0.46	4	
ES-VDA	Semi-Nat	-	0.61	0.83	0.63	0.69	0.61	0.83	0.12	3	**1.11**
	mean	1.75	1.55	1.87	1.58	1.63					
	min	0.06	0.05	0.09	0.08	0.07					
	max	8.78	7.53	10.89	7.20	8.11					
	n	58	60	57	58	68					

Table S4.5: Annual average NH_3 concentration measured in the NEU 1 DELTA® network and comparison with UNECE critical levels of NH_3 concentrations (annual mean), showing percentage exceedances for all sites and according to sites grouped by ecosystem type.

Country	ID	Ecosystem type	Annual averaged NH_3 (µg m^{-3})					% of sites in exceedance of UNECE Critical Levels of NH_3 concentrations (annual mean)
			mean	min	max	sd	N	
Germany	DE-Kli	Crops	1.88	1.59	2.20	0.26	4	**ALL sites (*n* = 64)**
Ukraine	UA-Pet	Crops	2.38	1.50	3.55	0.88	4	**mean = 1.98** µg NH_3 m^{-3}
Slovakia	SK07	Crops	3.30	2.42	4.84	1.09	4	> 1 µg NH_3 m^{-3} = 63 %
UK	UK-ESa	Crops	3.46	1.70	5.22	2.48	2	> 3 µg NH_3 m^{-3} = 27 %
France	FR-Gri	Crops	4.02	3.30	5.09	0.78	4	
Italy	IT-PoV	Crops	4.41	4.07	5.05	0.44	4	**Crops (*n* = 10)**
Denmark	DK-Ris	Crops	5.26	4.36	6.15	1.27	2	**mean = 4.63** µg NH_3 m^{-3}
Belgium	BE-Lon	Crops	5.77	4.18	8.92	2.15	4	> 1 µg NH_3 m^{-3} = 100 %
Germany	DE-Geb	Crops	5.97	3.49	10.66	3.29	4	> 3 µg NH_3 m^{-3} = 80 %
Italy	IT-BCi	Crops	9.85	8.28	13.22	2.28	4	
Finland	FI-Hyy	Forests	0.11	0.09	0.13	0.02	4	
Sweden	SE-Sk2	Forests	0.14	0.09	0.18	0.06	2	**Forests (*n* = 34)**
UK	UK-Gri	Forests	0.16	0.16	0.16	-	1	**mean = 1.27** µg NH_3 m^{-3}
Finland	FI-Sod	Forests	0.17	0.06	0.24	0.08	4	
Norway	NO-Bir	Forests	0.29	0.28	0.30	0.02	2	> 1 µg NH_3 m^{-3} = 50 %
Sweden	SE-Nor	Forests	0.32	0.11	0.54	0.17	4	> 3 µg NH_3 m^{-3} = 12 %
Russia	RU-Fyo	Forests	0.39	0.32	0.51	0.08	4	
France	FR-Ren	Forests	0.40	0.30	0.62	0.15	4	
Belgium	BE-Vie	Forests	0.45	0.35	0.56	0.09	4	*(SK04/SK04P and FR-Fgs/FR-FgsP = parallel measurements)*
France	FR-Bil	Forests	0.52	0.52	0.52	-	1	
France	FR-Pue	Forests	0.54	0.47	0.58	0.05	4	
Czech Rep.	CZ-BK1	Forests	0.58	0.50	0.67	0.09	3	
Slovakia	SK06	Forests	0.61	0.55	0.67	0.05	4	
Germany	DE-Wet	Forests	0.66	0.37	0.92	0.23	4	
Italy	IT-Col	Forests	0.68	0.63	0.74	0.05	4	
Slovakia	SK04	Forests	0.72	0.66	0.76	0.05	4	
Slovakia	SK04P	Forests	0.68	0.54	0.89	0.19	3	
Germany	DE-Tha	Forests	0.95	0.64	1.17	0.26	4	
France	FR-Hes	Forests	1.06	0.93	1.24	0.14	4	
Germany	DE-Hai	Forests	1.08	0.82	1.30	0.26	4	
Portugal	PT-Mi1	Forests	1.11	1.04	1.14	0.06	3	
Spain	ES-LMa	Forests	1.18	0.87	1.56	0.31	4	
France	FR-Fon	Forests	1.25	0.97	1.43	0.21	4	
France	FR-LBr	Forests	1.39	1.18	1.60	0.30	2	
Italy	IT-SR	Forests	1.47	0.71	3.09	1.11	4	
Switzerland	CH-Lae	Forests	1.52	1.36	1.79	0.20	4	
Denmark	DK-Sor	Forests	1.54	1.53	1.55	0.01	4	
Spain	ES-ES1	Forests	1.63	1.12	1.89	0.36	4	
Italy	IT-Ro2	Forests	1.97	1.57	2.59	0.43	4	
Portugal	PT-Esp	Forests	2.05	1.73	2.57	0.36	4	
France	FR-Fgs	Forests	2.43	2.43	2.44	0.01	2	
France	FR-FgsP	Forests	2.34	2.34	2.34	-	1	
Germany	DE-Hog	Forests	3.11	2.77	3.87	0.51	4	
Belgium	BE-Bra	Forests	3.40	3.12	3.89	0.34	4	
Netherlands	NL-Loo	Forests	3.83	3.04	4.91	0.80	4	
Netherlands	NL-Spe	Forests	4.92	4.52	5.42	0.38	4	
Germany	DE-Gri	Grass	1.10	0.96	1.21	0.10	4	
UK	UK-EBu	Grass	1.34	0.93	1.68	0.37	4	**Grassland (*n* = 9)**
UK	UK-EBuP	Grass	1.39	1.18	1.65	0.23	3	**mean = 2.62** µg NH_3 m^{-3}
Denmark	DK-Rim	Grass	1.47	1.46	1.48	0.01	2	
France	FR-Lq2	Grass	1.53	1.32	1.76	0.21	4	> 1 µg NH_3 m^{-3} = 100 %
Ireland	IE-Car	Grass	2.08	1.74	2.69	0.43	4	> 3 µg NH_3 m^{-3} = 33 %
Ireland	IE-Dri	Grass	2.81	2.16	3.50	0.67	3	
Switzerland	CH-Oe1	Grass	3.57	2.63	4.40	0.75	4	
UK	UK-Sol	Grass	3.83	2.88	4.79	1.35	2	*(UK-EBu/UK-EBuP = parallel measurement)*
Netherlands	NL-Ca1	Grass	7.13	6.80	7.64	0.36	4	
Finland	FI-Lom	Semi-Nat	0.09	0.07	0.11	0.02	4	
Italy	IT-Amp	Semi-Nat	0.69	0.63	0.74	0.08	2	**Semi-natural (SN) (*n* = 11)**
Denmark	DK-Brj	Semi-Nat	0.77	0.77	0.77	-	1	**mean = 1.34** µg NH_3 m^{-3}
Finland	FI-Kaa	Semi-Nat	0.79	0.35	1.22	0.62	2	
UK	UK-AMo	Semi-Nat	0.81	0.75	0.87	0.06	4	> 1 µg NH_3 m^{-3} = 36 %
UK	UK-AMoP	Semi-Nat	0.79	0.74	0.84	0.05	4	> 3 µg NH_3 m^{-3} = 18 %
Spain	ES-VDA	Semi-Nat	0.84	0.74	1.01	0.15	3	
Italy	IT-MBo	Semi-Nat	0.90	0.80	0.99	0.08	4	
Poland	PL-Pol	Semi-Nat	1.42	0.95	2.21	0.56	4	*(UK-AMo/UK-AMoP = parallel measurement)*
Germany	DE-Meh	Semi-Nat	2.34	2.10	2.73	0.34	3	
Hungary	HU-Bug	Semi-Nat	3.18	2.64	3.73	0.51	4	
Netherlands	NL-Hor	Semi-Nat	3.52	3.00	4.58	0.74	4	

Table S4.6: Annual mean particulate NH_4^+ concentrations measured in the NEU DELTA® network and summary statistics.

Site	Ecosystem type	NH_4^+-N (µg m^{-3})				Summary statistics					Group Mean
		2007	2008	2009	2010	mean	min	max	sd	N	
UK-ESa	Crops	0.99	0.41	-	-	0.70	0.41	0.99	0.41	2	
DE-Geb	Crops	1.13	1.05	1.25	1.17	1.15	1.05	1.25	0.08	4	
FR-Gri	Crops	1.15	0.73	0.97	0.86	0.93	0.73	1.15	0.18	4	
DE-Kli	Crops	1.06	1.05	1.06	1.11	1.07	1.05	1.11	0.03	4	
BE-Lon	Crops	1.01	0.82	1.32	1.58	1.18	0.82	1.58	0.34	4	
UA-Pet	Crops	1.16	1.70	0.91	0.89	1.17	0.89	1.70	0.38	4	
IT-BCi	Crops	1.38	1.33	0.83	0.98	1.13	0.83	1.38	0.27	4	
IT-PoV	Crops	2.53	2.22	1.58	1.44	1.94	1.44	2.53	0.52	4	
DK-Ris	Crops	0.49	0.62	-	-	0.56	0.49	0.62	0.09	2	
SK07	Crops	1.44	1.59	1.05	1.01	1.27	1.01	1.59	0.29	4	**1.11**
FR-Bil	Forest	-	-	-	0.38	0.38	0.38	0.38	-	1	
NO-Bir	Forest	-	-	0.21	0.23	0.22	0.21	0.23	0.01	2	
CZ-BK1	Forest	0.94	0.85	-	0.74	0.84	0.74	0.94	0.10	3	
BE-Bra	Forest	0.87	0.98	1.20	1.45	1.13	0.87	1.45	0.26	4	
IT-Col	Forest	-	0.48	0.52	0.39	0.46	0.39	0.52	0.07	3	
ES-ES1	Forest	0.77	1.03	1.02	0.77	0.90	0.77	1.03	0.15	4	
PT-Esp	Forest	1.03	0.67	0.51	0.70	0.73	0.51	1.03	0.22	4	
FR-Fon	Forest	1.14	0.79	0.94	0.82	0.92	0.79	1.14	0.16	4	
FR-Fgs	Forest	-	-	0.89	0.71	0.80	0.71	0.89	0.13	2	
FR-FgsP	Forest	-	-	-	0.69	0.69	0.69	0.69	-	1	
RU-Fyo	Forest	0.49	0.42	0.33	0.49	0.43	0.33	0.49	0.08	4	
UK-Gri	Forest	0.20	-	-	-	0.20	0.20	0.20	-	1	
DE-Hai	Forest	1.03	0.86	0.96	0.84	0.92	0.84	1.03	0.09	4	
FR-Hes	Forest	0.86	0.75	0.80	0.79	0.80	0.75	0.86	0.05	4	
DE-Hog	Forest	0.98	1.07	1.02	0.90	0.99	0.90	1.07	0.07	4	
FI-Hyy	Forest	0.17	0.09	0.19	0.25	0.18	0.09	0.25	0.07	4	
CH-Lae	Forest	1.12	0.77	0.85	0.90	0.91	0.77	1.12	0.15	4	
ES-LMa	Forest	0.37	0.54	0.47	0.50	0.47	0.37	0.54	0.07	4	
FR-LBr	Forest	0.69	0.48	-	-	0.59	0.48	0.69	0.15	2	
NL-Loo	Forest	1.60	1.60	1.34	1.18	1.43	1.18	1.60	0.21	4	
PT-Mi1	Forest	0.92	0.48	0.38	-	0.59	0.38	0.92	0.29	3	
SE-Nor	Forest	0.10	0.12	0.26	0.28	0.19	0.10	0.28	0.09	4	
FR-Pue	Forest	0.54	0.38	0.43	0.38	0.43	0.38	0.54	0.08	4	
FR-Ren	Forest	0.59	0.46	0.41	0.29	0.44	0.29	0.59	0.12	4	
IT-Ro2	Forest	0.83	0.81	0.70	0.70	0.76	0.70	0.83	0.07	4	
IT-SRo	Forest	0.85	0.94	0.65	0.68	0.78	0.65	0.94	0.14	4	
SK04	Forest	0.74	0.73	0.60	0.55	0.66	0.55	0.74	0.09	4	
SK04P	Forest	0.74	0.79	0.58	0.53	0.66	0.53	0.79	0.12	4	
SK06	Forest	0.75	0.69	0.60	0.60	0.66	0.60	0.75	0.07	4	
SE-Sk2	Forest	0.18	0.12	-	-	0.15	0.12	0.18	0.04	2	
FI-Sod	Forest	0.02	0.10	0.13	0.27	0.13	0.02	0.27	0.10	4	
DK-Sor	Forest	0.60	0.49	0.64	0.56	0.57	0.49	0.64	0.06	4	
NL-Spe	Forest	1.30	1.34	1.35	1.23	1.31	1.23	1.35	0.05	4	
DE-Tha	Forest	0.89	0.85	1.02	0.92	0.92	0.85	1.02	0.07	4	
BE-Vie	Forest	0.52	0.35	0.42	0.79	0.52	0.35	0.79	0.19	4	
DE-Wet	Forest	0.89	0.71	0.81	0.73	0.79	0.71	0.89	0.08	4	**0.65**
UK-EBu	Grass	0.44	0.33	0.38	0.30	0.36	0.30	0.44	0.06	4	
UK-EBuP	Grass	0.45	0.37	0.33	-	0.38	0.33	0.45	0.06	3	
NL-Ca1	Grass	1.92	1.47	1.40	1.44	1.56	1.40	1.92	0.24	4	
IE-Car	Grass	0.58	0.60	0.44	0.48	0.53	0.44	0.60	0.08	4	
IE-Dri	Grass	0.50	0.57	0.31	-	0.46	0.31	0.57	0.13	3	
DE-Gri	Grass	0.96	0.83	0.89	0.95	0.91	0.83	0.96	0.06	4	
FR-Lq2	Grass	0.54	0.36	0.45	0.39	0.44	0.36	0.54	0.08	4	
CH-Oe1	Grass	1.32	0.99	0.87	0.97	1.04	0.87	1.32	0.20	4	
DK-Rim	Grass	0.66	0.50	-	-	0.58	0.50	0.66	0.11	2	
UK-Sol	Grass	-	-	0.40	0.45	0.43	0.40	0.45	0.04	2	**0.67**
IT-Amp	Semi-Nat	0.50	0.46	-	-	0.48	0.46	0.50	0.03	2	
UK-AMo	Semi-Nat	0.42	0.33	0.32	0.28	0.34	0.28	0.42	0.06	4	
UK-AMoP	Semi-Nat	0.37	0.29	0.24	0.35	0.31	0.24	0.37	0.06	4	
DK-Brj	Semi-Nat	-	-	-	0.90	0.90	0.90	0.90	-	1	
HU-Bug	Semi-Nat	1.39	1.12	0.89	1.22	1.16	0.89	1.39	0.21	4	
NL-Hor	Semi-Nat	1.47	1.28	1.47	1.45	1.42	1.28	1.47	0.09	4	
FI-Kaa	Semi-Nat	-	-	0.34	0.16	0.25	0.16	0.34	0.13	2	
FI-Lom	Semi-Nat	0.24	0.08	0.05	0.22	0.15	0.05	0.24	0.10	4	
DE-Meh	Semi-Nat	-	1.15	1.13	1.09	1.12	1.09	1.15	0.03	3	
IT-MBo	Semi-Nat	0.82	0.66	0.55	0.64	0.67	0.55	0.82	0.11	4	
PL-Pol	Semi-Nat	1.30	0.90	0.96	1.22	1.10	0.90	1.30	0.19	4	
ES-VDA	Semi-Nat	-	0.52	0.40	0.62	0.51	0.40	0.62	0.11	3	**0.70**
	mean	0.84	0.75	0.72	0.75	0.73					
	min	0.02	0.08	0.05	0.16	0.13					
	max	2.53	2.22	1.58	1.58	1.94					
	n	58	60	57	58	68					

Table S4.7: Annual mean HNO_3 gas concentrations measured in the NEU DELTA® network and summary statistics.

Site	Ecosystem type	HNO_3-N (µg m^{-3})				Summary statistics					Group Mean
		2007	2008	2009	2010	mean	min	max	sd	N	
UK-ESa	Crops	0.12	0.12	-	-	0.12	0.12	0.12	0.00	2	
DE-Geb	Crops	0.26	0.25	0.29	0.34	0.29	0.25	0.34	0.04	4	
FR-Gri	Crops	0.54	0.37	0.40	0.39	0.43	0.37	0.54	0.08	4	
DE-Kli	Crops	0.32	0.30	0.31	0.37	0.33	0.30	0.37	0.03	4	
BE-Lon	Crops	0.26	0.32	0.37	0.37	0.33	0.26	0.37	0.05	4	
UA-Pet	Crops	0.38	0.33	0.31	0.32	0.34	0.31	0.38	0.03	4	
IT-BCi	Crops	0.38	0.38	0.43	0.32	0.38	0.32	0.43	0.05	4	
IT-PoV	Crops	0.44	0.44	0.40	0.43	0.43	0.40	0.44	0.02	4	
DK-Ris	Crops	0.14	0.17	-	-	0.16	0.14	0.17	0.02	2	
SK07	Crops	0.37	0.32	0.38	0.41	0.37	0.32	0.41	0.04	4	**0.32**
FR-Bil	Forest	-	-	-	0.17	0.17	0.17	0.17	-	1	
NO-Bir	Forest	-	-	0.09	0.08	0.09	0.08	0.09	0.01	2	
CZ-BK1	Forest	0.39	0.42	-	0.34	0.38	0.34	0.42	0.04	3	
BE-Bra	Forest	0.52	0.45	0.49	0.43	0.47	0.43	0.52	0.04	4	
IT-Col	Forest	-	0.12	0.16	0.12	0.13	0.12	0.16	0.02	3	
ES-ES1	Forest	0.33	0.32	0.27	0.27	0.30	0.27	0.33	0.03	4	
PT-Esp	Forest	0.47	0.32	0.32	0.33	0.36	0.32	0.47	0.07	4	
FR-Fon	Forest	0.46	0.35	0.39	0.41	0.40	0.35	0.46	0.05	4	
FR-Fgs	Forest	-	-	0.19	0.19	0.19	0.19	0.19	0.00	2	
*FR-FgsP	Forest	-	-	-	*(0.08)	-	-	-	-	-	
RU-Fyo	Forest	0.15	0.13	0.13	0.17	0.15	0.13	0.17	0.02	4	
UK-Gri	Forest	0.06	-	-	-	0.06	0.06	0.06	-	1	
DE-Hai	Forest	0.23	0.21	0.20	0.31	0.24	0.20	0.31	0.05	4	
FR-Hes	Forest	0.40	0.31	0.32	0.37	0.35	0.31	0.40	0.04	4	
DE-Hog	Forest	0.34	0.35	0.32	0.36	0.34	0.32	0.36	0.02	4	
FI-Hyy	Forest	0.12	0.09	0.10	0.10	0.10	0.09	0.12	0.01	4	
CH-Lae	Forest	0.37	0.34	0.36	0.38	0.36	0.34	0.38	0.02	4	
ES-LMa	Forest	0.24	0.22	0.26	0.25	0.24	0.22	0.26	0.02	4	
FR-LBr	Forest	0.32	0.25	-	-	0.29	0.25	0.32	0.05	2	
NL-Loo	Forest	0.32	0.23	0.28	0.26	0.27	0.23	0.32	0.04	4	
PT-Mi1	Forest	0.32	0.18	0.19	-	0.23	0.18	0.32	0.08	3	
SE-Nor	Forest	0.06	0.04	0.05	0.05	0.05	0.04	0.06	0.01	4	
FR-Pue	Forest	0.26	0.19	0.22	0.22	0.22	0.19	0.26	0.03	4	
FR-Ren	Forest	0.09	0.09	0.09	0.08	0.09	0.08	0.09	0.01	4	
IT-Ro2	Forest	0.21	0.26	0.27	0.23	0.24	0.21	0.27	0.03	4	
IT-SR	Forest	0.36	0.26	0.25	0.21	0.27	0.21	0.36	0.06	4	
SK04	Forest	0.22	0.17	0.18	0.21	0.20	0.17	0.22	0.02	4	
SK04P	Forest	0.22	0.21	0.25	0.21	0.22	0.21	0.25	0.02	4	
SK06	Forest	0.24	0.20	0.22	0.23	0.22	0.20	0.24	0.02	4	
SE-Sk2	Forest	0.08	0.06	-	-	0.07	0.06	0.08	0.01	2	
FI-Sod	Forest	0.06	0.04	0.04	0.06	0.05	0.04	0.06	0.01	4	
DK-Sor	Forest	0.25	0.23	0.20	0.19	0.22	0.19	0.25	0.03	4	
NL-Spe	Forest	0.36	0.36	0.42	0.43	0.39	0.36	0.43	0.04	4	
DE-Tha	Forest	0.32	0.25	0.26	0.32	0.29	0.25	0.32	0.04	4	
BE-Vie	Forest	0.18	0.12	0.09	0.13	0.13	0.09	0.18	0.04	4	
DE-Wet	Forest	0.26	0.26	0.28	0.35	0.29	0.26	0.35	0.04	4	**0.23**
UK-EBu	Grass	0.12	0.11	0.09	0.11	0.11	0.09	0.12	0.01	4	
UK-EBuP	Grass	0.12	0.12	0.10	-	0.11	0.10	0.12	0.01	3	
NL-Ca1	Grass	0.36	0.45	0.43	0.43	0.42	0.36	0.45	0.04	4	
IE-Car	Grass	0.11	0.10	0.09	0.12	0.11	0.09	0.12	0.01	4	
IE-Dri	Grass	0.07	0.07	0.05	-	0.06	0.05	0.07	0.01	3	
DE-Gri	Grass	0.33	0.38	0.28	0.41	0.35	0.28	0.41	0.06	4	
FR-Lq2	Grass	0.15	0.10	0.13	0.14	0.13	0.10	0.15	0.02	4	
CH-Oe1	Grass	0.43	0.39	0.39	0.38	0.40	0.38	0.43	0.02	4	
DK-Rim	Grass	0.24	0.23	-	-	0.24	0.23	0.24	0.01	2	
UK-Sol	Grass	-	-	0.07	0.11	0.09	0.07	0.11	0.03	2	**0.20**
IT-Amp	Semi-Nat	0.15	0.13	-	-	0.14	0.13	0.15	0.01	2	
UK-AMo	Semi-Nat	0.09	0.09	0.08	0.10	0.09	0.08	0.10	0.01	4	
UK-AMoP	Semi-Nat	-	-	-	-	-	-	-	-	-	
DK-Brj	Semi-Nat	-	-	-	0.17	0.17	0.17	0.17	-	1	
HU-Bug	Semi-Nat	0.29	0.30	0.35	0.30	0.31	0.29	0.35	0.03	4	
NL-Hor	Semi-Nat	0.35	0.31	0.33	0.36	0.34	0.31	0.36	0.02	4	
FI-Kaa	Semi-Nat	-	-	0.02	0.03	0.03	0.02	0.03	0.01	2	
FI-Lom	Semi-Nat	0.04	0.04	0.02	0.05	0.04	0.02	0.05	0.01	4	
DE-Meh	Semi-Nat	-	0.32	0.30	0.33	0.32	0.30	0.33	0.02	3	
IT-MBo	Semi-Nat	0.23	0.21	0.19	0.21	0.21	0.19	0.23	0.02	4	
PL-Pol	Semi-Nat	0.26	0.26	0.25	0.36	0.28	0.25	0.36	0.05	4	
ES-VDA	Semi-Nat	-	0.08	0.09	0.07	0.08	0.07	0.09	0.01	3	**0.18**
	mean	0.26	0.23	0.23	0.25	0.23					
	min	0.04	0.04	0.02	0.03	0.03					
	max	0.54	0.45	0.49	0.43	0.47					
	n	57	59	56	56	66					

**Different DELTA® denuder sample train using NaCl coated denuders to collect HNO_3*

Table S4.8: Annual mean particulate NO_3^- concentrations measured in the NEU DELTA® network and summary statistics.

Site	Ecosystem type	pNO_3^--N (µg m^{-3})				Summary statistics					Group Mean
		2007	2008	2009	2010	mean	min	max	sd	N	
UK-ESa	Crops	0.23	0.25	-	-	0.24	0.23	0.25	0.01	2	
DE-Geb	Crops	0.50	0.62	0.76	0.49	0.59	0.49	0.76	0.13	4	
FR-Gri	Crops	0.88	0.64	0.70	0.62	0.71	0.62	0.88	0.12	4	
DE-Kli	Crops	0.57	0.50	0.55	0.42	0.51	0.42	0.57	0.07	4	
BE-Lon	Crops	0.72	0.67	1.29	0.56	0.81	0.56	1.29	0.33	4	
UA-Pet	Crops	0.50	0.46	0.34	0.39	0.42	0.34	0.50	0.07	4	
IT-BCi	Crops	0.76	0.70	0.56	0.49	0.63	0.49	0.76	0.12	4	
IT-PoV	Crops	1.49	1.36	1.03	0.83	1.18	0.83	1.49	0.30	4	
DK-Ris	Crops	0.48	0.34	-	-	0.41	0.34	0.48	0.10	2	
SK07	Crops	0.67	0.60	0.51	0.43	0.55	0.43	0.67	0.10	4	**0.61**
FR-Bil	Forest	-	-	-	0.28	0.28	0.28	0.28	-	1	
NO-Bir	Forest	-	-	0.09	0.10	0.10	0.09	0.10	0.01	2	
CZ-BK1	Forest	0.37	0.42	-	0.29	0.36	0.29	0.42	0.07	3	
BE-Bra	Forest	0.90	0.79	0.91	0.71	0.83	0.71	0.91	0.10	4	
IT-Col	Forest	-	0.24	0.22	0.22	0.23	0.22	0.24	0.01	3	
ES-ES1	Forest	0.75	1.23	1.02	0.84	0.96	0.75	1.23	0.21	4	
PT-Esp	Forest	0.54	0.51	0.43	0.52	0.50	0.43	0.54	0.05	4	
FR-Fon	Forest	0.80	0.57	0.66	0.54	0.64	0.54	0.80	0.12	4	
FR-Fgs	Forest	-	-	0.60	0.48	0.54	0.48	0.60	0.08	2	
FR-FgsP	Forest	-	-	-	0.56	-	-	-	-	-	
RU-Fyo	Forest	0.14	0.15	0.10	0.16	0.14	0.10	0.16	0.03	4	
UK-Gri	Forest	0.11	-	-	-	0.11	0.11	0.11	-	1	
DE-Hai	Forest	0.48	0.40	0.64	0.41	0.48	0.40	0.64	0.11	4	
FR-Hes	Forest	0.53	0.44	0.47	0.47	0.48	0.44	0.53	0.04	4	
DE-Hog	Forest	0.45	0.54	0.67	0.48	0.54	0.45	0.67	0.10	4	
FI-Hyy	Forest	0.06	0.04	0.04	0.04	0.05	0.04	0.06	0.01	4	
CH-Lae	Forest	0.64	0.56	0.44	0.48	0.53	0.44	0.64	0.09	4	
ES-LMa	Forest	0.32	0.43	0.30	0.23	0.32	0.23	0.43	0.08	4	
FR-LBr	Forest	0.52	0.39	-	-	0.46	0.39	0.52	0.09	2	
NL-Loo	Forest	0.92	0.66	1.05	0.54	0.79	0.54	1.05	0.23	4	
PT-Mi1	Forest	0.42	0.33	0.28	-	0.34	0.28	0.42	0.07	3	
SE-Nor	Forest	0.06	0.05	0.04	0.05	0.05	0.04	0.06	0.01	4	
FR-Pue	Forest	0.33	0.27	0.31	0.27	0.30	0.27	0.33	0.03	4	
FR-Ren	Forest	0.27	0.25	0.21	0.19	0.23	0.19	0.27	0.04	4	
IT-Ro2	Forest	0.54	0.48	0.41	0.33	0.44	0.33	0.54	0.09	4	
IT-SR	Forest	0.68	0.56	0.34	0.45	0.51	0.34	0.68	0.15	4	
SK04	Forest	0.28	0.22	0.20	0.19	0.22	0.19	0.28	0.04	4	
SK04P	Forest	0.26	0.23	0.17	0.18	0.21	0.17	0.26	0.04	4	
SK06	Forest	0.26	0.23	0.17	0.20	0.22	0.17	0.26	0.04	4	
SE-Sk2	Forest	0.07	0.07	-	-	0.07	0.07	0.07	0.00	2	
FI-Sod	Forest	0.03	0.02	0.02	0.01	0.02	0.01	0.03	0.01	4	
DK-Sor	Forest	0.63	0.55	0.63	0.50	0.58	0.50	0.63	0.06	4	
NL-Spe	Forest	0.98	0.85	0.94	0.77	0.89	0.77	0.98	0.09	4	
DE-Tha	Forest	0.37	0.42	0.55	0.38	0.43	0.37	0.55	0.08	4	
BE-Vie	Forest	0.40	0.33	0.59	0.31	0.41	0.31	0.59	0.13	4	
DE-Wet	Forest	0.47	0.38	0.38	0.40	0.41	0.38	0.47	0.04	4	**0.39**
UK-EBu	Grass	0.28	0.23	0.22	0.23	0.24	0.22	0.28	0.03	4	
UK-EBuP	Grass	0.27	0.25	0.25	-	0.26	0.25	0.27	0.01	3	
NL-Ca1	Grass	1.22	1.08	1.02	0.68	1.00	0.68	1.22	0.23	4	
IE-Car	Grass	0.30	0.36	0.26	0.28	0.30	0.26	0.36	0.04	4	
IE-Dri	Grass	0.28	0.30	0.22	-	0.27	0.22	0.30	0.04	3	
DE-Gri	Grass	0.47	0.46	0.46	0.42	0.45	0.42	0.47	0.02	4	
FR-Lq2	Grass	0.30	0.21	0.27	0.24	0.26	0.21	0.30	0.04	4	
CH-Oe1	Grass	0.73	0.59	0.48	0.56	0.59	0.48	0.73	0.10	4	
DK-Rim	Grass	0.64	0.47	-	-	0.56	0.47	0.64	0.12	2	
UK-Sol	Grass	-	-	0.24	0.26	0.25	0.24	0.26	0.01	2	**0.42**
IT-Amp	Semi-Nat	0.22	0.21	-	-	0.22	0.21	0.22	0.01	2	
UK-AMo	Semi-Nat	0.24	0.22	0.21	0.19	0.22	0.19	0.24	0.02	4	
UK-AMoP	Semi-Nat	-	-	-	-	-	-	-	-	-	
DK-Brj	Semi-Nat	-	-	-	0.39	0.39	0.39	0.39	-	1	
HU-Bug	Semi-Nat	0.48	0.44	0.37	0.40	0.42	0.37	0.48	0.05	4	
NL-Hor	Semi-Nat	1.13	0.79	1.13	0.93	1.00	0.79	1.13	0.17	4	
FI-Kaa	Semi-Nat	-	-	0.01	0.01	0.01	0.01	0.01	0.00	2	
FI-Lom	Semi-Nat	0.02	0.01	0.01	0.01	0.01	0.01	0.02	0.01	4	
DE-Meh	Semi-Nat	-	0.57	0.67	0.55	0.60	0.55	0.67	0.06	3	
IT-MBo	Semi-Nat	0.51	0.43	0.27	0.34	0.39	0.27	0.51	0.10	4	
PL-Pol	Semi-Nat	0.50	0.42	0.35	0.45	0.43	0.35	0.50	0.06	4	
ES-VDA	Semi-Nat	-	0.27	0.21	0.17	0.22	0.17	0.27	0.05	3	**0.35**
	mean	0.49	0.44	0.45	0.38	0.42					
	min	0.02	0.01	0.01	0.01	0.01					
	max	1.49	1.36	1.29	0.93	1.18					
	n	57	59	56	57	66					

Table S4.9: Annual mean SO_2 gas concentrations measured in the NEU DELTA® network and summary statistics.

Site	Ecocystem type	SO_2-S (µg m^{-3})				Summary statistics					Group Mean
		2007	2008	2009	2010	mean	min	max	sd	N	
UK-ESa	Crops	0.70	0.59	-	-	0.65	0.59	0.70	0.08	2	
DE-Geb	Crops	0.58	0.45	0.42	0.68	0.53	0.42	0.68	0.12	4	
FR-Gri	Crops	0.78	0.53	0.47	0.50	0.57	0.47	0.78	0.14	4	
DE-Kli	Crops	1.80	1.46	1.60	2.32	1.80	1.46	2.32	0.38	4	
BE-Lon	Crops	1.17	0.94	0.78	0.75	0.91	0.75	1.17	0.19	4	
UA-Pet	Crops	1.26	1.30	1.35	1.44	1.34	1.26	1.44	0.08	4	
IT-BCi	Crops	0.75	0.78	1.18	0.60	0.83	0.60	1.18	0.25	4	
IT-PoV	Crops	0.98	0.85	0.69	0.77	0.82	0.69	0.98	0.12	4	
DK-Ris	Crops	0.34	0.28	-	-	0.31	0.28	0.34	0.04	2	
SK07	Crops	1.00	0.85	0.79	1.05	0.92	0.79	1.05	0.12	4	**0.87**
FR-Bil	Forest	-	-	-	0.21	0.21	0.21	0.21	-	1	
NO-Bir	Forest	-	-	0.07	0.10	0.09	0.07	0.10	0.02	2	
CZ-BK1	Forest	2.52	2.27	-	2.14	2.31	2.14	2.52	0.19	3	
BE-Bra	Forest	3.55	2.69	2.05	1.37	2.42	1.37	3.55	0.93	4	
IT-Col	Forest	-	0.13	0.15	0.12	0.13	0.12	0.15	0.02	3	
ES-ES1	Forest	0.89	0.76	0.59	0.52	0.69	0.52	0.89	0.17	4	
PT-Esp	Forest	0.97	0.74	0.66	0.63	0.75	0.63	0.97	0.15	4	
FR-Fon	Forest	0.72	0.48	0.44	0.43	0.52	0.43	0.72	0.14	4	
FR-Fgs	Forest	-	-	0.39	0.38	0.39	0.38	0.39	0.01	2	
FR-FgsP	Forest	-	-	-	-	-	-	-	-	-	
RU-Fyo	Forest	0.47	0.43	0.50	0.55	0.49	0.43	0.55	0.05	4	
UK-Gri	Forest	0.14	-	-	-	0.14	0.14	0.14	-	1	
DE-Hai	Forest	0.50	0.35	0.33	0.67	0.46	0.33	0.67	0.16	4	
FR-Hes	Forest	0.60	0.51	0.45	0.53	0.52	0.45	0.60	0.06	4	
DE-Hog	Forest	0.46	0.38	0.35	0.39	0.40	0.35	0.46	0.05	4	
FI-Hyy	Forest	0.31	0.20	0.31	0.27	0.27	0.20	0.31	0.05	4	
CH-Lae	Forest	0.56	0.49	0.41	0.39	0.46	0.39	0.56	0.08	4	
ES-LMa	Forest	0.26	0.27	0.16	0.21	0.23	0.16	0.27	0.05	4	
FR-LBr	Forest	0.48	0.31	-	-	0.40	0.31	0.48	0.12	2	
NL-Loo	Forest	0.74	0.52	0.53	0.48	0.57	0.48	0.74	0.12	4	
PT-Mi1	Forest	0.71	0.42	0.28	-	0.47	0.28	0.71	0.22	3	
SE-Nor	Forest	0.10	0.06	0.08	0.09	0.08	0.06	0.10	0.02	4	
FR-Pue	Forest	0.34	0.21	0.24	0.24	0.26	0.21	0.34	0.06	4	
FR-Ren	Forest	0.10	0.08	0.08	0.13	0.10	0.08	0.13	0.02	4	
IT-Ro2	Forest	0.40	0.36	0.36	0.34	0.37	0.34	0.40	0.03	4	
IT-SR	Forest	0.68	0.46	0.39	0.30	0.46	0.30	0.68	0.16	4	
SK04	Forest	0.63	0.48	0.47	0.60	0.55	0.47	0.63	0.08	4	
SK04P	Forest	0.73	0.61	0.58	0.58	0.63	0.58	0.73	0.07	4	
SK06	Forest	1.06	0.82	0.58	0.80	0.82	0.58	1.06	0.20	4	
SE-Sk2	Forest	0.10	0.08	-	-	0.09	0.08	0.10	0.01	2	
FI-Sod	Forest	0.29	0.28	0.27	0.31	0.29	0.27	0.31	0.02	4	
DK-Sor	Forest	0.51	0.48	0.43	0.40	0.46	0.40	0.51	0.05	4	
NL-Spe	Forest	0.82	0.75	0.70	0.63	0.73	0.63	0.82	0.08	4	
DE-Tha	Forest	1.31	0.99	1.14	1.53	1.24	0.99	1.53	0.23	4	
BE-Vie	Forest	0.38	0.22	0.19	0.22	0.25	0.19	0.38	0.09	4	
DE-Wet	Forest	0.76	0.56	0.66	0.90	0.72	0.56	0.90	0.15	4	**0.54**
UK-EBu	Grass	0.65	0.42	0.28	0.58	0.48	0.28	0.65	0.17	4	
UK-EBuP	Grass	0.64	0.47	0.34	-	0.48	0.34	0.64	0.15	3	
NL-Ca1	Grass	1.12	1.17	0.81	0.79	0.97	0.79	1.17	0.20	4	
IE-Car	Grass	0.29	0.24	0.20	0.24	0.24	0.20	0.29	0.04	4	
IE-Dri	Grass	0.25	0.19	0.17	-	0.20	0.17	0.25	0.04	3	
DE-Gri	Grass	1.31	1.15	1.06	1.66	1.30	1.06	1.66	0.26	4	
FR-Lq2	Grass	0.19	0.14	0.13	0.14	0.15	0.13	0.19	0.03	4	
CH-Oe1	Grass	1.48	1.28	0.43	0.37	0.89	0.37	1.48	0.57	4	
DK-Rim	Grass	0.39	0.35	-	-	0.37	0.35	0.39	0.03	2	
UK-Sol	Grass	-	-	0.19	0.25	0.22	0.19	0.25	0.04	2	**0.53**
IT-Amp	Semi-Nat	0.15	0.13	-	-	0.14	0.13	0.15	0.01	2	
UK-AMo	Semi-Nat	0.45	0.29	0.26	0.47	0.37	0.26	0.47	0.11	4	
UK-AMoP	Semi-Nat	-	-	-	-	-	-	-	-	-	
DK-Brj	Semi-Nat	-	-	-	0.42	0.42	0.42	0.42	-	1	
HU-Bug	Semi-Nat	0.96	1.27	1.28	1.31	1.21	0.96	1.31	0.16	4	
NL-Hor	Semi-Nat	0.78	0.71	0.81	0.63	0.73	0.63	0.81	0.08	4	
FI-Kaa	Semi-Nat	-	-	0.36	0.57	0.47	0.36	0.57	0.15	2	
FI-Lom	Semi-Nat	0.14	0.16	0.14	0.07	0.13	0.07	0.16	0.04	4	
DE-Meh	Semi-Nat	-	0.56	0.48	0.89	0.64	0.48	0.89	0.22	3	
IT-MBo	Semi-Nat	0.20	0.16	0.16	0.16	0.17	0.16	0.20	0.02	4	
PL-Pol	Semi-Nat	1.13	0.95	0.84	1.46	1.10	0.84	1.46	0.27	4	
ES-VDA	Semi-Nat	-	0.17	0.13	0.12	0.14	0.12	0.17	0.03	3	**0.50**
	mean	0.73	0.60	0.52	0.62	0.58					
	min	0.10	0.06	0.07	0.07	0.08					
	max	3.55	2.69	2.05	2.32	2.42					
	n	57	59	56	56	66					

Table S4.10: Annual mean particulate SO_4^{2-} concentrations measured in the NEU DELTA® network and summary statistics.

Site	Ecosystem type	pSO_4^{2-}-N (µg m^{-3})				Summary statistics					Group Mean
		2007	2008	2009	2010	mean	min	max	sd	N	
UK-ESa	Crops	0.21	0.22	-	-	0.22	0.21	0.22	0.01	2	
DE-Geb	Crops	0.57	0.51	0.56	0.32	0.49	0.32	0.57	0.12	4	
FR-Gri	Crops	0.53	0.41	0.39	0.34	0.42	0.34	0.53	0.08	4	
DE-Kli	Crops	0.60	0.46	0.51	0.41	0.50	0.41	0.60	0.08	4	
BE-Lon	Crops	1.20	1.00	1.37	0.90	1.12	0.90	1.37	0.21	4	
UA-Pet	Crops	0.83	1.15	0.71	0.57	0.82	0.57	1.15	0.25	4	
IT-BCi	Crops	0.91	1.08	0.56	0.63	0.80	0.56	1.08	0.24	4	
IT-PoV	Crops	0.87	0.75	0.54	0.43	0.65	0.43	0.87	0.20	4	
DK-Ris	Crops	0.78	0.55	-	-	0.67	0.55	0.78	0.16	2	
SK07	Crops	0.81	0.63	0.55	0.44	0.61	0.44	0.81	0.16	4	**0.63**
FR-Bil	Forest	-	-	-	0.27	0.27	0.27	0.27	-	1	
NO-Bir	Forest	-	-	0.35	0.34	0.35	0.34	0.35	0.01	2	
CZ-BK1	Forest	0.68	0.96	-	0.48	0.71	0.48	0.96	0.24	3	
BE-Bra	Forest	1.56	1.32	1.16	0.88	1.23	0.88	1.56	0.29	4	
IT-Col	Forest	-	0.30	0.25	0.21	0.25	0.21	0.30	0.05	3	
ES-ES1	Forest	1.23	1.14	0.93	0.73	1.01	0.73	1.23	0.22	4	
PT-Esp	Forest	0.55	0.67	0.38	0.57	0.54	0.38	0.67	0.12	4	
FR-Fon	Forest	0.53	0.39	0.38	0.29	0.40	0.29	0.53	0.10	4	
FR-Fgs	Forest	-	-	0.36	0.29	0.33	0.29	0.36	0.05	2	
FR-FgsP	Forest	-	-	-	-	-	-	-	-	-	
RU-Fyo	Forest	0.47	0.66	0.29	0.57	0.50	0.29	0.66	0.16	4	
UK-Gri	Forest	0.11	-	-	-	0.11	0.11	0.11	-	1	
DE-Hai	Forest	0.52	0.32	0.53	0.29	0.42	0.29	0.53	0.13	4	
FR-Hes	Forest	0.40	0.35	0.36	0.31	0.36	0.31	0.40	0.04	4	
DE-Hog	Forest	0.41	0.47	0.42	0.23	0.38	0.23	0.47	0.11	4	
FI-Hyy	Forest	0.47	0.42	0.52	0.43	0.46	0.42	0.52	0.05	4	
CH-Lae	Forest	0.47	0.59	0.37	0.37	0.45	0.37	0.59	0.10	4	
ES-LMa	Forest	0.72	0.57	0.51	0.65	0.61	0.51	0.72	0.09	4	
FR-LBr	Forest	0.46	0.33	-	-	0.40	0.33	0.46	0.09	2	
NL-Loo	Forest	0.64	0.49	0.68	0.30	0.53	0.30	0.68	0.17	4	
PT-Mi1	Forest	0.73	0.97	0.27	-	0.66	0.27	0.97	0.36	3	
SE-Nor	Forest	0.40	0.30	0.39	0.37	0.37	0.30	0.40	0.05	4	
FR-Pue	Forest	0.38	0.28	0.30	0.22	0.30	0.22	0.38	0.07	4	
FR-Ren	Forest	0.21	0.18	0.23	0.17	0.20	0.17	0.23	0.03	4	
IT-Ro2	Forest	0.51	0.54	0.43	0.38	0.47	0.38	0.54	0.07	4	
IT-SR	Forest	0.73	0.62	0.38	0.42	0.54	0.38	0.73	0.17	4	
SK04	Forest	0.67	0.42	0.37	0.36	0.46	0.36	0.67	0.15	4	
SK04P	Forest	0.57	0.43	0.34	0.29	0.41	0.29	0.57	0.12	4	
SK06	Forest	0.60	0.47	0.37	0.36	0.45	0.36	0.60	0.11	4	
SE-Sk2	Forest	0.42	0.35	-	-	0.39	0.35	0.42	0.05	2	
FI-Sod	Forest	0.36	0.35	0.53	0.41	0.41	0.35	0.53	0.08	4	
DK-Sor	Forest	0.88	0.68	0.77	0.76	0.77	0.68	0.88	0.08	4	
NL-Spe	Forest	0.58	0.64	0.58	0.42	0.56	0.42	0.64	0.09	4	
DE-Tha	Forest	0.49	0.45	0.55	0.33	0.46	0.33	0.55	0.09	4	
BE-Vie	Forest	0.86	0.70	0.62	0.88	0.77	0.62	0.88	0.13	4	
DE-Wet	Forest	0.46	0.32	0.34	0.28	0.35	0.28	0.46	0.08	4	**0.48**
UK-EBu	Grass	0.26	0.17	0.13	0.17	0.18	0.13	0.26	0.05	4	
UK-EBuP	Grass	0.25	0.20	0.17	-	0.21	0.17	0.25	0.04	3	
NL-Ca1	Grass	1.10	0.74	0.63	0.39	0.72	0.39	1.10	0.30	4	
IE-Car	Grass	0.26	0.31	0.25	0.23	0.26	0.23	0.31	0.03	4	
IE-Dri	Grass	0.25	0.28	0.22	-	0.25	0.22	0.28	0.03	3	
DE-Gri	Grass	0.49	0.51	0.48	0.35	0.46	0.35	0.51	0.07	4	
FR-Lq2	Grass	0.26	0.19	0.23	0.16	0.21	0.16	0.26	0.04	4	
CH-Oe1	Grass	0.58	0.63	0.32	0.40	0.48	0.32	0.63	0.15	4	
DK-Rim	Grass	0.82	0.74	-	-	0.78	0.74	0.82	0.06	2	
UK-Sol	Grass	-	-	0.24	0.18	0.21	0.18	0.24	0.04	2	**0.38**
IT-Amp	Semi-Nat	0.34	0.31	-	-	0.33	0.31	0.34	0.02	2	
UK-AMo	Semi-Nat	0.23	0.19	0.16	0.16	0.19	0.16	0.23	0.03	4	
UK-AMoP	Semi-Nat	-	-	-	-	-	-	-	-	-	
DK-Brj	Semi-Nat	-	-	-	0.67	0.67	0.67	0.67	-	1	
HU-Bug	Semi-Nat	0.72	0.82	0.62	0.49	0.66	0.49	0.82	0.14	4	
NL-Hor	Semi-Nat	0.77	0.53	0.78	0.55	0.66	0.53	0.78	0.14	4	
FI-Kaa	Semi-Nat	-	-	0.18	0.25	0.22	0.18	0.25	0.05	2	
FI-Lom	Semi-Nat	0.24	0.24	0.30	0.28	0.27	0.24	0.30	0.03	4	
DE-Meh	Semi-Nat	-	0.49	0.48	0.32	0.43	0.32	0.49	0.10	3	
IT-MBo	Semi-Nat	0.39	0.47	0.28	0.30	0.36	0.28	0.47	0.09	4	
PL-Pol	Semi-Nat	0.69	0.70	0.45	0.59	0.61	0.45	0.70	0.12	4	
ES-VDA	Semi-Nat	-	0.39	0.41	0.37	0.39	0.37	0.41	0.02	3	**0.43**
	mean	0.58	0.53	0.46	0.41	0.48					
	min	0.11	0.17	0.13	0.16	0.11					
	max	1.56	1.32	1.37	0.90	1.23					
	n	57	59	56	56	66					

Table S4.11: Annual mean HCl gas concentrations measured in the NEU DELTA® network and summary statistics.

Site	Ecosystem type	HCl-Cl⁻ (µg m⁻³)				Summary statistics					Group Mean
		2007	2008	2009	2010	mean	min	max	sd	N	
UK-ESa	Crops	0.21	0.30	-	-	0.26	0.21	0.30	0.06	2	
DE-Geb	Crops	0.12	0.19	0.23	0.25	0.20	0.12	0.25	0.06	4	
FR-Gri	Crops	0.39	0.19	0.29	0.29	0.29	0.19	0.39	0.08	4	
DE-Kli	Crops	0.16	0.19	0.19	0.24	0.20	0.16	0.24	0.03	4	
BE-Lon	Crops	0.48	0.22	0.57	0.15	0.36	0.15	0.57	0.20	4	
UA-Pet	Crops	0.29	0.23	0.18	0.22	0.23	0.18	0.29	0.05	4	
IT-BCi	Crops	0.40	0.36	0.32	0.40	0.37	0.32	0.40	0.04	4	
IT-PoV	Crops	0.17	0.18	0.17	0.06	0.15	0.06	0.18	0.06	4	
DK-Ris	Crops	0.25	0.16	-	-	0.21	0.16	0.25	0.06	2	
SK07	Crops	0.23	0.09	0.19	0.05	0.14	0.05	0.23	0.08	4	**0.24**
FR-Bil	Forest	-	-	-	0.34	0.34	0.34	0.34	-	1	
NO-Bir	Forest	-	-	0.46	0.23	0.35	0.23	0.46	0.16	2	
CZ-BK1	Forest	0.27	0.26	-	0.20	0.24	0.20	0.27	0.04	3	
BE-Bra	Forest	0.54	0.26	0.45	0.19	0.36	0.19	0.54	0.16	4	
IT-Col	Forest	-	0.19	0.17	0.06	0.14	0.06	0.19	0.07	3	
ES-ES1	Forest	0.40	0.53	0.27	0.22	0.36	0.22	0.53	0.14	4	
PT-Esp	Forest	0.51	0.51	0.44	0.58	0.51	0.44	0.58	0.06	4	
FR-Fon	Forest	0.31	0.26	0.33	0.26	0.29	0.26	0.33	0.04	4	
FR-Fgs	Forest	-	-	0.24	0.27	0.26	0.24	0.27	0.02	2	
FR-FgsP	Forest	-	-	-	-	-	-	-	-	-	
RU-Fyo	Forest	0.06	0.06	0.06	0.10	0.07	0.06	0.10	0.02	4	
UK-Gri	Forest	0.16	-	-	-	0.16	0.16	0.16	-	1	
DE-Hai	Forest	0.09	0.12	0.11	0.32	0.16	0.09	0.32	0.11	4	
FR-Hes	Forest	0.19	0.15	0.17	0.19	0.18	0.15	0.19	0.02	4	
DE-Hog	Forest	0.08	0.09	0.10	0.16	0.11	0.08	0.16	0.04	4	
FI-Hyy	Forest	0.13	0.07	0.42	0.17	0.20	0.07	0.42	0.15	4	
CH-Lae	Forest	0.11	0.11	0.10	0.18	0.13	0.10	0.18	0.04	4	
ES-LMa	Forest	0.22	0.45	0.16	0.15	0.25	0.15	0.45	0.14	4	
FR-LBr	Forest	0.37	0.26	-	-	0.32	0.26	0.37	0.08	2	
NL-Loo	Forest	0.24	0.13	0.22	0.15	0.19	0.13	0.24	0.05	4	
PT-Mi1	Forest	0.26	0.28	0.19	-	0.24	0.19	0.28	0.05	3	
SE-Nor	Forest	0.18	0.06	0.26	0.08	0.15	0.06	0.26	0.09	4	
FR-Pue	Forest	0.27	0.16	0.26	0.26	0.24	0.16	0.27	0.05	4	
FR-Ren	Forest	0.05	0.01	0.10	0.09	0.06	0.01	0.10	0.04	4	
IT-Ro2	Forest	0.36	0.39	0.25	0.14	0.29	0.14	0.39	0.11	4	
IT-SR	Forest	0.53	0.36	0.35	0.13	0.34	0.13	0.53	0.16	4	
SK04	Forest	0.13	0.08	0.10	0.05	0.09	0.05	0.13	0.03	4	
SK04P	Forest	0.09	0.14	0.20	0.03	0.12	0.03	0.20	0.07	4	
SK06	Forest	0.20	0.10	0.09	0.02	0.10	0.02	0.20	0.07	4	
SE-Sk2	Forest	0.16	0.18	-	-	0.17	0.16	0.18	0.01	2	
FI-Sod	Forest	0.16	0.18	0.25	0.10	0.17	0.10	0.25	0.06	4	
DK-Sor	Forest	0.39	0.36	0.40	0.21	0.34	0.21	0.40	0.09	4	
NL-Spe	Forest	0.40	0.41	0.50	0.49	0.45	0.40	0.50	0.05	4	
DE-Tha	Forest	0.17	0.13	0.14	0.22	0.17	0.13	0.22	0.04	4	
BE-Vie	Forest	0.13	0.08	0.26	0.09	0.14	0.08	0.26	0.08	4	
DE-Wet	Forest	0.12	0.16	0.16	0.28	0.18	0.12	0.28	0.07	4	**0.22**
UK-EBu	Grass	0.28	0.20	0.15	0.19	0.21	0.15	0.28	0.05	4	
UK-EBuP	Grass	0.22	0.21	0.20	-	0.21	0.20	0.22	0.01	3	
NL-Ca1	Grass	0.29	0.46	0.37	0.37	0.37	0.29	0.46	0.07	4	
IE-Car	Grass	0.24	0.15	0.19	0.24	0.21	0.15	0.24	0.04	4	
IE-Dri	Grass	0.21	0.14	0.26	-	0.20	0.14	0.26	0.06	3	
DE-Gri	Grass	0.16	0.30	0.20	0.31	0.24	0.16	0.31	0.07	4	
FR-Lq2	Grass	0.16	0.10	0.14	0.13	0.13	0.10	0.16	0.03	4	
CH-Oe1	Grass	0.09	0.09	0.08	0.16	0.11	0.08	0.16	0.04	4	
DK-Rim	Grass	0.34	0.19	-	-	0.27	0.19	0.34	0.11	2	
UK-Sol	Grass	-	-	0.11	0.17	0.14	0.11	0.17	0.04	2	**0.21**
IT-Amp	Semi-Nat	0.17	0.21	-	-	0.19	0.17	0.21	0.03	2	
UK-AMo	Semi-Nat	0.22	0.19	0.19	0.18	0.20	0.18	0.22	0.02	4	
UK-AMoP	Semi-Nat	-	-	-	-	-	-	-	-	-	
DK-Brj	Semi-Nat	-	-	-	0.26	0.26	0.26	0.26	-	1	
HU-Bug	Semi-Nat	0.12	0.10	0.07	0.10	0.10	0.07	0.12	0.02	4	
NL-Hor	Semi-Nat	0.20	0.32	0.35	0.97	0.46	0.20	0.97	0.35	4	
FI-Kaa	Semi-Nat	-	-	0.26	0.09	0.18	0.09	0.26	0.12	2	
FI-Lom	Semi-Nat	0.15	0.04	0.19	0.54	0.23	0.04	0.54	0.22	4	
DE-Meh	Semi-Nat	-	0.24	0.20	0.30	0.25	0.20	0.30	0.05	3	
IT-MBo	Semi-Nat	0.11	0.20	0.37	0.32	0.25	0.11	0.37	0.12	4	
PL-Pol	Semi-Nat	0.15	0.16	0.12	0.39	0.21	0.12	0.39	0.12	4	
ES-VDA	Semi-Nat	-	0.11	0.10	0.07	0.09	0.07	0.11	0.02	3	**0.22**
	mean	0.23	0.20	0.23	0.22	0.22					
	min	0.05	0.01	0.06	0.02	0.06					
	max	0.54	0.53	0.57	0.97	0.51					
	n	57	59	56	56	66					

Table S4.12: Annual mean particulate Cl^- concentrations measured in the NEU DELTA® network and summary statistics.

Site	Ecosystem type	pCl⁻ (µg m⁻³)				Summary statistics					Group Mean
		2007	2008	2009	2010	mean	min	max	sd	N	
UK-ESa	Crops	1.18	1.23	-	-	1.21	1.18	1.23	0.04	2	
DE-Geb	Crops	0.33	0.45	0.30	0.31	0.35	0.30	0.45	0.07	4	
FR-Gri	Crops	1.07	0.98	0.79	0.41	0.81	0.41	1.07	0.29	4	
DE-Kli	Crops	0.36	0.30	0.23	0.40	0.32	0.23	0.40	0.07	4	
BE-Lon	Crops	0.37	0.36	0.29	0.14	0.29	0.14	0.37	0.11	4	
UA-Pet	Crops	0.41	0.41	0.24	0.43	0.37	0.24	0.43	0.09	4	
IT-BCi	Crops	1.54	1.41	0.88	2.12	1.49	0.88	2.12	0.51	4	
IT-PoV	Crops	0.34	0.47	0.33	0.31	0.36	0.31	0.47	0.07	4	
DK-Ris	Crops	0.36	0.30	-	-	0.33	0.30	0.36	0.04	2	
SK07	Crops	0.53	0.28	0.20	0.23	0.31	0.20	0.53	0.15	4	**0.58**
FR-Bil	Forest	-	-	-	0.80	0.80	0.80	0.80	-	1	
NO-Bir	Forest	-	-	0.37	0.16	0.27	0.16	0.37	0.15	2	
CZ-BK1	Forest	0.29	0.29	-	0.17	0.25	0.17	0.29	0.07	3	
BE-Bra	Forest	0.67	0.60	0.41	0.29	0.49	0.29	0.67	0.17	4	
IT-Col	Forest	-	0.33	0.54	0.45	0.44	0.33	0.54	0.11	3	
ES-ES1	Forest	0.99	1.06	0.55	0.64	0.81	0.55	1.06	0.25	4	
PT-Esp	Forest	1.09	1.27	1.51	1.72	1.40	1.09	1.72	0.28	4	
FR-Fon	Forest	0.99	0.83	0.82	0.42	0.77	0.42	0.99	0.24	4	
FR-Fgs	Forest	-	-	1.47	0.96	1.22	0.96	1.47	0.36	2	
FR-FgsP	Forest	-	-	-	1.11	-	-	-	-	-	
RU-Fyo	Forest	0.14	0.12	0.07	0.22	0.14	0.07	0.22	0.06	4	
UK-Gri	Forest	0.85	-	-	-	0.85	0.85	0.85	-	1	
DE-Hai	Forest	0.36	0.32	0.22	0.23	0.28	0.22	0.36	0.07	4	
FR-Hes	Forest	0.45	0.35	0.25	0.03	0.27	0.03	0.45	0.18	4	
DE-Hog	Forest	0.12	0.15	0.17	0.12	0.14	0.12	0.17	0.02	4	
FI-Hyy	Forest	0.06	0.04	-	-	0.05	0.04	0.06	0.01	2	
CH-Lae	Forest	0.21	0.18	0.16	0.14	0.17	0.14	0.21	0.03	4	
ES-LMa	Forest	0.14	0.38	0.09	0.19	0.20	0.09	0.38	0.13	4	
FR-LBr	Forest	1.50	1.29	-	-	1.40	1.29	1.50	0.15	2	
NL-Loo	Forest	1.19	0.67	0.79	0.58	0.81	0.58	1.19	0.27	4	
PT-Mi1	Forest	1.04	0.96	0.90	-	0.97	0.90	1.04	0.07	3	
SE-Nor	Forest	0.08	0.08	0.04	0.02	0.06	0.02	0.08	0.03	4	
FR-Pue	Forest	0.52	0.50	0.54	0.18	0.44	0.18	0.54	0.17	4	
FR-Ren	Forest	0.12	0.17	0.15	-	0.15	0.12	0.17	0.03	3	
IT-Ro2	Forest	0.99	0.68	0.83	0.73	0.81	0.68	0.99	0.14	4	
IT-SR	Forest	2.60	1.92	1.16	1.68	1.84	1.16	2.60	0.60	4	
SK04	Forest	0.41	0.26	0.17	0.24	0.27	0.17	0.41	0.10	4	
SK04P	Forest	0.39	0.28	0.17	0.22	0.27	0.17	0.39	0.09	4	
SK06	Forest	0.35	0.25	0.17	0.30	0.27	0.17	0.35	0.08	4	
SE-Sk2	Forest	0.09	0.09	-	-	0.09	0.09	0.09	0.00	2	
FI-Sod	Forest	0.07	0.06	0.06	0.06	0.06	0.06	0.07	0.01	4	
DK-Sor	Forest	0.59	0.78	0.46	0.28	0.53	0.28	0.78	0.21	4	
NL-Spe	Forest	1.61	1.21	0.80	0.96	1.15	0.80	1.61	0.35	4	
DE-Tha	Forest	0.27	0.24	0.22	0.23	0.24	0.22	0.27	0.02	4	
BE-Vie	Forest	0.13	0.09	0.17	0.03	0.11	0.03	0.17	0.06	4	
DE-Wet	Forest	0.25	0.22	0.16	0.21	0.21	0.16	0.25	0.04	4	**0.52**
UK-EBu	Grass	1.38	0.86	1.04	1.11	1.10	0.86	1.38	0.22	4	
UK-EBuP	Grass	1.33	1.02	1.27	-	1.21	1.02	1.33	0.16	3	
NL-Ca1	Grass	1.02	1.20	0.93	0.88	1.01	0.88	1.20	0.14	4	
IE-Car	Grass	1.85	1.78	1.82	1.02	1.62	1.02	1.85	0.40	4	
IE-Dri	Grass	1.94	1.94	1.69	-	1.86	1.69	1.94	0.14	3	
DE-Gri	Grass	0.29	0.29	0.18	0.33	0.27	0.18	0.33	0.06	4	
FR-Lq2	Grass	0.35	0.28	0.23	0.01	0.22	0.01	0.35	0.15	4	
CH-Oe1	Grass	0.23	0.20	0.17	0.21	0.20	0.17	0.23	0.02	4	
DK-Rim	Grass	0.95	0.81	-	-	0.88	0.81	0.95	0.10	2	
UK-Sol	Grass	-	-	1.87	1.01	1.44	1.01	1.87	0.61	2	**0.98**
IT-Amp	Semi-Nat	0.29	0.25	-	-	0.27	0.25	0.29	0.03	2	
UK-AMo	Semi-Nat	1.27	1.16	1.00	1.02	1.11	1.00	1.27	0.13	4	
UK-AMoP	Semi-Nat	-	-	-	-	-	-	-	-	-	
DK-Brj	Semi-Nat	-	-	-	0.21	0.21	0.21	0.21	-	1	
HU-Bug	Semi-Nat	0.23	0.16	0.10	0.10	0.15	0.10	0.23	0.06	4	
NL-Hor	Semi-Nat	1.28	1.23	1.31	1.20	1.26	1.20	1.31	0.05	4	
FI-Kaa	Semi-Nat	-	-	0.11	0.19	0.15	0.11	0.19	0.06	2	
FI-Lom	Semi-Nat	0.13	0.06	0.06	0.02	0.07	0.02	0.13	0.05	4	
DE-Meh	Semi-Nat	-	0.44	0.31	0.31	0.35	0.31	0.44	0.08	3	
IT-MBo	Semi-Nat	0.12	0.12	0.08	0.09	0.10	0.08	0.12	0.02	4	
PL-Pol	Semi-Nat	0.59	0.44	0.28	0.30	0.40	0.28	0.59	0.14	4	
ES-VDA	Semi-Nat	-	0.04	0.04	0.05	0.04	0.04	0.05	0.01	3	**0.37**
	mean	0.67	0.58	0.53	0.47	0.57					
	min	0.06	0.04	0.04	0.01	0.04					
	max	2.60	1.94	1.87	2.12	1.86					
	n	57	59	55	55	66					

Table S4.13: Annual mean particulate Na^+ concentrations measured in the NEU DELTA® network and summary statistics.

Site	Ecosystem type	pNa^+ (µg m^{-3})				Summary statistics					Group Mean
		2007	2008	2009	2010	mean	min	max	sd	N	
UK-ESa	Crops	0.61	0.76	-	-	0.69	0.61	0.76	0.11	2	
DE-Geb	Crops	0.18	0.31	0.21	0.12	0.21	0.12	0.31	0.08	4	
FR-Gri	Crops	0.63	0.66	0.60	0.43	0.58	0.43	0.66	0.10	4	
DE-Kli	Crops	0.22	0.23	0.13	0.13	0.18	0.13	0.23	0.05	4	
BE-Lon	Crops	0.78	0.60	0.71	0.42	0.63	0.42	0.78	0.16	4	
UA-Pet	Crops	0.25	0.32	0.19	0.28	0.26	0.19	0.32	0.05	4	
IT-BCi	Crops	1.21	1.09	0.80	1.14	1.06	0.80	1.21	0.18	4	
IT-PoV	Crops	0.23	0.24	0.15	0.18	0.20	0.15	0.24	0.04	4	
DK-Ris	Crops	0.91	1.13	-	-	1.02	0.91	1.13	0.16	2	
SK07	Crops	0.13	0.13	0.09	0.08	0.11	0.08	0.13	0.03	4	**0.49**
FR-Bil	Forest	-	-	-	0.62	0.62	0.62	0.62	-	1	
NO-Bir	Forest	-	-	0.58	0.28	0.43	0.28	0.58	0.21	2	
CZ-BK1	Forest	0.20	0.27	-	0.09	0.19	0.09	0.27	0.09	3	
BE-Bra	Forest	1.09	1.15	1.03	0.69	0.99	0.69	1.15	0.21	4	
IT-Col	Forest	-	0.26	0.37	0.21	0.28	0.21	0.37	0.08	3	
ES-ES1	Forest	2.30	1.46	1.10	0.94	1.45	0.94	2.30	0.61	4	
PT-Esp	Forest	0.80	1.07	1.15	1.18	1.05	0.80	1.18	0.17	4	
FR-Fon	Forest	0.56	0.62	0.55	0.44	0.54	0.44	0.62	0.07	4	
FR-Fgs	Forest	-	-	0.82	0.67	0.75	0.67	0.82	0.11	2	
FR-FgsP	Forest	-	-	-	0.71	-	-	-	-	-	
RU-Fyo	Forest	0.08	0.09	0.04	0.10	0.08	0.04	0.10	0.03	4	
UK-Gri	Forest	0.38	-	-	-	0.38	0.38	0.38	-	1	
DE-Hai	Forest	0.18	0.22	0.14	0.10	0.16	0.10	0.22	0.05	4	
FR-Hes	Forest	0.20	0.23	0.24	0.18	0.21	0.18	0.24	0.03	4	
DE-Hog	Forest	0.05	0.12	0.09	0.07	0.08	0.05	0.12	0.03	4	
FI-Hyy	Forest	0.21	0.20	-	-	0.21	0.20	0.21	0.01	2	
CH-Lae	Forest	0.20	0.18	0.16	0.10	0.16	0.10	0.20	0.04	4	
ES-LMa	Forest	0.32	0.40	0.30	0.28	0.33	0.28	0.40	0.05	4	
FR-LBr	Forest	1.05	0.91	-	-	0.98	0.91	1.05	0.10	2	
NL-Loo	Forest	0.80	0.47	0.54	0.41	0.56	0.41	0.80	0.17	4	
PT-Mi1	Forest	1.00	0.79	0.74	-	0.84	0.74	1.00	0.14	3	
SE-Nor	Forest	0.20	0.31	0.22	0.13	0.22	0.13	0.31	0.07	4	
FR-Pue	Forest	0.33	0.41	0.44	0.33	0.38	0.33	0.44	0.06	4	
FR-Ren	Forest	0.00	0.14	0.01	-	0.05	0.00	0.14	0.08	3	
IT-Ro2	Forest	0.56	0.59	0.53	0.63	0.58	0.53	0.63	0.04	4	
IT-SR	Forest	1.56	1.42	0.76	0.88	1.16	0.76	1.56	0.39	4	
SK04	Forest	0.38	0.10	0.06	0.03	0.14	0.03	0.38	0.16	4	
SK04P	Forest	0.17	0.10	0.09	0.05	0.10	0.05	0.17	0.05	4	
SK06	Forest	0.18	0.20	0.13	0.12	0.16	0.12	0.20	0.04	4	
SE-Sk2	Forest	0.23	0.17	-	-	0.20	0.17	0.23	0.04	2	
FI-Sod	Forest	0.18	0.15	0.16	0.15	0.16	0.15	0.18	0.01	4	
DK-Sor	Forest	1.03	1.04	0.98	0.62	0.92	0.62	1.04	0.20	4	
NL-Spe	Forest	1.33	0.78	0.46	0.35	0.73	0.35	1.33	0.44	4	
DE-Tha	Forest	0.17	0.27	0.15	0.09	0.17	0.09	0.27	0.07	4	
BE-Vie	Forest	0.37	0.35	0.35	0.20	0.32	0.20	0.37	0.08	4	
DE-Wet	Forest	0.11	0.17	0.10	0.10	0.12	0.10	0.17	0.03	4	**0.45**
UK-EBu	Grass	0.75	0.60	0.67	0.60	0.66	0.60	0.75	0.07	4	
UK-EBuP	Grass	0.68	0.66	0.61	-	0.65	0.61	0.68	0.04	3	
NL-Ca1	Grass	0.80	0.70	0.52	0.42	0.61	0.42	0.80	0.17	4	
IE-Car	Grass	0.97	0.99	0.93	0.65	0.89	0.65	0.99	0.16	4	
IE-Dri	Grass	1.02	1.12	0.89	-	1.01	0.89	1.12	0.12	3	
DE-Gri	Grass	0.15	0.21	0.09	0.07	0.13	0.07	0.21	0.06	4	
FR-Lq2	Grass	0.22	0.23	0.19	0.17	0.20	0.17	0.23	0.03	4	
CH-Oe1	Grass	0.23	0.16	0.15	0.17	0.18	0.15	0.23	0.04	4	
DK-Rim	Grass	1.05	1.52	-	-	1.29	1.05	1.52	0.33	2	
UK-Sol	Grass	-	-	1.00	0.67	0.84	0.67	1.00	0.23	2	**0.64**
IT-Amp	Semi-Nat	0.24	0.39	-	-	0.32	0.24	0.39	0.11	2	
UK-AMo	Semi-Nat	0.67	0.64	0.65	0.48	0.61	0.48	0.67	0.09	4	
UK-AMoP	Semi-Nat	-	-	-	-	-	-	-	-	-	
DK-Brj	Semi-Nat	-	-	-	0.63	0.63	0.63	0.63	-	1	
HU-Bug	Semi-Nat	0.13	0.12	0.08	0.07	0.10	0.07	0.13	0.03	4	
NL-Hor	Semi-Nat	0.98	0.77	0.51	0.74	0.75	0.51	0.98	0.19	4	
FI-Kaa	Semi-Nat	-	-	0.10	0.17	0.14	0.10	0.17	0.05	2	
FI-Lom	Semi-Nat	0.18	0.12	0.13	0.08	0.13	0.08	0.18	0.04	4	
DE-Meh	Semi-Nat	-	0.28	0.14	0.13	0.18	0.13	0.28	0.08	3	
IT-MBo	Semi-Nat	0.12	0.09	0.16	0.16	0.13	0.09	0.16	0.03	4	
PL-Pol	Semi-Nat	0.43	0.26	0.16	0.18	0.26	0.16	0.43	0.12	4	
ES-VDA	Semi-Nat	-	0.12	0.12	0.07	0.10	0.07	0.12	0.03	3	**0.30**
	mean	0.53	0.49	0.40	0.35	0.46					
	min	0.00	0.09	0.01	0.03	0.05					
	max	2.30	1.52	1.15	1.18	1.45					
	n	57	59	55	55	66					

Table S4.14: Annual wet deposition of inorganic components (kg ha^{-1} yr^{-1}) estimated from Rotenkamp bulk precipitation collectors in the NEU bulk wet deposition network and percentage composition by mass measured. The data shown are 2-year averaged deposition, made between 2008 and 2010, except at 5 sites with 1 year of measurement only (BE-Vie, FR-Fgs, FR-LBr, DE-Wet, IT-BCi).

Site ID / Ecosystem type		Annual Wet Deposition (kg ha^{-1} yr^{-1})											% contribution to total (by mass)					
		NH_4^+-N	NO_3^--N	SO_4^{2-}-S	ss-SO_4^{2-}-S	nss-SO_4^{2-}-S	Cl^-	H^+	Na^+	Ca^{2+}	K^+	Mg^{2+}	NH_4^+-N	NO_3^--N	SO_4^{2-}-S	nss-SO_4^{2-}-S	Na^++Cl^-	Ca^{2+}+K^++Mg^{2+}
*BE-Vie	F	3.67	2.38	4.10	0.42	3.69	8.03	0.13	4.94	4.31	2.35	1.20	11.8%	7.6%	13.2%	11.9%	41.7%	25.3%
FR-Bil	F	1.25	0.65	2.70	1.73	0.96	36.8	0.09	20.6	2.34	1.50	2.18	1.8%	1.0%	4.0%	1.4%	84.3%	8.8%
FR-Pue	F	2.33	3.35	3.55	0.86	2.68	17.0	0.10	10.3	3.85	1.17	1.33	5.4%	7.8%	8.3%	6.3%	63.4%	14.8%
FR-Fon	F	0.72	0.61	1.52	0.23	1.29	4.37	0.12	2.78	2.30	0.94	0.46	5.2%	4.4%	11.0%	9.3%	51.7%	26.7%
*FR-Fgs	F	3.20	2.06	3.68	0.87	2.81	18.4	0.05	10.4	1.64	0.49	1.18	7.8%	5.0%	9.0%	6.9%	70.1%	8.1%
*FR-LBr	F	1.86	3.31	6.84	2.57	4.27	59.9	0.02	30.6	5.50	1.75	4.23	1.6%	2.9%	6.0%	3.7%	79.4%	10.1%
DE-Gri	G	3.80	4.00	4.26	0.17	4.09	3.51	0.20	2.06	2.38	1.07	0.44	17.5%	18.4%	19.6%	18.8%	25.6%	17.9%
*DE-Wet	F	5.00	5.33	4.60	0.27	4.33	4.91	0.31	3.21	1.94	0.73	0.59	18.8%	20.0%	17.3%	16.3%	30.5%	12.2%
DE-Hai	F	3.19	4.14	3.36	0.22	3.14	3.51	0.22	2.57	1.86	1.31	0.41	15.5%	20.1%	16.3%	15.3%	29.6%	17.4%
IT-SoR	F	2.20	3.22	6.84	3.23	3.61	70.1	0.18	38.5	8.16	2.65	4.62	1.6%	2.4%	5.0%	2.6%	79.6%	11.3%
IT-Ro2	F	3.36	1.57	4.07	1.07	3.00	22.7	0.08	12.8	8.47	1.97	2.07	5.9%	2.8%	7.1%	5.3%	62.1%	21.9%
*IT-BCi	C	5.09	2.54	5.51	2.09	3.41	47.3	0.00	24.9	13.0	5.27	3.61	4.7%	2.4%	5.1%	3.2%	67.3%	20.4%
PL-wet	SN	2.21	2.31	2.69	0.11	2.57	2.42	0.11	1.36	1.77	0.69	0.34	15.9%	16.6%	19.3%	18.5%	27.2%	20.1%
ES-Lma	F	12.4	4.38	3.93	0.53	3.39	13.0	0.00	6.35	14.7	4.52	2.22	20.2%	7.1%	6.4%	5.5%	31.5%	34.8%
ES-VDA	SN	14.6	6.03	7.74	0.38	7.36	9.38	0.01	4.55	25.0	2.99	1.72	20.3%	8.4%	10.7%	10.2%	19.3%	41.3%
ES-ES1	F	1.66	2.47	4.67	1.16	3.51	24.4	0.01	13.8	8.95	1.59	2.11	2.8%	4.1%	7.8%	5.9%	64.0%	21.2%
CH-Lae	F	2.82	2.56	2.64	0.11	2.53	2.24	0.13	1.28	2.93	2.05	0.39	16.6%	15.0%	15.5%	14.9%	20.7%	31.5%
mean		4.1	3.0	4.3	0.9	3.3	20.5	0.1	11.2	6.4	1.9	1.7	10.2%	8.6%	10.7%	9.2%	49.9%	20.2%
min		0.7	0.6	1.5	0.1	1.0	2.2	0.0	1.3	1.6	0.5	0.3	1.6%	1.0%	4.0%	1.4%	19.3%	8.1%
max		14.6	6.0	7.7	3.2	7.4	70.1	0.3	38.5	25.0	5.3	4.6	20.3%	20.1%	19.6%	18.8%	84.3%	41.3%
N		17	17	17	17	17	17	17	17	17	17	17.	17	17	17	17	17	17

*1 year of data only